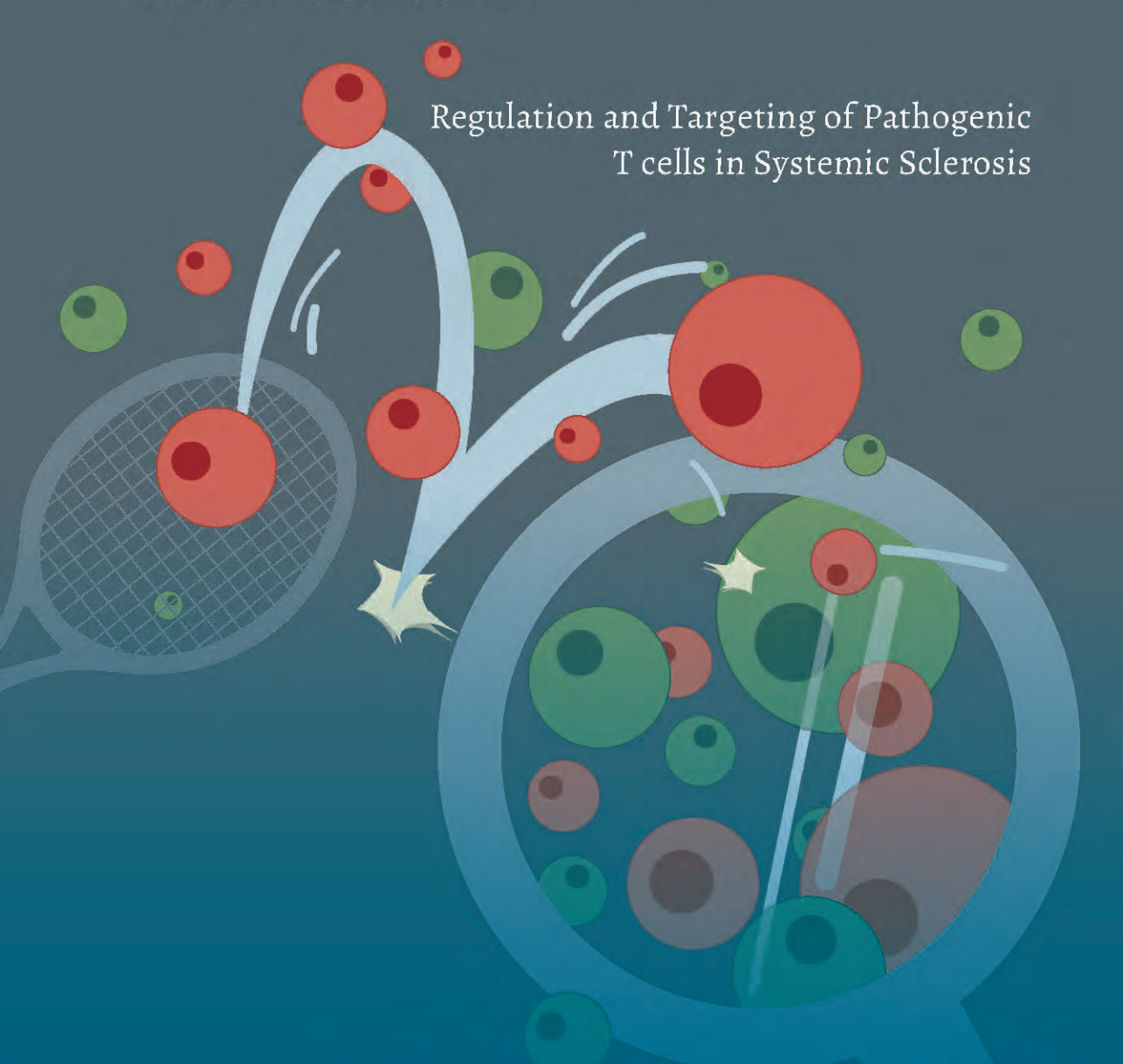
Redefining Autoimmune T Cell Pathology in Connective Tissue Disorders



Theodoros Ioannis Papadimitriou

RADBOUD UNIVERSITY PRESS

Radboud Dissertation Series

Redefining Autoimmune T Cell Pathology in Connective Tissue Disorders

Regulation and Targeting of Pathogenic T cells in Systemic Sclerosis

Theodoros Ioannis Papadimitriou



Printing costs for this thesis have been partially covered by Philikos B.V.

Redefining Autoimmune T Cell Pathology in Connective Tissue Disorders

Regulation and Targeting of Pathogenic T cells in Systemic Sclerosis

Theodoros Ioannis Papadimitriou

Radboud Dissertation Series

ISSN: 2950-2772 (Online); 2950-2780 (Print)

Published by RADBOUD UNIVERSITY PRESS Postbus 9100, 6500 HA Nijmegen, The Netherlands www.radbouduniversitypress.nl

Design: Proefschrift AIO | Guus Gijben Cover: Proefschrift AIO | Guus Gijben

Printing: DPN Rikken/Pumbo

ISBN: 9789465151144

DOI: 10.54195/9789465151144

Free download at: https://doi.org/10.54195/9789465151144

© 2025 Theodoros Ioannis Papadimitriou

RADBOUD UNIVERSITY PRESS

This is an Open Access book published under the terms of Creative Commons Attribution-Noncommercial-NoDerivatives International license (CC BY-NC-ND 4.0). This license allows reusers to copy and distribute the material in any medium or format in unadapted form only, for noncommercial purposes only, and only so long as attribution is given to the creator, see http://creativecommons.org/licenses/by-nc-nd/4.0/.

Redefining Autoimmune T Cell Pathology in Connective Tissue Disorders

Regulation and Targeting of Pathogenic T cells in Systemic Sclerosis

Proefschrift ter verkrijging van de graad van doctor aan de Radboud Universiteit Nijmegen op gezag van de rector magnificus prof. dr. J.M. Sanders, volgens besluit van het college voor promoties in het openbaar te verdedigen op

> woensdag 19 november 2025 om 14.30 uur precies

> > door

Theodoros Ioannis Papadimitriou geboren op 3 februari 1993 te Athene, Griekenland

Promotor:

Prof. dr. P.M. van der Kraan

Copromotoren:

Dr. J.P.M. Koenen

Dr. R.M. Thurlings

Dr. A.P.M. van Caam

Manuscriptcommissie:

Prof. dr. A.B. van Spriel

Prof. dr. E.C. de Jong

Prof. dr. A. Bozec (Friedrich-Alexander-Universität Erlangen-Nürnberg, Duitsland)

Redefining Autoimmune T Cell Pathology in Connective Tissue Disorders

Regulation and Targeting of Pathogenic T cells in Systemic Sclerosis

Dissertation to obtain the degree of doctor from Radboud University Nijmegen on the authority of the Rector Magnificus prof. dr. J.M. Sanders, according to the decision of the Doctorate Board to be defended in public on

Wednesday, November 19, 2025 at 2:30 pm

by

Theodoros Ioannis Papadimitriou born on February 3, 1993 in Athens, Greece

PhD supervisor:

Prof. dr. P.M. van der Kraan

PhD co-supervisors:

Dr. J.P.M. Koenen Dr. R.M. Thurlings

Dr. A.P.M. van Caam

Manuscript Committee:

Prof. dr. A.B. van Spriel

Prof. dr. E.C. de Jong

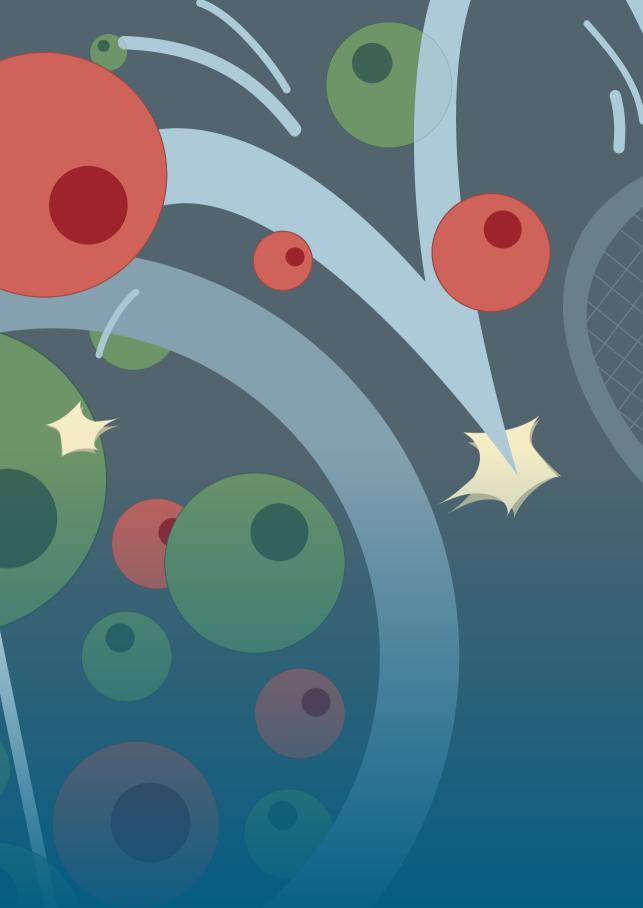
Prof. dr. A. Bozec (Friedrich-Alexander-University of Erlangen-Nürnberg, Germany)

Table of content

Abstract of thesis and outline	11
Chapter 1 General Introduction and outline	15
	13
Chapter 2 Therapeutic options for systemic sclerosis: current and future	41
perspectives in tackling immune-mediated fibrosis	71
Biomedicines 2022, 10, 316.	
Chapter 3	
CD7 activation regulates cytotoxicity-driven pathology in systemic sclerosis, yielding a target for selective cell depletion	93
Annals of the Rheumatic Diseases. 2024 Mar 12;83(4):488-498.	
Chapter 4	
Novel 3D hydrogel model shows that CD8+T cells drive myofibroblast activation and contraction via JAK/STAT3 and TGFβ signalling	137
iScience (Cell Press).	
Chapter 5	
Systemic sclerosis-associated pulmonary arterial hypertension is	175
characterized by a distinct peripheral T helper cell profile Rheumatology (Oxford). 2024 Sep 1;63(9):2525-2534.	
Chapter 6	
Interferon-responsive autoreactive CD4+ T cells restrict systemic	211
autoimmunity via TRAIL Submitted.	
Saomittea.	

Chapter 7

General Discussion and future perspectives	271
Summary of the thesis (Nederlandse samenvatting)	310
Research Data Management Plan	316
List of publications	318
Acknowledgements	320
Portfolio	328
Abbreviations	330
Curriculum vitae	340



Abstract of thesis and outline

The primary aim of this thesis is to investigate how pathogenic autoreactive T cell responses manifest in systemic sclerosis (SSc) and other connective tissue diseases (CTDs) such as Sjogren's syndrome (SjS). By elucidating the underlying mechanisms of these immune responses, this work seeks to advance the understanding of disease pathophysiology and inform the development of targeted T cell therapies with improved specificity, reduced side effects, and broader applicability to diverse SSc and CTD patient populations. To achieve this, a comprehensive toolkit that integrates advanced imaging, single-cell multiomic technologies, in silico approaches, and functional assays was developed to detect and analyze adaptive immune responses driving SSc and other related CTDs such as SjS.

Chapter 2 reviews current knowledge on the pathophysiology of SSc, with a particular focus on the heterogeneous nature of the disease and the critical roles of adaptive immune responses, especially T cell-mediated mechanisms, in its clinical manifestations. This review also evaluates the therapies that have been tested, their molecular targets, and their potential efficacy in clinical trials. By identifying unmet clinical needs, this narrative review aims to guide research towards novel disease hallmarks, specifically within adaptive immune responses, for which limited effective therapies are currently available.

In **Chapter 3**, we performed single-cell transcriptomic and proteomic analyses in the affected skin, lungs and blood samples from 4 SSc patient cohorts (a total of 165 SSc patients vs. 80 healthy individuals) to analyze disease-relevant differences in the phenotype and regulation of T cell responses in SSc affected tissues. We further investigated the potential therapeutic effects of T cell costimulatory modulation through functional assays and in a severely affected SSc patient treated under compassionate use with a novel anti-CD3/CD7 immunotoxin therapy that selectively depletes activated T cells.

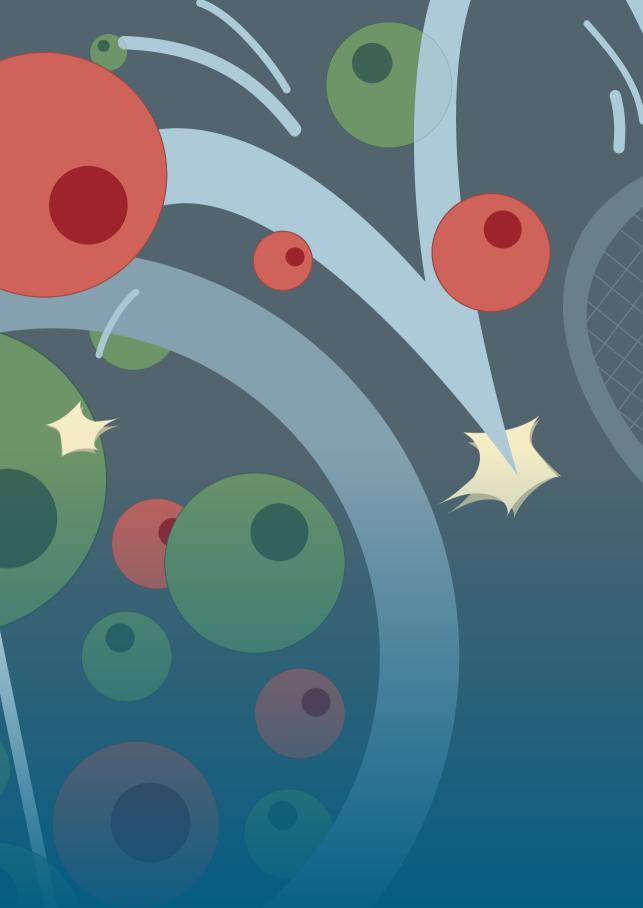
In **Chapter 4**, we developed an advanced 3D fibrogel contraction in vitro model to investigate T cell-mediated skin pathology in SSc, focusing on key hallmarks such as fibrosis and stiffness. This model provides a platform to unravel the molecular mechanisms through which T cells contribute to pro-fibrotic disease manifestations. Additionally, it enables high-throughput testing of preclinical efficacy for existing and novel therapeutic approaches targeting both T cell- and fibroblast-driven disease pathways.

Chapter 5 of this thesis focuses on examining the involvement of T cells in disease pathogenesis of a subgroup of severely affected SSc patients with severe

vasculopathy (presence of pulmonary arterial hypertension). In this chapter, we apply multi-color flow cytometry to identify whether and which peripheral T cell subsets associate with vascular severity in SSc. Analysis is performed in a wellstratified cohort of SSc patients with or without presence of pulmonary arterial hypertension (PAH) and age- and sex- matched healthy controls and patients with non-autoimmune PAH and examines whether expansion of certain T cell populations in SSc PAH patients may be used as a biomarker to assist early diagnosis of this life-threatening complication.

In Chapter 6, the focus shifts from blood and affected tissues to lymph nodes aiming to investigate whether pathogenic T cell responses in SSc tissues are orchestrated by locoregional lymph nodes. In this chapter, on top of general T cell responses, specific focus on the phenotype and function of nuclear-antigen specific T cells is given. To address this, we employ positron emission tomographycomputed tomography (PET-CT) imaging, single-cell multiomics, and ex vivo antigen stimulation assays for a first-of-its-kind analysis of autoreactive (nuclear antigen-specific) T cell responses in matched lymph nodes, blood, and skin biopsies from SSc patients. Parallel analyses in patients with SiS are included to identify overlapping and distinct immune responses to nuclear antigens in SSc compared to other CTDs like SjS. This chapter further explores the role of a novel SSc-specific lymph node TRAIL+ CD4+ T cell cluster in shaping antigen-presenting cell (APC)-mediated B cell pathology in systemic autoimmunity through a series of functional assays.

Finally, Chapter 7 provides a summary of the studies presented in this thesis, discusses their findings in the context of current literature, and offers perspectives for future research directions.



Chapter 1

General Introduction and outline

Rheumatic autoimmune connective tissue diseases: clinical manifestations, immune mechanisms, and therapeutic challenges

Rheumatic diseases encompass a diverse group of disorders characterized by inflammation, autoimmunity, and musculoskeletal involvement, often leading to chronic pain, disability, and systemic complications. Among these, systemic autoimmune CTDs represent a subset that primarily affects connective tissues and internal organs through immune-mediated mechanisms. These disorders include systemic lupus erythematosus (SLE), SSc, SjS, and polymyositis, each exhibiting unique but overlapping clinical manifestations. SLE is characterized by a relapsing-remitting course with multi-organ involvement, including arthritis, nephritis, and neuropsychiatric symptoms, driven by immune complex deposition and widespread inflammation [1]. SSc primarily presents with progressive fibrosis affecting the skin and internal organs, accompanied by vascular dysfunction and life-threatening complications such as pulmonary arterial hypertension [2]. SiS predominantly targets exocrine glands, causing severe dry mouth and eyes, with systemic features ranging from arthritis to interstitial lung disease [3]. Polymyositis, a form of inflammatory myopathy, manifests as proximal muscle weakness due to immune-mediated fiber destruction. The disease course varies from mild to severe, with complications such as pulmonary fibrosis, cardiovascular involvement, and increased malignancy risk [4]. Prognosis depends on organ involvement, with SSc and severe lupus nephritis carrying higher morbidity and mortality. Treatment strategies focus on immunosuppression, including corticosteroids, disease-modifying antirheumatic drugs (DMARDs), and targeted biologic therapies, aimed at modulating autoreactive immune responses and preventing irreversible organ damage [5].

CTDs affect up to 3% of the global population with SjS, SLE and SSc accounting for 0.5-3%, 0.9-1% and 0.2%, respectively [6]. CTDs represent a significant global health burden due to their chronic nature, complex pathophysiology, and substantial impact on patients' quality of life. These conditions are characterized by autoimmunemediated damage to connective tissues in the absence of an inciting infectious pathogen, leading to diverse manifestations such as fibrosis, multi-organ dysfunction, and systemic inflammation. They are classified as autoimmune because they involve the presence of autoantibodies (e.g. antinuclear antibodies) [7, 8] and are driven by autoreactive T cell and B cell responses in affected and locoregional lymphoreticular tissues due to failure of immune tolerance towards self-antigens [9, 10]. These immune cells interact in various ways to induce specific disease features [11].

Translational research reveals variability in the adaptive immune cell responses involved across different CTDs [12, 13]. Certain T cell and B cell subsets have been implicated in clinical symptoms characterizing SSc, SjS, and SLE. While each CTD exhibits distinct organ damage—e.g., skin and lungs in SSc, salivary glands in SiS common to all CTDs is the loss of self-tolerance, where self-reactive T cells escape immune regulation and become activated, often through APCs. These biological processes and the role of certain T cell subsets are discussed in detail in coming sections of this introduction.

The heterogeneity and overlapping features of CTDs complicate diagnosis and treatment, leading to delayed interventions and progressive disease. The oftensubtle initial complaints, such as Raynaud's phenomenon—characterized by episodes of reduced blood flow to the fingers and toes triggered by cold or stress, causing color changes, pain, or numbness—and sicca symptoms, which involve dryness of the eyes and mouth due to reduced glandular secretion, further contribute to diagnostic challenges as these early manifestations are frequently overlooked or misattributed to other conditions. Additionally, the lack of precise diagnostic tests hinders early detection, making it difficult to initiate timely treatment. Despite advances in understanding their underlying mechanisms, effective therapies remain limited, with many treatments primarily targeting symptoms rather than addressing the root cause. While there have been significant advancements in treatments for more prevalent autoimmune diseases such as rheumatoid arthritis, an unmet need exists for less common systemic autoimmune diseases [14]. This is partly due to their low prevalence and variability in affected tissues and immune mechanisms among patients, making disease activity hard to measure and complicating the assessment of treatment effects. Current imaging modalities and functional assays have limited sensitivity and specificity in detecting and analyzing autoreactive immune cells, which hampers diagnosis, monitoring of disease activity and the development of targeted therapies aimed at these cells.

This clinical and diagnostic gap underscores the need for continued research to better characterize how autoreactive immune responses develop both systemically and at the level of individual affected tissues. Such efforts are essential to improve our understanding of disease pathophysiology, to identify leads for tests for early diagnosis of disease onset and complications and to identify novel therapeutic targets. Ultimately, this will enhance outcomes for individuals suffering from these debilitating diseases.

Systemic sclerosis, Scleroderma

SSc, also known as scleroderma, is a rare rheumatic autoimmune CTD that affects approximately 2 out of 10,000 individuals worldwide [15]. SSc, similarly to other autoimmune diseases is more prevalent in women (>80%) compared to men [16]. The disease can develop at any age, but patients are typically diagnosed between the ages of 40 and 50. SSc is characterized by inflammation, progressive microvascular damage and generalized fibrosis in the skin and visceral organs that is caused by aberrant synthesis of extracellular matrix. SSc presents a wide range of clinical manifestations, from symptoms like Raynaud's phenomenon and fatique to more severe complications such as pulmonary arterial hypertension and lung fibrosis [17].

This thesis is centered around SSc because it exhibits one of the highest morbidity and mortality rates among systemic autoimmune CTDs [18]. Additionally, our research center has a strong clinical and experimental focus on SSc, including the largest national cohort and participation in the European Scleroderma Trials and Research (EUSTAR) group, a leading international network dedicated to advancing research, clinical care, and treatment development for SSc. While immunosuppressive therapy achieves disease remission in a proportion of patients, not all patients respond to treatment. Beyond the disease itself, this can lead to loss of work productivity and limitations in social activities. Even those who do respond require lifelong treatment with expensive therapies, creating a significant financial burden on patients and society [19].

Systemic sclerosis: disease subtypes and stages

The clinical presentation of SSc is highly heterogeneous, ranging from limited skin involvement to widespread skin thickening accompanied by severe internal organ damage. Early clinical manifestations include vasculopathy marked by Raynaud's phenomenon and puffy fingers (Figure 1), sometimes accompanied by nonspecific signs such as gastrointestinal reflux, joint pain, and fatigue, which may precede more definitive manifestations by several years [17]. Early disease processes (<3 years after diagnosis) are thought to be molecularly characterized by a highly inflammatory phase. In part of the patients with long standing/late disease inflammation regresses, while in others the inflammatory and profibrotic processes evolve and spread to internal organs and tissues [20].

Skin thickening is a hallmark of the disease and allows for classification into two clinical subsets: limited cutaneous systemic sclerosis (IcSSc) and diffuse cutaneous systemic sclerosis (dcSSc). In lcSSc (approximately 2/3 of patients), skin involvement is restricted to the face and areas distal to the elbows and knees, while dcSSc (approximately 1/3 of patients) features more widespread skin thickening, including proximal regions. Diffuse cutaneous SSc is more commonly associated with severe organ complications, such as heart, lung, and kidney involvement. Furthermore, these subsets also differ in their autoantibody profiles, which often provide additional insights into disease classification and prognosis [21].

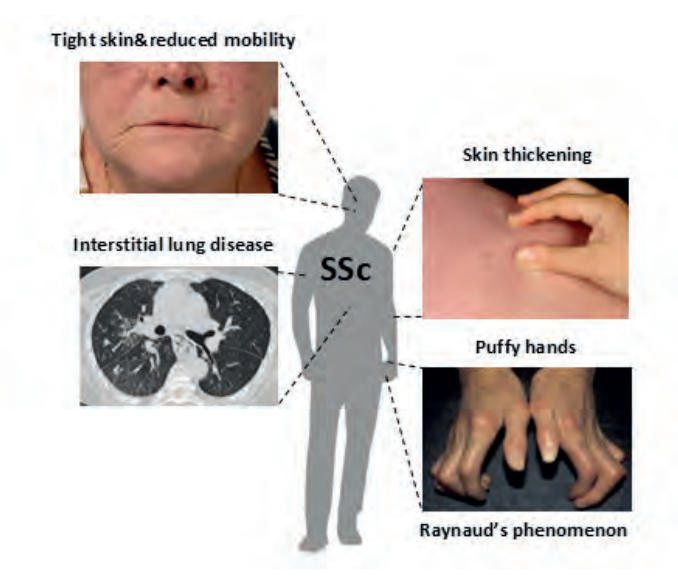


Figure 1. Schematic representation of common SSc clinical symptoms.

Pathogenesis of systemic sclerosis: mechanisms of vasculopathy, autoimmunity, and fibrosis

Similar to most other inflammatory diseases the precise etiopathogenesis of SSc is unknown, but its development is multifactorial, involving genetic predisposition, environmental triggers, epigenetics, ischemia-reperfusion stress, and viral infections [22-29]. However, none of these factors have been identified as the central cause. Vasculopathy, fibrosis and autoimmune inflammation are the main disease hallmarks in SSc pathophysiology (Figure 2). Although significant debate persists within the SSc community regarding the sequence of these events, it is widely accepted that disease is only sustained when the immune system, vascular endothelium, and connective tissue repair system are concurrently dysregulated [30].

To begin, vasculopathy is key in SSc pathogenesis because approximately 95% of patients experience Raynaud's phenomenon (RP) early on. RP results from vascular abnormalities, particularly affecting endothelial cells. Endothelial cell dysfunction initiates autocrine and paracrine activation of immune and stromal cells, driven by autoantibody-induced autoimmunity. Scleroderma-specific autoantibodies (antiscl70, anti-centromere, anti-RNA polymerase, Th/To) activate endothelial cells, increasing inflammatory and fibrotic responses, such as IL-6, collagen, α-SMA, and TGF-β production [31].

Regarding the involvement of the immune system in SSc two general etiologic scenarios are considered (Figure 3). First, an occult viral infection or exposure to environmental particles might cause chronic activation of innate immune mechanisms and directly induce SSc pathologic features [32-34]. Tissue infiltration by B and T cells might be a secondary response to viral antigens or an immunoregulatory phenomenon. Second and more likely because of a large and increasing body of evidence, SSc might be an autoimmune disease. In brief, SSc is genetically associated with certain MHC class II alleles and the B cell genes BANK1 and BLK [35]. Furthermore, SSc is associated with pathologic signs of aberrant T and B cell responses and specific autoantibodies that exert direct pathologic effects on SSc related cells, such as fibroblasts and endothelial cells [36, 37]. Finally, SSc is responsive to myeloablation with autologous stem cell transplantation (ASCT) and B and T cell directed drugs [38-41]. Following the second scenario of SSc etiology, hereafter these pathologic features in relation to SSc main disease hallmarks are described in greater detail.

The **adaptive immune system** plays a key role, with B cells and plasma cells generating SSc-specific autoantibodies, driving autoimmunity and inflammation [42, 43]. Autoreactive T cells are also major players in SSc pathogenesis, with Th1 cells initiating inflammation and Th2-associated cytokines such as interleukin 4 and other fibroproliferative cytokines that drive fibrosis in skin and internal organs [44]. The innate immune system is also involved. Mast cells, natural killer cells, dendritic cells, neutrophils, and monocytes/macrophages promote inflammation and fibrosis. Monocyte/macrophage plasticity enables progression from inflammation to fibrosis. Dendritic cells and Th1 cells produce type I interferons, enhancing inflammatory responses. Neutrophils contribute through reactive oxygen species (ROS) production, infiltrating tissues in the skin and lungs.

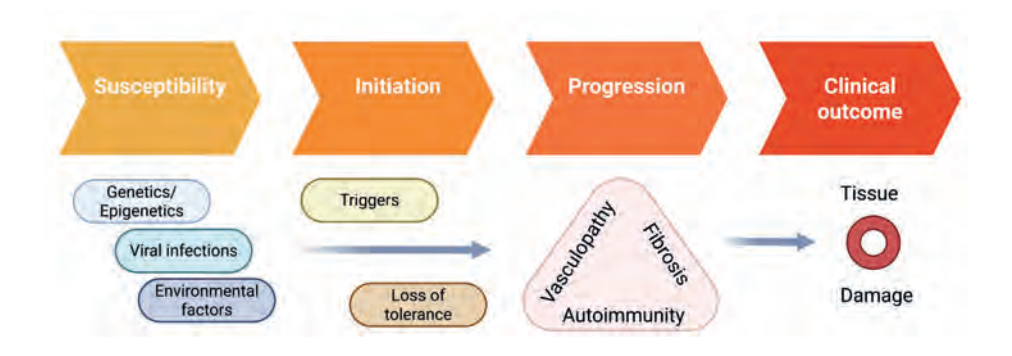


Figure 2. SSc etiopathogenesis and disease progression.

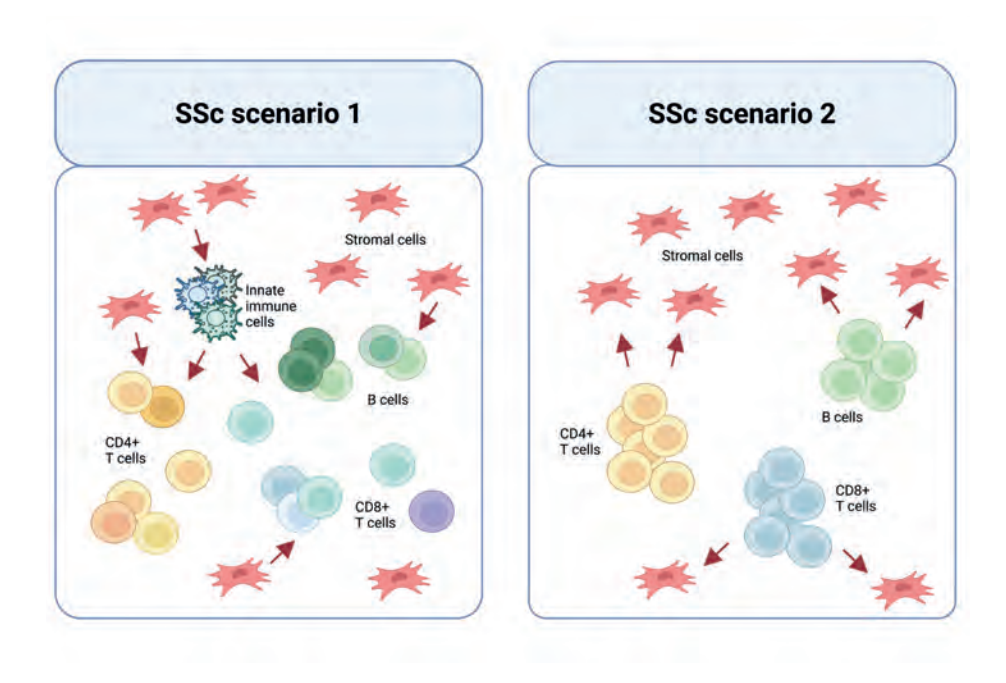


Figure 3. Scenarios of the involvement of the immune system in SSc disease pathophysiology.

Fibroblasts are central effector cells in SSc fibrosis. Upon activation, they transdifferentiate into myofibroblasts, producing extracellular matrix (ECM) components like α-SMA. Early disease fibroblasts release inflammatory cytokines (e.g., IL-6), chemokines (CXCL8-11), and fibrotic proteins (e.g., CTGF). As fibrosis progresses, hypoxia and stress trigger fibroblasts to produce profibrotic cytokines (e.g., TGF-β) and resist apoptosis. Additionally, epithelial and endothelial cells can undergo epithelial/endothelial-mesenchymal transition (EMT), adopt fibroblastlike properties, further contributing to fibrosis.

In summary, SSc pathogenesis involves vascular dysfunction, immune activation, and fibroblast-driven fibrosis. Autoimmunity, mediated by innate and adaptive immune responses, leads to endothelial activation and fibrotic changes, creating a self-sustaining inflammatory-fibrotic cycle. Immune cells, endothelial cells and fibroblasts interact via soluble mediators or by forming complex networks and that establishes additional interactions with various cell types, notably keratinocytes, pericytes, platelets, and adipocytes (Figure 4). The pathophysiology of SSc and the contribution of the immune cells involved is discussed in greater detail in chapter 2 of this thesis.

Key cell interactions in SSc pathogenesis

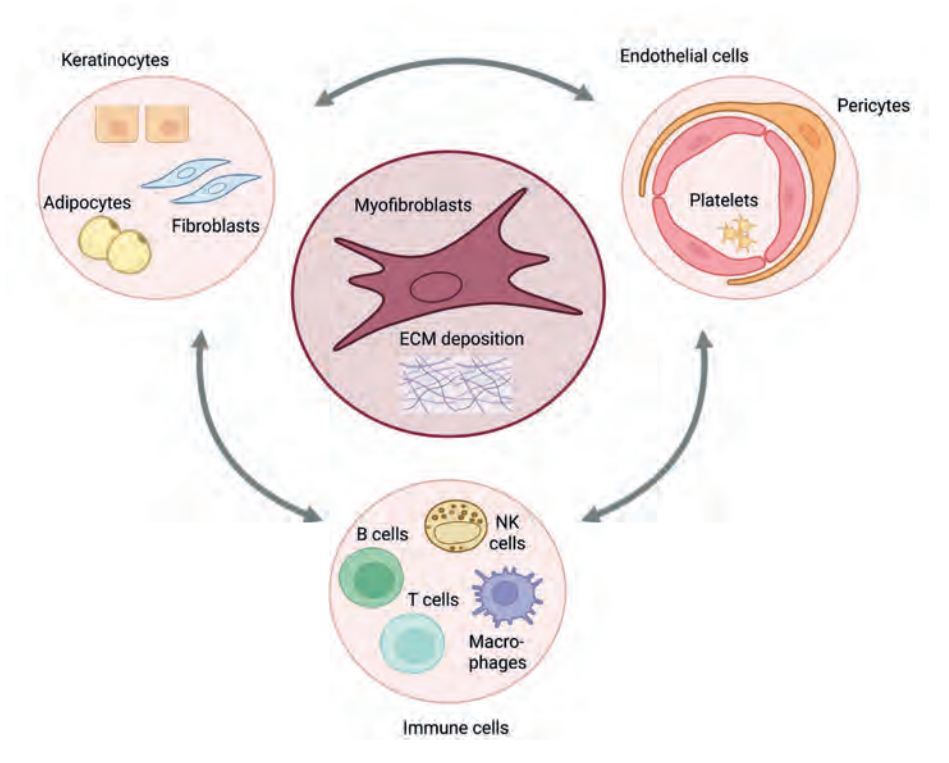


Figure 4. Pathogenesis of SSc: Complex Interactions Among Immune Cells, Endothelial Cells, and Fibroblasts.

Autoantigens and autoantibodies in systemic sclerosis: triggers, immune responses, and clinical implications

SSc has been associated with various environmental stimuli that may induce autoimmunity. These stimuli range from infections such as retroviruses and cytomegalovirus (CMV), to exposure to environmental toxins like silica, organic solvents, paint, industrial solvents, toxic oil, bleomycin and other drugs [45]. A particularly intriguing observation is the increased persistence of fetal cells and micro chimerism in women with SSc, suggesting a possible link between pregnancy and the development of autoimmunity in this disease [46]. These environmental exposures likely contribute to the formation of autoantigens that trigger the autoimmune response in SSc. Retroviruses and CMV are thought to induce autoantigen formation through molecular mimicry or by subverting antiviral immune responses [32, 33, 37], highlighting the complex relationship between infection and autoimmunity.

Furthermore, non-infectious stimuli, such as environmental toxins, may induce oxidative stress, other forms of cellular damage, or cell death. These processes are well documented in SSc, with increased levels of particles released from stressed or damaged tissues, such as hyaluronan, high mobility group box 1, S100A8/9, and nucleosomes, which contribute to the inflammatory environment [47]. Notably, bleomycin, a drug that induces oxidative stress, chromosome breaks, and apoptosis in fibroblasts, endothelial cells, and immunocytes, triggers a pro-fibrotic response in SSc [48]. Moreover, metals ingested in the context of ischemia-reperfusion injury have been shown to generate unique protein fragments containing SSc-associated autoantigens [49], further underscoring the role of environmental factors in the formation of autoantigens.

Connecting these findings, the stimuli discussed above have been shown to cause fibroblasts from SSc patients to undergo significant alterations in centromeric DNA, leading to DNA damage and chromosomal instability. These nuclear abnormalities can activate the cGAS-STING pathway, which is implicated in the production of proinflammatory cytokines, contributing to the autoimmune response seen in SSc [50]. This mechanism provides a direct link between environmental triggers and the activation of the immune system.

One of the earliest clinical manifestations of SSc is an exaggerated or late-onset Raynaud's phenomenon, characterized by abnormal thermal regulation of blood flow in the digital arteries. The pathogenesis of Raynaud's phenomenon has been attributed to endothelial damage, increased vasoconstriction, and reduced blood flow [51]. As oxidative stress is a major trigger for endothelial injury in SSc, it is often observed in the affected skin and lungs, with early pathological features, such as apoptosis, occurring in endothelial and perivascular cells [52]. This damage results in a perivascular infiltrate of macrophages, T cells, and B cells, further amplifying the autoimmune response. Apoptosis also leads to the extrusion of microparticles, which contain potential nuclear autoantigens like DNA topoisomerase I and centromere protein B, alongside immunostimulatory damage-associated particles [53, 54]. These microparticles may serve as potent stimuli for the induction of autoreactive cells, thus perpetuating the disease cycle. In conclusion, environmental stimuli, including infections and toxins contribute to the formation of autoantigens that drive autoimmune responses in SSc. These factors, combined with genetic predisposition, lead to endothelial damage and immune dysregulation, which are central to the disease's progression. Understanding these interactions is crucial for developing targeted diagnostic and therapeutic strategies for SSc.

As environmental stimuli and genetic factors contribute to the formation of autoantigens in SSc, these self-antigens are presented to autoreactive T cells, leading to the production of autoantibodies by autoreactive plasma cells. A central role for autoreactive T cell-mediated autoantibody production is supported by the positive associations between genetic predisposition to SSc and specific HLA class II alleles (e.g. HLA-DRB1/DPB1/DQB1) and disease severity [23, 55-57]. Most patients with SSc produce class-switched serum IgG antinuclear antibodies targeting various ribonucleoprotein and DNA-associated complexes, such as topoisomerase I (ScI-70), centromere proteins (CENP-A and CENP-B), Th/To, and RNA polymerases I/III [58]. Other autoantibodies directed against cell surface antigens, such as against intercellular adhesion molecule 1 (ICAM-1), endothelin-1 type A receptor (ETAR), angiotensin II type 1 receptor (AT1R), platelet derived growth factor (PDGF) receptor, CD22 and against endothelial cells (proteins unknown), co-occur with other autoantibodies and also occur in other CTDs [59].

Detection of more than one antinuclear autoantibodies in SSc patients is rare and between patients with different autoantibody profiles remarkably different clinical manifestations can be observed. For instance, anti-centromere is positive in 16-40% of patients and has been associated with limited cutaneous scleroderma and presence of digital ulcers. In addition, 20-40 % of the patients are sera positive for ScI-70 which is associated with diffuse cutaneous SSc and more severe organ involvement. Anti-RNA polymerase is present in 5-30% and is often predictive of patients at risk of renal crisis but less risk of pulmonary involvement [60]. Although the presence of autoantibodies in SSc is prevalent and disease-specific, it is yet unknown whether they are pathogenic or epiphenomena.

T cells are important players in SSc disease pathogenesis

T cells play a pivotal role in the pathogenesis of systemic sclerosis (SSc), contributing to inflammation, vascular damage, and fibrosis through distinct functional subsets. The balance and activity of CD4+ αβ T helper cells (Th1, Th2, Th17, Tfh and Tph) or T regulatory cells (Tregs), and cytotoxic CD8+ T cells (CTLs) are central to SSc pathology, with each subset exerting unique and often contrasting effects.

Th1 cells, characterized by their IL-12 induced production of interferon-gamma (IFN-v), exhibit a dual role in SSc. IFN-v suppresses collagen synthesis and promotes ECM breakdown by inducing matrix metalloproteinases (MMPs), which have antifibrotic effects [61]. However, conflicting evidence from animal models suggests Th1-like responses may also play a role in inflammation-driven skin fibrosis [62]. One possible explanation for these opposing effects may be that Th1 cells exert stage-dependent functions in SSc. In early disease, IFN-y may help limit fibrosis by reducing collagen deposition and enhancing ECM degradation. However, in later stages, persistent Th1 cytokine activity, including elevated IL-12 levels, may sustain chronic inflammation, promote macrophage activation toward a pro-inflammatory M1 phenotype, and indirectly contribute to fibrosis through prolonged immune activation and oxidative stress [63, 64]. Notably, Th1 responses appear diminished in lesional skin compared to systemic Th2 activity [65-67], reflecting a complex interplay between these T helper subsets.

Th2 cells are thought to be major drivers of fibrosis in SSc through the production of pro-fibrotic cytokines IL-4, IL-5, and IL-13. These cytokines activate fibroblasts, promoting excessive ECM deposition and collagen production, hallmark features of SSc pathology [68, 69]. Elevated levels of Th2 cytokines, particularly IL-4 and IL-13, have been detected in SSc skin lesions, correlating strongly with disease severity and the extent of fibrosis [70]. CD30, a marker of Th2 activation, has also been found in higher concentrations in SSc serum and skin tissues, further reinforcing the role of Th2 skewing in disease pathogenesis [71]. The dominance of Th2 responses over Th1 has long been associated with the fibrotic process in SSc.

Th17 cells have gained increasing attention as key players in SSc, bridging innate and adaptive immune responses. These cells produce cytokines such as IL-17, IL-21, and IL-22, which promote inflammation, activation of endothelial cells and fibroblasts, ultimately contributing to both vascular dysfunction and fibrosis [72]. Elevated Th17 frequencies have been observed in both peripheral blood and affected tissues of SSc patients, with IL-17 levels correlating with disease activity and severity, as measured by skin scores and organ involvement [73]. IL-17 induces the recruitment of monocytes and amplifies pro-inflammatory pathways, which are critical in early SSc pathology. Furthermore, IL-17 synergizes with IL-9, linking Th17 and Th9 responses in tissue damage. This interaction amplifies fibroblast activation and extracellular matrix deposition, promoting excessive collagen production and fibrosis. Additionally, IL-9 enhances mast cell survival and degranulation, leading to the release of proteases and pro-inflammatory mediators that exacerbate vascular injury and tissue remodeling in SSc [74, 75].

T follicular helper (Tfh) cells and T peripheral helper (Tph) cells are additional T helper subsets that are thought to contribute to SSc by driving B cell activation and autoantibody production [76]. Tfh cells, which are localized in germinal centers of secondary lymphoid organs, produce IL-21 and IL-17 and promote B cell maturation and antibody class switching and production of autoantibodies contributing to SSc pathology [77]. Elevated levels of circulating Tfh cells correlate with disease severity and fibrosis [78], while Tfh-like cells infiltrating lesional skin exacerbate local inflammation and skin fibrosis [79]. In contrast, Tph cells, localized in inflamed peripheral tissues, share functional similarities with Tfh cells but secrete CXCL13 and IL-21 to stimulate B cells locally [76]. Elevated CXCL13 production in lesional skin [80] and serum [81] correlates with disease severity, suggesting a role for Tph cells in perivascular inflammation and vascular dysfunction, particularly in early disease stages.

Conversely, T regulatory cells (Tregs), which are essential for maintaining immune tolerance and controlling inflammation [82], are often reduced or functionally impaired in SSc patients [83-85]. Reduced Treg activity exacerbates the Th17/Treg imbalance, which has been closely associated with increased inflammation and fibrosis [86]. While some studies report elevated Treg frequencies [87] in early SSc, others observe reduced Treg numbers [88] or impaired suppressive function in advanced stages, indicating dynamic changes in Treg behavior during disease progression. Notably, a skewed Th17/Treg ratio has been implicated as a potential biomarker for disease severity, progression, and activity [86].

Cytotoxic T cells (CTLs), particularly CD8+T cells, are also thought to contribute to SSc pathology, with evidence suggesting their involvement in endothelial damage and inflammation. In early dcSSc), CD8+T cells infiltrate lesional skin and induce apoptosis of endothelial cells, which may trigger vascular damage and initiate fibrosis [89].

Additionally, CD8+ T cells have been shown to secrete IL-4 and IL-13, cytokines traditionally associated with Th2 responses, thus contributing to fibrosis alongside their cytotoxic functions [90, 91]. Interestingly, CD4+ cytotoxic T lymphocytes (CD4 CTLs) have also been identified as key contributors to SSc, particularly in vascular dysfunction, due to their perforin- and granzyme-mediated cytotoxic effects on endothelial cells [92].

Together, these T cell subsets exhibit intricate and overlapping roles in SSc pathology. Th2, Th17, Tfh, and Tph cells predominantly promote fibrosis, inflammation, and autoimmunity, while Tregs attempt to suppress these responses, often inadequately. Th1 cells appear to have stage-specific roles, with potential antifibrotic effects in later disease phases. CTLs, on the other hand, play a significant role in vascular injury and tissue damage, particularly in early disease. The interplay between these subsets not only highlights the complexity of immune dysregulation in SSc but also suggests their potential as biomarkers for disease diagnosis, activity monitoring, and therapeutic targets.

Moreover, non-conventional γδ T cells and CD4, CD8 double positive T cells [93, 94], although present in lower numbers in SSc affected tissues and blood circulation, have been shown to produce high levels of IL-4, suggesting they may combine helper and cytotoxic functions and as such possibly contribute to neo-epitope formation and recognition [94].

Despite the significant insights gained from studies on T cell subsets in SSc, important knowledge gaps remain. First, much of the current understanding is derived from analyses of peripheral blood, with relatively fewer studies examining affected tissues and none exploring T cell responses within patients' lymph nodes. This represents a critical gap, as antigen-specific and potentially autoreactive T cell responses are primarily initiated and regulated within locoregional lymph nodes. Second, it remains unclear whether the observed T cell responses are truly antigen-specific and autoreactive or are instead bystander responses arising from a generalized inflammatory environment. Addressing these gaps is essential for unraveling the mechanisms driving T cell-mediated immune dysregulation in SSc and for identifying precise therapeutic targets.

Autoreactive T cells and antigen-specific immunotherapies in SSc

Autoimmune diseases, including SSc, arise from a breakdown of immune tolerance, where immune responses against self-antigens become pathogenic, resulting in localized or systemic inflammation. Examples of localized antigen-specific inflammation include Graves' disease [95] and type 1 diabetes [96], diseases affecting a single organ (thyroid and pancreas respectively). Autoimmunity can also present as a systemic condition, driven by immune responses to ubiquitous autoantigens like DNA topoisomerase I (ScI70), which is associated with severe dcSSc. [97]. The immune system maintains self-tolerance through mechanisms that delete or suppress autoreactive T cells, with regulatory T (Treg) cells playing a central role. However, such regulatory mechanisms are defective in SSc [98] and other CTDs [99], resulting in autoimmunity and inflammation. As previously discussed, recent research highlights specific T cell subsets and their cytokines as contributors to SSc pathogenesis by influencing autoimmunity, inflammation, and fibrosis, however, the antigen specificity of infiltrating T cells remains unknown. Antigenspecificity of infiltrating T cells towards nuclear and cytosolic antigens has been determined in RA [100, 101] synovium and SLE kidneys and urine samples [102], showing their enrichment in severely affected patients and their involvement in disease progression. Autoreactive T cells are also found in healthy individuals, where they play a role in promoting tolerance. This presents a significant challenge in developing antigen-specific therapies for autoimmune diseases. Consequently, these therapies must be designed to target autoreactive lymphocytes that drive disease while sparing those that contribute to health. Achieving this requires a thorough understanding of the specificity and pathogenic characteristics of autoreactive lymphocytes, distinguishing them from those crucial for maintaining health. Antigen-specific approaches have demonstrated success in animal models of autoimmunity and show promise in phase I and II clinical trials of localized autoimmune diseases such as type 1 diabetes and multiple sclerosis, with larger trials currently underway using various methods to achieve antigen-specific tolerance [103]. However, in systemic autoimmunity [104-107] challenges persist, including identifying the antigens targeted by the autoimmune response, tailoring treatments to the specific immune pathology of each disease, avoiding off-target effects or the promotion of autoimmunity, and ensuring that these therapies are accessible and provide lasting results.

DNA topoisomerase I specific CD4+ T cells have been detected in blood circulation of ScI70 seropositive only SSc patients and their frequency was correlated with interstitial lung disease [108]. However, further research is needed to explore the presence and function of these cells in tissues affected by SSc and in draining lymph nodes to better understand their role within the affected tissues. In this context, it is essential to distinguish between the pathogenic and regulatory roles of autoreactive T cells in SSc, as this differentiation will inform the development of novel therapeutic approaches aimed at either eliminating or tolerizing these cells.

Autoreactive immune responses in SjS compared to SSc

Loss of tolerance to self-antigens is not exclusive to SSc but is a fundamental process in the pathogenesis of all CTDs. While the specific autoantigens involved vary between CTDs, some are shared across multiple conditions. Each CTD affects different tissues, and the degree of immune cell involvement in these tissues also varies. It remains unclear whether the differences in disease manifestations and **immune responses** are directly attributable to the **distinct autoantigens** involved in each condition. However, evidence from experimental animal models of CTDs supports this hypothesis. For instance, in addition to SSc, SiS also involves reactivity to nuclear antigens (NAgs), yet the two diseases exhibit markedly different clinical presentations and immune responses within affected tissues. Therefore, a comparative study of antinuclear antigen responses in these two CTDs could provide valuable insights into how specific autoantigen responses drive diseasespecific immune mechanisms.

The vast majority of patients with SiS show autoreactivity against the nuclear antigens Ro60 and La. Detection of these autoantibodies in SiS patients' serum assists diagnosis and, similarly to seropositivity for Scl70 in SSc, is associated with severe and progressive disease. While at the cellular level, cytotoxic T cells and NK cells are known to play a prominent role in the tissue pathology of SSc, particularly in the skin and lungs [92], in SjS-affected salivary glands, there is a more pronounced involvement of B-helper CD4+ T cells [109] and autoreactive B cells [110].

Recent research has highlighted the role of distinct cell death pathways, molecular mimicry, oxidative stress and epitope spreading in the autoimmune mechanisms underlying SiS and SSc. In both diseases, cell death processes lead to the release of intracellular antigens and subsequent activation of the immune system. In SjS, the apoptosis of epithelial cells of the salivary glands and their defective clearance leads to activation of autoreactive T cells and B cells [111]. In SSc, necroptosis and pyroptosis are the predominant forms of cell death and lead to the release of damage-associated molecular patterns that contribute to fibrosis, vasculopathy and enhanced immune activation [112, 113].

These processes are thought to contribute to the development of autoimmunity through mechanisms such as cross-reactivity between self-antigens and microbial components, and the progressive diversification of immune responses over time [114]. To begin with, molecular mimicry seems to play an important role in both SjS and SSc. In SjS, it has been proposed that the autoantigen Ro60, a ribonucleoprotein, might share structural similarities with antigens present in gut bacteria. This mimicry could trigger an immune response against Ro60, leading to the autoimmune damage seen in SjS [115]. Similarly, molecular mimicry is also implicated in SSc, where interactions between host immune cells and microbial antigens may drive disease pathology. Studies suggest that HLA and autoantibodies are critical factors in defining SSc subtypes and determining the risk of the disease in different ethnic populations. This underscores the potential role of microbial antigen mimicry in initiating immune responses in genetically predisposed individuals [116]. In SjS, oxidative stress has been implicated in the dysregulation of immune tolerance. Specifically, oxidative stress in keratinocytes may cause the translocation of Ro60 from intracellular compartments to the cell surface, where it becomes accessible for presentation to T cells. This process could trigger the activation of autoreactive T cells, further contributing to the development of SiS by promoting immune responses against self-antigens [117]. Oxidative stress is also believed to contribute to the autoimmune aspect of scleroderma, as demonstrated in a mouse study where oxidation of DNA topoisomerase I induced autoimmunity, promoting the production of anti-topoisomerase I antibodies, increased fibroblast proliferation, enhanced type I collagen mRNA synthesis, and elevated H₂O₂ production by endothelial cells [118].

Finally, epitope spreading, a process in which the immune system progressively targets additional self-peptides beyond the initial antigen, plays a crucial role in the diversification of the autoimmune response in SiS, but not as prominently in SSc [119]. In SjS, epitope spreading often occurs, where patients display two dominant HLA class II polymorphisms that respond to multiple self-peptides. This differs from the situation in SSc, where a single HLA class II polymorphism is more frequently associated with the response to a single peptide [120]. This suggests that in SjS, the immune system may become increasingly dysregulated over time, progressively targeting a wider array of self-antigens, while in SSc, the response remains more narrowly focused. However, whether reactivity towards distinct nuclear antigens is involved in the observed divergent adaptive immune responses in patients' affected tissues is still elusive.

To better understand the differences in how antigen-specific T cells are involved or regulated in SSc versus SjS, it is essential to conduct detailed phenotypic and functional analyses of the affected tissues in patients. In this context, studying antigen-specific T cell responses not only in the affected tissues but also in the **locoregional lymph nodes** is crucial. These lymph nodes contain follicular dendritic cells, which play a key role in antigen presentation and the activation or regulation of T cells. Additionally, protective immune responses against pathogens are

initiated and propagated in inflamed lymph nodes. Given the evidence supporting molecular mimicry in the initiation of autoimmune responses, examining these responses in locoregional lymph nodes becomes particularly valuable.

Unmet clinical need

SSc exhibits a broad spectrum of clinical manifestations and disease stages. The lack of well-established biomarkers to predict disease progression and treatment response poses significant challenges to early diagnosis and the prevention of severe complications in later stages. To date, there is no disease-modifying treatment available for SSc and there is no universally agreed-upon treatment protocol. Existing treatments for SSc, such as methotrexate, cyclophosphamide and mycophenolate, primarily focus on managing inflammatory processes and slowing disease progression (detailed review of the efficacy of current therapies is provided in Chapter 2). However, their efficacy is often limited, and they may not adequately target the underlying cause of disease in SSc, which is loss of immune self-tolerance [121-124].

Only ASCT [125] and most recently anti-CD19 CAR-T cell therapy [126] can cause long-term disease remission. These therapies eliminate also the autoreactive immune cells and that shows the involvement of adaptive immunity in SSc. However, both approaches are highly invasive, accompanied by high mortality rates and are applicable only to a small subset of SSc patients—specifically, those with severe and progressive disease who possess sufficient overall health to tolerate the procedure. In addition, even though lymphocyte depletion shows promise, these therapies lack antigen specificity and lead to significant immunosuppression, including diminished vaccine responses and increased risk of infections. Therefore, novel specific treatments need to be developed and tested in trials to better treat SSc with the ultimate goal of specific targeting of autoreactive responses to achieve durable disease remission by maintaining a protective immune response.

To better understand why treatments work or fail and to assist the development program of novel treatments, it would be of great benefit to have tools to analyze cellular mechanisms central to SSc pathogenesis, such as failure of immune selftolerance by auto-reactive T and B cells. Identifying and characterizing antigenspecific immune responses has been challenging due to the low frequency of these cells and unavailability of adequate biopsies from patient affected tissues and draining lymph nodes. However, recent technological advances including activation induced marker assays, HLA tetramers and single-cell RNA sequencing allow researchers to identify potentially pathogenic T cells and validate their specificity. Further development and successful application of these tools will facilitate the pressing need for the development of novel therapies that specifically target the autoreactive immune responses driving key disease hallmarks in SSc. The development of such targeted treatments has the potential to enhance patient outcomes, achieve long-term disease remission with fewer side effects, and, most importantly, offer broader applicability across a wider SSc patient population.

Aim and outline of the thesis

The primary aim of this thesis is to elucidate how pathogenic autoreactive T cell responses manifest in SSc and other CTDs such as SiS. By elucidating the underlying mechanisms of these immune responses, this work seeks to advance the understanding of disease pathophysiology and inform the development of targeted T cell therapies with improved specificity, reduced side effects, and broader applicability to diverse SSc and CTD patient populations. To achieve this, we developed a comprehensive toolkit that integrates advanced PET imaging, singlecell multiomic technologies, in silico approaches, multiplex immunohistochemistry and functional in vitro assays to detect, spatially localize and analyze adaptive immune responses driving SSc and other related CTD pathology within patients' active lymph nodes and affected tissues.

In Chapter 2, the current knowledge on the pathophysiology of SSc is reviewed, with a particular focus on the heterogeneous nature of the disease and the critical roles of adaptive immune responses, especially T cell-mediated mechanisms, in its clinical manifestations. This review also evaluates the therapies that have been tested, their molecular targets, and their potential efficacy in clinical trials. By identifying unmet clinical needs, this narrative review aims to guide research towards novel disease hallmarks, specifically within adaptive immune responses, for which no effective therapies are currently available.

In Chapter 3, we performed single-cell transcriptomic and proteomic analyses in the affected skin, lungs and blood samples from 4 SSc patient cohorts (a total of 165 SSc vs 80 healthy individuals) to analyze disease-relevant differences in the phenotype and regulation of T cell responses in SSc affected tissues. We further investigated the potential therapeutic effects of T cell costimulatory modulation through functional assays and in a severely affected SSc patient treated under compassionate use with a novel anti-CD3/CD7 immunotoxin therapy that selectively depletes activated T cells.

In Chapter 4, we developed an advanced 3D hydrogel contraction in vitro model to investigate T cell-mediated skin pathology in SSc, focusing on key hallmarks such as fibrosis and stiffness. This model provides a platform to unravel the molecular mechanisms through which T cells contribute to pro-fibrotic disease manifestations. Additionally, it enables high-throughput testing of preclinical efficacy for existing and novel therapeutic approaches targeting both T cell- and fibroblast-driven disease pathways.

Chapter 5 of this thesis focuses on examining the involvement of T cells in disease pathogenesis of a subgroup of severely affected SSc patients with severe vasculopathy (presence of pulmonary arterial hypertension). In this chapter, we apply multi-color flow cytometry to identify whether and which peripheral T cell subsets associate with vascular severity in SSc. Analysis is performed in a well stratified cohort of SSc patients with or without presence of PAH and age and sex matched healthy controls and patients with non-autoimmune PAH and examines whether expansion of certain T cell populations in SSc PAH patients may be used as a biomarker to assist early diagnosis of this life-threatening complication.

In Chapter 6, the focus shifts from blood and affected tissues to lymph nodes to investigate whether pathogenic T cell responses in SSc tissues are orchestrated by locoregional lymph nodes. In this chapter on top of general T cell responses, specific focus on the phenotype and function of nuclear-antigen specific T cells is given. To address this, we employ PET-CT imaging, single-cell multiomics, and ex vivo antigen stimulation assays for a first-of-its-kind analysis of autoreactive (nuclear antigen-specific) T cell responses in matched lymph nodes, blood, and skin biopsies from SSc patients. Parallel analyses in patients with SiS are included to identify overlapping and distinct immune responses to nuclear antigens in SSc compared to other CTDs like SjS. This chapter further explores the role of a novel SSc-specific lymph node T cell cluster in shaping APC-mediated B cell pathology in systemic autoimmunity through a series of functional assays.

Finally, Chapter 7 provides a summary of the studies presented in this thesis, discusses their findings in the context of current literature, and offers perspectives for future research directions.

References

- 1 Rose, J., Autoimmune Connective Tissue Diseases: Systemic Lupus Erythematosus and Rheumatoid Arthritis. Emerg Med Clin North Am, 2022. 40(1): p. 179-191.
- Abraham, D.J., et al., An international perspective on the future of systemic sclerosis research. Nature 2. Reviews Rheumatology, 2025. 21(3): p. 174-187.
- 3. Baldini, C., et al., Update on the pathophysiology and treatment of primary Sjögren syndrome. Nature Reviews Rheumatology, 2024. 20(8): p. 473-491.
- Lundberg, I.E., M. de Visser, and V.P. Werth, Classification of myositis. Nature Reviews Rheumatology, 4. 2018. **14**(5): p. 269-278.
- Feldmann, M., et al., 25 years of biologic DMARDs in rheumatology. Nature Reviews Rheumatology, 5. 2023. 19(12): p. 761-766.
- 6. Gaubitz, M., Epidemiology of connective tissue disorders. Rheumatology (Oxford), 2006. 45 Suppl 3: p. iii3-4.
- Didier, K., et al., Autoantibodies Associated With Connective Tissue Diseases: What Meaning for 7. Clinicians? Frontiers in Immunology, 2018. 9.
- Suurmond, J. and B. Diamond, Autoantibodies in systemic autoimmune diseases: specificity and pathogenicity. J Clin Invest, 2015. 125(6): p. 2194-202.
- Rao, D.A., The rise of peripheral Thelper cells in autoimmune disease. Nature Reviews Rheumatology, 2019. 15(8): p. 453-454.
- 10. Rubin, S.J.S., M.S. Bloom, and W.H. Robinson, B cell checkpoints in autoimmune rheumatic diseases. Nature Reviews Rheumatology, 2019. 15(5): p. 303-315.
- 11. Petersone, L., et al., T Cell/B Cell Collaboration and Autoimmunity: An Intimate Relationship. Frontiers in Immunology, 2018. 9.
- 12. Townsend, M.J., J.G. Monroe, and A.C. Chan, B cell targeted therapies in human autoimmune diseases: an updated perspective. Immunol Rev, 2010. 237(1): p. 264-83.
- 13. Vincze, K., et al., Peripheral CD4+ T cell changes in connective tissue diseases. Cytokine & Growth Factor Reviews, 2018. 43: p. 16-24.
- 14. Winthrop, K.L., et al., Unmet need in rheumatology: reports from the Advances in Targeted Therapies meeting, 2022. Ann Rheum Dis, 2023. 82(5): p. 594-598.
- 15. Bairkdar, M., et al., Incidence and prevalence of systemic sclerosis globally: a comprehensive systematic review and meta-analysis. Rheumatology, 2021. 60(7): p. 3121-3133.
- 16. Hughes, M., et al., Gender-related differences in systemic sclerosis. Autoimmunity Reviews, 2020. 19(4): p. 102494.
- 17. Denton, C.P. and D. Khanna, Systemic sclerosis. The Lancet, 2017. 390(10103): p. 1685-1699.
- 18. Kouchit, Y., L. Morand, and N. Martis, Mortality and its risk factors in critically ill patients with connective tissue diseases: A meta-analysis. European Journal of Internal Medicine, 2022. 98: p. 83-92.
- 19. Bournia, V.K., et al., All-cause mortality in systemic rheumatic diseases under treatment compared with the general population, 2015-2019. RMD Open, 2021. **7**(3).
- 20. van Caam, A., et al., Unraveling SSc Pathophysiology; The Myofibroblast. Front Immunol, 2018. 9: p. 2452.
- 21. Herrick, A.L., S. Assassi, and C.P. Denton, Skin involvement in early diffuse cutaneous systemic sclerosis: an unmet clinical need. Nat Rev Rheumatol, 2022. 18(5): p. 276-285.
- 22. Ferri, C., et al., Insights into the knowledge of complex diseases: Environmental infectious/toxic agents as potential etiopathogenetic factors of systemic sclerosis. J Autoimmun, 2021. 124: p. 102727.

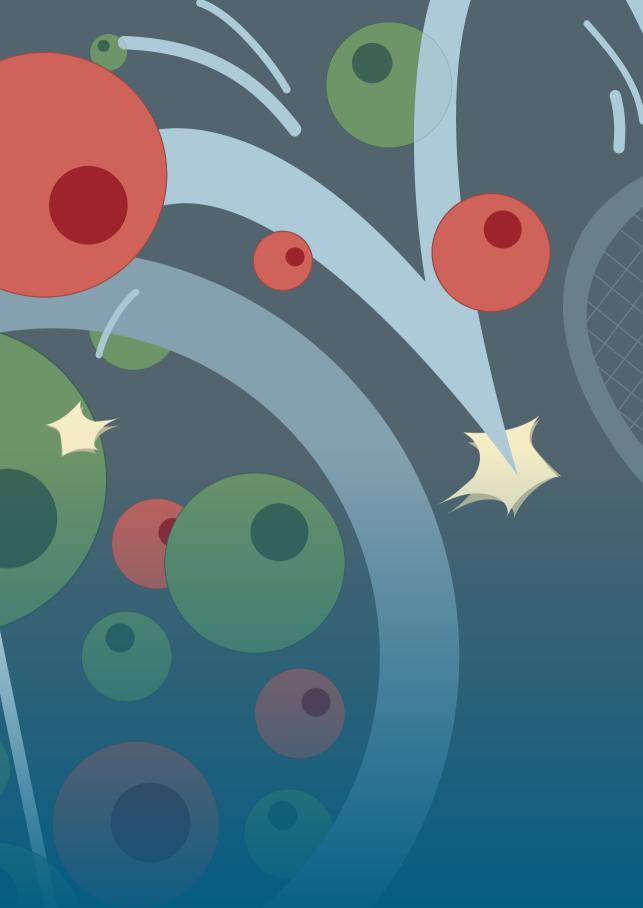
- 23. Ota, Y. and M. Kuwana, Updates on genetics in systemic sclerosis. Inflammation and Regeneration, 2021. **41**(1): p. 17.
- 24. Ouchene, L., et al., Toward Understanding of Environmental Risk Factors in Systemic Sclerosis [Formula: see text]. J Cutan Med Surg, 2021. 25(2): p. 188-204.
- 25. Tsou, P.-S., J. Varga, and S. O'Reilly, Advances in epigenetics in systemic sclerosis: molecular mechanisms and therapeutic potential. Nature Reviews Rheumatology, 2021. 17(10): p. 596-607.
- 26. Henderson, J., J. Distler, and S. O'Reilly, The Role of Epigenetic Modifications in Systemic Sclerosis: A Druggable Target. Trends in Molecular Medicine, 2019. 25(5): p. 395-411.
- 27. Moroncini, G., et al., Role of viral infections in the etiopathogenesis of systemic sclerosis. Clinical and experimental rheumatology, 2013. 31.
- 28. Dziedzic, R., et al., Increased oxidative stress response in circulating blood of systemic sclerosis patients - relation to disease characteristics and inflammatory blood biomarkers. Seminars in Arthritis and Rheumatism, 2023. 62: p. 152228.
- 29. Doridot, L., et al., Implication of oxidative stress in the pathogenesis of systemic sclerosis via inflammation, autoimmunity and fibrosis. Redox Biology, 2019. 25: p. 101122.
- 30. Stern, E.P. and C.P. Denton, The Pathogenesis of Systemic Sclerosis. Rheumatic Disease Clinics of North America, 2015. 41(3): p. 367-382.
- 31. Ota, Y. and M. Kuwana, Endothelial cells and endothelial progenitor cells in the pathogenesis of systemic sclerosis. Eur J Rheumatol, 2020. 7(Suppl 3): p. S139-s146.
- 32. Maul, G.G., et al., Determination of an epitope of the diffuse systemic sclerosis marker antigen DNA topoisomerase I: sequence similarity with retroviral p30gag protein suggests a possible cause for autoimmunity in systemic sclerosis. Proc Natl Acad Sci U S A, 1989. 86(21): p. 8492-6.
- 33. Radić, M., D. Martinović Kaliterna, and J. Radić, Infectious disease as aetiological factor in the pathogenesis of systemic sclerosis. Neth J Med, 2010. 68(11): p. 348-53.
- 34. Elkon, K.B., Review: Cell Death, Nucleic Acids, and Immunity: Inflammation Beyond the Grave. Arthritis Rheumatol, 2018. 70(6): p. 805-816.
- 35. Coustet, B., et al., Independent replication and meta analysis of association studies establish TNFSF4 as a susceptibility gene preferentially associated with the subset of anticentromere-positive patients with systemic sclerosis. J Rheumatol, 2012. 39(5): p. 997-1003.
- 36. Yoshizaki, A., et al., Immunization with DNA topoisomerase I and Freund's complete adjuvant induces skin and lung fibrosis and autoimmunity via interleukin-6 signalling. Arthritis Rheum, 2011. 63(11): p. 3575-85.
- 37. Lunardi, C., et al., Systemic sclerosis immunoglobulin G autoantibodies bind the human cytomegalovirus late protein UL94 and induce apoptosis in human endothelial cells. Nat Med, 2000. **6**(10): p. 1183-6.
- 38. Jordan, S., et al., Effects and safety of rituximab in systemic sclerosis: an analysis from the European Scleroderma Trial and Research (EUSTAR) group. Ann Rheum Dis, 2015. 74(6): p. 1188-94.
- 39. Gordon, J.K., et al., Belimumab for the Treatment of Early Diffuse Systemic Sclerosis: Results of a Randomized, Double-Blind, Placebo-Controlled, Pilot Trial. Arthritis Rheumatol, 2018. 70(2): p. 308-316.
- 40. Chakravarty, E.F., et al., Gene expression changes reflect clinical response in a placebo-controlled randomized trial of abatacept in patients with diffuse cutaneous systemic sclerosis. Arthritis Res Ther, 2015. 17(1): p. 159.

- 41. van Laar, J.M., et al., Autologous hematopoietic stem cell transplantation vs intravenous pulse cyclophosphamide in diffuse cutaneous systemic sclerosis: a randomized clinical trial. Jama, 2014. 311(24): p. 2490-8.
- 42. Thoreau, B., B. Chaigne, and L. Mouthon, Role of B cell in the Pathogenesis of Systemic Sclerosis. Front Immunol, 2022. 13: p. 933468.
- 43. Fukasawa, T., et al., The role of B cells in systemic sclerosis. J Dermatol, 2024. 51(7): p. 904-913.
- 44. Teske, N. and N. Fett, Recent Advances in Treatment of Systemic Sclerosis and Morphea. American Journal of Clinical Dermatology, 2024. 25(2): p. 213-226.
- 45. De Martinis, M., et al., An overview of environmental risk factors in systemic sclerosis. Expert Rev Clin Immunol, 2016. 12(4): p. 465-78.
- 46. Johnson, K.L., et al., Fetal cell microchimerism in tissue from multiple sites in women with systemic sclerosis. Arthritis Rheum, 2001. 44(8): p. 1848-54.
- 47. Yamamoto, T. and K. Nishioka, Possible role of apoptosis in the pathogenesis of bleomycin-induced scleroderma. J Invest Dermatol, 2004. 122(1): p. 44-50.
- 48. Casciola-Rosen, L., F. Wigley, and A. Rosen, Scleroderma autoantigens are uniquely fragmented by metal-catalyzed oxidation reactions: implications for pathogenesis. J Exp Med, 1997. 185(1): p. 71-9.
- 49. Sgonc, R., et al., Endothelial cell apoptosis is a primary pathogenetic event underlying skin lesions in avian and human scleroderma. J Clin Invest, 1996. 98(3): p. 785-92.
- 50. Paul, S., et al., Centromere defects, chromosome instability, and cGAS-STING activation in systemic sclerosis. Nature Communications, 2022. 13(1): p. 7074.
- 51. Herrick, A.L., Pathogenesis of Raynaud's phenomenon. Rheumatology, 2005. 44(5): p. 587-596.
- 52. Hénault, J., et al., DNA topoisomerase I binding to fibroblasts induces monocyte adhesion and activation in the presence of anti-topoisomerase I autoantibodies from systemic sclerosis patients. Arthritis Rheum, 2006. **54**(3): p. 963-73.
- 53. Michalska-Jakubus, M., et al., Anti-endothelial cell antibodies do not correlate with disease activity in systemic sclerosis. Postepy Dermatol Alergol, 2018. 35(2): p. 185-191.
- 54. Koenig, M., et al., Autoantibodies and microvascular damage are independent predictive factors for the progression of Raynaud's phenomenon to systemic sclerosis: a twenty-year prospective study of 586 patients, with validation of proposed criteria for early systemic sclerosis. Arthritis Rheum, 2008. 58(12): p. 3902-12.
- 55. Hanson, A.L., et al., Contribution of HLA and KIR Alleles to Systemic Sclerosis Susceptibility and Immunological and Clinical Disease Subtypes. Frontiers in Genetics, 2022. 13.
- Kuwana, M., et al., Association of human leukocyte antigen class II genes with autoantibody profiles, but not with disease susceptibility in Japanese patients with systemic sclerosis. Intern Med, 1999. 38(4): p. 336-44.
- 57. Kuwana, M., et al., The HLA-DR and DQ genes control the autoimmune response to DNA topoisomerase I in systemic sclerosis (scleroderma). J Clin Invest, 1993. 92(3): p. 1296-301.
- 58. Alkema, W., et al., Autoantibody profiles in systemic sclerosis; a comparison of diagnostic tests. Autoimmunity, 2021. 54(3): p. 148-155.
- 59. Schachna, L., et al., Recognition of Granzyme B-generated autoantigen fragments in scleroderma patients with ischemic digital loss. Arthritis Rheum, 2002. 46(7): p. 1873-84.
- 60. Walker, J.G. and M.J. Fritzler, Update on autoantibodies in systemic sclerosis. Curr Opin Rheumatol, 2007. 19(6): p. 580-91.
- 61. Wynn, T.A., Fibrotic disease and the T(H) 1/T(H)2 paradigm. Nat Rev Immunol, 2004. 4(8): p. 583-94.
- 62. Roderfeld, M., et al., Bone marrow transplantation improves hepatic fibrosis in Abcb4-/- mice via Th1 response and matrix metalloproteinase activity. Gut, 2012. 61(6): p. 907-16.

- 63. Sato, S., et al., Levels of interleukin 12, a cytokine of type 1 helper T cells, are elevated in sera from patients with systemic sclerosis. J Rheumatol, 2000. 27(12): p. 2838-42.
- 64. Valentini, G., et al., Peripheral blood T lymphocytes from systemic sclerosis patients show both Th1 and Th2 activation. J Clin Immunol, 2001. 21(3): p. 210-7.
- 65. Boin, F., et al., T cell polarization identifies distinct clinical phenotypes in scleroderma luna disease. Arthritis Rheum, 2008. 58(4): p. 1165-74.
- 66. Scaletti, C., et al., Th2-oriented profile of male offspring T cells present in women with systemic sclerosis and reactive with maternal major histocompatibility complex antigens. Arthritis Rheum, 2002. **46**(2): p. 445-50.
- 67. Parel, Y., et al., Presence of CD4+CD8+ double-positive T cells with very high interleukin-4 production potential in lesional skin of patients with systemic sclerosis. Arthritis Rheum, 2007. **56**(10): p. 3459-67.
- 68. Zhang, M. and S. Zhang, T Cells in Fibrosis and Fibrotic Diseases. Front Immunol, 2020. 11: p. 1142.
- 69. Gieseck, R.L., 3rd, M.S. Wilson, and T.A. Wynn, Type 2 immunity in tissue repair and fibrosis. Nat Rev Immunol, 2018. 18(1): p. 62-76.
- 70. Nguyen, J.K., et al., The IL-4/IL-13 axis in skin fibrosis and scarring: mechanistic concepts and therapeutic targets. Arch Dermatol Res, 2020. 312(2): p. 81-92.
- 71. Mavalia, C., et al., Type 2 helper T cell predominance and high CD30 expression in systemic sclerosis. Am J Pathol, 1997. 151(6): p. 1751-8.
- 72. Speeckaert, R., et al., The many faces of interleukin-17 in inflammatory skin diseases. Br J Dermatol, 2016. **175**(5): p. 892-901.
- 73. Guo, R.H., et al., Changes in peripheral T-lymphocyte subsets and serum cytokines in patients with systemic sclerosis. Front Pharmacol, 2022. 13: p. 986199.
- 74. Chen, Z. and J.J. O'Shea, Th17 cells: a new fate for differentiating helper T cells. Immunol Res, 2008. **41**(2): p. 87-102.
- 75. Fossiez, F., et al., T cell interleukin-17 induces stromal cells to produce proinflammatory and hematopoietic cytokines. J Exp Med, 1996. 183(6): p. 2593-603.
- 76. Yoshitomi, H. and H. Ueno, Shared and distinct roles of T peripheral helper and T follicular helper cells in human diseases. Cellular & Molecular Immunology, 2021. 18(3): p. 523-527.
- 77. Kayser, C. and M.J. Fritzler, Autoantibodies in systemic sclerosis: unanswered questions. Front Immunol, 2015. 6: p. 167.
- 78. Ricard, L., et al., Circulating follicular helper T cells are increased in systemic sclerosis and promote plasmablast differentiation through the IL-21 pathway which can be inhibited by ruxolitinib. Ann Rheum Dis, 2019. 78(4): p. 539-550.
- 79. Taylor, D.K., et al., T follicular helper-like cells contribute to skin fibrosis. Sci Transl Med, 2018.
- 80. Gaydosik, A.M., et al., Single-cell transcriptome analysis identifies skin-specific T cell responses in systemic sclerosis. Ann Rheum Dis, 2021. 80(11): p. 1453-1460.
- 81. Wutte, N., et al., CXCL13 and B cell activating factor as putative biomarkers in systemic sclerosis. Br J Dermatol, 2013. 169(3): p. 723-5.
- 82. Kondělková, K., et al., Regulatory T cells (TREG) and their roles in immune system with respect to immunopathological disorders. Acta Medica (Hradec Kralove), 2010. 53(2): p. 73-7.
- 83. Banica, L., et al., Quantification and molecular characterization of regulatory T cells in connective tissue diseases. Autoimmunity, 2009. 42(1): p. 41-9.
- 84. Antiga, E., et al., Regulatory T cells in the skin lesions and blood of patients with systemic sclerosis and morphoea. Br J Dermatol, 2010. 162(5): p. 1056-63.

- 85. Papp, G., et al., Altered T cell and regulatory cell repertoire in patients with diffuse cutaneous systemic sclerosis. Scand J Rheumatol, 2011. 40(3): p. 205-10.
- 86. Mo, C., et al., Imbalance between Thelper 17 and regulatory T cell subsets plays a significant role in the pathogenesis of systemic sclerosis. Biomed Pharmacother, 2018. 108: p. 177-183.
- 87. Radstake, T.R., et al., Increased frequency and compromised function of T regulatory cells in systemic sclerosis (SSc) is related to a diminished CD69 and TGFbeta expression. PLoS One, 2009. 4(6): p. e5981.
- 88. Kataoka, H., et al., Decreased expression of Runx1 and lowered proportion of Foxp3* CD25* CD4* regulatory T cells in systemic sclerosis. Mod Rheumatol, 2015. 25(1): p. 90-5.
- 89. Fuschiotti, P., Current perspectives on the role of CD8+ T cells in systemic sclerosis. Immunol Lett, 2018. 195: p. 55-60.
- 90. Fuschiotti, P., T.A. Medsger, Jr., and P.A. Morel, Effector CD8+ T cells in systemic sclerosis patients produce abnormally high levels of interleukin-13 associated with increased skin fibrosis. Arthritis Rheum, 2009. 60(4): p. 1119-28.
- 91. Luzina, I.G., et al., Occurrence of an activated, profibrotic pattern of gene expression in lung CD8+ T cells from scleroderma patients. Arthritis Rheum, 2003. 48(8): p. 2262-74.
- 92. Maehara, T., et al., Cytotoxic CD4+ T lymphocytes may induce endothelial cell apoptosis in systemic sclerosis. J Clin Invest, 2020. 130(5): p. 2451-2464.
- 93. Scharffetter, K., B. Lankat-Buttgereit, and T. Krieg, Localization of collagen mRNA in normal and scleroderma skin by in-situ hybridization. Eur J Clin Invest, 1988. 18(1): p. 9-17.
- 94. Atamas, S.P., et al., Production of type 2 cytokines by CD8+ lung cells is associated with greater decline in pulmonary function in patients with systemic sclerosis. Arthritis Rheum, 1999. 42(6): p. 1168-78.
- 95. Lanzolla, G., M. Marinò, and F. Menconi, Graves disease: latest understanding of pathogenesis and treatment options. Nat Rev Endocrinol, 2024. 20(11): p. 647-660.
- 96. Long, S.A. and J.H. Buckner, Clinical and experimental treatment of type 1 diabetes. Clin Exp Immunol, 2022. **210**(2): p. 105-113.
- 97. Roofeh, D. and D. Khanna, Management of systemic sclerosis: the first five years. Curr Opin Rheumatol, 2020. **32**(3): p. 228-237.
- 98. Frantz, C., et al., Regulatory T Cells in Systemic Sclerosis. Front Immunol, 2018. 9: p. 2356.
- 99. Dominguez-Villar, M. and D.A. Hafler, Regulatory T cells in autoimmune disease. Nature Immunology, 2018. 19(7): p. 665-673.
- 100. Rims, C., et al., Antigen-specific T cell frequency and phenotype mirrors disease activity in DRB1*04:04+ rheumatoid arthritis patients. Clin Exp Immunol, 2024.
- 101. Moon, J.-S., et al., Cytotoxic CD8+ T cells target citrullinated antigens in rheumatoid arthritis. Nature Communications, 2023. 14(1): p. 319.
- 102. Abdirama, D., et al., Nuclear antigen-reactive CD4+ T cells expand in active systemic lupus erythematosus, produce effector cytokines, and invade the kidneys. Kidney International, 2021. 99(1): p. 238-246.
- 103. Buckner, J.H., Antigen-specific immunotherapies for autoimmune disease. Nature Reviews Rheumatology, 2025. 21(2): p. 88-97.
- 104. Verheijden, G.F., et al., Human cartilage glycoprotein-39 as a candidate autoantigen in rheumatoid arthritis. Arthritis Rheum, 1997. 40(6): p. 1115-25.
- 105. Landewé, R.B., et al., Intranasal administration of recombinant human cartilage glycoprotein-39 as a treatment for rheumatoid arthritis: a phase II, multicentre, double-blind, randomised, placebocontrolled, parallel-group, dose-finding trial. Ann Rheum Dis, 2010. 69(9): p. 1655-9.

- 106. Urowitz, M.B., D.A. Isenberg, and D.J. Wallace, Safety and efficacy of hCDR1 (Edratide) in patients with active systemic lupus erythematosus: results of phase II study. Lupus Sci Med, 2015. 2(1): p. e000104.
- 107. Wang, Y., et al., The Therapeutic Strategies for SLE by Targeting Anti-dsDNA Antibodies. Clin Rev Allergy Immunol, 2022. 63(2): p. 152-165.
- 108. Fava, A., et al., Frequency of circulating topoisomerase-I-specific CD4 T cells predicts presence and progression of interstitial lung disease in scleroderma. Arthritis Res Ther, 2016. 18(1): p. 99.
- 109. Jin, L., et al., CD4+CXCR5+ follicular helper T cells in salivary gland promote B cells maturation in patients with primary Sjogren's syndrome. Int J Clin Exp Pathol, 2014. 7(5): p. 1988-96.
- 110. Broeren, M.G.A., et al., Proteogenomic analysis of the autoreactive B cell repertoire in blood and tissues of patients with Sjögren's syndrome. Ann Rheum Dis, 2022. 81(5): p. 644-652.
- 111. Verstappen, G.M., et al., Epithelial-immune cell interplay in primary Sjögren syndrome salivary gland pathogenesis. Nature Reviews Rheumatology, 2021. 17(6): p. 333-348.
- 112. Liu, X., F. Lu, and X. Chen, Examination of the role of necroptotic damage-associated molecular patterns in tissue fibrosis. Front Immunol, 2022. 13: p. 886374.
- 113. Yang, H., et al., Pyroptosis executor gasdermin D plays a key role in scleroderma and bleomycin-induced skin fibrosis. Cell Death Discovery, 2022. 8(1): p. 183.
- 114. Tong, L., V. Koh, and B.Y. Thong, Review of autoantigens in Sjögren's syndrome: an update. J Inflamm Res, 2017. **10**: p. 97-105.
- 115. Greiling, T.M., et al., Commensal orthologs of the human autoantigen Ro60 as triggers of autoimmunity in lupus. Science Translational Medicine, 2018. 10(434): p. eaan2306.
- 116. Gourh, P., et al., HLA and autoantibodies define scleroderma subtypes and risk in African and European Americans and suggest a role for molecular mimicry. Proc Natl Acad Sci U S A, 2020. 117(1): p. 552-562.
- 117. Saegusa, J., et al., Oxidative stress mediates cell surface expression of SS-A/Ro antigen on keratinocytes. Free Radical Biology and Medicine, 2002. 32(10): p. 1006-1016.
- 118. Servettaz, A., et al., Selective oxidation of DNA topoisomerase 1 induces systemic sclerosis in the mouse. J Immunol, 2009. 182(9): p. 5855-64.
- 119. Routsias, J.G. and A.G. Tzioufas, B cell epitopes of the intracellular autoantiaens Ro/SSA and La/SSB: Tools to study the regulation of the autoimmune response. Journal of Autoimmunity, 2010. 35(3): p. 256-264.
- 120. Rischmueller, M., et al., HLA class II phenotype controls diversification of the autoantibody response in primary Sjögren's syndrome (pSS). Clinical and Experimental Immunology, 2001. 111(2): p. 365-371.
- 121. Johnson, S.R., et al., Shifting our thinking about uncommon disease trials: the case of methotrexate in scleroderma. J Rheumatol, 2009. 36(2): p. 323-9.
- 122. Tashkin, D.P., et al., Cyclophosphamide versus placebo in scleroderma lung disease. N Engl J Med, 2006. 354(25): p. 2655-66.
- 123. Walker, K.M. and J. Pope, Treatment of systemic sclerosis complications: what to use when first-line treatment fails--a consensus of systemic sclerosis experts. Semin Arthritis Rheum, 2012. 42(1): p. 42-55.
- 124. Liossis, S.N., A. Bounas, and A.P. Andonopoulos, Mycophenolate mofetil as first-line treatment improves clinically evident early scleroderma lung disease. Rheumatology (Oxford), 2006. 45(8): p. 1005-8.
- 125. Joerg, H., et al., Autologous stem cell transplantation for progressive systemic sclerosis: a prospective non-interventional study from the European Society for Blood and Marrow Transplantation Autoimmune Disease Working Party. Haematologica, 2021. 106(2): p. 375-383.
- 126. Müller, F., et al., CD19 CAR T cell Therapy in Autoimmune Disease A Case Series with Follow-up. N Engl J Med, 2024. **390**(8): p. 687-700.



Chapter 2

Therapeutic Options for Systemic Sclerosis: Current and Future Perspectives in Tackling Immune-Mediated Fibrosis

Theodoros Ioannis Papadimitriou, Arjan van Caam, Peter M. van der Kraan and Rogier M. Thurlings

Biomedicines 2022, 10, 316. https://doi.org/10.3390/biomedicines10020316

Abstract

Systemic sclerosis (SSc) is a severe autoimmune, rheumatic disease, characterized by excessive fibrosis of the skin and visceral organs. SSc is accompanied by high morbidity and mortality rates, and unfortunately, few disease-modifying therapies are currently available. Inflammation, vasculopathy, and fibrosis are the key hallmarks of SSc pathology. In this narrative review, we ex-amine the relationship between inflammation and fibrosis and provide an overview of the efficacy of current and novel treatment options in diminishing SSc-related fibrosis based on selected clinical trials. To do this, we first discuss inflammatory pathways of both the innate and acquired immune systems that are associated with SSc pathophysiology. Secondly, we review evidence supporting the use of first-line therapies in SSc patients. In addition, T cell-, B cell-, and cytokine-specific treatments that have been utilized in SSc are explored. Finally, the potential effectiveness of tyrosine kinase inhibitors and other novel therapeutic approaches in reducing fibrosis is highlighted.

Keywords

systemic sclerosis; immune cells; anti-inflammatory; therapy; fibrosis

Introduction

Systemic sclerosis (SSc) is a severe rheumatic, autoimmune disease which affects up to 20 people per 100,000 and women up to nine times more often than men [1-3]. Inflammation, vasculopathy, and fibrosis are the key hallmarks of SSc. Patients suffer from fibrotic skin lesions, and as the disease progresses, the function of internal organs, including the heart, lungs, gastrointestinal tract, and kidneys deteriorate due to fibrosis. The disease has a high morbidity and greatly negatively affects the quality of life and life expectancy of patients.

Although the pathophysiology of SSc has not been elucidated yet, the immune system has been hypothesized as an important driver of the disease (*Figure 1*). SSc patients exhibit disease-specific autoantibodies, and a typical cytokine profile in their blood indicating immune cell activation. This profile is characterized by increased T helper 2 (Th2) and decreased T helper 1 (Th1) cytokines [4,5]. Furthermore, in skin biopsies of early disease patients, perivascular accumulation of immune cells, such as CD4+ and CD8+ cytotoxic T cells (CTLs), can be observed [6]. This immune activation can cause (or is maybe a response to) capillary damage, which leads to capillary breakdown, adherence of platelets, and activation of pro-fibrotic pathways. Additionally, vascular injury causes damage and apoptosis of endothelial cells. The release of internal damage-associated molecular patterns (DAMPs) increases microvascular permeability which causes additional recruitment of immune cells to the endothelium and therefore increased immune cell activation and inflammation [7].

Activation of the immune system is also linked to fibrosis. For example, Th2 cytokines, such as interleukin (IL)-4 and -13, can activate myofibroblasts [8]. Myofibroblasts are a strongly pro-fibrotic cell type which produces large amounts of extracellular matrix (ECM) molecules and matrix-strengthening enzymes. Furthermore, these cells also excrete growth factors and cytokines that worsen inflammation [9]. IL-4, IL-6, and transforming growth factor (TGF)-β are the predominant fibrogenic cytokines that cause subendothelial accumulation of fibrous tissue, leading to aberrant vascular remodeling [10]. In turn, this aberrant vascular remodeling makes the capillaries more prone to damage, fueling an immune response.

The important role of the immune system in the pathogenesis of SSc is further supported by the fact that autologous hematopoietic stem cell transplantation (ASCT) can induce long-term disease remission in patients with SSc. However, ASCT is accompanied by a high mortality rate (~10%) and is only administered in the most severe cases of SSc [11]. Currently, there is no specific and effective diseasemodifying treatment available, which, regarding the severity of the disease, results in an unmet medical need. Presently, mainly broad-spectrum immunosuppressive and anti-inflammatory drugs, developed for other autoimmune diseases, are used to treat SSc. In this narrative review, we discuss the effectiveness of the currently used and/or investigated agents in diminishing skin and lung fibrosis in scleroderma patients. For this, we first provide an overview of the main pathogenic pathways that are implicated in the disease. Secondly, drugs targeting these pathways are assessed for their treatment efficacy based on results from selected clinical trials. To write this review, the databases PubMed and clinicaltrials, gov were used to search for publications up to November 2021. Combinations of Medical Subject Headings (MeSH) terms referring to SSc ("Systemic sclerosis" OR "Scleroderma, Systemic") and drugs of interest, e.g., "methotrexate", were included in the search strategy.

The Role of Immune Cells in SSc-Related Inflammation and Fibrosis

A large body of evidence suggests that both the innate and the adaptive immune system are involved in the fibrogenesis of SSc.

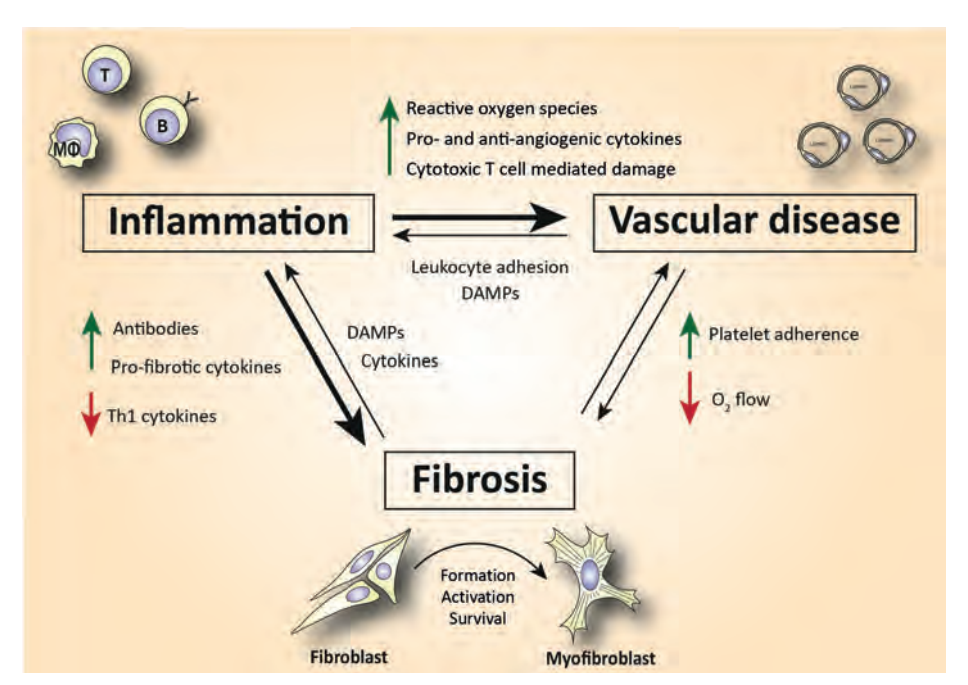


Figure 1. Simplified schematic representation of the complex interplay between inflammation, vasculopathy, and fibrosis in SSc. Abbreviations: Th1 = T helper type 1 cells; DAMPs = damageassociated molecular patterns; T = T lymphocyte; B = B lymphocyte; $M\Phi = macrophage$.

The Role of Innate Immunity in SSc

The innate immune system mediates the immediate defensive response against pathogens and chemical or mechanical damage. An increased number of macrophages, mast cells, type 2 innate-like lymphoid cells, eosinophils, and plasmacytoid dendritic cells have been identified in SSc tissues [12]. The induction of excessive numbers of myofibroblasts that are observed in SSc is partly mediated by the previously mentioned innate immune cells. Other innate immune cell types such as platelets, neutrophils, and natural killer cells have also been found to be dysregulated in SSc pathology. However, only a few studies highlighting their role in SSc have been published. Thus, in this review, we focus on the cells of the innate immune system that are well characterized in SSc.

Macrophages

Macrophages are effector phagocytotic cells specialized in eliminating pathogens. These cells play an essential role in homeostatic manifestations related to the disposal of internal waste products and tissue repair. Monocyte-derived macrophages can be found in the blood circulation under inflammatory conditions but are prevalent in all human tissues as tissue-resident macrophages. However, macrophages exhibit a highly heterogeneous phenotype that is regulated by their microenvironment. Under the influence of certain inflammatory mediators, macrophages can be polarized in vitro towards a classically activated (M1) inflammatory phenotype or an alternatively activated (M2) tissue repair phenotype. M2 macrophages are often characterized by the secretion of large amounts of IL-10, TGF-β, and other pro-fibrotic cytokines such as IL-4, IL-6, and IL-13 that play an essential role in wound healing and tissue repair (Figure 2). These cytokines are also known to induce fibrosis by activating myofibroblasts [13]. On the other hand, in states of chronic tissue repair, M2 macrophages can also exhibit anti-fibrotic functions that lower the progression of fibrosis by suppressing local T helper cell responses and decreasing the production of ECM by (myo) fibroblasts [14,15]. Furthermore, to a certain extent, M1 and M2 phenotypes are artificial in vitro cell states. In vivo, different types of anti-inflammatory and anti-fibrotic macrophages have been reported in the process of wound healing, repair, and fibrosis [16].

In SSc, transcriptomic and immunohistochemistry studies identified a prominent pro-fibrotic M2 macrophage signature in patients' skin and lung lesions that was correlated with an increased skin score and disease severity [17–19]. In addition, a dominant M2 monocyte signature has also been observed in SSc blood [20]. This notion suggests a role of M2 macrophages in the immunopathogenesis of SSc. The importance of macrophages in regulating fibrosis is further supported by the observation that mice lacking macrophages (with the use of liposomal chlodronate) exhibit reduced bleomycin-induced lung fibrosis [21]. In skin lesions, M2 macrophages are characterized by overexpression of the scavenger receptor CD163 or CD204 [22]. The number of CD163+ or CD204+ cells was found to be significantly expanded in SSc compared to healthy skin [23]. Strikingly, these activated macrophages were localized not only in the perivascular areas, but also between thickened collagen fibers. This indicates a potential role of tissueinfiltrating macrophages in the development of fibrosis [24]. However, it is worth mentioning that bone marrow-derived mesenchymal progenitors such as monocytes and fibrocytes may also be implicated in SSc-related fibrosis. These cells are able to migrate from the circulation to affected tissues such as the lungs, where they differentiate into activated (myo)fibroblasts [25]. Of note, it has been reported that fibrocytes were only detected in patients with connective tissue disorders (including SSc) and not in healthy donors [26]. In SSc, the frequency of circulating fibrocytes was positively correlated with an increased dermal thickness [27]. Furthermore, in a very recent single-cell RNA sequencing (sc-RNA seq) study, highly proliferating macrophages were only found in SSc and not healthy skin and were correlated with increased skin fibrosis [28]. All in all, the role of macrophages in fibrotic activation in SSc is prominent, but the signalling pathways characterizing their aberrant activation remain poorly understood. In addition, their role as regulators of the disease, in combination with deciphering a potential role of antifibrotic macrophages in SSc, warrants further research. Unraveling the pathogenic mechanisms by which macrophages mediate fibrosis will likely contribute to targeted therapies that reduce fibrosis and ameliorate inflammation in SSc and other connective tissue disorders. To this end, future therapeutic options should opt to reduce the activation/number of activated pro-fibrotic and pro-inflammatory macrophages while boosting the activity of the anti-inflammatory and antifibrotic ones.

Eosinophils and Mast Cells

As we discussed previously, serum levels of the cytokines IL-4, IL-10, and IL-13 are elevated in SSc patients and are correlated with increased fibrosis and disease severity. Meanwhile, IL-4 and IL-13 play an essential role in eosinophil-mediated inflammation, suggesting a potential role of eosinophils in SSc pathology [29,30]. Eosinophils are granulocytes derived from the myeloid stem cells that are part of the innate immune system. Elevated levels of eosinophils have been described in SSc and other diseases of the connective tissue [31]. In the peripheral blood of early untreated SSc patients, eosinophil counts were higher compared to patients with other major collagen diseases such as dermatomyositis, Sjogren's syndrome, and

systemic lupus erythematosus. Furthermore, eosinophil counts were significantly correlated with severe interstitial lung disease (ILD) and an increased skin thickness in patients with SSc, but not in patients with other collagen diseases [32]. In addition, the presence of skin ulcers in SSc has been associated with elevated counts of peripheral blood eosinophils [33]. Collectively, these results implicate eosinophils in the pathogenesis of SSc including the hallmarks of inflammation and vascular dysfunction. However, studies exploring the exact mechanism of inflammation or ulcer formation are lacking.

Another cell type of the innate immune system derived from myeloid stem cells is mast cells. Mast cells have been detected in SSc tissues and can exhibit profibrotic manifestations. Elevated infiltration of mast cells has been found in various SSc tissues including the skin and salivary glands [34-36]. Mast cell infiltration has been correlated with more severe disease phenotypes. Except for their wellestablished role in immediate inflammatory and allergic reactions, these cells are also implicated in cardiac, renal, and pulmonary fibrosis. Mast cells have been linked to fibrosis by their ability to produce pro-fibrotic cytokines such as IL-4, IL-6, IL-13, tumor necrosis factor alpha (TNF-α), platelet-derived growth factor (PDGF), and TGF-ß [37]. This way, mast cells stimulate the production and activity of myofibroblasts (Figure 2).

Serotonin is another molecule that is produced by mast cells. Serotonin can directly increase ECM deposition in primary skin fibroblasts in a TGFβ-dependent manner [38]. In addition, mast cells produce tryptase, a serine proteinase which triggers fibroblast proliferation and collagen production [39]. It was also demonstrated that fibroblast proliferation in patients' lungs can be caused by mast cell-related histamine release [40]. More specifically, human primary lung fibroblasts that were cultured in the presence of physiologically relevant concentrations of histamine exhibited increased cell proliferation that was mediated through an H2 histamine receptor on the fibroblasts. Interestingly, the observed fibroblast proliferation was inhibited by an H2 antagonist, empowering the role of histamine release in fibroblast proliferation. Of note, mast cell depletion with phototherapy ameliorates SSc fibrosis in vivo [41]. Thus, targeting mast cells in systemic sclerosis might be an effective treatment approach. We believe that exploring the immunopathogenic role of eosinophils and mast cells with the currently available novel arsenal of biomolecular techniques will unveil new innate pathogenic pathways that could pave the way for novel treatment approaches.

New Players: Innate Lymphoid Cells and Plasmacytoid Dendritic Cells

Among the family of innate immune cells, a highly interesting tissue-resident cell type that was recently shown to be involved in SSc is innate lymphoid cells (ILCs). These cells are derived from common lymphoid progenitors such as adaptive immune cells, but they lack rearranged antigen receptors. Therefore, ILCs do not exhibit antigen-specific responses but are characterized by a functional diversity similar to that of T lymphocytes. These cells have been categorized into distinct subtypes based on their cytokine and transcriptome profile. One of these subtypes is ILC2, which is identified by the expression of the transcription factor GATA-3. As with Th2 cells, ILC2s predominantly produce IL-4, IL-5, and IL-13 [42].

Intriguingly, locally accumulating ILC2s have emerged as a pivotal source of profibrotic cytokines in inflammatory and fibrotic diseases [43]. Studies using the carbon tetrachloride (CCl4)-induced liver fibrosis mouse model showed that ILC2s mediate liver fibrosis by producing the pro-fibrotic cytokine IL-13 [44]. This observation suggests that ILC2s may stimulate the activation of fibroblasts and thus increase tissue fibrosis. Indeed, ILC2 counts are significantly increased in both the skin and peripheral blood from patients with SSc compared to healthy controls. and their numbers are correlated with an increased skin thickness [45,46]. This notion is further supported by studies that have shown an elevated expression of the ILC2 cytokines IL-25, IL-33, and thymic stromal lymphopoietin (TSLP) in both the serum and skin of patients with SSc [46–48]. From a mechanistic point of view, TGF-β and IL-10 are two cytokines that have been implicated in ILC2-mediated skin fibrosis in SSc. Elevated TGF-β enhanced the in vitro pro-fibrotic function of ILC2s by increasing the activation of myofibroblasts and downregulating the levels of IL-10. Downregulation of IL-10 increased the production of collagen by dermal fibroblasts. In the same study, TGF-β inhibition combined with IL-10 administration prevented fibrotic manifestations in a mouse model recapitulating SSc [49]. Although there is a limited number of studies associating ILC2s in the pathogenesis of SSc, we believe that findings implicating TGF-β in their potential fibrotic mechanism might be promising in utilizing alternative therapeutic strategies that are based on TGF-β blocking.

Plasmacytoid dendritic cells (pDCs) are innate immune cells that secrete large amounts of interferon (IFN) and mediate Toll-like receptor (TLR)-induced inflammation in autoimmunity, pDCs have been recently detected in the sclerotic skin of patients with SSc. These cells were found to be chronically activated and characterized by an elevated expression of chemokine (C-X-C motif) ligand 4 (CXCL4) and IFN-α in a TLR8-dependent manner [28,50]. CXCL4 has been identified

as a biomarker that is associated with severe disease and lung fibrosis in SSc [51]. pDCs have also been detected in bronchoalveolar lavage fluids of patients with SSc, and their levels were correlated with increased lung fibrosis [52]. Compared to patients with idiopathic pulmonary fibrosis (IPF), SSc-ILD-infiltrating pDCs exhibited a stronger IFN and stress response gene signature, suggesting that these cells demonstrate disease-specific mechanisms in SSc [53]. Recent research has provided mounting evidence suggesting that SSc is an IFN-driven disease [54]. Indeed, an elevated expression of type 1 IFN signalling (IFN-α, IRF5, IRF7, IRF8) and its inducible genes (IL-6, STAT1, STAT3) have been illustrated in tissue biopsies, the peripheral blood, and serum of SSc patients and was correlated with disease severity [55]. In the blood circulation, on the other hand, numbers of pDCs were decreased in SSc patients compared to healthy controls, probably due to their accumulation in the fibrotic skin [56]. Additionally, pDCs are well known for their prevalent antigen-presenting role. As we discussed, SSc is characterized by autoimmunity, and the presence of multiple antinuclear antibodies has been reported in patients' serum. DNA topoisomerase I (topol) is the most prevalent autoantibody in SSc and is correlated with increased disease severity and mortality [57]. Mice administered with topol-loaded pDCs exhibited robust autoantibody production accompanied by long-term lung and skin fibrosis [58]. Furthermore, pDC depletion in the bleomycin mouse model attenuates skin and lung fibrosis and improves clinical scores. Interestingly, numbers of B and T lymphocytes were also reduced in mouse lungs, demonstrating an important role of pDCs in ongoing innate and adaptive immune abnormalities [50,52].

The Role of Adaptive Immunity in SSc

Activation of the innate immune system in SSc is essential in activating the adaptive immune response by presentation of antigens with parallel expression of dangerindicating molecules. This activation is mediated either by cell-cell interactions, or by the release of soluble mediators [59]. We will now briefly discuss the role of T and B lymphocytes in SSc pathogenesis (Table 1), to better explain the possible treatment options.

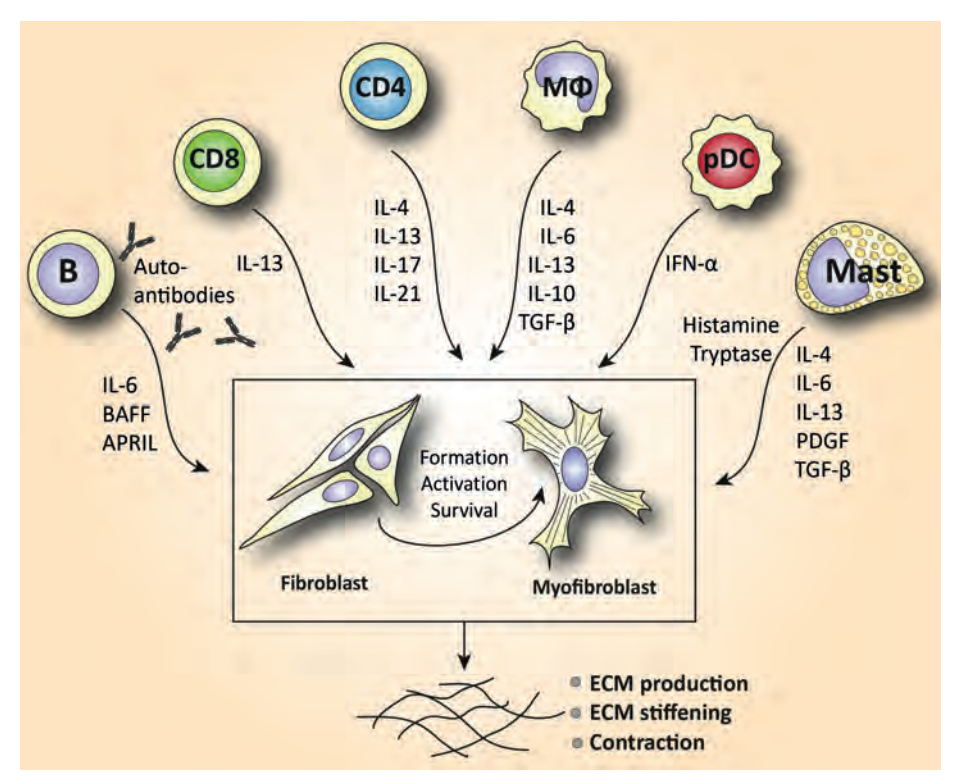


Figure 2. An overview of the main pathogenic mechanisms by which T cells, B cells, macrophages, mast cells, and plasmacytoid dendritic cells may contribute to (pro-)fibrotic manifestations in SSc immunopathology. Abbreviations: $M\Phi$ = macrophages; B = B lymphocyte; CD8 = cytotoxic T cell; CD4 = T helper cell; pDC = plasmacytoid dendritic cell; TGF- β = transforming growth factor- β ; BAFF = B cell activating factor; APRIL = A proliferation-inducing ligand; PDGF = platelet-derived growth factor; ECM = extracellular matrix.

T Lymphocytes

The role of T helper lymphocytes is well characterized in SSc pathology. Th1, Th2, and Th17 subtypes have been paid the most attention. However, it should be noted that these subtype classifications have been derived from in vitro studies. In vivo, these subsets have been implicated in various types of pathogens. In chronic inflammatory diseases, they have been shown to exhibit a certain extent of plasticity and multifunctionality. In Th2-associated pathologies (including SSc), additional T cell subtypes such as Th9 and Th22 cells have also been characterized. However, their specific importance still remains to be determined. Studies implicating T helper cell subsets in SSc pathogenesis have mostly utilized older conventional research techniques such as immunohistochemistry in SSc skin and flow cytometry in patients' blood. Elevated production of the Th2-associated cytokines IL-4, IL-13, and IL-10 and the Th17 signature cytokine IL-17 have been demonstrated in SSc

tissues and the blood circulation [4,60-63] (Figure 2). These studies suggested that SSc is driven by Th2- and Th17-type mechanisms. Elevated IL-4 levels have been associated with increased collagen production in fibroblasts and higher production of TGF-β. TGF-β directly triggers collagen production and ECM deposition but also inhibits the expression of matrix metalloproteinases [64]. An increased level of IL-17 is implicated in fibrosis and SSc-like manifestations [65]. IL-17 not only increases the proliferation of fibroblasts but also promotes the expression of TNF-α and IL-1 from macrophages which, in turn, triggers collagen, IL-6, and PDGF production from fibroblasts. In addition, IL-17 triggers the endothelial cell production of IL-1, IL-6, intracellular adhesion molecule 1 (ICAM-1), and vascular cell adhesion molecule 1 (VCAM-1) [66] (Figure 3). These adhesion molecules further interact with circulating leukocytes and facilitate their migration to and accumulation at the fibrotic sites [67]. In addition to elevated Th2 and Th17 cytokines, SSc patients exhibit a reduced expression of the anti-fibrotic Th1 cytokine IFN-y, and this further suggests a decreased anti-fibrotic capacity [63]. A T helper cell subset which could play a protective role in SSc pathology is regulatory T cells (Tregs). Tregs maintain immunological self-tolerance, and their depletion has been associated with spontaneous autoimmunity. A plethora of animal studies and a few clinical studies have shown a potentially beneficial effect of Treg administration in various autoimmune diseases [68]. In SSc, the majority of the published literature illustrates a decreased frequency and functional ability of circulating Tregs. However, data on the frequency of tissue-resident Tregs are scarce and contradictory [69]. Overall, the mechanisms of circulating and tissue-resident T helper cell subsets that drive fibrosis are not precisely determined. It is to be proven if mechanisms such as T cell tolerance, anergy, and exhaustion are protective or deleterious in fibrogenesis.

Novel techniques such as single-cell RNA sequencing and confocal immunofluorescence microscopy have provided us with essential tools to gain a deep understanding of the phenotype and function of tissue-infiltrating T cells. Utilization of these newly available techniques reveals the heterogeneity of T cell responses and opens avenues for detecting patient-specific T cell subsets. For example, quantitative analyses of skin-resident cells showed that early diffuse cutaneous systemic sclerosis (dcSSc) skin was predominantly infiltrated by granzyme A-producing CD8+ and CD4+ CTLs. Th1, Th2, and Th17 cells were also detected but in much lower amounts. This study unveiled that CD4 T cells in SSc may directly induce cell death, a function that deviates from their conventional role in promoting effector immune responses from other lymphocytes. CD4+ and CD8+ CTLs exhibited the ability to drive fibrosis and contribute to vasculopathy (Figure 3) via the secretion of pro-inflammatory cytokines such as IL-1β and/or by inducing cytotoxicity-mediated apoptosis of stromal cells, leading to exuberant tissue remodeling [6]. The importance of CTLs in SSc pathogenesis is further supported by another recent study identifying the genome-wide expression of cytotoxic genes in SSc skin such as perforin and granzymes B, K, and H. Of note, the observed cytotoxic gene signature was positively correlated with skin thickness [70,71]. Furthermore, a prominent infiltration of IL-13-producing CD8+ CTLs was observed in skin biopsies early in SSc pathogenesis (<3 years), implicating a potentially important role of CTLs in the disease onset [72] (*Figure 2*). This notion is further supported by earlier studies that paid attention to the role of the CTL-mediated apoptosis induced by granzyme B in the initiation of systemic autoimmunity. The unique fragments generated by granzyme B degranulation represent an exclusive source of autoantigens, and these self-protein fragments are recognized by autoantibodies in a subset of SSc patients [73].

Another example of a recently identified CD4+ T cell subset in SSc pathology is follicular helper T (Tfh) cells. Tfh cells are specialized in providing help to B cells in lymph nodes by stimulating proliferation, class switching, and somatic hypermutation. These cells have not only been found in lymph nodes but have also recently been detected in the blood circulation where they are referred to as T peripheral helper (Tph) cells [74]. A key cytokine in Tph function is IL-21. Strikingly, in SSc patients, elevated counts of Tph cells have been shown to promote plasmablast differentiation through an IL-21-mediated pathway [75]. Furthermore, increased infiltration of inducible T cell co-stimulator (ICOS)+ Tfh-like cells has been observed in the skin of SSc patients. The presence of these cells in the skin of sclerodermous graft-versus-host disease mice was strongly linked to increased skin fibrosis. Interestingly, both the depletion of ICOS+ (including Tph depletion) cells and neutralization of IL-21 exhibited a significant reduction in skin fibrosis. Tfh cells activate fibroblasts in vitro. Co-culture of Tfh and fibroblasts resulted in increased expression of α -smooth muscle actin (α -SMA) on the activated myofibroblasts [76]. α-SMA is a key marker of activated myofibroblasts, and its expression is linked to a fibrotic phenotype. The importance of skin-resident Tfh-like cells in the pathology of SSc is also supported by an sc-RNAseg study that unraveled the heterogeneity of T cell responses in patients' skin biopsies. In this study, a distinct CXCL13+ Tfh-like subset that secretes factors promoting B cell responses and autoantibody production was only found in SSc-inflamed tissue [77]. In light of these new findings, developing drug strategies to target the newly described pathogenic T cell subsets is expected to set the milestones for potential personalized therapy in SSc.

B Lymphocytes

B lymphocytes are the second major component of our adaptive immune response. Mounting evidence suggests that B cell homeostasis in the blood of SSc patients is aberrant. Autoantibody production caused by loss of self-tolerance is an important hallmark in SSc pathogenesis. Autoantibodies such as anti-DNA topoisomerase I, anti-centromere, and anti-RNA polymerase antibodies have been detected in the sera of more than 95% of scleroderma patients [78].

The prominent infiltration of B cells in SSc tissues including the skin and lungs suggests their involvement in the disease pathogenesis [79]. Similar to T cells, earlier studies revealed their presence in sclerotic skin by utilizing mainly immunohistochemistry techniques. In a recent sc-RNAseg study, a prominent B cell gene signature was detected in the skin of 69% of early dSSc patients [80]. In a different study, B cell infiltration was associated with skin progression in early diffuse disease. In this study, infiltration of plasma cells was also evident in the sclerotic skin [81]. Thus, B cell skin infiltration seems to be linked to skin progression early in the disease onset and in patients with dcSSc. However, the robustness of this correlation needs to be validated in a larger cohort of patients.

More specifically, B cells in SSc are characterized by elevated numbers of IL-6producing effector B cells (Beffs) and decreased numbers of IL-10-producing regulatory B cells (Bregs). Because Bregs suppress and Beffs enhance the immune response through the production of cytokines, this change might impact the inflammatory process. Of note, in SSc, elevated IL-6 and reduced IL-10 levels have been detected in serum/plasma, which is possibly explained by this B cell imbalance. A possible cause for this change might be the altered presence of the cytokines B cell activating factor (BAFF) and A proliferation-inducing ligand (APRIL) in SSc blood [82]. BAFF and APRIL are potent activators of B cells. These cytokines stimulate the production of effector B cells and suppress the generation of regulatory B cells. Elevated serum levels of BAFF and APRIL have been documented in SSc and are correlated with skin thickening, disease severity, and increased IL-6 production by Beffs [83] (Figure 2). Interestingly, it has been demonstrated that BAFF inhibition decreased skin fibrosis in a murine model of SSc [84].

Importantly, not only the numbers of Beffs but also the phenotype of these cells is altered in SSc. To elaborate, SSc patients are characterized by an increased naïve (CD19+CD27-) and a reduced activated memory B (CD19+CD27+) cell phenotype that is accompanied by overexpressed pro-apoptotic and activation markers such as CD95, CD86, and human leukocyte antigen-DR isotype (HLA-DR) [4,85-88]. In

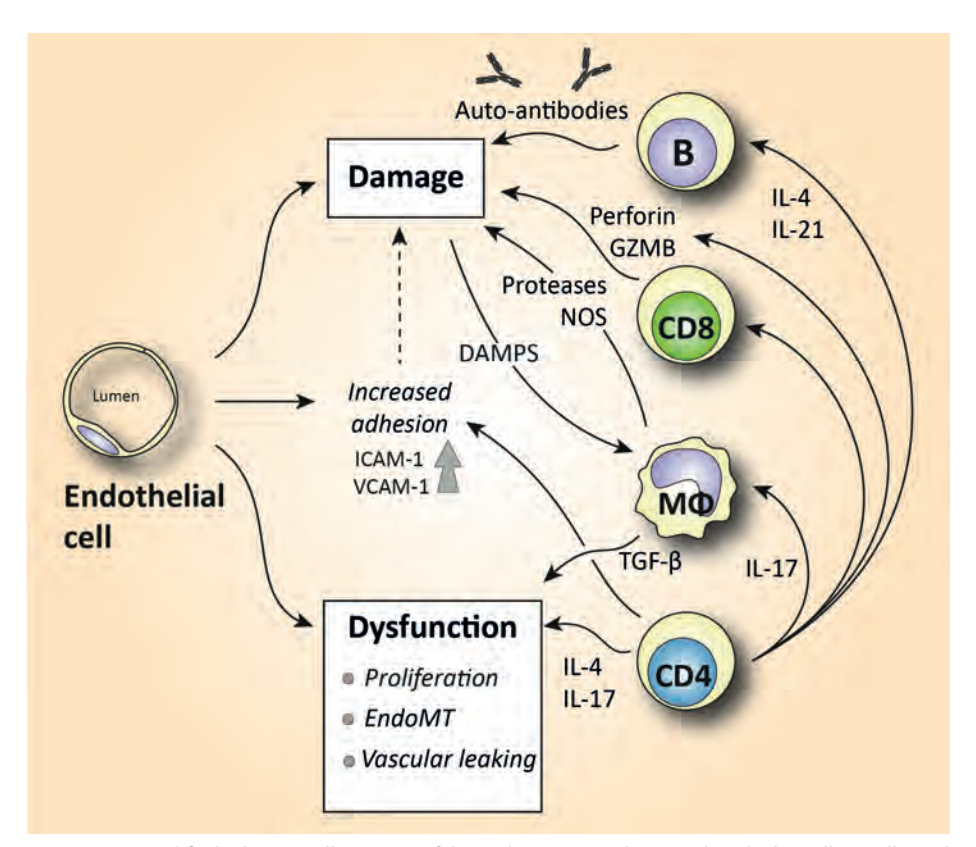


Figure 3. A simplified schematic illustration of the pathogenic mechanisms by which T cells, B cells, and macrophages may be involved in the vascular abnormalities that characterize SSc immunopathology. Abbreviations: ICAM-1 = intercellular adhesion molecule 1; VCAM-1 = vascular cell adhesion molecule 1; EndoMT = endothelial-to-mesenchymal transition; GZMB = granzyme B; NOS = nitric oxide synthase; DAMPs = damage-associated molecular patterns; MΦ = macrophages; B = B lymphocyte; CD4= T helper cell; CD8 = cytotoxic T cell; TGF- β = transforming growth factor- β .

addition, the cell surface phenotype of B cells is also changed in SSc. Significant overexpression of CD19 on the surface of B cells has been illustrated in SSc patients and was correlated with SSc-ILD [89,90]. However, in a recent study exploring lymphocyte subset aberrations between early dcSSc patients and healthy donors, the frequency of CD19+ B cells in the peripheral blood was similar [4]. CD19 is a positive B cell regulator that activates B cells through their B cell receptor (BCR) signalling. B cell hyperactivation through CD19-BCR signalling may be associated with the prevalent autoantibody production in SSc. Data from transgenic mouse models show that CD19-deficient mice have decreased serum autoantibodies. while overexpression of CD19 causes increased serum autoantibody production [91,92]. In addition, humans with homozygous mutations in the CD19 gene suffer from an antibody deficiency syndrome that impairs the response of mature B cells

in antigen stimulation [93]. In conclusion, in addition to B cells which have been documented to stimulate fibrosis with the release of cytokines, intriguingly, autoantibodies with direct pro-fibrotic effects and autoantibodies against the PDGF receptor have also been documented in SSc [94]. These autoantibodies seem to induce fibrosis by facilitating the conversion of the fibroblast to the myofibroblast phenotype [95] (Figure 2).

Table 1. Function of the primary cell types implicated in SSc pathogenesis both in the blood circulation and at the site of fibrosis.

Cell Type	Function
Endothelial cell	Platelet adhesion activates fibrotic pathways. Increased microvascular permeability causes leukocyte adhesion to the endothelium, leading to increased inflammation [7].
Monocyte/Macrophage	A prominent M2 macrophage signature increases levels of pro-fibrotic cytokines such as IL-4, IL-6, and IL-13 and correlates with elevated tissue fibrosis [17–20].
Eosinophil	Elevated eosinophil counts in the peripheral blood are associated with severe lung disease and presence of skin ulcers [31–33].
Mast cell	Release of cytokines and growth factors such as IL-4, IL-6, IL-13, TNF-a, PDGF, and TGF-β activates myofibroblasts to produce collagen [37]. Tryptase and histamine release triggers fibroblast proliferation [38,39].
Innate lymphoid cell	Increased production of the ILC2 cytokines IL-25, IL-33, and TSLP in serum and skin mediates fibrosis in a TGF- β -dependent manner [43–49].
Plasmacytoid dendritic cell	Elevated numbers of CXCL4+- and IFN-a-producing pDCs in skin and lungs are involved in increased fibrotic manifestations mediated by TLR8 activation [28,50,52].
T lymphocyte	Skin is predominantly infiltrated by CD4+ and CD8+ cytotoxic T cells that produce pro-fibrotic cytokines and cause apoptosis to epithelial cells [6,72]. Increased IL-21-producing Tph cells promote plasmablast differentiation and increase activation of myofibroblasts [75,77]. In the peripheral blood, SSc patients are characterized by increased Th2 and Th17 numbers compared to healthy donors [4,60,63].
B lymphocyte	Elevated BAFF and APRIL are correlated with skin thickening [81,83]. Increased IL-6-producing Beffs increase inflammation, while decreased IL-10-producing Bregs exhibit a reduced capacity for immunosuppression [82]. In SSc peripheral blood, an increase in naïve and a decrease in activated memory B cells is observed compared to healthy controls [4,85,87,91].

SSc First-Line Anti-Inflammatory Treatment

Now that we have discussed the role of immune cells in SSc, we will address the efficacy of treatment approaches. According to current recommendations from the European League against Rheumatism (EULAR), methotrexate (MTX) is considered as a first-line treatment in early dcSSc [96]. Other therapeutic strategies include administration of synthetic corticosteroids or low-dose (2 mg/kg) administration of cyclophosphamide (CYC) for 1 year, continued by conservation therapy with mycophenolate mofetil (MMF) [97], or first-line therapy with MMF. These therapies represent the broad-spectrum anti-inflammatory drugs (Table 2) that have been extensively used in SSc, and thus we will start discussing them first.

Synthetic Corticosteroids

To begin with, synthetic corticosteroids (CS) such as prednisolone, hydrocortisone, methylprednisolone, and dexamethasone are the oldest anti-inflammatory and immunosuppressive agents that have been extensively used in scleroderma and other rheumatic diseases. These compounds modulate the activation of all immune cells including macrophages and T and B lymphocytes but also affect the function of fibroblasts and endothelial cells. They still remain a cornerstone in the treatment of SSc as, due to their strong immunosuppressive and anti-inflammatory properties, they are able to halt inflammatory, vascular, and fibrotic manifestations (all key hallmarks of SSc pathogenesis) [98]. Retrospective case-control studies have shown that CS may improve muscle and joint inflammation and severe skin fibrosis [99–101], but to our knowledge, there is still no well-controlled, double-blind, placebocontrolled study to justify these indications. On the other hand, a high dose of prednisolone has been associated with an increased risk of scleroderma renal crisis [102–104]. This is a very severe and life-threatening complication and thus, in SSc, doses of prednisolone >10-15 mg are avoided. Administration of corticosteroids as monotherapy is not recommended. The addition of steroidsparing agents such as MMF in the treatment scheme reduces doses of steroids along with their side effects and steroid requirements. In clinical practice, the use of CS in SSc is limited and restricted to the more inflammatory than profibrotic manifestations such as arthritis and myositis. It is worth mentioning that CS still represent the mainstay of treatment for SSc patients with primary heart disease manifestations.

Methotrexate

MTX was developed as a cytotoxic folic acid analogue that inhibits purine and pyrimidine synthesis when administered at a high dosage. This means that it blocks cell proliferation, including that of immune cells. It was initially used to treat cancer

and, at much lower dosages, rheumatoid arthritis (RA) [105]. Its extended use in RA suggests an important anti-inflammatory role. The exact mechanism of action at the dosage that is used for RA and SSc is not fully understood yet, but several mechanisms have been postulated to contribute to its anti-inflammatory function. It seems that MTX does not directly induce apoptosis of T cells and fibroblasts but rather increases their sensitivity to apoptosis by modulating cell survival signalling pathways. In contrast, MTX directly depletes monocytes in vitro by inducing their apoptosis [106]. Two small-scale randomized control trials (RCTs) in early dcSSC patients have evaluated the use of 15 mg MTX per week for 6 months [107,108]. The total skin score (TSS) was used as the primary endpoint to evaluate skin fibrosis. In both studies, a small but not statistically significant improvement in skin fibrosis was observed. Interestingly, continuation of the therapy up to 1 year showed a statistically significant improvement in the primary endpoints. Based on these observations, the EULAR [96] supported the use of MTX in skin manifestations in early dcSSC. However, a follow-up study [107] did not confirm the initial promising results in the long run. Taken together, data evaluating the effectiveness of MTX in reducing skin fibrosis are contradictory, and thus treatment guidelines supporting the use of MTX are mostly based on the positive experience of expert physicians with MTX.

Cyclophosphamide

CYC is another cytotoxic agent that targets fast-dividing cells such as tumor cells and proliferative T and B cells. Its use in autoimmune diseases is attributed to inhibition of regulatory and helper T cell proliferation, leading to their suppression. Suppression of helper and regulatory T cells leads to declined gene expression of pro-inflammatory cytokines, such as interleukin-2, and attenuated production of the fibrogenic TGF-β and the immunoregulatory IL-10, respectively [109,110]. In addition, lymphocyte depletion can decrease the production of antibodies (including autoantibodies) [111]. These observations suggest a potential role of CYC in diminishing fibrosis in patients with SSc-ILD. In the scleroderma lung study (SLC), 158 patients with SSc-ILD received 2 mg/kg of CYC or placebo orally for 12 months. The primary endpoint was the absolute difference in predicted forced vital capacity (FVC) which is a prediction of the patient's lung function. Secondary endpoints included measurement of skin thickening with the modified Rodman skin thickness score (mRSS) and monitoring of lung function with high-resolution computed tomography (CT) scans. It was observed that the CYC group exhibited reduced skin fibrosis and thoracic fibrosis after the 12-month treatment compared to baseline (p = 0.014) [112,113]. All in all, CYC showed a measurable but small effect on improving the lung function of SSc patients. However, the use of CYC is limited due to severe toxicity notifications including leucopenia and thrombocytopenia. Thus, according to EULAR [96], the usage of CYC is only recommended in patients with progressive ILD.

Mycophenolate Mofetil

Another broad-spectrum agent that has been used in SSc treatment is MMF. MMF causes selective depletion of quanosine nucleotides in T and B lymphocytes. It inhibits their proliferation and therefore suppresses immune-associated responses and antibody formation [114]. Indeed, SSc patients receiving MMF exhibit decreased numbers of T helper cells (implicated in various SSc pathogenic manifestations) compared to patients with no immunosuppressive treatment [115]. Strikingly, MMF treatment inhibits the infiltration of myeloid cells including tissue-resident macrophages in the skin of patients with SSc. Furthermore, treatment with MMF is strongly associated with a reduced inflammatory gene signature in the sclerotic skin [116]. Although MMF has been traditionally regarded as a lymphocytetargeting drug, in vitro and clinical evidence shows its anti-fibrotic capacity by decreasing the proliferation of human fibroblasts [117]. The results from the Scleroderma Lung Study I and II suggest the efficacy of MMF in SSc patients with severe lung fibrosis. More specifically, treatment with 3 gr/day of MMF for 2 years resulted in a significantly improved percentage of predicted FVC and mRSS [118]. The effect of MMF has also been evaluated on patients with mild SSc-ILD (FVC ≥ 70% predicted). In this double-blind, placebo-controlled, randomized clinical trial [119], MMF was well tolerated while exhibiting an observed but not statistically significant improvement in FVC and mRSS scores. In the Scleroderma Lung Study, previous results of MMF were compared with results from oral CYC administration (2.0 mg/kg per day), followed by placebo administration for 1 more year. The adjusted percentage of the predicted FVC after 24 months improved by 2.19 with MMF and 2.88 with CYC. However, no statistically significant differences among the two treatment groups were observed, and thus the superiority of MMF compared to CYC is not justified. In the European Scleroderma Observational Study (ESOS), MMF was further compared with MTX, CYC, or "no immunosuppressant" [1]. This was a multicenter, prospective, observational cohort of 326 patients with early dcSSc (up to 3 years of onset of skin thickening) with a 24-month duration. After 12 months of treatment, a statistically significant reduction in mRSS was observed in all groups compared to baseline measurements. To sum up, results from clinical trials regarding the anti-fibrotic efficacy of MMF are also conflicting, and there are no signs revealing its superiority to MTX and CYC. Similar to MTX, the recommendation for first-line MMF treatment in patients with SSc-associated ILD has been based on positive clinical experience with the drug, and its beneficial safety profile [120]. The use of MMF in improving lung fibrosis of SSc-ILD has also been supported by a large number of small retrospective cohort studies [121–125].

Autologous Hematopoietic Stem Cell Transplantation

ASCT has been utilized in treating autoimmune disorders resistant to conventional immunosuppressive therapy for more than 20 years now [126]. ASCT is the only potential disease-modifying treatment in SSc, and it has been proposed for patients with early and rapidly progressive dcSSc who have a high mortality prognosis, but in whom advanced organ involvement has not started vet [127]. Autologous stem cell transplantation begins with the isolation of the patient's CD34+ cells. Then, B and T cells are depleted using a high dose of cyclophosphamide and anti-thymocyte globulin. The last step includes the transplantation of the patient's stem cells that were isolated, resulting in the repopulation of the lymphocytes [128]. According to clinical data, ASCT shows promising results in improving mortality rates, reducing skin thickness, and enhancing lung function [129,130]. Two randomized clinical trials evaluating the safety and efficacy of ASCT in SSc have been completed thus far. First, in the Cyclophosphamide or Transplantation (SCOT) trial (NCT00860548), it was observed that myeloablative CD34+-selected ASCT was more effective in diminishing skin fibrosis than CYC administration alone. However, the mortality rates of the participants during the first year after the transplantation were as high as 10%. Treatment-related deaths as well as cancer and infection were the causes of death in these participants. Among them, infection was the leading cause, due to the suppression of the immune system. Furthermore, the possibility of relapsing was also prevalent. Secondly, in the Autologous Stem Cell Transplantation International Scleroderma (ASTIS) study [131], ASCT was compared with CYC pulse therapy in 156 rapidly progressive diffuse SSc patients. In the first year, eight patients from the ASCT group compared to none in the CYC group died. However, parameters such as longterm event-free survival, overall survival, mRSS score, and FVC were significantly improved in the ASCT-treated patients. The increased mortality rates counteract transplantation's benefit, putting experts in a difficult judging position [132]. However, to date, no disease-modifying anti-rheumatic drug has been shown to effectively reduce patients' morbidity in the long term. ASCT, on the other hand, has shown a remarkable reversal of skin fibrosis accompanied by improved lung and internal organ function. In view of the outcomes of the previously described RCTs, the new EULAR recommendations [96] suggest that experts consider ASCT for the treatment of rapidly progressive SSc patients at risk of organ failure. It is believed that treatment-related mortality can be reduced by a more careful exclusion of patients with compromised heart function and by applying ASCT in earlier stages of the disease, enabling selected patients to benefit from this treatment. There are currently four ongoing clinical trials evaluating the effectiveness and safety of ASCT in SSc (NCT01895244, NCT01413100, NCT04464434, NCT03630211). The results from these studies are expected to shed light on the safety and efficacy of autologous ASCT in a better stratified SSc patient population.

Evaluation of Cell-Specific Anti-Inflammatory Treatment

On the road towards personalized therapy in SSc, specific elimination of pathogenic innate or adaptive immune cell populations could be promising in alleviating fibrosis and reducing the morbidity of the side effects of broad immunosuppression. Of note, there are no clinical trials evaluating drugs depleting innate immune cell populations. On the other hand, several trials (*Table 3*) have evaluated the efficacy of B and T cell-depletive therapies in SSc, and thus we begin with addressing treatments targeting these cells first [133].

B Cell-Specific Treatment

To begin with B cell-specific treatment, rituximab (RTX), belimumab, and inebilizumab are the three representative monoclonal antibodies that have been used.

Rituximab

Rituximab is a chimeric anti-CD20 monoclonal antibody that binds to both immature and mature B lymphocytes expressing CD20 on their surface (including the pathogenic Beffs) and eliminates them (*Figure 4*). Of note, RTX does not consistently succeed in depleting B cells in tissues [134,135], and antibodyproducing plasma cells are not targeted by RTX, since they lack the CD20 surface antigen [136]. Indeed, in a small, randomized, double-bind, placebo-controlled trial, treatment with RTX was not associated with reduced fibrosis but caused significant depletion of naïve and memory B cells in the peripheral blood and sclerodermaassociated dermal lesions [137]. As expected from RTX's mode of action, various plasma cells and autoantibody titters did not show a statistically significant change after treatment. The potential anti-fibrotic effect of RTX is supported by histopathological observations suggesting a reduced dermal hyalinized collagen content and myofibroblast count [138]. As we discussed, IL-6 is a cytokine largely produced by activated B cells that shows pro-fibrotic capacity. In a small, openlabel study where RTX significantly improved patients' skin scores, it was observed that patients had elevated basal levels of IL-6 in biopsies from their skin lesions. IL-6 levels decreased from 3.7 5.3 pg/mL at baseline to 0.6 0.9 pg/mL (p = 0.02) six months post-treatment. Furthermore, after treatment 7/9 patients exhibited a complete depletion of B cells in skin lesions. Thus, interestingly, the RTX-associated skin thickness was correlated with B cell depletion and IL-6 reduction in patients'

 Table 2. Clinical trials conducted for the evaluation of broad-spectrum treatment in SSc.

Drug	Target	Type of Trial(s)	Duration (Months)	Patients	Results
Methotrexate (MTX)	Exact anti-inflammatory role is unknown	Multicenter, double-blind			
		1. RCT [108]	1.6	1. 29 early dSSc	1. Mean TSS 21.61 at baseline, 19.96 (<i>p</i> = 0.135) 6 months after
		2. RCT [107]	2.12	2. 71 early dSSc	2. Mean TSS 18.3 at baseline, 14.5 ($p = 0.027$) 12 months post-treatment
Cyclophosphamide (CYC)	Inhibition and suppression of Thelper and regulatory T cells	Double-blind, RCT (SLC) [112]	12	158 SSc-ILD	2. 53% ($p < 0.03$) improvement in predicted FVC and 3.02 ($p = 0.08$) unit improvement in mRSS in CYC's favor
Mycophenolate mofetil (MMF)	T and B cell depletion	1. Double-blind, RCT (SLC II) [118]	1.24	1. 69 SSc-ILD	 Percentage of predicted FVC improved from 67 to 75, and mRSS decreased from 14.5 at baseline to 10 24 months post-treatment
		2. Double-blind RCT [119]	2.6	2.41 mild SSc-ILD	2. No statistically significant improvement in mRSS and FVC scores
Autologous hematopoietic stem cell transplantation (ASCT)	Depletion of T and B cells, followed by stem cell transplantation	1. Open-label, multicenter RCT (SCOT) (NCT00860548)	1.54	1. 75 severe SSc	1. ASCT more effective in diminishing skin fibrosis compared to CYC (-19.9 vs. -8.8 , $p < 0.001$) and shows greater event-free survival
		2. Open-label, multicenter RCT (ASTIS) [131]	2.24	2. 156 early dcSSc	2. Overall survival, mRSS, and FVC significantly improved with ASCT compared to CYC (67% of 1404 pairwise comparisons in favor of ASCT vs. 33% in CYC, $p=0.01$)

skin [139]. This observation further empowers the mechanism and role of RTX in skin fibrosis.

The potential efficacy of treating SSc patients with RTX has been extensively evaluated by Daoussis and colleagues. In an open-label, randomized, 1-year study, weekly administration of RTX (375 mg/m2) for 4 weeks at baseline and after 6 months on top of each patient's standard treatment compared to standard treatment alone was assessed. Patients that received RTX showed a significantly increased median percentage of FVC accompanied by a further improvement in the diffusing capacity for carbon monoxide (DLCO). Furthermore, skin improvement was also evident when evaluated both clinically and histologically [140]. In a more recent (2017) multicenter, open-label study, the same group of researchers compared administration of 4 infusions of RTX at a dose of 375 mg/m2 once weekly every 6 months with controls receiving traditional therapies (MTX, azathioprine, MMF). In a 4-year follow-up, the RTX group showed a reduced mRSS score of 14.72 10.52 compared to 17.78 9.48 in the control group (p = 0.31). Patients enrolled in this study exhibited a significant improvement in FVC and stabilization of pulmonary function tests (PFTs) [141]. In the latest open-label, randomized, headto-head clinical trial, 60 anti-scl70-positive early dcSSc patients randomly received either monthly pulses of CYC (500 mg/m2) or 1 g of RTX at 0 and 15 days. In the RTX group, there was a significant improvement in the percentage of FVC, while patients receiving CYC experienced deterioration of their lung function. Both groups exhibited a similar improvement in skin scores, but the safety profile of RTX was better [142].

Furthermore, B cell depletion may be an efficient and well-tolerated adjuvant treatment for SSc-associated pulmonary arterial hypertension (SSc-PAH). In a multicenter, double-blind, randomized, placebo-controlled, proof-of-concept trial, 57 SSc patients on standard medical therapy received two doses of either 1 gr RTX or placebo in a 2-week interval [143]. To evaluate the effect on PAH, the change in the 6 min walk distance (6MWD) was the primary outcome. Twenty-four weeks after treatment, patients in the RTX arm exhibited an estimated change of 23.6 \pm 8.8 m compared to 0.4 ± 9.7 m in the control arm (p = 0.03). The beneficial results of RTX in diminishing skin fibrosis have also been demonstrated in a number of case or pilot studies [144–148]. Most of these studies, however, were open label, often lacked a control group, and included heterogeneous patient populations and concurrent treatments. Interestingly, the fact that RTX shows positive results in reducing skin fibrosis and alleviating PAH and ILD, together with being more potent than traditional medications and well tolerated in all studies, suggests a promising

role in scleroderma medication options. However, a phase III randomized control study will be required to verify its safety and efficacy in patients.

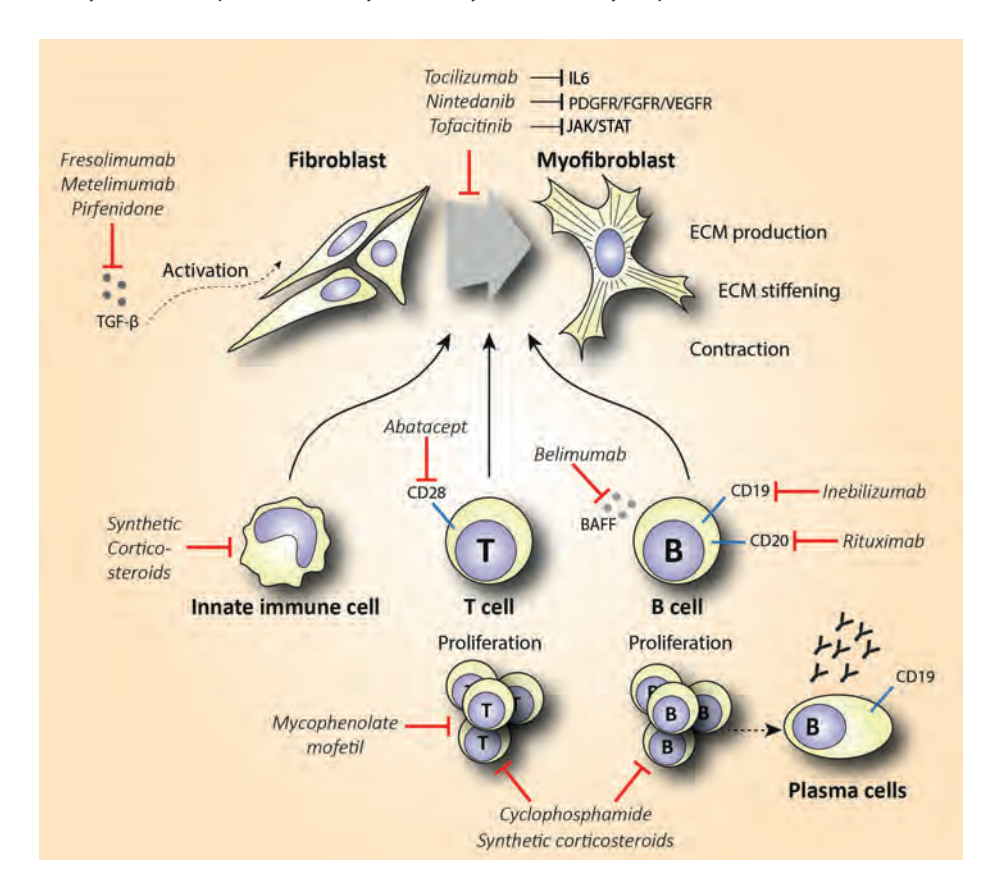


Figure 4. Schematic representation of the mechanism of action of synthetic corticosteroids (CS), mycophenolate mofetil, cyclophosphamide, inebilizumab, rituximab, belimumab, abatacept, nintedanib, tocilizumab, tofacitinib, fresolimumab, metelimumab, and pirfenidone in reducing fibrosis in SSc. Abbreviations: ECM = extracellular matrix; TGF- β = transforming growth factor- β .

Inebilizumab and Belimumab

Since depletion of CD20+ B cells does not consistently deplete B cells in tissues and does not eliminate plasma cells, developing monoclonal antibodies that target the bone marrow-resident pro- and pre-B cell co-receptor CD19 might be a more effective B cell-depletive approach (Figure 4). The efficacy of a humanized anti-CD19 monoclonal antibody, inebilizumab (MEDI-551), in reducing SSc fibrosis was assessed in a phase I randomized, double-blind, placebo-controlled study [149]. This therapy effectively depleted both B cells and plasma cells in the skin and blood of SSc patients in a dose-dependent manner. Furthermore, an improved skin score was observed in all patients, suggesting a role of inebilizumab in halting skin fibrosis. Strikingly, patients with an elevated plasma cell signature at inclusion showed greater improvement in mRSS compared to the patients that had normal or lower plasma cell counts [150].

Belimumab is another human monoclonal antibody targeting the soluble BAFF cytokine, a member of the tumor necrosis factor ligand superfamily that was a breakthrough in the treatment of systemic lupus erythematosus (Figure 4). This monoclonal antibody prevents the binding of BAFF to receptors on B cells and inhibits the survival of B cells, including the autoreactive ones. It further decreases the differentiation of B cells into immunoglobulin-producing plasma cells [151]. In a randomized, double-blind, placebo-controlled, pilot trial, 20 patients with dcSSc recently treated with MMF (1 gr twice a day) were administered 10 mg/kg of belimumab i.v., or placebo. Belimumab administration improved the mRSS score from 27 to 18 (p = 0.039), while the improvement in the placebo group was from 28 to 21 (p = 0.023). Patients with improved mRSS exhibited a significant reduction in both B cell and pro-fibrotic gene expression. However, the results of this small pilot study were not statistically significant, and larger trials should be conducted in order to make treatment recommendations [152]. A study evaluating the combination therapy of belimumab and RTX in SSc is currently pending (NCT03844061).

T Cell-Specific Treatment

The elevated infiltration of cytotoxic T cells in SSc-affected skin and lungs, along with the increased Th2 pro-fibrotic cytokine levels in the serum of SSc patients, suggests that targeting T cells could be a promising treatment option in SSc. T cell-specific treatment has shown encouraging results in other inflammatory diseases such as RA [153]. The biologicals that have been used either directly affect T cell activity by reducing their number, or they indirectly interact with cytokines expressed by T cells. Abatacept is the main representative of the former category, and it causes T cell deactivation by blocking CD28 (Figure 4), a molecule that is essential for T cell activation mediated by antigen-presenting cells (APCs) [154]. CD28 knockout mice exhibited decreased fibrosis in comparison with the wild type in bleomycin-induced fibrosis [155]. In 2015, the efficacy of abatacept in attenuating fibrosis was examined in a placebo-controlled RCT that included 10 patients with dcSSc [156]. Five out of seven patients that received abatacept showed a ≥30% decrease in mRSS, while this improvement was shown in one out of the three controls. Interestingly, patients with decreased mRSS also showed reduced CD28 gene expression along with decreased expression of genes associated with T cell proliferation. This empowers the proposed mechanism of abatacept's action. Recently, a phase II, multicenter,

double-blind, randomized, placebo-controlled trial assessed the safety and efficacy of subcutaneous administration of abatacept in 88 dcSSc patients [157]. The results failed to show a statistically significant improvement in mRSS (primary outcome) in the abatacept arm, but secondary outcomes reflecting patients' disability and quality of life were significantly improved in favor of the abatacept group. Of note, patients were stratified into inflammatory, normal-like, and fibroproliferative subgroups based on molecular gene expression data of their skin biopsies. Patients with an inflammatory intrinsic gene expression showed a larger decrease in mRSS compared to the other groups. Interestingly, the improvement in the skin score was associated with decreased gene expression of immune pathways including cytotoxic T lymphocyte-associated protein 4 (CTLA-4) and CD28 (targets of abatacept). These results are novel regarding the potentially targeted mechanism of action of abatacept as an inflammation immunomodulator. Furthermore, abatacept exhibits a good safety profile and seems to decrease joint involvement and related disability [158,159]. Based on these studies, abatacept seems to be effective in treating scleroderma-associated joint inflammation, but studies with a larger number of participants (phase III) are required to evaluate its anti-fibrotic effect.

Targeting Cytokine Production

An alternative option to T cell treatment may be targeting cytokines and growth factors (Table 4), such as IL-6, IL-1, IL-2, and TGF-β, that are produced by multiple pathological cell types in SSc. Tocilizumab (TCZ) is a monoclonal antibody that inhibits IL-6 signalling, by blocking the IL-6 receptor (Figure 4), and is effective in treating patients with juvenile idiopathic arthritis and RA [160,161]. Multiple studies have evaluated the use of TCZ in systemic sclerosis as well. Among these studies, there is one open-label, phase II, randomized controlled study (faSScinate) [162] that evaluated the efficacy and safety of a 24-week treatment with TCZ in reducing fibrosis. The observed difference of 2.70 units in mRSS was not statistically significant (p = 0.0579). However, the interesting findings of this study arise from a probable correlation between decreased IL-6 levels and TGF- β function. More specifically, researchers cultured fibroblasts from patients' skin biopsies at baseline and 24 weeks after treatment and showed that the IL-6 reduction was correlated with decreased TGF-B-related gene expression, suggesting a role of TCZ in reducing fibrosis [163]. The European Scleroderma Trials and Research (EUSTAR) observational study also evaluated the use of TCZ in SSc-associated joint and muscle inflammation, compared to abatacept. Similar to abatacept, the reduction of 3 units in mRSS between baseline and post-treatment was not significant (p = 0.109), but a significant improvement in joint function was observed [158]. A number of case

 Table 3.
 Representation of the studies evaluating the role of B and T cell-specific treatments in SSc.

Drug	Target	Type of Trial(s)	Duration (Months)	Patients	Results
Rituximab (RTX)	Anti-CD20 B cell depletion	1. Double-blind, RCT [137]	1.24	1. 16 early SSc	1. B cell depletion in blood did not improve mRSS and FVC scores
		2. Open-label trial [139]	2.54	2. 9 dcSSc	2. Median decrease in mRSS of 43.3% ($p=0.001$) accompanied by reduction in IL-6 levels
		3. Open-label RCT [140]	3.24	3. 14 SSc	3. FVC improved by 10.25% in RTX and reduced by 5.04% in the placebo group ($p=0.0018$). RTX arm: mRSS improvement of 13.5 vs. 8.37 in placebo, 12 months post-treatment ($p<0.001$)
		4. Multicenter, open- label trial [141]	4.48	4. 51 SSc-ILD	 No significant change in mRSS, but lung function improved significantly
		5. Open-label RCT [142]	5.6	5. 60 early dSSc	5. Significant improvement in RTX vs. CYC in median percentage of FVC (67.52 vs. 58.06 , $p=0.003$), but not in mRSS scores
		6. Multicenter, double- blind RCT [143]	9.9	6. 57 SSc-PAH	6. RTX arm: the improvement in median 6MWD was 25.5 m compared to 0.4 m in placebo ($p=0.03$) after 48 weeks
Inebilizumab (MEDI-551)	Anti-CD19 B cell depletion	Multicenter, double- blind RCT [149]	е	28 SSc	Depletion of B and plasma cells was correlated with improved mRSS and reduced expression of fibrotic genes in skin biopsies
Belimumab	Inhibition of B cell survival by blocking BAFF	Double-blind RCT [152]	13	20 dcSSc	mRSS score improved from 27 to 18 ($p=0.039$), while in placebo group from 28 to 21 ($p=0.023$)
Abatacept	CD28 blocking	1. RCT [156]	1.10	1. 6 dcSSc	1.5/7 patients and 1/3 controls showed >30% improved mRSS
	T cell depletion	2.Multicenter, double- blind RCT [157]	2.12	2.88 dcSSc	2. No significant improvement in mRSS, but secondary outcomes related to quality of life improved significantly

series have shown similar results [164–168]. Post hoc analysis of the results from the faSScinate study [162] showed that considerably fewer patients treated with TCZ compared to placebo exhibited a decline in their lung function. These participants were also characterized by a reduced expression of pro-fibrotic genes, suggesting that TCZ treatment may be associated with preserved lung function. These promising results, together with the unmet medical need for effective fibrosisreducing treatment, supported the exploration of TCZ in a phase III clinical trial (focuSSed) [169]. In this very recent randomized, double-blind, placebo-controlled, multicenter trial, 210 dcSSc patients were administered subcutaneous TCZ (162 mg) or placebo weekly for 48 weeks. The reduction in mRSS at the endpoint compared to baseline levels was -6.14 for TCZ and -4.41 for placebo, with the adjusted difference of -1.73 not being able to show statistically significant results (p = 0.10). Interestingly, the change in the FVC percentage predicted at week 48 was in favor of the TCZ arm, expressed as a difference in the least squares mean of 4.2 (p = 0.0002). These results further support the protective role of TCZ in preserving lung function. This was later investigated by stratifying the same patients according to the level of lung involvement [170]. Lung involvement was evaluated by serial spirometry, high-resolution chest CT, and quantitative interstitial lung disease (QILD) and fibrosis scores. Strikingly, TCZ was effective in stabilizing and thus preventing the progression of early SSc-ILD in all patient groups, irrespective of the severity of lung involvement. These results likely highlight the importance of targeting the immunoinflammatory, early fibrotic stage of SSc pathology. Taking everything together, TCZ does not seem to significantly improve skin fibrosis, but it seems to serve as a safe treatment option to preserve patients' lung function. Thus, TCZ has now been approved by the US Food and Drug Administration (FDA) to treat SSc-ILD.

Based on the elevated levels of IL-1 and IL-2 and their role in inflammation and fibrosis in SSc, the potential effect of the monoclonal antibodies rilonacept and basiliximab in tackling SSc-associated fibrosis has been examined lately. Rilonacept is an anti-inflammatory treatment that has been approved by the FDA as a therapy for cryopyrin-associated periodic syndromes [171]. Its potential use in SSc depends on the fact that it blocks IL-1\(\text{signalling} \) by binding with IL-1\(\text{\text{a}} \) and preventing its reaction with cell surface receptors, therefore reducing IL-1-triggered inflammation. The results from a double-blind, placebo-controlled, randomized trial did not support this hypothesis, as no changes were observed in mRSS between treatment and placebo. In addition, the researchers measured IL-1-regulated gene expression from explants obtained from patients' skin, and similarly, no difference was found [172]. Regarding IL-2 expression, basiliximab is an anti-CD25 monoclonal antibody that inhibits the IL-2 receptor and is used for the treatment of kidney allograft rejection as it inhibits the activation and proliferation of T cells [173]. The selective inhibition of IL-2 cytokines seems promising in counteracting the Th2 predominance in SSc lesions, but is this associated with reduced fibrosis? The results from a case study in which a patient with early dcSSC was treated with a combination of CYC, prednisolone, and basiliximab showed a decrease in mRSS from 24 at baseline to 19 six months post-treatment [174]. The same research group, 4 years later, conducted a small-scale open-label study including 10 patients with dcSSC [175]. The median mRSS was reduced from 26/51 to 11/51 at week 68 (p = 0.015). Furthermore, the median predicted FVC between baseline and 44 weeks after treatment increased from 82.1% to 88.4%. The observed trend towards an improvement in skin disease cannot be attributed to basiliximab alone as the patients also received other immunosuppressive treatments and there was no control group to compare with. Therefore, whether basiliximab can attenuate fibrosis is still unclear.

Another important inflammatory and pro-fibrotic mediator in SSc is TGF-B. Currently, drugs targeting the TGF-B pathway are under investigation mainly for diseases such as cancer. In SSc, the possible efficacy in reducing fibrosis by blocking TGF-β has been examined with the use of the monoclonal antibodies fresolimumab and metelimumab (*Figure 4*). In a small-scale, open-label, single-center study, fresolimumab, a high-affinity TGF-β-inactivating monoclonal antibody, reduced TGF-\(\beta\)-dependent gene expression in skin biopsies. Furthermore, fresolimumab administration was accompanied by an average reduction of 8 units in mRSS at 11 weeks post-treatment [176]. On the other hand, metelimumab's administration did not show similar encouraging effects. The effect of metelimumab has been examined in a randomized, double-blind, placebo-controlled trial in 45 patients with early (<18 months) dcSSc. All patients experienced an improvement in mRSS, but this improvement was not statistically significant (p = 0.49). Furthermore, the drug's administration was related to increased morbidity. A large number of severe adverse effects were reported, with skin ulceration and worsening of breathlessness being the most prominent [177]. With the results provided, TGF-β targeting exhibits conflicting results. Currently, several other compounds that target this pathway are under investigation. Those that target TGF-β signalling by inhibiting integrin expression have, thus far, shown promising results in reducing fibrosis in animal models [178].

Pirfenidone is a small molecule agent that interferes with TGF- β signalling and has potential interest in attenuating SSc-associated fibrosis. Pirfenidone is a pyridine derivative that is widely used in IPF, as it reduces fibroblast proliferation and

TGF-β-induced collagen production in primary skin fibroblasts [179] (Figure 4). However, the molecular target of pirfenidone remains unknown. Of note, only one open-label, phase II study (LOTUSS) has evaluated the safety and tolerability of pirfenidone in patients with SSc-ILD. The results of this study did not confirm the IPF observed beneficial effect of pirfenidone in the treatment of ILD in scleroderma patients, as there was no difference in the predicted FVC between baseline and post-treatment [180]. This inability to improve clinical primary outcomes is also reflected molecularly, since serum levels of TNF- α and TGF- β did not significantly differ between treated and untreated patients. These outcomes are in line with the neutral effect on lung function reported by retrospective case studies of SSc patients with ILD that were treated with pirfenidone [181,182]. Given the documented efficacy of pirfenidone in IPF and the overlapping pathogenic manifestations between IPF and SSc-ILD, further investigation of the potential anti-fibrotic effect of pirfenidone in patients with SSc-ILD is needed. In this regard, two phase II and one phase III, multicenter, double-blind, randomized, placebo-controlled trials that are evaluating the efficacy of pirfenidone in diminishing skin fibrosis in SSc-ILD are currently recruiting and may reinforce the potential anti-fibrotic role of pirfenidone in the near future (NCT03068234, NCT03221257, NCT03856853).

Emerging Therapies with Tyrosine Kinase Inhibitors

Tyrosine kinases are enzymes that use adenosine triphosphate (ATP) to transfer a phosphate group to intracellular proteins. Phosphorylation of proteins by kinases is vital for signal transduction and regulation of cell proliferation, differentiation, migration, and development. The pathological activation of tyrosine kinases (TKs) is crucial in multiple disease processes such as carcinogenesis, vascular remodeling, and fibrogenesis [183,184]. Furthermore, in inflammatory lesions, tyrosine kinases are also activated through over-production of growth factors and/or cytokines from the tissues [185]. Several current studies suggest that inhibiting tyrosine kinases may lead to effective anti-inflammatory therapy. Of note, targeting TK activity is feasible with monoclonal antibodies designed to target the extracellular domains of the receptors, or with small molecules that enter the cytoplasm and bind to intracellular catalytic domains of both receptor and non-receptor TKs [186] (Table 5).

 Table 4. Clinical trials and other studies that evaluated the role of cytokine targeting treatment in SSc.

Drug	Target	Type of Trial(s)	Duration (Months)	Patients	Results
Tocilizumab (TCZ)	Inhibits IL-6 signalling	1. Open-label RCT (faSScinate) [162]	1.24	1.87 early SSc	1. Insignificant change in mRSS, but IL-6 reduction was correlated with decreased TGF- β expression
		2. EUSTAR observational study [158]	2.5	2. 189 SSc- polyarthritis and myopathy	2. No statistically significant change in mRSS, but remarkable improvement in joint function
		3. Multicenter, double-blind RCT (focuSSed) [169]	3.12	3. 210 dcSSc	3. Change of -1.73 in mRSS between treated and placebo groups was not statistically significant ($p=0.10$), but the 4.2% improvement in predicted FVC was ($p=0.0002$)
Rilonacept	Blocks IL-1b signalling	Double-blind RCT [172]	5 weeks	19 dcSSc	No changes in mRSS between treatment and placebo
Basiliximab	Anti-CD25-mediated inhibition of IL-2 inhibits T cell activation and proliferation	Small-scale, open- label study [175]	17	10 dcSSc	Median mRSS reduced from 26/51 to 11/51 at week 68 (p = 0.015) Median predicted FVC between baseline and 44 weeks after treatment increased from 82.1% to 88.4%
Fresolimumab	Blocks TGF-β signalling	Small-scale, open- label study [176]	9	15 dcSSc	Reduction of 8 units in mRSS score (p < 0.001) Reduced expression of TGF- β -regulated genes in skin biopsies (p < 0.049)
Metelimumab	Blocks TGF-β signalling	Double-blind RCT [177]	9	45 early SSc	No statistically significant change in mRSS scores
Pirfenidone	Reduces fibroblast proliferation and TGF-β- induced collagen production in primary skin fibroblasts	Open-label, phase II study (LOTUSS) [180]	4	63 SSc-ILD	No difference in the predicted FVC between baseline and post-treatment

Indolinone-Derived Small Molecule Tyrosine Kinase Inhibitors

Imatinib mesylate is the principal compound among the small molecule TK inhibitors and was approved by the FDA in 2001 for the treatment of chronic myelogenous leukemia, to block the Ab1 kinase activity [187]. Its use in SSc has been examined due to its ability to inhibit the PDGF receptor and TGF-β signalling pathways [188]. Several case studies [188-192] have examined the efficacy and tolerability of imatinib in scleroderma patients. Moderate improvement in skin scores and predicted FVC has been reported, along with a large number of adverse effects. From a mechanistic point of view, imatinib successfully depleted patients' pDCs, immune cells that play an important role in the disease's pathogenesis [192,193]. Of note, treatment with imatinib exhibited a reduced amount of pathogenic IL-4-producing T cells in bronchoalveolar lavage of SSc patients, which was accompanied by elevated numbers of total T helper cells. Based on this observation, it could be suggested that imatinib's anti-fibrotic capacity could be mediated via shifting the Th2 response to a non-type 2 T helper phenotype [190]. In an openlabel, multicenter study, 16 out of 27 patients with early dcSSc completed a six-month imatinib administration. The mean decrease in mRSS was 21% compared to baseline; however, five patients exhibited severe adverse effects including generalized edema, erosive gastritis, anemia, upper respiratory tract infection, neutropenia, and neutropenic infection [193]. Therefore, based on the moderate improvement and the severe adverse effects that were observed, the use of the imatinib's analog nilotinib was proposed.

Nilotinib has the same mechanism of action as imatinib, but it is 20-30-fold more potent and has a more favorable toxicity profile [194]. The use of nilotinib in SSc has been tested in an open-label, single-arm, phase II trial that included 10 scleroderma patients. In this trial, nilotinib was well tolerated by the majority of the participants (7/10), with only a few cases of increased edema and mild QTc prolongation being reported. Furthermore, it was observed to be promising in reducing mRSS scores in patients with early and active disease (reduction of 16%, p = 0.02, and 23%, p = 0.01, at 6- and 12-months post-treatment, respectively) [195]. Furthermore, data from skin gene expression profiling showed that patients responding to treatment were characterized by elevated TGF-β signalling. Interestingly, the expression of TGF-β signalling genes was significantly reduced after these patients were treated with nilotinib. This observation empowers the mechanism of action of nilotinib and supports its potential anti-fibrotic effect. However, the progression into phase III trials will help to validate its efficacy in reducing fibrosis and determine its limitations concerning potential side effects.

The last indolinone-derived small molecule inhibitor that will be discussed is nintedanib. Nintedanib inhibits a plethora of molecules implicated in fibroblast activation such as PDGF receptor, fibroblast growth factor receptor (FGFR), and vascular endothelial growth factor receptor (VEGFR) (Figure 4). In vitro and animal data support the anti-fibrotic effect of nintedanib in inhibiting crucial pathways in the initiation and progression of lung fibrosis. For instance, nintedanib inhibits the secretion of the pro-fibrotic cytokines IL-4, IL-5, and IL-13 in the peripheral blood of SSc patients. In addition, its anti-fibrotic effect is partly mediated by preventing the polarization towards the pro-fibrotic M2 macrophages [196]. Nintedanib may also exert its anti-fibrotic efficacy by restraining the migration and differentiation of fibroblasts and fibrocytes. Interestingly, in vitro data have shown that nintedanib downregulates the transition of fibrocytes towards myofibroblasts, and thus the pro-fibrotic effect of the latter is reduced [197,198]. Nintedanib has received FDA approval for the treatment of IPF. Since IPF shares pathogenic commonalities with SSc-ILD, the use of nintedanib to reduce lung fibrosis in patients with SSc-ILD has been recently evaluated in the SENSCIS trial [199]. This trial included 576 patients with SSc-ILD that were randomly assigned (1:1 ratio) to receive 150 mg of nintedanib two times daily or placebo for 52 weeks. Deterioration of lung function in the nintedanib arm was significantly lower compared to the control group. More specifically, the adjusted annual rate of decline in FVC was -52.4 mL in patients treated with nintedanib compared to -93.3 mL in the placebo group (p = 0.04). Based on the results of this study, in 2019, nintedanib was the first FDAapproved treatment for patients with SSc-ILD [200]. It is worth mentioning that no significant clinical benefit was observed in skin fibrosis measured by mRSS over a 1-year period. To our knowledge, no clinical data verifying the in vitro and in vivo anti-fibrotic mechanisms have been published to date. An open-label, extension trial, assessing the long-term safety and efficacy of nintedanib in 444 SSc-ILD patients, is ongoing and expected to provide data on prolonged nintedanib therapy and its exact mechanism of action in SSc patients (NCT03313180).

Tofacitinib

Except for the Ab1 and PDGF tyrosine kinases, the inhibition of Janus kinases (JAK) is another potential treatment with anti-inflammatory properties. Recent data provide evidence that the JAK/STAT signalling pathway is highly activated in SSc skin biopsies [201]. Tofacitinib is a small molecule JAK inhibitor, with a structure similar to ATP, and has been used in the treatment of RA. Regarding its mechanism of action, it enters the cell with passive diffusion and binds to the ATP site of the JAK1 and JAK3 receptors. As a result, it inhibits the phosphorylation and activation of signal transducer and activator of transcription proteins (STATS), which leads to the downregulation of IL-6 expression [202] (Figure 4). In view of this mechanism, the use of tofacitinib in SSc might be of interest. The results from an observational study suggest tofacitinib as a potential treatment in reducing skin thickening of patients with refractory dcSSc [203]. More specifically, tofacitinib-treated patients showed a significantly shorter response time compared to the conventional immunosuppressive group, with a mean change of -3.7 (p = 0.001) in mRSS already 1-month post-treatment. After 6 months of treatment, the mean change in mRSS was even greater between the two groups (-10.0 tofacitinib vs. -4.1 conventional immunosuppressants, p = 0.026). Similarly, in another pilot study, patients treated with tofacitinib showed a significantly higher improvement in skin fibrosis compared to patients treated with MTX [204]. These results indicate that tofacitinib might be even more effective in reducing fibrosis than conventional immunosuppressants. further showing a quicker and higher response rate. The tolerability and efficacy of tofacitinib have been recently evaluated in a small clinical phase I/II trial in 15 SSc patients. According to the preliminary results, tofacitinib is well tolerated and shows a trend towards improving fibrosis (NCT03274076). Further evaluation of tofacitinib in dcSSc seems warranted.

Table 5. Clinical trials evaluating the efficacy of tyrosine kinase inhibitors in SSc treatment.

Drug	Target	Type of Trial(s)	Duration (Months)	Patients	Results
lmatinib mesylate	Inhibits PDGFR and TGF-β signalling	Multicenter, open-label RCT [193]	6	27 dcSSc	Mean decrease in mRSS was 21% compared to baseline ($p < 0.001$)
Nilotinib	Same as imatinib, but 20–30-fold more potent	Open-label, single-arm trial [195]	8	10 early dcSSc	Promising reduction of 23% in mRSS 12 months post-treatment $(p = 0.01)$
Nintedanib	Inhibits PDGFR, FGFR, and VEGFR signalling	Double-blind RCT (SENSCIS) [199]	13	576 SSc-ILD	Adjusted annual rate of decline in FVC -52.4 mL compared to -93.3 mL in the placebo group ($p = 0.04$)
Tofacitinib	Inhibits JAK/ STAT signalling	Double- blind RCT (NCT03274076)	6	15 dcSSc	Preliminary data show a trend towards improved fibrosis

Conclusions and Future Perspectives

SSc is a disabling, chronic, autoimmune disease accompanied by high mortality and morbidity rates. In this review, we examined the potential effects of antiinflammatory and immunosuppressive treatments in attenuating fibrosis. To do this, we evaluated the first-line, generalized as well as cell- and cytokine-specific anti-inflammatory and anti-fibrotic treatments, including the main therapies that have been used or are currently being tested in clinical trials.

To begin, among the broad-spectrum treatments, MTX has been well tolerated, but its efficacy in reducing fibrosis is still controversial. Although CYC's use seems efficient in reducing fibrosis, its high toxicity limits its use, and it has now been replaced with MMF. MMF is well tolerated, but its use has not been fully examined. On the other hand, cellular targeting of inflammation with molecules that reduce the number of B or T cells, such as rituximab, belimumab, and abatacept, has exhibited a potential effect in diminishing fibrosis compared to broad-spectrum immunosuppressants. Furthermore, the cytokine signalling-specific antibodies rilonacept, basiliximab, fresolimumab, and metelimumab show a trend towards reducing fibrosis, but the lack of large phase III trials limits their potential addition to SSc treatment guidelines. Among the TK inhibitors, nintedanib and tofacitinib are two promising therapies in halting SSc-related fibrosis. Based on encouraging outcomes from large phase III RCTs, tocilizumab and nintedanib have been FDA approved for the treatment of SSc-ILD. On the positive side, ASCT shows increased event-free and improved overall survival rates, but its use is limited to younger patients with early dcSSc that fulfill a list of very strict inclusion criteria. Careful patient selection is vital in reducing the relatively high mortality rates that accompany ASCT.

In conclusion, we are in a new era of a multitude of clinical trials with drugs targeting specific pathogenic cells and biological pathways related to SSc. Several antiinflammatory treatments have been used or tested in SSc patients, but only a mild to moderate improvement in reducing fibrosis has been demonstrated. However, the level of published evidence on the effectiveness of each tested drug varies greatly among case series and observational studies, and only a few RCTs have been conducted [205]. Thus, conclusions and comparisons between the efficacy of different drugs should be handled with caution. The anti-inflammatory approaches described show a trend towards reducing fibrosis, but the effect is moderate and, in many cases, controversial. The lack of complete understanding of the pathophysiology and the rare frequency of the disease are two obvious arguments that support this conclusion. Furthermore, SSc is a very complex and heterogeneous disease, and the traditional classification of the patients into the limited or diffuse

form based on the severity of skin involvement is an oversimplification. Lately, multiple studies have utilized intrinsic gene expression analyses to classify SSc patients into four categories: the inflammatory, fibroproliferative, limited, and normal-like subsets [206]. It is currently not certain if these categories are reflective of stable disease states that differ between patients. Other studies suggest that they concern different stages of the SSc disease process [80]. Various disease manifestations of SSc, such as ILD, pulmonary hypertension, and gastrointestinal disease, develop with a time course that differs from that of the skin manifestations. The underlying maladaptive innate and adaptive immune responses likely differ between these pathologies. Taken together, we believe that in-depth insight and measurement tools of the pathological processes may yield markers to determine the biological processes driving specific disease manifestations. Such markers will help to determine the best treatment approach in individual cases.

Furthermore, targeted drug selection is expected to show more remarkable results in the anti-inflammatory therapies that have been mentioned. Additionally, to understand if new drugs are effective, there is also a need for a better understanding of the pathological processes driving disease features. The use of novel and advanced molecular tools such as single-cell RNA sequencing is constantly advancing our knowledge about novel pathogenic cytokines, antibodies, and genes implicated in the pathogenesis of SSc. This knowledge will facilitate more personalized treatments. For example, scleroderma patients that exhibit high amounts of the Th2 cytokines IL-4 and IL-13 early after diagnosis, or those with prominent ILD, could be treated with immunotoxins or monoclonal antibodies that have been designed to block the IL-4 or IL-13 pathway and have shown promising results in anti-tumor, IPF, and asthma treatment. Another suggestion for future studies would be to evaluate the outcome of combined biological therapies.

Author Contributions: Conceptualization, T.-I.P., A.v.C. and R.M.T.; writing of the original draft preparation, T.-I.P.; writing of review and editing T.-I.P., A.v.C., P.M.v.d.K. and R.M.T. All authors have read and agreed to the published version of the manuscript.

Funding: This research received no external funding. **Institutional Review Board Statement:** Not applicable.

Informed Consent Statement: Not applicable.

Data Availability Statement: Not applicable. No new data were generated or analyzed in this study.

Conflicts of Interest: The authors declare no conflict of interest.

References

- Herrick, A.L.; Pan, X.; Peytrignet, S.; Lunt, M.; Hesselstrand, R.; Mouthon, L.; Silman, A.; Brown, E.; Czirják, L.; Distler, J.H.W.; et al. Treatment outcome in early diffuse cutaneous systemic sclerosis: The European Scleroderma Observational Study (ESOS). Ann. Rheum. Dis. 2017, 76, 1207-1218. https://doi.org/10.1136/annrheumdis-2016-210503.
- 2. Pellar, R.E.; Pope, J.E. Evidence-based management of systemic sclerosis: Navigating recommendations and guidelines. Semin. Arthritis Rheum. 2017, 46, https://doi.org/10.1016/j.semarthrit.2016.12.003.
- Lee, J.J.; Pope, J.E. Emerging drugs and therapeutics for systemic sclerosis. Expert Opin. Emerg. Drugs 2016, 21, 421-430. https://doi.org/10.1080/14728214.2016.1257607.
- Fox, D.A.; Lundy, S.K.; Whitfield, M.L.; Berrocal, V.; Campbell, P.; Rasmussen, S.; Ohara, R.; Stinson, A.; Gurrea-Rubio, M.; Wiewiora, E.; et al. Lymphocyte subset abnormalities in early diffuse cutaneous systemic sclerosis. Arthritis Res. Ther. 2021, 23, 10. https://doi.org/10.1186/s13075-020-02383-w.
- 5. Liu, M.; Wu, W.; Sun, X.; Yang, J.; Xu, J.; Fu, W.; Li, M. New insights into CD4+ T cell abnormalities in systemic sclerosis. Cytokine Growth Factor Rev. 2016, 28, 31-36. https://doi.org/10.1016/j. cytogfr.2015.12.002.
- Maehara, T.; Kaneko, N.; Perugino, C.A.; Mattoo, H.; Kers, J.; Allard-Chamard, H.; Mahajan, V.S.; Liu, H.; Murphy, S.J.; Ghebremichael, M.; et al. Cytotoxic CD4+ T lymphocytes may induce endothelial cell apoptosis in systemic sclerosis. J. Clin. Investig. 2020, 130, 2451-2464. https://doi.org/10.1172/JCI131700.
- Henderson, J.; Bhattacharyya, S.; Varga, J.; O'Reilly, S. Targeting TLRs and the inflammasome in systemic sclerosis. Pharmacol. Ther. 2018, 192, 163-169. https://doi.org/10.1016/j. pharmthera.2018.08.003.
- Fuschiotti, P. T cells and cytokines in systemic sclerosis. Curr. Opin. Rheumatol. 2018, 30, 594–599.
- Romano, E.; Rosa, I.; Fioretto, B.S.; Matucci-Cerinic, M.; Manetti, M. New Insights into Profibrotic Myofibroblast Formation in Systemic Sclerosis: When the Vascular Wall Becomes the Enemy. Life 2021, 11, 610. https://doi.org/10.3390/life11070610.
- 10. Bruni, C.; Frech, T.; Manetti, M.; Rossi, F.W.; Furst, D.E.; De Paulis, A.; Rivellese, F.; Guiducci, S.; Matucci-Cerinic, M.; Bellando-Randone, S. Vascular Leaking, a Pivotal and Early Pathogenetic Event in Systemic Sclerosis: Should the Door Be Closed? Front. Immunol. 2018, 9, 2045. https://doi.org/10.3389/fimmu.2018.02045.
- 11. Host, L.; Nikpour, M.; Calderone, A.; Cannell, P.; Roddy, J. Autologous stem cell transplantation in systemic sclerosis: A systematic review. Clin. Exp. Rheumatol. 2017, 35, S198–S207.
- 12. Laurent, P.; Sisirak, V.; Lazaro, E.; Richez, C.; Duffau, P.; Blanco, P.; Truchetet, M.-E.; Contin-Bordes, C. Innate Immunity in Systemic Sclerosis Fibrosis: Recent Advances. Front. Immunol. 2018, 9, 1702. https://doi.org/10.3389/fimmu.2018.01702.
- 13. van Caam, A.; Vonk, M.; van den Hoogen, F.; van Lent, P.; van der Kraan, P. Unraveling SSc Pathophysiology; The Myofibroblast. Front. Immunol. 2018, 9, 2452. https://doi.org/10.3389/ fimmu.2018.02452.
- 14. Pesce, J.T.; Ramalingam, T.R.; Mentink-Kane, M.M.; Wilson, M.S.; El Kasmi, K.C.; Smith, A.M.; Thompson, R.W.; Cheever, A.W.; Murray, P.J.; Wynn, T.A. Arginase-1-expressing macrophages suppress Th2 cytokine-driven inflammation and fibrosis. PLoS Pathog. 2009, 5, e1000371. https://doi.org/10.1371/journal.ppat.1000371.

- 15. Ostuni, R.; Kratochvill, F.; Murray, P.J.; Natoli, G. Macrophages and cancer: From mechanisms to therapeutic implications. Trends Immunol. 2015, 36, 229-239. https://doi.org/10.1016/j. it.2015.02.004.
- 16. Wynn, T.A.; Vannella, K.M. Macrophages in Tissue Repair, Regeneration, and Fibrosis. Immunity **2016**, 44, 450–462. https://doi.org/10.1016/j.immuni.2016.02.015.
- 17. Christmann, R.B.; Sampaio-Barros, P.; Stifano, G.; Borges, C.L.; de Carvalho, C.R.; Kairalla, R.; Parra, E.R.; Spira, A.; Simms, R.; Capellozzi, V.L.; et al. Association of Interferon- and transforming growth factor β-regulated genes and macrophage activation with systemic sclerosis-related progressive lung fibrosis. Arthritis Rheumatol. 2014, 66, 714–725. https://doi.org/10.1002/art.38288.
- 18. Assassi, S.; Swindell, W.R.; Wu, M.; Tan, F.D.; Khanna, D.; Furst, D.E.; Tashkin, D.P.; Jahan-Tigh, R.R.; Mayes, M.D.; Gudjonsson, J.E.; et al. Dissecting the heterogeneity of skin gene expression patterns in systemic sclerosis. Arthritis Rheumatol. 2015, 67, 3016-3026. https://doi.org/10.1002/ art.39289.
- 19. Rudnik, M.; Hukara, A.; Kocherova, I.; Jordan, S.; Schniering, J.; Milleret, V.; Ehrbar, M.; Klingel, K.; Feghali-Bostwick, C.; Distler, O.; et al. Elevated Fibronectin Levels in Profibrotic CD14(+) Monocytes and CD14(+) Macrophages in Systemic Sclerosis. Front. Immunol. 2021, 12, 642891. https://doi.org/10.3389/fimmu.2021.642891.
- 20. Soldano, S.; Trombetta, A.C.; Contini, P.; Tomatis, V.; Ruaro, B.; Brizzolara, R.; Montagna, P.; Sulli, A.; Paolino, S.; Pizzorni, C.; et al. Increase in circulating cells coexpressing M1 and M2 macrophage surface markers in patients with systemic sclerosis. Ann. Rheum. Dis. 2018, 77, 1842-1845. https://doi.org/10.1136/annrheumdis-2018-213648.
- 21. Gibbons, M.A.; MacKinnon, A.C.; Ramachandran, P.; Dhaliwal, K.; Duffin, R.; Phythian-Adams, A.T.; Van Rooijen, N.; Haslett, C.; Howie, S.E.; Simpson, A.J.; et al. Ly6Chimonocytes direct alternatively activated profibrotic macrophage regulation of lung fibrosis. Am. J. Respir. Crit. Care Med. 2011, 184, 569-581. https://doi.org/10.1164/rccm.201010-1719OC.
- 22. Cutolo, M.; Soldano, S.; Smith, V. Pathophysiology of systemic sclerosis: Current understanding and new insights. Expert Rev. Clin. Immunol. 2019, 15, 753-764. https://doi.org/10.1080/174466 6X.2019.1614915.
- 23. Higashi-Kuwata, N.; Jinnin, M.; Makino, T.; Fukushima, S.; Inoue, Y.; Muchemwa, F.C.; Yonemura, Y.; Komohara, Y.; Takeya, M.; Mitsuya, H.; et al. Characterization of monocyte/macrophage subsets in the skin and peripheral blood derived from patients with systemic sclerosis. Arthritis Res. Ther. **2010**, 12, R128. https://doi.org/10.1186/ar3066.
- 24. Manetti, M. Deciphering the alternatively activated (M2) phenotype of macrophages in scleroderma. Exp. Dermatol. 2015, 24, 576–578. https://doi.org/10.1111/exd.12727.
- 25. Bhattacharyya, S.; Wei, J.; Tourtellotte, W.G.; Hinchcliff, M.; Gottardi, C.G.; Varga, J. Fibrosis in systemic sclerosis: Common and unique pathobiology. Fibrogenesis Tissue Repair 2012, 5 (Suppl. S1), \$18-\$18. https://doi.org/10.1186/1755-1536-5-\$1-\$18.
- 26. Borie, R.; Quesnel, C.; Phin, S.; Debray, M.-P.; Marchal-Somme, J.; Tiev, K.; Bonay, M.; Fabre, A.; Soler, P.; Dehoux, M.; et al. Detection of alveolar fibrocytes in idiopathic pulmonary fibrosis and systemic sclerosis. PLoS ONE 2013, 8, e53736. https://doi.org/10.1371/journal.pone.0053736.
- 27. Ruaro, B.; Soldano, S.; Smith, V.; Paolino, S.; Contini, P.; Montagna, P.; Pizzorni, C.; Casabella, A.; Tardito, S.; Sulli, A.; et al. Correlation between circulating fibrocytes and dermal thickness in limited cutaneous systemic sclerosis patients: A pilot study. Rheumatol. Int. 2019, 39, 1369–1376. https://doi.org/10.1007/s00296-019-04315-7.

- 28. Xue, D.; Tabib, T.; Morse, C.; Yang, Y.; Domsic, R.; Khanna, D.; Lafyatis, R. Expansion of FCGR3A(+) macrophages, FCN1(+) mo-DC, and plasmacytoid dendritic cells associated with severe skin disease in systemic sclerosis. Arthritis Rheumatol. 2021, 74, 2, 329-341. https://doi.org/10.1002/ art.41813.
- 29. Pope, S.M.; Brandt, E.B.; Mishra, A.; Hogan, S.P.; Zimmermann, N.; Matthaei, K.I.; Foster, P.S.; Rothenberg, M.E. IL-13 induces eosinophil recruitment into the lung by an IL-5- and eotaxindependent mechanism. J. Allergy Clin. Immunol. 2001, 108, 594-601. https://doi.org/10.1067/ mai.2001.118600.
- 30. Chen, L.; Grabowski, K.A.; Xin, J.-P.; Coleman, J.; Huang, Z.; Espiritu, B.; Alkan, S.; Xie, H.B.; Zhu, Y.; White, F.A.; et al. IL-4 induces differentiation and expansion of Th2 cytokine-producing eosinophils. J. Immunol. 2004, 172, 2059-2066. https://doi.org/10.4049/jimmunol.172.4.2059.
- 31. Falanga, V.; Medsger, T.A.J. Frequency, levels, and significance of blood eosinophilia in systemic sclerosis, localized scleroderma, and eosinophilic fasciitis. J. Am. Acad. Dermatol. 1987, 17, 648-656. https://doi.org/10.1016/s0190-9622(87)70251-5.
- 32. Ando, K.; Nakashita, T.; Kaneko, N.; Takahashi, K.; Motojima, S. Associations between peripheral blood eosinophil counts in patients with systemic sclerosis and disease severity. Springerplus 2016, 5, 1401. https://doi.org/10.1186/s40064-016-3106-4.
- 33. Hara, T.; Ikeda, T.; Inaba, Y.; Kunimoto, K.; Mikita, N.; Kaminaka, C.; Kanazawa, N.; Yamamoto, Y.; Tabata, K.; Fujii, T.; et al. Peripheral blood eosinophilia is associated with the presence of skin ulcers in patients with systemic sclerosis. J. Dermatol. 2019, 46, 334-337. https://doi.org/10.1111/1346-8138.14774.
- 34. Saigusa, R.; Asano, Y.; Yamashita, T.; Takahashi, T.; Nakamura, K.; Miura, S.; Ichimura, Y.; Toyama, T.; Taniquchi, T.; Sumida, H.; et al. Systemic sclerosis complicated with localized scleroderma-like lesions induced by Köbner phenomenon. J. Dermatol. Sci. 2018, 89, 282-289. https://doi.org/10.1016/j.jdermsci.2017.12.005.
- 35. Hebbar, M.; Gillot, J.M.; Hachulla, E.; Lassalle, P.; Hatron, P.Y.; Devulder, B.; Janin, A. Early expression of E-selectin, tumor necrosis factor alpha, and mast cell infiltration in the salivary glands of patients with systemic sclerosis. Arthritis Rheum. 1996, 39, 1161-1165. https://doi.org/10.1002/ art.1780390713.
- 36. Bagnato, G.; Roberts, W.N.; Sciortino, D.; Sangari, D.; Cirmi, S.; Ravenell, R.L.; Navarra, M.; Bagnato, G.; Gangemi, S. Mastocytosis and systemic sclerosis: A clinical association. Clin. Mol. Allergy 2016, 14, 13. https://doi.org/10.1186/s12948-016-0050-3.
- 37. Yukawa, S.; Yamaoka, K.; Sawamukai, N.; Shimajiri, S.; Kubo, S.; Miyagawa, I.; Sonomoto, K.; Saito, K.; Tanaka, Y. Dermal mast cell density in fingers reflects severity of skin sclerosis in systemic sclerosis. Mod. Rheumatol. 2013, 23, 1151-1157. https://doi.org/10.3109/s10165-012-0813-8.
- 38. Dees, C.; Akhmetshina, A.; Zerr, P.; Reich, N.; Palumbo, K.; Horn, A.; Jüngel, A.; Beyer, C.; Krönke, G.; Zwerina, J.; et al. Platelet-derived serotonin links vascular disease and tissue fibrosis. J. Exp. Med. 2011, 208, 961-972. https://doi.org/10.1084/jem.20101629.
- 39. Prieto-García, A.; Zheng, D.; Adachi, R.; Xing, W.; Lane, W.S.; Chung, K.; Anderson, P.; Hansbro, P.M.; Castells, M.; Stevens, R.L. Mast cell restricted mouse and human tryptase-heparin complexes hinder thrombin-induced coagulation of plasma and the generation of fibrin by proteolytically destroying fibrinogen. J. Biol. Chem. 2012, 287, 7834-7844. https://doi.org/10.1074/jbc. M111.325712.
- 40. Jordana, M.; Befus, A.D.; Newhouse, M.T.; Bienenstock, J.; Gauldie, J. Effect of histamine on proliferation of normal human adult lung fibroblasts. Thorax 1988, 43, 552-558. https://doi.org/10.1136/thx.43.7.552.

- 41. Karpec, D.; Rudys, R.; Leonaviciene, L.; Mackiewicz, Z.; Bradunaite, R.; Kirdaite, G.; Venalis, A. The safety and efficacy of light emitting diodes-based ultraviolet A1 phototherapy in bleomycininduced scleroderma in mice. Adv. Med. Sci. 2018, 63, 152-159. https://doi.org/10.1016/j. advms.2017.09.001.
- 42. Kabata, H.; Moro, K.; Koyasu, S. The group 2 innate lymphoid cell (ILC2) regulatory network and its underlying mechanisms. Immunol. Rev. 2018, 286, 37-52. https://doi.org/10.1111/imr.12706.
- 43. Klose, C.S.N.; Artis, D. Innate lymphoid cells as regulators of immunity, inflammation and tissue homeostasis. Nat. Immunol. 2016, 17, 765-774. https://doi.org/10.1038/ni.3489.
- 44. McHedlidze, T.; Waldner, M.; Zopf, S.; Walker, J.; Rankin, A.L.; Schuchmann, M.; Voehringer, D.; McKenzie, A.N.J.; Neurath, M.F.; Pflanz, S.; et al. Interleukin-33-dependent innate lymphoid cells mediate hepatic fibrosis. Immunity 2013, 39, 357-371. https://doi.org/10.1016/j. immuni.2013.07.018.
- 45. Wohlfahrt, T.; Usherenko, S.; Englbrecht, M.; Dees, C.; Weber, S.; Beyer, C.; Gelse, K.; Distler, O.; Schett, G.; Distler, J.H.W.; et al. Type 2 innate lymphoid cell counts are increased in patients with systemic sclerosis and correlate with the extent of fibrosis. Ann. Rheum. Dis. 2016, 75, 623-626. https://doi.org/10.1136/annrheumdis-2015-207388.
- 46. Truchetet, M.-E.; Demoures, B.; Eduardo Guimaraes, J.; Bertrand, A.; Laurent, P.; Jolivel, V.; Douchet, I.; Jacquemin, C.; Khoryati, L.; Duffau, P.; et al. Platelets Induce Thymic Stromal Lymphopoietin Production by Endothelial Cells: Contribution to Fibrosis in Human Systemic Sclerosis. Arthritis Rheumatol. 2016, 68, 2784-2794. https://doi.org/10.1002/art.39817.
- 47. Manetti, M.; Guiducci, S.; Ceccarelli, C.; Romano, E.; Bellando-Randone, S.; Conforti, M.L.; Ibba-Manneschi, L.; Matucci-Cerinic, M. Increased circulating levels of interleukin 33 in systemic sclerosis correlate with early disease stage and microvascular involvement. Ann. Rheum. Dis. **2011**, 70, 1876–1878. https://doi.org/10.1136/ard.2010.148247.
- 48. La Barbera, L.; Lo Pizzo, M.; DI Liberto, D.; Schinocca, C.; Ruscitti, P.; Giacomelli, R.; Dieli, F.; Ciccia, F.; Guggino, G. POS0326 role of the IL-25 / IL-17RB Axis in TH9 Polarization in Patients with Progressive Systemic Sclerosis. Ann. Rheum. Dis. 2021, 80, 390-391. https://doi.org/10.1136/ annrheumdis-2021-eular.3814.
- 49. Laurent, P.; Allard, B.; Manicki, P.; Jolivel, V.; Levionnois, E.; Jeljeli, M.; Henrot, P.; Izotte, J.; Leleu, D.; Groppi, A.; et al. TGFβ promotes low IL10-producing ILC2 with profibrotic ability involved in skin fibrosis in systemic sclerosis. Ann. Rheum. Dis. 2021, 80, 1594–1603. https://doi.org/10.1136/ annrheumdis-2020-219748.
- 50. Ah Kioon, M.D.; Tripodo, C.; Fernandez, D.; Kirou, K.A.; Spiera, R.F.; Crow, M.K.; Gordon, J.K.; Barrat, F.J. Plasmacytoid dendritic cells promote systemic sclerosis with a key role for TLR8. Sci. Transl. Med. 2018, 10, 8458. https://doi.org/10.1126/scitranslmed.aam8458.
- 51. van Bon, L.; Affandi, A.J.; Broen, J.; Christmann, R.B.; Marijnissen, R.J.; Stawski, L.; Farina, G.A.; Stifano, G.; Mathes, A.L.; Cossu, M.; et al. Proteome-wide analysis and CXCL4 as a biomarker in systemic sclerosis. N. Engl. J. Med. 2014, 370, 433-443. https://doi.org/10.1056/NEJMoa1114576.
- 52. Kafaja, S.; Valera, I.; Divekar, A.A.; Saggar, R.; Abtin, F.; Furst, D.E.; Khanna, D.; Singh, R.R. pDCs in lung and skin fibrosis in a bleomycin-induced model and patients with systemic sclerosis. JCI Insight 2018, 3, 98380. https://doi.org/10.1172/jci.insight.98380.
- 53. Valenzi, E.; Tabib, T.; Papazoglou, A.; Sembrat, J.; Trejo Bittar, H.E.; Rojas, M.; Lafyatis, R. Disparate Interferon Signalling and Shared Aberrant Basaloid Cells in Single-Cell Profiling of Idiopathic Pulmonary Fibrosis and Systemic Sclerosis-Associated Interstitial Lung Disease. Front. Immunol. 2021, 12, 595811. https://doi.org/10.3389/fimmu.2021.595811.
- 54. Skauq, B.; Assassi, S. Type I interferon dysregulation in Systemic Sclerosis. Cytokine 2020, 132, 154635. https://doi.org/10.1016/j.cyto.2018.12.018.

- 55. Wu, M.; Assassi, S. The Role of Type 1 Interferon in Systemic Sclerosis. Front. Immunol. 2013, 4, 266. https://doi.org/10.3389/fimmu.2013.00266.
- 56. van der Kroef, M.; van den Hoogen, L.L.; Mertens, J.S.; Blokland, S.L.M.; Haskett, S.; Devaprasad, A.; Carvalheiro, T.; Chouri, E.; Vazirpanah, N.; Cossu, M.; et al. Cytometry by time of flight identifies distinct signatures in patients with systemic sclerosis, systemic lupus erythematosus and Sjögrens syndrome. Eur. J. Immunol. 2020, 50, 119-129. https://doi.org/10.1002/eji.201948129.
- 57. Alkema, W.; Koenen, H.; Kersten, B.E.; Kaffa, C.; Dinnissen, J.W.B.; Damoiseaux, J.G.M.C.; Joosten, I.; Driessen-Diks, S.; van der Molen, R.G.; Vonk, M.C.; et al. Autoantibody profiles in systemic sclerosis; a comparison of diagnostic tests. Autoimmunity 2021, 54, 148-155. https://doi.org/10.1080/089 16934.2021.1907842.
- 58. Mehta, H.; Goulet, P.-O.; Nguyen, V.; Pérez, G.; Koenig, M.; Senécal, J.-L.; Sarfati, M. Topoisomerase I peptide-loaded dendritic cells induce autoantibody response as well as skin and lung fibrosis. Autoimmunity 2016, 49, 503-513. https://doi.org/10.1080/08916934.2016.1230848.
- 59. Asano, Y. Systemic sclerosis. J. Dermatol. 2018, 45, 128-138. https://doi.org/10.1111/1346-8138.14153.
- 60. O'Reilly, S.; Hugle, T.; van Laar, J.M. T cells in systemic sclerosis: A reappraisal. Rheumatology 2012, 51, 1540–1549. https://doi.org/10.1093/rheumatology/kes090.
- 61. Boin, F.; De Fanis, U.; Bartlett, S.J.; Wigley, F.M.; Rosen, A. T Cell polarization indentifies distinct clinical phenotypes in scleroderma lung disease. Arththritis Rheum. 2008, 58, 1165-1174. https://doi.org/10.1002/art.23406.T.
- 62. Lonati, P.A.; Brembilla, N.C.; Montanari, E.; Fontao, L.; Gabrielli, A.; Vettori, S.; Valentini, G.; Laffitte, E.; Kaya, G.; Meroni, P.L.; et al. High IL-17E and Low IL-17C dermal expression identifies a fibrosis-specific motif common to morphea and systemic sclerosis. PLoS ONE 2014, 9, e0105008. https://doi.org/10.1371/journal.pone.0105008.
- 63. Budzyńska-Włodarczyk, J.; Michalska-Jakubus, M.M.; Kowal, M.; Krasowska, D. Evaluation of serum concentrations of the selected cytokines in patients with localized scleroderma. Postep. Dermatol. I Alergol. 2016, 33, 47-51. https://doi.org/10.5114/pdia.2015.48044.
- 64. Ayers, N.B.; Sun, C.-M.; Chen, S.-Y. Transforming growth factor-β signalling in systemic sclerosis. J. Biomed. Res. 2018, 32, 3-12. https://doi.org/10.7555/JBR.31.20170034.
- 65. Gonçalves, R.S.G.; Pereira, M.C.; Dantas, A.T.; de Almeida, A.R.; Margues, C.D.L.; Rego, M.J.B.M.; Pitta, I.R.; Duarte, A.L.B.P.; Pitta, M.G.R. IL-17 and related cytokines involved in systemic sclerosis: Perspectives. Autoimmunity 2018, 51, 1-9. https://doi.org/10.1080/08916934.2017.1416467.
- Rafael-Vidal, C.; Pérez, N.; Altabás, I.; Garcia, S.; Pego-Reigosa, J.M. Blocking IL-17: A Promising Strategy in the Treatment of Systemic Rheumatic Diseases. Int. J. Mol. Sci. 2020, 21, 7100. https://doi.org/10.3390/ijms21197100.
- 67. Kalfin, R.; Righi, A.; Del Rosso, A.; Bagchi, D.; Generini, S.; Guiducci, S.; Cerinic, M.M.; Das, D.K. Activin, a grape seed-derived proanthocyanidin extract, reduces plasma levels of oxidative stress and adhesion molecules (ICAM-1, VCAM-1 and E-selectin) in systemic sclerosis. Free Radic. Res. 2002, 36, 819-825. https://doi.org/10.1080/1071576021000005249.
- 68. Romano, M.; Fanelli, G.; Albany, C.J.; Giganti, G.; Lombardi, G. Past, Present, and Future of Regulatory T Cell Therapy in Transplantation and Autoimmunity. Front. Immunol. 2019, 10, 43. https://doi.org/10.3389/fimmu.2019.00043.
- 69. Frantz, C.; Auffray, C.; Avouac, J.; Allanore, Y. Regulatory T Cells in Systemic Sclerosis. Front. Immunol. 2018, 9, 2358. https://doi.org/10.3389/fimmu.2018.02356.
- 70. Milano, A.; Pendergrass, S.A.; Sargent, J.L.; George, L.K.; McCalmont, T.H.; Connolly, M.K.; Whitfield, M.L. Molecular subsets in the gene expression signatures of scleroderma skin. PLoS ONE 2008, 3, e2696. https://doi.org/10.1371/journal.pone.0002696.

- 71. Rice, L.M.; Stifano, G.; Ziemek, J.; Lafyatis, R. Local skin gene expression reflects both local and systemic skin disease in patients with systemic sclerosis. Rheumatology 2016, 55, 377-379. https://doi.org/10.1093/rheumatology/kev335.
- 72. Fuschiotti, P. Current perspectives on the role of CD8+T cells in systemic sclerosis. Immunol. Lett. **2018**, 195, 55–60. https://doi.org/10.1016/j.imlet.2017.10.002.
- 73. Casciola-Rosen, L.; Andrade, F.; Ulanet, D.; Wong, W.B.; Rosen, A. Cleavage by granzyme B is strongly predictive of autoantigen status: Implications for initiation of autoimmunity, J. Exp. Med. 1999, 190, 815-826. https://doi.org/10.1084/jem.190.6.815.
- 74. Morita, R.; Schmitt, N.; Bentebibel, S.-E.; Ranganathan, R.; Bourdery, L.; Zurawski, G.; Foucat, E.; Dullaers, M.; Oh, S.; Sabzghabaei, N.; et al. Human blood CXCR5(+)CD4(+) T cells are counterparts of T follicular cells and contain specific subsets that differentially support antibody secretion. Immunity **2011**, 34, 108–121. https://doi.org/10.1016/j.immuni.2010.12.012.
- 75. Ricard, L.; Jachiet, V.; Malard, F.; Ye, Y.; Stocker, N.; Rivière, S.; Senet, P.; Monfort, J.-B.; Fain, O.; Mohty, M.; et al. Circulating follicular helper T cells are increased in systemic sclerosis and promote plasmablast differentiation through the IL-21 pathway which can be inhibited by ruxolitinib. Ann. Rheum. Dis. 2019, 78, 539-550. https://doi.org/10.1136/annrheumdis-2018-214382.
- 76. Taylor, D.K.; Mittereder, N.; Kuta, E.; Delaney, T.; Burwell, T.; Dacosta, K.; Zhao, W.; Cheng, L.I.; Brown, C.; Boutrin, A.; et al. T follicular helper-like cells contribute to skin fibrosis. Sci. Transl. Med. 2018, 10, 5307. https://doi.org/10.1126/scitranslmed.aaf5307.
- 77. Gaydosik, A.M.; Tabib, T.; Domsic, R.; Khanna, D.; Lafyatis, R.; Fuschiotti, P. Single-cell transcriptome analysis identifies skin-specific T cell responses in systemic sclerosis. Ann. Rheum. Dis. 2021, 80, 14, 1453-1460, annrheumdis-2021-220209. https://doi.org/10.1136/annrheumdis-2021-220209.
- 78. Mahler, M.; Hudson, M.; Bentow, C.; Roup, F.; Beretta, L.; Pilar Simeón, C.; Guillén-Del-Castillo, A.; Casas, S.; Fritzler, M.J. Autoantibodies to stratify systemic sclerosis patients into clinically actionable subsets. Autoimmun. Rev. 2020, 19, 102583. https://doi.org/10.1016/j. autrev.2020.102583.
- 79. Melissaropoulos, K.; Daoussis, D. B cells in systemic sclerosis: From pathophysiology to treatment. Clin. Rheumatol. 2021, 40, 2621-2631. https://doi.org/10.1007/s10067-021-05665-z.
- 80. Skaug, B.; Khanna, D.; Swindell, W.R.; Hinchcliff, M.E.; Frech, T.M.; Steen, V.D.; Hant, F.N.; Gordon, J.K.; Shah, A.A.; Zhu, L.; et al. Global skin gene expression analysis of early diffuse cutaneous systemic sclerosis shows a prominent innate and adaptive inflammatory profile. Ann. Rheum. Dis. 2020, 79, 379-386. https://doi.org/10.1136/annrheumdis-2019-215894.
- 81. Bosello, S.; Angelucci, C.; Lama, G.; Alivernini, S.; Proietti, G.; Tolusso, B.; Sica, G.; Gremese, E.; Ferraccioli, G. Characterization of inflammatory cell infiltrate of scleroderma skin: B cells and skin score progression. Arthritis Res. Ther. 2018, 20, 75. https://doi.org/10.1186/s13075-018-1569-0.
- 82. Matsushita, T.; Kobayashi, T.; Mizumaki, K.; Kano, M.; Sawada, T.; Tennichi, M.; Okamura, A.; Hamaguchi, Y.; Iwakura, Y.; Hasegawa, M.; et al. BAFF inhibition attenuates fibrosis in scleroderma by modulating the regulatory and effector B cell balance. Sci. Adv. 2018, 4, eaas9944. https://doi.org/10.1126/sciadv.aas9944.
- 83. Matsushita, T.; Hasegawa, M.; Yanaba, K.; Kodera, M.; Takehara, K.; Sato, S. Elevated serum BAFF levels in patients with systemic sclerosis: Enhanced BAFF signalling in systemic sclerosis B lymphocytes. Arthritis Rheum. 2006, 54, 192-201. https://doi.org/10.1002/art.21526.
- 84. Matsushita, T.; Fujimoto, M.; Hasegawa, M.; Matsushita, Y.; Komura, K.; Ogawa, F.; Watanabe, R.; Takehara, K.; Sato, S. BAFF antagonist attenuates the development of skin fibrosis in tight-skin mice. J. Investig. Dermatol. 2007, 127, 2772–2780. https://doi.org/10.1038/sj.jid.5700919.
- 85. Soto, L.; Ferrier, A.; Aravena, O.; Fonseca, E.; Berendsen, J.; Biere, A.; Bueno, D.; Ramos, V.; Aguillón, J.C.; Catalán, D. Systemic Sclerosis Patients Present Alterations in the Expression of

- Molecules Involved in B cell Regulation. Front. Immunol. 2015, 6, 496. https://doi.org/10.3389/ fimmu.2015.00496.
- Dumoitier, N.; Chaigne, B.; Régent, A.; Lofek, S.; Mhibik, M.; Dorfmüller, P.; Terrier, B.; London, J.; Bérezné, A.; Tamas, N.; et al. Scleroderma Peripheral B Lymphocytes Secrete Interleukin-6 and Transforming Growth Factor β and Activate Fibroblasts. *Arthritis Rheumatol.* **2017**, *69*, 1078–1089. https://doi.org/10.1002/art.40016.
- 87. Forestier, A.; Guerrier, T.; Jouvray, M.; Giovannelli, J.; Lefèvre, G.; Sobanski, V.; Hauspie, C.; Hachulla, E.; Hatron, P.-Y.; Zéphir, H.; et al. Altered B lymphocyte homeostasis and functions in systemic sclerosis. Autoimmun. Rev. 2018, 17, 244-255. https://doi.org/10.1016/j.autrev.2017.10.015.
- 88. Sato, S.; Fujimoto, M.; Hasegawa, M.; Takehara, K. Altered blood B lymphocyte homeostasis in systemic sclerosis: Expanded naive B cells and diminished but activated memory B cells. Arthritis Rheum. 2004, 50, 1918-1927. https://doi.org/10.1002/art.20274.
- 89. Sato, S.; Hasegawa, M.; Fujimoto, M.; Tedder, T.F.; Takehara, K. Quantitative genetic variation in CD19 expression correlates with autoimmunity. J. Immunol. 2000, 165, 6635-6643. https://doi.org/10.4049/jimmunol.165.11.6635.
- 90. Wilfong, E.M.; Vowell, K.N.; Bunn, K.E.; Rizzi, E.; Annapureddy, N.; Dudenhofer, R.B.; Barnado, A.; Bonami, R.H.; Johnson, J.E.; Crofford, L.J.; et al. CD19 + CD21lo/neg cells are increased in systemic sclerosis-associated interstitial lung disease. Clin. Exp. Med. 2021. https://doi.org/10.1007/ s10238-021-00745-5.
- 91. Asano, N.; Fujimoto, M.; Yazawa, N.; Shirasawa, S.; Hasegawa, M.; Okochi, H.; Tamaki, K.; Tedder, T.F.; Sato, S. B Lymphocyte signalling established by the CD19/CD22 loop regulates autoimmunity in the tight-skin mouse. Am. J. Pathol. 2004, 165, 641-650. https://doi.org/10.1016/S0002-9440(10)63328-7.
- 92. Sato, S.; Ono, N.; Steeber, D.A.; Pisetsky, D.S.; Tedder, T.F. CD19 regulates B lymphocyte signalling thresholds critical for the development of B-1 lineage cells and autoimmunity. J. Immunol. 1996, 157, 4371-4378.
- 93. van Zelm, M.C.; Reisli, I.; van der Burg, M.; Castaño, D.; van Noesel, C.J.M.; van Tol, M.J.D.; Woellner, C.; Grimbacher, B.; Patiño, P.J.; van Dongen, J.J.M.; et al. An antibody-deficiency syndrome due to mutations in the CD19 gene. N. Engl. J. Med. 2006, 354, 1901-1912. https://doi.org/10.1056/ NEJMoa051568.
- 94. Terrier, B.; Tamby, M.C.; Camoin, L.; Guilpain, P.; Bérezné, A.; Tamas, N.; Broussard, C.; Hotellier, F.; Humbert, M.; Simonneau, G.; et al. Antifibroblast antibodies from systemic sclerosis patients bind to {alpha}-enolase and are associated with interstitial lung disease. Ann. Rheum. Dis. 2010, 69, 428-433. https://doi.org/10.1136/ard.2008.104299.
- 95. Baroni, S.S.; Santillo, M.; Bevilacqua, F.; Luchetti, M.; Spadoni, T.; Mancini, M.; Fraticelli, P.; Sambo, P.; Funaro, A.; Kazlauskas, A.; et al. Stimulatory autoantibodies to the PDGF receptor in systemic sclerosis. N. Engl. J. Med. 2006, 354, 2667-2676. https://doi.org/10.1056/NEJMoa052955.
- 96. Kowal-Bielecka, O.; Fransen, J.; Avouac, J.; Becker, M.; Kulak, A.; Allanore, Y.; Distler, O.; Clements, P.; Cutolo, M.; Czirjak, L.; et al. Update of EULAR recommendations for the treatment of systemic sclerosis. Ann. Rheum. Dis. 2017, 76, 1327-1339. https://doi.org/10.1136/ annrheumdis-2016-209909.
- 97. Denton, C.P.; Hughes, M.; Gak, N.; Vila, J.; Buch, M.H.; Chakravarty, K.; Fligelstone, K.; Gompels, L.L.; Griffiths, B.; Herrick, A.L.; et al. BSR and BHPR guideline for the treatment of systemic sclerosis. Rheumatology 2016, 55, 1906–1910. https://doi.org/10.1093/rheumatology/kew224.
- 98. Iudici, M. What should clinicians know about the use of glucocorticoids in systemic sclerosis? Mod. Rheumatol. 2017, 27, 919-923. https://doi.org/10.1080/14397595.2016.1270796.

- 99. Shah, A.A.; Wigley, F.M. My approach to the treatment of scleroderma. Mayo Clin. Proc. 2013, 88, 377-393. https://doi.org/10.1016/j.mayocp.2013.01.018.
- 100. Uy, G.L.; Duncavage, E.J.; Chang, G.S.; Jacoby, M.A.; Miller, C.A.; Shao, J.; Heath, S.; Elliott, K.; Fulton, R.S.; Fronick, C.C.; et al. HHS Public Access 2017, 31, 872-881. https://doi.org/10.1038/ leu.2016.282.Dynamic.
- 101. Lundberg, I.; Kratz, A.K.; Alexanderson, H.; Patarroyo, M. Decreased expression of interleukin-1α, interleukin-1\(\beta \), and cell adhesion molecules in muscle tissue following corticosteroid treatment in patients with polymyositis and dermatomyositis. Arthritis Rheum. 2000, 43, 336-348. https://doi.org/10.1002/1529-0131(200002)43:2<336::AID-ANR13>3.0.CO;2-V.
- 102. Steen, V.D.; Medsger, T.A. Case-control study of corticosteroids and other drugs that either precipitate or protect from the development of scleroderma renal crisis. Arthritis Rheum. 1998, 41, 1613-1619. https://doi.org/10.1002/1529-0131(199809)41:9<1613::AID-ART11>3.0.CO;2-O.
- 103. Cozzi, F.; Marson, P.; Cardarelli, S.; Favaro, M.; Tison, T.; Tonello, M.; Pigatto, E.; De Silvestro, G.; Punzi, L.; Doria, A. Prognosis of scleroderma renal crisis: A long-term observational study. Nephrol. Dial. Transplant. 2012, 27, 4398–4403. https://doi.org/10.1093/ndt/gfs317.
- 104. Zanatta, E.; Polito, P.; Favaro, M.; Larosa, M.; Marson, P.; Cozzi, F.; Doria, A. Therapy of scleroderma renal crisis: State of the art. Autoimmun. Rev. 2018, 17, 882-889. https://doi.org/10.1016/j. autrev.2018.03.012.
- 105. Maksimovic, V.; Pavlovic-Popovic, Z.; Vukmirovic, S.; Cvejic, J.; Mooranian, A.; Al-Salami, H.; Mikov, M.; Golocorbin-Kon, S. Molecular mechanism of action and pharmacokinetic properties of methotrexate. Mol. Biol. Rep. 2020, 47, 4699-4708. https://doi.org/10.1007/s11033-020-05481-9.
- 106. Cronstein, B.N.; Aune, T.M. Methotrexate and its mechanisms of action in inflammatory arthritis. Nat. Rev. Rheumatol. 2020, 16, 145-154. https://doi.org/10.1038/s41584-020-0373-9.
- 107. Pope, J.E.; Bellamy, N.; Seibold, J.R.; Baron, M.; Ellman, M.; Carette, S.; Smith, C.D.; Chalmers, I.M.; Hong, P.; O'Hanlon, D.; et al. A randomized, controlled trial of methotrexate versus placebo in early diffuse scleroderma. Arthritis Rheum. 2001, 44, 1351-1358. https://doi.org/10.1002/1529-0131(200106)44:6<1351::AID-ART227>3.0.CO;2-I.
- 108. van den Hoogen, F.H.; Boerbooms, A.M.; Swaak, A.J.; Rasker, J.J.; van Lier, H.J.; van de Putte, L.B. Comparison of methotrexate with placebo in the treatment of systemic sclerosis: A 24 week randomized double-blind trial, followed by a 24 week observational trial. Br. J. Rheumatol. 1996, 35, 364-372. https://doi.org/10.1093/rheumatology/35.4.364.
- 109. Ghiringhelli, F.; Larmonier, N.; Schmitt, E.; Parcellier, A.; Cathelin, D.; Garrido, C.; Chauffert, B.; Solary, E.; Bonnotte, B.; Martin, F. CD4+CD25+ regulatory T cells suppress tumor immunity but are sensitive to cyclophosphamide which allows immunotherapy of established tumors to be curative. Eur. J. Immunol. 2004, 34, 336-344. https://doi.org/10.1002/eji.200324181.
- 110. Wachsmuth, L.P.; Patterson, M.T.; Eckhaus, M.A.; Venzon, D.J.; Gress, R.E.; Kanakry, C.G. Posttransplantation cyclophosphamide prevents graft-versus-host disease by inducing alloreactive T cell dysfunction and suppression. J. Clin. Investig. 2019, 129, 2357–2373. https://doi.org/10.1172/JCI124218.
- 111. Bruni, C.; Shirai, Y.; Kuwana, M.; Matucci-Cerinic, M. Cyclophosphamide: Similarities and differences in the treatment of SSc and SLE. Lupus 2019, 28, 571-574. https://doi.org/10.1177/0961203319840433.
- 112. Tashkin, D.P.; Elashoff, R.; Clements, P.J.; Goldin, J.; Roth, M.D.; Furst, D.E.; Arriola, E.; Silver, R.; Strange, C.; Bolster, M.; et al. Cyclophosphamide versus Placebo in Scleroderma Lung Disease. N. Engl. J. Med. 2006, 354, 2655–2666. https://doi.org/10.1056/NEJMoa055120.
- 113. Goldin, J.; Elashoff, R.; Kim, H.J.; Yan, X.; Lynch, D.; Strollo, D.; Roth, M.D.; Clements, P.; Furst, D.E.; Khanna, D.; et al. Treatment of scleroderma-interstitial lung disease with cyclophosphamide is

- associated with less progressive fibrosis on serial thoracic high-resolution CT scan than placebo: Findings from the scleroderma lung study. Chest 2009, 136, 1333-1340. https://doi.org/10.1378/ chest.09-0108.
- 114. Broen, J.C.A.; van Laar, J.M. Mycophenolate mofetil, azathioprine and tacrolimus: Mechanisms in rheumatology. Nat. Rev. Rheumatol. 2020, 16, 167-178. https://doi.org/10.1038/s41584-020-0374-8.
- 115. Gernert, M.; Tony, H.-P.; Schwaneck, E.C.; Gadeholt, O.; Fröhlich, M.; Portegys, J.; Strunz, P.-P.; Schmalzing, M. Lymphocyte subsets in the peripheral blood are disturbed in systemic sclerosis patients and can be changed by immunosuppressive medication. Rheumatol. Int. 2021, 1-9. https://doi.org/10.1007/s00296-021-05034-8.
- 116. Hinchcliff, M.; Toledo, D.M.; Taroni, J.N.; Wood, T.A.; Franks, J.M.; Ball, M.S.; Hoffmann, A.; Amin, S.M.; Tan, A.U.; Tom, K.; et al. Mycophenolate Mofetil Treatment of Systemic Sclerosis Reduces Myeloid Cell Numbers and Attenuates the Inflammatory Gene Signature in Skin. J. Investig. Dermatol. **2018**, 138, 1301–1310. https://doi.org/10.1016/j.jid.2018.01.006.
- 117. Morath, C.; Reuter, H.; Simon, V.; Krautkramer, E.; Muranyi, W.; Schwenger, V.; Goulimari, P.; Grosse, R.; Hahn, M.; Lichter, P.; et al. Effects of mycophenolic acid on human fibroblast proliferation, migration and adhesion in vitro and in vivo. Am. J. Transplant. Off. J. Am. Soc. Transplant. Am. Soc. Transpl. Surg. 2008, 8, 1786–1797. https://doi.org/10.1111/j.1600-6143.2008.02322.x.
- 118. Volkmann, E.R.; Tashkin, D.P.; Li, N.; Roth, M.D.; Khanna, D.; Hoffmann-Vold, A.-M.; Kim, G.; Goldin, J.; Clements, P.J.; Furst, D.E.; et al. Mycophenolate Mofetil Versus Placebo for Systemic Sclerosis-Related Interstitial Lung Disease: An Analysis of Scleroderma Lung Studies I and II. Arthritis Rheumatol. 2017, 69, 1451-1460. https://doi.org/10.1002/art.40114.
- 119. Naidu, G.S.R.S.N.K.; Sharma, S.K.; Adarsh, M.B.; Dhir, V.; Sinha, A.; Dhooria, S.; Jain, S. Effect of mycophenolate mofetil (MMF) on systemic sclerosis-related interstitial lung disease with mildly impaired lung function: A double-blind, placebo-controlled, randomized trial. Rheumatol. Int. 2020, 40, 207-216. https://doi.org/10.1007/s00296-019-04481-8.
- 120. Tashkin, D.P.; Roth, M.D.; Clements, P.J.; Furst, D.E.; Khanna, D.; Kleerup, E.C.; Goldin, J.; Arriola, E.; Volkmann, E.R.; Kafaja, S.; et al. Mycophenolate mofetil versus oral cyclophosphamide in scleroderma-related interstitial lung disease (SLS II): A randomised controlled, double-blind, parallel group trial. Lancet. Respir. Med. 2016, 4, 708-719. https://doi.org/10.1016/S2213-2600(16)30152-7.
- 121. Gerbino, A.J.; Goss, C.H.; Molitor, J.A. Effect of mycophenolate mofetil on pulmonary function in scleroderma-associated interstitial lung disease. Chest 2008, 133, 455-460. https://doi. org/10.1378/chest.06-2861.
- 122. Morganroth, P.A.; Kreider, M.E.; Werth, V.P. Mycophenolate mofetil for interstitial lung disease in dermatomyositis. Arthritis Care Res. 2010, 62, 1496–1501. https://doi.org/10.1002/acr.20212.
- 123. Stratton, R.J.; Wilson, H.; Black, C.M. Pilot study of anti-thymocyte globulin plus mycophenolate mofetil in recent-onset diffuse scleroderma. Rheumatology 2001, 40, 84-88. https://doi.org/10.1093/rheumatology/40.1.84.
- 124. Simeón-Aznar, C.P.; Fonollosa-Plá, V.; Tolosa-Vilella, C.; Selva-O'Callaghan, A.; Solans-Laqué, R.; Vilardell-Tarrés, M. Effect of mycophenolate sodium in scleroderma-related interstitial lung disease. Clin. Rheumatol. 2011, 30, 1393-1398. https://doi.org/10.1007/s10067-011-1823-1.
- 125. Yilmaz, N.; Can, M.; Kocakaya, D.; Karakurt, S.; Yavuz, S. Two-year experience with mycophenolate mofetil in patients with scleroderma lung disease: A case series. Int. J. Rheum. Dis. 2014, 17, 923-928. https://doi.org/10.1111/1756-185X.12399.
- 126. Binks, M.; Passweg, J.R.; Furst, D.; McSweeney, P.; Sullivan, K.; Besenthal, C.; Finke, J.; Peter, H.H.; van Laar, J.; Breedveld, F.C.; et al. Phase I/II trial of autologous stem cell transplantation in systemic

- sclerosis: Procedure related mortality and impact on skin disease. Ann. Rheum. Dis. 2001, 60, 577– 584. https://doi.org/10.1136/ard.60.6.577.
- 127. Walker, U.A.; Saketkoo, L.A.; Distler, O. Haematopoietic stem cell transplantation in systemic sclerosis. RMD Open 2018, 4, e000533. https://doi.org/10.1136/rmdopen-2017-000533.
- 128. Zeher, M.: Papp, G.: Nakken, B.: Szodoray, P. Hematopoietic stem cell transplantation in autoimmune disorders: From immune-regulatory processes to clinical implications. Autoimmun. Rev. 2017, 16, 817–825. https://doi.org/10.1016/j.autrev.2017.05.020.
- 129. Farge, D.; Passweg, J.; van Laar, J.M.; Marjanovic, Z.; Besenthal, C.; Finke, J.; Peter, H.H.; Breedveld, F.C.; Fibbe, W.E.; Black, C.; et al. Autologous stem cell transplantation in the treatment of systemic sclerosis: Report from the EBMT/EULAR Registry. Ann. Rheum. Dis. 2004, 63, 974-981. https://doi.org/10.1136/ard.2003.011205.
- 130. Burt, R.K.; Shah, S.J.; Dill, K.; Grant, T.; Gheorghiade, M.; Schroeder, J.; Craig, R.; Hirano, I.; Marshall, K.; Ruderman, E.; et al. Autologous non-myeloablative haemopoietic stem-cell transplantation compared with pulse cyclophosphamide once per month for systemic sclerosis (ASSIST): An open-label, randomised phase 2 trial. Lancet 2011, 378, 498-506. https://doi.org/10.1016/S0140-6736(11)60982-3.
- 131. van Laar, J.M.; Farge, D.; Sont, J.K.; Naraghi, K.; Marjanovic, Z.; Larghero, J.; Schuerwegh, A.J.; Marijt, E.W.A.; Vonk, M.C.; Schattenberg, A. V; et al. Autologous hematopoietic stem cell transplantation vs intravenous pulse cyclophosphamide in diffuse cutaneous systemic sclerosis: A randomized clinical trial. JAMA 2014, 311, 2490-2498. https://doi.org/10.1001/jama.2014.6368.
- 132. Sullivan, K.M.; Goldmuntz, E.A.; Keyes-Elstein, L.; McSweeney, P.A.; Pinckney, A.; Welch, B.; Mayes, M.D.; Nash, R.A.; Crofford, L.J.; Eggleston, B.; et al. Myeloablative Autologous Stem-Cell Transplantation for Severe Scleroderma. N. Engl. J. Med. 2018, 378, 35–47.
- 133. Katsiari, C.G.; Simopoulou, T.; Alexiou, I.; Sakkas, L.I. Immunotherapy of systemic sclerosis. Hum. Vaccin. Immunother. 2018, 14, 2559-2567. https://doi.org/10.1080/21645515.2018.1491508.
- 134. Ramwadhdoebe, T.H.; van Baarsen, L.G.M.; Boumans, M.J.H.; Bruijnen, S.T.G.; Safy, M.; Berger, F.H.; Semmelink, J.F.; van der Laken, C.J.; Gerlag, D.M.; Thurlings, R.M.; et al. Effect of rituximab treatment on T and B cell subsets in lymph node biopsies of patients with rheumatoid arthritis. Rheumatology 2019, 58, 1075-1085. https://doi.org/10.1093/rheumatology/key428.
- 135. Thurlings, R.M.; Vos, K.; Wijbrandts, C.A.; Zwinderman, A.H.; Gerlag, D.M.; Tak, P.P. Synovial tissue response to rituximab: Mechanism of action and identification of biomarkers of response. Ann. Rheum. Dis. 2008, 67, 917-925. https://doi.org/10.1136/ard.2007.080960.
- 136. Bergantini, L.; d'Alessandro, M.; Cameli, P.; Vietri, L.; Vagaggini, C.; Perrone, A.; Sestini, P.; Frediani, B.; Bargagli, E. Effects of rituximab therapy on B cell differentiation and depletion. Clin. Rheumatol. 2020, 39, 1415-1421. https://doi.org/10.1007/s10067-020-04996-7.
- 137. Boonstra, M.; Meijs, J.; Dorjée, A.L.; Marsan, N.A.; Schouffoer, A.; Ninaber, M.K.; Quint, K.D.; Bonte-Mineur, F.; Huizinga, T.W.J.; Scherer, H.U.; et al. Rituximab in early systemic sclerosis. RMD Open 2017, 3, e000384. https://doi.org/10.1136/rmdopen-2016-000384.
- 138. Smith, V.; Van Praet, J.T.; Vandooren, B.; Van Der Cruyssen, B.; Naeyaert, J.M.; Decuman, S.; Elewaut, D.; De Keyser, F. Rituximab in diffuse cutaneous systemic sclerosis: An open-label clinical and histopathological study. Ann. Rheum. Dis. 2010, 69, 193-197. https://doi.org/10.1136/ ard.2008.095463.
- 139. Bosello, S.; De Santis, M.; Lama, G.; Spanò, C.; Angelucci, C.; Tolusso, B.; Sica, G.; Ferraccioli, G. B cell depletion in diffuse progressive systemic sclerosis: Safety, skin score modification and IL-6 modulation in an up to thirty-six months follow-up open-label trial. Arthritis Res. Ther. 2010, 12, R54-R54. https://doi.org/10.1186/ar2965.

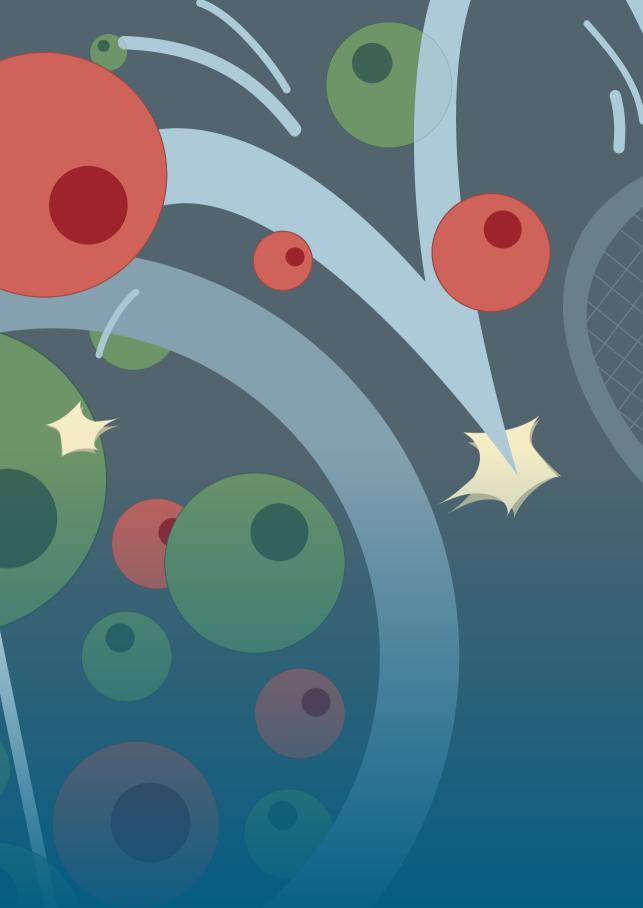
- 140. Daoussis, D.; Liossis, S.-N.C.; Tsamandas, A.C.; Kalogeropoulou, C.; Kazantzi, A.; Sirinian, C.; Karampetsou, M.; Yiannopoulos, G.; Andonopoulos, A.P. Experience with rituximab in scleroderma: Results from a 1-year, proof-of-principle study. Rheumatology 2010, 49, 271-280. https://doi.org/10.1093/rheumatology/kep093.
- 141. Daoussis, D.; Melissaropoulos, K.; Sakellaropoulos, G.; Antonopoulos, I.; Markatseli, T.E.; Simopoulou, T.; Georgiou, P.; Andonopoulos, A.P.; Drosos, A.A.; Sakkas, L.; et al. A multicenter, open-label, comparative study of B cell depletion therapy with Rituximab for systemic sclerosis-associated interstitial lung disease. Semin. Arthritis Rheum. 2017, 46, 625-631. https://doi.org/10.1016/j.semarthrit.2016.10.003.
- 142. Sircar, G.; Goswami, R.P.; Sircar, D.; Ghosh, A.; Ghosh, P. Intravenous cyclophosphamide vs rituximab for the treatment of early diffuse scleroderma lung disease: Open label, randomized, controlled trial. Rheumatology 2018, 57, 2106-2113. https://doi.org/10.1093/rheumatology/ key213.
- 143. Zamanian, R.T.; Badesch, D.; Chung, L.; Domsic, R.T.; Medsger, T.; Pinckney, A.; Keyes-Elstein, L.; D'Aveta, C.; Spychala, M.; White, R.J.; et al. Safety and Efficacy of B cell Depletion with Rituximab for the Treatment of Systemic Sclerosis-associated Pulmonary Arterial Hypertension: A Multicenter, Double-Blind, Randomized, Placebo-controlled Trial. Am. J. Respir. Crit. Care Med. 2021, 204, 209-221. https://doi.org/10.1164/rccm.202009-3481OC.
- 144. Lafyatis, R.; Kissin, E.; York, M.; Farina, G.; Viger, K.; Fritzler, M.J.; Merkel, P.A.; Simms, R.W. B cell depletion with rituximab in patients with diffuse cutaneous systemic sclerosis. Arthritis Rheum. 2009, 60, 578-583. https://doi.org/10.1002/art.24249.
- 145. Jordan, S.; Distler, J.H.W.; Maurer, B.; Huscher, D.; Van Laar, J.M.; Allanore, Y.; Distler, O.; Kvien, T.K.; Airo, P.; Sancho, J.J.A.; et al. Effects and safety of rituximab in systemic sclerosis: An analysis from the European Scleroderma Trial and Research (EUSTAR) group. Ann. Rheum. Dis. 2015, 74, 1188-1194. https://doi.org/10.1136/annrheumdis-2013-204522.
- 146. Moazedi-Fuerst, F.C.; Kielhauser, S.M.; Brickmann, K.; Hermann, J.; Lutfi, A.; Meilinger, M.; Brezinschek, H.P.; Graninger, W.B. Rituximab for systemic sclerosis: Arrest of pulmonary disease progression in five cases. Results of a lower dosage and shorter interval regimen. Scand. J. Rheumatol. 2014, 43, 257-258. https://doi.org/10.3109/03009742.2013.869617.
- 147. Yılmaz, D.D.; Borekci, S.; Musellim, B. Comparison of the effectiveness of cyclophosphamide and rituximab treatment in patients with systemic sclerosis-related interstitial lung diseases: A retrospective, observational cohort study. Clin. Rheumatol. 2021, 40, 4071-4079. https://doi.org/10.1007/s10067-021-05785-6.
- 148. Giuggioli, D.; Lumetti, F.; Colaci, M.; Fallahi, P.; Antonelli, A.; Ferri, C. Rituximab in the treatment of patients with systemic sclerosis. Our experience and review of the literature. Autoimmun. Rev. **2015**, 14, 1072–1078. https://doi.org/10.1016/j.autrev.2015.07.008.
- 149. Schiopu, E.; Chatterjee, S.; Hsu, V.; Flor, A.; Cimbora, D.; Patra, K.; Yao, W.; Li, J.; Streicher, K.; McKeever, K.; et al. Safety and tolerability of an anti-CD19 monoclonal antibody, MEDI-551, in subjects with systemic sclerosis: A phase I, randomized, placebo-controlled, escalating singledose study. Arthritis Res. Ther. 2016, 18, 131. https://doi.org/10.1186/s13075-016-1021-2.
- 150. Streicher, K.; Sridhar, S.; Kuziora, M.; Morehouse, C.A.; Higgs, B.W.; Sebastian, Y.; Groves, C.J.; Pilataxi, F.; Brohawn, P.Z.; Herbst, R.; et al. Baseline Plasma Cell Gene Signature Predicts Improvement in Systemic Sclerosis Skin Scores Following Treatment With Inebilizumab (MEDI-551) and Correlates with Disease Activity in Systemic Lupus Erythematosus and Chronic Obstructive Pulmonary Disease. Arthritis Rheumatol. 2018, 70, 2087-2095. https://doi.org/10.1002/art.40656.
- 151. Guerreiro Castro, S.; Isenberg, D.A. Belimumab in systemic lupus erythematosus (SLE): Evidence-to-date and clinical usefulness. Ther. Adv. Musculoskelet. Dis. 2017, 9, 75-85. https://doi.org/10.1177/1759720X17690474.

- 152. Gordon, J.K.; Martyanov, V.; Franks, J.M.; Bernstein, E.J.; Szymonifka, J.; Magro, C.; Wildman, H.F.; Wood, T.A.; Whitfield, M.L.; Spiera, R.F. Belimumab for the Treatment of Early Diffuse Systemic Sclerosis: Results of a Randomized, Double-Blind, Placebo-Controlled, Pilot Trial. Arthritis Rheumatol. 2018, 70, 308-316. https://doi.org/10.1002/art.40358.
- 153. Abbasi, M.; Mousavi, M.J.; Jamalzehi, S.; Alimohammadi, R.; Bezvan, M.H.; Mohammadi, H.; Aslani, S. Strategies toward rheumatoid arthritis therapy; the old and the new. J. Cell. Physiol. 2019, 234, 10018-10031. https://doi.org/10.1002/jcp.27860.
- 154. Nie, J.; Li, Y.Y.; Zheng, S.G.; Tsun, A.; Li, B. FOXP3+ Treg Cells and Gender Bias in Autoimmune Diseases. Front. Immunol. 2015, 6, 493. https://doi.org/10.3389/fimmu.2015.00493.
- 155. Okazaki, T.; Nakao, A.; Nakano, H.; Takahashi, F.; Takahashi, K.; Shimozato, O.; Takeda, K.; Yagita, H.; Okumura, K. Impairment of Bleomycin-Induced Lung Fibrosis in CD28-Deficient Mice. J. Immunol. 2001, 167, 1977–1981. https://doi.org/10.4049/jimmunol.167.4.1977.
- 156. Chakravarty, E.F.; Martyanov, V.; Fiorentino, D.; Wood, T.A.; Haddon, D.J.; Jarrell, J.A.; Utz, P.J.; Genovese, M.C.; Whitfield, M.L.; Chung, L. Gene expression changes reflect clinical response in a placebo-controlled randomized trial of abatacept in patients with diffuse cutaneous systemic sclerosis. Arthritis Res. Ther. 2015, 17, 159. https://doi.org/10.1186/s13075-015-0669-3.
- 157. Khanna, D.; Spino, C.; Johnson, S.; Chung, L.; Whitfield, M.L.; Denton, C.P.; Berrocal, V.; Franks, J.; Mehta, B.; Molitor, J.; et al. Abatacept in Early Diffuse Cutaneous Systemic Sclerosis: Results of a Phase II Investigator-Initiated, Multicenter, Double-Blind, Randomized, Placebo-Controlled Trial. Arthritis Rheumatol. 2020, 72, 125–136. https://doi.org/10.1002/art.41055.
- 158. Elhai, M.; Meunier, M.; Matucci-Cerinic, M.; Maurer, B.; Riemekasten, G.; Leturcq, T.; Pellerito, R.; Von Muhlen, C.A.; Vacca, A.; Airo, P.; et al. Outcomes of patients with systemic sclerosis-associated polyarthritis and myopathy treated with tocilizumab or abatacept: A EUSTAR observational study. Ann. Rheum. Dis. 2013, 72, 1217-1220. https://doi.org/10.1136/annrheumdis-2012-202657.
- 159. Castellví, I.; Elhai, M.; Bruni, C.; Airò, P.; Jordan, S.; Beretta, L.; Codullo, V.; Montecucco, C.M.; Bokarewa, M.; lannonne, F.; et al. Safety and effectiveness of abatacept in systemic sclerosis: The EUSTAR experience. Semin. Arthritis Rheum. 2020, 50, 1489–1493. https://doi.org/10.1016/j. semarthrit.2019.12.004.
- 160. Turnier, J.L.; Brunner, H.I. Tocilizumab for treating juvenile idiopathic arthritis. Expert Opin. Biol. Ther. 2016, 16, 559-566. https://doi.org/10.1517/14712598.2016.1150997.
- 161. Scott, L.J. Tocilizumab: A Review in Rheumatoid Arthritis. Drugs 2017, 77, 1865-1879. https://doi.org/10.1007/s40265-017-0829-7.
- 162. Khanna, D.; Denton, C.P.; Lin, C.J.F.; van Laar, J.M.; Frech, T.M.; Anderson, M.E.; Baron, M.; Chung, L.; Fierlbeck, G.; Lakshminarayanan, S.; et al. Safety and efficacy of subcutaneous tocilizumab in systemic sclerosis: Results from the open-label period of a phase II randomised controlled trial (faSScinate). Ann. Rheum. Dis. 2018, 77, 212-220. https://doi.org/10.1136/ annrheumdis-2017-211682.
- 163. Denton, C.P.; Ong, V.H.; Xu, S.; Chen-Harris, H.; Modrusan, Z.; Lafyatis, R.; Khanna, D.; Jahreis, A.; Siegel, J.; Sornasse, T. Therapeutic interleukin-6 blockade reverses transforming growth factor-beta pathway activation in dermal fibroblasts: Insights from the faSScinate clinical trial in systemic sclerosis. Ann. Rheum. Dis. 2018, 77, 1362-1371. https://doi.org/10.1136/ annrheumdis-2018-213031.
- 164. Kono, M.; Yasuda, S.; Kono, M.; Atsumi, T. Tocilizumab reduced production of systemic sclerosisrelated autoantibodies and anti-cyclic citrullinated protein antibodies in two patients with overlapping systemic sclerosis and rheumatoid arthritis. Scand. J. Rheumatol. 2018, 47, 248–250. https://doi.org/10.1080/03009742.2017.1297482.

- 165. Shima, Y.; Hosen, N.; Hirano, T.; Arimitsu, J.; Nishida, S.; Hagihara, K.; Narazaki, M.; Ogata, A.; Tanaka, T.; Kishimoto, T.; et al. Expansion of range of joint motion following treatment of systemic sclerosis with tocilizumab. Mod. Rheumatol. 2013, 25, 134-137. https://doi.org/10.1007/s10165-013-0855-6.
- 166. Kondo, M.; Murakawa, Y.; Matsumura, T.; Matsumoto, O.; Taira, M.; Moriyama, M.; Sumita, Y.; Yamaguchi, S. A case of overlap syndrome successfully treated with tocilizumab: A hopeful treatment strategy for refractory dermatomyositis? Rheumatology 2014, 53, 1907-1908.
- 167. Fernandes das Neves, M.; Oliveira, S.; Amaral, M.C.; Delgado Alves, J. Treatment of systemic sclerosis with tocilizumab. Rheumatology 2015, 54, 371–372.
- 168. Saito, E.; Sato, S.; Noqi, S.; Sasaki, N.; Chinen, N.; Honda, K.; Wakabayashi, T.; Yamada, C.; Nakamura, N.; Suzuki, Y. A case of rheumatoid arthritis and limited systemic sclerosis overlap successfully treated with tocilizumab for arthritis and concomitant generalized lymphadenopathy and primary biliary cirrhosis. Case Rep. Rheumatol. 2014, 2014, 386328. https://doi.org/10.1155/2014/386328.
- 169. Khanna, D.; Lin, C.J.F.; Furst, D.E.; Goldin, J.; Kim, G.; Kuwana, M.; Allanore, Y.; Matucci-Cerinic, M.; Distler, O.; Shima, Y.; et al. Tocilizumab in systemic sclerosis: A randomised, double-blind, placebo-controlled, phase 3 trial. Lancet Respir. Med. 2020, 8, 963-974. https://doi.org/10.1016/ S2213-2600(20)30318-0.
- 170. Roofeh, D.; Lin, C.J.F.; Goldin, J.; Kim, G.H.; Furst, D.E.; Denton, C.P.; Huang, S.; Khanna, D. Tocilizumab Prevents Progression of Early Systemic Sclerosis-Associated Interstitial Lung Disease. Arthritis Rheumatol. 2021, 73, 1301-1310. https://doi.org/10.1002/art.41668.
- 171. Hoffman, H.M. Rilonacept for the treatment of cryopyrin-associated periodic syndromes (CAPS). Expert Opin. Biol. Ther. 2009, 9, 519–531. https://doi.org/10.1517/14712590902875518.
- 172. Mantero, J.C.; Kishore, N.; Ziemek, J.; Stifano, G.; Zammitti, C.; Khanna, D.; Gordon, J.K.; Spiera, R.; Zhang, Y.; Simms, R.W.; et al. Randomised, double-blind, placebo-controlled trial of IL1-trap, rilonacept, in systemic sclerosis. A phase I/II biomarker trial. Clin. Exp. Rheumatol. 2018, 36 (Suppl. S1), 146-149.
- 173. Tan, J.; Yang, S.; Wu, W. Basiliximab (Simulect) reduces acute rejection among sensitized kidney allograft recipients. Transplant. Proc. 2005, 37, 903-905. https://doi.org/10.1016/j. transproceed.2005.01.071.
- 174. Scherer, H.U.; Burmester, G.-R.; Riemekasten, G. Targeting activated T cells: Successful use of anti-CD25 monoclonal antibody basiliximab in a patient with systemic sclerosis. Ann. Rheum. Dis. 2006, 65, 1245–1247. https://doi.org/10.1136/ard.2005.046938.
- 175. Becker, M.O.; Brückner, C.; Scherer, H.U.; Wassermann, N.; Humrich, J.Y.; Hanitsch, L.G.; Schneider, U.; Kawald, A.; Hanke, K.; Burmester, G.R.; et al. The monoclonal anti-CD25 antibody basiliximab for the treatment of progressive systemic sclerosis: An open-label study. Ann. Rheum. Dis. 2011, 70, 1340-1341. https://doi.org/10.1136/ard.2010.137935.
- 176. Rice, L.M.; Padilla, C.M.; McLaughlin, S.R.; Mathes, A.; Ziemek, J.; Goummih, S.; Nakerakanti, S.; York, M.; Farina, G.; Whitfield, M.L.; et al. Fresolimumab treatment decreases biomarkers and improves clinical symptoms in systemic sclerosis patients. J. Clin. Investig. 2015, 125, 2795–2807. https://doi.org/10.1172/JCI77958.
- 177. Denton, C.P.; Merkel, P.A.; Furst, D.E.; Khanna, D.; Emery, P.; Hsu, V.M.; Silliman, N.; Streisand, J.; Powell, J.; Akesson, A.; et al. Recombinant human anti-transforming growth factor beta1 antibody therapy in systemic sclerosis: A multicenter, randomized, placebo-controlled phase I/II trial of CAT-192. Arthritis Rheum. 2007, 56, 323–333. https://doi.org/10.1002/art.22289.
- 178. Gerber, E.E.; Gallo, E.M.; Fontana, S.C.; Davis, E.C.; Wigley, F.M.; Huso, D.L.; Dietz, H.C. Integrinmodulating therapy prevents fibrosis and autoimmunity in mouse models of scleroderma. Nature 2013, 503, 126-130. https://doi.org/10.1038/nature12614.

- 179. Lehtonen, S.T.; Veijola, A.; Karvonen, H.; Lappi-Blanco, E.; Sormunen, R.; Korpela, S.; Zagai, U.; Sköld, M.C.; Kaarteenaho, R. Pirfenidone and nintedanib modulate properties of fibroblasts and myofibroblasts in idiopathic pulmonary fibrosis. Respir. Res. 2016, 17, 14. https://doi.org/10.1186/ s12931-016-0328-5.
- 180. Khanna, D.; Albera, C.; Fischer, A.; Khalidi, N.; Raghu, G.; Chung, L.; Chen, D.; Schiopu, E.; Tagliaferri, M.; Seibold, J.R.; et al. An open-label, phase II study of the safety and tolerability of pirfenidone in patients with scleroderma-associated interstitial lung disease: The LOTUSS trial. J. Rheumatol. 2016, 43, 1672-1679. https://doi.org/10.3899/jrheum.151322.
- 181. Huang, H.; Feng, R.E.; Li, S.; Xu, K.; Bi, Y.L.; Xu, Z.J. A case report: The efficacy of pirfenidone in a Chinese patient with progressive systemic sclerosis-associated interstitial lung disease: A CAREcompliant article. Medicine 2016, 95, e4113. https://doi.org/10.1097/MD.000000000004113.
- 182. Miura, Y.; Saito, T.; Fujita, K.; Tsunoda, Y.; Tanaka, T.; Takoi, H.; Yatagai, Y.; Rin, S.; Sekine, A.; Hayashihara, K.; et al. Clinical experience with pirfenidone in five patients with sclerodermarelated interstitial lung disease. Sarcoidosis Vasc. Diffus. Lung Dis. 2014, 31, 235–238.
- 183. Zarrin, A.A.; Bao, K.; Lupardus, P.; Vucic, D. Kinase inhibition in autoimmunity and inflammation. Nat. Rev. Drug Discov. 2021, 20, 39-63. https://doi.org/10.1038/s41573-020-0082-8.
- 184. Pottier, C.; Fresnais, M.; Gilon, M.; Jérusalem, G.; Longuespée, R.; Sounni, N.E. Tyrosine Kinase Inhibitors in Cancer: Breakthrough and Challenges of Targeted Therapy. Cancers 2020, 12, 731. https://doi.org/10.3390/cancers12030731.
- 185. Tamura, T.; Koch, A. Tyrosine Kinases as Targets for Anti-Inflammatory Therapy. Anti-Inflamm. Anti-Allergy Agents Med. Chem. 2007, 6, 47-60. https://doi.org/10.2174/187152307779939732.
- 186. Iwamoto, N.; Distler, J.H.W.; Distler, O. Tyrosine kinase inhibitors in the treatment of systemic sclerosis: From animal models to clinical trials. Curr. Rheumatol. Rep. 2011, 13, 21-27. https://doi.org/10.1007/s11926-010-0142-x.
- 187. Gajski, G.; Gerić, M.; Domijan, A.-M.; Golubović, I.; Garaj-Vrhovac, V. Evaluation of oxidative stress responses in human circulating blood cells after imatinib mesylate treatment—Implications to its mechanism of action. Saudi Pharm. J. 2019, 27, 1216-1221. https://doi.org/10.1016/j. jsps.2019.10.005.
- 188. Haddon, D.J.; Wand, H.E.; Jarrell, J.A.; Spiera, R.F.; Utz, P.J.; Gordon, J.K.; Chung, L.S. Proteomic Analysis of Sera from Individuals with Diffuse Cutaneous Systemic Sclerosis Reveals a Multianalyte Signature Associated with Clinical Improvement during Imatinib Mesylate Treatment. J. Rheumatol. 2017, 44, 631-638. https://doi.org/10.3899/jrheum.160833.
- 189. Spiera, R.F.; Gordon, J.K.; Mersten, J.N.; Magro, C.M.; Mehta, M.; Wildman, H.F.; Kloiber, S.; Kirou, K.A.; Lyman, S.; Crow, M.K. Imatinib mesylate (Gleevec) in the treatment of diffuse cutaneous systemic sclerosis: Results of a 1-year, phase IIa, single-arm, open-label clinical trial. Ann. Rheum. Dis. 2011, 70, 1003-1009. https://doi.org/10.1136/ard.2010.143974.
- 190. Divekar, A.A.; Khanna, D.; Abtin, F.; Maranian, P.; Saggar, R.; Saggar, R.; Furst, D.E.; Singh, R.R. Treatment with imatinib results in reduced IL-4-producing T cells, but increased CD4(+) T cells in the broncho-alveolar lavage of patients with systemic sclerosis. Clin. Immunol. 2011, 141, 293– 303. https://doi.org/10.1016/j.clim.2011.08.010.
- 191. Chung, L.; Fiorentino, D.F.; Benbarak, M.J.; Adler, A.S.; Mariano, M.M.; Paniagua, R.T.; Milano, A.; Connolly, M.K.; Ratiner, B.D.; Wiskocil, R.L.; et al. Molecular framework for response to imatinib mesylate in systemic sclerosis. Arthritis Rheum. 2009, 60, 584–591. https://doi.org/10.1002/art.24221.
- 192. Fraticelli, P.; Gabrielli, B.; Pomponio, G.; Valentini, G.; Bosello, S.; Riboldi, P.; Gerosa, M.; Faggioli, P.; Giacomelli, R.; Del Papa, N.; et al. Low-dose oral imatinib in the treatment of systemic sclerosis interstitial lung disease unresponsive to cyclophosphamide: A phase II pilot study. Arthritis Res. Ther. 2014, 16, R144. https://doi.org/10.1186/ar4606.

- 193. Khanna, D.; Saggar, R.; Mayes, M.D.; Abtin, F.; Clements, P.J.; Maranian, P.; Assassi, S.; Saggar, R.; Singh, R.R.; Furst, D.E. A one-year, phase I/IIa, open-label pilot trial of imatinib mesylate in the treatment of systemic sclerosis-associated active interstitial lung disease. Arthritis Rheum. 2011, 63, 3540-3546. https://doi.org/10.1002/art.30548.
- 194. Bradeen, H.A.; Eide, C.A.; O'Hare, T.; Johnson, K.J.; Willis, S.G.; Lee, F.Y.; Druker, B.J.; Deininger, M.W. Comparison of imatinib mesylate, dasatinib (BMS-354825), and nilotinib (AMN107) in an N-ethyl-N-nitrosourea (ENU)-based mutagenesis screen: High efficacy of drug combinations. Blood 2006, 108, 2332-2338. https://doi.org/10.1182/blood-2006-02-004580.
- 195. Gordon, J.K.; Martyanov, V.; Magro, C.; Wildman, H.F.; Wood, T.A.; Huang, W.-T.; Crow, M.K.; Whitfield, M.L.; Spiera, R.F. Nilotinib (Tasigna™) in the treatment of early diffuse systemic sclerosis: An open-label, pilot clinical trial. Arthritis Res. Ther. 2015, 17, 213. https://doi.org/10.1186/s13075-015-0721-3.
- 196. Wollin, L.; Distler, J.H.W.; Redente, E.F.; Riches, D.W.H.; Stowasser, S.; Schlenker-Herceg, R.; Maher, T.M.; Kolb, M. Potential of nintedanib in treatment of progressive fibrosing interstitial lung diseases. Eur. Respir. J. 2019, 54, 1900161. https://doi.org/10.1183/13993003.00161-2019.
- 197. Sato, S.; Shinohara, S.; Hayashi, S.; Morizumi, S.; Abe, S.; Okazaki, H.; Chen, Y.; Goto, H.; Aono, Y.; Ogawa, H.; et al. Anti-fibrotic efficacy of nintedanib in pulmonary fibrosis via the inhibition of fibrocyte activity. Respir. Res. 2017, 18, 172. https://doi.org/10.1186/s12931-017-0654-2.
- 198. Cutolo, M.; Gotelli, E.; Montagna, P.; Tardito, S.; Paolino, S.; Pizzorni, C.; Sulli, A.; Smith, V.; Soldano, S. Nintedanib downregulates the transition of cultured systemic sclerosis fibrocytes into myofibroblasts and their pro-fibrotic activity. Arthritis Res. Ther. 2021, 23, 205. https://doi.org/10.1186/s13075-021-02555-2.
- 199. Distler, O.; Highland, K.B.; Gahlemann, M.; Azuma, A.; Fischer, A.; Mayes, M.D.; Raghu, G.; Sauter, W.; Girard, M.; Alves, M.; et al. Nintedanib for Systemic Sclerosis-Associated Interstitial Lung Disease. N. Engl. J. Med. 2019, 380, 2518-2528. https://doi.org/10.1056/NEJMoa1903076.
- 200. Bruni, T.; Varone, F. The adoption of nintedanib in systemic sclerosis: The SENSCIS study. Breathe 2020, 16, 200005. https://doi.org/10.1183/20734735.0005-2020.
- 201. Wang, W.; Bhattacharyya, S.; Marangoni, R.G.; Carns, M.; Dennis-Aren, K.; Yeldandi, A.; Wei, J.; Varga, J. The JAK/STAT pathway is activated in systemic sclerosis and is effectively targeted by tofacitinib. J. Scleroderma Relat. Disord. 2019, 5, 40-50. https://doi.org/10.1177/2397198319865367.
- 202. Kucharz, E.J.; Stajszczyk, M.; Kotulska-Kucharz, A.; Batko, B.; Brzosko, M.; Jeka, S.; Leszczyński, P.; Majdan, M.; Olesińska, M.; Samborski, W.; et al. Tofacitinib in the treatment of patients with rheumatoid arthritis: Position statement of experts of the Polish Society for Rheumatology. Reumatologia **2018**, *56*, 203–211. https://doi.org/10.5114/reum.2018.77971.
- 203. You, H.; Xu, D.; Hou, Y.; Zhou, J.; Wang, Q.; Li, M.; Zeng, X. Tofacitinib as a possible treatment for skin thickening in diffuse cutaneous systemic sclerosis. Rheumatology 2021, 60, 2472-2477. https://doi.org/10.1093/rheumatology/keaa613.
- 204. Karalilova, R.V.; Batalov, Z.A.; Sapundzhieva, T.L.; Matucci-Cerinic, M.; Batalov, A.Z. Tofacitinib in the treatment of skin and musculoskeletal involvement in patients with systemic sclerosis, evaluated by ultrasound. Rheumatol. Int. 2021, 41, 1743-1753. https://doi.org/10.1007/s00296-021-04956-7.
- 205. Vonk, M.C.; Smith, V.; Sfikakis, P.P.; Cutolo, M.; del Galdo, F.; Seibold, J.R. Pharmacological treatments for SSc-ILD: Systematic review and critical appraisal of the evidence. Autoimmun. Rev. **2021**, 20, 102978. https://doi.org/10.1016/j.autrev.2021.102978.
- 206. Lepri, G.; Hughes, M.; Bruni, C.; Cerinic, M.M.; Randone, S.B. Recent advances steer the future of systemic sclerosis toward precision medicine. Clin. Rheumatol. 2020, 39, 1-4. https://doi.org/10.1007/s10067-019-04834-5.



Chapter 3

CD7 activation regulates cytotoxicity-driven pathology in systemic sclerosis, yielding a target for selective cell depletion

Theodoros Ioannis Papadimitriou, Prashant Singh, Arjan PM van Caam, Birgitte Walgreen, Mark AJ Gorris, Elly Vitters, Iris van Ingen, Marije Koenders, Ruben L Smeets, Madelon Vonk, I Jolanda M de Vries, Peter M van der Kraan, Ypke V.J.M. van Oosterhout, Martijn A Huijnen, Hans JPM Koenen, Rogier M Thurlings

Ann Rheum Dis. 2024 Mar 12;83(4):488-498. doi: 10.1136/ard-2023-224827.

Abstract

Objectives. Cytotoxic T cells and NK cells are central effector cells in cancer and infections. Their effector response is regulated by activating and inhibitory receptors. The regulation of these cells in systemic autoimmune diseases such as systemic sclerosis (SSc) is less defined.

Methods. We conducted ex vivo analysis of affected skin and blood samples from 4 SSc patient cohorts (a total of 165 SSc vs. 80 healthy individuals) using singlecell transcriptomics, flow cytometry and multiplex immunofluorescence staining. We further analyzed the effects of co-stimulatory modulation in functional assays, and in a severely affected SSc patient who was treated on compassionate use with a novel anti-CD3/CD7 bispecific immunotoxin treatment.

Results. Here, we show that SSc affected skin contains proliferating, cytotoxic T cells and NK cells. These cells selectively express the co-stimulatory molecule CD7 in association with cytotoxic, pro-inflammatory and pro-fibrotic genes, especially in recent-onset and severe disease. We demonstrate that CD7 regulates the cytolytic activity of T cells and NK cells and that selective depletion of CD7+ cells prevents cytotoxic cell-induced fibroblast contraction and inhibits their pro-fibrotic phenotype. Finally, anti-CD3/CD7 directed depletive treatment eliminated CD7+ skin cells and stabilized disease manifestations in a severely affected SSc patient.

Conclusion. Together the findings imply co-stimulatory molecules as key regulators of cytotoxicity-driven pathology in systemic autoimmune disease, yielding CD7 as a novel target for selective depletion of pathogenic cells.

Keywords

Cytotoxic lymphocytes, skin, CD7, immunotherapy

WHAT IS ALREADY KNOWN ON THIS TOPIC

- Cytotoxic immune cells are prevalent in systemic sclerosis (SSc) affected skin and their presence is involved in endothelial cell dysfunction and fibroblast activation.
- 2. Autologous stem cell transplantation (ASCT) can achieve long-term remission in severe cases of SSc, but it is a high risk procedure applicable only to a limited amount (10%) of patients.

WHAT THIS STUDY ADDS

- SSc skin cytotoxicity-driven pathology is regulated by activated T cells and NK cells that upregulate the co-stimulatory receptor CD7 in association with a pro-inflammatory and pro-fibrotic gene signature, particularly in recent-onset and severe disease.
- Selective elimination of CD7⁺ T cells and NK cells with a novel bi-specific 4 anti-CD3/CD7 immunotoxin prevented cytotoxic cell-induced myofibroblast contraction and activation and stabilized disease progress in a severely affected SSc patient that was treated on compassionate use.

HOW THIS STUDY MIGHT AFFECT RESEARCH, PRACTICE OR POLICY

Our results highlight the key role of co-stimulatory receptors in regulating cytotoxicity induced pathology in systemic autoimmunity, rendering a promising therapeutic strategy for mitigating tissue inflammation and fibrosis in connective tissue disorders such as SSc.

Introduction

Systemic sclerosis (SSc) is a systemic autoimmune disease that is characterized by vasculopathy, inflammation and progressive fibrosis of skin and internal organs (1). Autoimmunity in SSc is directed against nuclear autoantigens, which can be aberrantly presented by endothelial cells and fibroblasts due to hypoxic stress and serve as antigenic targets (2). This is exemplified by the development of a dysregulated Raynaud's phenomenon as the first and principal disease manifestation. T lymphocytes have been detected in SSc-affected tissues and multiple studies have suggested their potential involvement in the observed fibrosis and vasculopathy through the production of cytokines such as interleukin (IL)-4, IL-13, and IL-17 (3). Unexpectedly, a recent study showed a prominent role for cytotoxic T cells in mediating SSc skin pathology (4). Furthermore, an epigenetic study implicated natural killer (NK) and CD8⁺ T cells in SSc pathogenesis (5).

In chronic inflammatory conditions, T cell activation is restricted to prevent unwarranted inflammatory side-effects. Activation of antigen-specific CD4⁺ T cells is regulated by professional antigen-presenting cells via major histocompatibility complex (MHC) class II-controlled processes. Regulatory mechanisms are less defined for cytotoxic T cells and NK cells because these depend on non-MHC class Il receptors and these are expressed ubiquitously in inflamed tissue. In chronic infections and malignancies, activation of cytotoxic T cells and NK cells has been shown to be regulated by an interplay between co-stimulatory and inhibitory receptors (6). Animal models indicate that similar mechanisms may operate in cytotoxic autoimmunity (7). Still, the exact role of T cells in SSc pathogenesis is yet to be defined. On the one hand, genetic studies have proven that human leukocyte antigen genes (HLAs) corresponding to MHC class II confer susceptibility to SSc (8). On the other hand, treatment with the T cell directed drug cytotoxic T-lymphocyteassociated antigen 4 (CTLA-4) immunoglobulin (abatacept) has shown limited clinical efficacy (9).

Here, we hypothesize that co-stimulatory receptors, independent of CTLA-4, regulate cytotoxic cell-driven pathologic processes in SSc. Furthermore, we hypothesize that these processes can be alleviated by therapeutic targeting of such receptors. We conducted analyses of affected skin and blood at the single cell, protein and spatial level in 4 separate SSc patient cohorts. Furthermore, we analyzed the effects of co-stimulatory modulation in ex vivo functional assays, and in a severely affected SSc patient who was treated on compassionate use with a novel combination of anti-CD3/CD7 immunotoxins (CD3/CD7-IT).

Methods

Detailed methods are provided in **online supplemental methods**.

Results

SSc skin contains increased numbers of activated cytotoxic T and NK cells with a cytotoxic, pro-inflammatory and pro-fibrotic signature

T and NK cell subsets may upregulate co-stimulatory receptors to direct the autoimmune inflammatory process in SSc. To gain a comprehensive profiling of skin infiltrating lymphocytes, we analyzed T and NK cell clusters (n=5.061 cells) from a scRNAseq dataset of affected skin of 97 SSc patients compared to healthy skin from 56 individuals, as part of a larger dataset that was published recently (GSE195452) (10) (Supp. Figure 1). To enhance confidence, we comparatively analyzed another single-cell RNA transcriptome dataset containing 2,126 cells from 9 healthy and 12 SSc skin biopsies (GSE138669) (11) (**Supp. Figure 2**).

First, we analyzed T cells and NK cells in skin single-cell datasets based on differential gene expression of known lineage-specific genes (GSE195452, GSE138669). Among the transcriptionally distinct cell subtypes that were detected (Supp. Figure 1A, 2A), the following three were significantly expanded (q< 0.05 for all comparisons) in SSc compared to healthy skin in both datasets: proliferating T cells, CD8+ cytotoxic T cells, and NK cells (Figure 1A, B). We verified the presence of these T and NK cell subsets at the protein level in SSc affected skin in an additional cohort of 24 SSc patients (Figure 1C). In addition, increased infiltration of cytotoxic CD8+ T cells and CD56+ NK cells was further apparent in biopsies from the affected compared to matched non-affected skin in 71% and 83% of SSc patients respectively (n=24, p= 0.06 and p< 0.001 respectively) (*Figure 1D, E*). In the affected SSc skin, cytotoxic T cells and NK cells were primarily present in perivascular areas while a smaller amount of these cells was infiltrated around blood vessels of the non-affected skin (Figure 1D).

Next, we analyzed the potential function of these enriched cell populations in SSc skin. For this, we used gene set enrichment analyses based on each cluster with Wiki pathways as reference dataset. Both the skin cytotoxic T and NK cell clusters from each sc-dataset were not only associated with cell cytolytic pathways but were also the only clusters from SSc skin that were specifically enriched for gene sets related to lung fibrosis, pro-inflammatory and pro-fibrotic manifestations relative

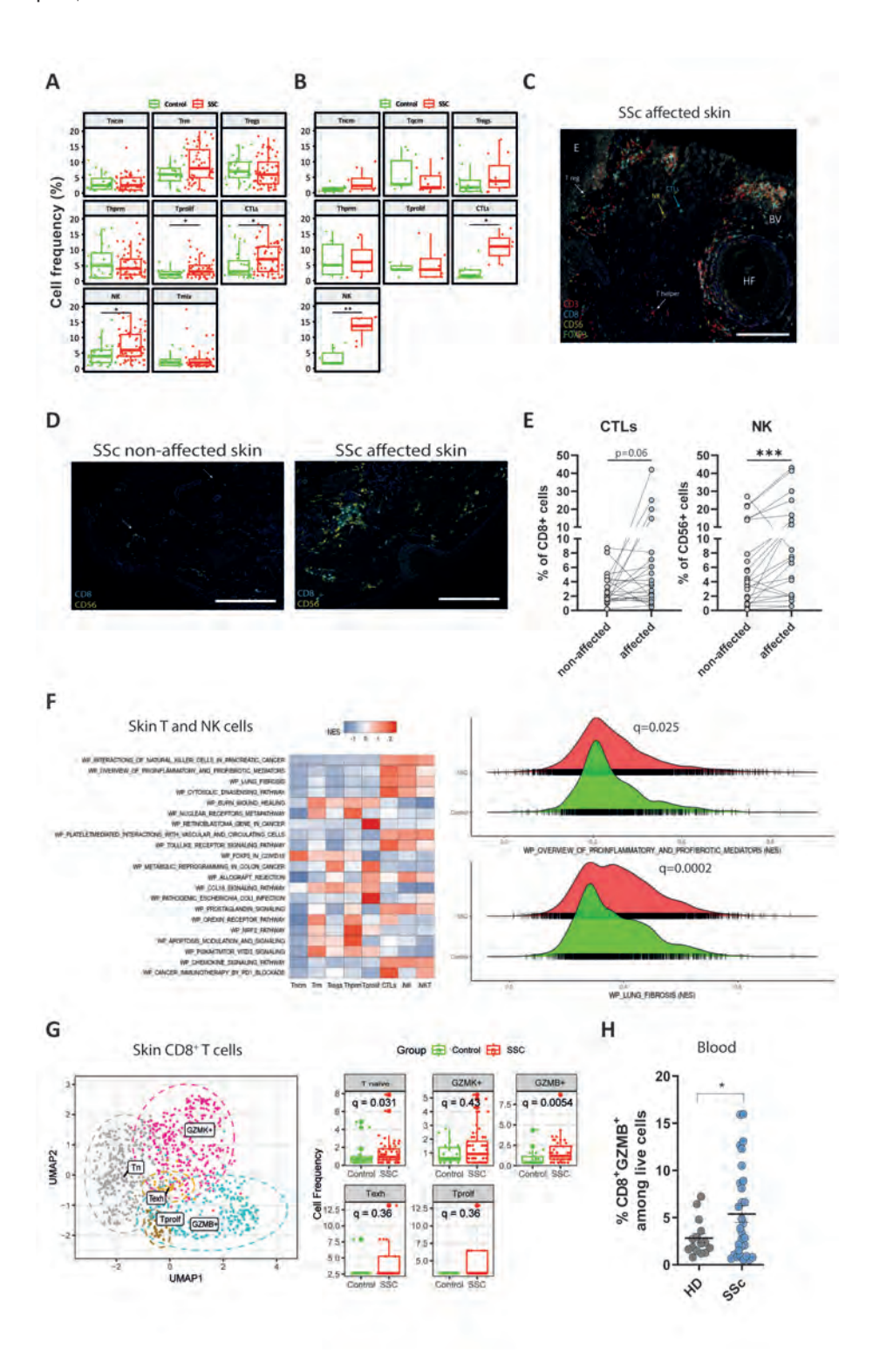


Figure 1. Increased frequency of pro-fibrotic cytotoxic T and NK cells in SSc skin. A Frequencies of T and NK cell clusters in the skin of (n= 56) Healthy Donors (HD) compared to (n=97) patients with systemic sclerosis (SSc) (GSE195452), **B** Frequencies of T and NK cell clusters in the skin of (n= 9) HD compared to (n=12) patients with SSc (GSE138669). Abbreviations: tissue-resident memory T cells (Trm), cytotoxic T cells (CTLs), regulatory T cells (Tregs), hypofunctional tissue resident T cells (Thprm), naïve/central memory (Tncm), proliferating T cells (Tprolif), NK cells (NK), quiescent tissue- resident T cells (Tgcm). For both panels A and B, values are represented as variation in cell counts (in %) and statistics were performed with Wilcox-Test, corrected for multiple comparisons. Only the adjusted p-values (q) of the statistically significant comparisons are shown, *q<0.05, **q<0.01. **C** Representative multicolor immunofluorescence composite image of T helper CD3+CD8- (red), cytotoxic CD8+ (cyan), regulatory FOXP3+ (green) T cells and CD56+CD3- (yellow) NK cells in SSc affected skin. Abbreviations: hair follicle (HF), epidermis (E), blood vessel (BV). Scale 50 µm. D Immunofluorescence composite images of infiltrated cytotoxic CD8+ (cyan) T cells and CD56+CD3- (yellow) NK cells of the non-affected versus the affected skin from a representative SSc patient with early diffuse disease. **E** Percentages (%) of cytotoxic T (CD3+CD8+) and NK cells (CD56+CD3-) in matched non-affected versus affected SSc skin (n=24 SSc patients). Values are represented as % of CD8+ or CD56+ cells compared to all cells (DAPI+) present in each biopsy (excluding the rich in keratinocytes epidermis layer). Statistics were performed with non-parametric Wilconxon test, ***p<0.001. F (left) Gene set enrichment analysis of skin T and NK cell clusters with Wiki pathways as reference dataset. Examples of top pathways (p < 0.001) represented by NK and CTL clusters are shown. Statistics were performed with Kolmogorov-Smirnov test. (right) Comparison of the enrichment scores of the "Overview of proinflammatory and profibrotic mediators" (q=0.025) and "Lung fibrosis" (q=0.0002) pathways in HD (green) versus SSc (red) skin T and NK cell clusters (here for GSE195452, Supp. Figure 2C for GSE138669). G (left) UMAP displaying 5 transcriptionally different CD8+ T cell clusters in skin of (n=56) HD and (n=97) SSc, n=977 cells. Based on the top differentially expressed genes, clusters were annotated as naïve (T naive), Granzyme K+ (GZMK+), Granzyme B+ (GZMB+), exhausted (Texh) and proliferating (Tprolif). (right) Cell frequency of CD8+T cell clusters between HD and SSc. H Percentage of Granzyme B (GZMB) expressing CD8+T cells in peripheral blood of (n=15) HD and (n=30) SSc. Values are represented as % of total live peripheral blood mononuclear cells, *p<0.05.

to healthy skin (Figure 1F, Supp. Figure 2C). These pathways included pro-fibrotic genes such as TGFB1, XCL1, OSM, CCL4, IL4, IL17, FGF and PDGF (for a complete overview see Supp. Figure 3). This indicates that cytotoxic cells are not only involved in cytotoxicity but also in directing pro-fibrotic pathophysiological processes.

In recent studies in chronic inflammatory conditions, CD8+ T cells were shown to mainly exert a cytokine mediated function instead of their conventional cytotoxic effects with an important role of granzyme K (12). Therefore, we performed a focused analysis of CD8+ T cells. In skin, at the sc-RNAseq level, the following CD8+ sub-clusters were formed: naïve, proliferating, skin resident exhausted like, granzyme K (GZMK⁺) and granzyme B (GZMB⁺) positive effector cells. Of these, only the subset of CD8 effector GZMB+ cells were significantly enriched in SSc skin (Figure 1G, Supp. Figure 1D). Flow cytometry analysis in blood also showed increased (2-fold) presence of CD8+GZMB+ cells in SSc compared to healthy donors (Figure 1H).

Expanded CD8+ T and NK cells in the affected skin and lungs of systemic sclerosis patients are characterized by upregulation of the CD7 co-stimulatory molecule

The activity of cytotoxic T cells and NK cells is closely regulated by an interplay between activating and inhibitory cell surface receptors. In chronic infection and malignancies, T and NK cell cytotoxic functions have been shown to be restricted by inhibitory receptors (13-15). Therefore, we compared expression of known T and NK cell activating and inhibitory receptors between immune cells of healthy and SSc skin. Of the inhibitory receptors, LAG3 was expressed in a proportion of CD8+GZMB+ T cells in SSc skin. The expression of TIGIT, CTLA4 and HAVCR2 (TIM-3) did not show any significant difference between healthy and SSc skin while PDCD1 (PD-1) was only expressed in a few naïve/central memory CD8+ T cells together with FOXP3 (Supp. Figure 1E). Of the activating receptors, CD69 and CD7 were upregulated in CD8+GZMB+T cells whilst SSc NK cells exhibited elevated expression of CD7, TNFRSF9 (CD137) and CD28. In the cluster of proliferating SSc T cells, CD40LG was downregulated and CD28 expression was decreased in SSc versus healthy skin (Figure 2A). Of these, CD7 was expressed by almost all the cells in these clusters and also showed the strongest upregulation in patients compared to controls (α <0.001) (Figure 2A, B). In a further attempt to identify differences in cytotoxic T and NK cell activation between healthy and SSc individuals, we used an alternative unbiased approach based on the FindConservedMarker function implemented in Seurat. (to find features that are conserved between the groups, i.e- healthy donors and SSc). This approach confirmed enrichment of cytotoxic genes and CD7 in cytotoxic T cells and NK cells of SSc patients compared to healthy controls. No other activating or inhibitory receptors were enriched in SSc in this analysis (Figure 2C). These observations suggest that CD7 co-stimulation may be involved in SSc skin T and NK cell activation.

To validate these results at the protein level, we performed CD7 and CD3 immunohistochemistry in SSc skin tissue. The total amount of CD3+ T cells was higher even though statistically non-significant in the affected SSc skin (mean number of CD3+T cells: 15.8 affected versus 6.1 in non-affected) (*Supp. Figure 4A, B*). Strikingly, an increased infiltration of CD7+ cells was specifically found in the perivascular areas (*Supp Figure 4C*) of affected compared to the non-affected SSc skin (*Figure 2D*). Furthermore, in SSc skin, CD7 was found to be co-expressed with CD8 and CD56 positive cells, while no expression on CD3+CD8-cells could be observed (*Figure 2E*).

Recently, an increased presence of tissue resident cytotoxic T and NK cells was also described in SSc lungs (16). Thus, we next evaluated CD7 expression in SSc lung tissue compared to healthy. In accordance with our data in skin, CD7 was selectively expressed in lung cytotoxic T cells and NK cells and its expression in SSc CD8+T cells and CD56+ NK cells was significantly higher (2-fold increase) compared to healthy counterparts (Figure 2F). In conclusion, CD7 is a co-stimulatory receptor that is significantly upregulated in disease related cytotoxic immune cell populations in both the affected skin and lungs of patients with SSc.

CD7 co-stimulation is involved in T and NK cell cytotoxic and profibrotic processes

CD7 is selectively expressed in skin T cells and NK cells (Supp. Figure 4D). This receptor is upregulated after TCR ligation and activated by its ligand, SECTM1 (17). SECTM1 is a transmembrane protein produced by thymic epithelial cells and fibroblasts and induced by IFN-y in professional antigen-presenting cells. CD7 activation by SECTM1 has been shown to augment CD4+ and CD8+ T cell effector functions (18). To gain insight on the function of CD7 in SSc, we analyzed expression of SECTM1 in skin stromal and immune cells. In our dataset, SECTM1 as expected was primarily detected in skin myeloid cells including monocytes, macrophages and dendritic cells. Furthermore, SECTM1 was also expressed by cells in the fibroblast cluster characterized by increased expression of PTGDS (Figure 3A). Interestingly, it was previously reported that this fibroblast subtype is marked by high expression of MHC class I genes compared to other skin fibroblast subsets, suggesting that the SECTM1-CD7 axis may be important in T and NK cell activation (**Supp. Figure 5A**). Notably, T cell and NK cell CD7 expression was positively correlated with IFNG, while expression of its receptor (IFNGR1) positively correlated with SECTM1 in fibroblasts and antigen presenting cells (Supp. Figure 5B, C). This suggests an IFN-y driven SECTM1-CD7 axis in SSc skin.

From a clinical perspective, SSc is a heterogeneous disease with various disease subtypes and phases. Thus, we next analyzed CD7 gene expression in subgrouping of SSc patients with limited (ISSc) versus diffuse (dSSc) cutaneous and early (≤ 3 years from first non-Raynaud symptom) versus late disease. We found that CD7 was significantly upregulated in early diffuse SSc compared to late disease (Figure 3B) and CD7 expression was further associated with patients exhibiting increased skin score (p=0.03) (Figure 3C). CD7 skin expression was not associated with the presence of interstitial lung disease (ILD). Furthermore, CD7 expression was similar between treatment naïve and patients that were receiving immunosuppressive medication, suggesting that currently used therapeutic approaches do not seem to directly target this activation axis (*Figure 3D*).

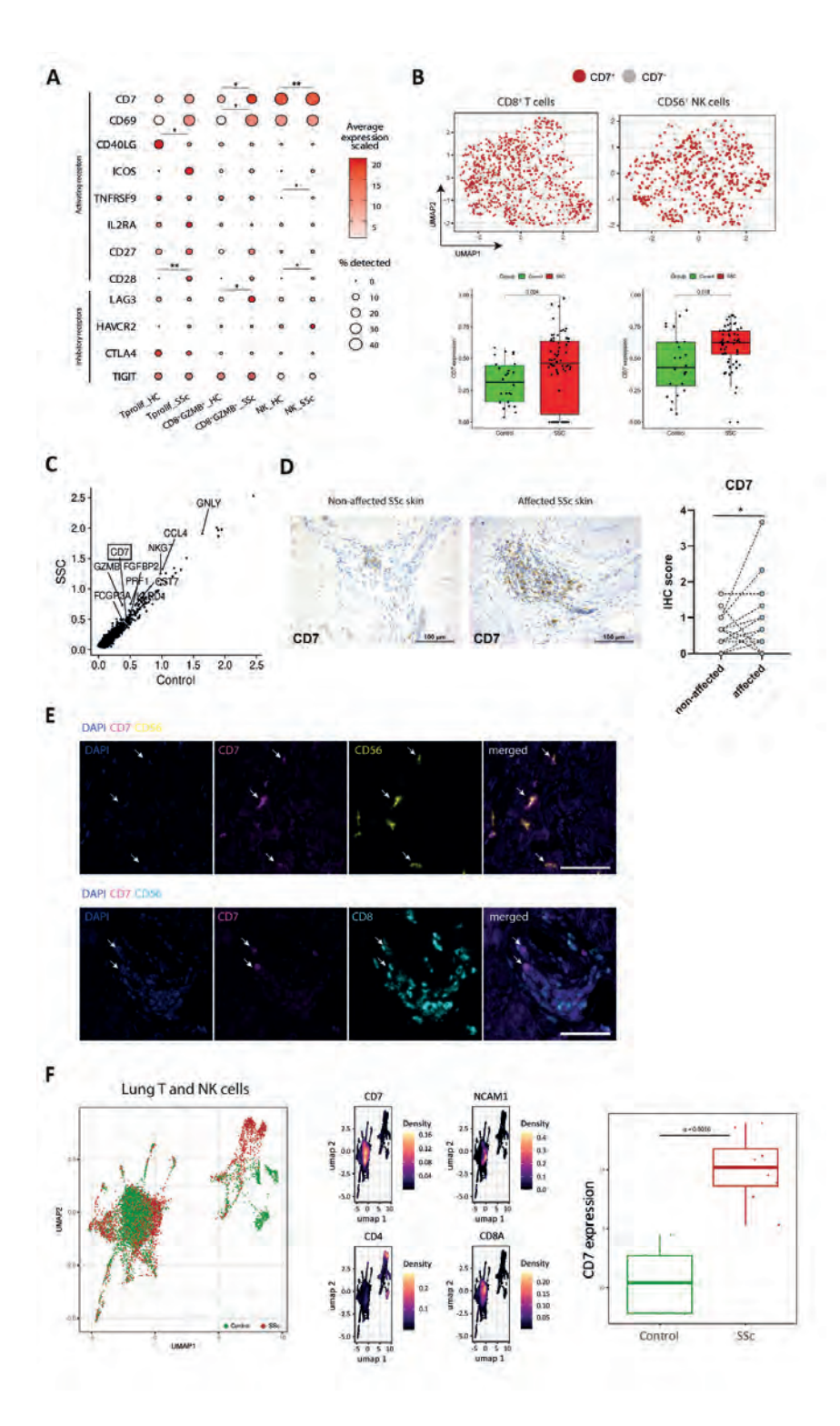


Figure 2. CD7 upregulation associates with activation of cytotoxic T and NK cells in SSc affected skin and lungs. A 2-D dot plots comparing the gene expression of selected activating and inhibitory costimulatory receptors in Tprolif, CD8+GZMB+ and NK clusters between HD and SSc (circle size shows the percentage of cells expressing each gene and color intensity depicts average expression while numbers indicate average of normalized counts). B (top) UMAPs representing positive (red) and negative (grey) gene expression of CD7 among CD8+T cells (left) and CD56+NK cells (right). (bottom) Intensity of CD7 normalized gene expression between HD and SSc among CD8+T cells (left) and CD56+ NK cells (right). **C** Scatter plot with gene expression values highlighting genes that are specifically enriched in skin T and NK cells of patients with SSc compared to HD. D Representative photos of CD7 immunohistochemistry (IHC) staining of the affected and non-affected skin biopsies from a SSc patient, accompanied by quantification of CD7 IHC scores (n=20). Non-parametric sign test, *p<0.05. **E** Immunofluorescence microscopy showing co-expression of CD7 with CD8⁺ T and CD56⁺ NK cells in early dSSc skin. A representative experiment is depicted in scale of 100 µm. F (left) UMAP displaying T and NK cells from control (healthy) (n=6) and SSc (n=7) lung tissues from patients with interstitial lung disease (GSE128169). (middle) Density plots showing gene expression density of CD7, NCAM1 (CD56), CD4 and CD8A. (Right) CD7 gene expression counts (normalized) between control and SSc lung T and NK cells (each dot represents the average CD7 expression per donor).

To further explore the function of CD7+ T cells, we analyzed the response to activation of cells purified from blood. In SSc blood, a larger fraction of CD8+CD7+ cells were detected compared to healthy individuals (18% of total CD3+ cells in SSc vs 12% in HD) (Figure 3E). The CD7+CD8+T cells from SSc patients upon short (t=4 hours) stimulation with phorbol myristate acetate (PMA) and ionomycin produced significantly more granzyme B (MFI: 40000 in SSc vs 34000 in HD). In addition, SSc CD8+CD7+ T cells were also characterized by increased co-expression of the profibrotic cytokines IL-4 and IL-13 (among CD8+ T cells: 2.5% IL-13+ and 40% IL-4+) compared to CD8+CD7+ cells of healthy controls (among CD8+ T cells: 1% IL-13+ and 30% IL-4+) (Figure 3F). Taken together, these data indicate that CD8+T and NK cells that exhibit cytotoxic and pro-fibrotic properties in SSc, are characterized by increased CD7 expression.

To test the involvement of CD7 in T and NK cell cytotoxicity, we co-cultured healthy peripheral blood mononuclear cells (PBMCs) (n=6) with K562 cancer cells and evaluated T and NK cell cytolytic activity by measuring the release of lactate dehydrogenase (LDH) from the damaged target cells. Interestingly, while blockage of the CD7 receptor did not affect the cell viability of T and NK cells, it was accompanied by significant reduction in their cytolytic capacity towards K562 cells (Figure 3G). This observation suggests that CD7 co-stimulation is important for an efficient cytotoxic response.

In addition, we observed above that SSc skin cytotoxic T and NK cells showed disease-related enrichment of pathways associated with lung fibrosis and proinflammatory/pro-fibrotic manifestations. To explore the potential involvement

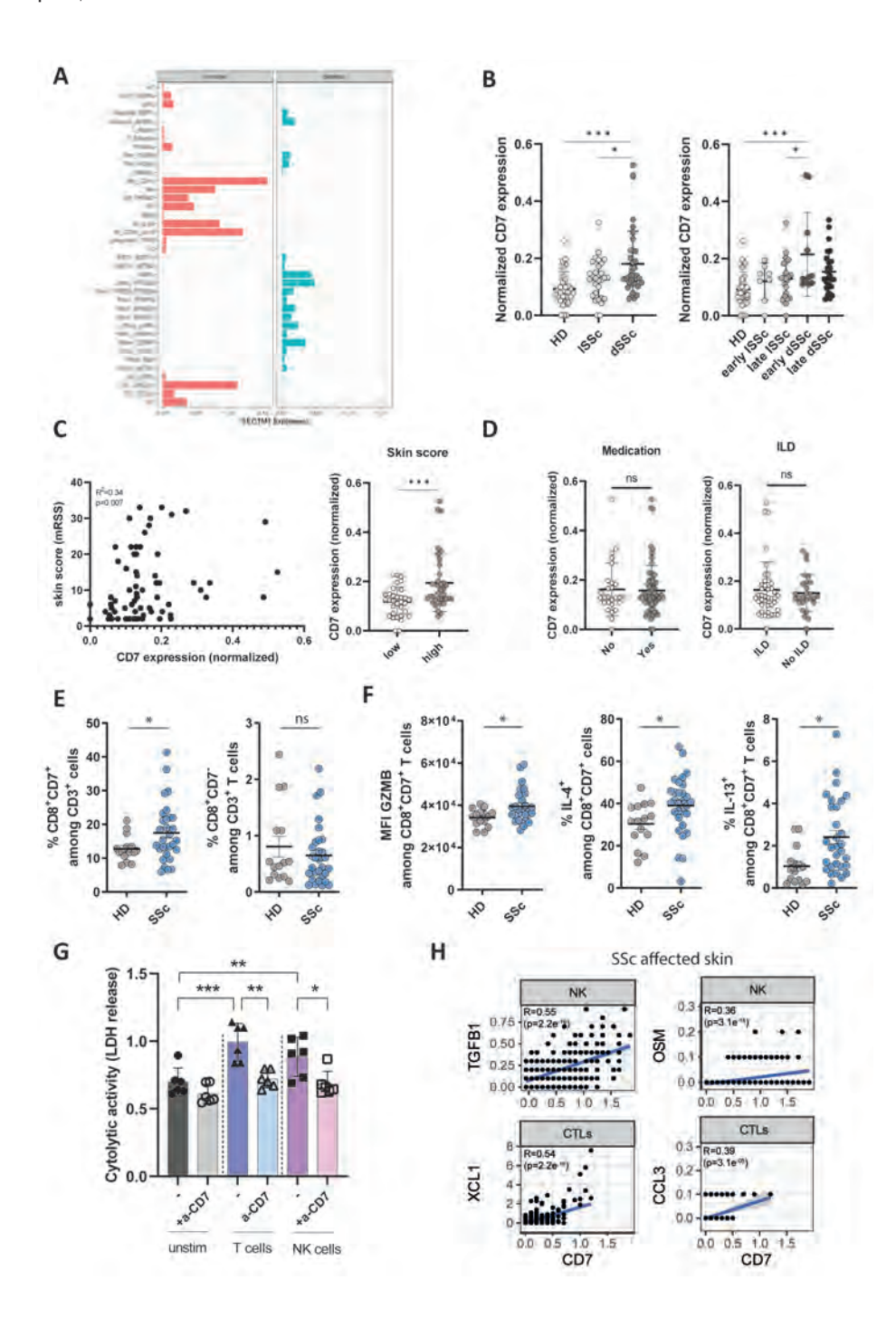


Figure 3. CD7 co-stimulation plays an essential role in T and NK cell cytotoxic and pro-fibrotic manifestations. A SECTM1 log normalized gene expression among skin immune and stromal cell subsets (GSE195452). Annotations of the depicted cell clusters were retrieved from Gur et al. (10). **B** Subgroup analysis of *CD7* normalized gene expression among healthy individuals (HD), and systemic sclerosis (SSc) patients with early versus late limited cutaneous SSc (ISSc) or diffuse cutaneous (dSSc) disease. Early disease was defined as ≤3 years from initial diagnosis. One-way ANOVA with Tukey's multiple comparisons test, *p<0.05, ***p<0.001 **C** (left) Scatter plot showing correlation of *CD7* normalized gene expression with skin score. Each circle represents a single SSc patient. Spearman r=0.34, p=0.07. (right) Normalized CD7 gene expression between SSc patients with low versus high skin scores. The distinction between low and high skin score was as described previously (10). **D** Normalized CD7 gene expression between SSc patients that were treatment naïve or treated with immunosuppressive medication and between SSc patients with or without the presence of interstitial lung disease (ILD). **E** Percentage of CD8+CD7+ and CD8+CD7-T cells in peripheral blood of (n=15) HD and (n=30) SSc. Values are represented as % of total CD3+T cells, *p<0.05. F Expression (Mean Fluorescence Intensity) of Granzyme B (GZMB) and percentage of IL-4+/IL-13+ cells between HDs and SSc CD8⁺CD7⁺ T cells. Expression levels of GZMB are presented as mean fluorescence intensity (MFI) and values of IL-4+/IL-13+ cells are represented as percentage of positive cells among the CD8+CD7+ T cell compartment. Student's t-test, *p<0.05. **G** Cytolytic activity of T and NK cells in a co-culture with K562 target cells was quantified by measuring Lactate dehydrogenase (LDH) release of the target cells. T cells and NK cells were stimulated with anti-CD3/CD28 and IL-2/IL-15 respectively and anti-CD7 was added to block CD7 co-stimulation. Unstim refers to control cells that were not stimulated. Statistical comparisons between groups were performed with ordinary one-way ANOVA with Tukey's multiple comparisons test *p<0.05, **p<0.01, **p<0.001. **H** Pair-wise correlation plots between *CD7* and *XCL1*, TGB1, OSM, MMP9 gene expression within the NK or cytotoxic T cell (CTLs) clusters in SSc affected skin (GSE195452).

of CD7 in the observed pro-fibrotic manifestations of the cytotoxic skin cells, we obtained and merged the gene lists associated with those pathways and performed pairwise correlations with CD7 (Supp Figure 3). Notably, CD7 gene expression in SSc affected skin was positively correlated with expression of profibrotic mediators such as XCL1 (19, 20) and CCL3 (21, 22) in cytotoxic lymphocytes (CTLs) and TGFB1 (23, 24) and OSM (25, 26) in NK cells (Figure 3H). From these observations, it is suggested that CD7 co-stimulation regulates both T and NK cell mediated cytotoxicity and fibrosis.

In vitro elimination of the expanded and activated CD7+T and NK cell subsets by targeted immunotoxin treatment halts fibroblast contraction

The selective upregulation of CD7 expression in cytotoxic T and NK cells in SSc skin can serve as target for therapeutic modulation but also for selective depletion of these cells. For this, we utilized a combination of anti-CD3/CD7 immunotoxins (CD3/CD7-IT) developed to target alloreactive activated T cells and NK cells in graft versus host disease (GvHD) (27). In cultured PBMCs isolated from patients' blood, a significant killing efficacy (>85% cells eliminated) of CD3/CD7-IT was only observed

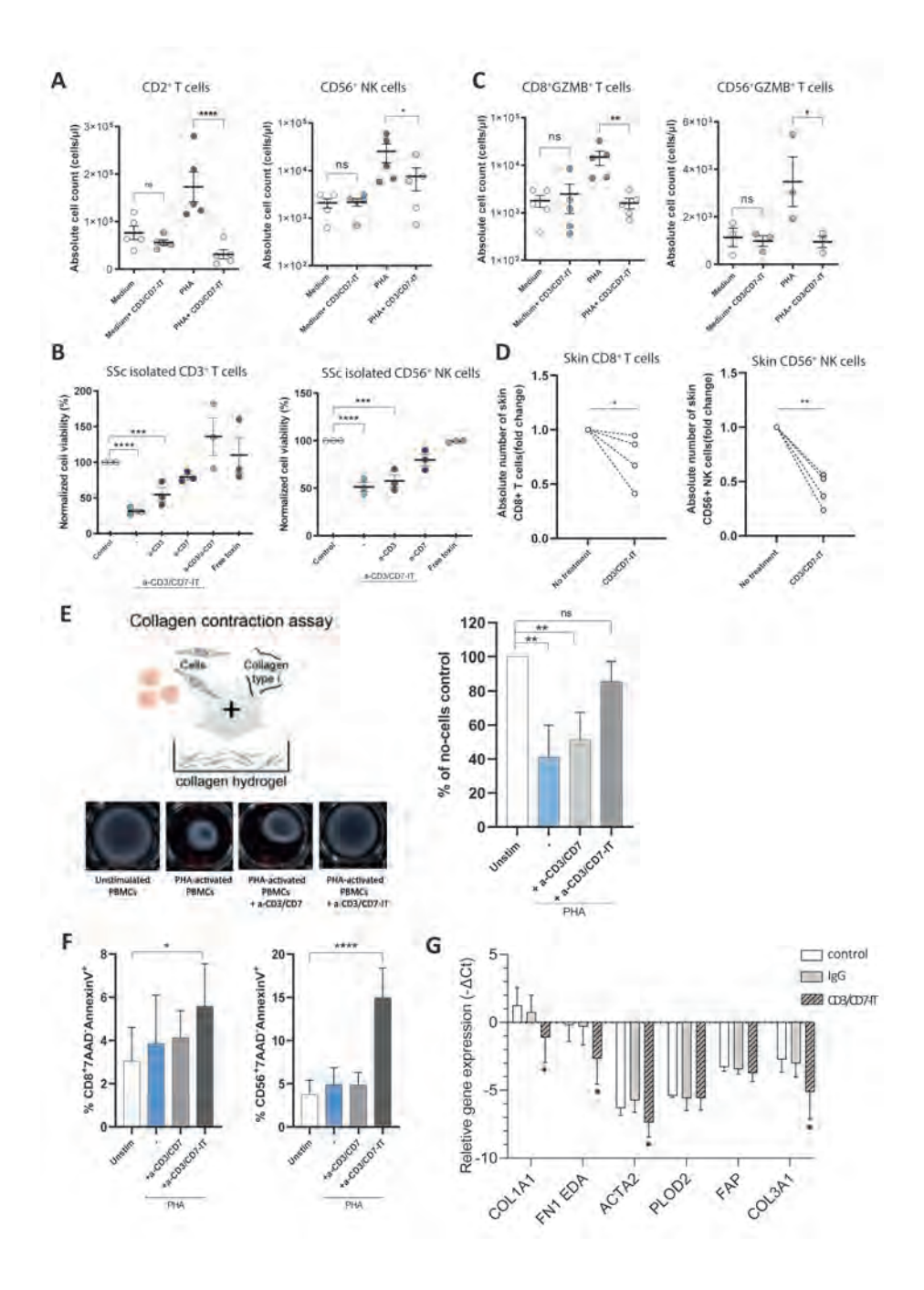


Figure 4. Targeted immunotoxin mediated depletion of activated CD7+ T and NK cells prevents fibroblast contraction and decreases myofibroblast phenotype. A Flow cytometric quantification of CD3/CD7-IT-induced cell death exhibiting absolute cell counts (cells/ul) of CD2+T and CD56+ NK cells in PBMCs isolated from (n=5) SSc patients. **B** Percentage of normalized cell viability of CD3⁺T and CD56⁺ NK cells isolated from SSc (n=3) PBMCs. C Flow cytometric quantification of CD3/CD7-IT-induced cell death illustrating absolute cell counts (cells/µl) of CD8+GZMB+ T and CD56+GZMB+ NK cells in PBMCs isolated from (n=5) SSc patients. D Flow cytometric quantification of CD3/CD7-IT-induced cell death towards CD8+ T and CD56+ NK cells in ex vivo skin explants (n=4). Paired t-test, *p<0.05, **p<0.01. E Schematic representation of our in vitro hydrogel collagen contraction assay in the developed 3D model with co-cultured primary skin fibroblasts and PBMCs. The level of contraction was quantified compared to no-cells control and plotted graphically on the right (n=3). Bars are mean ±SD. An image of a representative experiment is depicted on the bottom of this panel. F The percentage of proapoptotic cytotoxic T (CD8+7-AAD-Annexin V+) and NK (CD56+7-AAD-Annexin V+) cells in the depicted conditions was measured with flow cytometry of the enzymatically digested collagen plugs (n=5). **G** IaG or CD3.CD7-IT treated PBMCS were co-cultured with primary dermal fibroblasts in the developed 3D hydrogel collagen co-culture model and fibroblasts were analyzed for expression of genes reflective of a myofibroblast phenotype. Values represent relative gene expression (- Δ Ct) as measured with qPCR. GAPDH and RPS27A were used as reference genes. Data represents mean ± SEM. Statistical comparisons between three or more groups were performed with ordinary one-way ANOVA with Tukey's multiple comparisons test, *p<0.05, **p<0.01, ***p<0.001. Abbreviations: Phytohemagglutinin (PHA), Immunotoxin (IT), Peripheral blood mononuclear cells (PBMCs).

towards the activated T cells and NK cells (Figure 4A). The combination of CD3 and CD7 immunotoxins had an additive effect on the killing efficacy towards T cells, while NK cells (CD3-CD56+CD7+) as expected were predominantly targeted by the CD7-IT (Figure 4B). Of note, treatment with CD3/CD7-IT also effectively depleted the potentially pathogenic CD8+GZMB+ T cells and CD56+GZMB+ NK cells (Figure 4C). IL-2 production was 9-fold decreased upon treatment (Supp. Figure 6A), supporting that anti-CD3/CD7-IT treatment selectively depleted the activated T cells and NK cells. The surviving CD8+T cells in the CD3/CD7-IT treated condition exhibited a clear alteration in their memory/maturation status: decreased CD8 effector and increased memory and naïve phenotype, showing killing specificity towards effector cells (Supp. Figure 6B). Additionally, upon post-treatment stimulation with PHA, the CD8+ T cells that survived treatment showed diminished cell proliferation (decreased % CD8+Ki-67+ cells) and production of cytotoxic (GZMB) and pro-fibrotic molecules (IL-4) compared to their non-treated counterparts (Supp. Figure 6C). Importantly, treatment with anti-CD3/CD7-IT had no effect on the number nor on the cell viability of CD19⁺ B cells and CD14⁺ M2 monocytes/ macrophages (Supp. Figure 6D, E). Next, we used ex vivo whole skin cultures and showed that upon treatment with anti-CD3/CD7-IT, both numbers of CD8+ T cells and CD56⁺ NK cells were significantly reduced compared to the untreated condition (Figure 4D).

As we achieved specific elimination of the potentially pathogenic CD7⁺ T cells and NK cells, we next evaluated whether this depletion exhibits therapeutic relevance. Fibrosis accompanied by skin tightening is the main disease hallmark of SSc, so we developed a novel 3D collagen fibroblast: immune cell co-culture hydrogel model that enables to study fibroblast contractility (*Figure 4E*). In this model, spontaneous fibroblast contraction happened in the presence of allogeneic PBMCs and the level of contraction was significantly larger in the presence of PHA-activated PBMCs. PHA upregulates CD3 and CD7 expression on T cells and CD7 on NK cells (Supp. Figure 6F, G), so this model mimics the effector functions of the potentially pathogenic immune cell subsets on fibroblasts in vitro. Fibroblasts that were cocultured with sorted CD7+T cells and NK cells exhibited increased contractility and a higher expression of IL-6, collagen type 1 and alpha smooth muscle actin (a-SMA) compared to fibroblasts co-cultured with CD7⁻ cells (Supp Figure 7). Next, we pretreated PHA-activated PBMCs with 0.33 nM a-CD3/CD7 antibodies or CD3/CD7-IT and showed that only upon immunotoxin treatment, fibroblast contraction was significantly reduced compared to PHA activated PBMCs (Figure 4E). Under these conditions (24 hrs of co-culture), the percentage of necrotic CD8+ or CD56+ cells was not (vet) significantly affected (**Supp. Figure 6H**). However, we observed a sharp increase in apoptotic CD8+ and CD56+ cells (Figure 4F). Interestingly, fibroblasts that were co-cultured with CD3/CD7-IT treated PBMCs exhibited a decreased gene expression of COL1A1, FN1 and ACTA2 (Figure 4G), indicating a lowered profibrotic phenotype.

Administration of bispecific CD3/CD7-IT treatment in the first patient with SSc effectively eliminates pathogenic CD7+ cells in blood and skin

A 34-year-old male patient with severe diffuse cutaneous SSc showed disease progression following autologous hematopoietic stem cell transplantation (ASCT) that did not respond to treatment with mycophenolate mofetil, prednisone and rituximab. The patient had developed severely invalidating diffuse skin fibrosis (a modified Rodnan skin score of 27), joint contractures, high inflammation parameters with ESR 49 mm/Hour (< 15mm/Hour) and CRP 78 mg/L and joint contractures. He was bedridden with a very poor prognosis and was therefore treated with CD3/CD7-IT as last resort. Treatment resulted in a depletion of circulating and skin-resident T cells and NK cells, and a normalization of C-reactive protein (CRP) levels from 131 mg/L to 27 mg/L after four weeks, which CRP levels then further decreased to normal after 5 months. His functional status stabilized, with an observed increase in quality of life, yet with a persistent invalidation due to severe skin-tightening and joint contractures that proved irreversible. The patient died 1.5 years after CD3/CD7-IT treatment from disease complications.

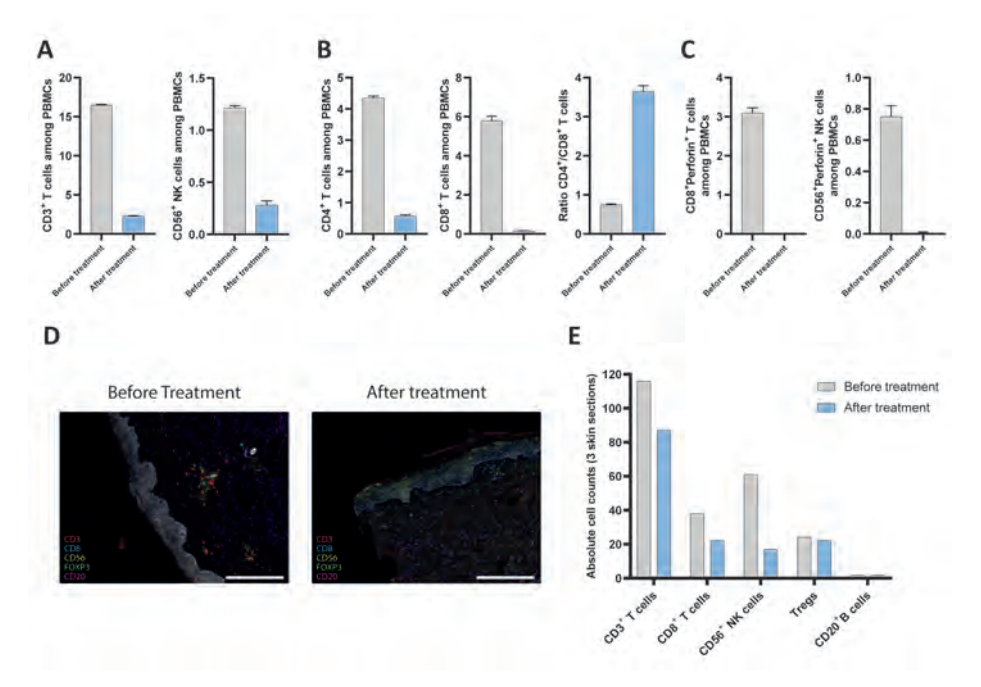


Figure 5. Treatment with a-CD3/CD7-IT depletes cytotoxic T and NK cells in an early dSSc patient's blood and skin. Percentage of **A** CD3⁺T and CD56⁺ NK cells **B** CD4⁺T and CD8⁺T cells **C** CD8⁺Perforin⁺T and CD56⁺Perforin⁺ NK cells in SSc patient's peripheral blood before and after treatment with a-CD3/ CD7-IT. Values are represented as % of total live peripheral blood mononuclear cells (PBMCs). **B** (right) Ratio of CD4+/CD8+ T cells before and after treatment. **D** Representative immunofluorescent images and **E** quantification of lymphocyte subsets in the patient's affected skin before versus after treatment.

Biologic responses to CD3/CD7-IT treatment were measured with flow cytometry in patient's blood and multiplex immunofluorescent staining in skin pre- and post- drug administration. Consistent with the expected in vitro effect, treatment with CD3/CD7-IT directed a profound elimination of circulating T cells and NK cells. Already one week after administration, the amount of circulating T cells and NK cells was reduced by 86% and 77% respectively (Figure 5A). CD8+ T cells were preferentially targeted by CD3/CD7-IT compared to CD4⁺ T cells. More specifically, the percentage of CD8⁺T cells exhibits a 37-fold decrease while CD4⁺T cells show an 8-fold reduction. (Figure 5B). We further explored the killing efficacy of CD3/CD7-IT towards effector cytotoxic T cell and NK cell populations. Effector cytotoxic T cells were characterized as CD8+Perforin+ and NK cells as CD56+Perforin+. Interestingly, both CD8⁺Perforin⁺ and CD56⁺Perforin⁺ cell populations were completely depleted (100%) in this patient's blood (*Figure 5C*). The therapeutic effectiveness towards skin-resident T and NK cells was then evaluated with multiplex immunofluorescence staining of skin biopsies before and after treatment. Post-treatment, skin biopsies showed a remarkable reduction in immune cell infiltration (*Figure 5D*). More specifically, absolute cell counts of CD3+T cells, CD8+T cells and CD56+NK cells were all considerably reduced post treatment. Importantly, the numbers of CD3+FOXP3+ regulatory T cells and CD20+B cells were not affected (*Figure 5E*). While the treatment outcome was considered positive and clinically meaningful, we expect even greater benefit when CD3/CD7-IT is applied earlier in the course of the disease, when the inflammatory component is more prominent and the fibrotic process not yet irreversible.

Discussion

Here, we show that SSc affected skin contains increased numbers of proliferating T cells, cytotoxic T cells and NK cells. These cells exhibit a cytotoxic, pro-inflammatory and pro-fibrotic gene signature. When focusing on their co-stimulatory and inhibitory molecule expression, these cells express the co-stimulatory molecule CD7 in association with pro-inflammatory and pro-fibrotic genes, especially in recent-onset and severe disease. Furthermore, we show that CD7 regulates cytolytic activity of cytotoxic T cells and NK cells and that selective depletion of CD7+ cells prevents cytotoxic cell induced fibroblast contraction by halting their pro-fibrotic phenotype. Finally, CD3/CD7 directed depletive treatment depleted CD7+ cells and stabilized disease manifestations in a severely affected SSc patient.

The role of T cells in mediating the pathology of SSc has been a subject of controversy. The importance of the immune system, however, is highlighted by recent observations indicating that in treatment with ASCT, long-term remission of SSc disease manifestations can be achieved (27). CD4+T cells have been considered as main effector cells since genetic studies indicated that some MHC class II polymorphisms confer a risk of acquiring SSc (5, 8, 28). Recently, however, MHC class II polymorphisms were shown to confer not so much risk on SSc incidence as on the development of disease related autoantibodies that precede development of clinical disease in a proportion of cases (29). Because of its' fibrotic clinical manifestations, SSc has been considered a T helper type 2 (Th2) mediated disease (30, 31). However, epigenetic studies revealed gene transcription in cytotoxic T cells and NK cells in SSc patients with disease risk loci (5). Also, SSc skin was found to be predominantly infiltrated by cytotoxic T cells, in proximity to pre-apoptotic

endothelial cells (4). Another recent study associated increased infiltration of IFN-v producing effector T cells and NK cells in SSc skin to fibrotic activation of fibroblast subsets (10). Our study confirms these data, and our functional analyses suggest that SSc skin disease is driven by T cells and NK cells that produce cytotoxic proteins such as granzyme B and perforin, induce fibroblast contractility and myofibroblastic phenotype, and produce well described pro-fibrotic mediators such as TGFB1, XCL1, CCL3 and OSM. This suggests that increased cytotoxicity in SSc skin may be associated with induction of the fibrotic pathology of the disease.

Our study addresses the question how the cytotoxic immune response in SSc is regulated. Cytotoxic T cells and NK cells are central effector cells in cancer and infections. Their effector response is tightly regulated by the expression of activating and inhibitory surface receptors (32). Here we find that cytotoxic cells in SSc consistently express high levels of CD7. Of interest, IFN-y, a key cytokine in cytotoxic immune responses, is the main inducer of SECTM1, the ligand of CD7 (18). This suggests that SECTM1-CD7 interaction is part of an IFN-y driven feedback loop that enhances cytotoxic responses in SSc skin.

The other side of the coin is that in chronic viral infection and cancer cytotoxic cells develop reduced and altered effector functions due to a process termed exhaustion. Exhaustion involves increased expression of inhibitory receptors such as PD-1, LAG-3, TIM-3 and CTLA-4 (33). The extent of exhaustion varies from dysfunction to anergy or clonal deletion and is determined by factors such as antigen abundance and TCR affinity. The mechanisms in autoimmunity are less certain. In a model of autoimmunity activation of autoreactive CD8+ cytotoxic T cells was restrained by LAG-3 (7). T cell exhaustion in patients with systemic autoimmune disease has mainly been investigated and described in peripheral blood samples and not in tissues where autoantigen presentation occurs (34, 35). We found that in SSc skin compared to healthy skin a subset of cytotoxic T cells expressed LAG3, suggesting a restrained phenotype. Only a few cytotoxic T cells expressed PD-1 in conjunction with FOXP3, suggesting they are regulatory T cells. Taken together, cytotoxic lymphocytes in SSc skin are characterized by an activating rather than an exhausted profile.

This study reconfirms the importance of autoimmunity in driving SSc pathology. This is clinically relevant since ASCT can cure the disease but is a high-risk procedure and only applicable to a very restricted group (<10%) of SSc patients (27). Other currently used broad immunosuppressive treatments do not cure the disease and can only slow down fibrosis to a limited extent. Selective targeting of activated lymphocytes may represent a more selective and safer treatment for SSc. Thus, we utilized a novel combination of anti-CD3/CD7-IT that has been developed to deplete activated alloreactive T cells and NK cells for the treatment of GvHD (36). We gave proof of concept that treatment with a-CD3/CD7-IT, can selectively deplete the activated cytotoxic T cells and NK cells in blood and SSc affected skin. Because of its depletive nature, anti-CD3/CD7-IT is administered as single treatment and that furthers support its favorable safety profile. In line with this notion, CD7 targeting therapeutic approaches have shown clinical efficacy and safety in kidney transplantation patients (36, 37). Previously, we showed that anti-CD3/CD7 immunotoxin treatment was well tolerated and increased survival rates in patients with acute GvHD. Similarly to ASCT, a significant increase in the diversity of T cell repertoires that entailed new polyclonal T cell populations was observed, suggesting the efficacy of our treatment approach in rebalancing the immune composition (36).

Our study comes along with some limitations. First, the analyzed sc-RNA seq datasets lack T cell receptor (TCR) sequencing and this hampers the investigation of (auto)antigen-specific T cell responses. In future studies, it is of importance to examine whether the cytotoxic T cells are clonally expanded and autoreactive or bystander-activated cells. Secondly, our results suggest that prevention of fibroblast contraction is mediated by CD7+ cytotoxic lymphocytes. However, additional research is needed to investigate if autoantibodies and other immune cell subsets such as macrophages contribute to this process. Finally, the safety and clinical efficacy of the CD3/CD7-IT for treatment of SSc needs to be investigated in a well-designed and prospective study. Given the large SSc heterogeneity, and since CD7 upregulation was profound in patients with early diffuse disease, our results suggest that this SSc subpopulation is expected to benefit from such a therapeutic approach in particular.

In conclusion, we found that CD7 activation regulates cellular cytotoxicity-driven pathologic processes in SSc. Together the findings imply co-stimulatory molecules as key regulators of cytotoxicity-driven pathology in systemic autoimmune disease, yielding a flag for selective depletion of pathogenic cells.

Online supplemental methods

Study design

The objective of this study was to delineate the role of co-stimulatory receptors in regulating cytotoxic cell driven pathologic processes in the affected skin of patients with systemic sclerosis (SSc) and examine whether therapeutic targeting of such receptors halts SSc pathology. To address these questions, we performed single-cell RNA sequencing analysis of two separate SSc cohorts (total of n= 109 SSc and n= 65 healthy individuals) containing skin cells from SSc and healthy individuals and used multiplex immunohistochemistry for spatial imaging (n=24) and multi-color flow cytometry for protein level confirmation. We further analyzed the effects of costimulatory modulation in functional assays using (i) stimulation/ inhibition of primary lymphocytes from SSc individuals with recombinant proteins, (ii) blocking antibodies in co-cultures of lymphocytes with K562 target cells and (iii) in a fibroblast/immune cell co-culture collagen contraction assay that serves as a disease-relevant in-vitro model to mimic SSc tight and hard skin. Treatment efficacy of a novel combination of bispecific anti-CD3/CD7 targeting immunotoxin was evaluated (i) in lymphocytes from SSc individuals' blood, (ii) ex vivo skin cultures and (iii) in a severely affected SSc patient who was treated on compassionate use with a novel anti-CD3/7 immunotoxin (CD3/CD7-IT) treatment. Functional experiments were performed with multiple biological and technical replicates as mentioned in each figure's legend and in each assay's methods description.

Patient and public involvement

This research incorporated the active participation of patients in its design and execution. Two patient research partners were proactively involved in the design of primary research questions and methods of patient recruitment by structured interviews and regular, interactive discussions. Patient research partners were trained in the context of STAP ("Key To Active Participation"), an initiative of the department of rheumatic diseases of the Radboud University Medical Centre (Nijmegen, the Netherlands) to establish a patient panel within the hospital setting to provide support for rheumatology research (38). The involvement of patients and their families in disseminating the results of this study in patient organizations played a central role in motivating community engagement both during and after the study.

Patients

Our study was approved by the local research ethics committee of Radboud University Medical Center, the Netherlands (study numbers: NL57997.091.16, NL67672.091.18). All procedures regarding patient participation followed the Declaration of Helsinki principles were performed in accordance with the relevant Dutch legislation regarding reviewal by an accredited research ethics committee, with the file number 2021-8193. All patients (aged >18) that donated whole blood and skin biopsies, were diagnosed with established systemic sclerosis disease according to the ACR 1980 preliminary classification criteria(39). SSc patients with overlapping syndromes were not included in our study. Blood samples from age and sex matched healthy volunteers were collected from Sanquin bloodbank (project number: NVT 0397-02) from individuals that consented on donating blood for medical research. All patients agreed to participate in the study before blood withdrawal or skin biopsy acquisition. For analyses were we examined the relationship between CD7 normalized mean gene expression and selected patient clinical characteristics, SSc patients' clinical data were received as part of a previous publication(10).

Immunotoxins

The anti-CD3/CD7 combination of immunotoxins (CD3/CD7-IT) as referred to in this article contains a 1:1 mixture (w/w) of the murine monoclonal antibodies SPV-T3a (anti-CD3) and WT1 (anti-CD7) that are both conjugated to recombinant ricin toxin A as has been previously described (36, 40).

Peripheral blood mononuclear cell (PBMC) isolation, cryopreservation and culture

PBMCs were isolated from patients' (n=30) and healthy donors' (n=15) peripheral blood by Ficoll Pacque PLUS density centrifugation and cultured in complete RPMI medium 1640+ GlutaMAXTM (Gibco, ref 72400-021) supplemented with 100 IU/ml penicillin, 100 mg/ml streptomycin, 100 mg/L sodium pyruvate and 10% human pooled serum. PBMCs that were not processed immediately were cryopreserved and stored in liquid nitrogen until further use. To generate phytohemagglutinin (PHA)-activated T cells, PBMCs were first seeded in 96-well-u bottom plates (Greiner) at a cell density of 100,000 cells per well and then stimulated with 5 μ g/ml PHA (Roche, cat# 11082132001) for 24 hours at 37 °C, 5% CO2. To evaluate production of cytokines, prior to flow cytometric staining, PBMCs were stimulated for 4 hours at 37 °C, 5% CO2, with 12.5 ng/ml phorbol myristate acetate (Sigma), and 500 ng/ml ionomycin (Merck) in the presence of 5 μ g/ml brefeldin A (Merck).

Collection and cell culture of primary fibroblasts

Half piece of 4 mm diameter skin biopsies was placed in 24 well plates containing 2 ml DMEM Glutamax medium (Gibco, Waltham, MA, USA) that was supplemented

with 100 U/ml penicillin, 100 mg/ml streptomycin, 100 mg/L sodium pyruvate and 20% fetal calf serum. Plates were incubated in regular culture conditions (5% CO2, 37 °C, 95% humidity) for 2 weeks in which primary skin fibroblasts spontaneously grew out Medium was refreshed every 3-4 days. After outgrowth, primary fibroblasts were cultured in DMEM Glutamax medium (Gibco) that was supplemented with 100 U/ml penicillin, 100 mg/ml streptomycin, 100 mg/L sodium pyruvate and 10% fetal calf serum and used in experiments after passage 5.

Isolation, culture and cell viability of T cells, B cells and NK cells from SSc peripheral blood

Cryopreserved PBMCs from patients with systemic sclerosis were thawed and washed as previously described to isolate specific immune cell populations. CD3+ T cells were isolated with a magnetic negative selection according to the manufacturer's instructions (MojoSort pan CD3⁺ T cell isolation kit; Cat# 480021). CD19⁺ B cells were also isolated with negative selection using the MojoSort TM Human Pan B cell Isolation Kit (cat# 480082). Isolation of untouched CD56+ NK cells from SSc PBMCs was performed by using NK isolation kit (Miltenyi Biotec, cat# 130-092-657), according to manufacturer's protocol. After isolation, enriched CD3+ T cell, CD19+ B cell and CD56+ NK cell fractions exhibited more than 95% purity as evaluated by flow cytometry staining for CD3, CD19, CD56 markers. The isolated immune cell populations were cultured with XVIVO™ 15 medium (Lonza, cat# 04-418Q) at a density of 50,000 cells/well in 96-well u bottom plates (Greiner). To evaluate cell viability of the cells after different stimulation (24 hours) and treatment conditions (48 hours), the CellTiter-Glo® 2.0 Cell Viability Assay (Promega) was used as per manufacturer's instructions. Cells were also treated with 5 mM cycloheximide (Sigma, cat# 01810-1G) as positive control. Luminescence was measured with the use of CLARIOstar Plus (BMG LABTECH). For every experimental condition, 4 technical replicates were used and the average of them was used in further analysis. Experimental values were corrected for medium luminescence and were normalized to the control unstimulated and untreated conditions.

Monocytes isolation and differentiation to M2 macrophages

CD14⁺ monocytes were isolated from PBMCs with positive selection kit (Miltenyi Biotec, cat# 130-050-201) according to manufacturer's instructions. Monocytes were then seeded in 6-well plates at a cell density of 1 million cells per well at a volume of 2 ml in XVIVOTM 15 medium that was supplemented with 100 IU/ml penicillin, 100 mg/ml streptomycin and 2% human pooled serum. Differentiation towards M2-like macrophages was stimulated by adding 20 ng/ml rhM-CSF (R&D Systems, cat# 216-MC) and 10 ng/ml rhlL-4 (Biolegend, cat# 500815). The duration of culture was 7 days and medium with cytokines was refreshed at day 3. Cell viability of M2-like macrophages was evaluated with CellTiter-Glo® 2.0 Cell Viability Assay (Promega) as previously described.

Immunohistochemistry

Immunohistochemical analysis was performed on formalin fixed paraffin embedded (FFPE) skin biopsies of 20 patients with systemic sclerosis. Skin biopsies were obtained from both an affected and non-affected area of the forearm as diagnosed by an expert clinician via surgical excision with a 6-mm ø punch biopsy. In all cutaneous specimens staining for CD3 was used as a marker to evaluate T cell infiltration and CD7 to assess infiltration of activated T lymphocytes and NK cells. For the CD3 staining, slides were deparaffinized with xylol wash and rehydrated with ethanol. Antigen was retrieved in 10 mM sodium citrate buffer (pH 6.0) room temperature (RT). Blocking of the peroxidase activity was conducted by incubation with 3% H202 in or 30 min. Then, sections were incubated with the primary mouse CD3 anti-human monoclonal antibody (1:200 dilution in PBS containing 1% BSA; Clone F7.2.38; Dako; Cat# M7254) overnight at RT. Next, tissues were incubated with secondary antibody (BrightVision Poly-HRP, Immunologic DPVO55HRP) for 60 minutes at RT. 3'3'-diaminobenzene was used to visualize antibodies (bright DAB, Immunologic). Nuclei in all slides were counterstained with hematoxylin and mounted with a cover slip (Permount, Thermo-Fischer, Waltham, MA, USA). CD7 was immunohistochemically evaluated with the use of the Omnis automatic immunostainer (DAKO) according to manufacturer's standard procedures. In brief, FFPE tissues were deparaffinized, rehydrated and subjected to heat-mediated antigen retrieval (30 min at 97° C). Followingly, endogenous peroxidase was blocked and the primary mouse CD7 anti-human monoclonal antibody (ready to use, diluted in Envision Flex Antibody Diluent, clone CBC.37, DAKO; Cat# GA64361-2) was added for 20 min at RT. Secondary antibody (Envision Flex HRP, DAKO) was then applied for 20 min at RT. Antibody complex was developed with Envision Flex Substrate Working solution (DAKO) and nuclei were counterstained with hematoxylin. Human synovial/tonsil specimens were used as positive controls and skin sections without the primary antibodies as negative controls. Cellular infiltrates were examined through the whole surface of all sections (n=4) mounted per donor and condition and imaged with CaseViewer (v2.3.0.99276). CD3 positive cells were counted by 2 independent observers in four randomly selected fields and total number of positive cells was plotted as mean ± SD. CD7 positive staining was assessed using an arbitrary 0-4 semiquantitative scoring system of positively stained areas. This scoring was performed blindly by 2 independent observers. Expression of collagen type 1 (Goat Anti-Type I Collagen-UNLB, Southern Biotech, cat# 1310-01) in fibroblasts was also evaluated. Staining was performed similarly to CD3 marker with the exception that incubation with a secondary rabbit biotinylated anti-goat IgG antibody (Vector Laboratories, PK-6101) was performed for 30 minutes at room temperature. Values illustrated in the graphs represent mean \pm SD.

Multiplex immunohistochemistry staining and imaging of SSc skin

For multiplex immunofluorescent staining, 5 µm thick sections from matched affected and non-affected skin of 24 SSc patients were included. Slides were stained by an automated platform with the use of Opal 7-color Automation IHC kit (NEL801001KT; PerkinElmer) on the BOND RX IHC & ISH Research platform (Leica Biosystems) as it has been previously described (41). Incubation with primary and secondary antibodies was for 1 hour and 30 min respectively at RT. For the detection of skin lymphocyte cell populations the following antibodies were used; anti-CD56 (Cell Marque, 156R-94, clone MRQ-42) with Opal620, anti-CD8 (Dako, M7103, clone C8/144B, 1:200) with Opal690, anti-CD7 (Dako, GA64361-2, clone CBC.37, 1:30) with Opal480, anti-CD3 (Thermo Fisher, RM-9107, clone RM-9107, 1:200) with Opal520, anti-FOXP3 (eBioscience Affymetrix, 14-4777, clone 236A/ E7, 1:100) with Opal570 and anti-CD20 (ThermoFisher, MS-340, clone L26, 1:600) with Opal570. Slides were stained with DAPI for 5 minutes, washed and mounted with Fluoromount-G (SouthernBiotech, 0100-01). Slides were then scanned by the Automated Quantitative Pathology Imaging System (Vectra V.3.0.4, PerkinElmer) with using an overview of 4x magnification. Annotation of multispectral images of skin tissue was performed with Phenochart (V.1.0.9, PerkinElmer) and scanned at 20x magnification. Spectral unmixing of the Opal fluorophores was done by InForm software (V.2.4.2, PerkinElmer) and the multichannel images were then digitally merged. For quantitative analysis, digital scans containing whole skin biopsies (n=3 sections per biopsy per donor and condition) were quantified by QuPath-0.4.4 (42).

Single-cell RNA sequencing analysis

The single-cell count matrix (Cell by Gene) was obtained from two publicly available datasets, namely GSE195452, GSE138669 and GSE128169. Preprocessing of the data was performed using Seurat (version 4.3.0) (40). Quality control measures were implemented by filtering out cells with a high content of mitochondrial genes (>5%) and cells with gene counts per cell values below 200 or above 2000. Subsequently, CD3+ and/or CD7+ cells were sorted, resulting in the recovery of 2126 and 5061 high-quality cells from both datasets, respectively. Later, the CD8+ subset of cells was sorted from these cells for separate analyses.

For primary dimension reduction, non-negative matrix factorization was employed, followed by the application of UMAP: Uniform Manifold Approximation and Projection (43, 44) with Louvain clustering, as previously described by Singh et al. (45). The FindAllMarkers function of Seurat was then utilized to identify differentially expressed genes (DEGs) within each cluster, which were subsequently annotated based on the characteristics of these DEGs. An R package pheatmap (Kolde, R. (2019). pheatmap: Pretty Heatmaps (R package version 1.0.12)) was used to visualize the DEGs across the cell types/groups.

To assess DEGs between healthy and diseased individuals, the FindConservedMarker function of Seurat was employed. Additionally, the Wilcox-Test (46) was applied to test for differences in cell frequencies between healthy individuals and those with systemic sclerosis (SSc).

Single-Sample Gene Set Enrichment and Correlation analyses

To gain insights into the functional characteristics of each cell type, we performed single-sample gene set enrichment analysis (ssGSEA) using the escape R package (47) with WikiPathways from MsigDB (48) as the reference gene set collection.

An R function called *geom_tile* from ggplot2 package (Wickham, H. (2016). ggplot2: Elegant Graphics for Data Analysis (2nd ed.). Springer) was used to visualize the pathways across different cell types/groups. The difference in the distribution of Normalized Enrichment Scores (NES) between control and SSc group was tested using Kolmogorov-Smirnov test (49). To capture pathways associated with fibrosis and inflammation, we retrieved the gene list related to these processes and further augmented it by including CD7.

Performing correlations at the single-cell level can be noisy and biased by technical factors. Hence, we constructed a meta-cell object (from previously described Seurat object) comprising CD3/CD7+ cells, by employing the WGCNA R package (50). This object contains framework weighted gene co-expression to identify modules of highly correlated genes. Subsequently, from this meta-cell object was used to obtain pairwise correlations and p-values were computed using the Hmisc function from the Hmisc R package (Harrell Jr., F. E., & with contributions from Charles Dupont and many others (2020). Hmisc: Harrell Miscellaneous (R package version 4.8.0). An R package ComplexHeatmap (Gu, Z. (2016). ComplexHeatmap: Making Complex Heatmaps in R (R package version 2.10.0)) was used to visualize the correlations.

Flow cytometry analysis

Per donor, 1 x 106 PBMCs were first labeled with ViaKrome 808 fixable viability dye (1.5:1000 in PBS) for 30 min at 4 °C to exclude dead cells and then stained for 20 minutes at RT with fluorescently labeled extracellular antibodies (supplemental table 1). For intracellular stainings (supplemental table 2), cells were fixed with permeabilized using the Cyto-Fast™ Fix/Perm Buffer Set (Biolegend) according to manufacturer's quidelines. To facilitate detection of intracellular cytokines, cells were pre-stimulated with 12.5 ng/ml phorbol 12-myristate 13-acetate (PMA) (Sigma), 500ng/ml lonomycin (Merck) and 5 ug/ml brefeldin A (Merck) before staining. Samples were acquired on a Beckman Coulter Cytoflex LX 21-color flow cytometer immediately after staining.

Multi-parameter flow cytometric quantification of CD3/CD7-ITinduced cell death

To evaluate the killing efficacy of CD3/CD7-IT towards activated T and NK cells in vitro, we developed a model in which a 24-hour PHA (Roche) stimulation of PBMCs was used to mimic disease related T cell activation. PHA stimulation was accompanied by elevated surface expression of CD3 (2-fold increase in MFI) and CD7 (3-fold increase in MFI) antigens on cytotoxic CD8+GZMB+ T cells and CD7 (2-fold increase in MFI) on CD56+GZMB+ NK cells (Supp. Figure 6A, B). Nonactivated or PHA-activated (5 µg/ml) PBMCs were cultured for 24 hours at 37° C, 5% CO₂ before treated with CD3/CD7-immunotoxin (IT) for 48 hours. Based on previous studies, the in vitro clinically therapeutic concentration was between 1-5 nM. We titrated drug concentration (0-10 nM) based on its killing efficacy towards primary T cells, and we chose the lowest concentration exerting maximum killing efficacy. Concentration of the drug that was used in in-vitro experiments was 0.33 nM. Post treatment, cells were collected in 15 ml conical tubes, washed with PBS and processed for flow cytometric staining. Staining protocol for live/ dead, extracellular and intracellular markers followed as was previously described. CD2 was used to identify and characterize T cell populations, instead of CD3, due to possible modulation of the CD3 antigen from the CD3/CD7-IT treatment. To enable quantification of absolute cell counts, a fixed amount of counting beads (Precision Count BeadsTM, Biolegend, cat# 424902) was added in each sample prior to acquisition. Samples were acquired on a Beckman Coulter Cytoflex LX 21-color flow cytometer immediately after staining.

Ex vivo skin culture

Full thickness 6 mm diameter skin punch biopsies were obtained from the abdomen of 4 healthy individuals that underwent plastic surgery. All patients signed informed consent that their surgical leftover material will be used for research purposes. From each skin tissue, 4-6 punch biopsies were received and cut in half. To account for a potentially inequal infiltration of immune cells between skin biopsies, all skin pieces were pooled together and then distributed equally in the different experimental conditions. The skin tissue was cultured in 24-well plates in 1 ml of RPMI medium 1640 with 100 IU/ml rhIL-2 (Thermo Fischer, cat# 16-7027-85), 5 ug/ml PHA (Roche), growth supplements and antibiotics. Twenty-four hours later, samples were treated with 0.33 nM a-CD3/CD7-IT. After 48 hours, the skin pieces of each condition were used to obtain single-cell suspensions containing skin infiltrating lymphocytes for functional assays. Protocol that was used combines mechanical and enzymatic dissociation of the skin tissue and has been extensively described by He et al. (51).

Apoptosis assay

To distinguish early apoptotic cells from non-apoptotic and cells in late apoptosis/ necrosis, cells were first stained extracellularly with monoclonal antibodies of interest for 20 minutes at RT. Cells were then washed twice with cold PBS and resuspended in 100 μ l of a buffer containing 5 μ l 7-AAD (eBioscience, cat# 00-6993-50), 5 μ l Annexin V:FITC labeled (BD Pharmigen) and 0.15 μ l CaCl2 (1 M) in PBS. Samples were incubated in the dark at RT for 10 minutes and were acquired by flow cytometry (Gallios) immediately after staining. Cells being 7-AAD+AnnexinV+ are referred to as late apoptotic/necrotic cells while cells being 7-AAD-AnnexinV+ as early apoptotic. Live cells are negative for both 7-AAD and AnnexinV.

Cytokine measurements

Quantification of human cytokines and chemokines in culture supernatants were measured by Luminex. The Bio-Plex Pro Human Cytokine 27-plex Assay (Bio-Rad, cat# M500KCAF0Y) was used following the manufacturer's instructions. Samples were analyzed with BioPlex Manager 4 software (Bio-Rad Laboratories, Hercules, CA, USA).

LDH cytotoxicity assay

To assess cytotoxic capacity of cytotoxic T and NK cells, Lactate dehydrogenase (LDH) was measured in PBMC and K562 cell co-culture supernatants using a LDH-cytox kit according to manufacturer's protocol (Biolegend #426401). PBMCs and K562 cells were seeded into 96-well plates (F-bottom) in a 10:1 ratio, using triplicate wells. To augment cytotoxic function of CD8+ T cells and NK cells, PBMCs were stimulated overnight with 1 μg/ml anti-CD3/CD28 (Biolegend, cat# 317326, 302913) or 500 IU/ml IL-2 (Thermo Fischer, cat# 16-7027-85), 10 ng/ml IL-15 (Gibco,

PHC9154) respectively. To evaluate the involvement of CD7 receptor in T and NK cell cytotoxicity 330 nM of anti-CD7 (WT1) blocking antibody was used. Percentage of cytotoxic capacity was calculated according to the formula: %cytotoxicity= (experimental value-low control value)/(high control value-low control value) x 100. Low and high control values correspond to LDH levels of K562 cells alone without or after addition of lysis solution respectively.

Fibroblast and immune cell in vitro co-culture collagen contraction assav

Primary healthy human fibroblasts were detached with trypsin and were then brought to a cell density of 2 x 106 cells/ml. PBMCs from 5 healthy individuals were thawed and washed as previously described and stimulated/treated with the different experimental conditions mentioned in the results section. Cell suspension containing a mixture of PBMCs and fibroblasts in a 5:1 ratio was then prepared. To create the 3D collagen hydrogels, for every plug, 20 µl Minimal Essential Medium (Sigma-Aldrich, Saint Louis, CA, USA), 10 µL sodium bicarbonate (Gibco, Waltham, MA, USA), 150 µL soluble collagen (PureCol, type 1 collagen) and 90 µL cell suspension were sequentially mixed in a different tube and the respective order. After the suspension was delicately homogenized, 250 µl was added per well of 48-well plates. Thereafter, 750 µl of complete RPMI medium was added and the plugs were incubated under standard conditions for 24 or 48 hours. Spontaneous fibroblast contraction was macroscopically evaluated by scanning plates on a standard office flat-bed scanner. To quantify the area of contraction, generated images were analyzed with Fiji ImageJ. To further study the phenotype and function of this model's lymphocytes and fibroblasts, after macroscopic evaluation, the collagen plugs were enzymatically digested with a mixture of collagenase D, Dispase and DNase in plain RPMI medium supplemented with 100 U/ml penicillin, 100 mg/ml streptomycin for 1 hour at 37 °C on a roller. Reaction was stopped with the addition of complete RPMI medium containing 10% HPS and singlecell suspensions were then washed twice with PBS and used for flow cytometry analysis. To co-culture fibroblasts with CD7+ or CD7-T and NK cells (**Supp. Figure 7**) these cells were FACS sorted from PBMCs and seeded in the 3D collagen hydrogels.

RNA isolation and quantitative real-time PCR

RNA isolation was performed with the use of 500 µl of TRIzol (Sigma-Aldrich), according to the manufacturer's guidelines. After isolation, RNA concentration was quantified with a Nanodrop photospectrometer (Thermo Scientific, Waltham, MA, USA) and any genomic DNA was removed using DNAse I. Next, a maximum of 1 µg of RNA was reverse-transcribed into cDNA in a single step reverse transcriptase PCR at 37°C with the use of oligo dT primer and 200U M-MLV Reverse transcriptase (All Life Technologies) using a thermocycler. Gene expression in this cDNA was measured using 0.25 mM of validated primers (Biolegio, Nijmegen, the Netherlands: see supp. table 3) and SYBR green master mix (Applied Biosystems, Waltham, MA, USA) in a quantitative real-time polymerase chain reaction (qPCR). The relative gene expression (-ΔCt) was calculated based on the average of the following reference genes: *GAPDH* and *RPS27A*

Statistics

Data visualization of the results and comparisons for statistical significance between experimental groups were performed with R Studio (version 4.1.3) and the Prism software (Graphpad 9.0.0, San Diego, CA, USA). The exact statistical tests performed in every analysis/experiment are indicated in the figure legends.

Funding

This study was funded by Health Holland.

Author contributions

Conceptualization: R.M.T, T.I.P, H.J.P.M.K, Y.V.J.M.v.O

Methodology: R.M.T, T.I.P, A.P.M.v.C, H.J.P.M.K, P.S, M.A.H, I.J.M.d.V, M.K

Investigation: T.I.P, P.S

Visualization: T.I.P, A.P.M.v.C, P.S Funding acquisition: R.M.T

Project administration: R.M.T, T.I.P, H.J.P.M.K, P.M.vd.K

Performance and or supervision of the experiments: T.I.P, A.P.M.v.C, H.J.P.M.K, R.L.S,

B.W, E.V, M.A.J.G

Physicians involved in patient treatment and enrollment: R.M.T, I.v.I, M.V

Writing – original draft: T.I.P and R.M.T

Writing – review & editing: R.M.T, T.I.P, A.P.M.v.C, H.J.P.M.K, P.S, M.A.H, M.K, R.L.S

Competing interests

Y.V.J.M.v.O is an employee of Xenikos and owns stock in Xenikos. The remaining authors have no conflicts of interest to report.

Data availability statement

All data and GEO accession numbers that are required to assess the conclusions of this paper are presented in the paper's main and supplementary figures and materials and methods section.

Code availability

The single-cell RNA sequencing analyses presented in this study were performed with standard workflows and open-source R packages and software were utilized (Methods). Some analyses involved the development of custom-made codes. All the codes are available here; https://github.com/PrashINRA

Ethics statements

Patient consent for publication

Not applicable

Ethics approval

This study entails human participation and was approved by the Medical Ethical Committee of the Radboud University Medical Center, Nijmegen, the Netherlands (study numbers: NL57997.091.16, NL67672.091.18). Before participating in the study, participants provided informed consent.

Acknowledgments

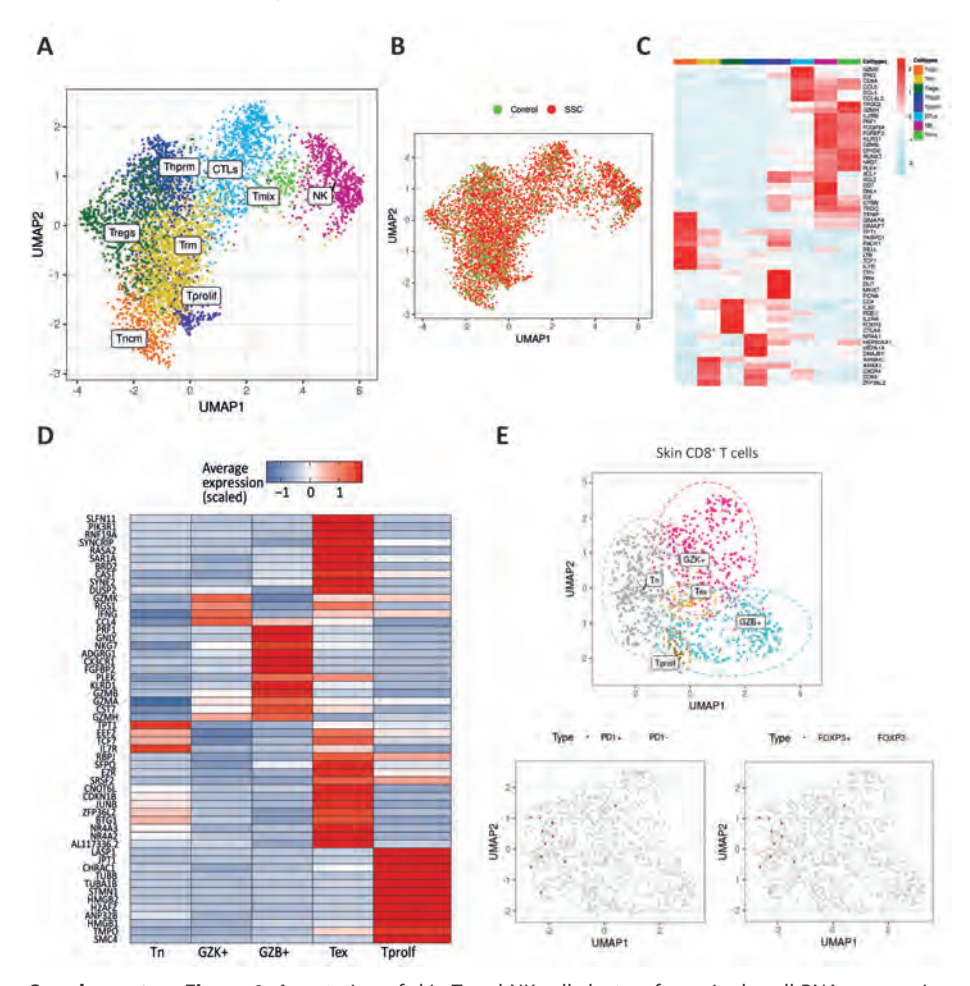
We thank Trisha Tee for processing the blood samples of the SSc patient treated with a-CD3/CD7-IT. We also want to thank Bram van Cranenbroek and the Radboud Technology Centre Flow Cytometry facility for their technical support in flow cytometry experiments and analysis.

- Truchetet ME, Brembilla NC, Chizzolini C. Current Concepts on the Pathogenesis of Systemic Sclerosis. Clin Rev Allergy Immunol. 2021.
- 2. Benfaremo D, Svegliati Baroni S, Manfredi L, Moroncini G, Gabrielli A. Putative functional pathogenic autoantibodies in systemic sclerosis. Eur J Rheumatol. 2020;7(Suppl 3):S181-S6.
- Papadimitriou TI, van Caam A, van der Kraan PM, Thurlings RM. Therapeutic Options for Systemic Sclerosis: Current and Future Perspectives in Tackling Immune-Mediated Fibrosis. Biomedicines. 2022;10(2).
- Maehara T, Kaneko N, Perugino CA, Mattoo H, Kers J, Allard-Chamard H, et al. Cytotoxic CD4+ T lymphocytes may induce endothelial cell apoptosis in systemic sclerosis. J Clin Invest. 2020;130(5):2451-64.
- Lopez-Isac E, Acosta-Herrera M, Kerick M, Assassi S, Satpathy AT, Granja J, et al. GWAS for systemic sclerosis identifies multiple risk loci and highlights fibrotic and vasculopathy pathways. Nat Commun. 2019;10(1):4955.
- Schnell A, Bod L, Madi A, Kuchroo VK. The yin and yang of co-inhibitory receptors: toward antitumor immunity without autoimmunity. Cell Res. 2020;30(4):285-99.
- Grebinoski S, Zhang Q, Cillo AR, Manne S, Xiao H, Brunazzi EA, et al. Autoreactive CD8(+) T cells are restrained by an exhaustion-like program that is maintained by LAG3. Nat Immunol. 2022;23(6):868-77.
- 8. Ishikawa Y, Terao C. Genetics of systemic sclerosis. J Scleroderma Relat Disord. 2020;5(3):192-201.
- 9. Khanna D, Spino C, Johnson S, Chung L, Whitfield ML, Denton CP, et al. Abatacept in Early Diffuse Cutaneous Systemic Sclerosis: Results of a Phase II Investigator-Initiated, Multicenter, Double-Blind, Randomized, Placebo-Controlled Trial. Arthritis Rheumatol. 2020;72(1):125-36.
- 10. Gur C, Wang SY, Sheban F, Zada M, Li B, Kharouf F, et al. LGR5 expressing skin fibroblasts define a major cellular hub perturbed in scleroderma. Cell. 2022;185(8):1373-88 e20.
- 11. Gaydosik AM, Tabib T, Domsic R, Khanna D, Lafyatis R, Fuschiotti P. Single-cell transcriptome analysis identifies skin-specific T cell responses in systemic sclerosis. Ann Rheum Dis. 2021;80(11):1453-60.
- 12. Jonsson AH, Zhang F, Dunlap G, Gomez-Rivas E, Watts GFM, Faust HJ, et al. Granzyme K(+) CD8 T cells form a core population in inflamed human tissue. Sci Transl Med. 2022;14(649):eabo0686.
- 13. Buckle I, Guillerey C. Inhibitory Receptors and Immune Checkpoints Regulating Natural Killer Cell Responses to Cancer. Cancers (Basel). 2021;13(17).
- Okwor CIA, Oh JS, Crawley AM, Cooper CL, Lee SH. Expression of Inhibitory Receptors on T and NK Cells Defines Immunological Phenotypes of HCV Patients with Advanced Liver Fibrosis. iScience. 2020;23(9):101513.
- 15. Xia A, Zhang Y, Xu J, Yin T, Lu XJ. T Cell Dysfunction in Cancer Immunity and Immunotherapy. Front Immunol. 2019;10:1719.
- Padilla CM, Valenzi E, Tabib T, Nazari B, Sembrat J, Rojas M, et al. Increased CD8+ tissue resident memory T cells, regulatory T cells, and activated natural killer cells in systemic sclerosis lungs. Rheumatology (Oxford). 2023.
- 17. Lyman SD, Escobar S, Rousseau AM, Armstrong A, Fanslow WC. Identification of CD7 as a cognate of the human K12 (SECTM1) protein. J Biol Chem. 2000;275(5):3431-7.

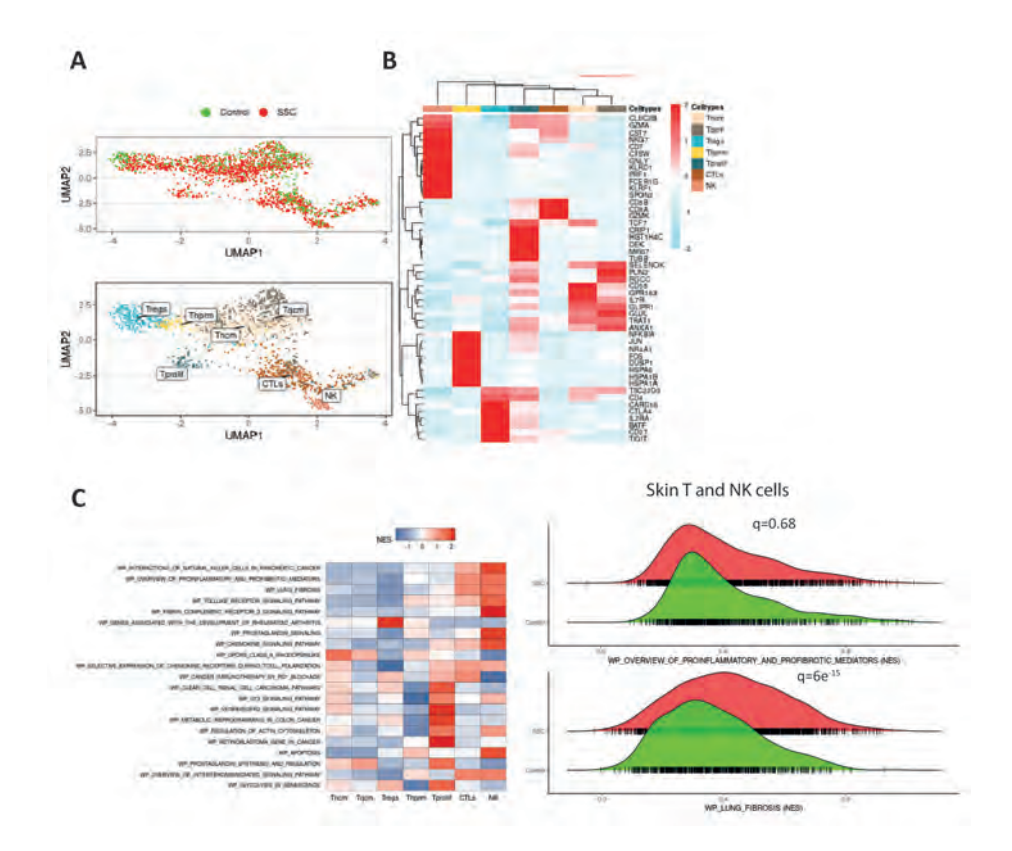
- 18. Wang T, Huang C, Lopez-Coral A, Slentz-Kesler KA, Xiao M, Wherry EJ, et al. K12/SECTM1, an interferon-gamma regulated molecule, synergizes with CD28 to costimulate human T cell proliferation. J Leukoc Biol. 2012;91(3):449-59.
- 19. Buskermolen JK, Roffel S, Gibbs S. Stimulation of oral fibroblast chemokine receptors identifies CCR3 and CCR4 as potential wound healing targets. J Cell Physiol. 2017;232(11):2996-3005.
- 20. Lei Y, Takahama Y. XCL1 and XCR1 in the immune system. Microbes and Infection. 2012;14(3):262-7.
- 21. Heinrichs D, Berres ML, Nellen A, Fischer P, Scholten D, Trautwein C, et al. The chemokine CCL3 promotes experimental liver fibrosis in mice. PLoS One. 2013;8(6):e66106.
- 22. Sahin H, Wasmuth HE. Chemokines in tissue fibrosis. Biochimica et Biophysica Acta (BBA) -Molecular Basis of Disease. 2013;1832(7):1041-8.
- 23. Frangogiannis NG. Transforming growth factor–β in tissue fibrosis. Journal of Experimental Medicine. 2020;217(3).
- 24. McCormick LL, Zhang Y, Tootell E, Gilliam AC. Anti-TGF-β Treatment Prevents Skin and Lung Fibrosis in Murine Sclerodermatous Graft-Versus-Host Disease: A Model for Human Scleroderma1. The Journal of Immunology. 1999;163(10):5693-9.
- 25. Matsuda M, Tsurusaki S, Miyata N, Saijou E, Okochi H, Miyajima A, et al. Oncostatin M causes liver fibrosis by regulating cooperation between hepatic stellate cells and macrophages in mice. Hepatology. 2018;67(1):296-312.
- 26. Stawski L, Trojanowska M. Oncostatin M and its role in fibrosis. Connect Tissue Res. 2019;60(1):40-9.
- 27. van Bijnen S, de Vries-Bouwstra J, van den Ende CH, Boonstra M, Kroft L, Geurts B, et al. Predictive factors for treatment-related mortality and major adverse events after autologous haematopoietic stem cell transplantation for systemic sclerosis: results of a long-term follow-up multicentre study. Ann Rheum Dis. 2020;79(8):1084-9.
- 28. Acosta-Herrera M, Kerick M, Lopéz-Isac E, Assassi S, Beretta L, Simeón-Aznar CP, et al. Comprehensive analysis of the major histocompatibility complex in systemic sclerosis identifies differential HLA associations by clinical and serological subtypes. Annals of the Rheumatic Diseases. 2021;80(8):1040-7.
- 29. Ota Y, Kuwana M. Updates on genetics in systemic sclerosis. Inflammation and Regeneration. 2021;41(1):17.
- 30. O'Reilly S, Hügle T, van Laar JM. T cells in systemic sclerosis: a reappraisal. Rheumatology. 2012;51(9):1540-9.
- 31. Jin W, Zheng Y, Zhu P. T cell abnormalities in systemic sclerosis. Autoimmunity Reviews. 2022;21(11):103185.
- 32. Collier JL, Weiss SA, Pauken KE, Sen DR, Sharpe AH. Not-so-opposite ends of the spectrum: CD8(+) T cell dysfunction across chronic infection, cancer and autoimmunity. Nat Immunol. 2021;22(7):809-19.
- 33. Huang Y, Jia A, Wang Y, Liu G. CD8(+) T cell exhaustion in anti-tumour immunity: The new insights for cancer immunotherapy. Immunology. 2023;168(1):30-48.
- 34. McKinney EF, Lee JC, Jayne DR, Lyons PA, Smith KG. T cell exhaustion, co-stimulation and clinical outcome in autoimmunity and infection. Nature. 2015;523(7562):612-6.
- 35. Fleury M, Belkina AC, Proctor EA, Zammitti C, Simms RW, Lauffenburger DA, et al. Increased Expression and Modulated Regulatory Activity of Coinhibitory Receptors PD-1, TIGIT, and TIM-3 in Lymphocytes From Patients With Systemic Sclerosis. Arthritis Rheumatol. 2018;70(4):566-77.

- 36. Groth C, van Groningen LFJ, Matos TR, Bremmers ME, Preijers F, Dolstra H, et al. Phase I/II Trial of a Combination of Anti-CD3/CD7 Immunotoxins for Steroid-Refractory Acute Graft-versus-Host Disease. Biol Blood Marrow Transplant. 2019;25(4):712-9.
- 37. Lazarovits AI, Rochon J, Banks L, Hollomby DJ, Muirhead N, Jevnikar AM, et al. Human mouse chimeric CD7 monoclonal antibody (SDZCHH380) for the prophylaxis of kidney transplant rejection. Transplant Proc. 1993;25(1 Pt 1):820-2.
- 38. de Wit MPT, Koenders MI, Neijland Y, van den Hoogen FHJ, van der Kraan PM, van de Loo FAJ, et al. Patient involvement in basic rheumatology research at Nijmegen: a three year's responsive evaluation of added value, pitfalls and conditions for success. BMC Rheumatology. 2022;6(1):66.
- Preliminary criteria for the classification of systemic sclerosis (scleroderma). Subcommittee for scleroderma criteria of the American Rheumatism Association Diagnostic and Therapeutic Criteria Committee. Arthritis Rheum. 1980;23(5):581-90.
- 40. van Oosterhout YV, van Emst L, Schattenberg AV, Tax WJ, Ruiter DJ, Spits H, et al. A combination of anti-CD3 and anti-CD7 ricin A-immunotoxins for the in vivo treatment of acute graft versus host disease. Blood. 2000;95(12):3693-701.
- 41. Gorris MAJ, van der Woude LL, Kroeze LI, Bol K, Verrijp K, Amir AL, et al. Paired primary and metastatic lesions of patients with ipilimumab-treated melanoma: high variation in lymphocyte infiltration and HLA-ABC expression whereas tumor mutational load is similar and correlates with clinical outcome. J Immunother Cancer. 2022;10(5).
- 42. Bankhead P, Loughrey MB, Fernández JA, Dombrowski Y, McArt DG, Dunne PD, et al. QuPath: Open source software for digital pathology image analysis. Scientific Reports. 2017;7(1):16878.
- 43. Stuart T, Butler A, Hoffman P, Hafemeister C, Papalexi E, Mauck WM, 3rd, et al. Comprehensive Integration of Single-Cell Data. Cell. 2019;177(7):1888-902 e21.
- 44. Becht E, McInnes L, Healy J, Dutertre CA, Kwok IWH, Ng LG, et al. Dimensionality reduction for visualizing single-cell data using UMAP. Nat Biotechnol. 2018.
- 45. Singh P, Zhai Y. Deciphering Hematopoiesis at single cell level through the lens of reduced dimensions. bioRxiv. 2022:2022.06.07.495099.
- 46. Wilcoxon F. Individual Comparisons by Ranking Methods. Biometrics Bulletin. 1945;1(6):80-3.
- 47. Borcherding N, Vishwakarma A, Voigt AP, Bellizzi A, Kaplan J, Nepple K, et al. Mapping the immune environment in clear cell renal carcinoma by single-cell genomics. Communications Biology. 2021;4(1):122.
- 48. Barbie DA, Tamayo P, Boehm JS, Kim SY, Moody SE, Dunn IF, et al. Systematic RNA interference reveals that oncogenic KRAS-driven cancers require TBK1. Nature. 2009;462(7269):108-12.
- 49. Antoneli F, Passos FM, Lopes LR, Briones MRS. A Kolmogorov-Smirnov test for the molecular clock based on Bayesian ensembles of phylogenies. PLoS One. 2018;13(1):e0190826.
- 50. Langfelder P, Horvath S. WGCNA: an R package for weighted correlation network analysis. BMC Bioinformatics. 2008;9(1):559.
- He X, de Oliveira VL, Keijsers R, Joosten I, Koenen HJ. Lymphocyte Isolation from Human Skin for Phenotypic Analysis and Ex Vivo Cell Culture. J Vis Exp. 2016(110):e52564.

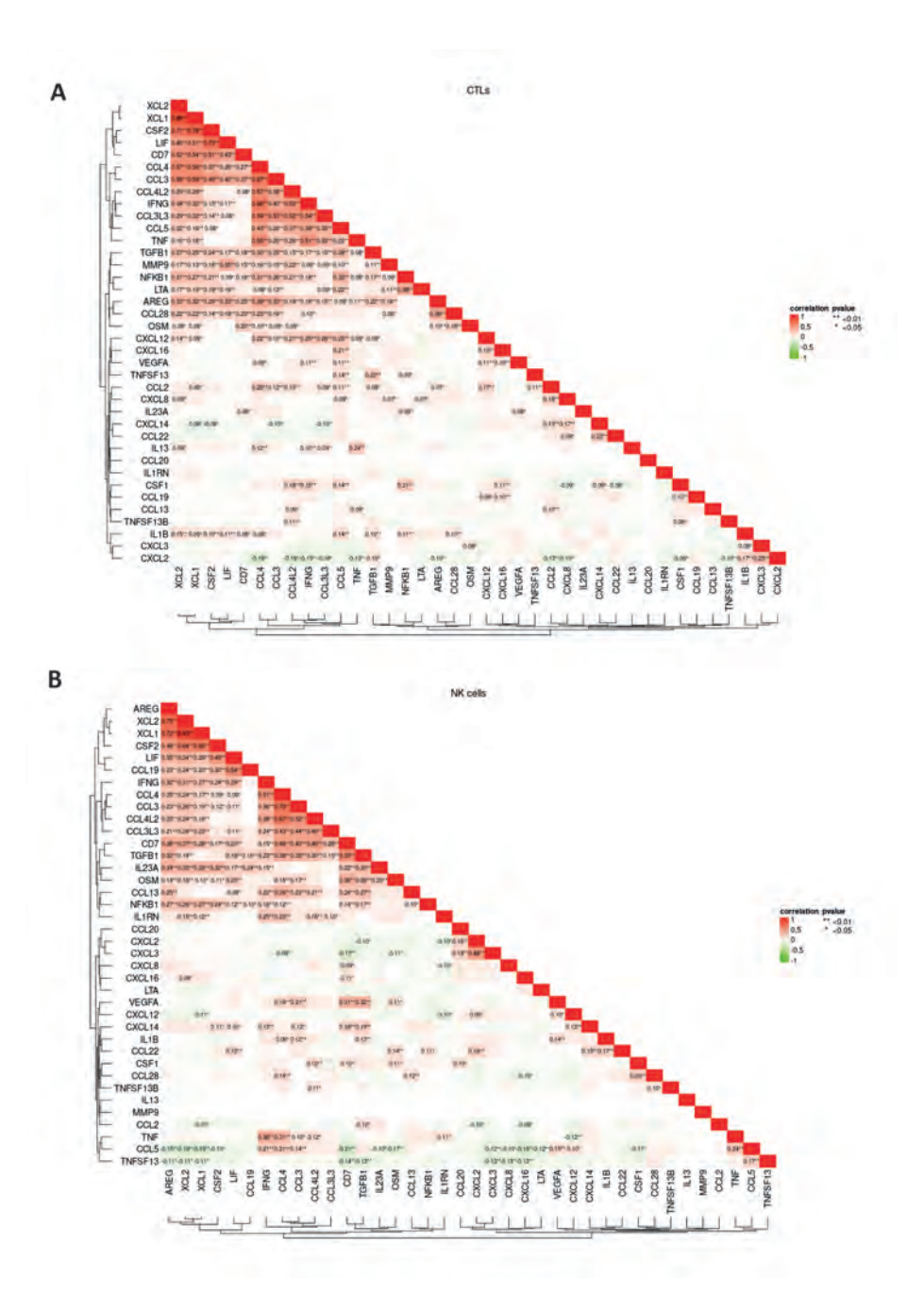
Supplementary Figures



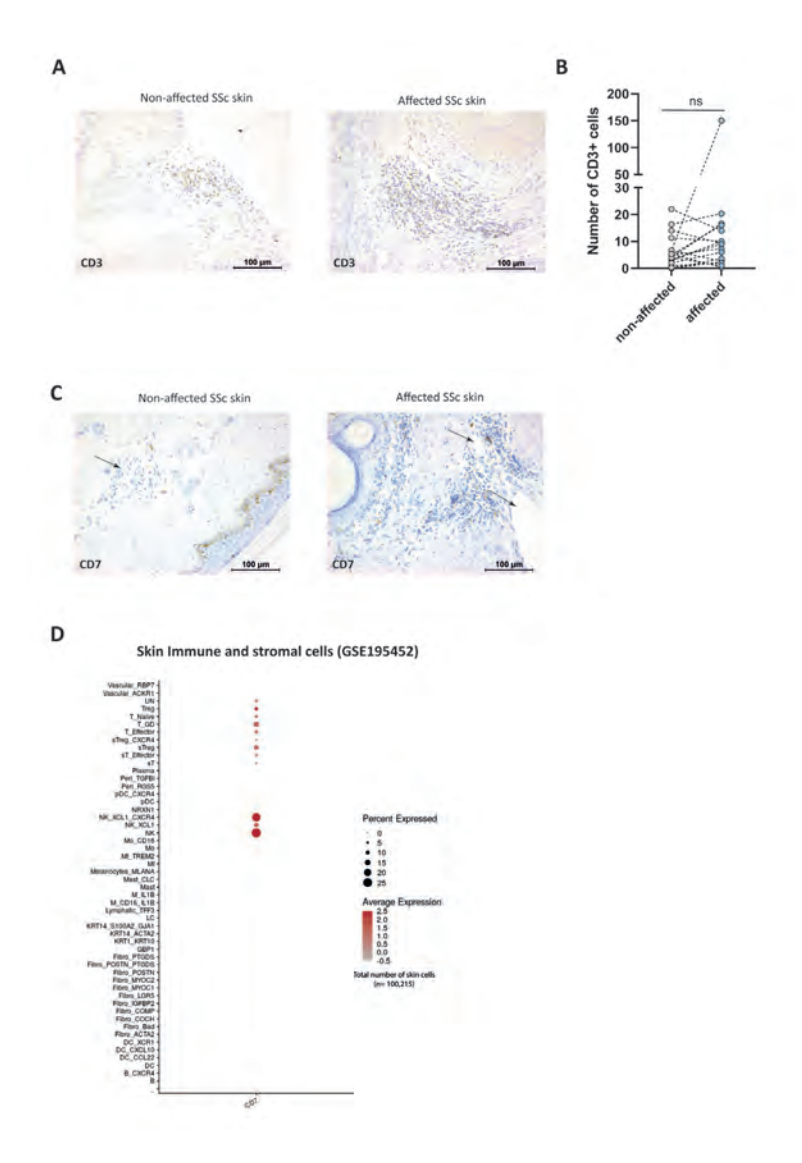
Supplementary Figure 1. Annotation of skin T and NK cell clusters from single cell RNA sequencing dataset GSE195452. A Unsupervised Uniform Manifold Approximation and Projection (UMAP) to visualize clustering of 5,061 cells detects 8 transcriptionally distinct cell clusters: tissue-resident memory T cells (Trm), cytotoxic T cells (CTLs), regulatory T cells (Tregs), hypofunctional tissue resident T cells (Thprm), naïve/central memory (Tncm), proliferating T cells (Tprolif) and NK cells (NK) and a cluster containing a mixture of MAIT, INKT CD8 $^+$ T and $\gamma\delta T$ cells (T mix). **B** UMAP showing the cells belonging to healthy individuals (control) or patients (SSc) C Heatmap illustrating the top 5 differentially expressed genes in each distinguished cell cluster: Trm (CD69, ZFP36L2, CXCR4, IL7R), CTLs (GZMK, IFNG, CCL5, CCL4, CD8A), Tregs (CD4, FOXP3, CTLA4, IL2RA), Thprm (NR4A1, CD69, CXCR4, DUSP1), Tncm (TCF7, SELL, IL7R), Tprolif (MKI67), NK (NKG7, FCGR3A, FGFBP2, KLRD1, GZMB, PRF1) and Tmix (CD8A, CCL5, TRGC2, NKG7, GZMB, PRF1, FCGR3A, FGFBP2, KLRD1). D Heatmap demonstrating the top 10 upregulated genes in each of the 5 different clusters of isolated CD8+T cells; naïve (Tn): IL7R, Granzyme K+ (GZK+): GZMK, IFNG, CCL4, Granzyme B+ (GZB+): PRF1, GNLY, NKG7, GZMB, GZMZ, GZMH, exhausted (Tex): NR4A2, NR4A3, and proliferating (Tprolif): LASP1, TMPO, ANP32B. E UMAP representing positive (red) and negative (grey) gene expression of PDCD1 (PD-1) among CD8+T cell clusters.



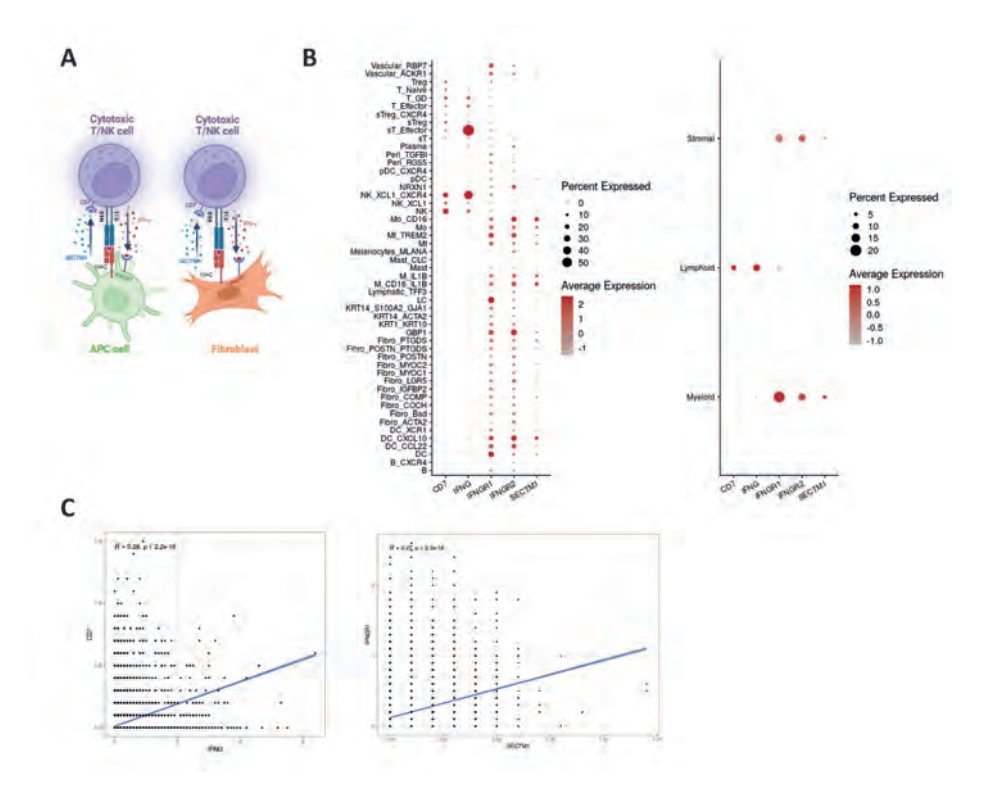
Supplementary Figure 2. Single cell RNA sequencing analysis of dataset GSE138669. A Unsupervised Uniform Manifold Approximation and Projection (UMAP) clustering of 2,126 cells determines 7 transcriptionally distinct cell clusters: quiescent tissue resident T cells (Tqcm), cytotoxic T cells (CTLs), regulatory T cells (Treqs), hypofunctional tissue resident T cells (Thprm), naïve/central memory (Tncm), proliferating T cells (Tprolif) and NK cells (NK). UMAP displaying the cells belonging to healthy individuals (control) or patients (SSc) is depicted on the top of this panel. **B** Heatmap of the top 10 differentially expressed genes in each distinguished cell cluster: Tqcm (CD69, IL7R, TCF7, SELL, ANXA1), CTLs (CD8A, GZMK, GZMA,), Tregs (CD4, CD27, CTLA4, IL2RA), Thprm (NR4A1, DUSP1), Tncm (TCF7, IL7R), Tprolif (MKI67), NK (NKG7, FCGR3A, KLRD1, PRF1). C (left) Gene set enrichment analysis with Wiki pathways as reference dataset. Examples of top pathways (p <1e-10) represented by NK and CTL clusters are shown. Statistics were performed with Kolmogorov-Smirnov (KS) test.(right) Comparison of the enrichment scores of the overview of proinflammatory and profibrotic (q=0.68) and lung fibrosis (q=6e⁻¹⁵) pathways in HD versus SSc skin T and NK cell clusters (here for GSE138669, **Fig 1** for GSE195452).



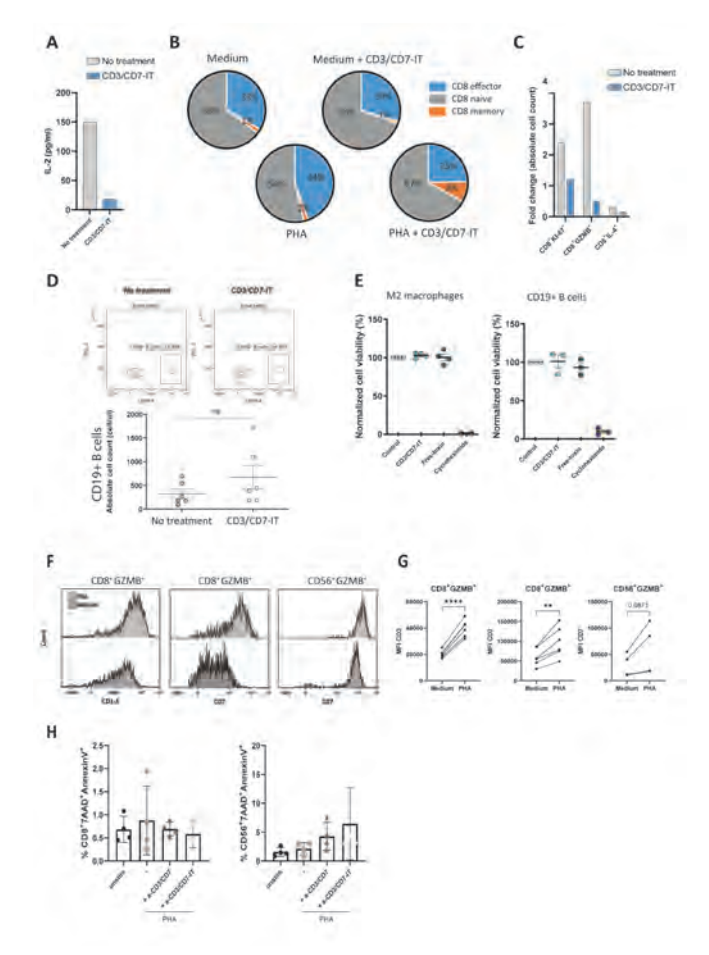
Supplementary Figure 3. Pairwise correlations of CD7 with pro-fibrotic genes. The Wiki gene pathways lung fibrosis and pro-inflammatory and pro-fibrotic manifestations were merged and potential correlation of CD7 gene expression with the included genes was evaluated separately for the cluster of **A** cytotoxic T cells (CTLs) and **B** NK cells. Statistical significance for every comparison was corrected for multiple comparisons and is presented as adjusted p value, *p<0.05, **p<0.01.



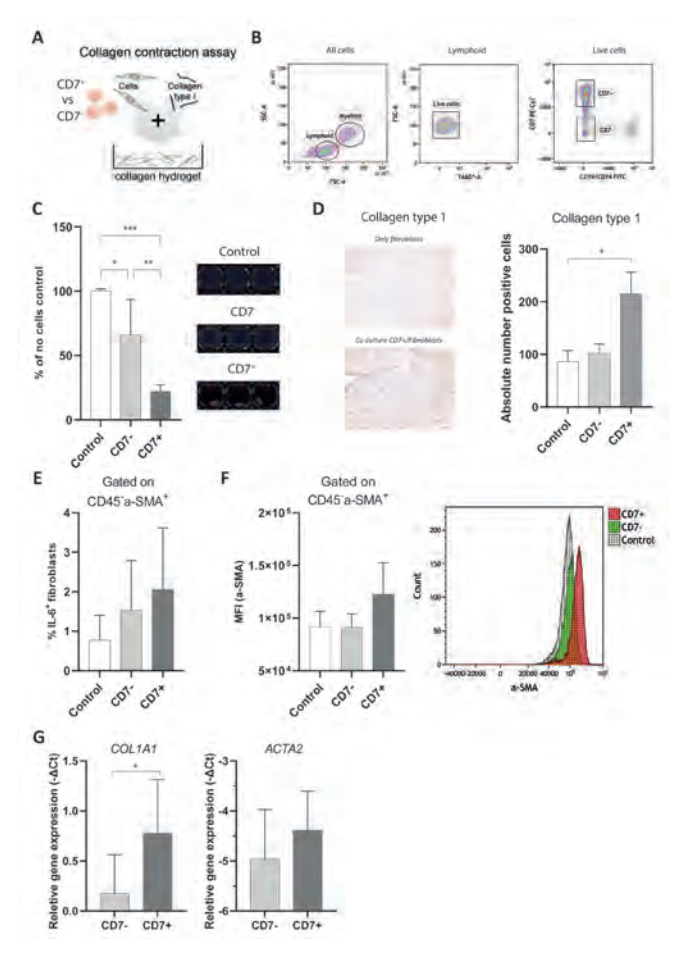
Supplementary figure 4. CD3 and CD7 immunohistochemistry in SSc affected versus non-affected skin of patients with systemic sclerosis. CD7 gene expression in skin immune and stromal cells is also depicted. **A** Representative images of CD3 immunohistochemistry (IHC) staining of the affected and non-affected skin biopsies from one SSc patient. Scale is $100 \, \mu m$. **B** Quantification of CD3+T cells in the affected vs non lesion SSc skin (n=20). Bars are mean \pm SD. Non-parametric Wilconxon test, p=0.19. **C** In SSc affected skin large infiltration of CD7+ cells is found in perivascular areas while in matched non-affected skin, a smaller number of CD7+ cells is present around blood vessels. Scale is $100 \, \mu m$. Here, representative images of one SSc patient with early diffuse disease are depicted. **D** 2-D dot plot comparing *CD7* gene expression in skin immune and stromal cells. Cell cluster annotations were retrieved from metadata information as have been described in the single-cell RNA sequencing dataset GSE195452. Circle size shows the percentage of cells expressing *CD7* and color intensity depicts average expression. Numbers indicate average of normalized counts.



Supplementary Figure 5. SECTM1-CD7 axis in activation of cytotoxic T and NK cells in SSc affected skin. A Schematic model for the proposed involvement of SECTM1-CD7 axis in cytotoxic T cell and NK cell activation (Created with BioRender.com). In SSc affected skin, CD7 and IFNG is predominantly expressed in cytotoxic T and NK cells while its receptor IFNGR and SECTM1 in antigen presenting cells (APCs) and stromal cells (mainly fibroblasts). This suggests a cytokine-mediated positive feedback loop in the communication between CD7+ cytotoxic immune cells and SECTM1 producing APCs and fibroblasts, with IFN-y being a key cytokine. B 2-D dot plots comparing expression levels of selected genes in skin immune (myeloid and lymphoid) and stromal cell populations. Cell cluster annotations were retrieved from metadata information as have been described in the single-cell RNA sequencing dataset GSE195452. Circle size shows the percentage of cells expressing each gene and color intensity depicts average expression. Numbers indicate average of normalized counts. C Pair-wise correlation plots in SSc affected skin (GSE195452) show a positive correlation between CD7/IFNG and SECTM1/IFNGR1. Abbreviations; TCR: T cell receptor, NKR: NK cell receptor, MHC: major histocompatibility complex, APC: antigen-presenting cell.



Supplementary Figure 6. CD3/CD7-IT specifically eliminates only the activated cytotoxic T and NK cells in vitro. A Concentration of IL-2 (pg/ml) was measured in cell supernatant of cells with or without treatment with a-CD3/CD7-IT B Pie charts illustrating the proportion of effector (CD8+CD45RA+CD27-), memory (CD8+CD45RA-CD27+) and naïve (CD8+CD45RA+CD27+) cells among the CD8+T cell population in the depicted stimulation and treatment culture conditions (percentages in the pie charts are mean values of n=6 SSc patients). C Response to TCR mediated (PHA) restimulation of cells treated with a-CD3/CD7-IT was evaluated by intracellular flow cytometry. Values are represented as fold change of the re-stimulated compared to the values before stimulation. D (Bottom) Comparison of absolute counts (cells/µl) of CD19+ B cells after in-vitro treatment with CD3/CD7-IT compared to non-treated peripheral blood mononuclear cells (n=6). (top) Representative flow cytometry plots of one experiment. E Normalized cell viability, of M2 macrophages and CD19+ B cells that were isolated from SSc patients' blood for the depicted different culture/treatment conditions. Cycloheximide was used a positive control. F Flow cytometric histograms of one representative experiment exhibiting elevated expression of CD3 and CD7 in CD8+GZMB+ cells and CD7 in CD56+GZMB+ NK cells upon stimulation with phytohemagglutinin (PHA) that is further quantified in G. CD3 and CD7 expression is presented as mean fluorescence intensity (MFI). Statistics were performed with Student's t-test, **p<0.01, ****p<0.0001 **H** The percentage of necrotic cytotoxic T (CD8+7-AAD+Annexin V+) and NK (CD56+7-AAD+Annexin V+) cells in the depicted conditions was measured with flow cytometry of the enzymatically digested collagen plugs (n=5).



Supplementary Figure 7. Fibroblasts co-cultured with CD7+ T cells and NK cells exhibit increased contractility that is accompanied by an elevated myofibroblast-like phenotype. A Schematic representation of the experimental design in the developed 3D in-vitro collagen contraction fibroblast: immune cell co-culture model. B Flow cytometry gating strategy that was used to sort CD7+ versus CD7⁻T cell and NK cell populations from healthy peripheral blood (n=3). First, we gated on the lymphoid cell population based on cell size (FSC) and granularity (SSC). Followingly, we excluded dead cells based on 7-AAD+ staining and we then sorted CD19-CD14- lymphoid cells that were either positive or negative for CD7 expression. C The level of fibroblast contraction was quantified compared to no-cells control and plotted graphically (n=3). Bars are mean ±SD. An image of a representative experiment is depicted on the right part of this panel. D (left) Representative images of Collagen type 1 immunohistochemistry of the collagen plugs that contained only fibroblasts or fibroblasts co-cultured with CD7⁺ T cells and NK cells. (right) Quantification of Collagen type 1 positive fibroblasts in control versus fibroblasts that were co-cultured with either CD7⁻ or CD7⁺ cells (n=3). Bars are mean ±SD. E The percentage of CD45 a-SMA+IL-6+ fibroblasts in the depicted conditions was measured with flow cytometry of the enzymatically digested collagen plugs (n=3). F Expression levels (mean fluorescence intensity-MFI) of a-SMA in CD45 a-SMA+ fibroblasts in the depicted conditions was measured with flow cytometry of the enzymatically digested collagen plugs (n=3). (right) Flow cytometry histograms of one representative experiment exhibiting increased expression of a-SMA in fibroblasts co-cultured

with CD7+ compared to CD7-T cells and NK cells is shown. G CD7+ versus CD7-T and NK cells (n=3) were co-cultured with primary dermal fibroblasts in the developed 3D hydrogel collagen co-culture model and fibroblasts were analyzed for expression of genes reflective of a myofibroblast phenotype such as COL1A1 and ACTA2. Values represent relative gene expression (-ΔCt) as measured with qPCR. *GAPDH* and *RPS27A* were used as reference genes. Data represents mean \pm SEM.

Supplementary materials

Supplementary Table 1. List of antibodies used for cell surface staining.

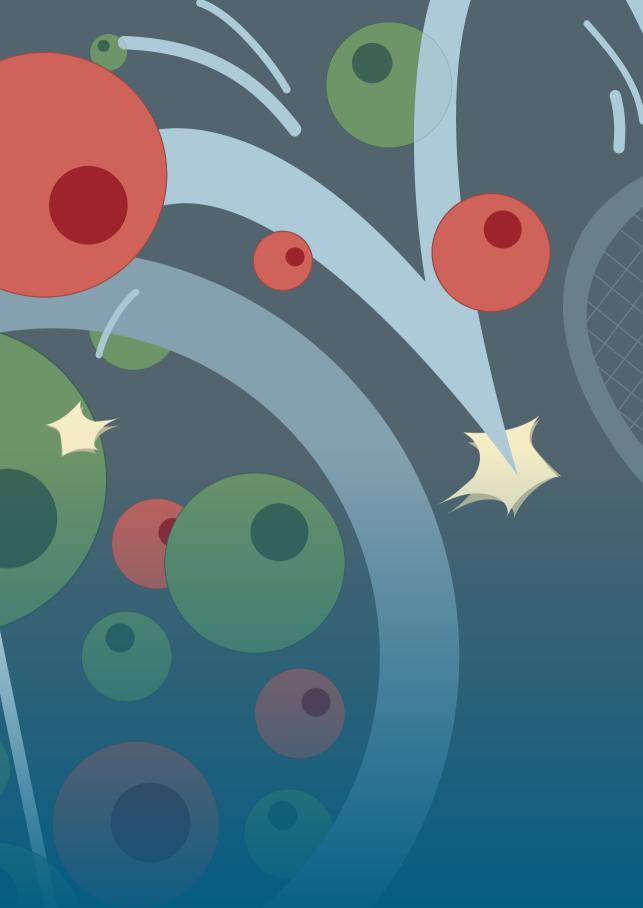
Antigen	Clone	Dilution	Fluorochrome	Supplier
CD4	RPA-T4	1:100	PerCP/Cy5.5	Biolegend
CD3	UCHT1	1:100	Alexa700	Biolegend
CD8a	RPA-T8	1:100	BV510	Biolegend
CD7	M-T701	1:20	BUV737	BD Biosciences
CD56	N901	1:50	APC	Beckman-Coulter
CD19	HIB19	1:25	BV605	Biolegend
CD2	S5.2	1:100	BUV737	BD Biosciences

Supplementary Table 2. List of antibodies used for intracellular staining.

Antigen	Clone	Dilution	Fluorochrome	Supplier
Granzyme B	GB11	1:15	FITC	Biolegend
Perforin	Dg9	1:15	FITC	ThermoFischer
IL-4	MP4-25D2	1:20	PE/Dazzle594	Biolegend
IL-13	JES10-5A2	1:20	PE/Cy7	Biolegend
Ki-67	B56	1:50	Alexa Fluor 647	BD Biosciences
a-SMA	1A4	1:20	Alexa Fluor 700	R&D systems
IL-6	MQ2-13A5	1:20	Pacific Blue	Biolegend

Supplementary Table 3. List of primer sequences used.

Gene	Forward primer 5'-3'	Forward primer 5'-3'
GAPDH	ATCTTCTTTTGCGTCGCCAG	TTCCCCATGGTGTCTGAGC
RPS27A	TGGCTGTCCTGAAATATTATAAGGT	CCCCAGCACCACATTCATCA
COL1A1	AGATCGAGAACATCCGGAG	AGTACTCTCCACTCTTCCAG
ACTA2	CTGACCCTGAAGTACCCGATA	GAGTGGTGCCAGATCTTTTCC
FN1 EDA	TTCAGACTGCAGTAACCAACAT	GGTCACCCTGTACCTGGAAAC
PLOD2	AAGACTCCCCTACTCCGGAAA	AGCAGTGGATAATAGCCTTCCAA
FAP	GCTTTGAAAAATATCCAGCTGCC	ACCACCATACACTTGAATTAGCA
COL3A1	CCTGGAATCTGTGAATCATGCC	TGCGAGTCCTCCTACTGCTA



Chapter 4

Novel 3D hydrogel model shows that CD8+ T cells drive myofibroblast activation and contraction via JAK/STAT3 and TGFβ signalling

Theodoros Ioannis Papadimitriou, Anne van Essen, Merel Willemse, Daphne Dorst, Elly Vitters, Birgitte Walgreen, Hans J.P.M Koenen, Peter van der Kraan, Marije Koenders, Rogier M. Thurlings, Arjan van Caam

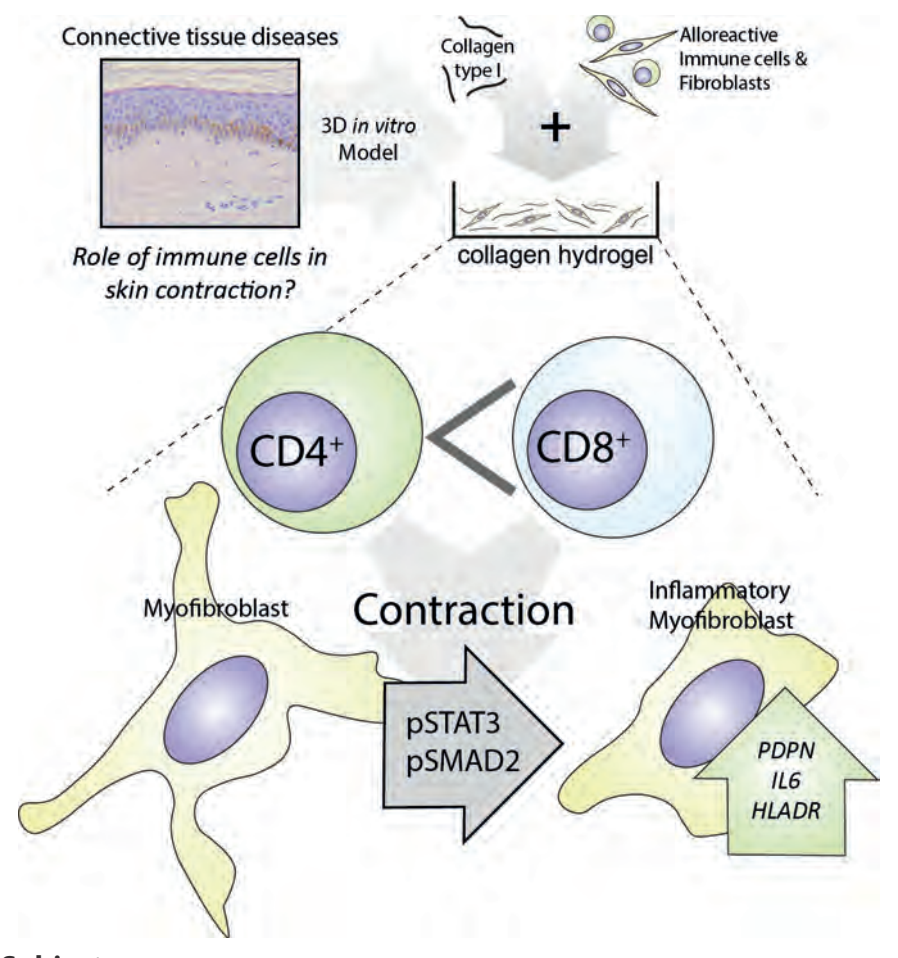
iScience (Cell Press).

- Allogeneic mismatching in 3D collagen contraction assays reveals a novel model to study immune-driven tissue contraction.
- CD8⁺ T cells induce stronger myofibroblast-mediated collagen contraction than CD4⁺ T cells, independent of cytotoxicity.
- Myofibroblast activation is regulated by distinct JAK/STAT3 and TGF β signalling pathways in CD4+ and CD8+T cell contexts.
- Dual inhibition of JAK/STAT3 and TGFβ pathways synergistically halts immunemediated myofibroblast contraction and activation.

Summary

Fibrosis, a leading cause of morbidity and mortality in rheumatic connective tissue diseases, is marked by CD8+ T cell and pro-fibrotic myofibroblast infiltration, though the role of CD8+ T cells in myofibroblast activity remains unexplored. To address this, we developed a 3D cell culture model of immunity-driven fibrosis by combining the classic mixed lymphocyte reaction and a 3D myofibroblast contractility model. Upon co-culture with either sorted CD4+ or CD8+ T cells, CD8+ T cells more strongly induced myofibroblast contraction and activation than CD4+ T cells. This was not associated with cytotoxicity but with increased IL-6 production by CD8+ T cells compared to CD4+ T cells and STAT3/TGF β -induced signalling in myofibroblasts. Use of either the JAK/STAT3-inhibitor tofacitinib or the TGF β receptor inhibitor SB-505124 blocked the activated myofibroblast phenotype, and combined use of both inhibitors had an additive effect on myofibroblast activation and contraction. Our findings reveal a previously underappreciated non-canonical role of CD8+ T cells in fibrosis, providing new lights into the mechanisms of the human immune system.

Graphical Abstract



Subject areas

myofibroblasts, CD8+T cells, contraction, fibrosis, cytokines

Fibrosis is characterized by an excessive accumulation of extracellular matrix (ECM) and increased tissue stiffness, leading to loss of tissue architecture and function. Generally, fibrosis is poorly reversible, making it a key complication in various diseases, including (rheumatic) autoimmune diseases such as systemic sclerosis (SSc) (1). Fibrosis has been estimated to be responsible for up to 45% of all deaths in the industrialized world (2). In SSc, fibrosis affects the skin and internal organs such as lungs, gastrointestinal tract and heart leading to a high morbidity and increased mortality (3).

A key cell type in fibrosis is the myofibroblast. This specialized type of fibroblast contributes to fibrosis in multiple ways. For example, myofibroblasts produce large amounts of ECM molecules such as collagen type 1 and fibronectin and make the ECM harder to degrade via expression of collagen crosslinking enzymes and tissue inhibitors of metalloproteinases. Importantly, the defining feature of myofibroblasts is their so-called stress fibers. These fibers, made of alpha smooth muscle actin (ACTA2) and (often) non muscle myosin type 2 (NMMII), give the cell contractile properties. Because myofibroblasts are tightly anchored to their environment via cell-cell adherence junctions and cell-matrix focal adhesion junctions, they can contract their environment, leading to tissue stiffness. Notably, increased tissue stiffness precedes matrix deposition in e.g. liver fibrosis (4), indicating that processes increasing tissue stiffness are a crucial initiating step in fibrosis and perpetuating the fibrotic response.

Formation and activation of myofibroblasts can be triggered by the immune system. Cytokines such as TGF β , IL-4, IL-6 and IL-13 have been described to induce and activate this cell type (5). Various immune cells, such as CD4+ T helper cells, can make these cytokines. Compared to the role of T helper cells in SSc, the role of cytotoxic T cells in myofibroblast formation and activation is less established; typically, these cells are associated with target cell lysis e.g. in anti-viral responses.

We and others recently showed increased numbers of cytotoxic CD8+ T cells in SSc skin and blood compared to healthy controls, especially in early disease processes (6-8). Remarkably, only a small number of CD4+ T helper cells was present in SSc skin, and their presence was similar to that of healthy skin. These observations suggest that CD8+ T cells may exhibit a more pronounced role in connective tissue disease (CTD) fibrosis pathogenesis compared to CD4+ T cells than is currently appreciated. This is intriguing given that HLA class II alleles—typically associated with CD4+

T cell responses—are the strongest genetic risk factors for SSc, while HLA class I associations in GWAS studies are less studied (9, 10). This idea is supported by recent observations of distinct subsets of CD8+T cells with non-canonical functions divergent from cytotoxicity (11). Such CD8+ T cell subsets have been described to produce T helper cytokines or exhibit regulatory functions (12). Additionally, cytotoxicity-related mechanisms have also been suggested to drive myofibroblast activation via DAMP production resulting from lysis of endothelial cells (13). The question of whether non-canonical CD8+ T cell functions are involved in myofibroblast activation and contraction in CTD, as opposed to cytotoxicity-related processes or CD4+ T helper functions, remains unanswered.

To address this question, we investigated the role of CD4+ versus CD8+ T cells in myofibroblast activation and contraction. For this, we developed a three-dimensional (3D) collagen hydrogel co-culture model comprising primary skin myofibroblasts and alloreactive immune cells. This novel model expands upon classical mixed lymphocyte reaction assays, which have been widely used to evaluate the efficacy and immunogenicity of compounds in vitro and are considered a physiologically relevant approach for studying T cell activation and function. (14), We modified this classical model by incorporating a 3D collagen environment and myofibroblasts to simulate T cell activation, function, and interactions within a fibrotic-like microenvironment, similar to that of the skin. We found that immune cell-mediated myofibroblast contraction and activation was predominantly attributed to cytokine producing CD8+ T cells rather than CD4+ T cells. This process could be halted by inhibiting either JAK/STAT3 or TGFβ signalling. Importantly, combined inhibition showed an additive effect and completely blocked myofibroblast activation and contraction. These data indicate a greater involvement of CD8+ T cells compared to CD4+T cells in myofibroblast activation, suggesting that therapeutic approaches targeting both CD8+T cell cytokine production and myofibroblast activation might be beneficial in mitigating immune cell mediated tissue fibrosis.

Results

Co-culture of myofibroblasts with immune cells induces myofibroblast activation and spontaneous contraction

To gain insight into how the interaction between immune cells and myofibroblasts may lead to tissue fibrosis in CTD, we set out to establish a humanized in vitro 3D model to study immune cell mediated myofibroblast activation and contraction. In this model, primary human skin myofibroblasts were co-cultured with allogeneic

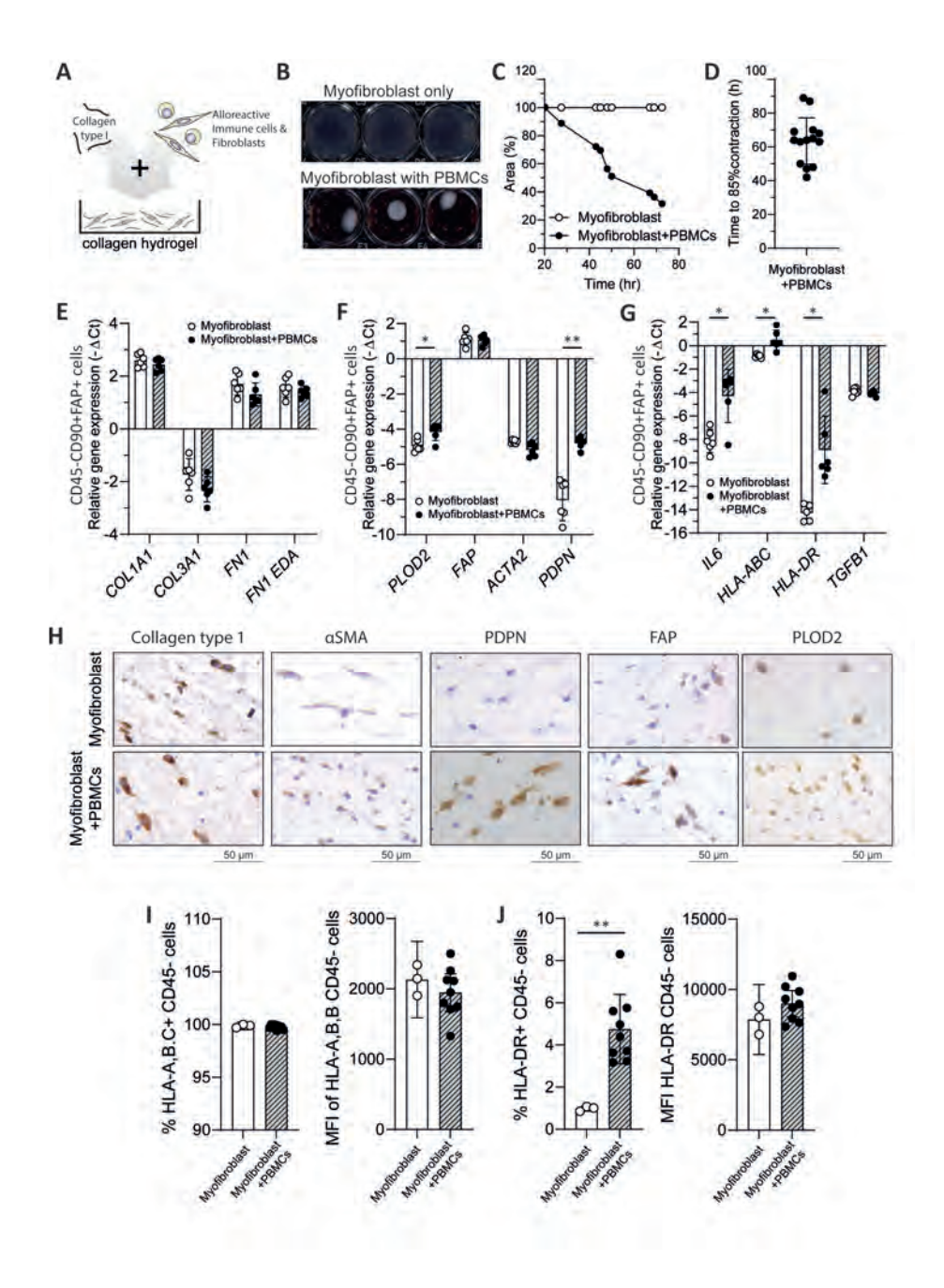


Figure 1. The co-culture of myofibroblasts with immune cells triggers their activation and leads to spontaneous myofibroblast contraction. (A) Schematic illustration of the developed 3D collagen hydrogel contraction model, incorporating co-cultured primary skin myofibroblasts and PBMCs. (B) Representative image exhibiting macroscopic evaluation of myofibroblast contraction in absence or presence of PBMCs. (C) The extent of contraction is quantified relative to the no-cell control and is graphically illustrated for one representative donor over the course of time. (D) Time required until 85% of myofibroblast contraction is reached for each PBMC donor (n=14). (E) Myofibroblasts from collagen hydrogels in absence or presence of PBMCs (n=6 per group) were FACs sorted as the CD45-CD90+FAP+ cell population and analyzed with qPCR for gene expression of markers reflective of (E) ECM production, (F) myofibroblast activation, (G) cytokine production and antigen-presentation capacity, GAPDH, TBP and RPS27A were used as reference genes. (H) Representative images of Collagen Type I, aSMA, PDPN, FAP and PLOD2 immunohistochemistry from collagen hydrogels containing either myofibroblasts alone or myofibroblasts co-cultured with PBMCs. Scale is 50 µm. The percentage of (I) CD45-HLA-A,B,C+ myofibroblasts and HLA-A,B,C mean fluorescence intensity (MFI) (J) CD45-HLA-DR+ myofibroblasts and HLA-DR MFI in the depicted conditions was measured with flow cytometry of the enzymatically digested hydrogels (n=3 myofibroblast only, n=10 myofibroblast + PBMCs). Statistics were performed with two-way ANOVA corrected with Sidak's multiple comparisons test for panels E-G and two-way ANOVA corrected with Tukey's post hoc test for panels I-J. In the panels above, each dot represents one donor.

peripheral blood mononuclear cells (PBMCs) in a collagen type 1 hydrogel (schematic representation of the model is illustrated in *Figure 1A*). Alloreactivity was used to mimic autoreactive immunity in SSc because both are characterized by T cell responses against fibroblast antigens. Co-culturing of PBMCs with myofibroblasts at a 5:1 ratio induced spontaneous hydrogel contraction (Figure 1B, C), resulting in an average of approximately 85% within 72 hours (Figure 1D). In contrast, myofibroblasts cultured alone showed no contraction (Figure 1B, C). The amount and speed of contraction depended on the PBMCs: myofibroblasts ratio (Supplemental Figure 1). In addition, we tested multiple primary skin myofibroblast strains with similar effects (Supplemental Figure 2).

To better understand immune cell-mediated myofibroblast contraction, we further evaluated the effects of co-culture on myofibroblast biology at both the mRNA and protein levels. For mRNA expression, myofibroblasts were FACS sorted from enzymatically digested hydrogels based on CD45⁻, CD90⁺, and fibroblast activation protein (FAP)+ (Supplemental Figure 3 for the sorting strategy). At the mRNA level, co-culture did not affect the expression of ECM genes such as collagen type I or fibronectin, which are typically upregulated in pathological conditions involving excessive tissue fibrosis, such as SSc. (Figure 1E). On the other hand, we observed increased gene and protein expression of the collagen crosslinking enzyme PLOD2 (Figure 1F, H), which has been associated with pathological fibrosis (16). Co-culture also enhanced myofibroblast antigen presentation, as it induced the gene expression of HLA-ABC (i.e. MHC class 1) and gene and protein expression of HLA-DRB (i.e. MHC class II) (*Figure 1G*). This suggests that co-culture increases myofibroblast antigen presentation capacity, a pathological process also observed in the context of SSc (17). In addition, co-culture clearly induced *IL6* and podoplanin (*PDPN*) expression, two genes associated with pathologically activated myofibroblasts in e.g. rheumatoid arthritis (*Figure 1G*) (18-20). At the protein level, co-culture notably increased FAP and PDPN expression, as analysed by immunohistochemistry (IHC) (*Figure 1H*). Additionally, the elevated presence of HLA-DR+ myofibroblasts was verified at the protein level with flow cytometry (*Figure 1I, J*). Collectively, the developed in vitro model demonstrates that co-culturing skin myofibroblasts with PBMCs induces myofibroblast activation, contraction, and a phenotype with pathological features, highlighting immune-mediated alterations in myofibroblasts.

Co-culture of immune cells with myofibroblasts induces T cell activation, cytotoxicity and cytokine production

To examine the influence of myofibroblasts on the co-cultured immune cells, we performed multi-color flow cytometry on the single cells isolated after digestion of the collagen hydrogels at multiple timepoints (24, 48, 72 hours). Since our model was based on allogeneic mismatch, we evaluated the effect of the co-culture on both CD4+ T cell and CD8+ T cell activation. To assess this, we measured T cell activation markers (CD25, CD69, CD134) after 16 hours of co-culture and compared them to immune cells cultured in the collagen hydrogel without myofibroblasts. CD25 and CD69 were significantly induced in both T cell subtypes, while no difference in CD134 (OX40) expression was observed (Figure 2A). The largest effect on T cell activation was attributed to CD69 up-regulation, suggesting that T cells acquire a tissue-resident activation profile. Since cytokine production is a result of T cell activation, we examined the kinetics of T cell activation over extended culture periods by measuring IL-2 and IFNy expression for up to three days of co-culture. Initially, approximately 10% of T cells were positive for these cytokines, but the proportion of IL-2 and IFNy-expressing CD4+ and CD8+ T cells increased over time, reaching up to 80% at 72 hours (Figure 2B, C). Additionally, while the percentage of CD8+GZMB+/GZMK+ T cells did not change during this co-culture time-frame (Supplemental figure 4), CD8+ T cells showed a time dependent elevation of granzyme B expression that fits with their increased activation status (Figure 2D). In conclusion, myofibroblast activation, contraction, and pathogenic phenotype are accompanied by the induction of effector functions in both CD4+ and CD8+ activated T cells. Thus, our model extends beyond myofibroblast activation.

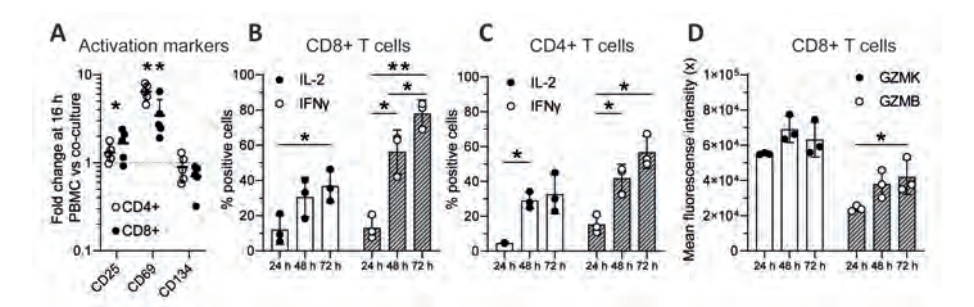


Figure 2. Co-culturing immune cells with myofibroblasts promotes T cell activation, granzyme expression, and cytokine production. (A) The expression of the activation markers CD25, CD69, CD134 on both CD4+ and CD8+ T cells was measured with flow cytometry of enzymatically digested myofibroblast and PBMC (n=5) hydrogels after 16 hours of co-culture. Values are represented as fold change compared to PBMCs cultured alone and statistics were performed with two-way ANOVA corrected with Tukey's post hoc test. Asterisks refer to both CD4+ and CD8+ T cell fold change statistical significance compared to PBMCs alone condition. Flow cytometric quantification of the percentage of IL-2 and IFNy positive CD8+ T cells (B) and CD4+ T cells (C) after 24, 48 and 72 hours of co-culture (n=3). (D) Mean fluorescence intensity of the expression of granzyme K (GZMK) and granzyme B (GZMB) in CD8+ T cells after 24, 48 and 72 hours of co-culture (n=3). Statistics for panels B-D were performed with two-way ANOVA corrected with Tukey's post hoc test. In the panels above, each dot represents one donor.

Myofibroblast contraction induced by immune cells is not driven by cvtotoxic mechanisms

Given that elevated myofibroblast contraction was linked to T cell activation, we next investigated whether this could be attributed to increased T cell cytotoxicity towards myofibroblasts as target cells. To determine if the enhanced contraction was associated with cell death or cell death-related fragments (which can trigger myofibroblast activation), we quantified myofibroblast cell death using flow cytometry and IHC. First, we assessed myofibroblast viability using a fixable viability dve in flow cytometric staining of single cells from the digested hydrogels. The presence of PBMCs did not negatively affect myofibroblast viability (*Figure 3A*). On IHC, a limited number of apoptotic cells expressing active caspase 3 were observed, and only a few cells showed an increased amount of double-stranded DNA breaks (yH2AX) when comparing myofibroblasts cultured alone to those co-cultured with PBMCs (Figure 3B). Further investigation using 7AAD and Annexin-V flow cytometric staining to measure early and late apoptosis, as well as necrosis of myofibroblasts, revealed only a small percentage (<5%) of dead or preapoptotic myofibroblasts in both short-term (24 hours) and long-term (72 hours) cultures (Figure 3C-F). Collectively, our data suggest that immune cell-mediated myofibroblast cell death is minimal and does not appear to be the primary mechanism driving myofibroblast activation and contraction.

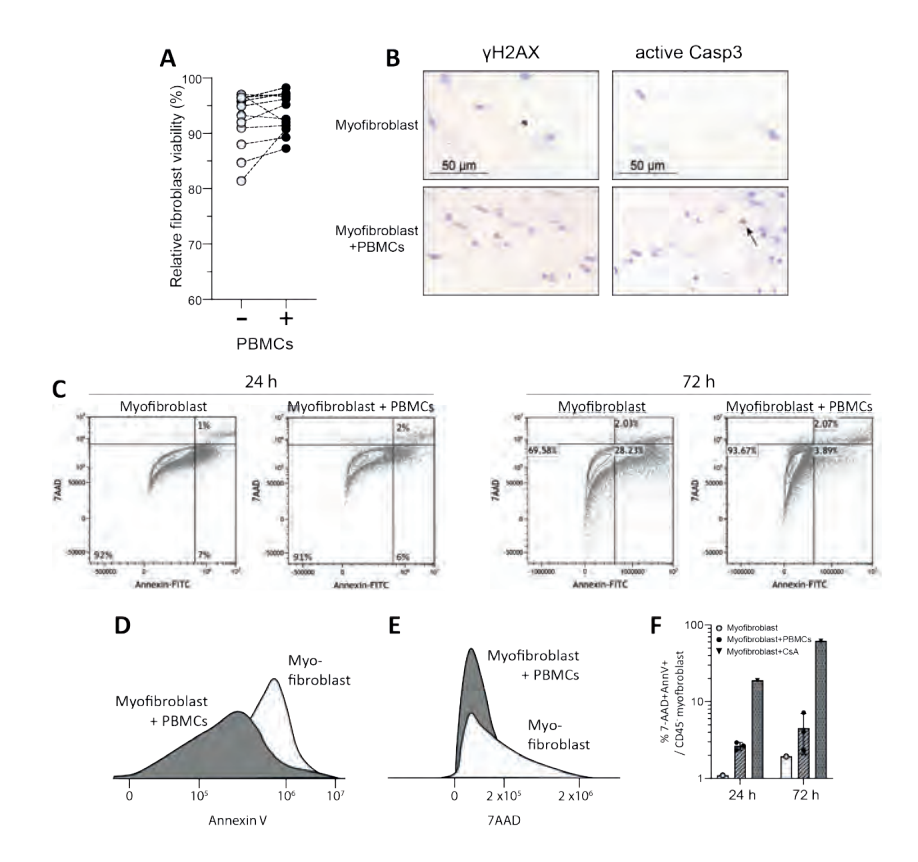


Figure 3. Immune cell-induced myofibroblast contraction is not dependent on cytotoxic mechanisms. (**A**) Percentage of relative myofibroblast viability in absence or presence of PBMCs, measured by flow cytometric viability staining. (**B**) Representative images of γH2AX and active caspase-3 immunohistochemistry from collagen hydrogels containing either myofibroblasts alone or myofibroblasts co-cultured with PBMCs. Scale is 50 μm. (**C**) Representative flow cytometry plots illustrating myofibroblast 7-AAD/ Annexin V staining at 24 and 72 hours of co-culture. Flow cytometry overlay histograms of one representative experiment comparing mean fluorescence intensity of (**D**) Annexin V and (**E**) 7-AAD staining between myofibroblast and myofibroblast+ PBMC conditions at 72 hrs. (**F**) Percentage of 7-AAD+/ AnnexinV+ CD45- myofibroblasts at 24 and 72 hours of cell culture alone or in presence of PBMCs (n=3). A condition with myofibroblasts treated with cyclosporin A (CsA) was used as positive control. In the panel A, each dot represents one donor.

Cytokine producing CD8+ T cells drive myofibroblast contraction

Recent data suggests a prevalent presence of CD8+ cytotoxic compared to CD4+ T helper cells in the affected tissues (skin, lungs, synovium) of patients with autoimmune mediated CTD (6, 7, 21). Therefore, we analyzed whether CD8+ T cells and CD4+ T cells were differentially linked to the observed myofibroblast contraction. To address this, we sorted CD3+ T cells, CD4+ T cells and CD8+ T cells through negative magnetic beads selection from healthy blood and co-cultured

them in the same cell concentration separately with myofibroblasts. All T cell populations induced myofibroblast contraction, and of note, CD8+ T cells induced significantly higher contraction compared to CD4+ T cells (Figure 4A). To further evaluate whether TCR signalling is required for the observed contraction, we used an anti-CD8 blocking antibody. Blocking the CD8 receptor resulted in a 25% decrease in myofibroblast contraction but did not completely inhibit it (Figure 4B), suggesting that mechanisms downstream of TCR activation are not the only way CD8+ T cells activate myofibroblasts. By transferring the supernatant from the myofibroblast: immune cell co-culture, we were able to trigger hydrogel contraction when added to new, unexposed hydrogel mono-cultured myofibroblasts. This suggests that soluble mediators, such as cytokines, are involved (Supplemental Figure 5). The supernatant was screened for a large panel of cytokines, detecting IL-6, IL-8 and IFNγ, while IL-1β, IL-2, IL-4, IL-5, IL-17, IL-12, IL-13, IL-10, IL-15, and IL-17 were undetectable

Given that supernatant transfer induced myofibroblast contraction in the absence of immune cells and in light of the recently described T helper cytokine production by CD8+ T cells (12), we compared the expression of T helper cytokines (i.e., IL-4, IL-13, IL-6, and IFNy) between CD4+ and CD8+ T cells to better understand their potential involvement in our model. We found that IL-4 was produced by both T cell subtypes, while IL-13 was only produced by CD4+ T cells (Figure 4C). In contrast to previous research on the pro-fibrotic role of these cytokines in SSc and other CTDs, it seems unlikely that they are the main drivers of the CD8+ T cell effects in this model. However, both the expression (Figure 4D) and production (Figure 4E) of the pro-inflammatory cytokine IL-6 were significantly elevated in CD8+ compared to CD4+ T cells, suggesting a potential role in the enhanced myofibroblast contraction.

STAT3 is a prominent intracellular mediator of IL-6 signalling. Therefore, we next used a luciferase construct to measure activity of this transcription factor: i.e. sisinduced element (SIE) driven luciferase expression. Co-culture of PBMCs with these reporter cells resulted in clear SIE-driven luciferase expression. Interestingly, we observed an oscillating SIE-driven luciferase expression reflecting a dynamic regulation over time (Figure 4F). We then sought to evaluate whether the elevated SIE response was attributed to cytokine production from PBMCs and CD8+ T cells. To do this, we pre-incubated whole PBMCs or isolated CD8+ T cells with the Golgi inhibitor BFA to block their cytokine production and then co-cultured them with myofibroblasts carrying the SIE luciferase construct. Cytokine blockade in both PBMCs and CD8+ T cells fully inhibited SIE activity (Figure 4G, H), showing that the elevated SIE-driven myofibroblast activity was likely mediated by secreted factors that among other activate STAT3 signalling. This hypothesis was confirmed by measuring cytokine levels such as IL-6 in the supernatant of these cultures, where pre-treatment of CD8+ T cells with BFA completely blocked IL-6 production (*Figure 4I*). Furthermore, blocking cytokine production in CD8+ T cell also halted myofibroblast gene expression of PDPN, IL-6 and HLA-DR (*Figure 4J*). In conclusion, the increased myofibroblast activation and contraction observed in our model is a dynamic process that requires interaction between cells and cytokines, and it appears to be predominantly driven by CD8+ T cells in a STAT3 signalling-dependent manner.

Co-culture mediated myofibroblast activation is dependent on JAK/ STAT and TGFß signalling

To further unravel the molecular mechanisms underlying STAT3 CD8+ T cell- and other well-known pro-fibrotic mechanisms such as TGF β - mediated myofibroblast contraction, we next evaluated myofibroblast expression of key downstream TGF β and JAK/STAT signalling molecules (pSMAD2 and pSTAT3, respectively) 72 hours after their co-culture with PBMCs. Both SMAD2 and STAT3 phosphorylation were highly activated in the presence of immune cells (*Figure 5A*). Interestingly, the expression of these markers was reciprocal, suggesting distinct myofibroblast mechanisms and functions.

To assess the potential reversibility of these processes, we treated PBMC: myofibroblast hydrogels with the JAK/STAT inhibitor tofacitinib and the TGF-B1 receptor (ALK4/5/7) inhibitor SB-505124 to evaluate their effects on myofibroblast contraction. Neither inhibitor negatively affected myofibroblast or immune cell viability (Supplemental Figure 6), but both significantly reduced myofibroblast contraction. Furthermore, the combination of both inhibitors exhibited an additive effect, almost completely preventing myofibroblast activation (Figure 5B, C). The involvement of JAK/STAT3 signalling was further verified by the efficacy of the JAK/ STAT-specific inhibitor stattic in significantly halting myofibroblast contraction (Figure 5D). All mentioned inhibitors were similarly effective in halting CD8+ T cell mediated myofibroblast contraction (Figure 5E). Gene expression analyses following immune-stromal co-culture revealed TGF\$\beta\$ transcripts in fibroblasts, monocytes/ macrophages, and lymphocytes, with marked upregulation in T cells (Supplemental Figure 7A, B). Functional assays using a TGFβ-responsive luciferase reporter further confirmed that co-culture supernatants activate the pathway in a TGFβ-dependent manner (**Supplemental Figure 7C**). These results suggest that TGF β and JAK/STAT signalling play key roles in mediating the elevated myofibroblast activation.

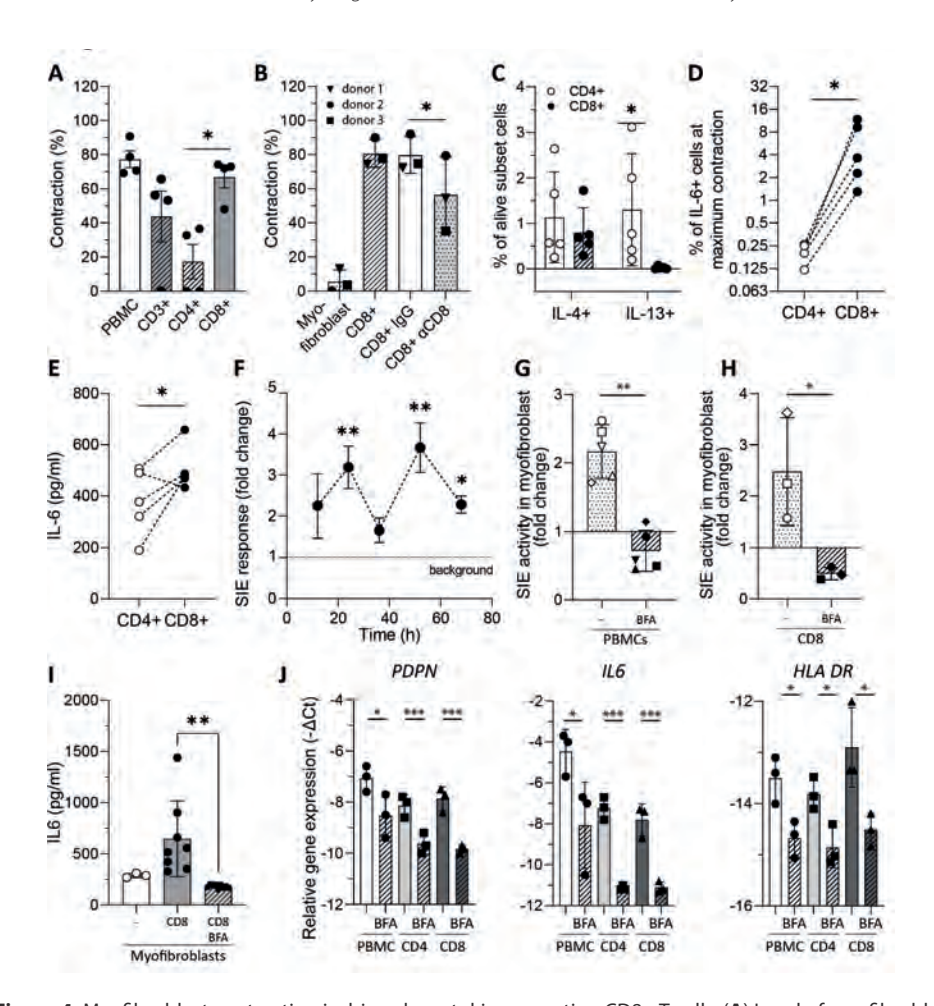


Figure 4. Myofibroblast contraction is driven by cytokine-secreting CD8+T cells. (A) Level of myofibroblast contraction after co-culture with PBMCs or sorted CD3+/CD4+/CD8+ T cells (n=4) at time of maximum contraction. (B) Level of myofibroblast contraction after co-culture with CD8+T cells in presence/absence of anti-CD8 monoclonal antibody or isotype control (n=3). Expression of IL-4 and IL-13 (C) and IL-6 (D) on CD4+ and CD8+ T cells was measured with intracellular flow cytometry of digested hydrogels containing PBMCs and myofibroblasts (n=5) at time of maximum contraction. (E) Production of IL-6 in the co-culture supernatant of myofibroblasts that were co-cultured with either CD4+ or CD8+ T cells. (F) SIE response of primary myofibroblast cell line was evaluated with the luciferase reporter assay after cells were incubated with supernatant from hydrogels containing myofibroblasts and PBMCs (n=3) that was collected at the depicted time points. Fold change of SIE activity in primary myofibroblast cell line incubated with supernatant from hydrogels containing myofibroblasts and (G) PBMCs or (H) CD8+ T cells that were cocultured for 24 hours. In depicted experimental conditions BFA was added to block release of cytokines. (I) Total IL-6 levels of co-cultures after 24 hours. (J) Primary skin myofibroblasts were cultured for 24 hours with cell culture supernatants obtained from myofibroblast hydrogels containing PBMCs, CD4+ T cells, or CD8+T cells in absence or presence of BFA. Myofibroblast relative gene expression of PDPN, IL-6 and HLA-DR was measured with qPCR and values are represented as - \Delta Ct. Statistics for panels A-B were performed with one-way repeated measures ANOVA, for panel C two-way repeated measures ANOVA with Tukey's post hoc test, for panels D-E, H paired t-test, for panel F, I one-way repeated measures ANOVA and for panel J two-way ANOVA with Tukey's post hoc test. In the panels above, each dot represents one donor. PBMCs; Peripheral Blood Mononuclear Cells, SIE; Sis-Inducible Element, BFA; Brefeldin A, PDPN; Podoplanin.

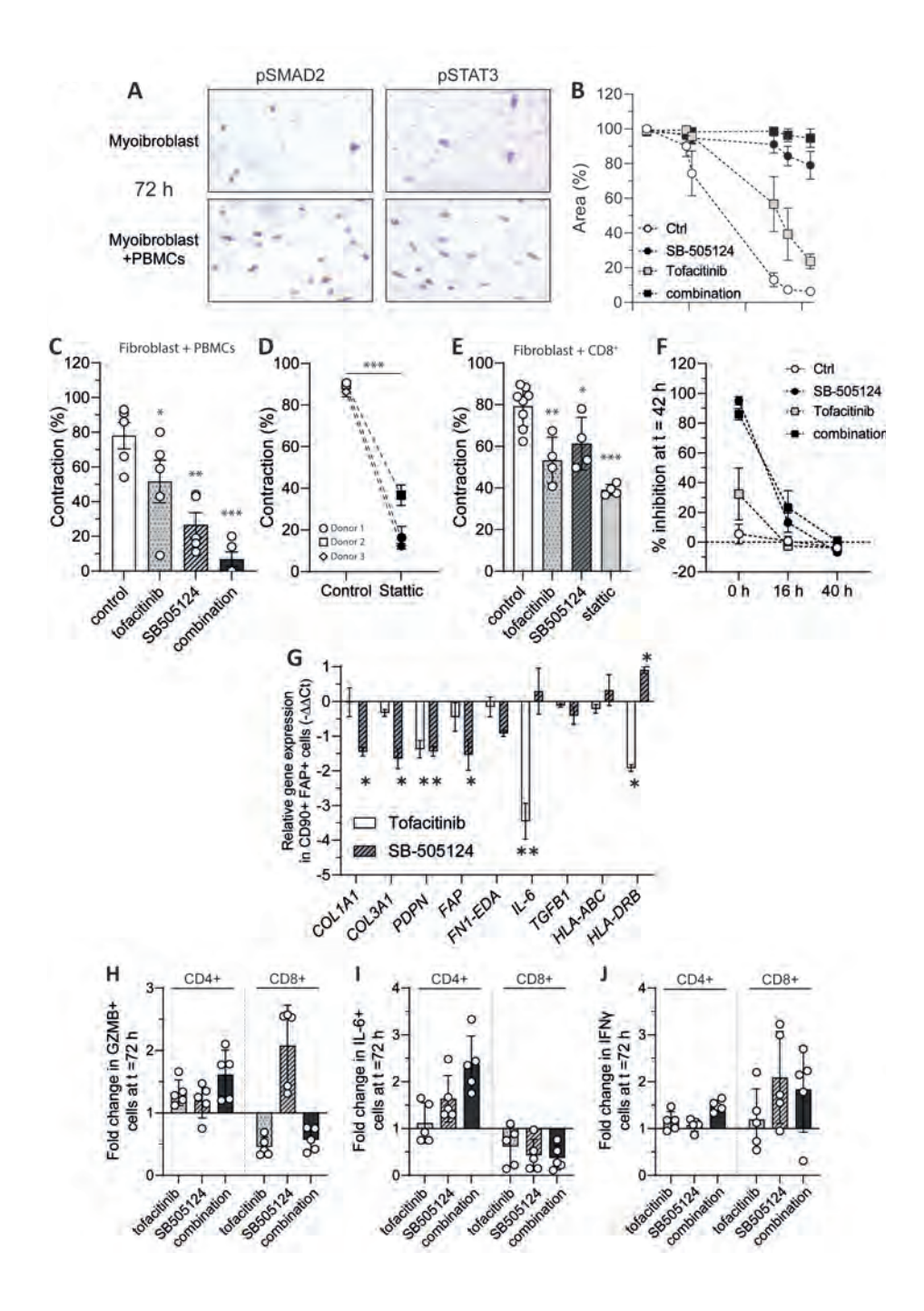


Figure 5. CD8+ T cell mediated myofibroblast activation is dependent on JAK/STAT and TGFβ signalling. (A) Representative images of pSMAD2 and pSTAT3 immunohistochemistry from collagen hydrogels containing either myofibroblasts alone or myofibroblasts co-cultured with PBMCs. Scale is 50 μm. (B) Level of myofibroblast contraction in myofibroblast: PBMCs hydrogels (n=5) that were treated with SB-505124 inhibitor, tofacitinib or a combination of the inhibitors (n=5). Graph represents meanSD myofibroblast contraction over time and the individual values at time of maximum contraction are depicted in panel (C). (D) Percentage of inhibition on myofibroblast contraction in PBMC:myofibroblast co-cultures treated with stattic (n=3). (E) CD8+ T:myofibroblast co-cultures were treated with the indicated inhibitors and the level of inhibition in myofibroblast contraction is indicated. (F) Percentage of inhibition in myofibroblast contraction after 42 hours treatment with the indicated inhibitors (n=5). Values are meanSD. In this experiment inhibitors were added at the beginning (t=0) or after 16 or 40 hours of culture. (G) Relative gene expression (- $\Delta\Delta$ Ct) of selected genes in sorted CD90+FAP+ myofibroblasts from PBMC/myofibroblast hydrogels that were treated with tofacitinib or SB-505124. From the same hydrogels, digested cells were subjected to flow cytometry staining to evaluate the effect of the inhibitors towards expression of (H) GZMB (I) IL-6 and (J) IFNy in both CD4+ and CD8+ T cells. Results are represented as fold change compared to control condition (n=5). Regarding statistics, for panels C, E one-way repeated measures ANOVA, for D paired t-test, for G two-way ANOVA corrected with Sidak's multiple comparisons test and for H-J two-way ANOVA with Tukey's post hoc test were used. In the panels above, each dot represents one donor. PBMCs: Peripheral Blood Mononuclear Cells.

To further investigate the kinetics of myofibroblast contraction inhibition by these inhibitors, we introduced them into the co-culture either at baseline or 16 and 40 hours after initiation. The addition of the inhibitors at 16 hours still showed an effect; however, when added after 40 hours, no effect was observed (Figure 5F). Since cytokines like IL-6 and TGFB can have direct effect towards myofibroblasts, we incubated hydrogel myofibroblast monocultures with increasing doses of IL-6 and TGFβ and witnessed that spontaneous contraction only happened after 7 days (Supplemental Figure 8), a time point not relevant to our model where immune cell mediated contraction happens within a maximum of three days, These observations suggest that the underlying molecular mechanisms of immune cell mediated myofibroblast contraction occur early in the model and are not reversible with later intervention.

In addition to the (kinetic) effect of the inhibition on myofibroblast contraction, we were also interested in its potential effect towards other myofibroblast functions such as ECM production, antigen presentation and activation. To address this, we analyzed the gene expression of FACs sorted CD45-CD90+FAP+ myofibroblasts that were treated or untreated with the aforementioned inhibitors. SB-505124 effectively halted pro-fibrotic myofibroblast phenotype by decreasing the expression of ECM and activation genes such as COL1A1, COL3A1, PDPN and FAP, while tofacitinib showed a significant reduction of myofibroblast IL-6 and HLA-DRB expression (Figure 5G).

Both inhibitors may also directly or indirectly affect immune cell function. Thus, we finally analyzed the effects of these inhibitors on CD8+ T cells and CD4+ T cells. The inhibitors did not significant affect CD4+ T cell cytokine production (IL-6 and IFNγ) (*Figure 5I, J*). Of note, tofacitinib, but not SB-505124, inhibited CD8+ T cell cytotoxic mediators, as indicated by reduced GZMB expression (*Figure 5H*). These findings further support the notion that CD8+ T cell, but not CD4+ T cell, cytokine production is driving myofibroblast activation. Interestingly, both tofacitinib and SB-505124 significantly reduced IL-6 production, but not IL-4, IL-13, or IFNγ, in CD8+ T cells (*Figure 5I*). In conclusion, these results suggest that myofibroblast activation depends on non-canonical cytokine producing CD8+ T cells, rather than exhibiting direct cytotoxicity, and that this activation can be reversed by targeting distinct immune cell and myofibroblast molecular pathways. Targeting both pathways shows an additive effect in halting T cell effector functions, myofibroblast activation, and contraction.

Discussion

Collagen contraction assays serve as models for tissue contraction, utilizing the observation that collagen hydrogels populated with cells undergo predictable and consistent contraction over time (22). In this study, we expanded upon current models by introducing allogeneic mismatching to mimic the interaction between auto-reactive immune cells and myofibroblasts, aiming to investigate how adaptive immune cells drive tissue contraction. Strikingly, CD8+ T cells were more effective at inducing myofibroblast contraction than CD4+ T cells, and this effect does not appear to be driven by cytotoxic mechanisms. Further analysis revealed that myofibroblast activation was dependent on JAK/STAT3 and TGF β signalling pathways, which function differently in CD4+ and CD8+ T cells. Notably, simultaneously targeting these pathways had an additive effect in halting hydrogel contraction, likely by inhibiting both T cell and myofibroblast activation.

We developed a novel 3D hydrogel co-culture model that induces spontaneous myofibroblast contraction through allogeneic immune cells. This model builds upon the classic mixed lymphocyte reaction model and a 3D myofibroblast contractility model. Our findings show that this model recapitulates key features of pathogenic myofibroblasts, including tissue contraction, expression of cross-linking enzymes, and activation and antigen-presentation. Co-culture strongly increased expression of activation markers such as FAP, PDPN, HLA type 2 and IL-6—markers of a myofibroblast phenotype associated with chronic inflammation, as seen

in conditions like rheumatoid arthritis, and indicative of immune crosstalk (23). However, no significant changes were observed in ECM molecules (e.g. COL1A1). This may reflect a shift toward an immunomodulatory phenotype, as evidenced by the upregulation of HLA-A, HLA-DR, and IL6, rather than a matrix-remodeling phenotype. This functional plasticity of myofibroblasts, shaped by cytokine cues such as interferon gamma, has been described in recent single-cell studies and highlights the dynamic interplay between immune signalling and fibroblast behavior in fibrotic environments (24). Future studies with extended culture times could further refine the model, providing deeper insights into immune cell-induced myofibroblast ECM production and deposition.

Mixed lymphocyte T cell alloreactivity depends on direct recognition of mismatched MHC class I or II molecules and/or of (allo)peptides presented by these MHC molecules (25). In mixed lymphocyte cultures, as well as, in vivo, approximately 5-10% of the T cell pool becomes activated in a highly polyclonal manner (14, 26) with a similar response for CD4+ and CD8+ T cell populations (27). In our experiments, expression of the classical T cell activation markers (28) CD25 (IL2R) and CD69 was strongly induced in both CD4+ and CD8+ populations after 24 hours of co-culture, but expression of CD134 (OX40) was not. However, kinetics of OX40 expression are slower than that of CD25 and CD69 and typically peak after 48 hours (28). Based on IL-2 and IFNy expression, we observed activation of 5-10% of CD4+ and CD8+ T cells similar as reported before, but these numbers further increased up to 40-80% after 72 hours. Possibly, cytokine-driven bystander activation (29) is involved in this further activation as we did not observe profound T cell proliferation in the time frame of our experiments. Taken together, our model recapitulated the features of a bona fide alloreactive response.

Despite similar activation levels of CD4+ T cells and CD8+ T cells, we observed stronger induction of hydrogel contraction by CD8+ T cells. This contraction is myofibroblast-dependent, as adding only PBMCs (or CD8+ T cells) (data not shown) to the hydrogels, or selectively deleting myofibroblasts, does not induce contraction (30). Thus, the more potent contraction indicates differential immune cell-mediated activation of myofibroblasts. Recently, distinct subsets of CD8+ T cells with noncanonical functions, that divert from cytotoxic killing effect, have been described such as producing T helper cytokines or exhibiting regulatory functions (12). Canonical functions of CD8+ T cells typically involve direct cytotoxic activity against infected or malignant cells, whereas non-canonical functions include roles in immune regulation and cytokine production (31). Strikingly, no significant CD8+ T cell-mediated cytotoxicity was observed; myofibroblast viability was higher in co-culture, and 7AAD/Annexin V staining revealed minimal apoptosis or necrosis in myofibroblasts. Additionally, activation of cleaved caspase-3 and detection of double-stranded DNA breaks (γH2AX) did not indicate apoptosis (32). This suggests that cytotoxicity mechanisms are unlikely to play a role in regulating contraction, and it is more likely that the interaction between CD8+ T cells and myofibroblasts involves non-canonical functions.

Non-canonical CD8+T cells are known to express T helper cytokines such as IL-4, IL-13, IL-6, and IFNy. In our experiments, we found a similar percentage of CD4+ and CD8+T cells expressing IL-4, but significantly more CD4+T cells expressed IL-13. In contrast, a higher proportion of CD8+T cells expressed IL-6, and overall IL-6 levels were elevated in CD8+T cell: myofibroblast co-cultures. These findings, combined with the strong inhibitory effect of tofacitinib, suggest that IL-6 may serve as an effector molecule mediating the effects of non-canonical CD8+T cells on myofibroblast activation and contraction. Additionally, the transfer of the contractile phenotype to naïve myofibroblasts through supernatant transfer supports the involvement of soluble mediators. This hypothesis is further supported by the observation that BFA, an inhibitor that blocks the trafficking of cytokines and growth factors from the endoplasmic reticulum to the Golgi apparatus in T cells, reduces myofibroblast activation at the gene expression level.

Mixed lymphocyte reaction (MLR) assays are essential in pre-clinical drug development for immunotherapies targeting cancer, inflammatory and transplantation-related diseases. These assays evaluate the safety and efficacy of targeting interactions between T cells and professional antigen-presenting cells (APCs) in an immunological context (33). To better understand immune-driven processes like fibrosis, it is essential to study T cell interactions with stromal cells, as these interactions are key to the orchestration of tissue adaptation. Therefore, our developed model offers added translational value compared to traditional MLR assays in studying the complex interactions between immune cells and stromal cells. These interactions are relevant in various pathological contexts, such as the pancreatic tumour microenvironment, graft-versus-host disease, and CTD pathology. SSc, a prototypic autoimmune CTD, is characterized by excessive myofibroblast activation and contraction in the skin and other affected organs. Notably, SSc is marked by a prominent influx of CD8+ T cells into the skin, especially in the early stages of the disease (34). However, it is yet poorly understood how these cells contribute to the excessive myofibroblast activation. Our work demonstrates that these cells might be directly involved in driving myofibroblast contraction. Further research into the detailed phenotype of these CD8+T cells in SSc is needed to support this claim.

While CD4+ T cells did activate fibroblasts, their impact was less significant, likely due to differences in signalling interactions or effector functions. In many CTDaffected tissues (including SSc-affected skin), a significantly higher infiltration of CD8+ T cells rather than CD4+ T cells, particularly in early disease stages, has been observed (21, 34, 35). Cytokine-producing CD8+ T cells are likely key drivers of fibrosis, contributing to tissue destruction. Importantly, our findings are consistent with emerging evidence that CD8+ T cells can adopt cytokine-producing roles similar to CD4+ T helper subsets in certain pathological contexts (11). Possibly, this could be a consequence of myofibroblast signalling or T cell-ECM interaction. as cancer associated myofibroblasts have been shown to suppress CD8+ T cell cytotoxicity (36), which has also been suggested for tumor ECM stiffness (37).

The myofibroblast-immune cell crosstalk was directly or indirectly driven by STAT3 signalling as the JAK/STAT3 inhibitor tofacitinib strongly reduced gene and protein expression of both HLA type 2 (HLA-DR) and IL-6. In addition, TGFβ signalling, via TGFBR1, strongly affected myofibroblast activity and gene expression. Both pathways are strongly associated with fibrotic diseases including SSc (5). Notably, a clear additive effect of inhibiting TGFβ and JAK/STAT3 signalling was observed on tissue contraction. Inhibiting these pathways had differential effects between CD4+ and CD8+ T cells. In CD8+ T cells, tofacitinib and SB-505124 had opposite effects on GZMB production, but in co-inhibition, tofacitinib was dominant in suppressing its expression. In CD4+ T cells, no such effect on GZMB expression was observed. Instead, IL-6 expression was modulated by these inhibitors in CD8+ T cells, in contrast to CD4+T cells. These observations underscore the heterogeneity of lymphocyte responses within a signalling network. Furthermore, our findings provide mechanistic evidence on the limited efficacy of anti-IL-6 monotherapy in CTDs such as scleroderma (38, 39) and suggest that combining anti-IL6 treatment with an anti-fibrotic agent such as SB-505124 might exhibit increased efficacy in halting tissue fibrosis in CTDs. A better understanding of such differential responses will contribute to the development of more effective treatments.

Limitations of the Study

While the developed 3D collagen hydrogel model provides new opportunities for translational research and high throughput drug screening, it comes along with certain limitations. Given that our model is based on MHC-driven T cell activation, we cannot exclude the possibility that the TCR-MHC interaction strength may be higher than that observed in autoimmune T cells. Since TCR signalling strength plays a critical role in determining T cell effector versus exhausted responses, our model may be biased toward the activation of certain T cell subsets. Although the

Conclusion

specific pathology.

In conclusion, this study provides valuable insights into the mechanisms by which CD8+ T cells can induce myofibroblast activation and contraction, primarily through cytokine-driven activation rather than cytotoxic mechanisms. The TGF β and JAK/STAT3 pathways were identified as critical regulators of this process, with dual inhibition demonstrating an additive effect in reducing contraction. These findings contribute to our understanding of the mechanisms underlying tissue fibrosis in systemic connective tissue diseases (CTDs). Moreover, they highlight the importance of targeting both immune and stromal cells in the treatment of fibrotic diseases.

Resource availability

Lead contact

Further information and requests should be addressed to the lead contact, Dr. Arjan van Caam (arjan.vancaam@radboudumc.nl).

Materials availability

This study did not generate new unique reagents.

Data and code availability

Not applicable.

Acknowledgements

We thank Monique Helsen for assistance with Luminex

Author contributions

Conceptualization: T.I.P, R.M.T, A.C ; execution of experiments and data analysis: T.I.P, A.E., M.W; technical support: E.V, B.W; funding acquisition: R.M.T; investigation: T.I.P, A.C, H.K, R.M.T; methodology: T.I.P, A.C, M.K, D.D, R.M.T; supervision: T.I.P, A.C, H.K, P.K, R.M.T; visualization: T.I.P, A.C; writing: T.I.P, A.C; reviewing & editing: T.I.P, A.C, A.E, D.D. M.K. H.K. R.M.T

Declaration of interests

The authors declare no competing interests.

Declaration of generative AI and AI-assisted technologies

No generative AI nor AI-assisted technologies were used in the writing process.

Supplemental information

Figures S1-S5, Tables S1-S4

STAR Methods

Key resources table

REAGENT or RESOURCE	SOURCE	IDENTIFIER
Antibodies		
Rabbit polyclonal anti-Collagen type 1 (COL1A1)	Merck	Cat#ABT257
Rabbit polyclonal Anti-alpha smooth muscle Actin	Abcam	Cat#ab5694
Purified anti-Podoplanin (Clone D2-40)	Biolegend	Cat#916605
Rabbit monoclonal anti-Fibroblast activation protein, alpha	Abcam	Cat#ab207178
Rabbit Phospho-SMAD2 (Ser465/467)/ SMAD3 (Ser423/425)	Cell Signalling	Cat#3108
Rabbit Phospho-Stat3 (Tyr705) (D3A7) XP	Cell Signalling	Cat#9145
Rabbit polyclonal Cleaved caspase-3 (Asp175)	Cell Signalling	Cat#9661
Rabbit polyclonal Phospho-Histone H2A.X (Ser139) (20E3)	Cell Signalling	Cat#9718
PerCP/Cyanine5.5 anti-human CD4 (Clone RPA-T4)	Biolegend	Cat#300530
APC/Cyanine7 anti-human CD3 (Clone UCHT1)	Biolegend	Cat#300425
Brilliant Violet 510™ anti-human CD8a (Clone RPA-T8)	Biolegend	Cat#301048
Brilliant Violet 510™ anti-human CD45 (Clone HI30)	Biolegend	Cat#304036
PE/Cyanine7 anti-human CD25 (Clone M-A251)	Biolegend	Cat#356108
FITC anti-human CD134 (OX40) (Clone ACT35)	Biolegend	Cat#350006
APC anti-human HLA-DR (Clone L243)	Biolegend	Cat#307609
APC anti-human HLA-A, B, C (Clone W6/32)	Biolegend	Cat#311409
APC anti-human CD90 (Thy-1) (Clone 5E10)	eBioscience	Cat#17-0909-42
APC anti-human Fibroblast Activation Protein alpha (Clone BLR150J)	R&D Systems	Cat#FAB3715A-025
Alexa Fluor700 anti-human CD69 (Clone FN50)	Biolegend	Cat#310922
PE anti-human IL-2 (Clone MQ1-17H12)	eBioscience	Cat#12-7029-42
PE/Dazzle594 anti-human IL-4 (Clone MP4-25D2)	Biolegend	Cat#500832
Alexa Fluor 700 anti-human IFN-γ (Clone B27)	Biolegend	Cat#506516
Pacific Blue anti-human IL-6 (Clone MQ2-13A5)	Biolegend	Cat#501114
PE/Cy7 anti-human IL-13 (Clone JES10-5A2)	Biolegend	Cat#501914
APC/Fire750 anti-human Granzyme B (Clone QA16A02)	Biolegend	Cat#372210
FITC anti-human Granzyme K (Clone GM26E7)	Biolegend	Cat#370508
Biological samples		
Human skin biopsies	Radboud University Medical Center	Study number: NL57997.091.16

REAGENT or RESOURCE	SOURCE	IDENTIFIER
Healthy human peripheral blood	Sanquin Blood Bank, the Netherlands	NA
Chemicals, peptides, and recombinant proteins		
Tofacitinib	LC Laboratories	Cat#T-1377
SB-505124	Sigma-Aldrich	Cat#HY-10431
Brefeldin-A	Merck	Cat#B7651
Collagenase D	Roche	Cat#COLLD-RO
DNase I	Roche	Cat#10104159001
Oligonucleotides		
Primers for GAPDH, RPS27a, TBP, COL1A1, COL3A1, FN1, FN1EDA, PLOD2, FAP, ACTA2, PDPN, IL6, HLA-ABC, HLA-DR, TGFB1, see Table S4	Merck	www.sigmaaldrich. com/NL/en/search/ order-primers?focus= products&page=1&pe rpage=30&sort=relev ance&term=order%20 primers&type=product
Software and algorithms		
ImageJ	U. S. National Institutes of Health, Bethesda, Maryland, USA	https://imagej.net/ ij/, 1997-2018
Kaluza Analysis Software, Version 2.1.3	Beckman Coulter	www.mybeckman. nl/flow-cytometry/ software/kaluza

Isolation and culture of primary skin myofibroblasts

Primary skin dermal myofibroblasts were isolated from 4 mm diameter skin biopsies of the forearm. Written informed consent was provided prior to the procedure (study number: NL57997.091.16). Biopsies were subsequently placed in a 24 wells plate with 2 ml DMEM Glutamax medium (Gibco, Waltham, MA, USA) supplemented with 100 U/ml penicillin, 100 mg/ml streptomycin, 100 mg/L pyruvate, and 20% fetal calf serum (FCS) in standard culture conditions (37 °C, 5% CO₂, 95% humidity) for 2 weeks to allow spontaneous outgrowth of primary myofibroblasts. Medium was partly refreshed every 3-4 days. Primary myofibroblasts were cultured on plastic in T175 flasks in DMEM Glutamax medium (Gibco) supplemented with 100 U/ml penicillin, 100 mg/ml streptomycin, 100 mg/L pyruvate, and 10% FCS. Medium was partly refreshed every 3-4 days. Myofibroblasts were used in experiments after passage 6. To validate our findings, Human Dermal Myofibroblasts (HDF) purchased from the American Type Culture Collection (PCS-201-012) were included as a reference strain.

Isolation and culture of peripheral blood mononuclear cells

Human peripheral blood mononuclear cells (PBMCs) were isolated from buffy coats (obtained from Sanquin, The Netherlands, (project number: NVT 0397-02) by Ficoll Pacque PLUS density centrifugation according to manufacturer's guidelines. Cells were cultured in RPMI medium 1640 + GlutaMAXTM (Gibco) supplemented with 100 U/ml penicillin, 100 mg/ml streptomycin, 100 mg/L pyruvate, and 10% Human Processed Serum (HPS). To aid detection of cytokines with flow cytometry, Brefeldin A (BFA) (5 μ g/ml) (Sigma-Aldrich) was added in the culture medium for 3 hours prior to enzymatic digestion (37 °C, 5% CO₂).

CD3+ T cells, CD4+ T cells and CD8+ T cells were isolated from PBMCs via negative selection with magnetic-activated cell sorting (MACS) kits (Biolegend: 480022, 480010, 480012) according to manufacturer's guidelines. Following isolation, the enriched fractions of CD3+ T cells, CD4+ T cells, and CD8+ T cells displayed purity levels exceeding 95%, assessed through flow cytometry staining targeting CD3, CD4, and CD8 antigens.

Myofibroblast and immune cell 3D co-culture hydrogel contraction model

To obtain a single cell suspension, myofibroblasts were washed twice with saline and detached from the culture flask with trypsin/EDTA at 37 °C. After detachment, trypsin was inactivated by adding 10 ml DMEM medium with 10% FCS. Cryopreserved PBMCs were thawed and washed twice with RPMI medium containing 10% HPS.

Next, the cells were seeded into the collagen hydrogel. Every hydrogel consisted of 20 μ l Minimum Essential Medium Eagle (Sigma-Aldrich), 10 μ l Sodium Bicarbonate 7.5% solution (Gibco), 150 μ l Type 1 Bovine Collagen Solution (Advanced BioMatrix) (3.1 mg/ml), and 90 μ l cell suspension. The cells in the hydrogel consisted of either 180 000 myofibroblasts alone, 1*10⁶ PBMCs alone, or 180 000 myofibroblasts with different cell concentrations of PBMCs/ CD3+ T/CD4+ T/CD8+ T cells. After the collagen-cell mixture was adequately homogenized, 250 μ l of mixture was pipetted per well in a 48 wells plate. The hydrogels solidified for 2 hours in the incubator at 37 °C and 5% CO₂. After solidification, 750 μ l RPMI medium 1640 + GlutaMAXTM (Gibco) supplemented with 100 U/ml penicillin, 100 mg/ml streptomycin, 100 mg/L

pyruvate, and 10% HPS was gently pipetted at the side of the wells. For all conditions in every experiment at least three technical replicates were used. Contraction was macroscopically evaluated by scanning the plates on a standard office flat-bed scanner with 600 dpi resolution. The size of the hydrogels was measured using Fiji software and was calculated as follows:

$$Contraction = \left(\frac{Area\ of\ hydrogel}{Area\ of\ uncontracted\ hydrogel}\right)*100\%$$

Pharmaceutical compounds

Tofacitinib (1 μM) (LC Laboratories), SB-505124 (5 μM) (Sigma-Aldrich) were added to the hydrogels by adding the compounds to the medium that was added after solidification of the hydrogels. In the experiments where we wanted to block cytokine production of immune cells, BFA (5 µg/ml) (Merck) was added to isolated immune cells (PBMCs, CD3+ T cells, CD4+ T cells or CD8+ T cells) for 4 hours before being washed away and cells were used for hydrogel co-cultures.

Enzymatic digestion of hydrogels

To obtain a single cell suspension of the myofibroblasts and PBMCs from the hydrogels in order to study phenotype and gene expression levels of cell populations of interest, hydrogels were enzymatically digested for 1 hour on a roller at 37 °C in 500 µl digestion mix containing collagenase D (Roche) (200 U/ml) and DNase I (Roche) (0.1 mg/ml) that were dissolved in PBS. Digestion enzymes were inactivated by adding 50 µl FCS. Hydrogels were then mechanically disrupted by careful pipetting up and down and subsequently spun down for 5 minutes at $300 \times g$. The supernatant was removed and the cells used for further processing.

Immunohistochemistry

Collagen hydrogels were formalin-fixed, paraffin-embedded (FFPE), and sectioned into 5.0 µm thick slices before being stained with hematoxylin and eosin (HE). For immunohistochemistry, the FFPE tissue sections underwent deparaffinization using xylene and rehydration with ethanol. Antigen retrieval was performed either in 10 mM sodium citrate buffer (pH 6.0) at room temperature or by heating the slides at 97°C for 10 minutes. Endogenous peroxidase activity was blocked with 3% H₂O₂ in PBS. Primary antibodies (detailed in **Supplementary Table 1**) and corresponding secondary antibodies (BrightVision Poly-HRP, Immunologic DPVO55HRP, or Envision Flex HRP, DAKO) were applied, followed by labeling with 3,3'-diaminobenzidine (bright DAB, Immunologic or DAKO). The sections were then counterstained with hematoxylin.

Antibody staining and flow cytometry

Approximately 1×10^6 cells per condition, were washed twice with PBS in a 96 well v-bottom and incubated with (1.5: 1000 PBS) Viakrome808 (Beckman Coulter) viability dye for 30 minutes at 4 °C in the dark. After washing, the extracellular staining was performed by adding 30 μ l staining buffer (PBS+1% BSA) buffer with extracellular antibodies for 20 minutes at room temperature protected from light. In case of intracellular staining, cells were fixed with 50 μ l Cyto-Fast Fix/Perm solution (Biolegend) for 20 minutes at room temperature. Subsequently, cells were washed twice with 10X Cyto-Fast Perm/Wash Buffer (Biolegend) before stained with intracellular antibodies for 20 minutes at room temperature in the dark. Eventually cells were washed twice and acquired in a Beckman Coulter Cytoflex LX 21-color flow cytometer. Flow cytometry data were analyzed using Kaluza software version 2.1.3 (Beckman Coulter). A list of all extracellular and intracellular antibodies used is provided (**Supplementary table 2, 3**).

For fluorescently activated cell sorting (FACs), cells from digested hydrogels were first filtered through a 70 µm cell strainer (Falcon) and the extracellular staining was performed as previously described while the viability dye efluor780 (eBioscience) was used (1:1000 in PBS). An overview of the gating strategy that was used to sort immune and stromal cell populations of interest is displayed in (**Supplementary figure 3**). Sorted cells were collected in 200 µl RPMI medium supplemented with 10% HPS, 100 mg/L pyruvate, and 1% Penicillin/Streptomycin. After centrifugation, the cell pellet was resuspended in 350 µl RLT buffer from the RNeasy Mini Kit (Qiagen) with 2-Mercaptoethanol (1:100) and stored at -20 °C until further processing.

RNA isolation and quantitative real-time PCR

RNA isolation was performed with the RNeasy Mini Kit (Qiagen) according to the manufacturer's manual. RNA concentrations were measured with a nanodrop photo-spectrometer. Amplification grade DNase 1 (Sigma-Aldrich) was incubated for 15 minutes on room temperature in 10X reaction buffer (Sigma-Aldrich). The reaction stopped with Stop Solution For DNase 1 Kit (Sigma-Aldrich) for 15 minutes and by incubation of the samples at 65 °C for 10 minutes subsequently. cDNA was produced with a single step RT-qPCR by the following procedure: Samples were incubated for 5 minutes at 25 °C, for 60 minutes at 39 °C, and for 5 minutes at 95 °C subsequently in a thermocycler. Produced cDNA was diluted 10x with water. To perform qPCR, samples with 5 μ l SYBR Green Master Mix (Applied biosystems), 2 μ l 1 μ M forward and reverse primer solution, and 3 μ l cDNA sample were incubated for 10 minutes at 95 °C, then 40 cycli followed including 15 seconds at 95 °C and

60 seconds at 60 °C. After the reaction a melt curve was included in the protocol to verify target specificity. Reference genes used were: GAPDH, RPS27a, and TBP. Sequences of forward and reverse primers are provided (Supplementary table 4). All primers were first validated for their efficacy. $-\Delta C_{\tau}$ values were calculated with the following formula:

 $-\Delta C_T = Average C_T$ of 3 reference genes $-C_T$ value of gene of interest

Reporter Luciferase Assay

Sis-inducible element (SIE) activity was evaluated in reporter constructs cloned in the same primary dermal myofibroblasts and were obtained from Neefies et al, 2021 (15). Reporter myofibroblasts were also used at a density of 200.000 cells per hydrogel. Recombinant IL-6 (Peprotech: 100-21C-2UG) (10 ng/ml) was used as positive control. After 24 h coculture, hydrogels were collected and centrifuged, after which 150 µl Assay Buffer with 50x substrate from the Nano-Glo Luciferase Assay kit (Promega) was added to the pellet. Luciferase was measured with a Clariostar (BMG Labtech). Emission was measured at 590 nm.

Apoptosis assay

To differentiate between early apoptotic cells, non-apoptotic cells or cells in late apoptosis/necrosis, single-cell suspensions from digested hydrogels were initially labeled extracellularly with specific monoclonal antibodies for 20 minutes at room temperature. Subsequently, the cells underwent two cold PBS washes and were suspended in 100 µl PBS containing 5 µl 7-AAD (eBioscience, cat# 00-6993-50), 5 µl AnnexinV:FITC labeled (BD Pharmigen), and 0.15 µl CaCl2 (1 M) in PBS. Following a 10-minute incubation in darkness at room temperature, the samples were promptly analyzed via flow cytometry (Cytoflex LX 13, BD) after staining. Cells positive for both 7-AAD and AnnexinV are designated as late apoptotic/necrotic, whereas those positive only for AnnexinV and negative for 7-AAD are considered early apoptotic. Live cells exhibit negativity for both 7-AAD and AnnexinV.

Cytokine measurements

Human cytokines present in culture supernatants were quantified using Luminex. The Bio-Plex Pro Human Cytokine 27-plex Assay (Bio-Rad, cat# M500KCAF0Y) was employed according to the manufacturer's guidelines. Analysis of the samples was conducted utilizing BioPlex Manager 4 software (Bio-Rad Laboratories, Hercules, CA, USA).

Statistical analysis

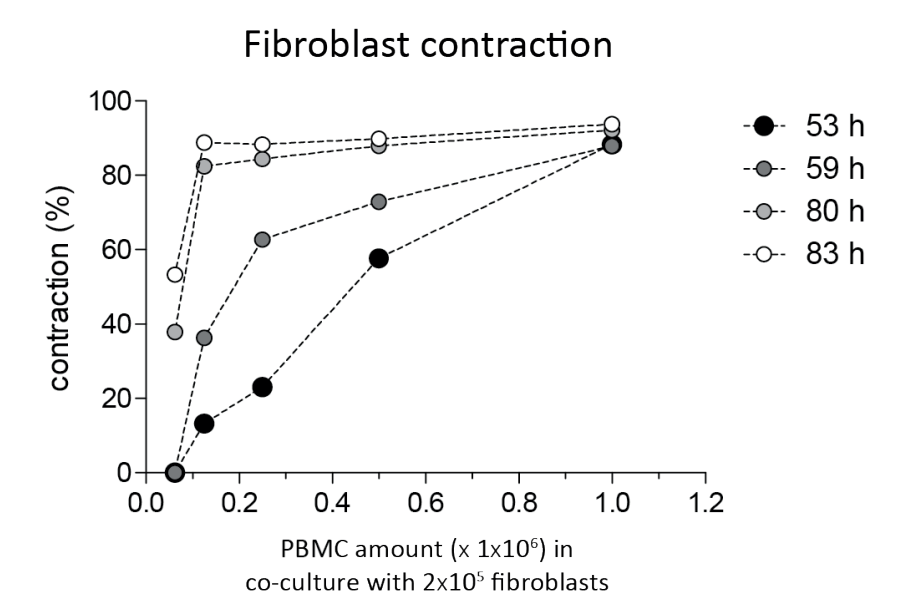
Statistical analyses were performed with GraphPad Prism version 10.0.3. Pairwise comparisons were analyzed with independent student's t test. For comparison of two groups a two-sided paired T test was utilized and for comparison of two or more groups a one-way or two-way (repeated measures) ANOVA was performed. P values below 0.05 were considered to be significant. For multiple comparisons, p values were adjusted for multiple testing with Tukey's or Dunnett's multiple comparison test. Specific statistical tests performed are mentioned in every figure's legend.

References

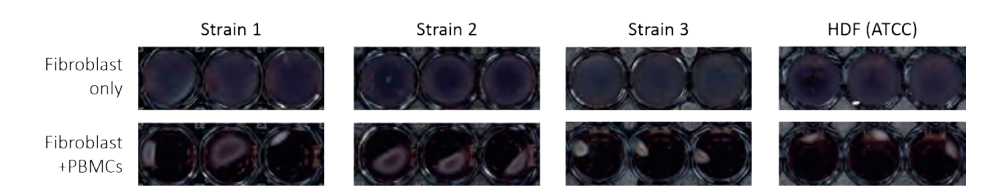
- Krieg T, Abraham D, Lafyatis R. Fibrosis in connective tissue disease: the role of the myofibroblast and fibroblast-epithelial cell interactions. Arthritis Research & Therapy. 2007;9(2):S4.
- Henderson NC, Rieder F, Wynn TA. Fibrosis: from mechanisms to medicines. Nature. 2. 2020:587(7835):555-66.
- 3 de Oliveira Martins LV, Oliveira SM, Silvatti J, de Amorim FG, Agapito Tito CV, Kayser C. Mortality in Systemic Sclerosis-Associated Interstitial Lung Disease in Brazil: A Real-Life, Long-Term Follow-up Observational Study. JCR: Journal of Clinical Rheumatology. 2022;28(2):e532-e8.
- Georges PC, Hui JJ, Gombos Z, McCormick ME, Wang AY, Uemura M, et al. Increased stiffness of the rat liver precedes matrix deposition: implications for fibrosis. Am J Physiol Gastrointest Liver Physiol. 2007;293(6):G1147-54.
- van Caam A, Vonk M, van den Hoogen F, van Lent P, van der Kraan P. Unraveling SSc Pathophysiology; The Myofibroblast. Front Immunol. 2018;9:2452.
- Papadimitriou TI, Singh P, Caam Av, Walgreen B, Gorris MAJ, Vitters EL, et al. CD7 activation regulates cytotoxicity-driven pathology in systemic sclerosis, yielding a target for selective cell depletion. Annals of the Rheumatic Diseases. 2023:ard-2023-224827.
- Padilla CM, Valenzi E, Tabib T, Nazari B, Sembrat J, Rojas M, et al. Increased CD8+ tissue resident memory T cells, regulatory T cells, and activated natural killer cells in systemic sclerosis lungs. Rheumatology (Oxford). 2023.
- Fuschiotti P. Current perspectives on the role of CD8+ T cells in systemic sclerosis. Immunol Lett. 2018;195:55-60.
- Ota Y, Kuwana M. Updates on genetics in systemic sclerosis. Inflammation and Regeneration. 2021:41(1):17.
- 10. Acosta-Herrera M, Kerick M, Lopéz-Isac E, Assassi S, Beretta L, Simeón-Aznar CP, et al. Comprehensive analysis of the major histocompatibility complex in systemic sclerosis identifies differential HLA associations by clinical and serological subtypes. Annals of the Rheumatic Diseases. 2021;80(8):1040-7.
- 11. Jonsson AH. Granzyme K(+) CD8 T cells in autoimmunity. Best Pract Res Clin Rheumatol.
- 12. Koh C-H, Lee S, Kwak M, Kim B-S, Chung Y. CD8 T cell subsets: heterogeneity, functions, and therapeutic potential. Experimental & Molecular Medicine. 2023;55(11):2287-99.
- 13. Maehara T, Kaneko N, Perugino CA, Mattoo H, Kers J, Allard-Chamard H, et al. Cytotoxic CD4+ T lymphocytes may induce endothelial cell apoptosis in systemic sclerosis. J Clin Invest. 2020;130(5):2451-64.
- 14. Kwon M, Choi YJ, Sa M, Park SH, Shin EC. Two-Round Mixed Lymphocyte Reaction for Evaluation of the Functional Activities of Anti-PD-1 and Immunomodulators. Immune Netw. 2018;18(6):e45.
- 15. Neefjes M, Housmans BAC, van den Akker GGH, van Rhijn LW, Welting TJM, van der Kraan PM. Reporter gene comparison demonstrates interference of complex body fluids with secreted luciferase activity. Sci Rep. 2021;11(1):1359.
- 16. Qi Y, Xu R. Roles of PLODs in Collagen Synthesis and Cancer Progression. Front Cell Dev Biol. 2018;6:66.
- 17. Gur C, Wang SY, Sheban F, Zada M, Li B, Kharouf F, et al. LGR5 expressing skin fibroblasts define a major cellular hub perturbed in scleroderma. Cell. 2022;185(8):1373-88.e20.

- 18. Symons RA, Colella F, Collins FL, Rafipay AJ, Kania K, McClure JJ, et al. Targeting the IL-6-Yap-Snail signalling axis in synovial fibroblasts ameliorates inflammatory arthritis. Ann Rheum Dis. 2022;81(2):214-24.
- 19. Mizoguchi F, Slowikowski K, Wei K, Marshall JL, Rao DA, Chang SK, et al. Functionally distinct disease-associated fibroblast subsets in rheumatoid arthritis. Nature Communications. 2018;9(1):789.
- 20. Croft AP, Naylor AJ, Marshall JL, Hardie DL, Zimmermann B, Turner J, et al. Rheumatoid synovial fibroblasts differentiate into distinct subsets in the presence of cytokines and cartilage. Arthritis Research & Therapy. 2016;18(1):270.
- 21. Moon J-S, Younis S, Ramadoss NS, Iyer R, Sheth K, Sharpe O, et al. Cytotoxic CD8+ T cells target citrullinated antigens in rheumatoid arthritis. Nature Communications. 2023;14(1):319.
- 22. Ngo P, Ramalingam P, Phillips JA, Furuta GT. Collagen gel contraction assay. Methods Mol Biol. 2006:341:103-9.
- 23. Davidson S, Coles M, Thomas T, Kollias G, Ludewig B, Turley S, et al. Fibroblasts as immune regulators in infection, inflammation and cancer. Nat Rev Immunol. 2021;21(11):704-17.
- 24. Younesi FS, Miller AE, Barker TH, Rossi FMV, Hinz B. Author Correction: Fibroblast and myofibroblast activation in normal tissue repair and fibrosis. Nature Reviews Molecular Cell Biology. 2024;25(8):671-.
- 25. Carnel N, Lancia HH, Guinier C, Benichou G. Pathways of Antigen Recognition by T Cells in Allograft Rejection. Transplantation. 2023;107(4):827-37.
- 26. DeWolf S, Grinshpun B, Savage T, Lau SP, Obradovic A, Shonts B, et al. Quantifying size and diversity of the human T cell alloresponse. JCI Insight. 2018;3(15).
- 27. Macedo C, Orkis EA, Popescu I, Elinoff BD, Zeevi A, Shapiro R, et al. Contribution of naïve and memory T cell populations to the human alloimmune response. Am J Transplant. 2009;9(9):2057-
- 28. Poloni C, Schonhofer C, Ivison S, Levings MK, Steiner TS, Cook L. T cell activation-induced marker assays in health and disease. Immunol Cell Biol. 2023;101(6):491-503.
- 29. Yosri M, Dokhan M, Aboagye E, Al Moussawy M, Abdelsamed HA. Mechanisms governing bystander activation of T cells. Front Immunol. 2024;15:1465889.
- 30. Dorst DN, van Caam APM, Vitters EL, Walgreen B, Helsen MMA, Klein C, et al. Fibroblast Activation Protein Targeted Photodynamic Therapy Selectively Kills Activated Skin Fibroblasts from Systemic Sclerosis Patients and Prevents Tissue Contraction. International Journal of Molecular Sciences. 2021;22(23):12681.
- 31. Koh CH, Lee S, Kwak M, Kim BS, Chung Y. CD8 T cell subsets: heterogeneity, functions, and therapeutic potential. Exp Mol Med. 2023;55(11):2287-99.
- 32. Kuo LJ, Yang LX. Gamma-H2AX a novel biomarker for DNA double-strand breaks. In Vivo. 2008;22(3):305-9.
- 33. Mehrotra A, Leventhal J, Purroy C, Cravedi P. Monitoring T cell alloreactivity. Transplantation Reviews. 2015;29(2):53-9.
- 34. Papadimitriou TI, Singh P, van Caam A, Walgreen B, Gorris MAJ, Vitters EL, et al. CD7 activation regulates cytotoxicity-driven pathology in systemic sclerosis, yielding a target for selective cell depletion. Ann Rheum Dis. 2024;83(4):488-98.
- 35. Kaneko N, Chen H, Perugino CA, Maehara T, Munemura R, Yokomizo S, et al. Cytotoxic CD8+T cells may be drivers of tissue destruction in Sjögren's syndrome. Scientific Reports. 2022;12(1):15427.

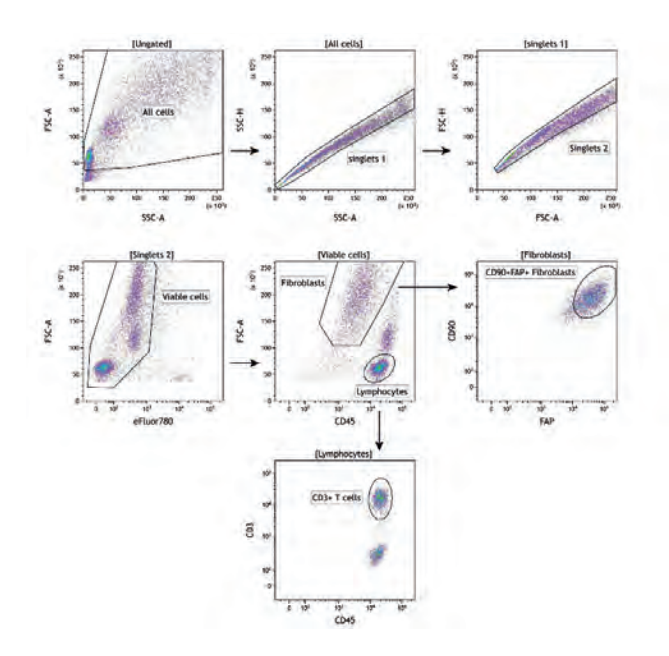
- 36. Freeman P, Mielgo A. Cancer-Associated Fibroblast Mediated Inhibition of CD8+ Cytotoxic T Cell Accumulation in Tumours: Mechanisms and Therapeutic Opportunities. Cancers (Basel). 2020;12(9).
- 37. Chirivì M, Maiullari F, Milan M, Presutti D, Cordiglieri C, Crosti M, et al. Tumor Extracellular Matrix Stiffness Promptly Modulates the Phenotype and Gene Expression of Infiltrating T Lymphocytes. Int J Mol Sci. 2021;22(11).
- 38. Khanna D, Lin CJF, Furst DE, Wagner B, Zucchetto M, Raghu G, et al. Long-Term Safety and Efficacy of Tocilizumab in Early Systemic Sclerosis-Interstitial Lung Disease: Open-Label Extension of a Phase 3 Randomized Controlled Trial. Am J Respir Crit Care Med. 2022;205(6):674-84.
- 39. Khanna D, Lin CJF, Furst DE, Goldin J, Kim G, Kuwana M, et al. Tocilizumab in systemic sclerosis: a randomised, double-blind, placebo-controlled, phase 3 trial. The Lancet Respiratory Medicine. 2020;8(10):963-74.
- 40. Pakshir P, Hinz B. The big five in fibrosis: Macrophages, myofibroblasts, matrix, mechanics, and miscommunication. Matrix Biology. 2018;68-69:81-93.



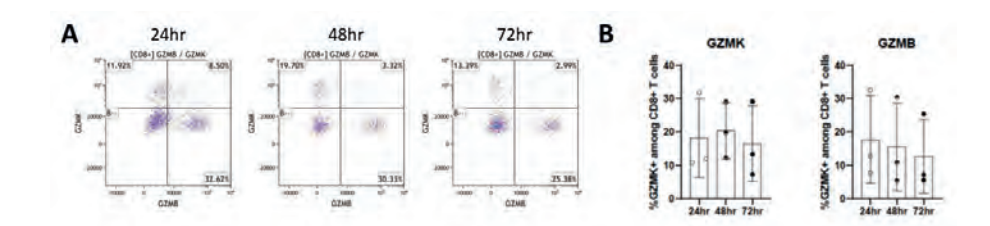
Supplemental figure 1. Contraction of hydrogels based on time and PBMC: myofibroblast ratio. Primary skin myofibroblasts were co-cultured with varying amounts of PBMCs in collagen type 1 hydrogels. The extent of hydrogel contraction was measured at specific time points as indicated. PBMCs; Peripheral Blood Mononuclear Cells.



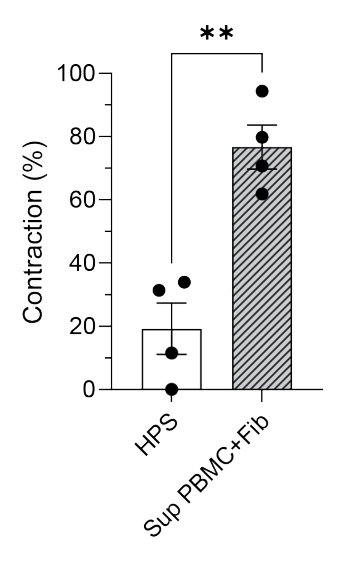
Supplemental figure 2. PBMC-myofibroblast co-culture induced hydrogel contraction in different myofibroblast strains. Four strains of primary skin myofibroblasts show strong contraction after 72 h of co-cultured with PBMCs in collagen type 1 hydrogels. This includes a primary normal dermal myofibroblasts (HDF) obtained from ATCC. PBMCs; Peripheral Blood Mononuclear Cells, HDF; Human Dermal Myofibroblasts, ATCC; American Type Culture Collection.



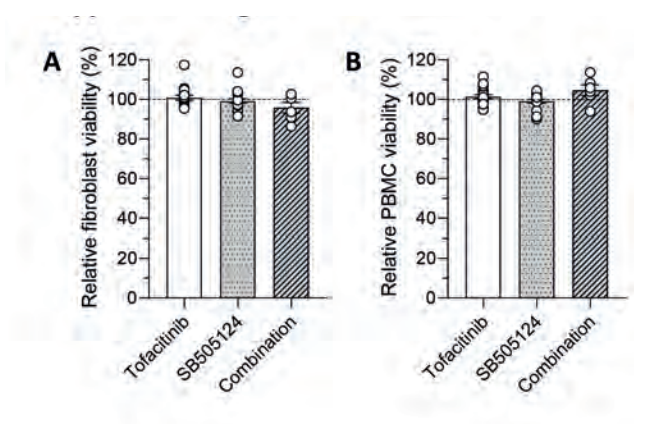
Supplemental figure 3. FACs gating strategy for sorting Myofibroblast and T cells for RNA analysis. Myofibroblasts were defined as CD45⁻, and CD90⁺, FAP⁺. FACs; Fluorescence-Activated Cell sorting.



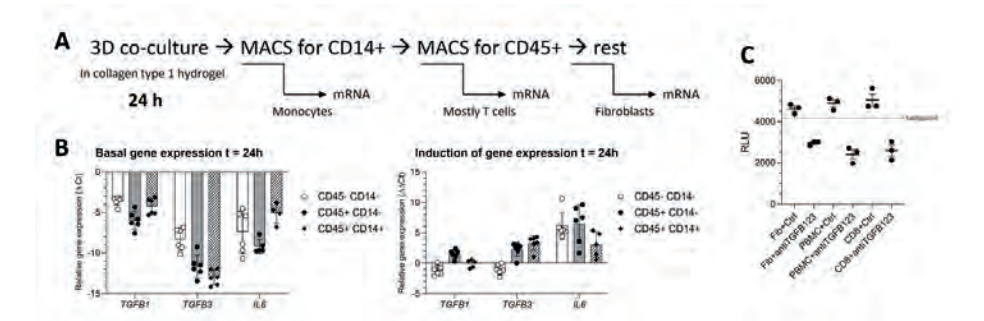
Supplemental figure 4. PBMC-myofibroblast co-culture does not affect the percentage of CD8+GZMB+ nor CD8+GZMK+ T cells. (A) Flow cytometry plots from one representative donor exhibit expression of GZMB and GZMK in CD8+T cells co-cultured with myofibroblasts for 24, 48 and 72 hours. (B) Graphic quantification of the percentage of CD8+GZMB+ and CD8+GZMK+ T cells from n=3 donors at 24, 48 and 72 hours of co-culture. PBMCs; Peripheral Blood Mononuclear Cells, GZMK; Granzyme K, GZMB; Granzyme B.



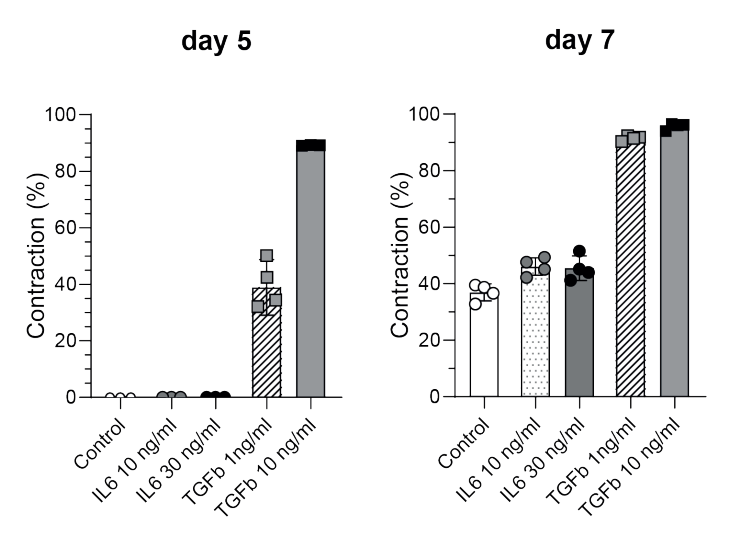
Supplemental figure 5. Co-culture supernatant transfer promotes hydrogel contraction in myofibroblast monoculture. Myofibroblasts and PBMCs were co-cultured for 72 hours, after which the supernatant was collected and centrifuged twice at 300 x g. This processed supernatant (20% v/v) was then added to the medium of fresh hydrogels containing only myofibroblasts. As a control, medium that had not been exposed to co-cultures (10% HPS) was used. The supernatant-induced contraction of myofibroblast monocultures was observed 1-2 days later compared to when immune cells are present. PBMCs; Peripheral Blood Mononuclear Cells, HPS; Human Pooled Serum.



Supplemental figure 6. No significant decrease in myofibroblast nor PBMC viability is observed with the inhibitors' treatment. Relative viability of myofibroblasts (A) and PBMCs (B) after 72-hour treatment with Tofacitinib ($0.5 \mu M$), SB505124 ($5 \mu M$) or the combination of both compared to vehicle control.



Supplemental figure 7. TGFβ signalling plays an essential role in immune-cell mediated myofibroblast contraction and activation. A) Schematic representation of the sorting strategy that was used to isolate fibroblasts (CD45-CD14-), monocytes/macrophages (CD45+CD14+) and CD45+CD14- immune cells (containing lymphocytes of which the largest amount is T cells) for RNA isolation 24 hours after co-culture. B) Basal gene expression (left) and induction of gene expression (right) of TGFB1, TGFB3 and IL6 in the sorted myofibroblasts, monocytes/macrophages and lymphocytes. Values are represented as relative gene expression (-ΔCt) III) RLU luciferase values of SBE expression in SBE reporter cells that were cultured with the designated supernatants and were treated with isotype (control) or anti-TGFB123 antibody for 1 hour at 37 degrees Celcius.



Supplemental figure 8. Spontaneous contraction of myofibroblast monoculture hydrogels under the influence of TGFB and IL6. Primary skin myofibroblasts were cultured in collagen hydrogels for 1 week and contraction was measured at day 5 and day 7. At day 5, no spontaneous contraction is observed in the controls yet, whereas at day 7 this can be observed. TGFβ clearly enhanced contraction, but IL-6 alone did not.

Supplementary materials

Supplementary Table 1. List of antibodies used for immunohistochemistry.

Antigen	Clone	Supplier	Identifier
Pro-collagen type 1	A1/COL1A1	Merck	ABT257
alpha-smooth muscle actin	polyclonal	Abcam	ab5694
Podoplanin	D2-40	Biolegend	916605
Myofibroblast activation protein	Monoclonal	Abcam	ab207178
Phospho-SMAD2 (Ser465/467)	138D4	CellSignalling	#3108
Phospho-Stat3 (Tyr705)	D3A7	CellSignalling	9145S
Cleaved caspase-3 (Asp175)	Polyclonal	CellSignalling	9661S
γH2AX	Polyclonal	CellSignalling	9718S

Supplementary Table 2. List of antibodies used for cell surface flow cytometry staining.

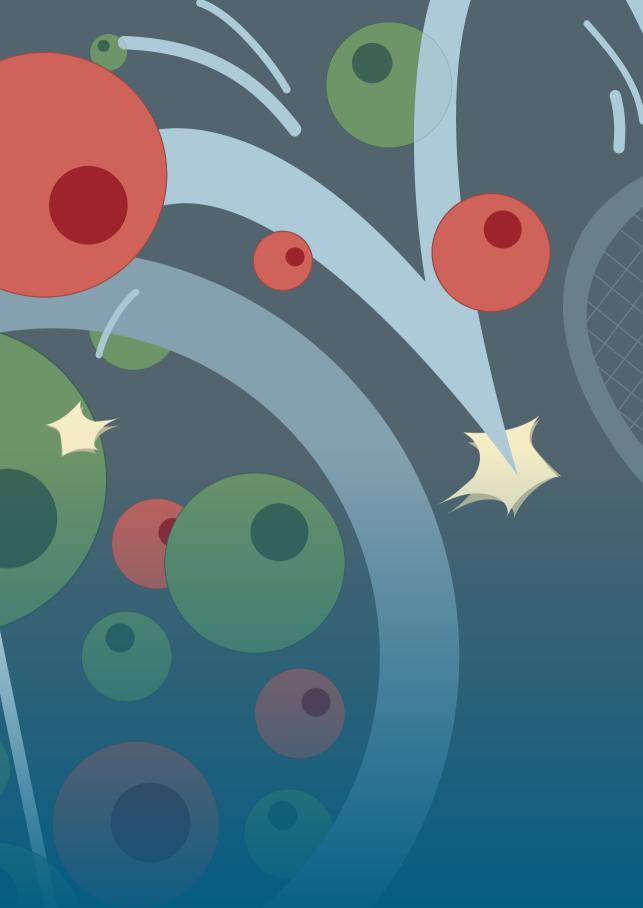
Antigen	Clone	Fluorochrome	Supplier	Identifier
CD4	RPA-T4	PerCP/Cy5.5	Biolegend	300530
CD3	UCHT1	Alexa Fluor700	Biolegend	300425
CD8a	RPA-T8	BV510	Biolegend	301048
CD45	HI30	BV510	Biolegend	304036
CD25	M-A251	PE/Cy7	Biolegend	356108
CD134 (OX40)	ACT35	FITC	Biolegend	350006
HLA-DR	L243	APC	Biolegend	307609
HLA-A,B,C	W6/32	APC	Biolegend	311409
CD90 (Thy-1)	5E10	APC	eBioscience	17-0909
FAP	BLR150J	APC	R&D Systems	FAB3715A-025
CD69	FN50	Alexa Fluor700	Biolegend	310922

Supplementary Table 3. List of antibodies used for intracellular flow cytometry staining.

Antigen	Clone	Fluorochrome	Supplier	Identifier
IL-2	MQ1-17H12	PE	eBioscience	12-7029-71
IL-4	MP4-25D2	PE/Dazzle594	Biolegend	500832
IFN-γ	B27	Alexa Fluor 700	Biolegend	506516
IL-6	MQ2-13A5	Pacific Blue	Biolegend	501114
IL-13	JES10-5A2	PE/Cy7	Biolegend	501914
Granzyme B	QA16A02	APC/Fire750	Biolegend	372210
Granzyme K	GM26E7	FITC	Biolegend	370508

Supplementary Table 4. List of primers used for qPCR.

Gene	FWD (5'à 3')	REV (5'à 3')
GAPDH	ATCTTCTTTTGCGTCGCCAG	TTCCCCATGGTGTCTGAGC
RPS27a	TGGCTGTCCTGAAATATTATAAGGT	CCCCAGCACCACATTCATCA
TBP	GCTTCGGAGAGTTCTGGGATTG	GCAGCAAACCGCTTGGGATTA
COL1A1	AGATCGAGAACATCCGGAG	AGTACTCTCCACTCTTCCAG
COL3A1	CCTGGAATCTGTGAATCATGCC	TGCGAGTCCTCCTACTGCTA
FN1	CCCAGTCCACAGCTATTCCT	TTCATTGGTCCGGTCTTCTC
FN1EDA	TTCAGACTGCAGTAACCAACAT	GGTCACCCTGTACCTGGAAAC
PLOD2	AAGACTCCCCTACTCCGGAAA	AGCAGTGGATAATAGCCTTCCAA
FAP	GCTTTGAAAAATATCCAGCTGCC	ACCACCATACACTTGAATTAGCA
ACTA2	CTGACCCTGAAGTACCCGATA	GAGTGGTGCCAGATCTTTTCC
PDPN	GGTGCAATCATCGTTGTGGTTA	TTCAGCTCTTTAGGGCGAGTAC
IL6	AGCCCACCGGGAACGA	GGACCGAAGGCGCTTGT
HLA-ABC	TACCTGGAGAACGGGAAGGA	GTGGCCTCATGGTCAGAGA
HLA-DR	CCCTGCAGCACCACAAC	GGAACCACCTGACTTCAATGC
TGFB1	GAGGTCACCCGCGTGCTA	TGCTTGAACTTGTCATAGATTTCGTT



Chapter 5

Systemic sclerosis-associated pulmonary arterial hypertension is characterized by a distinct peripheral T helper cell profile

Theodoros Ioannis Papadimitriou, Jacqueline MJ. Lemmers, Arjan PM. van Caam, Jacqueline Vos, Elly Vitters, Lizan Stinessen, Sander I van Leuven, Marije Koenders, Peter M. van der Kraan, Hans JPM Koenen, Ruben Smeets, Robin Nijveldt, Madelon C. Vonk, R. M Thurlings.

Rheumatology (Oxford). 2024 Sep 1;63(9):2525-2534. doi: 10.1093/rheumatology/keae190.

Abstract

Background/Objectives. Systemic sclerosis (SSc) is characterized by multiple clinical manifestations. Vasculopathy is a main disease hallmark and ranges in severity from an exacerbated Raynaud phenomenon to pulmonary arterial hypertension (PAH). The potential involvement of immune system in SSc associated vascular abnormalities is not clear. Here, we set out to study SSc-related immune parameters and determine if and which peripheral T cell subsets associate with vascular severity in SSc patients.

Methods. Peripheral blood and clinical data were collected from 30 SSc patients, 5 patients with idiopathic pulmonary arterial hypertension (IPAH) and 15 age and sexmatched healthy donors (HD). In this cross-sectional cohort SSc patients with PAH (n=15) were matched for their age, sex and medication with SSc patients with no signs of PAH (n=15). Lymphocyte subsets were quantified by multi-colour flow cytometry.

Results. SSc patients exhibited elevated percentages of T peripheral helper cells (Tph), CD4+GZMB+ T cells and decreased levels of Th1 cells compared to HD. Increased presence of both CD4+ and CD8+ exhausted-like (CD28-) T cells, characterized by raised cytokine and cytotoxic signature, was also observed in SSc compared to HD blood. Furthermore, IL-4 expressing CD4+CD8+ T cells were significantly increased in SSc peripheral blood. Interestingly, the presence of PAH in SSc was accompanied by a distinct T helper profile, characterized by raised percentages of Th17 and Tph cells.

Conclusion. SSc patients with severe vasculopathy (presence of PAH) exhibited a distinct pro-inflammatory and auto-antibody T cell profile, suggesting for a potential role of autoimmune inflammation in SSc vascular complications.

Keywords

Systemic sclerosis, vasculopathy, pulmonary arterial hypertension, T lymphocytes, biomarkers

Rheumatology key messages

- 1. CD4+ and CD8+ exhausted-like T cells (CD28-) are elevated in SSc peripheral blood and exhibit increased cytokine and cytotoxic signature.
- 2. Presence of pulmonary arterial hypertension in SSc individuals is characterized by a distinct pro-inflammatory T helper phenotype: elevated Th17 and T peripheral helper cells.

Introduction

Systemic sclerosis (SSc) is a rare autoimmune connective tissue disease and has the highest morbidity and mortality of all rheumatic diseases (1, 2). Hallmark characteristics of this disease are autoimmune inflammation, vasculopathy and fibrosis of skin and internal organs with a variable degree of severity. The vasculopathy is marked by gradual vascular impairment, affecting both small and large blood vessels. Peripheral vascular disease is universal in individuals diagnosed with SSc and prototypically occurs as the initial symptom of the disease. manifesting as a new or exaggerated Raynaud's phenomenon with microscopic nailfold capillary malformation. In severe cases vasoconstriction results in digital ulcers, which can also develop later in the disease course. In a subset of patients, central vasculopathy may be responsible for cardiac dysfunction and pulmonary arterial hypertension (PAH) typically later in the disease course (3).

The most severe vascular disease in SSc is pulmonary arterial hypertension (PAH),a devastating and progressive complication of SSc, which is among the leading causes of death (4). To date, there is no curative treatment available. Despite progress in the treatment of PAH, the quality of life is severely declined and survival of SSc-PAH patients remains poor (5). Moreover, vasoactive therapy is known to be less effective in SSc-PAH compared to the idiopathic form of PAH, whereas both share clinical and hemodynamic similarities (6, 7).

Current knowledge indicates that in connective-tissue diseases such as SSc, inflammatory processes contribute to vasculopathy. Recently we and others showed that cytotoxic T cells are present in perivascular infiltrates of affected skin in SSc and cause endothelial cell damage (8-10), especially early in the disease course. Other studies indicate that T cells may also mediate progression of PAH, especially by instigating changes in the pulmonary vasculature (11, 12). The vascular remodelling that characterizes SSc-PAH consists of intimal thickening of pulmonary arterioles and capillaries which is caused by intimal cell proliferation and deposition of extracellular matrix. Histologic analyses of pulmonary tissue from SSc-PAH patients have shown inflammatory cell infiltrates, such as of T and B lymphocytes and macrophages, in peri-vascular cell areas, and to a lesser extent in plexiform lesions (13-15). Possibly, these immune cells contribute to the (abnormal) vascular remodelling process and dysfunction. However, to date, the potential involvement of immune cells in manifestations of severe vascular dysfunction in SSc is poorly understood.

Various studies (16-19) report on the aberrations of different T cell cytotoxic (CTL) and T helper (Th) subsets that are linked with inflammatory and/or fibrotic manifestations of patients with SSc. However, the SSc associated immune cell subsets vary between disease components and between studies. Here we hypothesize that the relative contribution of distinct T cell subsets may differ according to SSc-associated vascular severity. To address that question, we performed in depth T lymphocyte immunophenotyping in a cross-sectional cohort (20) focused on the inclusion of SSc patients with or without the presence of PAH that were carefully matched for their age, sex, ethnicity and medication use.

Materials and Methods

Here, we set out to examine if and which peripheral T cell populations may associate with distinct vascular severity in patients with SSc. To answer this question, we utilized a multi-color 17-antigen flow cytometry panel (the detected T cell populations along with the extracellular and intracellular antigens that were used for their identification are presented in *supplementary tables 1, 2, 3*) to explore the relative contribution of multiple peripheral blood T cell subsets in distinct clinical manifestations of SSc. For a complete overview of the patient and healthy controls characteristics and the experimental methods, see *online supplementary methods and materials*. Ethics approval for the study was granted in accordance with the Dutch Code of Conduct for Health Research, the Dutch Code of Conduct for Responsible Use, the Dutch Personal Data Protection Act, and the Medical Treatment Agreement Act. The study, conducted at Radboudumc in Nijmegen, The Netherlands, was assigned File Number CMO: 2017-3979.

Results

Clinical and demographic features

Patients and healthy donors (HD) included in our study were of similar age, sex, and race distribution (p values not statistically significant). Approximately 80% of the SSc patients and controls were female with an age range from 57 to 76 years and disease duration from a minimum of 2.4 to a maximum of 19.9 years. Patients with idiopathic pulmonary arterial hypertension (IPAH) were all Caucasian females of similar age range. A complete overview of the baseline patient characteristics including demographics, laboratory values, clinical features, autoantibody and medication status is depicted in *Table 1* and *Supplementary table 4*. SSc patients

Table 1. Clinical characteristics of subjects included in the cross-sectional cohort study.

Baseline characteristics	SScN= 30	IPAHN=5	HDN=15	P value
Age in years, mean (SD)	67.6 (9.6)	63.0 (9.4)	63.2 (6.2)	0.46
Female, n (%)	25 (83)	5 (100)	12 (80)	0.95
Caucasian, n (%)	30 (100)	5 (100)	15 (100)	1.00
SSc duration in years, mean (SD)	10.1 (8.1)			
LcSSc, n, (%)	24 (80)			
Clinical SSc features				
PAH, n (%)	15 (50)	5 (100)		
ILD, n (%)	12 (40)	0		
Raynaud's Phenomenon, n (%)	29 (97)	0		
Digital Ulcers, n (%)	11/29 (38)	0		
Telangiectasias, n (%)	12/24 (50)	0		
mRSS, mean (SD)	4.1 (5)			
NYHA class, n (%)				
1.1	13 (43)	0		
2. II	6 (20)	5 (100)		
3. III	8 (27)	0		
IV	3 (10)	0		
<u>Laboratory results, mean (SD)</u>				
MDRD/GFR (ml/min/1.73m ²	63.4 (16.2)	72.2 (14.4)		
Creatinine (µmol/L)	86.6 (23.4)	78.2 (23.5)		
Urate (µmol/L))	0.35 (0.12)	0.36 (0.13)		
Nt-proBNP (pg/ml)	794 (1253)	96.6 (42)		
ANA positive, n (%)	26 (87)	2 (40)		
ENA positive, n (%)	19/24 (79)	0		

SSc: systemic sclerosis. IPAH: idiopathic pulmonary arterial hypertension. HD: healthy donors. S.D.: standard deviation. PAH: pulmonary arterial hypertension. ILD: Interstitial lung disease. mRSS: modified Rodnan skin score. NYHA: New York Heart Association. MDRD: Modification of Diet in Renal Disease. GFR: Glomerular Filtration Rate. Nt-proBNP: aminoterminal pro B-type natriuretic peptide. ANA: Antinuclear Antibody. ENA: extractable nuclear antigen. Statistics were performed with ordinary one-way ANOVA with Tukey's multiple comparisons test.

were clinically classified into either limited (80%) or diffuse cutaneous (20%) SSc according to the subclassification criteria of Leroy (21). All patients experienced symptoms of Raynaud's phenomenon, 40% of the patients had interstitial lung disease (ILD) on HRCT-scan despite preserved vital capacity (mean 92.5%, see *Supplementary table 4*) and 50% of the patients were diagnosed with SScassociated pulmonary arterial hypertension (PAH) (*Supplementary table 5*). SSc patients without PAH enrolled in this cross-sectional cohort were matched for their age, sex, ethnic background and medication with SSc patients with PAH and HD.

Deep flow cytometric quantification reveals differential presence of T cell subsets in blood of SSc patients compared to healthy donors

To determine potential differences between SSc and healthy peripheral blood T cell composition, we used multi-color flow cytometry. First, we analyzed general T cell characteristics between patients and healthy donors, starting with T cell numbers (for the gating strategy see **Supplementary Figure 1**). No differences were observed in overall and CD4⁺ T cell or CD8⁺ T cell subset percentages between SSc patients and HD. Furthermore, there was no significant effect of immunosuppressive or other medication in the percentage of these T cell populations. Of note, SSc patients exhibited an elevated expression of the CD4+CD8+ population in their CD3+ compartment (3.1% SSc vs 1.3% HCs, p= 0.0021) (Figure 1A). Next, we explored the composition of the T helper sub-groups in SSc patients versus healthy donors (Figure 1B, Supplementary Figure 2A-C). No differences were observed in the presence of Th2, Th9, Th17 and Th1-Th17 subsets in patients versus HD. However, the Th1 (CD4+CCR6-CXCR3+) compartment was significantly decreased in SSc patients compared to controls (SSc: 2.1% vs HD: 3.0% of live cells, p= 0.038). This is in line with previous reports describing a reduced ratio of Th1 versus Th2 cells (22, 23). Hereafter we analyzed the presence of a T helper subset important for B cell function; the peripheral helper cells (Tph). These cells are known for regulating B cell class switching, maturation and antibody production (24). Tph cells, characterized as CD4+PD-1high ICOShigh T cells that produce the T follicular/peripheral helper signature cytokine IL-21, were detected in both healthy and SSc blood, but the percentage of Tph in patients was twice as high as in healthy donors (SSc: 1.6% vs HD: 0.8 % of live cells, p=0.013) (*Figure 1B*).

Followingly, we explored CD8⁺ T cell function deeper by characterizing their maturation status. We observed a trend towards decreased CD8 naïve (CD8⁺CD45RA⁺CD27⁺) and increased effector (CD8⁺CD45RA⁺CD27⁻) and central memory (CD8⁺CD45RA⁻CD27⁺) T cells in SSc, however, none of these comparisons were statistically significant (*Figure 1C, Supplementary Figure 3A*).

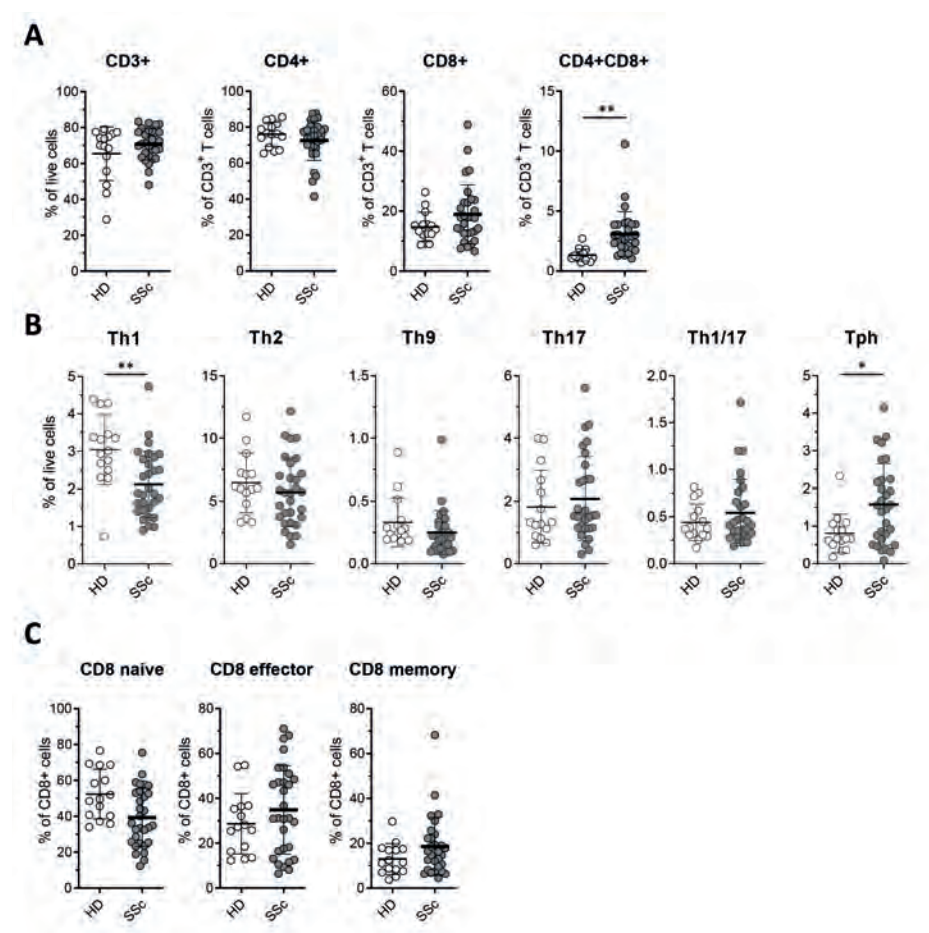


Figure 1. SSc patients are characterized by enriched presence of CD4+CD8+ T cells and Tph cells and decreased percentage of Th1 cells compared to age and sex matched HD. Percentages of circulating T cell subsets were detected with multi color flow cytometry in the peripheral blood of SSc patients (n=30) compared to HD (n=15). (A) No differences in percentages of CD3+, CD4+, CD8+ T cells between SSc and HD were observed. However elevated percentage of CD4+CD8+T cells was evident in SSc blood. Values are presented as percentage (%) of total live cells (B) Quantification of Th1, Th2, Th9, Th17, Th1-17 cell frequencies. Percentage of Th1 cells is greatly reduced in SSc patients while % of T peripheral helper (Tph) cells shows an elevated presence in SSc blood. Values are presented as % of total live cells. (C) No significant differences in percentages of naïve (CD8+CD45RA+CD27+), effector (CD8+CD45RA+CD27-) and central memory (CD8+CD45RA-CD27+) cytotoxic T cell populations were observed in SSc versus HD. Values are presented as percentage (%) of total live CD8+ T cells. (D) Comparison of percentage (%) of CD8+GZMB+ T cells (left) and CD4+GZMB+ T cells (right) between SSc patients and healthy donors. Values are presented as percentage (%) of total live cells. (E) Comparison of percentages of CD4+IL-4+, CD4+IL-13+, CD8+IL-4+, CD8+IL-13+ T cells between HD and SSc exhibits a prominent cytotoxic T cell pro-fibrotic signature in SSc blood. Values are presented as percentage (%) of total live cells. (F) A significantly higher fraction of CD4+CD8+T cells from SSc patients are also positive for IL-4 compared to the same cell type in HD. Statistical comparisons between groups were performed either with Student's t-test for normally distributed data or with Mann-Whitney U test for non-normally distributed data. In all cases values were corrected for multiple comparisons, * p<0.05, ** p<0.01.

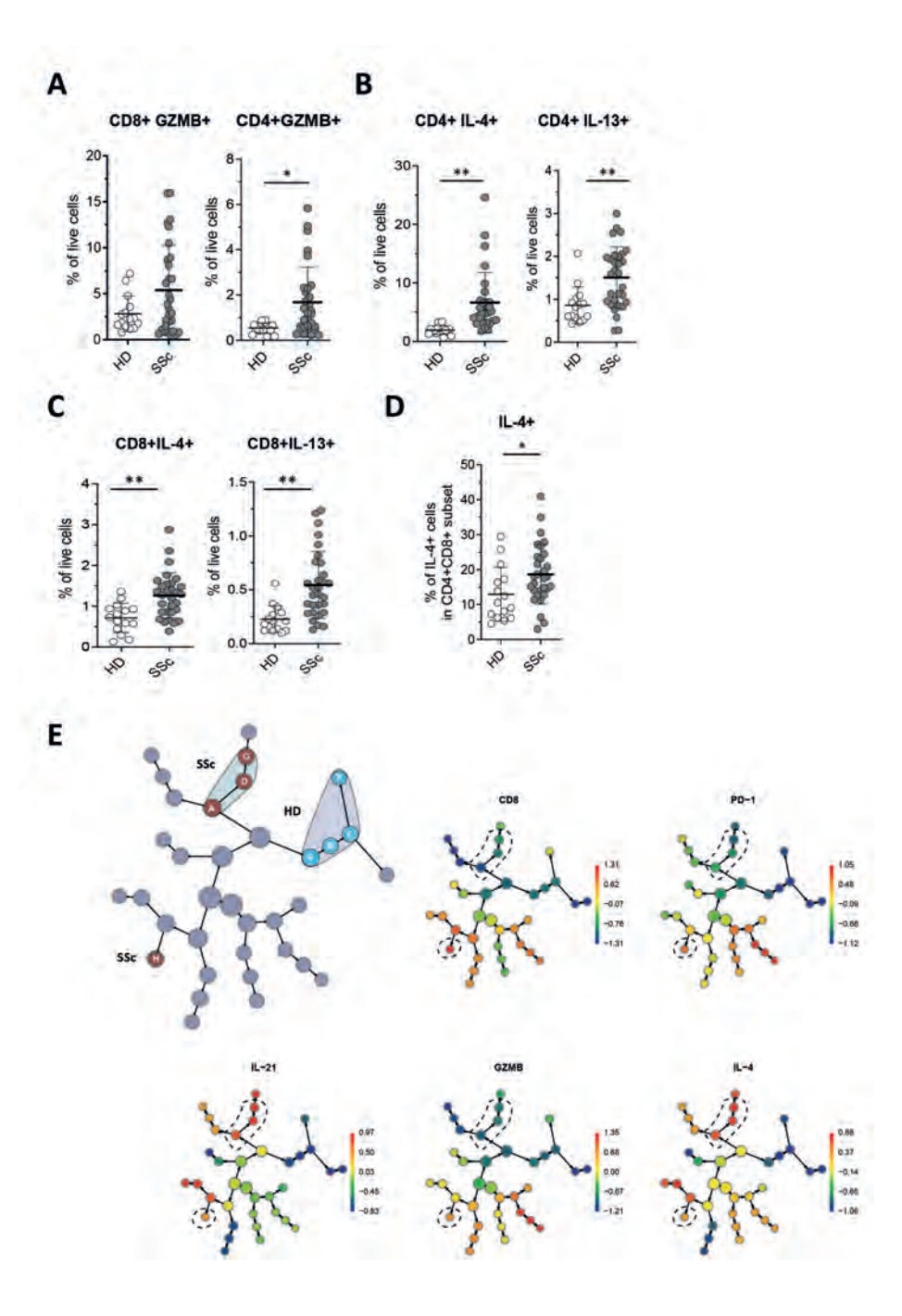


Figure 2. SSc patients exhibit a prevalent pro-fibrotic and cytotoxic T cell phenotype. Percentages of circulating T cell subsets were detected with multi color flow cytometry in the peripheral blood of SSc patients (n=30) compared to HD (n=15). Expression of granzyme B (GZMB), IL-4, IL-13 was measured with intracellular staining after cells were stimulated with PMA, lonomycin and BFA for 4 hours at 37° C. (A) Comparison of percentage (%) of CD8+GZMB+ T cells (left) and CD4+GZMB+ T cells (right) between SSc patients and healthy donors. Values are presented as percentage (%) of total live cells. (B-C) Comparison of percentages of CD4+IL-4+, CD4+IL-13+, CD8+IL-4+, CD8+IL-13+ T cells between HD and SSc exhibits a prominent cytotoxic T cell pro-fibrotic signature in SSc blood. Values are presented as percentage (%) of total live cells. (D) A significantly higher fraction of CD4+CD8+T cells from SSc patients are also positive for IL-4 compared to the same cell type in HD. (E) Classification of SSc and HD peripheral blood CD3+ T cells based on hierarchical clustering of the protein markers CD3, CD4, CD8, CCR4, CD28, CCR6, CXCR3, CD45RA, CD27, PD-1, ICOS, IL-4, IL-13, IL-21 and GZMB was used to detect cell populations of comparable marker expression and their abundance utilizing the CITRUS tool provided by Cytobank. 5,000 events were sampled per individual donor. The size of each node depicts the cell frequency. Prediction analysis for microarrays (PAM) clustering was performed to detect cell clusters contributing to SSc patients (red clusters) compared to HD (blue clusters). Citrus hierarchical "clustering trees" exhibiting the relationships of the detected nodes are also shown for selected markers and the color scales illustrates intensity of expression of each depicted marker per cluster and the size of each node shows the event frequency. Statistical comparisons between groups were performed either with Student's t-test for normally distributed data or with Mann-Whitney U test for non-normally distributed data. In all cases values were corrected for multiple comparisons, * p<0.05, ** p<0.01.

SSc individuals exhibit an elevated pro-fibrotic and cytotoxic T cell phenotype

Since we and others previously exhibited a prevalent cytotoxic immune cell response in the affected skin of patients with early SSc (8-10), we next examined whether such a cytotoxic signature is also evident in patients' blood circulation. There was no significant difference in percentage of GZMB+ CD8+T cells in circulation between SSc and HD (Figure 2A). Considering that recent literature suggests for a potential role of CD4⁺ cytotoxic T cells in promoting vascular dysfunction in skin of patients with early and diffuse SSc (8), we explored presence of this subset in peripheral blood. Indeed, cytotoxic CD4+ GZMB+ T cells (Supplementary Figure 3D, 4) could be readily detected in SSc patients, but were hardly distinguishable in healthy donors (SSc: 1.68 vs HD: 0.54 % of live cells, p=0.05) (*Figure 2A*).

Furthermore, accumulating evidence supports the pro-fibrotic role of the cytokines IL-4 and IL-13 in connective tissue diseases (25). As expected, expression of both IL-4 and IL-13 was significantly up-regulated in the CD4⁺ compartment of patients with SSc, revealing a prominent pro-fibrotic response (SSc: 6.63% CD4+IL-4+, 1.50% CD4+IL-13+ vs HD: 1.94% CD4+IL-4+, 0.85% CD4+IL-13+ of live cells, p= 0.002 and 0.007 respectively) (Figure 2B, Supplementary Figure 5). Interestingly, CD8+T cells from SSc patients also exhibited an elevated expression of pro-fibrotic cytokines such as IL-4 and IL-13, suggesting their potential involvement in disease-related

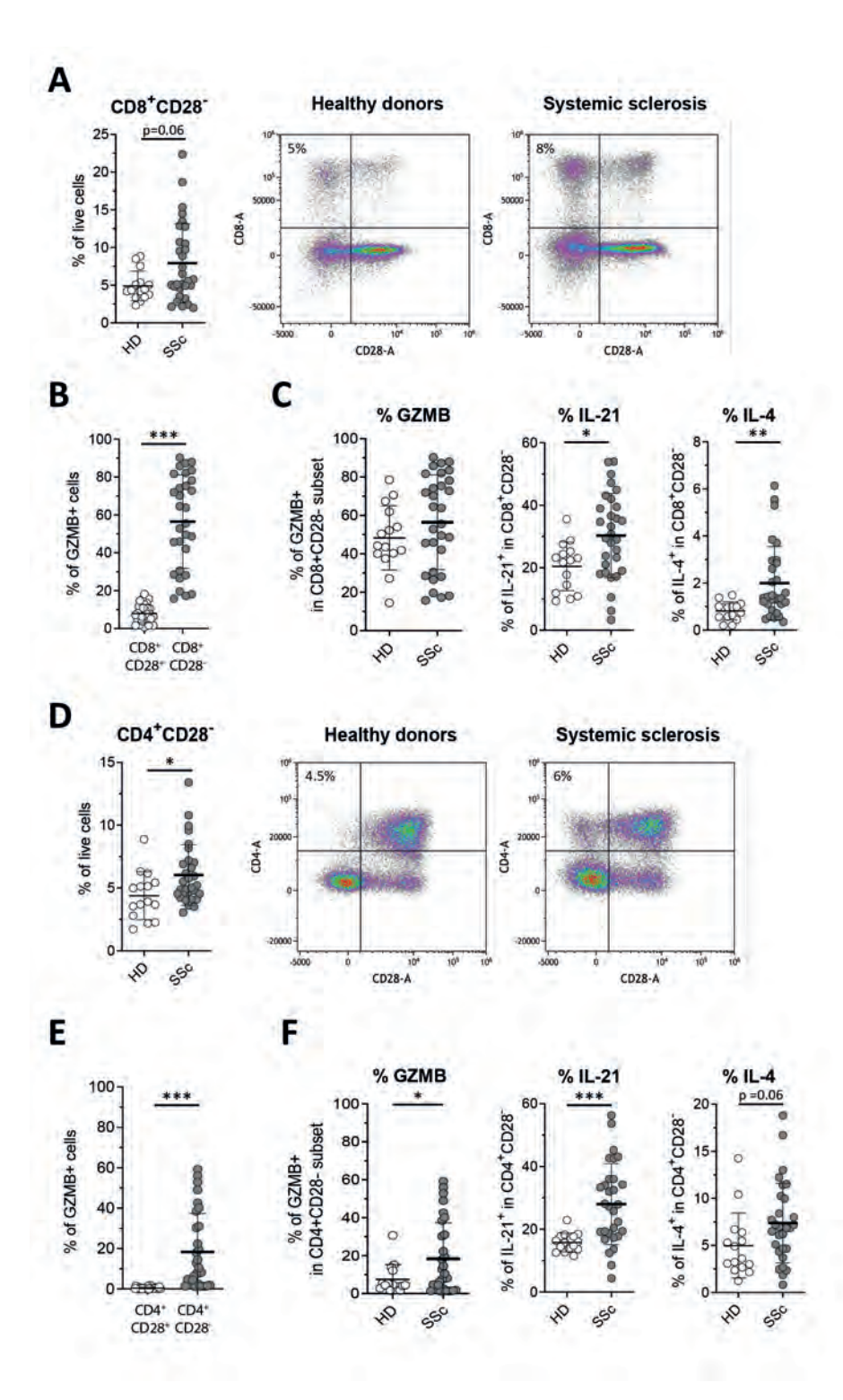


Figure 3. Increased presence of exhausted T cells in early SSc may facilitate key disease manifestations, such as cytotoxicity mediated tissue destruction, fibrosis and auto-antibody production. (A) CD8+CD28-T cells are expanded in SSc patients compared to HD. Values are presented as % of total live PBMCs. Representative flow cytometry plots of one HD and one SSc patient to identify CD8+CD28-T cells are illustrated. (B) Exhausted-like CD8+CD28-T cells show increased Granzyme B (GZMB) positivity in comparison to their effector CD8+CD28+ counterpart. Values are expressed as % of cells that are GZMB+ within CD8+CD28- and CD8+CD28+ T cell populations. (C) CD8+CD28- T cells from SSc patients exhibit significantly more GZMB+, IL-21+ and IL-4+ cells compared to the same cell type in HD. Values are presented as % of GZMB+/IL-21+/IL-4+ cells among the total CD8+CD28-T cells. (**D**) SSc patients are characterized by an elevated percentage of CD4+CD28-T cells compared to HD. Values are presented as % of total live PBMCs. (right) Representative flow cytometry plots of one HD and one SSc patient to identify CD4+CD28-T cells are also depicted. (E) Exhausted-like CD4+CD28-T cells show increased GZMB positivity in comparison to their effector CD4+CD28+ counterpart. Values are expressed as % of cells that are GZMB+ within CD4+CD28- and CD4+CD28+ T cell populations. (F) CD4+CD28- T cells from SSc patients exhibit significantly more GZMB+, IL-21+ and IL-4+ cells compared to the same cell type in HD. Values are presented as % of GZMB+/IL-21+/IL-4+ cells among the total CD4+CD28- T cells. Statistical comparisons between groups were performed either with Student's t-test for normally distributed data or with Mann-Whitney U test for non-normally distributed data. In all cases values were corrected for multiple comparisons, * p<0.05, ** p<0.01, ***p<0.001.

manifestations such as fibrosis (Figure 2C, Supplementary Figure 5). In addition, we previously observed an increased presence of CD4+CD8+ T cells in SSc blood. The functional and phenotypical properties of these double positive cells are still poorly understood. Of note and in accordance with earlier studies in SSc skin (26), this double positive population expressed significantly higher levels of the pro-fibrotic cytokine IL-4 in SSc compared to HD (18.7% SSc vs 12.9% HCs, p = 0.033) (*Figure 2D*).

To further investigate phenotypic features of the different T cell populations, we utilized the CITRUS tool on the Cytobank platform (27), employing unsupervised clustering based on similar descriptive features such as marker expression, correlating with assigned sample types (SSc versus HD and IPAH). The top four clusters with the highest stratification for predicting SSc disease (Figure 2E, Supplementary Figure 6) were characterized by elevated expression of CD8, PD-1, IL-4, IL-21 and GZMB (Figure 2E, Supplementary Figure 7). Collectively and in line with our supervised analysis, these results illustrate that SSc circulating T cells exhibit an increased pro-fibrotic (IL-4), cytotoxic (GZMB) and peripheral helper (IL-21) signature.

SSc blood is characterized by an increased exhausted-like T cell signature that is accompanied by an elevated cytokine and cytotoxic phenotype

Often, in patients with cancer and chronic inflammation, the early elevated cytotoxic T cell responses are attributed to exposure to certain (auto)-antigens and the inflammatory microenvironment. Antigen-specific T cell activation is a critical regulator of their effector functions. A key determinant of T cell activity is exhaustion (28). Long-term exposure to persistent antigen stimulation is usually associated with T cell anergy/exhaustion. T cell exhaustion is observed in many rheumatic diseases including rheumatoid arthritis and is often correlated with disease manifestations (29). Therefore, we next looked at T cell exhaustion in our dataset. Exhausted/ anergic T cells are characterized by loss of the co-stimulatory molecule CD28. In our cohort, the percentage of CD8+CD28- T cells (Figure 3A, Supplementary Figure 3B) was expanded in SSc patients compared to HD (7.92% in SSc vs 4.88% in HD, % of total live cells, p=0.06). It has been shown that in rheumatoid arthritis, T cell exhaustion leads to atypical cytotoxic properties (30). Indeed, in SSc blood, CD8+CD28-T cells showed on average a 6-fold higher GZMB expression compared to their CD28+ counterpart (Figure 3B). In line with this observation, our unsupervised analysis after dimensionality reduction and cell clustering with the CITRUS algorithm, we found that among the distinct CD8+ T cell clusters there was a clear distinction between clusters that were either GZMB+CD28- or GZMB-CD28+(Supplementary Figure 8). In addition, in SScCD8+CD28-Tcells, an elevated % of GZMB, IL-4 and IL-21 positive cells was detected compared to HD (Figure 3C). This observation points out a potential role of exhausted T cells in facilitating SSc disease processes related to cytotoxicity, fibrosis and auto-antibody production.

Furthermore, in patients with SSc increased percentage of exhausted-like CD4⁺ T cells (CD4⁺CD28⁻) compared to HD was also observed. (6.03% in SSc vs 4.38% in HD, % of total live cells, p= 0.032) (*Figure 3D*). Similarly to the anergic cytotoxic T cells, in CD4⁺CD28⁻ T cells an elevated GZMB expression was observed in comparison to CD4⁺CD28⁺ T cells (*Figure 3E*). In addition, more CD4⁺CD28⁻ T cells of SSc patients were positive for GZMB, IL-21 and IL-4 than those of healthy donors (*Figure 3F*). In conclusion, both CD4⁺ and CD8⁺ T cells were expanded in SSc blood and exhibited an increased cytotoxic and cytokine expressing profile compared to HD.

Presence of PAH in SSc individuals is associated with a distinct T helper profile: increased frequency of Th17 and Tph cells

Since several T cell subsets were found to be expanded in SSc blood, we further combined these data with clinical features of the included patients to understand

how such immunological differences may be related to distinct SSc clinical patterns (such as PAH) and disease severity. First, subgroup analysis showed that SSc individuals with active disease (patients that exhibited elevated skin score (mRSS) or developed a new organ complication that was attributed to SSc over a 6-month period before inclusion in our study) exhibited elevated numbers of CD4+ T cells (Figure 4A), suggesting that T helper responses may be associated with disease severity. Furthermore, in our patient cohort half of the SSc patients were diagnosed with PAH (SSc-PAH), while the rest were not (SSc-noPAH). These two patient groups were carefully matched for their sex, age and underlying medication and further compared with age and sex matched healthy controls (n=15) and also with patients with IPAH (n=5). We aimed to detect T cell subsets that were specifically related to patients with or without PAH, that could serve as candidate biomarkers, Strikingly, percentages of Th17 (CD4+CCR6+CXCR3-CCR4+) and Tph (PD-1+ICOS+IL-21+) cells were specifically up-regulated in SSc-PAH patients (Figure 4B). This reveals a distinct pro-inflammatory/peripheral T helper phenotype associated with the presence of PAH in SSc patients. Of note, no differences in CD8+T cell subsets were found. Patients with IPAH, did not show elevated percentages of Th17 nor Tph cells. On the other hand, Th2 cells characterized as CD4+CCR6-CXCR3-CCR4+ were significantly expanded in patients with IPAH, while the rest comparing groups shared similar percentages (Supplementary Figure 9). In conclusion, CD4 T cell inflammatory responses (Th17, Tph) are evident in SSc patients with prevalent vascular disease (PAH), suggesting for a potential role of autoimmune inflammation in SSc-associated vascular dysfunction.

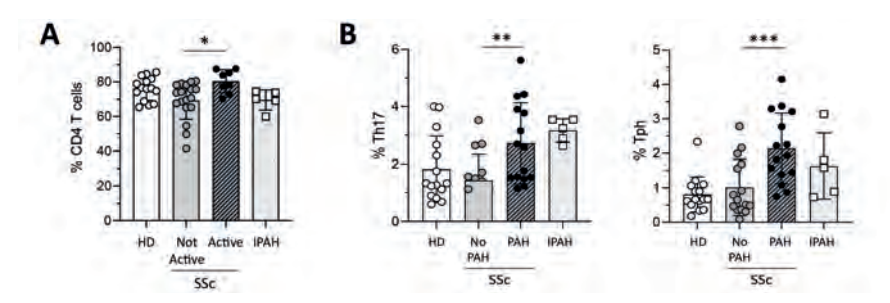


Figure 4. Presence of PAH in SSc is accompanied by a distinct T helper profile. (A) Comparison of percentages (%) of CD4+ T cells in patients with active versus not active disease shows elevated percentages of CD4+ T helper cells in patients with progressive disease. Patients with active disease exhibited elevated skin score (mRSS) or developed a new organ complication that was attributed to SSc over a 6-month period before inclusion in our study. (B) Comparison of percentages (%) of T cell subsets in SSc patients with and without the presence of PAH shows elevated percentages of Th17 and Tph cells in patients with SSc-associated PAH. Statistical comparisons between groups were performed with two-way ANOVA with Tukey's multiple comparisons test, *p<0.05, **p<0.01, ***p<0.001.

Immune dysregulation seems to play an important role in SSc pathogenesis. Recent observations suggest a prevalent T cell cytotoxic signature in the affected skin of patients with early diffuse SSc (8, 10). However, the potential involvement of T cell abnormalities in relation to prolonged SSc disease duration, severity and vascular complications such as PAH remains elusive. In the present study, we performed an in-depth flow cytometric analysis in SSc peripheral blood to explore the potential involvement of specific T cell subpopulations in SSc pathology and its distinct clinical manifestations such as PAH.

In accordance with previous studies (31, 32), we confirmed expansion of IL-4/IL-13 expressing CD4+ and CD8+ T cell populations in SSc blood circulation. For the first time, in SSc peripheral blood, we detected a CD4 and CD8 double positive population that may contribute to SSc pathology by producing excessive amounts of pro-fibrotic cytokines such as IL-4. Such a population has been previously described as exhibiting a very high IL-4 production in SSc lesional skin (26). Strikingly, a GZMB+ CD4+ cytotoxic T cell population was almost exclusively present in SSc individuals but was hardly detectable in healthy blood.

T cell exhaustion was prevalent in SSc blood for both T helper and cytotoxic cells. T cell dysfunction is increased with aging, cancer and chronic viral infections and the function of these cells can range from effector to immunosuppressive (33). In immune mediated inflammatory diseases such as systemic erythematosus lupus, type I diabetes mellitus and ANCA-associated vasculitis their presence is often associated with improved disease prognosis (34-36). Our analysis showed that exhausted T cells in SSc blood had elevated cytotoxic and cytokine producing phenotype compared to those present in healthy blood. This suggests that SSc blood contains "dysfunctional" T cells that are functionally active probably due to chronic auto-antigen presentation. Such a phenotype has been described before for the exhausted CD4⁺ T cell compartment in SSc blood (37). Of note, in our study we also observed elevated percentages of cytotoxic (CD8+) exhausted-like T cells in patients with SSc. Our data suggests that exhausted CD8+T cells are functionally adapted and may potentially exacerbate tissue destruction rather than being anergic. However, a closer examination of their functional role and their potential association with better or worse disease progression in further longitudinal analyses is needed.

Currently, PAH is one of the most severe complications of SSc that usually develops in later disease stages and although treatment options have proven to improve quality

of life and survival, it remains one of the main causes of death in SSc. The pathogenesis of SSc-PAH is still poorly understood and the intricate pathological characteristics of SSc make it challenging to address the role of the immune and vascular systems in the development of SSc-PAH. Here, we identified a prominent T helper phenotype in SSc PAH patients that is addressed by elevated numbers of circulating Th17 and Tph cells and thus suggests a potential role of T helper autoimmune inflammation in SSc vascular complications. Expansion of Th17 cells in SSc blood has been previously described (22, 38, 39), however, we are the first to report increased presence of these cells in SSc-PAH. Apart from their central role in SSc related fibrosis (40), IL-17 producing cells were shown to be involved in SSc vasculopathy through the recruitment of inflammatory cells to vascular endothelial cells leading to small vessel vasculopathy and fibrosis due to a faulty repair response. Possibly a similar mechanism occurs in the pulmonary arteries leading to its thickening and decreased lumen (18, 41).

We also observed increased T peripheral helper cells in SSc-PAH. This T cell subtype lacks CXCR5 expression but has a transcriptionally similar phenotype with T follicular helper cells that produce IL-21 and play an essential role in stimulating B cell differentiation to immunoglobulin secreting plasma cells. Interestingly, we recently identified IL-21 as one of the key cytokines defining SSc subtypes in a cohort of 346 patients (42). Importantly, in previous studies, (auto)- antibodies have been linked to risk of the development of PAH and this could be partially explained by the observed elevated Tph numbers in these patients (43-45). Increased numbers of circulating T follicular helper cells that promote plasmablast differentiation in an IL-21 dependent manner have also been reported in SSc-PAH patients (46). Taken together, these findings support the role of the immune system in SSc-PAH development. This is in line with current views on PAH pathophysiology (47).

This study has several strengths and limitations. First, most of the included patients received medication, including immunomodulatory and PAH modifying drugs. Such medication may affect T cell populations and skew the data. To address this point, we compared SSc patients with or without the presence of PAH that were matched for their medication use. Secondly, immune aging and sex ratio is often an important confounding factor in immunological studies. To account for this, we took special care to age and sex match the healthy volunteers included in our study with the enrolled SSc patients. Importantly, in this study we used cryopreserved PBMCs of the enrolled subjects and that enabled us to refrain from potential batch effects since all samples were processed, stained and acquired for flow cytometry at the same day. Finally, the lack of in vitro functional assays due to limited amount of cells from each donor is hampering a more in-depth investigation of the mechanisms behind the pathogenic role of Th17 and Tph expansion in SSc-PAH. In this regard, examining presence and function of these cells in the affected tissue would be essential in determining their potential pathogenicity.

To conclude, our results shed light on the SSc immune pathogenesis by determining several T cell aberrations in the peripheral blood of SSc patients compared to carefully age and sex matched healthy individuals. Of note, patients with PAH exhibited a distinct expansion of the pro-inflammatory Th17 and auto-antibody related Tph subsets, highlighting a potential role of autoimmune inflammation in SSc vascular complications. Our findings suggest the potential use of therapeutic approaches that target inflammation in the treatment course of PAH in SSc.

Authors contribution

T.I. Papadimitriou: Conceptualization, Formal Analysis, Investigation, Writing-Original Draft, Writing - Review & Editing, Visualization. J. Lemmers: Conceptualization, Patient Inclusion and clinical data collection, Writing - Review. A. van Caam: Conceptualization, Formal Analysis, Investigation, Writing - Review & Editing, Supervision. J. Vos: Patient Inclusion, Writing - Review. E. Vitters: Technical support. L. Stinessen: Technical support. M. Koenders: Writing - Review, Supervision. P. van der Kraan: Writing -Review, Project administration. H. Koenen: Supervision. R. Smeets: Supervision. R. Nijveldt: Supervision, Writing – Review. M. C. Vonk: Conceptualization, Supervision, Writing – Review, Project Administration. R. Thurlings: Conceptualization, Supervision, Writing - Review, Project Administration.

Ethics

Written informed consent was obtained from all included participants.

Acknowledgements

We want to thank Bram van Cranenbroek and the Radboud Technology Centre Flow Cytometry facility for their technical support in flow cytometry experiments.

Disclosure

The authors declare no conflicts of interest.

Funding

No source of funding for this work.

Data availability

Not applicable.

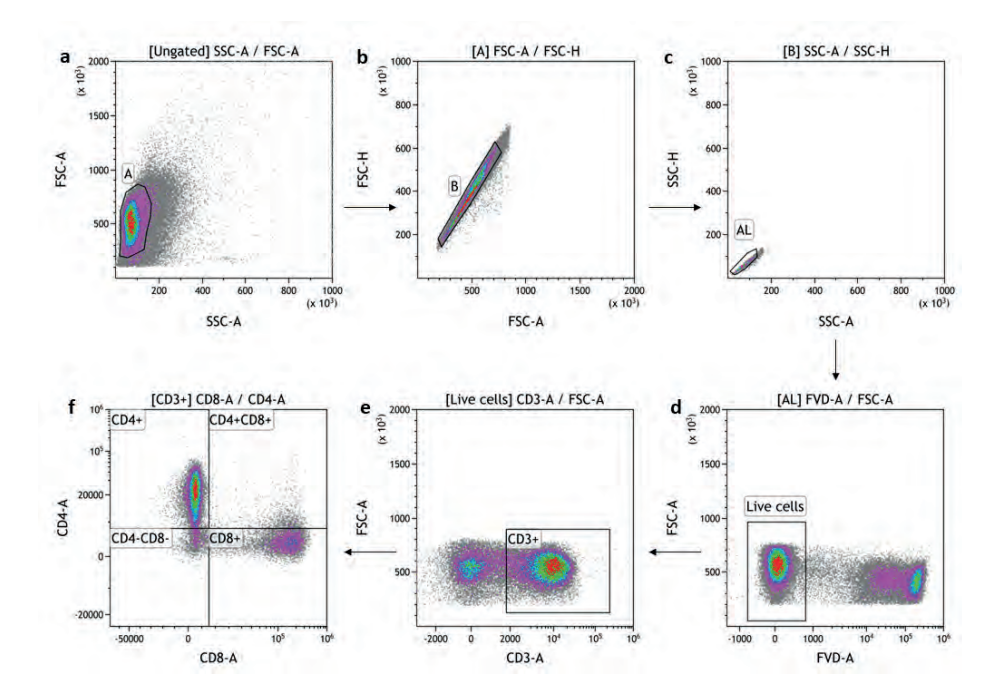
References

- 1. Denton CP, Khanna D. Systemic sclerosis. Lancet. 2017;390(10103):1685-99.
- 2. Papadimitriou TI, van Caam A, van der Kraan PM, Thurlings RM. Therapeutic Options for Systemic Sclerosis: Current and Future Perspectives in Tackling Immune-Mediated Fibrosis. Biomedicines. 2022:10(2).
- 3 Asano Y, Sato S. Vasculopathy in scleroderma. Semin Immunopathol. 2015;37(5):489-500.
- 4 Naranjo M, Hassoun PM. Systemic Sclerosis-Associated Pulmonary Hypertension: Spectrum and Impact. Diagnostics (Basel). 2021;11(5).
- 5. Galie N, Humbert M, Vachiery JL, Gibbs S, Lang I, Torbicki A, et al. 2015 ESC/ERS Guidelines for the diagnosis and treatment of pulmonary hypertension: The Joint Task Force for the Diagnosis and Treatment of Pulmonary Hypertension of the European Society of Cardiology (ESC) and the European Respiratory Society (ERS): Endorsed by: Association for European Paediatric and Congenital Cardiology (AEPC), International Society for Heart and Lung Transplantation (ISHLT). European heart journal. 2016;37(1):67-119.
- Hurdman J, Condliffe R, Elliot CA, Davies C, Hill C, Wild JM, et al. ASPIRE registry: assessing the Spectrum of Pulmonary hypertension Identified at a REferral centre. Eur Respir J. 2012;39(4):945-55.
- Launay D, Sitbon O, Hachulla E, Mouthon L, Gressin V, Rottat L, et al. Survival in systemic sclerosisassociated pulmonary arterial hypertension in the modern management era. Ann Rheum Dis. 2013;72(12):1940-6.
- Maehara T, Kaneko N, Perugino CA, Mattoo H, Kers J, Allard-Chamard H, et al. Cytotoxic CD4+ T lymphocytes may induce endothelial cell apoptosis in systemic sclerosis. J Clin Invest. 2020;130(5):2451-64.
- Gur C, Wang SY, Sheban F, Zada M, Li B, Kharouf F, et al. LGR5 expressing skin fibroblasts define a major cellular hub perturbed in scleroderma. Cell. 2022;185(8):1373-88 e20.
- 10. Papadimitriou TI, Singh P, Caam Av, Walgreen B, Gorris MAJ, Vitters EL, et al. CD7 activation regulates cytotoxicity-driven pathology in systemic sclerosis, yielding a target for selective cell depletion. Annals of the Rheumatic Diseases. 2023:ard-2023-224827.
- 11. Humbert M, Morrell NW, Archer SL, Stenmark KR, MacLean MR, Lang IM, et al. Cellular and molecular pathobiology of pulmonary arterial hypertension. J Am Coll Cardiol. 2004;43(12 Suppl S):13s-24s.
- 12. Dorfmüller P, Perros F, Balabanian K, Humbert M. Inflammation in pulmonary arterial hypertension. Eur Respir J. 2003;22(2):358-63.
- 13. Humbert M, Guignabert C, Bonnet S, Dorfmüller P, Klinger JR, Nicolls MR, et al. Pathology and pathobiology of pulmonary hypertension: state of the art and research perspectives. Eur Respir J. 2019;53(1).
- 14. Dorfmüller P, Humbert M, Perros F, Sanchez O, Simonneau G, Müller KM, et al. Fibrous remodeling of the pulmonary venous system in pulmonary arterial hypertension associated with connective tissue diseases. Hum Pathol. 2007;38(6):893-902.
- 15. Ramirez A, Varga J. Pulmonary arterial hypertension in systemic sclerosis: clinical manifestations, pathophysiology, evaluation, and management. Treat Respir Med. 2004;3(6):339-52.
- 16. Fuschiotti P. Current perspectives on the role of CD8+T cells in systemic sclerosis. Immunol Lett. 2018:195:55-60.
- 17. Frantz C, Auffray C, Avouac J, Allanore Y. Regulatory T Cells in Systemic Sclerosis. Front Immunol. 2018:9:2356.

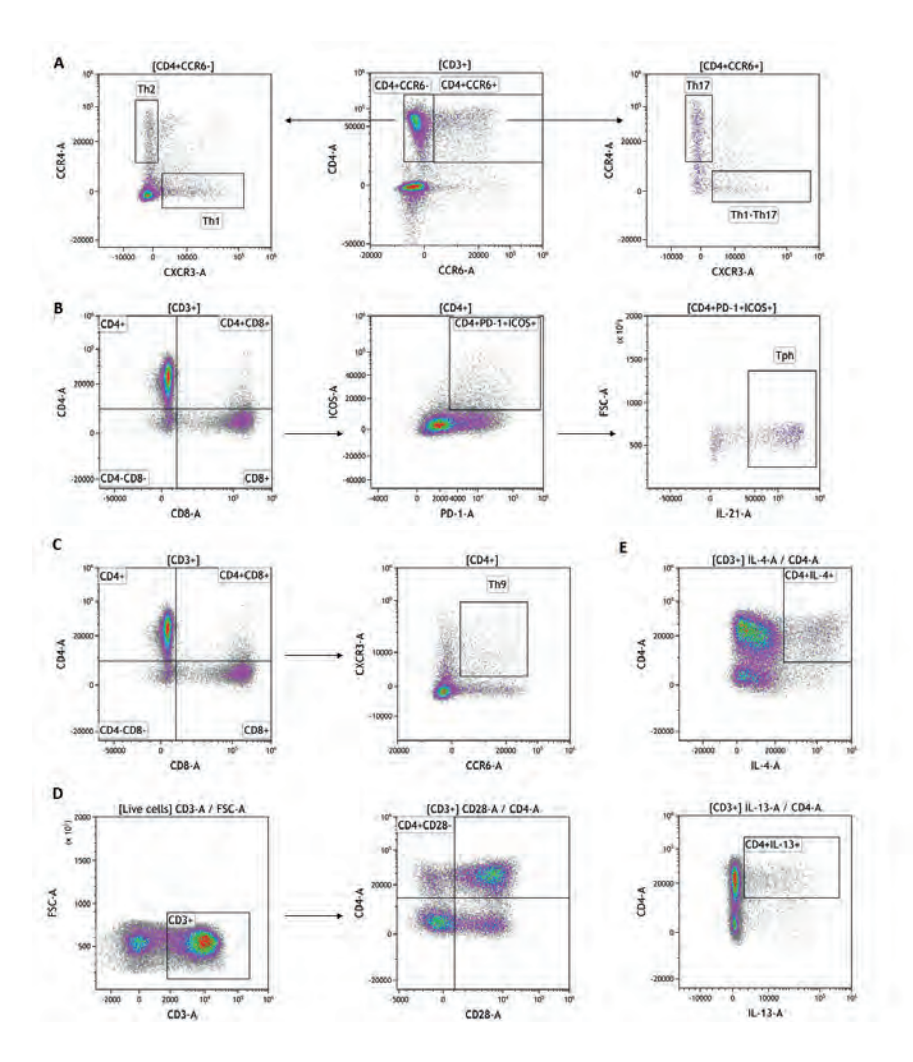
- 18. Rafael-Vidal C, Perez N, Altabas I, Garcia S, Pego-Reigosa JM. Blocking IL-17: A Promising Strategy in the Treatment of Systemic Rheumatic Diseases. Int J Mol Sci. 2020;21(19).
- 19. O'Reilly S, Hugle T, van Laar JM. T cells in systemic sclerosis: a reappraisal. Rheumatology (Oxford). 2012;51(9):1540-9.
- 20. Lemmers JM, van Caam AP, Kersten B, van den Ende CH, Knaapen H, van Dijk AP, et al. Nailfold capillaroscopy and candidate-biomarker levels in systemic sclerosis-associated pulmonary hypertension: A cross-sectional study. J Scleroderma Relat Disord. 2023;8(3):221-30.
- 21. LeRoy EC, Medsger TA, Jr. Criteria for the classification of early systemic sclerosis. J Rheumatol. 2001;28(7):1573-6.
- 22. Truchetet ME, Brembilla NC, Montanari E, Allanore Y, Chizzolini C. Increased frequency of circulating Th22 in addition to Th17 and Th2 lymphocytes in systemic sclerosis: association with interstitial lung disease. Arthritis Res Ther. 2011;13(5):R166.
- 23. Oliver SJ. The Th1/Th2 paradigm in the pathogenesis of scleroderma, and its modulation by thalidomide. Curr Rheumatol Rep. 2000;2(6):486-91.
- 24. Yoshitomi H, Ueno H. Shared and distinct roles of T peripheral helper and T follicular helper cells in human diseases. Cell Mol Immunol. 2021;18(3):523-7.
- 25. van Caam A, Vonk M, van den Hoogen F, van Lent P, van der Kraan P. Unraveling SSc Pathophysiology; The Myofibroblast. Front Immunol. 2018;9:2452.
- 26. Parel Y, Aurrand-Lions M, Scheja A, Dayer JM, Roosnek E, Chizzolini C. Presence of CD4+CD8+ double-positive T cells with very high interleukin-4 production potential in lesional skin of patients with systemic sclerosis. Arthritis Rheum. 2007;56(10):3459-67.
- 27. Kotecha N, Krutzik PO, Irish JM. Web-based analysis and publication of flow cytometry experiments. Curr Protoc Cytom. 2010; Chapter 10: Unit 10.7.
- 28. Wherry EJ. T cell exhaustion. Nat Immunol. 2011;12(6):492-9.
- 29. Gao Z, Feng Y, Xu J, Liang J. T cell exhaustion in immune-mediated inflammatory diseases: New implications for immunotherapy. Front Immunol. 2022;13:977394.
- 30. Warrington KJ, Takemura S, Goronzy JJ, Weyand CM. CD4+,CD28- T cells in rheumatoid arthritis patients combine features of the innate and adaptive immune systems. Arthritis Rheum. 2001;44(1):13-20.
- 31. Fox DA, Lundy SK, Whitfield ML, Berrocal V, Campbell P, Rasmussen S, et al. Lymphocyte subset abnormalities in early diffuse cutaneous systemic sclerosis. Arthritis Res Ther. 2021;23(1):10.
- 32. Gasparini G, Cozzani E, Parodi A. Interleukin-4 and interleukin-13 as possible therapeutic targets in systemic sclerosis. Cytokine. 2020;125:154799.
- 33. Gao Z, Feng Y, Xu J, Liang J. T cell exhaustion in immune-mediated inflammatory diseases: New implications for immunotherapy. Frontiers in Immunology. 2022;13.
- 34. McKinney EF, Lee JC, Jayne DR, Lyons PA, Smith KG. T cell exhaustion, co-stimulation and clinical outcome in autoimmunity and infection. Nature. 2015;523(7562):612-6.
- 35. Lima G, Treviño-Tello F, Atisha-Fregoso Y, Llorente L, Fragoso-Loyo H, Jakez-Ocampo J. Exhausted T cells in systemic lupus erythematosus patients in long-standing remission. Clin Exp Immunol. 2021;204(3):285-95.
- 36. Wiedeman AE, Muir VS, Rosasco MG, DeBerg HA, Presnell S, Haas B, et al. Autoreactive CD8+ T cell exhaustion distinguishes subjects with slow type 1 diabetes progression. J Clin Invest. 2020;130(1):480-90.
- 37. Paleja B, Low AHL, Kumar P, Saidin S, Lajam A, Nur Hazirah S, et al. Systemic Sclerosis Perturbs the Architecture of the Immunome. Frontiers in Immunology. 2020;11.

- 38. Rodriguez-Reyna TS, Furuzawa-Carballeda J, Cabiedes J, Fajardo-Hermosillo LD, Martinez-Reyes C, Diaz-Zamudio M, et al. Th17 peripheral cells are increased in diffuse cutaneous systemic sclerosis compared with limited illness: a cross-sectional study. Rheumatol Int. 2012;32(9):2653-60.
- 39. Radstake TR, van Bon L, Broen J, Hussiani A, Hesselstrand R, Wuttge DM, et al. The pronounced Th17 profile in systemic sclerosis (SSc) together with intracellular expression of TGFbeta and IFNgamma distinguishes SSc phenotypes. PLoS One. 2009;4(6):e5903.
- 40. Yang X, Yang J, Xing X, Wan L, Li M. Increased frequency of Th17 cells in systemic sclerosis is related to disease activity and collagen overproduction. Arthritis Res Ther. 2014;16(1):R4.
- 41. Wei L, Abraham D, Ong V. The Yin and Yang of IL-17 in Systemic Sclerosis. Front Immunol. 2022;13:885609.
- 42. Smeets RL, Kersten BE, Joosten I, Kaffa C, Alkema W, Koenen H, et al. Diagnostic profiles for precision medicine in systemic sclerosis; stepping forward from single biomarkers towards pathophysiological panels. Autoimmun Rev. 2020;19(5):102515.
- 43. Parthvi R, Sikachi RR, Agrawal A, Adial A, Vulisha A, Khanijo S, et al. Pulmonary hypertension associated with antiphospholipid antibody: Call for a screening tool? Intractable Rare Dis Res. 2017;6(3):163-71.
- 44. Nunes JPL, Cunha AC, Meirinhos T, Nunes A, Araujo PM, Godinho AR, et al. Prevalence of autoantibodies associated to pulmonary arterial hypertension in scleroderma - A review. Autoimmun Rev. 2018;17(12):1186-201.
- 45. Shu T, Xing Y, Wang J. Autoimmunity in Pulmonary Arterial Hypertension: Evidence for Local Immunoglobulin Production. Front Cardiovasc Med. 2021;8:680109.
- Ricard L, Jachiet V, Malard F, Ye Y, Stocker N, Riviere S, et al. Circulating follicular helper T cells are increased in systemic sclerosis and promote plasmablast differentiation through the IL-21 pathway which can be inhibited by ruxolitinib. Ann Rheum Dis. 2019;78(4):539-50.
- 47. Zhong Y, Yu PB. Decoding the Link Between Inflammation and Pulmonary Arterial Hypertension. Circulation. 2022;146(13):1023-5.

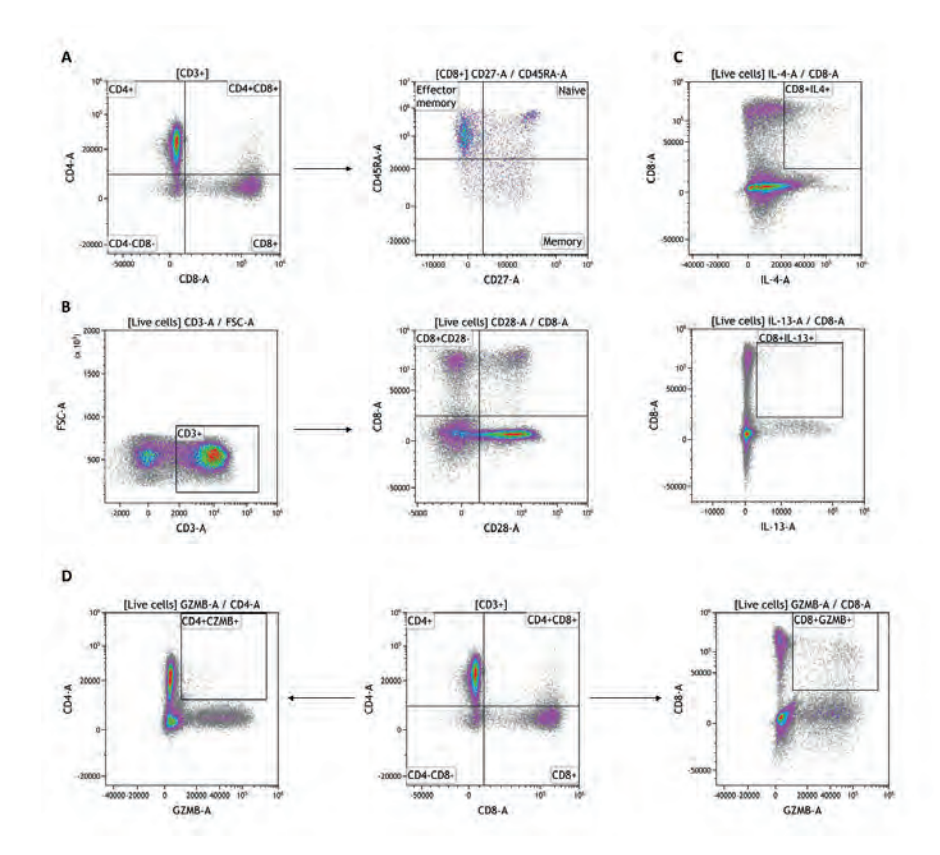
Supplementary Figures



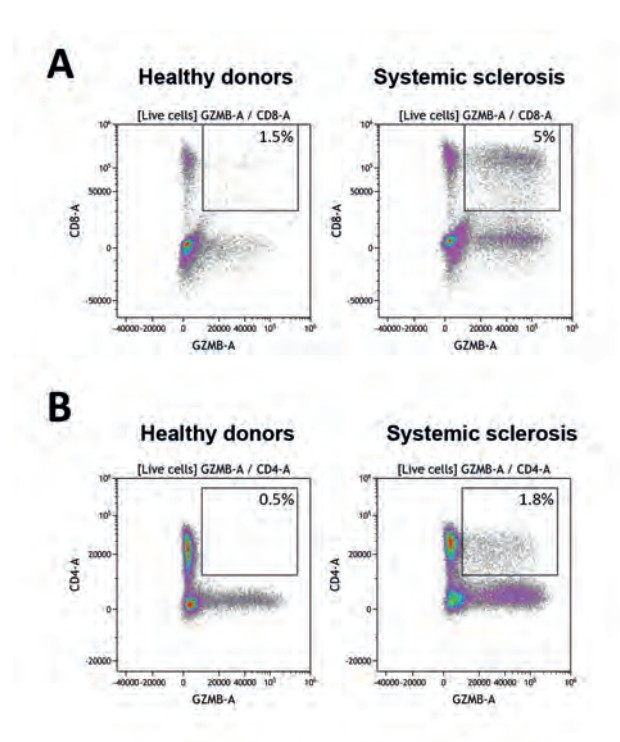
Supplementary Figure S1. Gating strategy for the detection of T helper (CD4⁺) T cells and cytotoxic (CD8⁺) T cells. In this figure FACs plots from one representative healthy donor sample are illustrated. (a) First debris is excluded and lymphocytes are selected based on their size and granularity when plotting cells for their forward and side scatter area (FSC-A and SSC-A respectively). Then, only the single cells are included for further analysis by plotting (b) their forward scatter area vs height and (c) side scatter area vs height. (d) FSC-A and fixable viability dye (FVD) emission are used to gate for the viable cells: FVD⁻. (e) Pan (CD3⁺) T cells are selected based on positive emission of the CD3 antibody when cells are plotted for FSC-A vs CD3. (f) CD3⁺ T cells are finally plotted for the emission of the antibodies CD4 and CD8 and cytotoxic T cells are gated as CD4⁺CD8⁺ and T helper cells as CD4⁺CD8⁻.



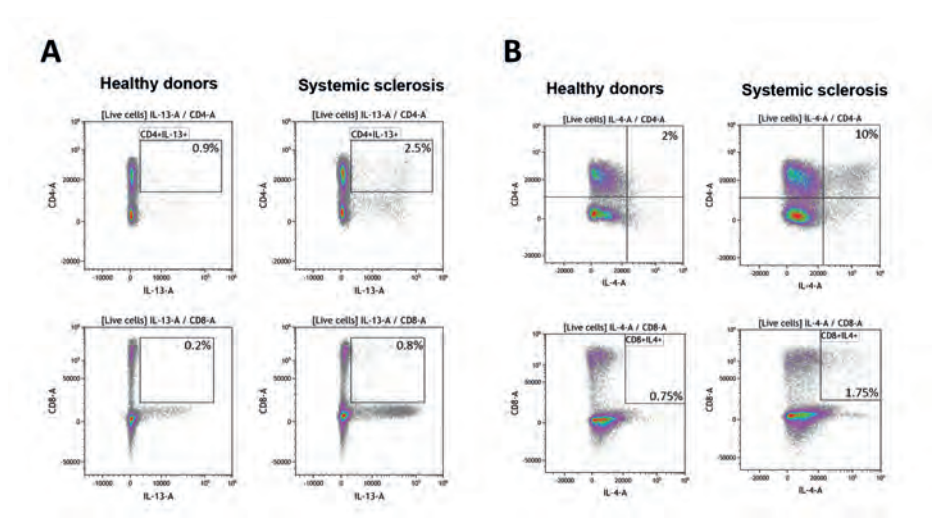
Supplementary Figure S2. Gating strategy for the detection of CD4⁺ T helper 1 (Th1), 2 (Th2), 17 (Th17), 9 (Th9) and T peripheral helper (Tph), exhausted and pro-fibrotic lymphocyte populations. (A) CD4⁺T lymphocytes can differentiate into various effector subpopulations including Th1, Th2, Th9, Th1/17 and Th17 subsets. Importantly, these subsets can be distinguished based on their chemokine receptor profile. Thus, to characterize the different T helper subsets, we used different combinations of the chemokine receptors CCR6, CCR4 and CXCR3 as has been described in literature (1-3). Live cells gated as shown in supplementary figure 1 are plotted for their CD4 vs CCR6 emission. Th1 cells are then gated as CD4⁺CCR6⁻CXCR3⁺CCR4⁻ and Th2 cells as CD4⁺CCR6⁻CXCR3⁻CCR4⁺. Th17 cells are gated as CD4+CCR6+CXCR3-CCR4+ and Th1-Th17 cells as CD4+CCR6+CXCR3+CCR4-. (B) T helper (CD4+) cells are plotted for ICOS vs PD-1 emission and the population CD4+PD-1+ICOS+ is then plotted for FSC vs IL-21 and Tph cells are gated as CD4+PD-1+ICOS+IL-21+. (C) Th9 cells are gated as CD4+CXCR3+CCR6+. (D) Exhausted T helper cells are gated as CD3+CD4+CD28. (E) Pro-fibrotic T helper cell populations are characterized as either CD4+IL-4+ or CD4+IL-13+.



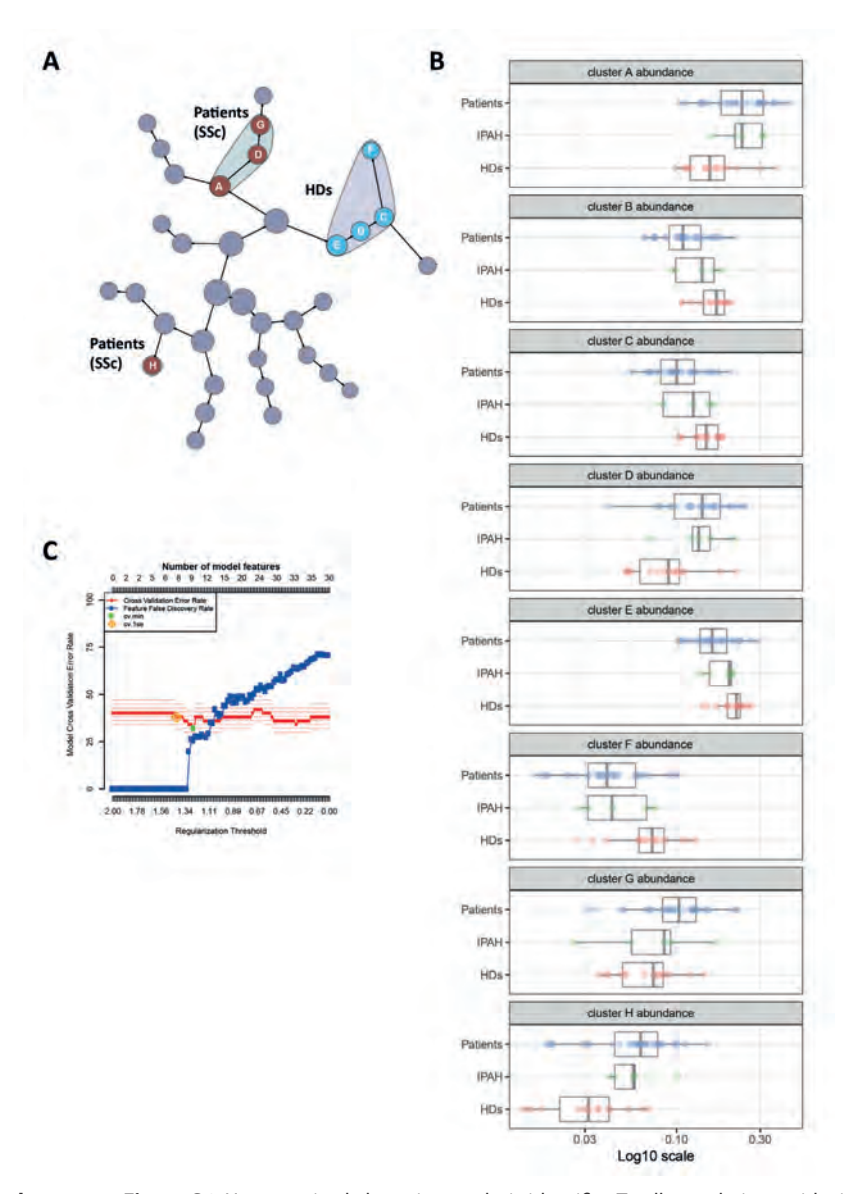
Supplementary Figure S3. Gating strategy for the detection of CD8⁺ T cell sub-populations. (**A**) Live CD8⁺CD4⁻ T cells are gated for their CD45RA vs CD27 emission and CD8⁺ T cells are characterized as naïve (CD54RA⁺CD27⁺), memory (CD45RA⁻CD27⁺) and effector memory (CD45RA⁺CD27⁻). (**B**) Exhausted cytotoxic T cells are detected as CD3⁺CD8⁺CD28⁻. (**C**) Cytotoxic pro-fibrotic T cells are recognized as CD8⁺IL-4⁺ or CD8⁺IL-13⁺. (**D**) Cytotoxic CD4⁺/CD8⁺T cells are characterized as CD3⁺CD4⁺CD8⁻GZMB⁺ and CD3⁺CD4⁻CD8⁺GZMB⁺ respectively.



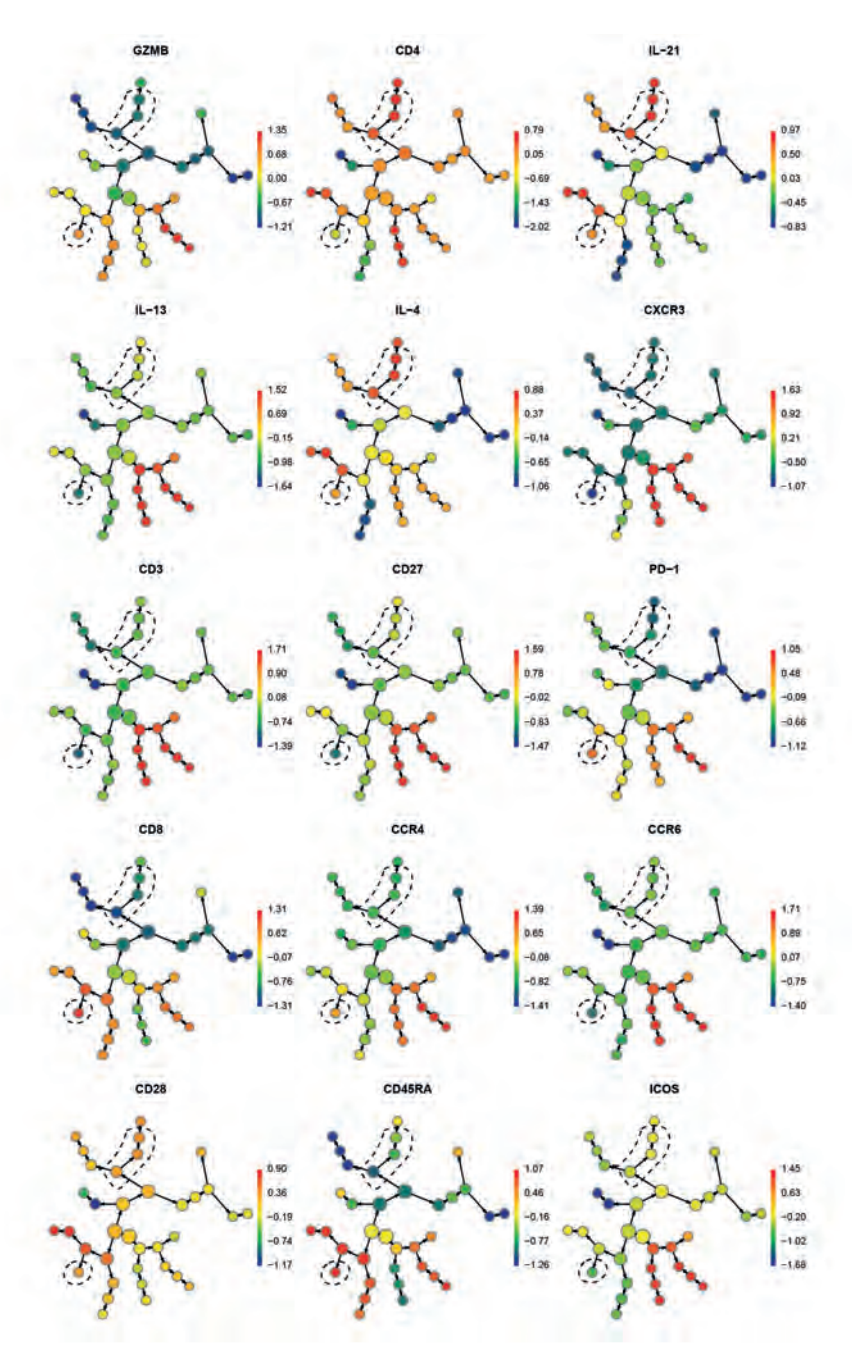
Supplementary Figure S4. Increased presence of GZMB expressing CD4+ T cells in SSc compared to HD. Representative flow cytometry plots exhibiting expression of Granzyme B (GZMB) in (A) CD8+ T cells and (B) CD4⁺ T cells in SSc and healthy (HD) blood.



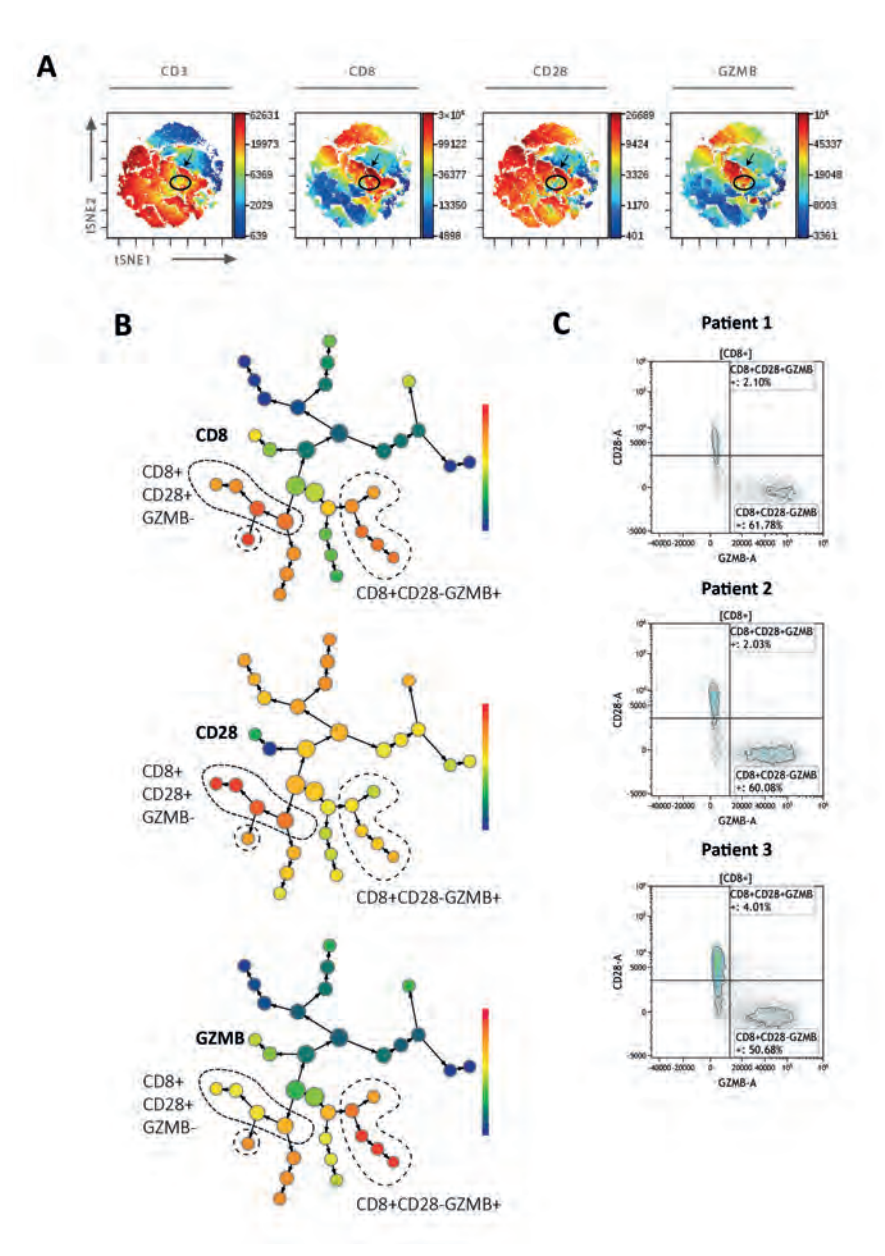
Supplementary Figure S5. T helper and cytotoxic T cells from SSc patients show increased profibrotic cytokine expression compared to HD. Representative flow cytometry plots showing expression of the cytokines (**A**) IL-13 and (**B**) IL-4 in CD4⁺T helper (up) and cytotoxic CD8⁺T (down) cells in healthy donors and in patients with systemic sclerosis.



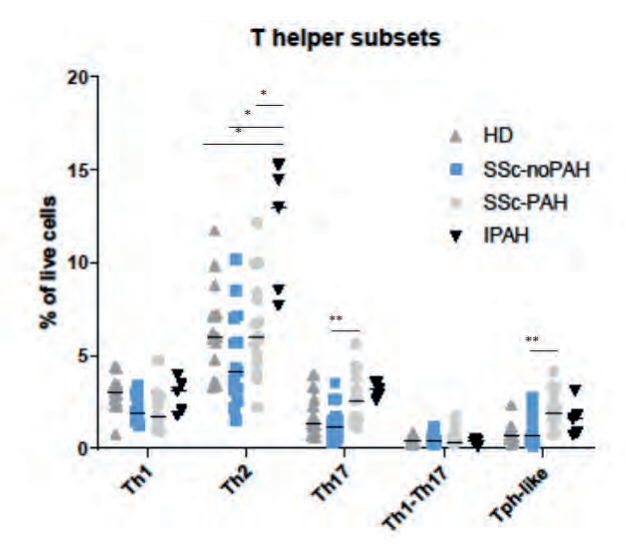
Supplementary Figure S6. Unsupervised clustering analysis identifies T cell populations with similar characteristics that are enriched either in SSc patients or HD. (A-B) Classification of SSc, IPAH patients' and HD peripheral blood CD3⁺ T cells based on hierarchical clustering of the protein markers CD3, CD4, CD8, CCR4, CD28, CCR6, CXCR3, CD45RA, CD27, PD-1, ICOS, IL-4, IL-13, IL-21 and GZMB was used to detect cell populations of comparable marker expression and their abundance utilizing the CITRUS tool provided by Cytobank. 5,000 events were sampled per each individual donor. The size of each node depicts the cell frequency. On the right (B) the cluster frequency relative to total events per sample is illustrated showing clusters that are enriched in either SSc patients or HD. (C) Prediction analysis for microarrays (PAM) clustering was performed to detect cell clusters contributing to SSc patients. Here, the graph showing the model error rate of this analysis is illustrated.



Supplementary Figure S7. Unsupervised CITRUS hierarchical clustering analysis reveals enriched expression of CD8, GZMB, IL-4 and IL-21 in patients with SSc. Citrus hierarchical "clustering trees" exhibiting the relationships of the detected nodes. The color scales illustrates the intensity of expression of each depicted marker per cluster and the size of each node shows the event frequency.



Supplementary Figure S8. CD8+CD28-GZMB+ T cells and CD8+CD28+GZMB- T cells represent distinct CD8+ cytotoxic T lymphocyte clusters. (A) Marker expression of CD3, CD8, CD28 and GZMB in the combined t-distributed Stochastic Neighbor Embedding (t-SNE) plots of all SSc patients. T-SNE analyses were performed using the Cytobank platform (1). For this analysis, automated compensation was applied before gating in every sample. (B) Plots showing the expression of CD8, CD28 and GZMB in clustering results from HD and SSc concatenated FCS files. For this analysis, clustering was performed by Citrus from Cytobank. Clusters highlighted with different dashed lines represent cells that are either CD8+CD28+GZMB- or CD8+CD28-GZMB+. (C) Representative flow cytometry plots from 3 SSc patients exhibiting populations of CD8+CD28+GZMB+ and CD8+CD28-GZMB+ T cells.



Supplementary Figure S9. Comparison of the frequencies of T helper subsets in SSc patients with or without PAH, healthy donors (HD) and patients with idiopathic PAH (IPAH). Patients with IPAH exhibit a predominant Th2 profile in their circulation compared to patients with SSc and HD. Values are represented as % of live cells. For the statistics, a two-way ANOVA with Tukey's multiple comparisons correction test was performed for each T helper subset within the four depicted groups, *p<0.05, **p<0.01. Only the statistically significant comparisons are illustrated in the graph.

References

- Fava A, Cimbro R, Wigley FM, Liu QR, Rosen A, Boin F. Frequency of circulating topoisomerase-lspecific CD4 T cells predicts presence and progression of interstitial lung disease in scleroderma. Arthritis Res Ther. 2016;18(1):99.
- Dulic S, Vasarhelyi Z, Sava F, Berta L, Szalay B, Toldi G, et al. T cell Subsets in Rheumatoid Arthritis Patients on Long-Term Anti-TNF or IL-6 Receptor Blocker Therapy. Mediators Inflamm. 2017;2017:6894374.
- Kara EE, Comerford I, Bastow CR, Fenix KA, Litchfield W, Handel TM, et al. Distinct chemokine receptor axes regulate Th9 cell trafficking to allergic and autoimmune inflammatory sites. J Immunol. 2013;191(3):1110-7.

Supplementary Data S1

Supplementary methods

Patient enrollment and clinical phenotyping

In this cross-sectional cohort study, peripheral blood samples were obtained from consecutive SSc-PAH patients and idiopathic pulmonary arterial hypertension (IPAH) patients treated at the pulmonary hypertension expert center of the Radboud University Niimegen Medical Centre who previously consented to the use of their clinical parameters and blood for scientific study (protocol NL66117.091.18). Samples from selected age and sex matched SSc patients without pulmonary arterial hypertension (PAH), treated at the outpatient department of Rheumatic Diseases, Radboudumc, Nijmegen between 22-03-2021 and 15-07-2021 were also included. Peripheral blood samples from healthy donors, age and sex matched, were acquired from Sanguin bloodbank (Project number NVT 0397-02). All patients consented to study participation before blood donation. This study complied with the Declaration of Helsinki and was carried out in accordance with the applicable Dutch legislation concerning reviewal by an accredited research ethics committee, file number 2021-8193.

Inclusion criteria

Patients eligible to participate in the study fulfilled the following criteria:

- 1. Fulfilment of the ACR/EULAR classification criteria for SSc (1),
- 2. Age \geq 18 years,
- 3. SSc-PAH and IPAH patients (WHO group 1) diagnosed by right heart catheterization, according to the ESC/ERS 2015 guidelines (2).

SSc patients with overlapping syndromes or with forms of pulmonary hypertension other than IPAH/SSc-PAH were excluded from our sample collection.

Clinical and demographic data were prospectively collected, including age, sex, Rodnan skin score, laboratory values including creatinine, urate and Nt-proBNP, New York Heart Association functional class (NYHA), six-minute walking distance (6MWD), pulmonary function test results and co-medication use at inclusion. In addition, data concerning medication, pulmonary function and Rodnan skin score were retrospectively collected up to 6 months before inclusion.

Peripheral blood mononuclear cell (PBMC) isolation and culture

PBMCs were isolated from whole blood with the use of Ficoll Pacque PLUS density gradient (GE Healthcare) as per the manufacturer's instructions. Harvested PBMCs were washed three times with PBS + 1.5% ACD-A and cryopreserved at a density of 10 to 20 x 10 $^{\circ}$ cells/ml. On the day of the experiment, PBMCs were rapidly thawed in warm (37 $^{\circ}$ C) complete (containing 10% of human pooled serum) culture RPMI medium and washed. Next, 5×10^{5} cells from each subject were plated on 96-well-u bottom plates (Greiner) and stimulated with 12.5 ng/ml phorbol myristate acetate (PMA) and 500 ng/ml ionomycin in the presence of 5 µg/ml brefeldin A for 4 hours at 37 $^{\circ}$ C, 5% CO₃.

Flow cytometry: preparation and staining of cells

To comprehensively characterize and compare the T lymphocyte immunome of SSc patients, we developed a 17-color flow cytometric immunophenotyping panel, consisting of both surface and intracellular markers. This panel allowed us to identify key T helper and cytotoxic T cell subsets (*Supplementary table 1*). Cells were first treated with 100 µl of ViaKrome 808 fixable viability dye (1.5 : 1000 in PBS) for 30 min on ice, before they were labeled with cell surface antibodies. Staining for cell surface molecules (*Supplementary table 2*) was performed for 20 minutes at room temperature (RT). For intracellular staining, Cyto-Fast™ Fix/Perm Buffer Set (Biolegend) was used for fixation and permeabilization of the cells as per manufacture's protocol. Cells were then labeled for 20 minutes at RT with intracellular antibodies (*Supplementary table 3*).

Flow cytometry analysis

Samples were analyzed on a Beckman Coulter Cytoflex LX 21-color flow cytometer, immediately after staining. All samples were stained and acquired the same day to reduce batch effect variation. Compensation was optimized using single stainings in UltraComp eBeads[™] (Thermo Fischer, cat #: 01-2222-41). Flow data were analyzed using Kaluza (v2.1.2) software. The gating strategy that was utilized is illustrated in *Supplementary figure 1*. The gaiting strategies of the different T helper and cytotoxic populations are depicted in *Supplementary figures 2 and 3*.

viSNE analysis

viSNE analyses were performed with using the web-based analysis software Cytobank (http://cytobank.org/) (3). Each individual file was first gated on live CD3+ T cells. Subsampling of events was conducted according to the visNE algorithm, with an analysis of 14,060 events per sample. CD3, CD4, CD8, CCR4, CD28, CCR6, CXCR3, CD45RA, CD27, PD-1, ICOS, IL-4, IL-13, IL-21 and GZMB were utilized to generate the t-SNE axes of the illustrated viSNE maps. The levels of each protein marker were normalized based on the maximum value observed for the respective channel within each donor

CITRUS clustering

In the context of unsupervised analysis, manually gated CD3+T lymphocytes were initially isolated using the Beckman Coulter plug-in of the Kaluza (v2.1.2) software. Subsequently, these extracted cells underwent further processing through the web-based analysis platform Cytobank (http://cytobank.org/) (3). The individual files were then grouped and categorized as SSc, HD and IPAH. Unsupervised clustering of lymphocyte and T cell frequencies was conducted using the CITRUS tool, with clustering based on abundance, setting a minimum cluster size of 2% of total cells and a false discovery rate of 1%. Cells were clustered based on the level of expression of the protein cell surface and intracellular markers described in the methods section "viSNE analysis". In the Citrus "cluster tree" the clustering hierarchy is illustrated and the nodes of the "cluster tree" were scaled based on cell frequency in each respective cluster. Clustering was evaluated using prediction analysis for microarrays (PAM). This predictive model aimed to identify features contributing to SSc specific immunophenotyping differences compared to HD and patients with IPAH.

Statistical analysis

Statistical significance comparisons between experimental groups were performed with GraphPad 9.0.0. For comparisons between SSc patients and healthy donors the Student's t-test corrected for multiple comparisons was performed for data that were normally distributed (for corrected for multiple comparisons data adjusted p values is reported). When dealing with non-normally distributed data, the Mann-Whitney U test corrected for multiple comparisons was performed. Normality in data distribution was evaluated using the Kolmegorov-Smirnov test. For statistical comparisons between the different subject groups (SSc-PAH, SSc-NoPAH, IPAH, HD) two-way ANOVA with Tukey's multiple comparisons test was performed.

Adjusted p values less than 0.05 were considered as statistically significant and are indicated in graphs with asterisks (p<0.05 *, p<0.01 ***, p< 0.001 ***). Results are expressed as mean \pm standard deviation. The specific statistical tests conducted for each analysis are mentioned in each figure's legend.

Supplementary materials

Supplementary Table S1. Definition of T cell subsets.

T cell subty	pe	Detection markers	
CD4 ⁺	Th1	CCR6 ⁻ CXCR3 ⁺ CCR4 ⁻	
	Th2	CCR6-CXCR3-CCR4+	
	Th17	CCR6+CXCR3-CCR4+	
	T peripheral helper	PD-1 ⁺ ICOS ⁺ IL-21 ⁺	
	Exhausted	CD28 ⁻	
	Cytotoxic	GZMB ⁺	
	Pro-fibrotic	IL-4+/IL-13+	
CD8 ⁺	Naïve	CD27 ⁺ CD45RA ⁺	
	Memory	CD27 ⁺ CD45RA ⁻	
	Effector memory	CD27 ⁻ CD45RA ⁺	
	Cytotoxic	GZMB ⁺	
	Exhausted	CD28 ⁻	
	Pro-fibrotic	IL-4+/IL-13+	

Supplementary Table S2. List of antibodies used for cell surface staining.

Antigen	Clone	Dilution	Fluorochrome	Supplier
CD4	RPA-T4	1:100	PerCP/Cy5.5	Biolegend
CXCR3	G025H7	1:20	APC	Biolegend
CD3	UCHT1	1:100	Alexa700	Biolegend
CD27	O323	1:10	APC/Cy7	Biolegend
PD-1	EH12.2H7	1:20	BV421	Biolegend
CD8a	RPA-T8	1:100	BV510	Biolegend
CCR4	L291H4	1:20	BV605	Biolegend
ICOS	C398.4A	1:100	BV711	Biolegend
CCR6	G034E3	1:20	BV785	Biolegend
CD28	CD28.2	1:20	BUV395	BD Biosciences
CD45RA	HI100	1:40	BUV496	BD Biosciences

Supplementary Table S3. List of antibodies used for intracellular staining.

Antigen	Clone	Dilution	Fluorochrome	Supplier
Granzyme B	GB11	1:15	FITC	Biolegend
IL-21	eBIO3A3-N2	1:12.5	PE	Biolegend
IL-4	MP4-25D2	1:20	PE/Dazzle594	Biolegend
IL-13	JES10-5A2	1:20	PE/Cy7	Biolegend

Supplementary Table S4. Additional baseline patient characteristics.

Baseline characteristics	SScN= 30	IPAHN=5	HDN=15
Autoantibody profiling (rest)			
ACA	15 (50)	0	
ATA	3 (10)	0	
ARA	2 (6.7)	0	
Other	8 (26.7)	0	
Unknown	4 (13.3)	2 (40)	
Pulmonary Function, mean (SD)			
1. VC % predicted	92.5 (22.4)	104.6(22.6)	
2. DLCO % predicted	51.4 (15.1)	72.8 (19.3)	
3. 6MWT (m)	409.4 (115.9)	447.6 (42.3)	
Medication use, n(%)			
4. Immunosuppression	16 (53.3)	0	
5. Diuretics	13 (43)	3 (60)	
6. Urate lowering Therapy	2 (6.7)	0	
7. Nifedipine	8 (27)	0	
8. PAH medication	17 (56)	5 (100)	

SSc: systemic sclerosis. IPAH: idiopathic pulmonary arterial hypertension. ACA: Anticentromere antibodies. ATA: Anti-topoisomerase antibodies. ARA: .Anti-reticulin antibodies. HD: healthy donors. S.D.: standard deviation. VC: Vital Capacity. DLCO: Diffusing Lung Capacity for carbon monoxide. 6MWT: 6-Minute Walk Test. PAH: Pulmonary Arterial Hypertension.

Supplementary Table S5. Clinical characteristics of patients with or without the presence of pulmonary arterial hypertension.

Baseline characteristics	SSc-PAH N= 15	SSc-NPAH N=15	IPAH N=5	HD N=15	P value
Age in years, mean (SD)	67.7 (10.4)	67.5 (8.9)	63.0 (9.4)	63.2 (6.2)	0.46
Female, n (%)	12 (80)	13 (86.7)	5 (100)	12 (80)	0.72
Caucasian, n (%)	15 (100)	15 (100)	5 (100)	15 (100)	1.00
SSc duration in years, mean (SD)	9.5 (7.1)	10.7 (9.2)			0.73
LcSSc, n, (%)	12 (80)	12 (80)			1.00
Clinical SSc features					
ILD, n (%)	6 (40)	6 (40)	0		
Raynaud's Phenomenon, n (%)	15 (100)	14 (93.3)	0		
Digital Ulcers, n (%)	3/14 (20)	8/15 (53.3)	0		
Telangiectasias, n (%)	8/9 (53.3)	4/15 (26.7)	0		
mRSS, mean (SD)	4.0 (4.4)	4.13 (5.6)			
NYHA class, n (%)					
9.1	0	13 (86.7)	0		
10. II	4 (26.7)	2 (13.3)	5 (100)		
11.	8 (53.3)	0	0		
12. IV	3 (20)	0	0		
Laboratory results, mean (SD)					
MDRD/GFR (ml/min/1.73m ²	59.6 (17.2)	67.3 (15.2)	72.2 (14.4)		
Creatinine (µmol/L)	93.5 (27.1)	79.7 (19.6)	78.2 (23.5)		
Urate (µmol/L))	0.39 (0.16)	0.30 (0.07)	0.36 (0.13)		
natron (pg/ml)	1419 (2301)	170 (206)	96.6 (42)		
ANA positive, n (%)	12 (80)	14 (93.3)	2 (40)		
ENA positive, n (%)	8/11	11/13	0		
ACA positive, n (%)	6 (40)	9 (60)	0		
ATA positive, n (%)	1 (6.7)	2 (13.3)	0		
ARA positive, n (%)	1 (6.7)	1 (6.7)	0		
Other, n (%)	4 (26.7)	4 (26.7)	0		
Unknown, n (%)	3 (20)	1 (6.6)	2 (40)		
Pulmonary Function, mean (SD)					
13. VC % predicted	87.9 (22.5)	97.1 (22.2)	104.6(22.6)		
14. DLCO % predicted	36.2 (12.5)	66.6 (17.7)	72.8 (19.3)		
15. 6MWT (m)	368.71 (104)	450 (127.8)	447.6 (42.3)		

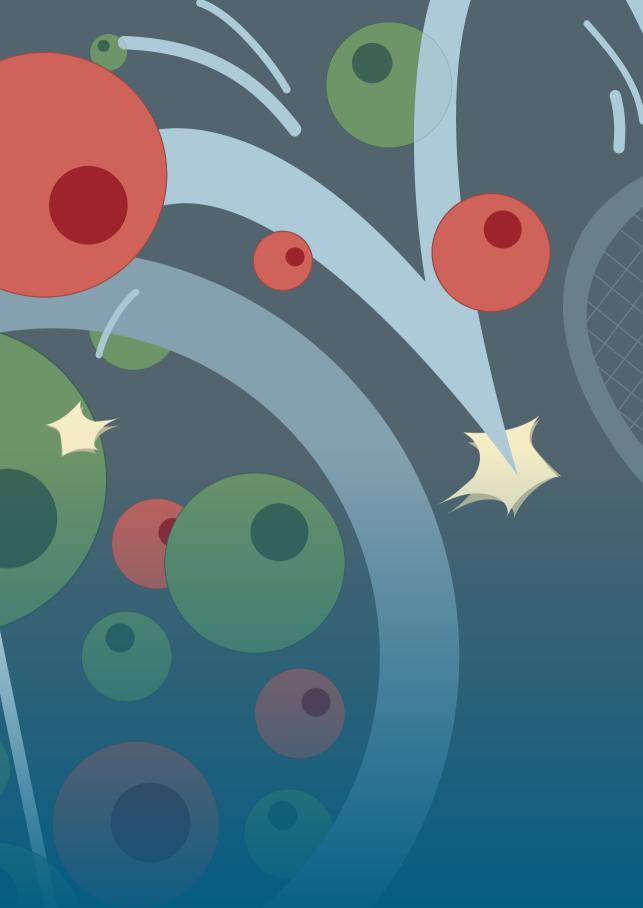
Supplementary Table S5. Continued

Baseline characteristics	SSc-PAH N= 15	SSc-NPAH N=15	IPAH N=5	HD N=15	P value
Medication use, n(%)					
16. Immunosuppression	8 (53.3)	8 (53.3)	0		
17. Diuretics	10 (66.7)	3 (20)	3 (60)		
18. Urate lowering Therapy	1 (6.7)	1 (6.7)	0		
19. Nifedipine	1 (6.7)	7 (46.7)	0		
20 . PH medication	14 (93.3)	3 (20)	5 (100)		

SSc-PAH: systemic sclerosis combined with pulmonary arterial hypertension. SSc-NPAH: systemic sclerosis with no pulmonary arterial hypertension. IPAH: idiopathic pulmonary arterial hypertension.. HD: healthy donors. S.D.: standard deviation. PAH: pulmonary arterial hypertension. ILD: Interstitial lung disease. mRSS: modified Rodnan skin score. NYHA: New York Heart Association. MDRD: Modification of Diet in Renal Disease. GFR: Glomerular Filtration Rate. Nt-proBNP: aminoterminal pro B-type natriuretic peptide. ANA: Antinuclear Antibody. ENA: extractable nuclear antigen. ACA: Anticentromere antibodies. ATA: Anti-topoisomerase antibodies. ARA: . Anti-reticulin antibodies. HD: healthy donors. S.D.: standard deviation. VC: Vital Capacity. DLCO: Diffusing Lung Capacity for carbon monoxide. 6MWT: 6-Minute Walk Test.

References

- van den Hoogen F, Khanna D, Fransen J, Johnson SR, Baron M, Tyndall A, et al. 2013 classification criteria for systemic sclerosis: an American college of rheumatology/European league against rheumatism collaborative initiative. Ann Rheum Dis. 2013;72(11):1747-55.
- Humbert M, Kovacs G, Hoeper MM, Badagliacca R, Berger RMF, Brida M, et al. 2022 ESC/ERS Guidelines for the diagnosis and treatment of pulmonary hypertension. European heart journal. 2022;43(38):3618-731.
- Kotecha N, Krutzik PO, Irish JM. Web-based analysis and publication of flow cytometry experiments. Curr Protoc Cytom. 2010; Chapter 10: Unit10.7.



Chapter 6

Interferon-responsive autoreactive CD4+ T cells restrict systemic autoimmunity via TRAIL

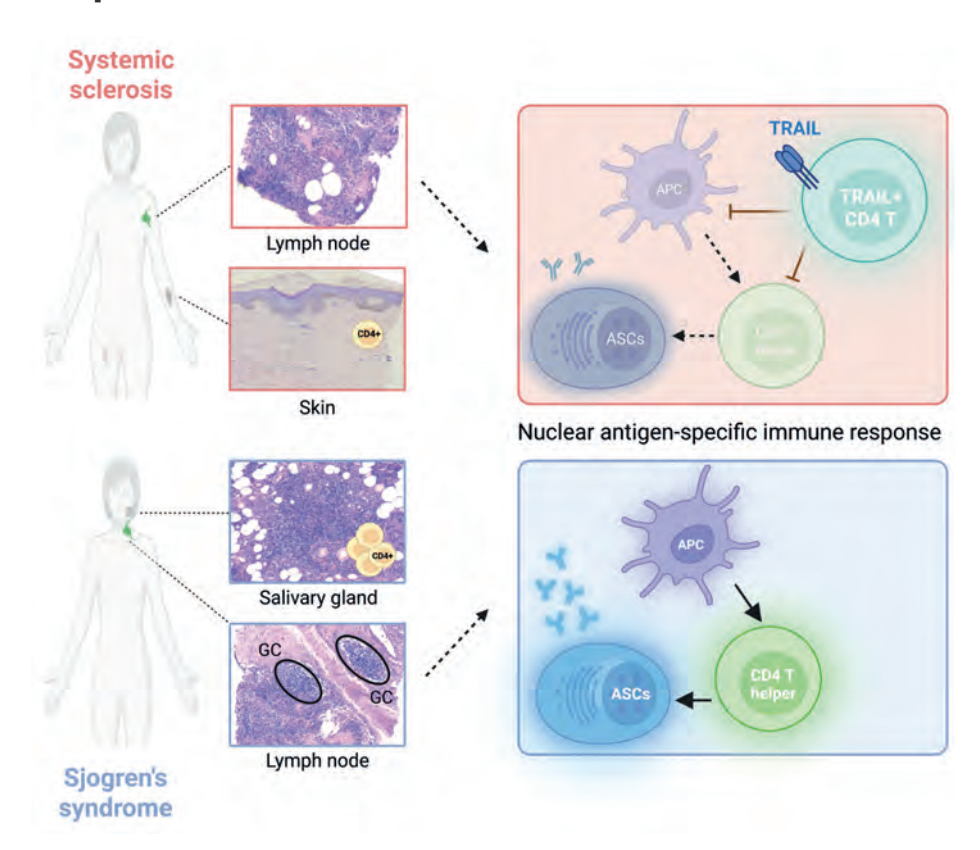
Theodoros Ioannis Papadimitriou, Prashant Singh, Arjan van Caam, Xuehui He, Konnie M. Hebeda, Birgitte Walgreen, Elly Vitters, Pim Kloosterman, Laura J. A. Wingens, Klaas W. Mulder, Madelon Vonk, I. Jolanda M. de Vries, Peter van der Kraan, Ruben L. Smeets, Erik Aarntzen, Hans Koenen, Martijn A. Huynen and Rogier M. Thurlings

Submitted.

Abstract

Recognition of nuclear antigens (NAgs) by CD4+ T cells is a key driver of systemic autoimmunity in connective tissue diseases (CTDs), but the infiltration and activation of CD4+ T cells in affected tissues widely differs. Studies in experimental animal models suggest that differences arise because immune responses targeting specific NAgs vary between CTDs; however, these models do not fully capture the complete spectrum of CTD. The comprehensive understanding of NAg-specific CD4+ T cell responses in human CTD remains elusive due to their rarity, challenging localization in lymphoid and diseased tissues, and the absence of imaging tools to detect autoreactive immune activity. To address this, we combined [18F]labeled thymidine PET imaging, multi-omics and T cell activation assays to biopsy, identify and compare NAg-specific T cells in immunologically active lymph nodes (LNs) and affected tissues of patients with immunologically divergent CTDs. In Sjogren's syndrome, active LNs and affected tissue contained NAg-specific effector CD4+ T cells, including B-helper T cells. In systemic sclerosis, active LNs contained CD4+TRAIL+ with interferon stimulated gene signature (ISG) T cells, while LNs and affected tissue lacked NAg-specific effector CD4+ T cells. Functional assays indicated that TRAIL+ CD4+ T cells suppressed the proliferation of CD4+ effector T cells and reduced the activation of antigen-presenting cells to restrict the generation of effector T cells, autoreactive plasma cells, and autoantibodies within reactive LNs. Taken together, this study provides improved understanding of the autoreactive response that drives pathology from locoregional LNs in autoimmune CTDs. Applying this knowledge will aid in the design and testing of novel tolerogenic therapies for autoimmune CTDs.

Graphical abstract



Introduction

Autoimmune connective tissue diseases (CTDs) are debilitating diseases accompanied by a poor quality of life and severe health deterioration (1). They are characterized by a fluctuating disease course, systemic and local inflammatory responses, and organ- and connective tissue-specific symptoms (2). Although the etiology of these diseases remains poorly understood, loss of tolerance due to self-antigen recognition by autoreactive CD4+ T-cells, is considered to play a central role (3). This is supported by genetic studies confirming that polymorphisms in the HLA region confer the highest risk for development of CTDs. In addition, CTDs are characterized by circulating autoantibodies against nuclear antigens, and HLA class II alleles are associated with their development (4, 5).

In contrast, recent immunopathogenic and multi-omics studies, that we and others performed, indicate that the infiltration and activation of CD4+ T-cells vary significantly across CTD affected tissues. Sjogren's syndrome (SjS) and systemic sclerosis (SSc) represent two CTDs at the opposite ends of this immunological spectrum. SjS is primarily characterized by chronic inflammation of salivary and lacrimal glands. These tissues exhibit a dense periductal infiltrate of effector CD4+ T-cell helper subsets (6, 7) and autoreactive B-cells (8). SSc on the other hand, is characterized by vasculopathy, autoimmune inflammation and fibrosis, leading to excessive extracellular matrix deposition in skin and internal organs such as heart, lungs and kidneys. In contrast with SjS, this involves a sparse perivascular immune cell infiltrate without an overt increase in CD4+ T-cells (9-11).

Hypothetically, these differences occur because the underlying immune responses targeting distinct nuclear antigens (NAgs) vary between different CTDs (12-14). The mechanisms driving NAg-directed immune responses have been primarily studied in experimental animal models of systemic autoimmunity (14, 15). In these models, aberrant activation of professional antigen-presenting cells (APCs) disrupts self-tolerance by presenting NAgs to CD4+ T-cells within lymphoid tissues (16, 17). This presentation initiates CD4+ T-cell activation against specific NAg epitopes, but the nature and strength of this activation differ depending on factors such as TCR–MHC affinity, antigen persistence and timing of exposure (18-20). Such variations lead to either weak extrafollicular or strong follicular NAg-directed humoral immune responses, dependent on the model (21). B-cell follicles within lymph nodes (LNs) are critical sites where APCs orchestrate interactions between CD4+ T-cells and B-cells, facilitating the development of adaptive immune responses. In contrast, extrafollicular regions support B-cell responses that occur with minimal or no CD4+

T-cell help (22). Importantly, regulatory T-cell subsets exert tolerogenic mechanisms to prevent autoreactive CD4+ T-cell activation in both follicular and extrafollicular sites (23). Consequently, the location and robustness of NAq-directed humoral responses in various models are at least partly determined by the efficiency with which regulatory T-cells suppress effector CD4+ T-cell activation within these distinct regions (24, 25).

In human CTD, the full spectrum of the NAq-directed immune response—including priming, activation, and regulation of NAg-specific CD4+ T-cells in LNs, circulation, and affected tissues—remains unexplored. This is primarily due to the challenge of localizing autoantigen-specific CD4+ T-cells, which are present in low numbers and reside in hard-to-access locoregional lymph nodes and disease-affected tissues. Additionally, there is a lack of imaging techniques capable of detecting and localizing the activity of autoreactive immune cells. As a result, NAg-specific CD4+ T-cells have primarily been detected in blood circulation, limiting understanding of their generation in LNs and their role in organ destruction (26, 27). Advancements in imaging, such as positron emission tomography (PET), allow sensitive visualization and quantification of biomolecular processes simultaneously at the whole-body scale. [18F]-labeled 3'-fluoro-3'-deoxy-thymidine ([18F] FLT) detects thymidine incorporation during DNA synthesis phases of cell proliferation (28) and has been used to visualize active LNs in clinical settings of both acute and chronic inflammation (29, 30).

Here, we hypothesized that the differences in CD4+ T-cell infiltration and activation in affected tissues of patients with SSc and SjS result from variations in the activation and regulation of NAg-specific CD4+ T-cell-mediated humoral immune responses originating in locoregional LNs. We used [18F] FLT PET imaging to identify lymph nodes containing proliferating lymphocytes. Followingly, we applied multimodal single-cell RNA sequencing combined with multiplex immunohistochemistry and functional assays to define the properties of NAg-specific CD4+ T-cell responses in blood. LNs and affected tissues.

We demonstrate that in SjS patients, FLT-positive LNs are marked by a higher presence of NAq-specific effector CD4+ T-cells that provide B-cell help. In contrast, CD4+ NAg-specific T-cells in active lymph nodes of SSc patients predominantly occurred as regulatory T-cells and as a novel, naïve-like CD4+ TRAIL+ with interferon stimulated gene signature (ISG) T-cell population. CD4+ TRAIL+ ISG T-cells displayed an immunoregulatory role by restricting APC-mediated activation and suppressing proliferation of CD4+ effector T cells leading to reduced formation of autoreactive plasma cells. This coincided with little infiltration and activation of NAg-specific CD4+ effector T-cells in SSc affected tissues, compared to extensive infiltration of these cells in SjS affected tissues. Together, our findings provide evidence of disease-specific differences in activation and regulation of NAg-specific humoral immunity within active LNs of patients with CTD, potentially explaining differences in CD4+ T-cell infiltration and activation in affected tissues. This has significant implications for the development of targeted and tolerogenic therapies.

Results

[18F] FLT PET scans distinguish active and quiescent lymph nodes in CTDs

To understand if the extent of CD4+ T-cell infiltration and activation in CTD-affected tissues is related to the immune response targeting distinct NAgs, we undertook a multimodal single-cell approach to characterize NAq-specific CD4+T-cell responses in the blood, affected tissues and locoregional LNs of patients with CTD. We selected treatment-naïve patients with SSc and SiS who had clinically active disease and were sero-positive for the NAgs anti-ScI70 and anti-Ro60/La (Figure 1A, B and Supplemental Table 1). Anti-ScI70 and anti-Ro60/La anti-nuclear antibodies are associated with a severe disease course in SSc and SiS, respectively. We performed [18F] FLT PET scans to identify affected tissues and active LNs in their vicinity. LNs showing increased [18F] FLT PET uptake were considered as "positive" while those with no or low uptake were classified as "negative" (Figure 1C). This imaging strategy guided the selective sampling of ultrasound-guided biopsies from positive and negative LNs. In patients with SjS, cervical LNs were biopsied (Figure 1D), while in patients with SSc, LNs from affected arms or legs were collected (Supplemental Figure 1 and Supplemental Table 1). In addition, biopsies of affected tissues were obtained from the same patients (salivary gland [SG] for SjS and skin for SSc).

Immunohistochemical analysis confirmed our earlier findings that salivary glands affected by SjS contained a large CD4+ T-cell infiltrate, whereas skin affected by SSc exhibited only a sparse CD4+ T-cell infiltrate (*Supplemental Figure 2A*). To confirm that FLT-PET guidance successfully identified LNs with proliferating lymphocytes, we analyzed lymphocyte retrieval from cell suspensions and examined immunohistochemical markers in tissue biopsies. In FLT-positive LNs (n=4 SSc and n=4 SjS), a higher number of total cells per biopsy and a higher fraction of lymphocytes were observed compared to FLT-negative LNs (n=2 SSc and n=2 SjS) (median yield 340,000 cells versus 105,162 cells respectively, with 66%

versus 40% lymphocytes) (Figure 1E). There was no difference in the total number of cells in FLT-positive LNs between SSc and SjS patients (Figure 1E). The number of proliferating cells, as assessed by Ki-67 immunohistochemistry, was also higher in FLT-positive compared to FLT-negative LNs (48% of Ki-67+ cells compared to 14%) and did not differ between SSc and SjS patients (Figure 1F). To determine whether cell proliferation was driven by APC-mediated T-cell and B-cell activation, we analyzed the presence of an adaptive immune response, by assessing CD21 expression, a marker for mature B-cells and follicular dendritic cells (FDCs) and by T-cell and B-cell clonality analysis. FLT-positive LNs contained an elevated number of CD21+ mature B-cells/FDCs in comparison to FLT-negative LNs (Figure 1G). Additionally, gene expression analysis revealed increased levels of MKI67 and the follicular markers CXCR5, BCL6 and CD38 in FLT-positive LNs (Figure 1H). Finally, clonality analysis demonstrated that FLT-positive LNs contained more expanded T- and B-cell clones compared to FLT-negative LNs (Figure 11). In summary, these findings indicate a more active adaptive immune response in FLT-positive LNs (active LNs) in both SSc and SiS.

Active lymph nodes of patients with SjS contain lymphocyte clusters and T helper cells providing B-cell help, and these occur less frequently in SSc

To further understand whether the differences in CD4+ T-cell infiltration observed in SiS and SSc affected tissues were linked to variations in the activation and regulation of NAg-directed immune responses within active LNs, we analyzed the type and interaction of adaptive immune cell subsets in active LNs, affected SG and skin. We first undertook a qualitative approach, using a semi-quantitative score to assess the level of T/B-cell clustering within APC rich lymphocyte areas, identified by the markers CD3, CD79A/CD20 and CD1c/CD21. In SjS affected SG we observed large and germinal center (GC)-like organized aggregates of APCs, T-cells and B-cells. In contrast, SSc affected skin contained small aggregates of APCs and T-cells, and no B-cells (Supplemental Figure 2B). Similar to SjS affected SG, active LNs of SjS patients contained large and GC-like organized aggregates of APCs, T-cells and B-cells. In contrast, in SSc active LNs T-cells, B-cells and APCs were dispersed throughout the biopsy (Figure 2A, B). These findings were confirmed by multiplex immunofluorescence staining (*Figure 2C, D*).

Since CD4+ T-cells orchestrate adaptive immune responses, providing essential help for B-cells to mature, class-switch and produce (auto)antibodies, we investigated whether differences in their presence and activation could explain the distinct structural organization between active LNs of SjS and SSc. To address this, we analyzed the T-cell populations of the same LNs using single-cell multi-omic

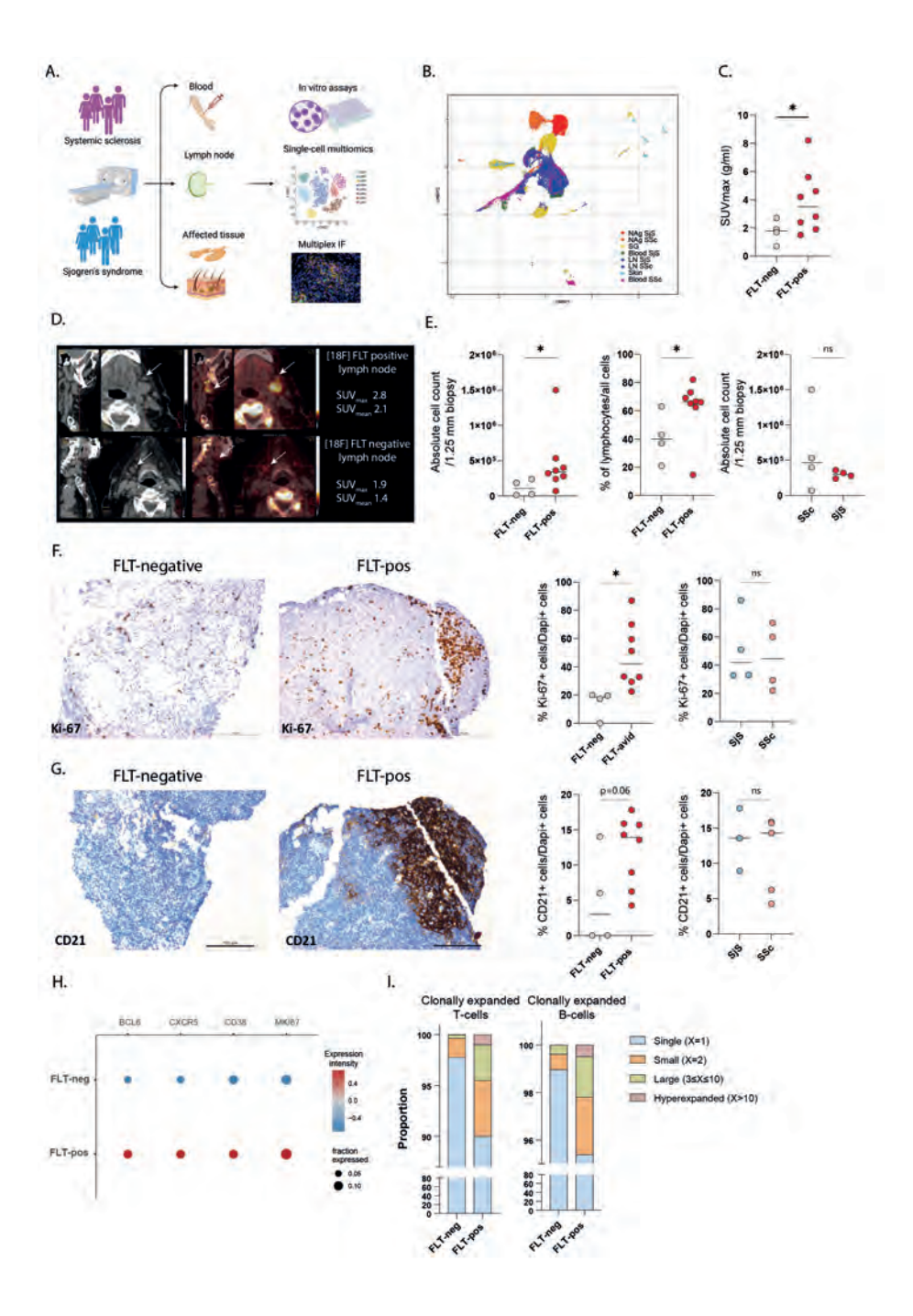


Figure 1. [18F] FLT PET scans allow identification of active lymph nodes containing clonally expanded T-cells and B-cells. (A) Overview of the experimental approach. Blood, lymph node (LN) and affected tissue (skin or salivary gland) samples from patients with SSc and SjS were isolated and processed for single-cell multimodal profiling (transcriptomics, proteomics, TCR/BCR sequencing). (B) UMAP displaying all cells recovered from SSc and SjS patients' tissues, blood and ex vivo NAg-specific T-cells. Each subpopulation is illustrated with a different color. (C) SUV_{max} values between FLT-positive and FLT-negative LNs. (D) Representative [18F] FLT PET/CT scan from the cervical area of a patient with SiS (n=4) exhibit with arrows detection, among the salivary gland draining lymph nodes, of a FLTpositive and a FLT-negative LN based on high or low [18F] FLT signal, represented with SUV_{mean} and SUV___ values (g/ml). (E) Absolute cell counts and % of CD45+ lymphocytes among all cells of each biopsy comparing FLT-positive versus FLT-negative LNs and FLT-positive LNs of patients with SiS versus SSc. Representative images of KI-67 (F) and CD21 (G) immunohistochemistry staining of FLT-negative and FLT-positive LN of a patient with SjS, accompanied by quantification of KI-67+ or CD21+ cells (n=4 FLT-negative, 4 FLT-positive SSc, 4 FLT-positive SiS LNs). (H) 2D dot plots comparing the gene expression of the depicted genes between FLT-positive and FLT-negative LNs. (I) Comparison of the proportion of clonally expanded T-cells and B-cells between FLT-negative/positive LNs. Each symbol and each horizontal line in (C), (E), (F), (G) represents one donor and mean value respectively. Statistical differences: two-tailed unpaired t test with significance set at *p<0.05.

analysis. We performed unsupervised whole transcriptome clustering of isolated T-cells, focusing on CD4+ T-cell populations (*Figure 3A*). CD4+ T-cell clusters were identified based on differentially expressed genes (DEGs), differentially expressed proteins (DEPs), canonical subset markers, and joint density of multiple features (Figure 3B, C and Supplemental Figure 3A, B). This analysis identified eight distinct CD4+ T-cell clusters: naïve, central memory (CM), regulatory (Tregs), TRAIL+ interferon-stimulated genes (TRAIL+ CD4 ISG), CD4 helper (a mix of Th2 and Th17 cells), activated (CD4 activ), T-cell helper providing B-cell help (a mix of extrafollicular helper and follicular helper T-cells [Tfh/ef]) and a small cluster of unknown (CD4 uk) identity. Compared to non-active LNs, SjS active LNs contained a significantly lower amount of naïve CD4+ T-cells and a higher percentage of effector CD4+ T-cells, including increased T-helper, T-fh/ef, CD4+ activ and TRAIL+ CD4+ ISG T-cells (Figure 3D). In contrast, SSc active LNs did not significantly differ in the amount of naive T-cells compared to the quiescent ones, and CD4+ T- cells mainly consisted of regulatory T-cells and TRAIL+ CD4+ ISG T-cells (Figure 3D). Finally, we analyzed the expanded TCR clones in each CD4+ T-cell cluster. T-helper cells and Tfh/ef exhibited the highest proportion of expanded T-cell clones, and their clonal expansion was more pronounced in SjS than in SSc (Figure 3E). Collectively, these results indicate that active LNs in both diseases show signs of an active memory CD4+ T-cell response. Only SiS active LNs harbor a B-cell helper T-cell response, consistent with the observed histological APC/B/T-cell interaction clusters in SjS. In contrast, SSc active LNs are characterized by an expanded TRAIL+ CD4+ ISG T-cell population, without an increased Treg/Teff ratio (Supplemental Figure 3C), which suggests that the TRAIL+ T-cells may exert a regulatory function that counteracts a CD4+ T-cell effector response, or that these concern effector CD4+ T-cells that are activated via an alternative pathway.

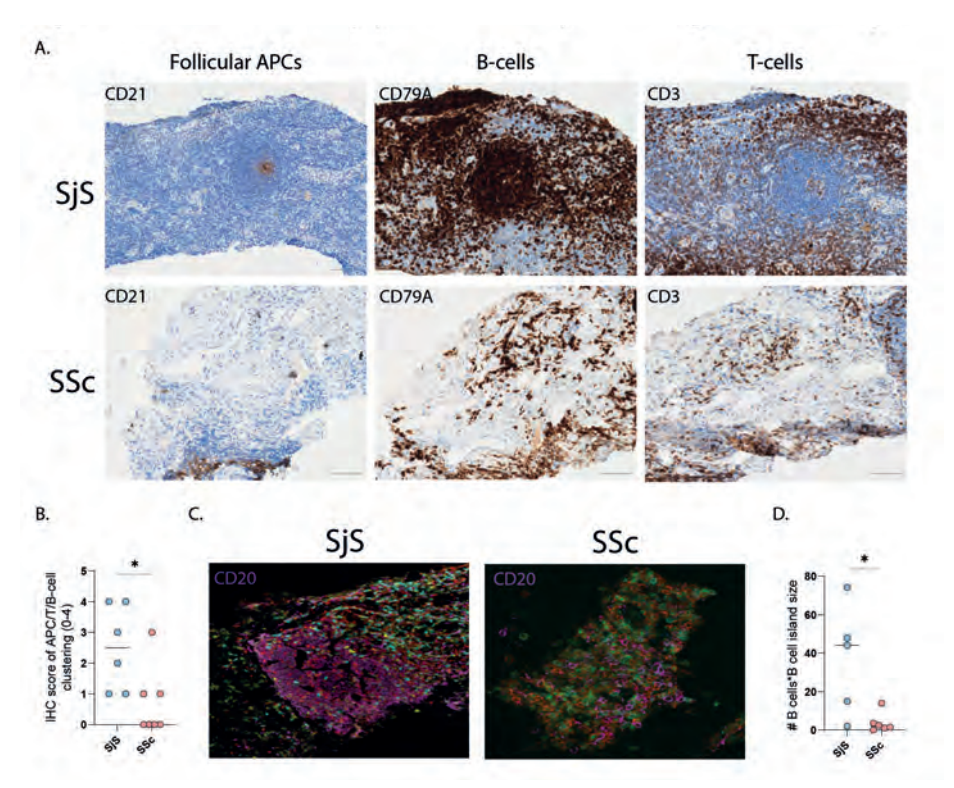


Figure 2. APC-T-B-cell interaction in SSc lymph nodes is limited compared to more organized and robust in SjS. (**A**) IHC stainings of representative SjS and SSc active LNs (n=12) for CD21, CD79A and CD3. Scale bars are 100 μm. (**B**) Semi-quantitative IHC score (values range from 0-4) for the quantification of the level of APC-T-B-cell clustering (n=6 SjS, n=7 SSc). (**C**) Representative Immunofluorescent images and (**D**) quantification of the number of B-cell islands multiplied by total B-cells per biopsy in SjS (n=5) and SSc (n=6) patients' active LNs. The following markers were used for the immunofluorescent staining; CD20 (purple), CD3 (red), CD56 (yellow), FOXP3 (green), CD8 (cyan). Each symbol and each horizontal line in (B), (D) represents one donor and mean value respectively. Statistical differences: two-tailed unpaired t test with significance set at *p<0.05.

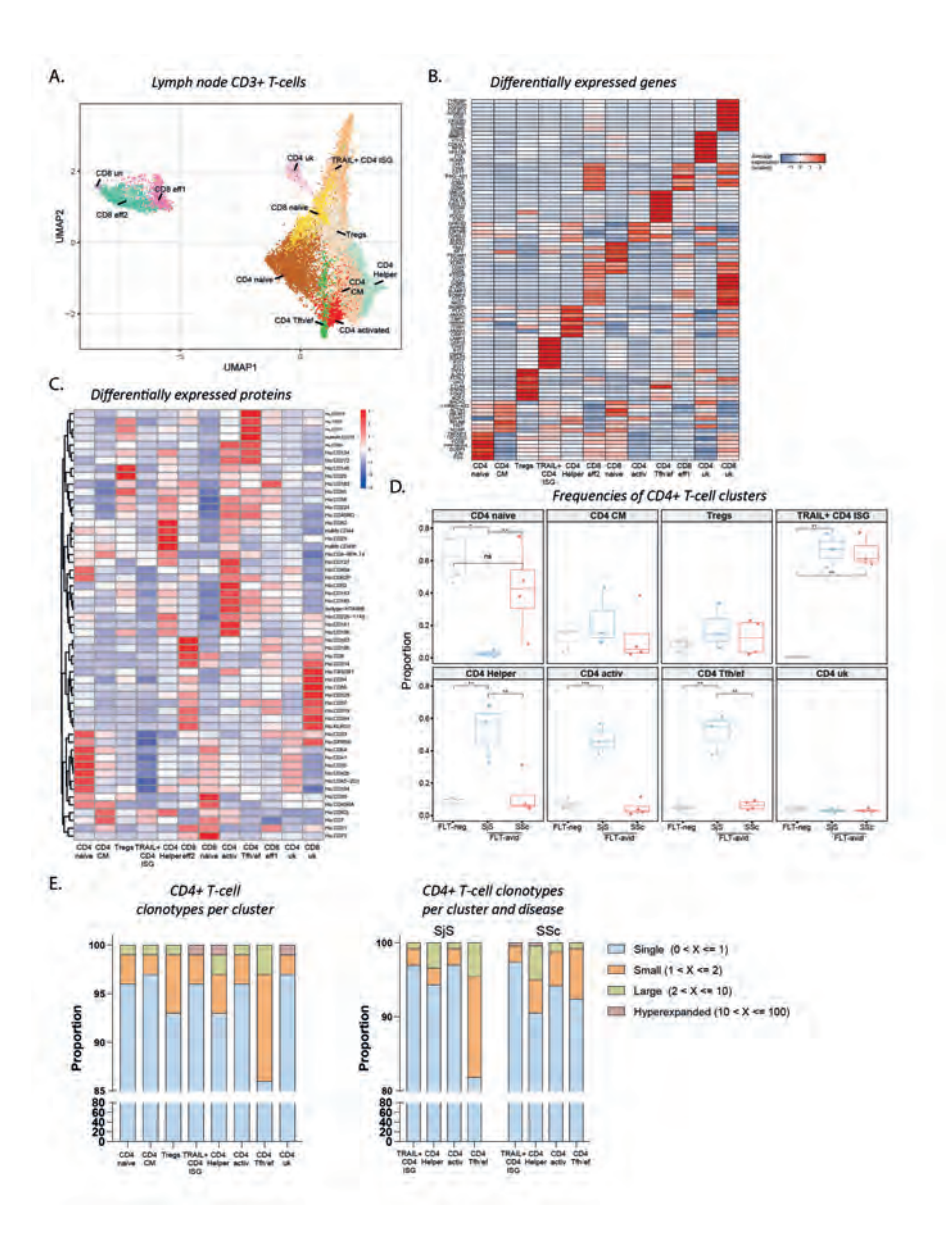


Figure 3. Single-cell analysis of active LNs reveals a more evident B helper CD4+ T-cell response in SjS compared to SSc. (A) UMAP plot of CD3+ T-cell subsets from patients' FLT negative and positive LNs. (B) Heatmap illustrating the top differentially expressed genes in each distinguished T-cell cluster. (C) Heatmap exhibiting the top differentially expressed proteins for each transcriptionally distinct T-cell cluster. (D) Frequencies of CD4+ T-cell clusters in the FLT negative (n=4) compared to FLT positive LNs of patients with SjS (n=4) and SSc (n=4). Values are presented as the percentage variation in cell counts. Statistical analysis was conducted using the Wilcoxon test, with correction for multiple comparisons, *q<0.05, **q<0.01, ***q<0.001. (E) Distribution (proportion) of clonally expanded T-cells based on clonotype size for each CD4+ T-cell cluster. For the clusters of TRAIL+CD4 ISG, CD4 Helper, CD4 activ and Tfh/ef clonal distribution between SjS and SSc is also illustrated to the right.

To understand the NAg-specificity of the observed T-cell responses, we analyzed CD4+ T-cells specific to the NAgs Ro60/La in SjS and Scl70 in SSc patients. Over the past decades, AIM assays have been used for high throughput detection of antigen-specific T-cells, primarily in the context of infectious diseases (31), and more recently for autoimmune diseases (32-34). Here, we validated the antigen-specificity of this assay for SjS and SSc NAgs, using HLA tetramers, MHC II blocking, APC and metabolism experiments (**Supplemental Figure 4, 5, 6** and methods for detailed description). Importantly, we also analyzed single-cell RNA and TCR sequencing of sorted AIM+ NAg-specific T-cells along with paired affected tissues and LNs, to validate that the AIM-assay enriched for memory antigen-specific T-cell clones shared between blood, LNs and affected tissues (Figure 5A, B).

Subsequently, we applied this assay to detect antigen-specific T-cells in the blood of SSc (n=45) and SjS (n=38) patients and healthy controls (n=30) (*Figure 4A, B*). In SjS blood, we observed a significantly larger amount (on average 20 times higher) of Ro60/La-specific T-cells compared to Scl70-specific T-cells in SSc blood (*Figure 4C*). Furthermore, Ro60/La-specific T-cells in SjS patients exhibited an elevated CD4+/CD8+ T-cell ratio compared to Scl70-specific T-cells in SSc (*Figure 4E*). Finally, Ro60/La-specific CD4+ T-cells in SjS exhibited elevated expression of the B-cell help markers CD40L, IL21 and were enriched for a CXCR5+PD-1+ICOS+ Tfh phenotype (*Figure 4F, G*). Ro60/La-specific T-cells were also detected in higher numbers in healthy controls compared to Scl70-specific T-cells, but these were predominantly naive compared to predominantly memory in SjS (*Figure 4D*). Taken together, circulating NAg-specific CD4+ T-cells are more prevalent and show more signs of B-cell help in SjS compared to SSc.

NAg-specific CD4+ T-cells in SjS active lymph nodes, affected tissues and blood display robust effector functions, whereas in SSc, they display regulatory functions

To extend the analysis of the activation and regulation of NAg-specific CD4+ T-cells beyond patients' blood to include affected tissues in SjS and SSc patients, we performed an integrated analysis using single-cell RNA sequencing and TCR sequencing of T-cell clones shared between AlM-enriched NAg-specific T-cells from blood, active LNs, and affected tissues. The AlM assay has been applied to various conditions, but the extent to which circulating AlM+ antigen-specific T-cells form migrating parts of tissue-resident T-cell clones has not yet been analyzed. To

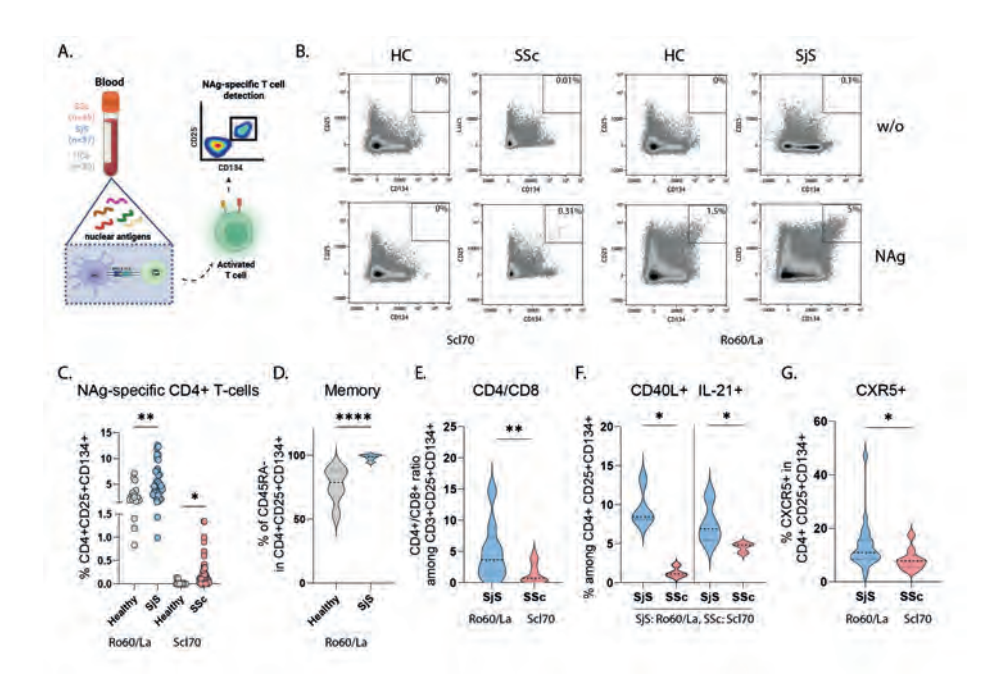


Figure 4. Circulating NAq-specific CD4+ T-cells exhibit elevated B-cell help activation in SjS compared to SSc. (A) Experimental workflow for the detection and characterization of NAg-specific T-cells in patients with SiS and SSc and healthy donors (HCs). (B) Representative flow cytometry plots exhibiting the detection of NAq-specific CD4+ T-cells identified as CD4+CD25+CD134+ after 16 hours of incubation of PBMCs with or without antigen (w/o) NAgs (ScI70 in 45 SSc patients, Ro60/La in 37 SjS). (C) Frequencies of NAg-specific T-cells in HCs (n=30), and patients with SjS (n=37) and SSc (n=45). (D) Percentage of memory (CD45RA-) CD4+ T-cells within NAq-specific CD4+CD25+CD134+ T-cells in HCs (n=6) and SjS patients (n=17). (E) Ratio of CD4+/CD8+ NAg-specific T-cells between SjS (n=37) and SSc (n=45). Violin plots representing the proportion of NAg-specific T-cells expressing (F) CD40L and IL-21 in NAq-specific CD4+ T cells (detected with the AIM assay as CD4+CD25+CD134+) were measured with flow cytometry on patients PBMCs that were stimulated with NAgs (ScI70 in SSc, Ro60/La in SjS); SjS (n=6/4) and SSc (n=6/4) and (G) CXCR5+PD-1+ICOS+ (Tfh) NAg-specific T cells; SjS (n=20) vs SSc (n=9). Each symbol and each horizontal line in (C) represent one donor and mean value respectively. Statistical differences: two-tailed unpaired t test with significance set at *p<0.05, **p<0.01, ****p<0.0001.

investigate this, we performed single-cell transcriptomics on FACs-sorted NAgspecific T-cells enriched from the blood of patients (n=5 SSc and n=4 SjS) using the AIM assay. This was paired with single-cell transcriptomics of blood, LN, and affected tissue T-cells from the same patients (Figure 5A). Overall, we found that 18% (2,300/13,000 cells) of AIM-enriched NAg-specific T-cells were part of clones that were also detected in tissue biopsies. When compared to blood T-cells, AIM enriched NAg-specific T-cell clones exhibited higher clonal expansion and the number of expanded AIM enriched NAg-specific T-cell clones that were also detected in LN (SjS; 104, SSC; 38) and affected tissue biopsies (SjS SG; 42, SSc skin; 3) was also larger compared to the number of shared expanded clones between T-cells in blood and LNs (SjS; 14, SSc; 8), and between T-cells in blood and affected tissues (SjS SG; 10, SSc skin; 1) (*Figure 5B*). Almost all NAg-specific CD4+ T-cells were memory cells (SjS; 99%, SSc; 99%) compared to ~48% memory T-cells in peripheral blood (SjS; 44%, SSc; 51%) (*Figure 5C*). Similarly, all NAg-specific CD4+ T-cell clones detected in LNs/affected tissues were memory T-cells, compared to 41% of all T-cells in LN being memory T-cells (SjS; 41%, SSc; 41%) and 82% in affected tissues (SjS SG; 72%, SSc skin; 91%) (*Figure 5D*). Together, this indicates that our approach was successful in enriching for tissue expanded memory T-cell clones.

To examine if the difference in CD4+ T-cell infiltration in affected tissues of SiS and SSc is mirrored by differences in the distribution, activation and regulation of NAgdirected CD4+ T-cells, we examined NAg-specific CD4+ T-cells in tissues, active LNs and blood. NAg-specific CD4+ T-cells were highly present in SjS SG, but none were found in SSc affected skin. Similarly, NAg-specific CD4+ T-cells were more abundant in SiS blood and active LNs, compared to NAg-specific CD4+ T-cells in SSc blood and LNs (Figure 5C). In SiS, the affected SG, active LNs and blood contained a large fraction of effector NAg-specific CD4+ T-cells, that displayed a diverse CD4 helper phenotype that included Tfh, Tef, Th2, and Th17 cells (Figure 5E, F, and Supplemental Figure 7). In contrast, NAg-specific CD4+ T-cell clones in SSc LNs and blood predominantly exhibited a central memory (CM), TRAIL+ ISG, and Treg phenotype (*Figure 5F*). The Tregs in SSc partly expressed markers of follicular Tregs (FOXP3 and BCL6) and partly of extrafollicular Tregs (FOXP3 and PRDM1). Finally, the ratio of NAq-specific CD4+ Tregs versus effector CD4+ T-cells was higher in SSc compared to SjS. Collectively, our findings show that in SjS patients, NAg-specific CD4+ T-cell responses are shared between blood, LNs and affected tissues, and mediate relatively robust follicular and extrafollicular humoral effector responses. In contrast, SSc is characterized by NAg-specific CD4+ T-cells exerting a regulatory, and TRAIL+ ISG directed response, coinciding with the generation of a weak CD4+ T-cell effector response and fewer NAq-specific CD4+ T-cells that migrate to blood and affected tissues.

A distinct T helper subtype of CD4+ TRAIL+ ISG T-cells is uniquely present in the extrafollicular areas of patients' active lymph nodes

Hypothetically, the absence of NAg-specific CD4+ effector T-cell subsets in SSc active LNs and affected skin is caused by counter-regulation by regulatory T-cells in active LNs. However, we only observed limited differences in NAg-specific Treg numbers in active LNs of SjS and SSc patients (*Figure 3D, 5F*). Of interest, our single-cell multimodal analysis did identify TRAIL+ CD4+ ISG T-cells that were

uniquely present in the active LNs of SSc and SjS patients. This cluster was relatively enriched in NAg-specific CD4+ T-cells in SSc patients (Figure 3D, 5F). Therefore, we questioned whether this subset exerted immunoregulatory or non-canonical effector functions. We capitalized on the presence of these cells in both diseases, which allowed us to analyze the inhibition of their effect in the context of a relatively robust (SjS) versus a relatively weak (SSc) effector humoral response.

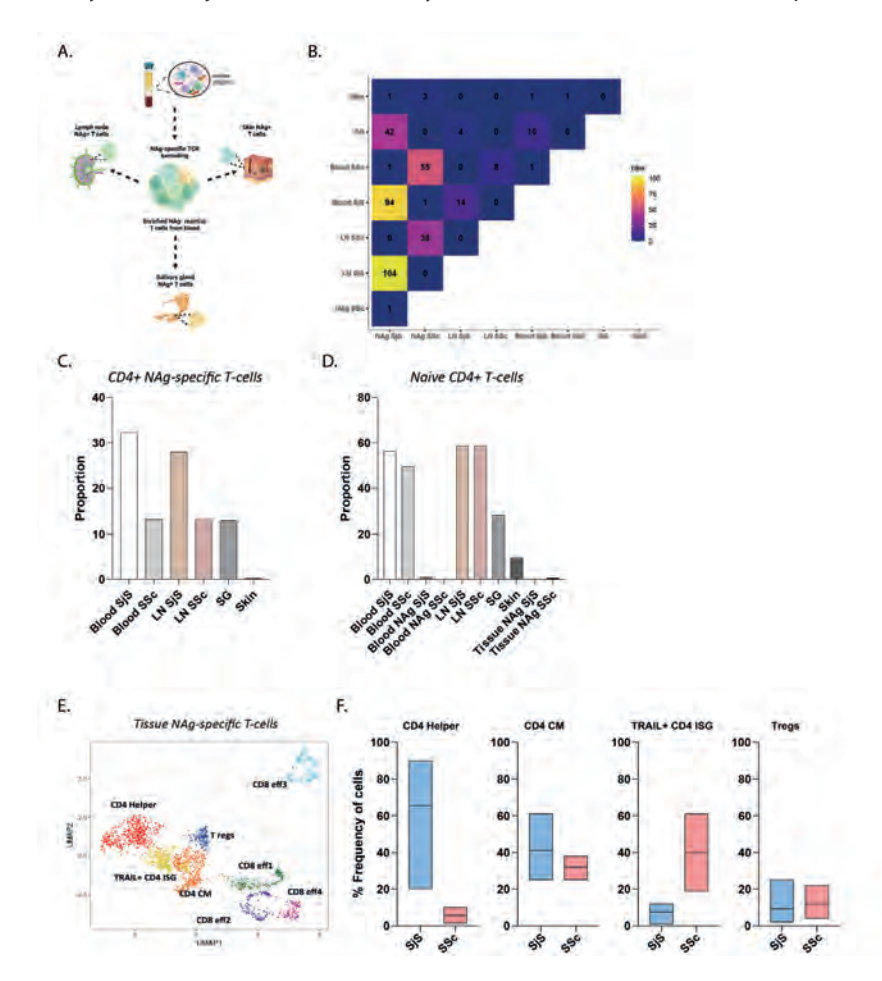


Figure 5. NAg-specific CD4+ T-cells in SjS active lymph nodes and SGs exhibit robust effector functions, whereas in SSc LNs, they display regulatory phenotypes. (A) Experimental workflow exhibiting the method used to detect and characterize NAg-specific T-cells in patients' active LNs (n=4 SSc, n=4 SjS), skin (n=2) and salivary glands (n=3). (B) Morisita overlap quantification of the number of matching T-cell lineages among different tissues and between blood enriched NAg-specific T-cells and T-cells in tissues. (C, D) Tissue distribution of naïve CD4+ NAq-specific T-cells and naïve CD4+ T-cells among patients' blood and tissues. (E) UMAP of NAg-specific CD3+ T-cells in patients' active LNs and affected tissues accompanied by (F) Cell frequency of NAg-specific CD4+ subpopulations between SjS and SSc.

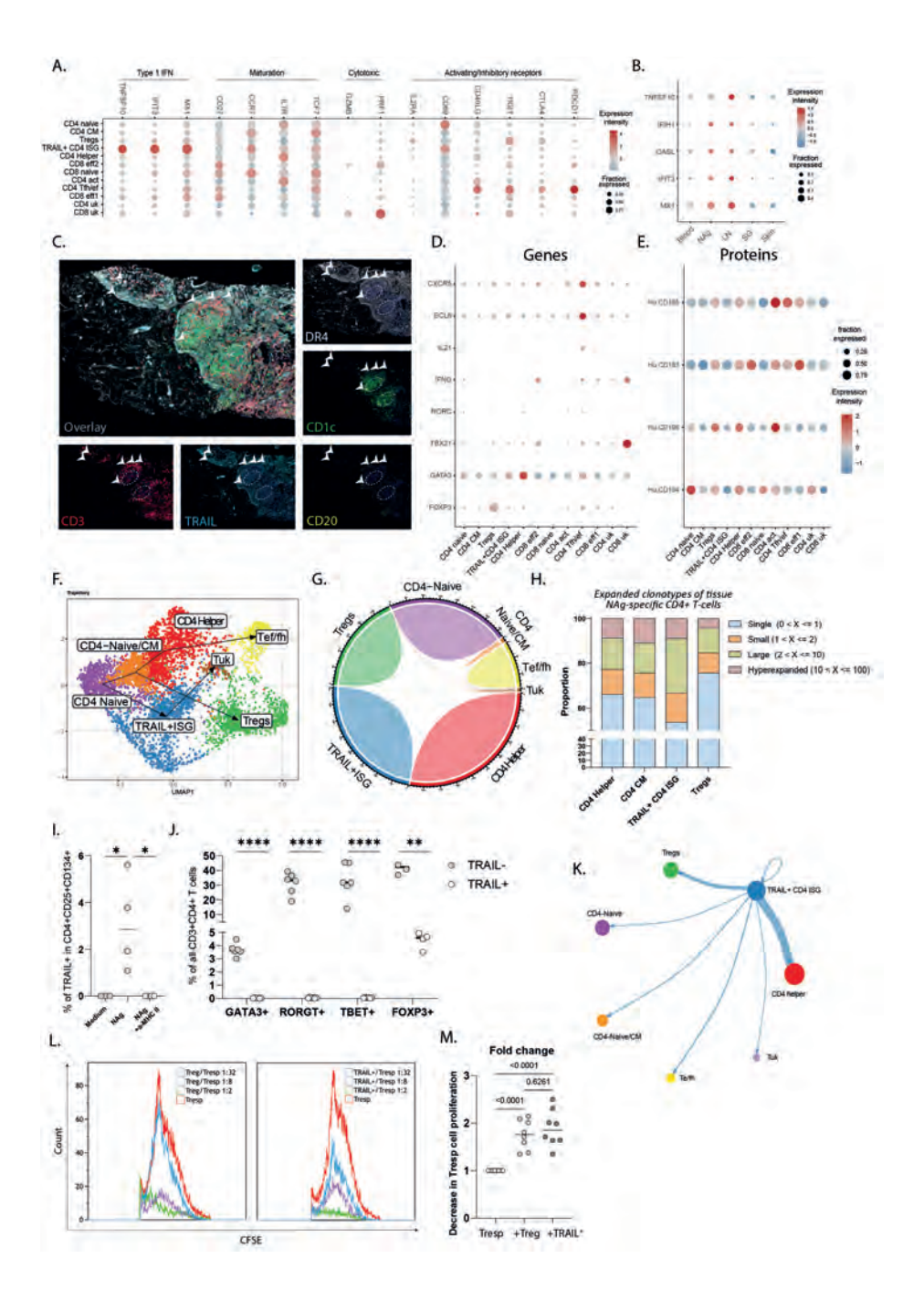


Figure 6. CD4+ TRAIL+ ISG T-cells render a distinct naive-like T helper subtype that is uniquely present in extrafollicular sites of patients' reactive LNs. 2D dot plots comparing gene expression of selected genes (A) per cluster (B) between blood, active LNs, affected tissues and NAg-specific T-cells. (C) Multicolor immunofluorescence staining of the depicted markers to visualize the spatial mapping of CD4+ TRAIL+ T-cells within reactive LNs. Scale bars are 100 µm. 2D dot plots comparing (D) gene and (E) protein expression of selected CD4+ T helper markers between CD4+ T-cell clusters. (F) Singlecell developmental trajectories of LN CD4+ T-cell clusters. (G) Cord diagram showing the TCR clonal overlap between the LN CD4+T-cell clusters. (H) Proportion of clonal lineages by clonal size within each cluster of NAq-specific CD4+ T-cells. (I) Proportion of NAq-specific CD4+CD25+CD134+ T-cells (n=4) expressing TRAIL after 16-hour incubation with Ro60/La antigens. (J) Flow cytometric quantification of GATA3, RORGT, TBET and FOXP3 expression between TRAIL- and TRAIL+ CD4+ T-cells (n=4/6). (K) Graphical representation of cell-cell edges (interactions) of TRAIL+ ISG CD4+ T cells with the rest CD4+ T-cell clusters, exhibiting high likelihood and specificity of interaction of TRAIL+ ISG CD4+ T cells with CD4 effector cells (thick blue line). (L) Overlay histogram flow cytometry plots illustrating proliferation of CD4 effector responsive cells (Tresp) that were cultured alone or in the presence of either regulatory T-cells (Tregs) or TRAIL+ CD4+ T-cells at indicated ratios (Treg/TRAIL+ CD4+ T: Tresp). Proliferation was measured with CFSE fluorescence emission and quantified as the fold change of the decrease in Tresp proliferation for all included donors (n=8) in (M). Each symbol and each horizontal line in (I), (J) and (M) represent one donor and mean value respectively. Statistical differences: in (I) ordinary one-way ANOVA, in (J) two-tailed paired t-test, *p<0.05, **p<0.01, ****p<0.0001.

To gain more insight into the identity of TRAIL+ CD4+ ISG T-cells, we analyzed their transcriptome, proteome and tissue localization using single-cell RNA sequencing, CITE-seg and multiplex immunofluorescence. For functional validation, we performed in vitro assays. TRAIL+ CD4+ T-cells have been studied for their dual roles in inducing cell death and regulating immune responses via binding of TRAIL to its receptors DR4 and DR5. CD4+ T-cells with ISG expression have been identified in single-cell analyses across various conditions, including viral infections, lupus, and rheumatoid arthritis (35-39). Here, the detected CD4+TRAIL+ISG T-cells were characterized by the expression of the death receptor TRAIL (TNFSF10) and a prominent type I ISG signature, including MX1, IFIH1, OASL, and IFITs (Figure 6A, Supplemental Figure 3B). Additionally, CD4+TRAIL+ ISG T-cells expressed type 1 interferon receptors (IFNAR1/2) and intracellular double stranded RNA receptors (DDX58, DHX58 and IFIH1) but did not express genes that mediate detection of intracellular DNA (cGAS or STING) (Supplemental Figure 3B). Gene expression analysis verified higher ISG intensity in LN and AIM enriched NAg-specific CD4+ T-cells compared to blood-derived T-cells (Figure 6B), supporting their antigenspecific activation within LNs influenced by type 1 interferon and/or dsRNA. We confirmed this responsiveness by culturing CD4+ T-cells in-vitro for 24 hours in the presence of IFNa or synthetic dsRNA analogs, which induced a robust upregulation of the ISG signature (Supplemental Figure 8).

Regarding their maturation stage, these cells exhibited a naïve-like phenotype (high SELL, CCR7; moderate CD27, IL7R) without markers of cytotoxicity, T-cell activation/exhaustion or follicular localization (low CXCR5, BCL6) (*Figure 6A, Supplemental Figure 3B*). This indicates a relatively quiescent extrafollicular state. Localization studies confirmed these cells occupy extrafollicular zones in active LNs, adjacent to germinal center-like structures in SjS or scattered near DR4+ APCs in SSc (*Figure 6C, Supplemental Figure 9*). The TRAIL+ CD4+ ISG T-cell cluster in patients' LNs was transcriptionally and phenotypically distinct from Th1, Th2, Th17, Tfh, and Treg subsets, lacking apparent gene expression of TBX21, GATA3, RORC, BCL6 and FOXP3 (Figure 6D) and protein expression of CXCR3 (CD183), CXCR5 (CD185), CCR4 (CD194) and CCR6 (CD196) compared to the CD4 effector and Treg clusters (*Figure 6E*).

Pseudo-time analysis of CD4+ T-cell differentiation positioned TRAIL+ CD4+ ISGT-cells along a distinct trajectory, separate from helper and regulatory T-cells, originating from naïve CD4+ T-cells (*Figure 6F, Supplemental Figure 10A-C*). TCR clonal overlap analysis showed minimal overlap with helper subsets and no overlap with Tregs, supporting their unique identity (*Figure 6G*). Differential dynamic gene expression analysis highlighted type I IFN-stimulation responsive genes (STAT1, MX1, ISG15), T-cell activation markers (CD69), and TCR signaling genes (LY6E) as key contributors to the transition of CD4+ naïve T-cells to the TRAIL+ ISG phenotype (*Supplemental Figure 10D*). In line with an antigen-specific induction, among tissue NAg-specific CD4+ T-cell clusters, TRAIL+ CD4+ ISG T-cells exhibited the largest clonal expansion compared to other CD4+ T-cell subsets (*Figure 6H*). In summary, CD4+TRAIL+ ISG T-cells exhibit characteristics of a uniquely expanded CD4+ T-cell subset with distinct extrafollicular lymph node localization.

TRAIL+ CD4+ ISG T-cells +are antigen-specific and can be induced in vitro from naïve T-cells by type 1 IFN and TCR stimulation

To better understand if TRAIL+ CD4+ ISG T-cells have a unique ontogeny we analyzed their induction in vitro. In the blood of patients, TRAIL expression was restricted to antigen-pulsed NAg-specific CD4+ T-cells and was absent after MHC class II blocking, confirming an antigen specific nature (*Figure 6I*). To study their induction, we stimulated and cultured naïve CD4+ T-cells, from both healthy controls and patients, with anti-CD3/CD28 in the presence of IL-2 (Th0) and IFNα (ISG T) to mimic type I interferon signaling. Neutralizing antibodies against IFNγ, IL-4, and IL-17 were added in the ISG T condition to prevent skewing towards classical Th1, Th2, or Th17 subsets. After five days, in the ISG T condition compared to Th0 condition, approximately 45% of the cells (n=4) displayed elevated expression of TRAIL (*Supplemental Figure 11A*)

and significant induction of an ISG signature (MX1, IFIH1, DDX58) (Supplemental Figure 11B) was observed in all donors (Supplemental Figure 11C).

TRAIL+ CD4+ ISG T-cells exhibit a unique immunoregulatory phenotype in autoreactive LNs

To study the potential effector functions of these cells, we analyzed the expression of CD4+ T-cell master transcription factors and effector molecules in the blood of healthy donors. Flow cytometry showed that TRAIL+ CD4+ T-cells, in contrast to TRAIL-CD4+ T-cells, lacked GATA3, RORGT, and T-BET expression. Interestingly, TRAIL+ CD4+ T-cells expressed FOXP3 as the solitary CD4+ T helper master transcription factor, although the abundance of FOXP3 expression was 10 times lower than in TRAIL- CD4+ T-cells (T-cell population including Tregs) (Figure 6J). When cultured in vitro in the presence of anti-CD3/CD28 and IFNa, compared to other effector T-cell subsets, CD4+TRAIL+ ISG T-cells displayed reduced IFNy production and increased expression of IL-10 and TRAIL (Supplemental Figure 11B). Cell-chat analysis of our scRNAseq T-cell dataset showed that TRAIL+ CD4+ T-cells exhibited a robust interaction with CD4+ effector T cells (Figure 6K). To investigate a potential immunoregulatory role, we compared the suppressive capacity of TRAIL+ CD4+ T-cells and conventional Tregs and we found that TRAIL+CD4+ T-cells directly suppress CD4+ effector T cell proliferation to a similar extent as conventional Tregs (Figure 6L, M).

To gain insight on function of TRAIL+ CD4+ T-cells in physiological settings we merged our scRNAseq T-cell dataset with a public dataset of T-cells from tonsils. Notably, both the frequency of TRAIL*CD4* T cells and the intensity of their ISG signature are elevated in lymph nodes compared to tonsils (22% vs 1.2%) (Supplemental Figure 12A-D). In SSc reactive lymph nodes, TRAIL+ CD4+ T-cells were significantly clonally expanded compared to SjS reactive LNs and tonsils (Supplemental Figure 12E). Furthermore, lymph node TRAIL+ CD4+ ISG T-cells expressed genes linked to immunoregulatory pathways (Supplemental Figure 12F, G), whereas in tonsils, their gene profile was more infection-related—underscoring their distinct expansion and distinct functional role in autoreactive lymph nodes. Together with their in vivo enrichment in active LNs and autoreactive features, this suggests that TRAIL+ CD4+ ISG+ T-cells may exert an immunoregulatory role in autoimmune CTDs within patients' reactive lymph nodes.

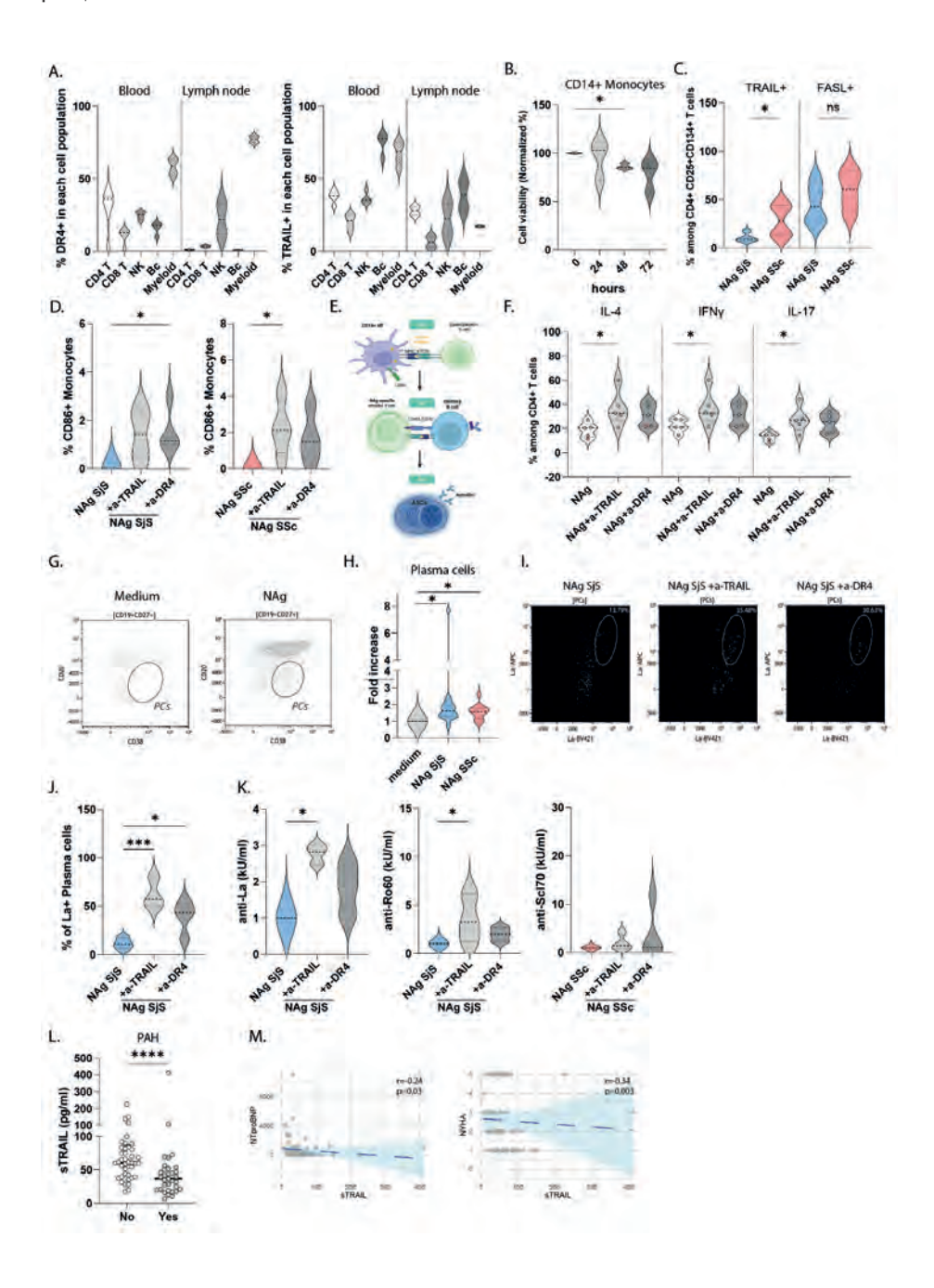


Figure 7. NAg-specific CD4+ TRAIL+ ISG T-cells restrict plasma cell formation by suppressing APC mediated autoreactive humoral responses. (A) Expression of TRAIL and TRAILR1 in blood/ LN immune cells. (B) Normalized cell viability of CD14+ monocytes incubated with soluble TRAIL. (C) Proportion of SjS (n=6) and SSc (n=6) NAg-specific T-cells expressing TRAIL and FASL. (D) Percentage of CD86+ CD14+ monocytes under stimulation (24 hours) of SiS and SSC PBMCs (n=4 each group). (E) Schematic representation of the in vitro mechanistic experiments unraveling the potential role of NAg-specific CD4+ TRAIL+ T-cells towards modulating APC/T/B cell interactions. (F) Proportion of CD4+ memory T-cells expressing IL-4, IFNy, IL-17. (G) Representative plots (n=10) illustrating in vitro generation of plasma cells that are further quantified in (H) as fold change increase on % of CD19+CD27+CD20^{low}CD38+ plasma cells/all live cells. (I) Flow cytometry plots of one representative experiment (n=4) showing detection of La-specific plasma cells in the absence/presence of TRAIL/TRAILR blockade. (J) Percentage of La-specific plasma cells among live plasma cells (n=4). (K) Quantification of autoantibody (anti-La/Ro60/ScI70) production in cell culture supernatants (n=6 per condition). (L) Quantification of soluble TRAIL in serum of SSc patients with (n=33) and without PAH (n=41). (M) Spearman correlation of soluble TRAIL with the clinical parameters N-terminal prohormone of brain natriuretic peptide (NTproBNP) and New York heart association functional class (NYHA). Statistics: in (A) two-tailed unpaired t test with significance set at *p<0.05; (C) RM oneway ANOVA, with Dunnett's multiple comparisons test, *p<0.05; in (D), (H), (J), (K) ordinary one-way ANOVA, with Tukey's multiple comparisons test, *p<0.05, ***p<0.001; in (F) non-parametric Kruskal-Wallis test, *p<0.05; in (L) two-tailed Mann-Whitney U test, ****p<0.0001 and each dot represents one donor (n=33 SSc patients with PAH and n=41 SSc patients without PAH).

APC dependent NAg-specific CD4+ T-cell mediated plasma cell generation is restricted by the TRAIL-DR4 axis

Tumor necrosis factor (TNF)-related apoptosis-inducing ligand (TRAIL) has been found to regulate immune responses through its death receptors, DR4 and DR5, and decoy receptors, DcR1 and DcR2 (40). In most studies, TRAIL induces apoptosis via DR4/5. However, target cells can be rescued from TRAIL-induced apoptosis by concurrent signaling mechanisms, such as CD40-CD40L, or by expressing DcR1/2 (41). It is less clear if TRAIL can also exert non-killing immunoregulatory effects. To better understand the role of TRAIL+ CD4+ ISG T-cells in SjS and SSc affected tissue pathology, we analyzed expression of TRAIL and its receptor DR4 on T-cells and other immune cell populations. In blood and LN, TRAIL was predominantly expressed by CD4+ T-cells, as well as by B-cells and monocytes, while its receptor DR4, was widely expressed on professional APCs (Figure 7A). These patterns suggested that TRAIL+ CD4+ T-cells might primarily interact directly with APCs. Supporting this hypothesis, TRAIL+ T-cells were not observed in affected tissues, but selectively found in patients' active LNs, in close proximity to DR4+ APCs, indicating potential cell-cell interactions (Supplemental Figure 9). Incubation of primary monocytes with soluble TRAIL reduced their viability by approximately 20% (Figure 7B), suggesting they are at least partially sensitive to TRAIL-DR4 mediated cell death.

As mentioned above, the presence of CD4+ TRAIL+ ISG T-cells was relatively increased in SSc blood and active LNs compared to SjS. Consistent with this, we observed elevated TRAIL expression in NAg-specific CD4+ T-cells in blood from SSc patients, while the expression of the death receptor ligand FASL did not differ (*Figure 7C*). In contrast, CD40L expression was increased in SjS NAg-specific CD4+ T-cells (*Figure 4F*). Along with a stronger follicular and extrafollicular T-cell response in SjS and the lack of follicular structures in SSc compared to SjS, these observations suggest that TRAIL+ CD4+ ISG T-cells might counteract CD40-CD40L—mediated GC-like interactions.

To validate such a potential involvement of the TRAIL-DR4 axis in NAg directed immune responses, NAg-stimulated PBMCs were cultured with or without TRAIL/DR4 blockade. TRAIL inhibition resulted in enhanced monocyte activation, marked by elevated CD86 expression (*Figure 7D*), confirming that TRAIL directly suppresses APC activation. Further co-culture experiments (*Figure 7E*) demonstrated that TRAIL blockade increased the number of NAg-specific IL-4, IL-17 and IFNy producing T-cells (*Figure 7F*). Finally, TRAIL/TRAIL receptor blockade significantly increased NAg-specific plasma cell formation (*Figure 7G, H*) and anti-nuclear antibody production (*Figure 7I, J, K*). The induction of autoreactive T-cell and B-cell responses was less pronounced in SSc compared to SjS, likely because of a relative lack of effector cells in SSc. These findings suggest that TRAIL may play a regulatory role in autoimmune CTD by suppressing APC activation and limiting generation of effector CD4+ T-cells and autoreactive plasma cells.

Clinically, serum levels of soluble TRAIL were significantly reduced in SSc patients with a disease course complicated by the development of severe vascular involvement, manifesting as pulmonary arterial hypertension (PAH), compared to those with less severe disease (*Figure 7L*). Additionally, systemic TRAIL concentration was negatively correlated with clinical parameters reflective of disease severity such as N-terminal prohormone of brain natriuretic peptide (NTproBNP) and New York heart association functional class (NYHA) (*Figure 7M*). Collectively, these findings suggest a protective role for TRAIL by restricting autoreactive T-cell and B-cell mediated disease severity.

Discussion

Antigen-specific CD4+ T-cell responses are propagated from affected tissues and locoregional active LNs. They orchestrate infection resolution and cancer targeting (42),

but are considered to cause autoimmune pathology in CTDs (43). The efficacy of autologous stem cell transplantation and anti-CD19 CAR T-cell therapy in treating autoimmune CTDs highlights the need to eliminate autoreactive responses (44, 45). However, poor understanding of mechanisms of immunological disease activity in CTDs hinder the development of safer, more personalized tolerogenic therapies. Here, we demonstrate that the contrast between limited CD4+ T-cell infiltration with fibrosis in SSc and extensive CD4+ T-cell infiltration with tissue destruction in SjS coincides with differences in autoreactive CD4+ T-cell activation and regulation within active I Ns.

Phenotypic and functional characterization of autoreactive responses in affected tissues and active LNs has been challenging due to difficulties in isolating these rare cell populations. Therefore, autoreactive T-cells have been extensively studied in patients' blood limiting insights on the systemic and local function of these cells. Here, [18F] FLT PET scans were used to detect active locoregional LNs and affected tissues, potentially enriched for autoreactive T-cells. We found that the [18F] FLTpositive LNs contained a higher number of proliferating immune cells compared to the [18F] FLT-negative ones, with enhanced formation of GC-like structures and clonal expansion of T-cells and B-cells. These findings align with previous studies in patients with melanoma and head and neck carcinomas (30, 46) suggesting that [18F] FLT PET scan may effectively sample active LNs enriched with disease-involved proliferating (likely autoreactive) immune cells.

Combining [18F] FLT-PET scans with multiplex immunohistochemistry, singlecell RNA sequencing, and NAg-specific T-cell activation assays, we found that SjS patients exhibit robust APC, B-cell, and T-cell interactions forming germinal centerlike structures in active LNs, resulting in broad autoreactive T-cell responses and extensive APC/CD4+ T-cell/B-cell aggregates in inflamed SGs. In contrast, SSc shows limited APC/T/B-cell interactions, partly due to extrafollicular NAq-specific CD4+ TRAIL+ ISG T-cells with immunoregulatory functions that restrict proliferation of effector CD4+ T-cells, generation of antibody-producing plasma cells, APC activation, and effector CD4+ T-cell-mediated B-cell help. This observation was further reflected in the elevated frequency of both follicular and extrafollicular T-cell subsets providing B-cell help in SjS compared to SSc. This noticeable observation may be explained by the strength of the innate immune response, which can trigger abnormal presentation of autoantigens, or by the inherent properties of the autoantigens themselves (47)—particularly Ro/SSA and La/SSB, which are highly immunogenic (48) and widely expressed in epithelial tissues. These factors may collectively drive persistent B-cell activation and promote the formation of tertiary lymphoid structures (49). Additionally, SSc patients displayed a modestly increased NAg-specific CD4+ Treg/effector cell ratio in active LNs and blood, consistent with previous findings of elevated Tregs in SSc blood with uncertain suppressive function (50, 51). These results align with studies in NOD mice showing that regulatory T-cell activity influences follicular versus extrafollicular humoral responses (23, 52) and with our earlier findings of increased skin-infiltrating CD8+ T-cells but not CD4+ T-cells in 135 SSc patients (9).

In contrast to the longstanding belief that autoreactive CD4+ T-cells primarily drive tissue damage in autoimmunity, our findings reveal distinct pathogenic and protective NAq-specific CD4+ T-cell responses across CTDs. In SiS, expanded NAg-specific CD4+ T-cells providing B-cell help at follicular and extrafollicular sites promote germinal center-like structures and produce high-affinity, autoreactive antibodies that drive tissue inflammation (53). However, such CD4+ T-cells were absent in SSc. Instead, we identified a novel TRAIL+ CD4+ ISG T-cell subset in SSc active LNs that likely contributes to prevention of autoimmune exacerbation by inhibiting APC activation, suppressing activation and proliferation of CD4+ effector cells and restricting antibody-producing plasma cells, possibly to counteract regulation of epitope spreading and affinity maturation. This finding is consistent with observations in SiS, where a broad range of antibody specificities is present (54), whereas in SSc, antibody diversity and titers are more limited (55). Additionally, our earlier findings indicate that tissue fibrosis in SSc is driven by profibrotic cytokine-producing cytotoxic T cells and NK cells, not pathogenic CD4+ T cells, raising the question of how pathogenic CD8+ T cells evade regulation by conventional Tregs or CD4+ TRAIL+ ISG T cells. Possibly, like professional regulatory T cells (56, 57), this novel regulatory CD4+ TRAIL+ T cell subset may have a preferential effect towards restricting autoreactive effector CD4+ rather than CD8+ T cell responses. To our knowledge, the differential effect of TRAIL on CD4+ and CD8+ effector T cells has not been adequately examined, but it has been shown that TRAIL inhibits formation of effector Th17 cells (58). In line with this hypothesis, CD4+CD25+ Tregs can suppress the function of CD4 effector T cells by upregulating TRAIL in a TRAIL/DR5 but not FAS/FASL dependent manner (59).

TRAIL is a type II transmembrane protein belonging to the TNF superfamily, closely resembling the FAS ligand. TRAIL triggers cell apoptosis by binding to its death receptors (DR4/DR5), which activates apoptosis signaling via the caspase cascade. However, primary immune cells are often resistant to TRAIL-induced death (60). The functional role of TRAIL, beyond its potential to kill cancer cells, is not well defined. CD4+ TRAIL+ T-cells have been primarily analyzed in peripheral blood and affected

tissues with vasculopathy and atherosclerosis, where they were found to contribute to disease activity by killing vascular smooth muscle cells (35-37). In these studies, no ISG gene signature in CD4+TRAIL+ T-cells was reported. In contrast, the unique and novel T-cell subset that we observed and termed CD4+ TRAIL+ ISG T-cells was primarily detected in the active LNs of SSc patients and rarely in the blood or affected tissues of patients with SSc and SjS. This subset was characterized by the combined expression of the death receptor TRAIL and a type I IFN gene signature specific to this cluster of cells. This novel CD4+ TRAIL+ ISG T-cell subset exhibits a naïve-like memory phenotype with features of autoreactivity, relative quiescence, and antigen specificity. Of interest, CD4+ ISG T-cells exhibiting antigen specificity and TCR expansion were recently described in patients with systemic lupus erythematosus (61). The ISG response program in these T-cells may have evolved as a regulatory mechanism to counteract proinflammatory autoreactive responses triggered by stromal tissue damage or viral infections that exploit APCs. As such, these cells may serve as a protective brake to control NAg-specific humoral immune responses associated with tissue damage.

SSc may feature a relative increase in these cells because of a low immunogenic autoantigen response, e.g. lacking CD40L stimulating signals, or because of a more anti-viral-like immune response. In previous work, we observed predominant activation of CD8+ T-cells and NK cells in patients with early and diffuse SSc, while in patients with late disease, complicated by PAH, we observed increased CD4+ helper T-cells in their peripheral blood (62). In our current study, we find that the latter correlates with decreased levels of soluble TRAIL in these patients. This likely suggests that a severe disease course in a subset of SSc patients may result, among other mechanisms, from the escape from a CD4+ TRAIL+ ISG T-cell regulatory response. Although, our current results do not fully prove the extent to which CD4+ TRAIL+ ISG T-cells influence the autoreactive response, their transcriptional and functional profiles provide new insights into T-cell-mediated autoimmunity, warranting further investigation into their role and therapeutic potential in animal models or in patients undergoing targeted treatment. Of note, a protective role of soluble TRAIL has been documented in animal models of other autoimmune diseases such as rheumatoid arthritis (38) diabetes type 1 (39) and autoimmune encephalomyelitis (58), but the source of secreted TRAIL and potential role of the described immunoregulatory CD4+ T-cell subset was not unveiled. Together, our findings provide evidence of disease-specific differences in activation and regulation of NAg-specific humoral immunity within active LNs of patients with CTD, related to differences in CD4+ T-cell infiltration and activation in affected tissues. This has significant implications for the development of targeted and tolerogenic therapies.

Our study comes along with some limitations. First, the study cohort of matched blood, LN and affected tissue biopsies consisted of patients with early, severe and progressive disease, limiting within patients' correlations between CD4+TRAIL+ ISG T-cells and clinical status. Secondly, although the AIM assay is commonly used to identify antigen-reactive CD4⁺ T cells, it has inherent limitations. Despite our validation efforts, including HLA-DR blocking, cytokine profiling, tetramer specificity and TCR analysis, which amongst others showed a large overlap between AIM reactive T-cells and tetramer positive T-cells, we cannot fully exclude the possibility of bystander activation, which may lead to some overestimation of antigen-specific T-cell responses. Furthermore, we did not investigate whether TRAIL blockade affects B-cell differentiation directly or indirectly. In oncological studies, it was shown that soluble TRAIL selectively induced apoptosis of germinal center-derived B-cell lymphomas (41). Future studies are needed to address this. In fact, a selective direct and/or indirect effect towards follicular and not extrafollicular B-cells may explain why in patients with SSc, where no clear GC-like formation in their active LNs was observed, anti-scl70 autoantibodies can still be detected.

Finally, several open questions remain; Why are NAg-specific CD4+ TRAIL+ ISG T-cells highly present in SSc active LNs but not in SjS? Is this regulated by the type of autoantigen (Ro/La bind RNA, while ScI70 binds DNA) or at the antigen-presentation level? Can we use these findings to design novel therapeutic approaches to tackle systemic autoimmune diseases, such as including adjuvants in tolerogenic vaccines that may divert the differentiation of antigen-specific T-cells towards an immunoregulatory TRAIL+ CD4+ ISG phenotype? Such novel therapies might benefit a broader spectrum of autoimmune diseases, including well-known B-cell mediated diseases such as lupus, rheumatoid arthritis, and multiple sclerosis.

Methods

Sex as a biological variable: Our study examined both male and female patients and similar findings are reported for both sexes.

Study design: The objective of this study was to examine the role of NAg-specific CD4+ T-cells in disrupting immune tolerance in CTDs. To address this question, we chose SSc and SjS as reference diseases because they are both immune responsive to NAgs but exhibit distinct clinical manifestations. First, we set out to conduct an in-depth characterization of NAg-specific T-cell responses in blood, LNs and

affected tissues of patients with SSc versus SjS. For this, we performed 3'-fluoro-3'-deoxy-thymidine [18F] FLT PET scans, to identify active LNs likely containing autoreactive T-cells. Ultrasound-guided biopsies were subsequently performed to obtain PET-positive and PET-negative LN samples. In addition, affected tissues (salivary gland or skin, for SjS and SSc respectively) from the same patients were also sampled. To obtain antigen-specific T-cells, ex vivo antigen-dependent T-cell stimulation assays were combined with paired blood, LN and affected tissue multimodal single-cell techniques (transcriptome, proteome, and TCR/BCR sequencing) to identify Ro60/La- and Scl70- specific CD4+ T-cells in patients with SjS and SSc respectively. Flow cytometry and multiplex immunofluorescence staining were used for validation and detailed analysis of spatial localization of the autoreactive cells. Finally, the functional role of NAg-specific T-cells and B-cells was evaluated with dedicated in-vitro co-culture assays.

Study participants: All SSc and SjS patients (aged >18) that donated whole blood (n=45 SSc and n=37 SiS) and/or LN (n=4 each disease), salivary gland (parotid) (n=3 SiS), skin (forearm) (n=2 SSc) biopsies, were diagnosed with established disease according to the ACR EULAR 2014 classification criteria (63) and European American consensus group classification criteria (64) respectively. SSc and SiS patients with overlapping syndromes were excluded from the study. SiS patients seropositive for anti-Ro60 and/or anti-La antibodies were included, while all SSc patients were seropositive for anti-ScI70 (anti-topoisomerase I). Diagnosis of early diffuse cutaneous SSc was performed according to the VEDOSS criteria (65) and presence of anti-Scl70 antibodies, a disease duration (from first non-Raynaud symptom) of < 3 years and progressive disease in the past year, as defined by either 1. an increase in mean Rodnan skin score (mRSS) > 10 points / > 25%, or 2. a decrease in forced vital lung capacity > 10%, because of an increase in interstitial lung disease. From all patients that donated tissue biopsies, paired peripheral blood mononuclear cells (PBMCs) were also available. Clinical characteristics for all patients are provided in Supplemental Table 1. Blood samples from healthy volunteers (n=30) were collected from Sanguin blood bank, Nijmegen, the Netherlands (project number: NVT 0397-02) from individuals that consented to donating blood for medical research.

PET/CT acquisition and analysis: All patients were instructed to drink 1 L of water before imaging and received 10 mg furosemide intravenously to stimulate urinary tracer excretion. An integrated PET-CT scanner (Biograph mCT, Siemens, Knoxville, TN, USA) was used for data acquisition. Emission images were acquired one hour after intravenous injection of 250±10% MBq of [18F] FLT (Cyclotron B.V., VU Medical Centre, Amsterdam, The Netherlands). The images were corrected for attenuation using low-dose CT and reconstructed using the ordered-subsets expectation maximization (OSEM) algorithm, following EANM guidelines [DOI 10.1007/s00259-014-2961-x]. Low-dose CT scan was used for anatomical correlation.

The PET/CT image sets were assessed by a certified nuclear medicine physician for the presence or absence of [18F] FLT uptake in LNs. Three-dimensional regions of interest were placed manually over every LN by using a CE-marked viewing software Agfa Enterprise on multiple slices. Maximum and mean standardized uptake values (SUV_{max}, SUV_{mean}) were derived for LNs of interest. LNs were annotated as negative when uptake of the tracer was not higher compared to the surrounding connective tissue and positive for uptake that was higher than the cutoff defined in preceding studies (29, 30).

Sample preparation: PBMCs were isolated from whole blood by using Ficoll-Paque PLUS (Sigma Aldrich, GE17-1440-03) density centrifugation and were cryopreserved as previously described (62) and stored in liquid nitrogen until future use. After thawing and washing, PBMCs where cultured in complete RPMI 1640 medium with GlutaMAX™ (Gibco, ref 72400-021), supplemented with 100 IU/ml penicillin, 100 mg/ml streptomycin, 100 mg/L sodium pyruvate, and 10% human pooled serum (HPS). LN biopsies (three-five 1.25 mm biopsies from each donor) obtained with the use of HistoCore autobiopsy system (cat # HC18100) were rinsed in complete RPMI medium in 6-well plates and with the help of a syringe staple passed through a 70 µm cell strainer to obtain single-cell suspensions. After washing with PBS, red blood cells were lysed using ice-cold erythrocyte lysis buffer (155 mM NH₂Cl, 12 mM KHCO₂, 0.1 mM EDTA in PBS) for 2 minutes at room temperature. For salivary gland and skin tissue disaggregation, tissue fragments were minced with a scalpel and enzymatically digested by using 0.1 mg/ml DNAse I (DN-25, Merck, Darmstadt, Germany) and 0.1 mg/ml Liberase TM (5401127001, Roche, Vienna, Austria) in plain RPMI 1640 for 60 minutes at 37 °C on a roller bank. For skin, 3-mm punch biopsies' mechanical dissociation was additionally used before and after enzymatic dissociation using a gentle MACs dissociator (program h skin 01). The digested fragments were passed through a 70 µm cell strainer to obtain a single-cell solution and washed with complete RPMI medium.

Sample preparation for single-cell RNA sequencing: For single-cell RNA sequencing experiments utilizing tissue biopsies and PBMCs, single-cell suspensions were washed twice with PBS before they were stained with Fc block (10 minutes at 4 °C; BD Biosciences, cat 564219), and then with CITE-seq antibody cocktail. For CITE-seq, cells were stained with the TotalSeq™-C Human Universal Cocktail, V1.0 (Biolegend,

cat#399905) according to the manufacturer's instructions. Then, viable single-cell suspensions were FACs sorted (Supplemental Figure 11A) in a BD FACSMelody™ Cell Sorter in cooled sorting tubes (4 °C) and immediately processed according to manufacturer's guidelines (10x Genomics) for Chromium Single Cell Immune Profiling using Chromium Next GEM Single-cell 5' Reagent Kits (v.2) and the recommended reagents, supplies and equipment. Sorted cells were loaded into the 10x chromium cell controller at a density of 1200 cells/ul to optimally capture up to 10,000 cells per sample. Quality control of the generated libraries was performed using the Oubit 1x dsDNA HS assay kit (Invitrogen) and the Bioanalyzer (Agilent). The sequencing of the barcoded cDNAs was performed on the Nextseg500 (Illumina) using paired end reads. The average sequencing depth was at least higher than 70K raw reads per cell.

Multimodal single-cell RNA sequencing analysis: Raw data were prepared for analysis using the Cell Ranger (v.7.2.0; 10x genomics) and FASTQ reads were aligned from gene expression (GEX), ADT/HTO and V(D)J sequencing libraries to the prebuilt GRCh38 human transcriptome. TRA and TRB sequences were annotated using the Cell Ranger VDJ function from 10x Genomics. Preprocessing of the raw data and subsequent analysis was performed in R (version 4.4.0) using the Seurat (5.1.0) package (66). Quality control measures of the count matrix were applied to filter out T-cells with a mitochondrial gene content exceeding 5% and cells with too low or too high feature counts per cell (customized for each dataset). Following this, CD3+ T-cells were computationally isolated and sorted for separate analyses based on unsupervised clustering and expression of CD3E/D/G. CD4+ T-cell clustering was then performed based on gene expression of CD4 measured by Seurat and CD4+ T-cell clusters were identified based on each cluster's differentially expressed genes (DEGs) and differentially expressed proteins (DEPs; a CITE-seg panel of 137 antibodies was used). Cell type annotation was further validated based on the expression (gene and protein) of canonical subset markers and with the use of joint density (32) to identify co-expressed genes relevant to certain T helper clusters. To ensure high purity and exclude CD4, CD8 double positive T-cells, we afterwards filtered out T-cells that had CD8A normalized mRNA expression levels greater than 1 (padj < 0.01 and log2FC > 0.5).

For primary dimensionality reduction, non-negative matrix factorization (NMF) was utilized, followed by Uniform Manifold Approximation and Projection (UMAP) and Louvain clustering using top 40 NMF components, as described by Singh et al. (67). Counts of the CITE-seq antibodies were normalized with the use of the centered log ratio transformed (CLR) counts. To identify DEGs and differentially DEPs within each transcriptionally distinct cluster, the *FindAllMarkers* function (with logistic regression; LR as testing method) in Seurat was employed. These DEGs and DEPs were annotated based on their characteristics, and the R package *pheatmap* (Kolde, R. (2019). *pheatmap: Pretty Heatmaps* (R package version 1.0.12) was used to visualize them across multiple cell types. Top DEGs and DEPs per cluster were statistically defined using LR test and the Benjamini-Hochberg method to adjust for multiple testing.

Integration of T-cell receptor clonotype analysis with single-cell RNA sequencing data: T-cell receptors (TCR)s were annotated using the Cell Ranger VDJ pipeline. The scRepertoire R package (v1.153) was utilized to identify and analyze TCR clonotypes based on TCR alpha and beta chains as well as CDR3 sequences. Clonotype data were integrated with Seurat to generate gene expression and cluster information using the combineExpression function. Cells sharing the same paired TCRαβ genes were annotated as belonging to the same clonal lineage. To visualize shared clones across clusters or tissues and to determine expanded TCR clonotypes in paired blood, LNs and affected tissue biopsies, a chord diagram was generated using the getCirclize function from the R package circlize. Heatmaps were created using the ComplexHeatmap R package (v2.13.153,55). Additionally, shared expanded TCR clonotypes in paired blood, LNs and affected tissue biopsies were visualized using the circlize R package. All scripts used for analysis of the bioinformatic data of this manuscript can be found here; https://github.com/PrashINRA/TRAIL_Manuscript.

Analysis of tissue NAq-specific TCR clonotypes paired with single-cell RNA sequencing data: To analyze TCR clonotypes shared between blood, LNs and affected tissues, we used paired single-cell RNA and TCR sequencing in all three compartments of SjS and SSc patients (blood, LNs, affected tissues). T-cells that had at least one annotated α and one annotated β chain in the TCR data were classified as matching if a cell in the paired tissue/blood data exhibited the exact same α and β chain composition. Only T-cells with at least one annotated α and one β chain were included in analyses comparing matching blood, LN and affected tissue cells. Two cells were considered part of the same T-cell clone if they shared both the exact same α and β chains, as determined by the amino acid sequence. If cells possessed multiple α and β chains, they were deemed matching only if all detected α and β chains were identical. This strict definition was applied to ensure that each pair of cells within the same clone exhibited complete similarity in their detected TCR chains, indicating with high probability that they originated from the same T-cell clone. TCR data was also used to quantify clonal expansion by counting the number of cells in each clonotype. Detection and characterization of NAg-specific T-cells in

the LNs and affected tissues were achieved through single-cell RNA sequencing, CITE-seg, and TCR sequencing across blood, LNs and affected tissues. TCR sequences derived from ex vivo blood NAg-specific T-cells, that were FACs sorted and subjected to single-cell RNA sequencing analysis, served as unique identifiers, akin to molecular barcodes, enabling the mapping of identical TCR sequences across blood, LNs, and affected tissues.

Flow cytometry and intracellular staining: 0.5-1 x 10⁶ PBMCs/single-cell suspensions were first labeled with ViaKrome 808 fixable viability dye (1.5:1000 in PBS) for 30 minutes at 4 °C to exclude dead cells, followed by staining with fluorescently labeled extracellular antibodies (Supplemental Table 2) for 20 minutes at room temperature. For intracellular antibody staining (Supplemental Table 3), cells were fixed and permeabilized using the Cyto-Fast™ Fix/Perm Buffer Set (Biolegend) according to the manufacturer's guidelines. To facilitate detection of intracellular cytokines, cells were pre-stimulated with 12.5 ng/ml phorbol 12-myristate 13-acetate (PMA) (Sigma), 500 ng/ml ionomycin (Merck), and 5 µg/ml brefeldin A (Merck) before staining. Samples were acquired on a Beckman Coulter Cytoflex LX 21-color flow cytometer immediately after staining.

To detect antigen-specific T-cells and B-cells with the use of fluorescent tetramers (Supplemental Table 4) the flow cytometric protocol was as described earlier with the addition that after cell viability staining, cells were incubated with designated fluorescent tetramers at room temperature in the dark for 30 minutes before the staining for extracellular markers was performed. Tetramers to detect Ro60-specific T-cells were obtained through the NIH Tetramer Core Facility (contract number 75N93020D00005). Streptavidin labeled tetramers to detect autoreactive Laspecific B-cells were kindly provided by Dr. Mathijs Broeren.

Activation induced marker assay: An activation induced marker (AIM) assay was used on top of antigen tetramer staining because it is a high throughput assay that can be applied to a larger number of patients without the need to determine their human leukocyte antigen (HLA) type. The AIM assay allowed identification of both foreign and auto-antigen specific T-cells with high sensitivity based on each different antigen stimulation (Supplemental Figure 4A).

Cryopreserved PBMCs were thawed and resuspended in RPMI 1640 with 10% HPS medium and seeded in 96-well u bottom plates with 250,000 cells per well (4-plo per condition). PBMCs were cultured for 16 hours at 37 °C and 5% CO₂ in the presence of negative control (DMSO vehicle), positive control (1 µg/ml) Staphylococcal enterotoxin B (SEB) (Sigma) and recombinant human proteins. Experimental replicates (quadruplicates) were conducted for all conditions. The human recombinant proteins comprised influenza A H1N1 nucleoprotein (NP, Sino Biological, 11675-V08B) at 2 µg/ml and La/SS-B ribonucleoprotein (La, Prospec, PRO-327), 60 kDa SS-A/Ro ribonucleoprotein (Ro60, Prospec, PRO-329), DNA topoisomerase 1 (ScI70, Prospec, ENZ-306) all at a concentration of 1 µg/ml. After a 16-hour incubation, cells were washed with PBS and used for flow cytometry staining. The gates for AIM+ T-cells were drawn based on increased expression of the early T-cell activation markers CD25/CD134 (OX40) as response to (auto)antigen stimulation (representative plots and gating strategy are provided in Figure 4B and Supplemental Figure 13B). In experiments where the AIM assay was combined with intracellular staining, after the 16-hour incubation, 5 μg/ml Brefeldin A (Merck) was added, and cells were cultured for additional 4 hours to facilitate detection of intracellular proteins. To block the interaction of HLA class II complex and CD4+ T-cells, 1 µg/ml of purified anti-human HLA-DR, DP, DQ (clone; Tü39, Biolegend, 361702) antibody was added simultaneously with antigen stimulation. Blocking of HLA class II-mediated antigen presentation with anti-HLA class II antibodies prevented NAg-induced T-cell activation (Supplemental Figure 4C). This suggests that CD4+ T-cell activation in response to anti-nuclear antigens is MHC II dependent. Of note, CD4+ AIM+ T-cells (NAg-specific) were more metabolically active in terms of protein translation compared to CD4+ AIM- T-cells as it was exemplified by elevated puromycin incorporation in AIM+ (NAq-specific) CD4+ T-cells (Supplemental Figure 4D). To further characterize the involvement of APCs in NAg-specific T-cell responses, patients' PBMCs were depleted by certain APC populations (CD19+ B-cells, CD14+ monocytes and panDCs) and T-cell activation after antigen stimulation was evaluated (Supplemental Figure 4E). Depletion of every APC population decreased T-cell response showing that all APCs in PBMCs are contributing to antigen presentation. Depletion of B-cells completely prevented the detection of CD4+CD40L+ T-cells, showing that in this assay B-cells also contribute as APCs through the CD40-CD40L axis (Supplemental Figure 4F).

AIM+ T-cells that were specific to the NAgs La, Ro60 and Scl70 were isolated using FACS (see for gating strategy Supplemental Figure 13B) and processed for single-cell RNA/TCR sequencing to analyze NAg-specific responses and generate NAg-specific TCR repertoire libraries. Single-cell RNA sequencing data analysis of NAg stimulated T-cells was performed with the same workflow that was previously described.

Flow cytometric quantification of puromycin incorporation: To quantify energy metabolism (protein translation) at the single-cell level, as previously described

(68), PBMCs were plated and cultured according to the AIM assay protocol, with the only modification being the exclusion of pyruvate from the medium. All conditions were tested in experimental triplicates. After 16 hours of stimulation with Ro60/La or ScI70 antigens, wells were treated with 10 µg/ml puromycin (Merck) for 15 minutes. After puromycin treatment, cells were washed with cold PBS and stained with ViaKrome 808 fixable cell viability fluorescent dye. This was followed by staining with primary conjugated antibodies against surface markers for 20 minutes at room temperature in FACS buffer (PBS + 1% BSA). Afterwards, cells were washed, fixed, and permeabilized using FOXP3 fixation and permeabilization buffer (ThermoFisher eBioscience) according to the manufacturer's instructions. Intracellular staining of anti-puromycin monoclonal antibody conjugated with Alexa Fluor 647 (Biolegend, cat#381507) was diluted in the permeabilization buffer and cells were incubated for 1 hour at 4°C. Samples were acquired on a Beckman Coulter Cytoflex LX 21-color flow cytometer immediately after staining.

Immunohistological analysis: LN, salivary gland and skin biopsies were formalin fixed, paraffin embedded (FFPE), sectioned (5.0 µm thickness) and subsequently stained with hematoxylin and eosin (HE). For immunohistochemistry, the FFPE tissue sections were deparaffinized with xylol and rehydrated with ethanol. Antigen retrieval was performed in a 10 mM sodium citrate buffer (pH 6.0) in water either at room temperature or by heating the slides for 30 minutes at 97° C. Blocking of endogenous peroxidase was conducted with the use of 3% H₂O₂ in PBS. Primary (Supplemental Table 5) and appropriate secondary (BrightVision Poly-HRP, Immunologic DPVO55HRP or Envision Flex HRP, DAKO) antibody labeling was performed with 3'3'-diaminobenzene (bright DAB, Immunologic or DAKO) reagent and sections were counterstained with hematoxylin. For multiplex immunofluorescent staining, slides were stained using an automated platform with the Opal 7-color Automation IHC kit (NEL801001KT; PerkinElmer) on the BOND RX IHC & ISH Research platform (Leica Biosystems), following previously described protocols (9). We refer to Supplemental Table 6 for a full list of the antibodies that were used. Slides were then scanned using the Automated Quantitative Pathology Imaging System (Vectra V.3.0.4, PerkinElmer) at 4x magnification for an overview. Multispectral images of tissue biopsies were annotated with Phenochart (V.1.0.9, PerkinElmer) and scanned at 20x magnification. Spectral unmixing of the Opal fluorophores was performed using InForm software (V.2.4.2, PerkinElmer), and the multichannel images were digitally merged. For quantitative analysis, digital scans of whole tissue biopsies (three sections per biopsy per donor) were quantified using QuPath-0.4.4 (69).

Co-culture suppression assays: The suppressive capacity of FACs sorted (see Supplemental Figure 11D for the gating strategy) CD4+CD25highTRAIL- Tregs and CD4+TRAIL+CD25- T-cells was assessed using co-culture suppression assays. Tregs and TRAIL+ CD4+ T cells were sorted from fresh blood PBMCs after CD4+ T-cell enrichment was performed with a MojoSort™ Human CD4 T Cell Isolation Kit (Biolegend, cat#480010) according to manufacturer's instructions and followingly co-cultured with CFSE-labeled CD4+CD25-TRAIL- responder T cells (Tresp) at varying ratios, in the presence of anti-CD3/anti-CD28 mAb-coated beads (ThermoFischer, cat#11131D), bead-to-cell ratio 1:5, for 3 days. Tresp proliferation was quantified by CFSE dilution, as previously described (70).

B-cell help immunoassay: To evaluate B-cell help function of NAg-specific memory CD4+ T-cells, we utilized a sensitive immunoassay, developed by Ansari et al. (71). In this assay, CD19+ B-cells, CD4+CD45RO+ memory T-cells and CD14+ monocytes were FACS sorted (Supplemental Figure 13C) from SSc and SjS patients' blood and co-cultured at 1:1:0.5 ratio with or without stimulation with recombinant human La, Ro60, ScI70 for 8 days at 37 °C and 5% CO2. Generation of (autoreactive) plasma cells was assessed with flow cytometry and plasma cells were gated as CD19+CD27+CD38++CD20low (Supplemental Figure 14). For detection of La-specific B-cells, La-APC/BV421 tetramers were used in the flow cytometric extracellular staining. To block TRAIL-TRAIL Receptor pathway signaling, recombinant human anti-TRAIL (Biolegend, 308202) and anti-TRAILR1/CD261 (DR4; Biolegend, 307201) antibodies were used at 10 μg/ml.

Quantification of anti-nuclear autoantibodies: To measure Ro60, La and ScI70-specific IgG antibodies in the co-culture supernatants of the B-cell help immunoassay experiments, an EliA Symphony assay (Thermo Fisher Scientific, Inc., Waltham, MA) was used as previously described (72). The analyses were conducted using an immunoassay analyzer (ImmunoCAP 250, Thermo Fisher Scientific, Inc.). Values are presented in kU/ml and were corrected based on the number of live B-cells per sample.

RNA isolation and quantitative real-time polymerase chain reaction: RNA isolation was carried out using RNAeasy (Qiagen) following the manufacturer's instructions. The RNA concentration was then measured with a Nanodrop spectrophotometer (Thermo Scientific, Waltham, MA, USA), and any genomic DNA was removed using DNase I. Up to 1 µg of RNA was reverse-transcribed into cDNA in a single-step reverse transcription PCR at 39°C using an oligo dT primer and 200U M-MLV reverse transcriptase (All Life Technologies) in a thermocycler. Gene expression

in the resulting cDNA was measured using 0.2 mM validated primers (Biolegio, Nijmegen, the Netherlands; see Supplemental Table 7) and SYBR Green master mix (Applied Biosystems, Waltham, MA, USA) in a quantitative real-time polymerase chain reaction (gPCR). Relative gene expression ($-\Delta$ Ct) was calculated based on the average expression of three reference genes: GAPDH, TBP and RPS27A.

Computational analysis of flow cytometry data: For dimensionality reduction of flow cytometry data, viSNE analyses were conducted using the web-based analysis software Cytobank (http://cytobank.org/) (73). Initially, each file was gated on live CD3+ T-cells and then on certain T-cell populations of interest for each analysis. Subsampling followed the visNE algorithm, analyzing 14,060 events per sample. The t-SNE axes of the viSNE maps were generated using the markers CD3, CD4, CD8, CCR4, CD25, CD69, CXCR5, CD28, CCR4, CCR6, CXCR3, CD45RA, CD27, PD-1, ICOS, CD154. The levels of each protein marker were normalized to the maximum value observed for the respective channel within each sample. For unsupervised analysis, T lymphocyte populations of interest were manually gated and isolated using the Beckman Coulter plug-in of Kaluza (v2.1.2) software. The files were categorized into comparison groups based on patient origin and T-cell population. Unsupervised clustering of lymphocyte and T-cell frequencies was performed with the CITRUS tool, using abundance-based clustering, a minimum cluster size of 2% of total cells, and a false discovery rate of 1%. Clustering was based on the expression levels of cell surface and intracellular markers from the viSNE analysis. The Citrus "cluster tree" illustrated the clustering hierarchy, with nodes scaled according to cell frequency in each cluster. Clustering was evaluated using prediction analysis for microarrays (PAM) to identify features that distinguish certain T-cell clusters with each other and/or certain T-cell clusters between patients with SiS and SSc.

To investigate patterns in marker expression profiles, principal component analysis (PCA) was performed on pseudo bulk flow cytometry data. Marker expression data were standardized prior to analysis using the prcomp function in R. PCA was conducted to compare marker expression profiles across experimental conditions. The resulting PCA scores were visualized using ggplot2, where donors were represented as individual points. With this analysis we observed that T-cells specific to different (auto)antigens (e.g. ScI70, Ro60/La, H1N1 Flu) detected with the AIM assay as CD4+CD25+CD134+ exhibited distinct T helper phenotypes (Supplemental Figure 4B), attributed to the distinct nature of each antigen stimulation.

Statistical analysis: Data visualization and statistical comparisons between experimental groups were carried out using R Studio (version 4.1.3) and Prism software (GraphPad 9.0.0, San Diego, CA, USA). Data are presented as means \pm SEM. Two-tailed unpaired Student's T-tests were used for comparisons between two groups, while one-way or two-way ANOVA with Tukey's multiple comparisons test or non-parametric Kruskal Wallis test was applied for comparisons among multiple groups. Spearman's correlation was used to analyze relationships between two variables that were not normally distributed. P values less than 0.05 were considered significant. To compare significance in cell frequency of single-cell RNA sequencing clusters the Wilcoxon test, corrected for multiple comparisons, was used. The specific statistical tests used for each analysis or experiment are detailed in the figure legends.

Study approval: This study was approved by the local research ethics committee of Radboud University Medical Center, the Netherlands (study number(s): NL 67672.091.18) and all participants provided signed informed consent according to the principles of the Declaration of Helsinki. All patient related procedures were executed in accordance with the relevant Dutch legislation and reviewed by an accredited research ethics committee.

Materials availability: This study did not generate new unique reagents.

Data and code availability: The datasets and scripts used in this manuscript can be found here; https://github.com/PrashINRA/TRAIL_Manuscript. This study did not generate any unique code.

Lead contact

Further information and requests should be addressed to the lead contact, Dr. Rogier Thurlings (Rogier.thurlings@radboudumc.nl).

Author contributions

T.I.P, H.K and R.M.T conceptualized the project. T.I.P executed the wet lab experiments and performed their data analysis. Technical support was provided by B.W, L.J.A.W and E.V. Bioinformatic analysis of single-cell RNA sequencing data was performed by P.S. P.K assisted with bioinformatic analyses at the revision process of the manuscript. Funding WAS acquired by R.M.T. This study investigation was carried out by T.I.P, A.C, H.K, I.J.M.V, M.A.H and R.M.T. Methodology was developed by T.I.P, P.S, A.C, R.L.S, K.W.M, I.J.M.V, E.A, M.A.H and R.M.T. Supervision was provided by A.C, X.H, H.K, P.K, R.L.S, E.A, I.J.M.V, M.A.H and R.M.T. Visualization was performed by T.I.P, K.M.H and E.A; The original draft was written by T.I.P and R.M.T, and the manuscript was reviewed and edited by T.I.P, A.C, X.H, H.K, K.W.M, M.V, E.A, I.J.M.V, M.A.H and R.M.T.

Declaration of generative AI and AI-assisted technologies

No generative AI nor AI-assisted technologies were used in the writing process.

Supplemental material

Supplemental Figures 1-14

Supplemental Tables 1-7

Acknowledgements

We acknowledge a. the work performed by our student Myrthe van der Waal in the optimization of the in vitro functional assays during her internship in our department of Rheumatology b. the work of Dr. Mark Gorris and Kiek Verrijp in setting up multiplex immunofluorescence panels. We thank Dr. Massis Krekorian for his assistance in the collection and processing of patients' biopsies for singlecell RNA sequencing, Annika Decker for her assistance in experiment evaluating antigen-presentation in AIM assay.

Conflict of interest

The authors have declared that no conflict of interest exists.

References

- 1. Spagnolo P, Cordier J-F, Cottin V. Connective tissue diseases, multimorbidity and the ageing lung. European Respiratory Journal. 2016;47(5):1535-58.
- 2. Resende ABL, Monteiro GP, Ramos CC, Lopes GS, Broekman LA, De Souza JM. Integrating the autoimmune connective tissue diseases for the medical student: A classification proposal based on pathogenesis and clinical phenotype. Heliyon. 2023;9(6).
- 3. Wieber K, Zimmer CL, Hertl M. Detection of autoreactive CD4+ T cells by MHC class II multimers in HLA-linked human autoimmune diseases. J Clin Invest. 2021;131(9).
- Mulhearn B, Tansley SL, McHugh NJ. Autoantibodies in connective tissue disease. Best Practice & Research Clinical Rheumatology. 2020;34(1):101462.
- 5. Ota Y, Kuwana M. Updates on genetics in systemic sclerosis. Inflammation and Regeneration. 2021;41(1):17.
- 6. Kwok SK, Lee J, Yu D, Kang KY, Cho ML, Kim HR, et al. A pathogenetic role for IL-21 in primary Sjögren syndrome. Nat Rev Rheumatol. 2015;11(6):368-74.
- 7. Nayar S, Turner JD, Asam S, Fennell E, Pugh M, Colafrancesco S, et al. Molecular and spatial analysis of tertiary lymphoid structures in Sjogren's syndrome. Nature Communications. 2025;16(1):5.
- 8. Broeren MGA, Wang JJ, Balzaretti G, Groenen P, van Schaik BDC, Chataway T, et al. Proteogenomic analysis of the autoreactive B cell repertoire in blood and tissues of patients with Sjögren's syndrome. Ann Rheum Dis. 2022;81(5):644-52.
- Papadimitriou TI, Singh P, van Caam A, Walgreen B, Gorris MAJ, Vitters EL, et al. CD7 activation regulates cytotoxicity-driven pathology in systemic sclerosis, yielding a target for selective cell depletion. Ann Rheum Dis. 2024;83(4):488-98.
- Padilla CM, Valenzi E, Tabib T, Nazari B, Sembrat J, Rojas M, et al. Increased CD8+ tissue resident memory T cells, regulatory T cells and activated natural killer cells in systemic sclerosis lungs. Rheumatology (Oxford). 2024;63(3):837-45.
- 11. Maehara T, Kaneko N, Perugino CA, Mattoo H, Kers J, Allard-Chamard H, et al. Cytotoxic CD4+ T lymphocytes may induce endothelial cell apoptosis in systemic sclerosis. The Journal of Clinical Investigation. 2020;130(5):2451-64.
- 12. Kramer K, Pecher AC, Henes J, Klein R. IgE autoantibodies to nuclear antigens in patients with different connective tissue diseases: re-evaluation and novel findings. Front Immunol. 2025;16:1483815.
- Mesa A, Somarelli JA, Wu W, Martinez L, Blom MB, Greidinger EL, et al. Differential immunoglobulin class-mediated responses to components of the U1 small nuclear ribonucleoprotein particle in systemic lupus erythematosus and mixed connective tissue disease. Lupus. 2013;22(13):1371-81.
- 14. Kondeti RD, Venkatesh K, Murthy D, Kameti S, Devi KS, Chandrika KV. A Study of Clinical Manifestations and their Association with Antinuclear Antibodies in Various Autoimmune Connective Tissue Disorders. Indian J Dermatol. 2023;68(4):486.
- 15. Aubin AM, Lombard-Vadnais F, Collin R, Aliesky HA, McLachlan SM, Lesage S. The NOD Mouse Beyond Autoimmune Diabetes. Front Immunol. 2022;13:874769.
- 16. Bouzahzah F, Jung S, Craft J. CD4+ T cells from lupus-prone mice avoid antigen-specific tolerance induction in vivo. J Immunol. 2003;170(2):741-8.
- 17. Busser BW, Adair BS, Erikson J, Laufer TM. Activation of diverse repertoires of autoreactive T cells enhances the loss of anti-dsDNA B cell tolerance. J Clin Invest. 2003;112(9):1361-71.

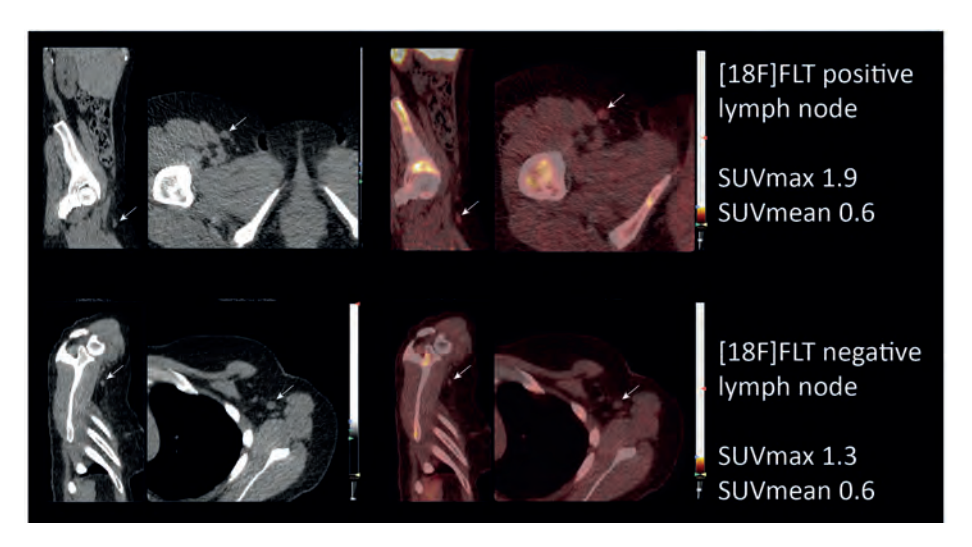
- 18. Krakowski ML, Owens T. The central nervous system environment controls effector CD4+ T cell cytokine profile in experimental allergic encephalomyelitis. Eur J Immunol. 1997;27(11):2840-7.
- 19. Gabrysová L, Wraith DC. Antigenic strength controls the generation of antigen-specific IL-10secreting T regulatory cells. Eur J Immunol. 2010;40(5):1386-95.
- 20. Smith MZ, Bastidas S, Karrer U, Oxenius A. Impact of antigen specificity on CD4+ T cell activation in chronic HIV-1 infection. BMC Infect Dis. 2013:13:100.
- 21. Sweet RA, Ols ML, Cullen JL, Milam AV, Yagita H, Shlomchik MJ. Facultative role for T cells in extrafollicular Toll-like receptor-dependent autoreactive B-cell responses in vivo. Proc Natl Acad Sci U S A. 2011;108(19):7932-7.
- 22. Elsner RA, Shlomchik MJ. Germinal Center and Extrafollicular B Cell Responses in Vaccination, Immunity, and Autoimmunity. Immunity. 2020;53(6):1136-50.
- 23. Pagan JD, Vlamakis H, Gaca A, Xavier RJ, Anthony RM. Modulating T Follicular Cells In Vivo Enhances Antigen-Specific Humoral Immunity. J Immunol. 2021;206(11):2583-95.
- 24. Wing JB, Ise W, Kurosaki T, Sakaguchi S. Regulatory T cells control antigen-specific expansion of Tfh cell number and humoral immune responses via the coreceptor CTLA-4. Immunity. 2014;41(6):1013-25.
- 25. Jang E, Cho WS, Cho ML, Park HJ, Oh HJ, Kang SM, et al. Foxp3+ regulatory T cells control humoral autoimmunity by suppressing the development of long-lived plasma cells. J Immunol. 2011;186(3):1546-53.
- 26. Fava A, Cimbro R, Wigley FM, Liu QR, Rosen A, Boin F. Frequency of circulating topoisomerase-lspecific CD4T cells predicts presence and progression of interstitial lung disease in scleroderma. Arthritis Res Ther. 2016;18(1):99.
- 27. Lu C, Pi X, Xu W, Qing P, Tang H, Li Y, et al. Clinical significance of T cell receptor repertoire in primary Sjogren's syndrome. eBioMedicine. 2022;84.
- 28. Shields AF, Grierson JR, Dohmen BM, Machulla HJ, Stayanoff JC, Lawhorn-Crews JM, et al. Imaging proliferation in vivo with [F-18]FLT and positron emission tomography. Nat Med. 1998;4(11):1334-6.
- 29. Troost EG, Vogel WV, Merkx MA, Slootweg PJ, Marres HA, Peeters WJ, et al. 18F-FLT PET does not discriminate between reactive and metastatic lymph nodes in primary head and neck cancer patients. J Nucl Med. 2007;48(5):726-35.
- 30. Aarntzen EH, Srinivas M, De Wilt JH, Jacobs JF, Lesterhuis WJ, Windhorst AD, et al. Early identification of antigen-specific immune responses in vivo by [18F]-labeled 3'-fluoro-3'-deoxythymidine ([18F]FLT) PET imaging. Proc Natl Acad Sci U S A. 2011;108(45):18396-9.
- 31. Poloni C, Schonhofer C, Ivison S, Levings MK, Steiner TS, Cook L. T-cell activation-induced marker assays in health and disease. Immunol Cell Biol. 2023;101(6):491-503.
- 32. Khaleel M, Jebrel A, Dunia MS. Artificial Intelligence in Computer Science: https://doi.org/10.5281/ zenodo.10937515. Int J Electr Eng and Sustain. 2024;2(2):01-21.
- 33. Moon JS, Younis S, Ramadoss NS, Iyer R, Sheth K, Sharpe O, et al. Cytotoxic CD8(+) T cells target citrullinated antigens in rheumatoid arthritis. Nat Commun. 2023;14(1):319.
- 34. Abdirama D, Tesch S, Grießbach A-S, von Spee-Mayer C, Humrich JY, Stervbo U, et al. Nuclear antigen-reactive CD4+ T cells expand in active systemic lupus erythematosus, produce effector cytokines, and invade the kidneys. Kidney International. 2021;99(1):238-46.
- 35. Sato K, Niessner A, Kopecky SL, Frye RL, Goronzy JJ, Weyand CM. TRAIL-expressing T cells induce apoptosis of vascular smooth muscle cells in the atherosclerotic plaque. J Exp Med. 2006:203(1):239-50.

- Kavurma MM, Schoppet M, Bobryshev YV, Khachigian LM, Bennett MR. TRAIL stimulates proliferation of vascular smooth muscle cells via activation of NF-kappaB and induction of insulin-like growth factor-1 receptor. J Biol Chem. 2008;283(12):7754-62.
- 37. Sato K, Nuki T, Gomita K, Weyand CM, Hagiwara N. Statins reduce endothelial cell apoptosis via inhibition of TRAIL expression on activated CD4 T cells in acute coronary syndrome. Atherosclerosis. 2010;213(1):33-9.
- 38. Chyuan IT, Tsai HF, Liao HJ, Wu CS, Hsu PN. An apoptosis-independent role of TRAIL in suppressing joint inflammation and inhibiting T-cell activation in inflammatory arthritis. Cell Mol Immunol. 2018;15(9):846-57.
- 39. Bossi F, Bernardi S, Zauli G, Secchiero P, Fabris B. TRAIL modulates the immune system and protects against the development of diabetes. J Immunol Res. 2015;2015:680749.
- 40. Daniels RA, Turley H, Kimberley FC, Liu XS, Mongkolsapaya J, Ch'En P, et al. Expression of TRAIL and TRAIL receptors in normal and malignant tissues. Cell Research. 2005;15(6):430-8.
- 41. Travert M, Ame-Thomas P, Pangault C, Morizot A, Micheau O, Semana G, et al. CD40 ligand protects from TRAIL-induced apoptosis in follicular lymphomas through NF-kappaB activation and up-regulation of c-FLIP and Bcl-xL. J Immunol. 2008;181(2):1001-11.
- 42. Norouzi M, Abdi S. Exploring the Role of the Lymphatic System in Immune Regulation: Implications for Autoimmunity, Cancer, and Infection. 2023.
- 43. Santambrogio L, Marrack P. The broad spectrum of pathogenic autoreactivity. Nature Reviews Immunology. 2023;23(2):69-70.
- 44. Henes J, Oliveira MC, Labopin M, Badoglio M, Scherer HU, Del Papa N, et al. Autologous stem cell transplantation for progressive systemic sclerosis: a prospective non-interventional study from the European Society for Blood and Marrow Transplantation Autoimmune Disease Working Party. Haematologica. 2021;106(2):375-83.
- 45. Müller F, Taubmann J, Bucci L, Wilhelm A, Bergmann C, Völkl S, et al. CD19 CAR T-Cell Therapy in Autoimmune Disease A Case Series with Follow-up. N Engl J Med. 2024;390(8):687-700.
- 46. Woolf DK, Beresford M, Li SP, Dowsett M, Sanghera B, Wong WL, et al. Evaluation of FLT-PET-CT as an imaging biomarker of proliferation in primary breast cancer. British Journal of Cancer. 2014;110(12):2847-54.
- 47. Ahlin E, Mathsson L, Eloranta ML, Jonsdottir T, Gunnarsson I, Rönnblom L, et al. Autoantibodies associated with RNA are more enriched than anti-dsDNA antibodies in circulating immune complexes in SLE. Lupus. 2012;21(6):586-95.
- 48. Naito R, Ohmura K, Higuchi S, Nakai W, Kohyama M, Mimori T, et al. Positive and negative regulation of the Fcγ receptor-stimulating activity of RNA-containing immune complexes by RNase. JCl Insight. 2023;8(16).
- 49. Vílchez-Oya F, Balastegui Martin H, García-Martínez E, Corominas H. Not all autoantibodies are clinically relevant. Classic and novel autoantibodies in Sjögren's syndrome: A critical review. Front Immunol. 2022;13:1003054.
- 50. Radstake TR, van Bon L, Broen J, Wenink M, Santegoets K, Deng Y, et al. Increased frequency and compromised function of T regulatory cells in systemic sclerosis (SSc) is related to a diminished CD69 and TGFbeta expression. PLoS One. 2009;4(6):e5981.
- 51. Jiang N, Li M, Zeng X. Correlation of Th17 cells and CD4*CD25* regulatory T cells with clinical parameters in patients with systemic sclerosis. Chin Med J (Engl). 2014;127(20):3557-61.
- 52. Hadaschik EN, Wei X, Leiss H, Heckmann B, Niederreiter B, Steiner G, et al. Regulatory T cell-deficient scurfy mice develop systemic autoimmune features resembling lupus-like disease. Arthritis Res Ther. 2015;17(1):35.

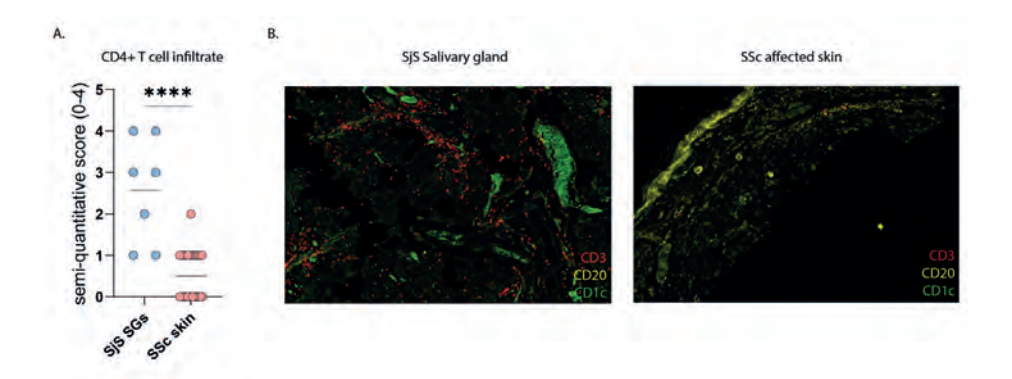
- 53. Chen W, Yang F, Xu G, Ma J, Lin J. Follicular helper T cells and follicular regulatory T cells in the immunopathology of primary Sjögren's syndrome. Journal of Leukocyte Biology. 2021;109(2):437-47.
- 54. Tong L, Koh V, Thong BY, Review of autoantigens in Siögren's syndrome: an update, J Inflamm Res. 2017:10:97-105.
- 55. Alkema W. Koenen H. Kersten BE, Kaffa C. Dinnissen JWB, Damoiseaux JGMC, et al. Autoantibody profiles in systemic sclerosis; a comparison of diagnostic tests. Autoimmunity. 2021;54(3):148-55.
- 56. Vignali DA, Collison LW, Workman CJ. How regulatory T cells work. Nat Rev Immunol. 2008;8(7):523-32.
- 57. Yang J, Brook MO, Carvalho-Gaspar M, Zhang J, Ramon HE, Sayegh MH, et al. Allograft rejection mediated by memory T cells is resistant to regulation. Proc Natl Acad Sci U S A. 2007;104(50):19954-9.
- 58. Chyuan IT, Tsai HF, Wu CS, Sung CC, Hsu PN. TRAIL-Mediated Suppression of T Cell Receptor Signaling Inhibits T Cell Activation and Inflammation in Experimental Autoimmune Encephalomyelitis. Front Immunol. 2018;9:15.
- 59. Ren X, Ye F, Jiang Z, Chu Y, Xiong S, Wang Y. Involvement of cellular death in TRAIL/DR5-dependent suppression induced by CD4(+)CD25(+) regulatory T cells. Cell Death Differ. 2007;14(12):2076-84.
- 60. Walczak H, Miller RE, Ariail K, Gliniak B, Griffith TS, Kubin M, et al. Tumoricidal activity of tumor necrosis factor-related apoptosis-inducing ligand in vivo. Nat Med. 1999;5(2):157-63.
- 61. Mori S, Kohyama M, Yasumizu Y, Tada A, Tanzawa K, Shishido T, et al. Neoself-antigens are the primary target for autoreactive T cells in human lupus. Cell. 2024;187(21):6071-87.e20.
- 62. Papadimitriou TI, Lemmers JMJ, van Caam APM, Vos JL, Vitters EL, Stinissen L, et al. Systemic sclerosis-associated pulmonary arterial hypertension is characterized by a distinct peripheral T helper cell profile. Rheumatology. 2024;63(9):2525-34.
- 63. van den Hoogen F, Khanna D, Fransen J, Johnson SR, Baron M, Tyndall A, et al. 2013 classification criteria for systemic sclerosis: an American College of Rheumatology/European League against Rheumatism collaborative initiative. Arthritis Rheum. 2013;65(11):2737-47.
- 64. Vitali C, Bombardieri S, Jonsson R, Moutsopoulos HM, Alexander EL, Carsons SE, et al. Classification criteria for Sjögren's syndrome: a revised version of the European criteria proposed by the American-European Consensus Group. Ann Rheum Dis. 2002;61(6):554-8.
- 65. Avouac J, Fransen J, Walker UA, Riccieri V, Smith V, Muller C, et al. Preliminary criteria for the very early diagnosis of systemic sclerosis: results of a Delphi Consensus Study from EULAR Scleroderma Trials and Research Group. Ann Rheum Dis. 2011;70(3):476-81.
- 66. Stuart T, Butler A, Hoffman P, Hafemeister C, Papalexi E, Mauck WM, 3rd, et al. Comprehensive Integration of Single-Cell Data. Cell. 2019;177(7):1888-902.e21.
- 67. Singh P, Zhai Y. Deciphering Hematopoiesis at single cell level through the lens of reduced dimensions. bioRxiv. 2022:2022.06.07.495099.
- 68. Argüello RJ, Combes AJ, Char R, Gigan JP, Baaziz AI, Bousiquot E, et al. SCENITH: A Flow Cytometry-Based Method to Functionally Profile Energy Metabolism with Single-Cell Resolution. Cell Metab. 2020;32(6):1063-75.e7.
- 69. Bankhead P, Loughrey MB, Fernández JA, Dombrowski Y, McArt DG, Dunne PD, et al. QuPath: Open source software for digital pathology image analysis. Scientific Reports. 2017;7(1):16878.
- 70. Koenen HJ, Fasse E, Joosten I. CD27/CFSE-based ex vivo selection of highly suppressive alloantigen-specific human regulatory T cells. J Immunol. 2005;174(12):7573-83.
- 71. Ansari A, Sachan S, Jit BP, Sharma A, Coshic P, Sette A, et al. An efficient immunoassay for the B cell help function of SARS-CoV-2-specific memory CD4(+) T cells. Cell Rep Methods. 2022;2(6):100224.

- 72. van der Molen RG, Hamann D, Jacobs JF, van der Meer A, de Jong J, Kramer C, et al. Anti-SSA antibodies are present in immunoglobulin preparations. Transfusion. 2015;55(4):832-7.
- 73. Kotecha N, Krutzik PO, Irish JM. Web-based analysis and publication of flow cytometry experiments. Curr Protoc Cytom. 2010;Chapter 10:Unit10.7.

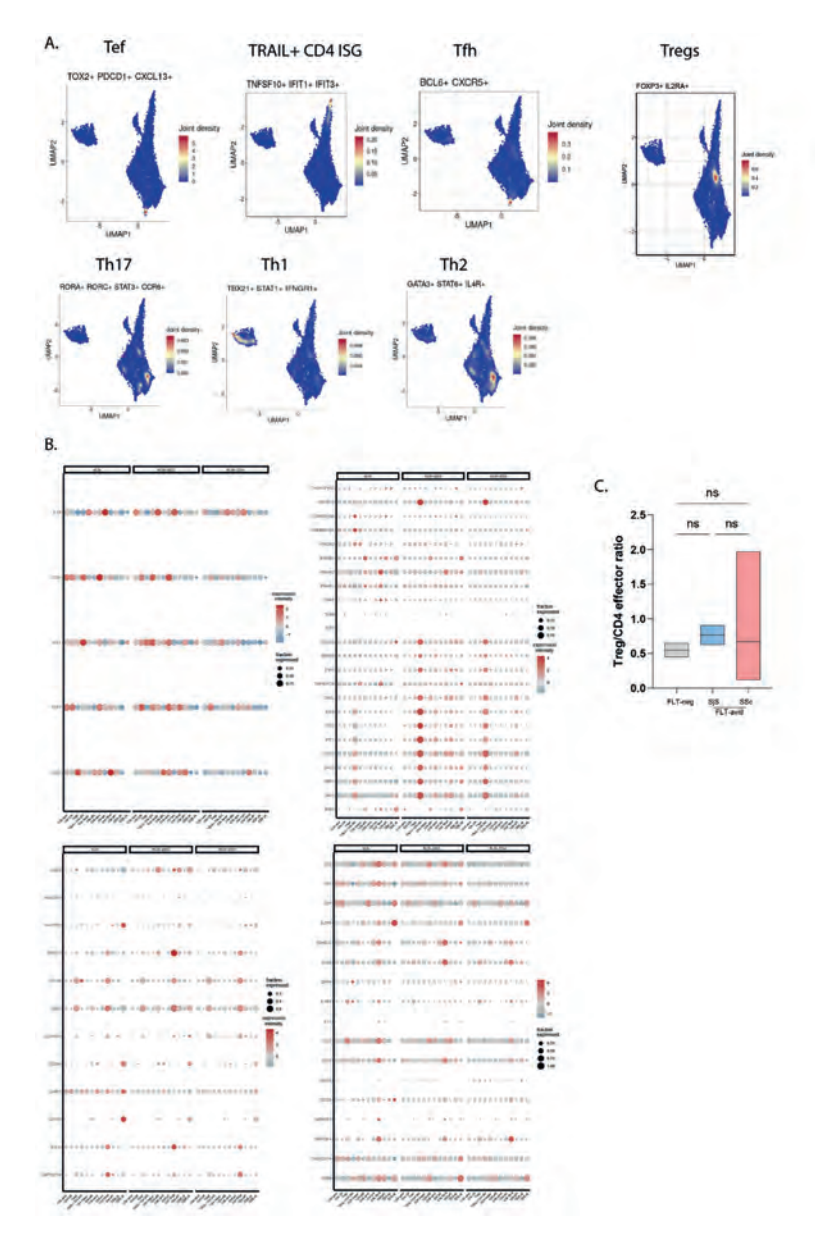
Supplementary Figures



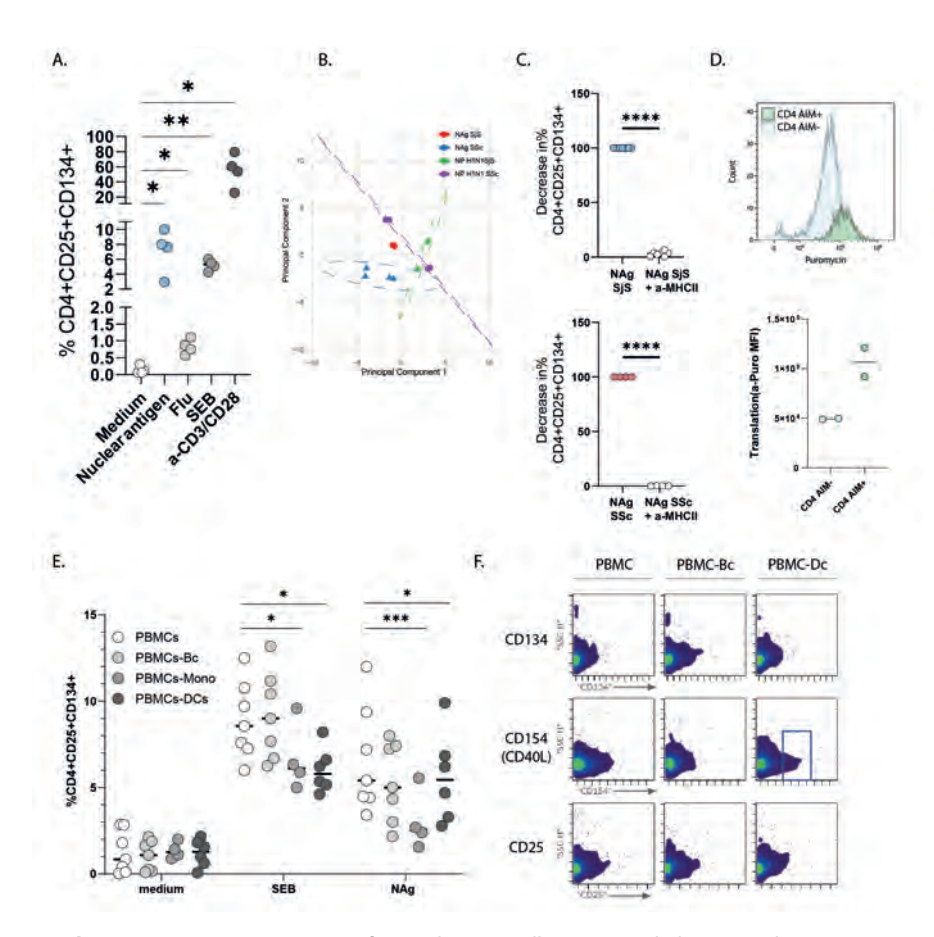
Supplementary Figure 1. Representative image of [18F] FLT PET/CT scan of a patient with SSc (n=4) exhibiting with arrows detection, among the affected skin draining lymph nodes, of a FLT-positive (inguinal right) and a FLT-negative (axillar left) LN based on high or low [18F] FLT signal represented with SUV_{mean} and SUV_{max} values (g/ml).



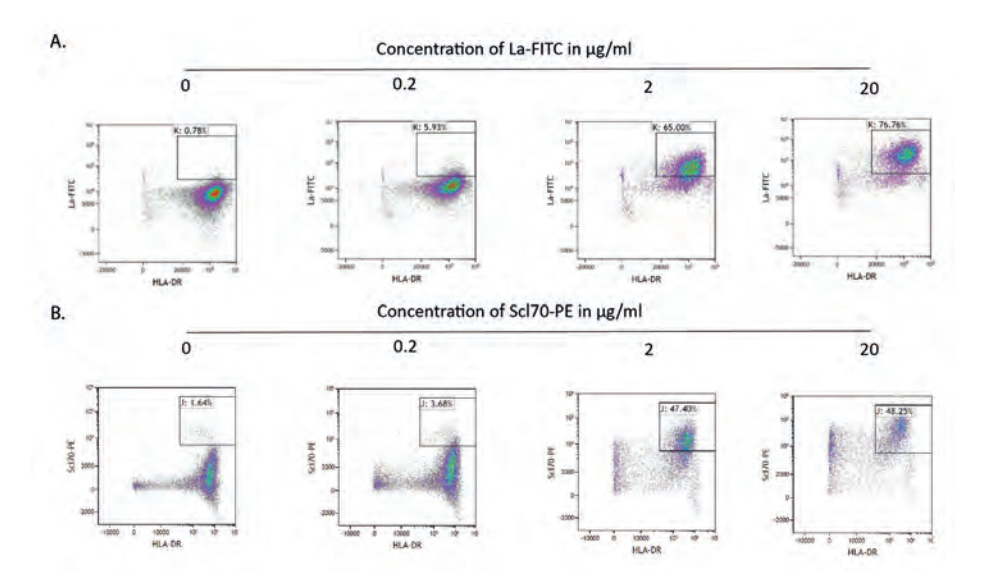
Supplementary Figure 2. Affected CTD of patients with SjS (salivary glands-SGs) exhibit higher infiltration of CD4+ T cell clusters compared to SSc affected skin. (A) Semi-quantitative score of CD4+ T-cell infiltration within affected SjS salivary glands (SGs) (n=7) and SSc affected skin (n=20). (B) Representative multiplex immunofluorescence stainings (n=7/20) exhibiting robust interaction between T-/B- cells withing APC rich areas in SjS SGs but not as prominent in SSc affected skin. Scale bars are 100 µm.



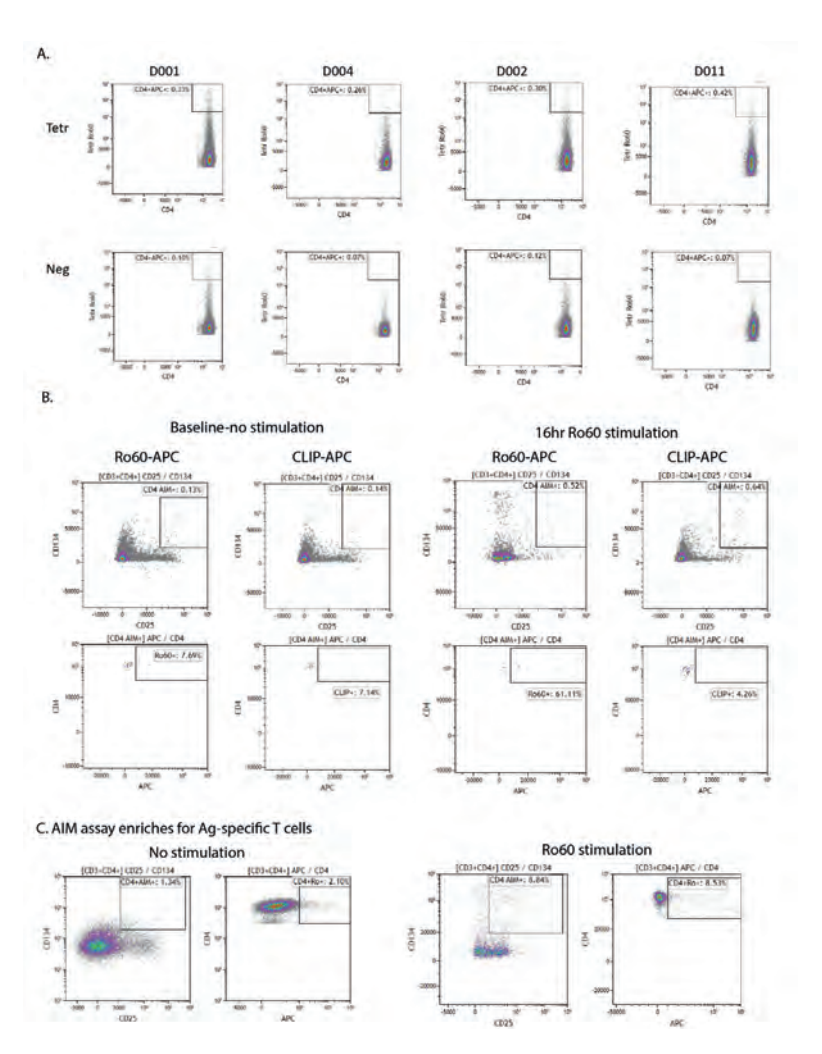
Supplementary Figure 3. Additional single-cell RNA and CITE-seq analyses that facilitated annotation of CD4+ T-cell subsets in patients' active and non-active lymph nodes. **(A)** 2D Joint Density plots of selected markers reflective of Tph, TRAIL+ ISG, Tfh, Treg, Th17, Th1, Th2 specific gene signatures. **(B)** 2D dot plots showing the percentage and level of gene expression of selected type I IFN signaling, maturation, cytotoxic and activating/inhibitory receptor genes between T-cell clusters identified in active and non-active lymph nodes. **(C)** Cell ratio of Tregs/CD4 effector T cells between negative and positive LNs of patients with SjS and SSc.



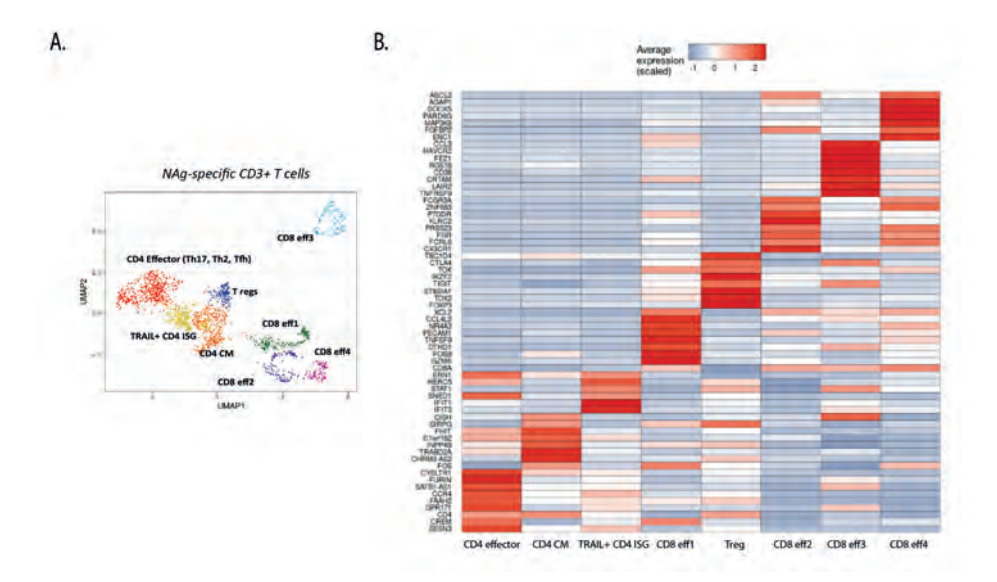
Supplementary Figure 4. NAq-specific circulating T-cells are expanded in SiS and SSc patients in an MHCII-dependent manner. (A) Frequencies of detected CD4+CD25+CD134+ T-cells (AIM+) in SjS patients' PBMCs (n=4) that were stimulated for 16 hrs with NAgs (Ro60/La), Flu H1N1 nucleoprotein (NP H1N1) antigens, staphylococcus enterotoxin B (SEB) and anti-CD3/CD28 monoclonal antibodies (moAb) as positive controls. (B) Pseudo-bulk principal component analysis (PCA) comparing the flow cytometric phenotype of NAg SjS, NAg SSc, NP H1N1 SjS and NP H1N1 SSc T-cell responses based on the expression of 15 T-cell extracellular markers (for PC1, 40.1% variance explained; for PC2, 28.92% variance explained) shows clear separation between H1N1 NP, NAg SSc and NAg SjS determining distinct phenotypes for each foreign or self Ag-specific T-cell response. (C) Normalized decrease in % of CD4+AIM+ (CD4+CD25+CD134+) response under ScI70 or Ro60/La stimulation and blockage or not of MHC II interactions with anti-HLA-DR/DQ/DP moAb. (D) Overlay flow cytometry histograms of one representative experiment (n=2) comparing expression of anti-Puromycin (translation level) between CD4+ AIM-T-cells (CD4+CD25+CD134+) and CD4+ AIM+T-cells (CD4+CD25-CD134-) accompanied by graphic quantification of anti-Puromycin MFI. (E) Frequencies of AIM+ (CD4+CD25+CD134+) T-cells in (n=3 SjS and 4 HCs) PBMCs that were further depleted from CD19+ B-cells, CD14+ monocytes or panDCs and stimulated with SEB and SjS NAgs (Ro60/La) antigens. (F) Density plots generated by Cytobank that contain pooled CD4+ T-cells from (n=4) SjS and illustrate expression of CD134, CD154 and CD25 in whole PBMCs and PBMCs depleted from B-cells or DCs. Statistics: in (A) RM one-way ANOVA, with Dunnett's multiple comparisons test, *p<0.05, **p<0.01; in (C) two-tailed paired t-test, ****p<0.0001; in (E) ordinary one-way ANOVA, with Tukey's multiple comparisons test, *p<0.05, ***p<0.001.



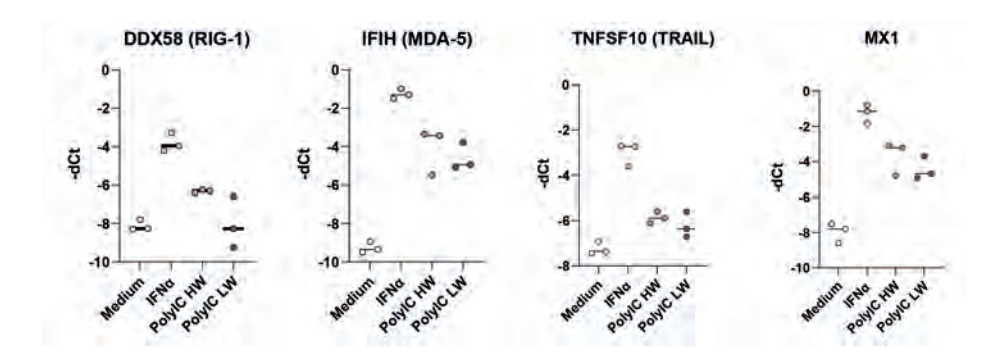
Supplementary Figure 5. The NAgs La and Scl70 are endocytosed by CD11c+ antigen-presenting cells of La+ SjS patients and Scl70+ SSc patients. Flow cytometric plots of the endocytosis of fluorescently labeled Scl70 and La proteins by CD11c+ cells in (**A**) SSc and (**B**) SjS PBMCs exhibiting that antigen-presenting cells uptake both autoantigens in a dose-dependent manner. PBMCs were incubated with increasing concentrations, ranging from 0-20 ug/ml, of Scl70-PE and La-FITC proteins.



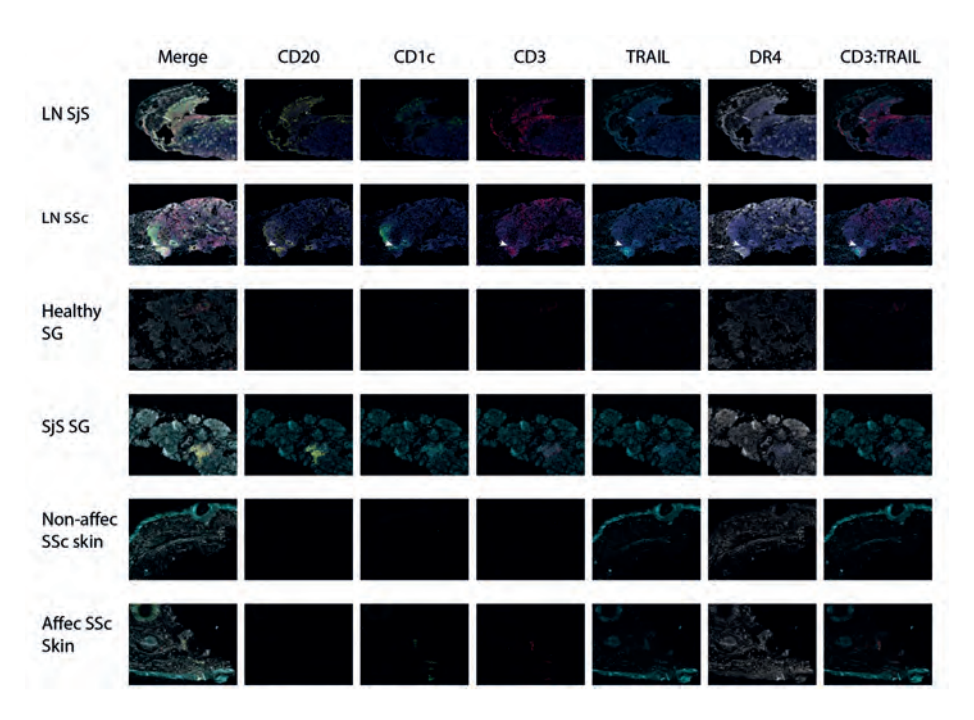
Supplementary Figure 6. Detection of NAq-specific T-cells with the AIM assay overlaps with detection of NAg-specific T-cells with tetramers. In 4 SiS patients with suitable HLA background, we performed AIM assay with the whole Ro60 antigen and combined with Ro60 (3 different peptides pooled) tetramer staining and found that the detection overlap between T-cell activation and tetramer staining was 60%. Furthermore, enrichment for antigen-specific T-cells with the AIM assay also enhanced detection of autoreactive T-cells with tetramers and a similar percentage of Ag-specific T-cells were detected between AIM assay and tetramer staining (Supp. figure 5C). Collectively, these findings determine the validity of AIM assay to detect autoreactive T-cells that are pulsed by monocytes, DCs and B-cells, including T follicular helper like (elevated CD40L). (A) Flow cytometry plots illustrate the detection of Ro60-specific CD4+ T-cells with the use of Ro60 tetramers conjugated with APC in 4 patients with SjS that are Ro60 seropositive. Results are compared with CLIP tetramers that were also conjugated with APC as negative controls. (B) Flow cytometric density plots of one representative experiment with PBMCs from SjS patient where tetramer staining in combination with the AIM assay was performed. An enriched number of Ro60-specific T-cells is detected at similar levels (C) with AIM assay markers and tetramer staining after 16-hour incubation of PBMCs with recombinant Ro60 protein. The overlap between AIM+ and tetramer+ cells is about 60%.



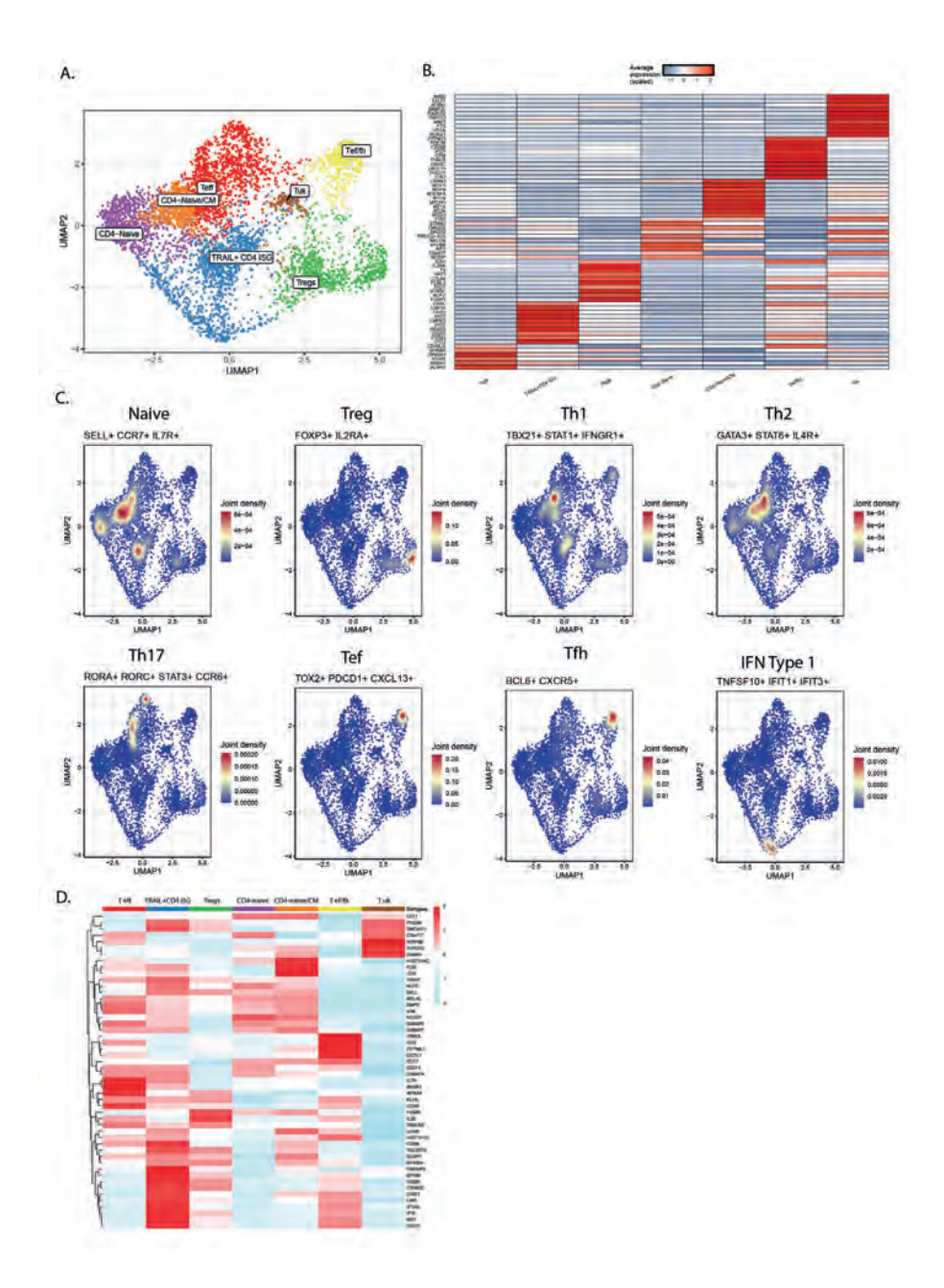
Supplementary Figure 7. Single-cell RNA sequencing of SjS and SSc patients' blood and tissue NAgspecific T-cells. Complementary graphs for figures 4 and 5. (**A**) UMAP to visualize the transcriptionally distinct T-cell clusters from tissue NAg-specific T-cells. (**B**) Heatmap illustrates the top 8 differentially expressed genes in each identified cell cluster of the tissue NAg-specific T-cells dataset.



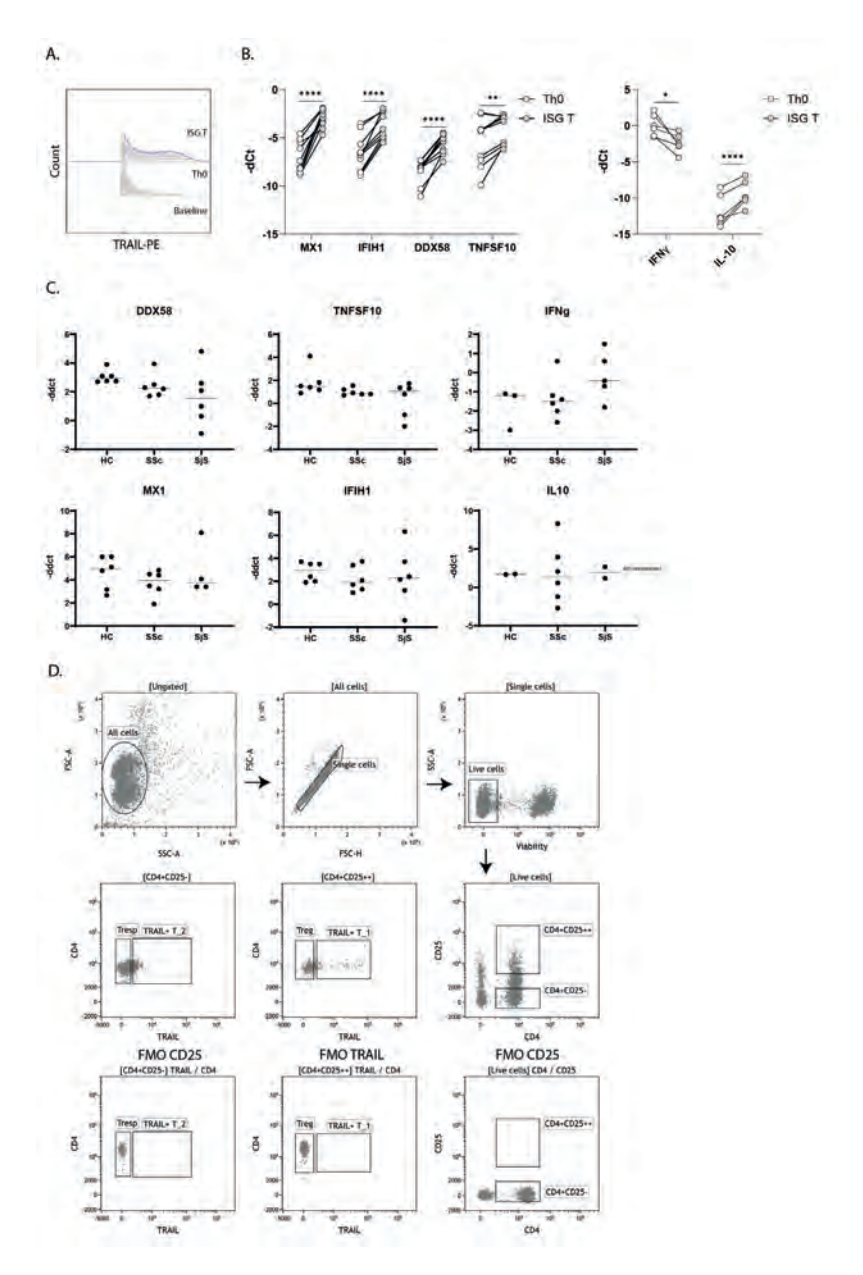
Supplementary Figure 8. CD4+ T-cells respond directly to poly IC by upregulating an ISG gene signature. CD4+ T-cells from healthy peripheral blood were MACs sorted and cultured for 24 hours with IFNα, HW (high molecular weight) and LW (low molecular weight) Poly IC. Relative gene expression (–dCt) of the type I IFN signaling genes *DDX58, IFIH, TNFSF10* and *MX1* was measured by qPCR.



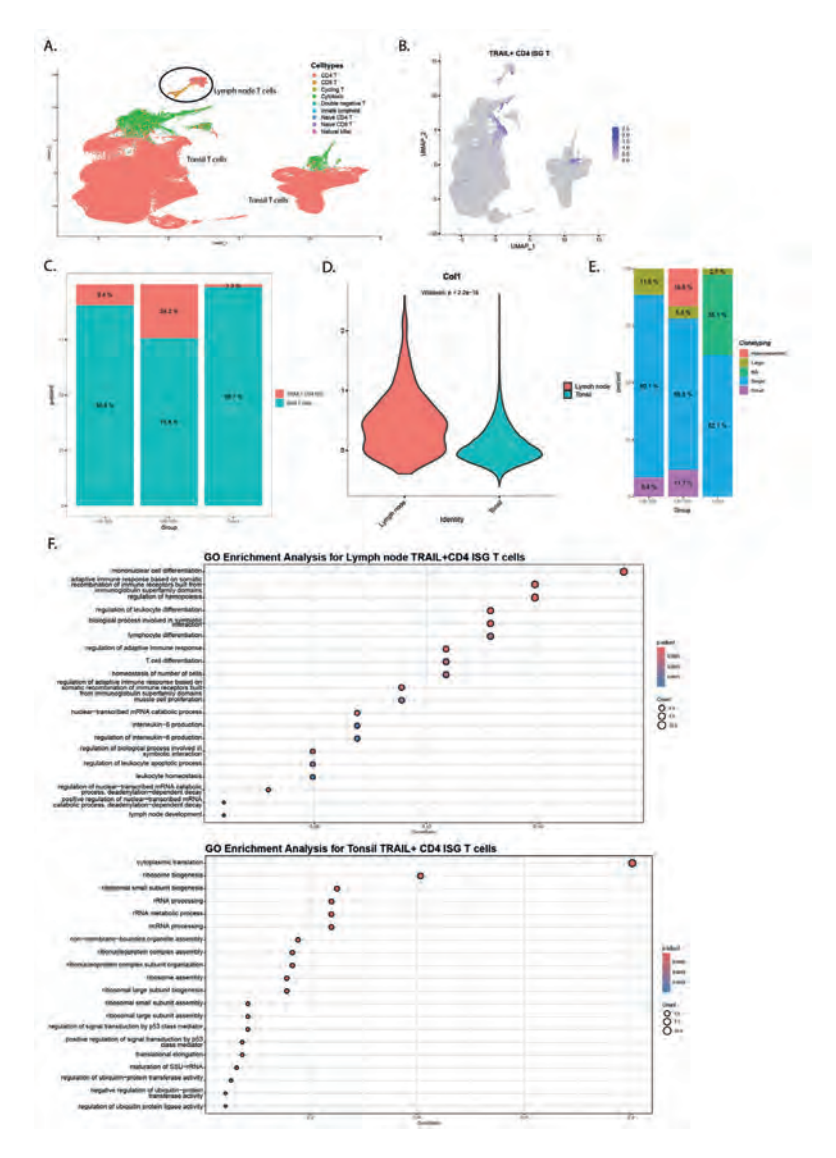
Supplementary Figure 9. Multiplex IF stainings for the spatial localization of TRAIL+ T-cells. (A) Immunofluorescence microscopy showing expression of CD20, CD1c, CD3, TRAIL, DR4 and coexpression of CD3 with TRAIL in LN SjS (n=6), LN SSc (n=7), healthy SG (n=2), SjS SG (n=7), non-affected and affected SSc skin (n=20). A representative experiment is depicted in scale of 100 μm .



Supplementary Figure 10. Focused subcluster single-cell RNA sequencing analysis of CD4+ T-cells to perform trajectory analysis. (**A**) UMAP of the transcriptionally distinct CD4+ T-cell clusters in patients' lymph nodes; CD4 naive, CD4 naive/CM, TRAIL+ CD4 ISG, T uk (unknown), Tregs, Tef/fh. (**B**) Heatmap illustrates the top 10 differentially expressed genes in each identified cell cluster of CD4+ LN T-cells. (**C**) 2D Joint Density plots of selected markers reflective of Naive, Treg, Th1, Th2, Th17, Tef, Tfh, IFN Type 1 specific gene signatures. (**D**) Differential dynamic genes (DYG) contributing to the clustering of each distinct CD4+ T-cell cluster.

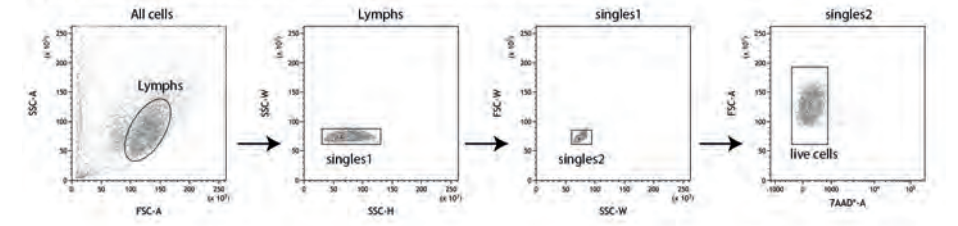


Supplementary Figure 11. (A) Overlay histograms of one experiment illustrating expression of TRAIL in baseline, Th0 and ISG differentiated T-cells. (B) Relative gene expression (-dCt) of the depicted genes measured with qPCR on Th0 or ISG differentiated T-cells (n=4). (C) Relative gene expression (-ddct) of the depicted genes comparing ISG T/Th0 differentiated cells from healthy controls (HC) and patients with SSc and SjS (n=6 per group). (D) Gating strategy that was used to sort TRAIL+ T cells (CD4+CD25-TRAIL-), Tregs (CD4+CD25++TRAIL-) and Tresp(onsive) cells (CD4+CD25-TRAIL-) for the CD4 effector proliferation suppression assay. Statistics for panel B were performed with ordinary oneway ANOVA with Tukey's multiple comparisons test, *p<0.05.

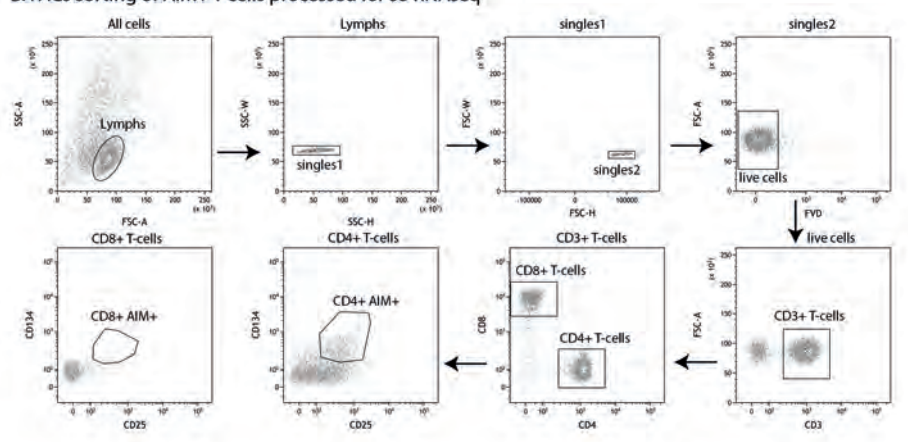


Supplementary Figure 12. CD4+TRAIL+ ISG T cells exhibit unique expansion and immunoregulatory functional role within autoreactive lymph nodes. For this analysis our single-cell RNAseq data from lymph node (LN) T cells of patients with SjS and SSc, were merged with single-cell RNAseq data of tonsils T-cells extracted from the atlas of human cells in the human tonsil [1] by Massoni-Badosa et al. (**A**) UMAP depicting the cell types present in the merged object of lymph node and tonsil T cells. (**B**) UMAP projection illustrating the presence and intensity of gene signature expression of TRAIL+ ISG CD4+ T cells. These cells were defined as expressing CD4, TNFSF10 and MX1 genes. (**C**) Bar graphs showing the frequency of TRAIL+ ISG CD4+ T cells between SSc/SjS reactive LNs and tonsils. (**D**) Violin plot comparing the intensity of ISG signature expression between LN and tonsil T-cells. (**E**) Bar graphs showing the percentage of expanded clones of TRAIL+ ISG CD4+ T cells between SSc/SjS reactive LNs and tonsils. (**F-G**) Gene ontology (GO) enrichment analysis based on the differentially expressed genes of TRAIL+ ISG CD4+ T cells in lymph node (top) versus tonsils (bottom).

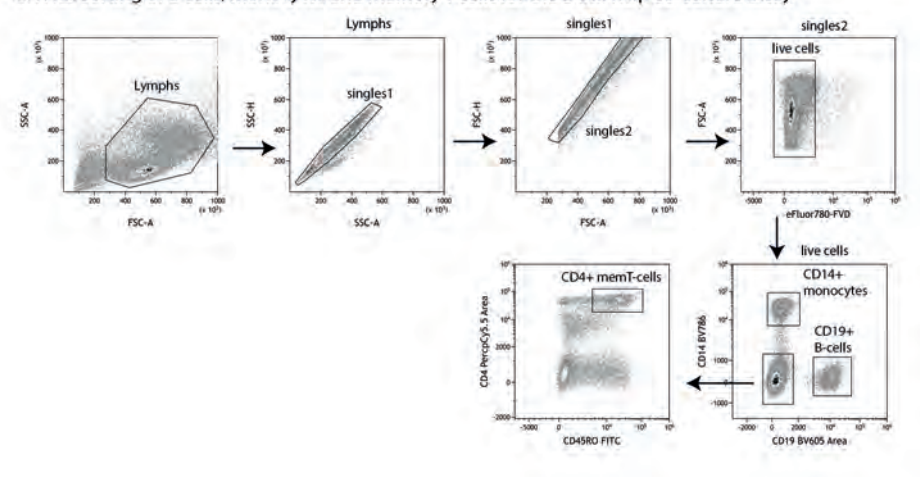
A. FACs sorting of live cells from tissues processed for sc-RNAseq



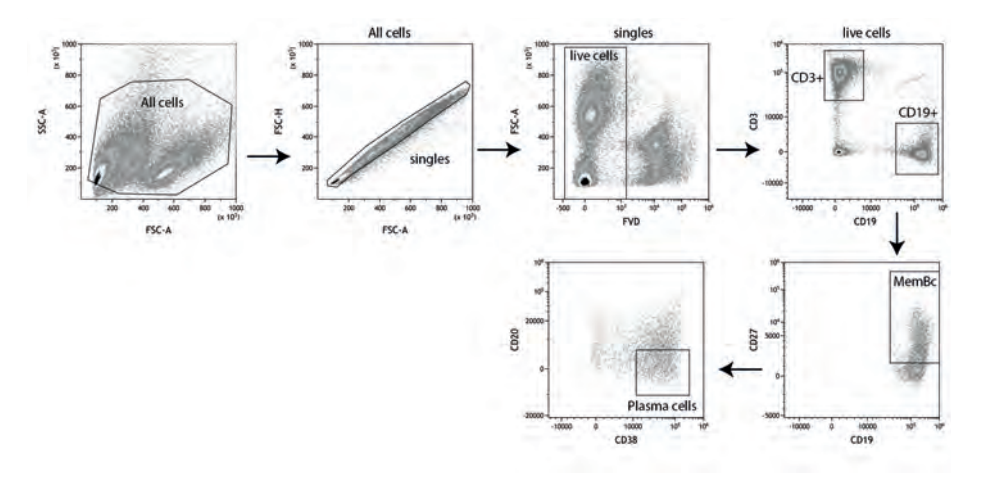
B. FACs sorting of AIM+ T cells processed for sc-RNAseq



C. FACs sorting of B cells, monocytes and memory T cells for the B cell help co-culture assay



Supplementary Figure 13. Gating strategies exhibiting fluorescently activated cell sorting (FACs) of (A) Viable lymph node lymphocytes that were subsequently processed for 10x single-cell RNA sequencing. (B) Viable AIM+ CD4+ T-cells and CD8+ T-cells that were subsequently processed for 10x single-cell RNA sequencing. (C) B-cells, monocytes and memory T-cells that were subsequently cocultured in vitro for the B-cell help immunoassay.



Supplementary Figure 14. Gating strategy for the identification of plasma cells related to results from the in vitro B-cell help assay that are illustrated in Figure 7.

References

1. Massoni-Badosa, R., et al., An atlas of cells in the human tonsil. Immunity, 2024. **57**(2): p. 379-399.e18.

Supplementary materials

Supplementary Table 1. List of SjS (top) and SSc (bottom) patients included in single-cell RNA sequencing experiments and their clinical characteristics.

)		-		
Patient ID	Sex	Progr sicca	essive	Swollen L glands	Lymphoma	IgM RF	lgG titer (mg/dl)	Cryoglobulin	Autoantibody status	ody Material processed for scRNAseq	
5,5001	Female	Yes		Yes N	No	Yes	21	No	Anti-SSA, SSB	Blood, LN	
SjS002	Male	Yes		No	Yes	Yes	29	Yes	Anti-SSA, SSB, RF	Blood, LN	
SjS003	Female	Yes		Yes N	No No	N _o	20	Yes	Anti-SSA, dsDNA	Blood, LN, SG	
SjS004	Male	Yes		No	No	Yes	6.7	Yes	Anti-SSA, RF	Blood, LN, SG	
SjS007	Female	No		No	No	Yes	9.8	Yes	Anti-SSA, SSB, RF	Blood, S	
Patient ID	Sex	Disease duration (Years)	Active disease	Increased ESR	ASCT	Active ulcers/ progressive P	Active ulcers/ progressive PAH	Comor	bidity	Autoantibody status	Material processed for scRNAseq
SSc006	Female	0.1	Yes	Yes	No	No		No	Scl	ScI70+	Blood, LN, skin
SSc008	Male	0.2	Yes	Yes	No	No		N	Scl	ScI70+	Blood, LN
SSc010	Female	0.5	Yes	Yes	No	No		No	Scl	ScI70+	Blood, LN, skin
SSc011	Male	_	Yes	Yes	o _N	No		No	Scl	ScI70+	Blood, LN

Antigen	Clone	Fluorochrome	Supplier	Identifier
CD4	RPA-T4	PerCP/Cy5.5	Biolegend	300530
CD3	UCHT1	Alexa700	Biolegend	300425
CD8a	RPA-T8	BV510	Biolegend	301048
CD14	M5E2	BV785	Biolegend	301839
CD56	N901	APC	Beckman-Coulter	318309
CD19	HIB19	BV605	Biolegend	302243
CD11c	B-ly6	BUV395	BD Biosciences	563787
CD45	HI30	BV510	Biolegend	304036
CD25	M-A251	PE/Cy7	Biolegend	356108
CD134 (OX40)	ACT35	FITC	Biolegend	350006
CD154	5C8	PE	Miltenyi Biotec	130-113-607
CD45RA	HI100	BUV496	BD Biosciences	750258
CD253 (TRAIL)	RIK-2	PE	Biolegend	308206
FASL	DX2	BV421	Biolegend	305623
CD20	B9E9	ECD	BD Biosciences	IM3607U
CD38	HB-7	PE/Cy7	Biolegend	356608
CD27	0323	APC/Cy7	Biolegend	302816
CD86	IT2.2	PerCP/Cy5.5	Biolegend	305420
HLA-DR	L243	APC	Biolegend	307609

Supplementary Table 3. List of antibodies used for intracellular staining.

Antigen	Clone	Fluorochrome	Supplier	Identifier
IL-21	mgalx21	PE	Invitrogen	12-7213-83
IL-4	MP4-25D2	PE/Dazzle594	Biolegend	500832
IFN-γ	B27	Alexa Fluor 700	Biolegend	506516
Ki-67	ki-67	Alexa Fluor 488	Biolegend	350532
IL-17A	BL168	BV421	Biolegend	512322
GATA-3	16E10A23	Alexa Fluor 488	Biolegend	653807
ROR gamma (t)	AFKJS-9	PE	ThermoFischer	12-6988-82
T-bet	4B10	Alexa Fluor 647	Biolegend	644803
FOXP3	PCH101	PE	ThermoFischer	12-4776-42
Puromycin	2A4	Alexa Fluor 647	Biolegend	381507

Supplementary Table 4. List of fluorescent tetramers used to detect antiquen-specific T and B-cells with flow cytometry.

Target	Peptide	HLA haplotype	HLA haplotype Fluorochrome Supplier	Supplier
B tetramers (negative)	LEIRAAFLRQRNTALRTEVAELEQEVQRLENEVSQYETRYGPLGGGGK	NA	PE	In house
La+ B-cells	GSGKGKVQFQGKKTKF	NA	APC	In house
La+ B-cells	GSGKGKVQFQGKKTKF	NA	BV421	In house
Ro-60+ T-cells	ELEVIHLIEEHRLVREHLLTNHLKS	DRB1*03:01	APC	NIH Tetramer Core facility
Ro-60+ T-cells	KTNTPADVFIVFTDNETFAG	DRB1*03:01	APC	NIH Tetramer Core facility
Ro-60+ T-cells	PCPVTTDMTLQQVLMAMSQIPAGGT	DRB1*03:01	APC	NIH Tetramer Core facility
Human CLIP (negative)	PVSKMRMATPLLMQA	DRB1*03:01	APC	NIH Tetramer Core facility

Supplementary Table 5. List of antibodies used for immunohistochemistry.

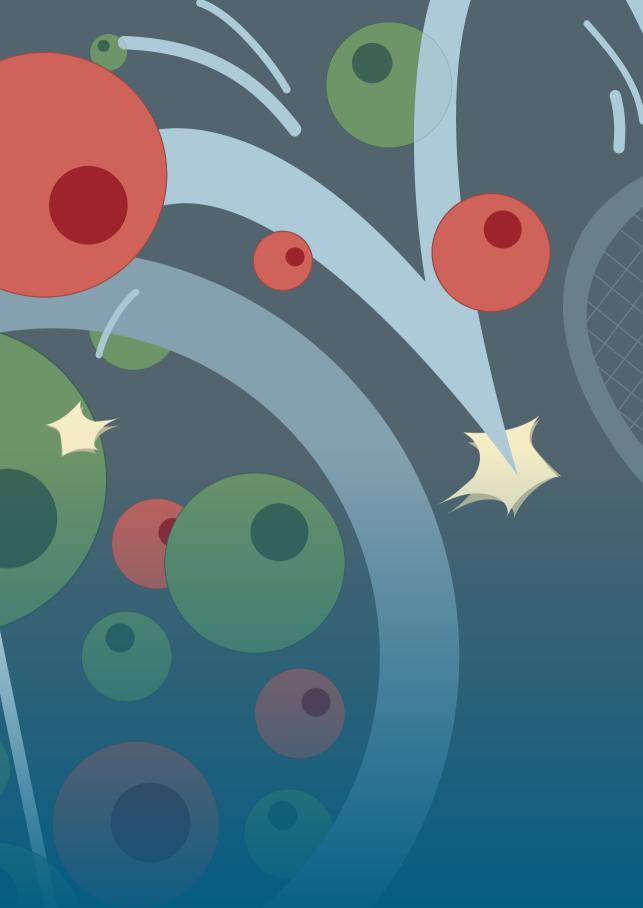
Antigen	Clone	Dilution	Supplier
CD21	1F8	Ready to use	Dako
CD3	Poly CD3	Ready to use	Dako
CD79a	JCB117	Ready to use	Dako

Supplementary Table 6. List of antibodies used for multiplex immunofluorescent staining.

Antigen	Clone	Dilution	Fluorochrome	Supplier
CD3	SP7	1:200	OPAL570	Invitrogen (#MA1-90582)
CD20	L26	1:300	OPAL480	Fischer Scientific (12651067)
CD1c (BDCA1)	2F4	1:150	OPAL520	Fischer Scientific (15766056)
CD253 (TRAIL)		1:1250	OPAL620	ThermoFischer (PA5-95476)
CD261 (DR4)		1:800	OPAL690	ThermoFischer (PA5-84201)

Supplementary Table 7. List of primer sequences used.

Gene	Forward primer 5'-3'	Reverse primer 5'-3'
GAPDH	ATCTTCTTTTGCGTCGCCAG	TTCCCCATGGTGTCTGAGC
RPS27A	TGGCTGTCCTGAAATATTATAAGGT	CCCCAGCACCACATTCATCA
MX1	CTCCGACACGAGTTCCACAA	ACTCAAAATTTTATGGCCTTCTTGA
IFIH1	CACTCTGGTGGACAAGCTTCT	GCAGCAGCAATCCGGTTTC
DDX58	TTCATGTCCACCTTCAGAAGTGT	TCATAGCAGGCAAAGCAAGCT
IFNG		
IL-10	AGGGCACCCAGTCTGAGAAC	GTCCAGCTGATCCTTCATTTGAAAG
TNFSF10	CCGTCAGCTCGTTAGAAAGATGAT	CCCAGTTATGTGAGCTGCTACT



Chapter 7

General Discussion and future perspectives

SSc is a complex rheumatic CTD characterized by vasculopathy, autoimmune inflammation, and fibrosis of the skin and visceral organs. It involves a loss of self-tolerance to nuclear antigens; however, unlike other nuclear antigen reactive CTDs such as SjS, SSc exhibits distinct immunopathological processes within disease-affected tissues. Both the initiation and progression of SSc are critically influenced by (auto)immune responses. However, its significant heterogeneity in manifestations, onset, and progression presents challenges for research and clinical management. Despite significant efforts, safe and universally applicable treatments (other than ASCT and potentially anti-CD19 CART cell therapy) that can modify the disease, as well as reliable biomarkers to predict and monitor the progression of SSc, have not yet been developed. This is mainly due to the incomplete understanding of the disease's underlying mechanisms and initiating factors.

This thesis explores the role of (autoreactive) T cell responses in driving the pathological processes of vasculopathy, fibrosis, and autoantibody-mediated tissue destruction in SSc and other CTDs such as Sjogren's syndrome. Key findings and their implications are summarized below, followed by an in-depth discussion of future therapeutic directions, aimed at translating laboratory insights into clinical applications.

Chapter 2 – Importance of the immune system in SSc and lack of safe and targeted curative treatments

Summary

The immune system is central to SSc pathogenesis, driving inflammation, vasculopathy, and fibrosis. T cells have a central role in orchestrating the strength, direction, specificity, location and duration of adaptive immune responses. Thus, due to their plasticity and functional diversity, T cells are pivotal in linking early inflammatory events to fibrotic and other pathogenic responses. Pro-fibrotic CD4+ and CD8+ T cells producing cytokines such as IL-4 and IL-13 have been detected in SSc-affected tissues and are thought to contribute to the observed fibrosis via extensive myofibroblast-mediated extracellular matrix deposition. Apart from the involvement of the pro-fibrotic Th2 cells, other T helper subsets such as Th17 and Tph and Tregs have been implicated in certain disease processes, though findings are often controversial and thus inconclusive. The role of cytotoxic T cells in SSc pathogenesis has not been adequately examined. Recent research has demonstrated an increased presence of cytotoxic T cells, rather than T helper cells, in SSc-affected skin, with their function linked to vascular damage through

the induction of endothelial cell apoptosis (1). While most studies have focused on examining T cell composition in patients' blood, some have investigated SScaffected tissues, providing valuable insights into the role of tissue-resident T cells in underlying disease processes. However, no study has comprehensively analyzed the regulation of (autoreactive) T cell responses simultaneously across blood, active lymph nodes, and affected tissues. Given the systemic nature of SSc, such an analysis is expected to significantly advance our understanding of disease pathogenesis.

Discussion points

Chapter 2 reviews the contributions of immune cells, including T cells, to SSc pathophysiology and evaluates current and emerging therapies targeting these cells. While immunosuppressive, anti-inflammatory, and anti-fibrotic treatments generally show limited efficacy in reducing fibrosis, certain advanced therapies, such as ASCT, have demonstrated significant effectiveness, achieving long-term remission in many patients. However, the ASCT process is associated with relatively high mortality rates, limiting its broader adoption despite its efficacy. Furthermore, anti-CD19 CAR T cell therapy, although still in its early stages and applied only in isolated cases, has shown promising results; however, its effects on reversing skin fibrosis appear to be limited. In both cases, disease remission results from elimination of the autoreactive immune cells and this highlights the importance of the immune system in SSc disease pathology. Both approaches face additional challenges, including high costs, severe side effects, and restricted applicability to the broader SSc patient population. Therefore, there is an urgent need to develop new therapies that can target autoreactive immune cells more specifically than ASCT and anti-CD19 CAR T. This is expected to reduce treatment-related sideeffects and most importantly to be applicable to a larger amount of patients.

Future perspectives

Advancing tools to identify and specifically target pathogenic (autoreactive) T cells could provide alternatives with fewer side effects, potentially obviating the need for intensive treatments like ASCT and CAR T cell therapy. However, effectively targeting pathogenic immune cells requires a better understanding of both local and systemic autoreactive immune responses and their regulatory mechanisms. Despite decades of research shedding light SSc disease mechanisms, several questions remain unanswered:

How are effector T cell responses regulated by co-stimulatory receptors within 1. affected tissues?

- 2. Are the T cells identified as pathogenic truly autoreactive and directly involved in underlying disease processes, or are they bystander T cells arising from a generalized inflammatory response?
- 3. Considering the systemic nature of SSc, how are effector T cell responses in affected tissues orchestrated by locoregional lymph nodes?
- 4. How do these T cell responses compare to the distinct autoreactive responses observed in other CTDs, and are they linked to the unique clinical manifestations of SSc?

Chapter 3 – CD7 as a marker to selectively eliminate pathogenic T and NK Cells in SSc-affected skin

According to the reviewed literature of chapter 2, adaptive immune responses play a central role in SSc pathology. Thus, in this chapter we set out to investigate disease-associated differences in the phenotype and regulation of T cells in SSc-affected tissues. To address this, we performed ex vivo analysis on affected skin, lung and blood samples from four cohorts of SSc patients (comprising 165 SSc patients and 80 healthy individuals) using single-cell transcriptomics, flow cytometry, and multiplex immunofluorescence staining. Additionally, we examined the effects of costimulatory modulation in functional assays and in a severely affected SSc patient who received compassionate use treatment with a novel anti-CD3/CD7 immunotoxin.

Summary

Chapter 3 identifies elevated CD7 co-stimulation as a marker of pathogenic T and NK cells in SSc-affected skin and lungs, offering a potential new avenue to therapeutically address immune-mediated affected tissue pathology. In this chapter, we demonstrate that SSc-affected skin exhibits an increased presence of proliferating T cells, cytotoxic T cells, and NK cells. These cells are characterized by a cytotoxic, proinflammatory, and profibrotic gene signature. Analyzing their costimulatory and inhibitory molecule expression revealed that these cytotoxic immune cells express the costimulatory molecule CD7, which is associated with proinflammatory and profibrotic genes such as *CCL3*, *TGFB1*, *OSM*, particularly in cases of recent-onset and severe disease. Additionally, we show that CD7 costimulation is involved in the effector and potentially pathogenic functions of cytotoxic T cells and NK cells, and that selective depletion of CD7+ activated T and NK cells inhibits immune cell-induced fibroblast contraction. Finally, a CD3/CD7-targeted depletive treatment successfully eliminated circulating and affected tissue

CD7+ T cells and NK cells and stabilized disease manifestations in a patient with severe dcSSc.

Discussion points

The findings of chapter 3 imply that costimulatory molecules like CD7 are key regulators of effector cytotoxic immune cell-driven tissue pathology in SSc, positioning CD7 as a novel target for therapeutic intervention.

The role of cytotoxic T cells and NK cells in SSc pathology has been a topic of controversy. For decades, research has primarily focused on understanding the pathogenic roles of T helper cells as the main effector cells in SSc and other systemic rheumatic autoimmune diseases (2). This emphasis has been driven largely by the genetic associations between MHC class II polymorphisms and the risk of developing systemic autoimmunity, including SSc (3, 4). However, recent findings from two large genome-wide association studies (GWAS) in SSc have identified risk associations involving MHC class I polymorphisms, suggesting their role in the development of SSc (5, 6). Traditionally, **CD8+ T cells** have been recognized as crucial defenders against viral infections and tumors. Yet, emerging evidence from studies in autoimmune diseases such as type 1 diabetes, multiple sclerosis, and Crohn's disease indicates that CD8+ T cells can cause autoimmunity by mistakenly recognizing self-antigens and inducing apoptosis in healthy cells, leading to tissue damage and inflammation (7).

This growing body of evidence, coupled with recent rheumatology studies highlighting the pathogenic role of cytotoxic T cells in systemic connective tissue disorders including rheumatoid arthritis (8-10), systemic lupus erythematosus (11, 12) and Sjogren's syndrome (13-15), —underscores the importance of investigating the involvement of cytotoxic T cells in SSc. Our focused analysis of the presence and function of T helper and cytotoxic T cells in SSc-affected skin and lungs from four independent SSc patient cohorts revealed a significantly larger presence of cytotoxic T cells with pro-fibrotic signature compared to T helper cells in affected tissues. This finding suggests that cytotoxic T cells are at least as important as if not more important than T helper cells in SSc pathology. Our results align with other recent studies that also emphasize the prominent role of cytotoxic rather than T helper cells in driving SSc-related skin (1, 16) and lung (17) pathology.

Our functional analyses indicate that cytotoxic T cells and NK cells play a dual role in mediating SSc skin pathology. Specifically, CD7+ cytotoxic T cells and NK cells express both cytotoxic and pro-fibrotic genes and are located in the vicinity of endothelial cells in SSc-affected skin biopsies. Functionally, CD7 co-stimulation is essential for CD8+ T cells and NK cells to exert their cytolytic activity against K562 cells, a human leukemia cell line commonly used in cytotoxicity assays due to its low expression of MHC class I molecules. Conversely, co-culture of CD7+ cells, compared to CD7- cells, with primary skin myofibroblasts resulted in enhanced myofibroblast activation and contraction without compromising cell viability. Furthermore, the selective elimination of CD7+ cells from PBMC: myofibroblast co-cultures effectively inhibited immune cell-mediated myofibroblast contraction. These findings suggest that CD7+ cytotoxic T cells and NK cells may contribute to vascular abnormalities through the release of cytotoxic molecules, such as granzyme B and perforin, which may damage endothelial cells. Simultaneously, their secretion of pro-fibrotic cytokines, including TGFβ, CCL3, and OSM, appears to promote myofibroblast formation and activation, a key feature of fibrosis. Supporting our findings, cytotoxic T cells have been detected in close proximity to pro-apoptotic endothelial cells (1) and identified as a primary source of other profibrotic cytokines, such as IL-13 (18).

CD8+ T cells display significant heterogeneity and plasticity in their maturation and effector functions, which are tightly regulated by the interplay between activating and inhibitory receptors. In chronic viral infections and cancer, cytotoxic cells often exhibit diminished and altered effector functions through a process known as exhaustion. This state is characterized by the upregulation of inhibitory receptors such as PD-1, LAG-3, TIM-3, and CTLA-4 (19). In autoimmune CTDs, the mechanisms underlying CD8+ T cell function are less well defined. Research in this context has predominantly focused on circulating cells rather than affected tissue-resident populations, hampering the understanding of their specific roles and contributions to disease pathology. In autoimmune diseases like type 1 diabetes (T1D), multiple sclerosis (MS)/experimental autoimmune encephalomyelitis (EAE), and vitiligo, tissue-resident CD8+ T cells have been extensively studied and are known to play a pivotal role in driving disease initiation and progression (20-22).

Interestingly, while maintaining effector functions, some autoreactive CD8+ T cells exhibit features of exhaustion, which may serve a protective role. Exhaustion reflects a hyporesponsive state, and in conditions like T1D and SLE, an increased presence of exhausted CD8+ T cells has been associated with slower disease progression and better prognosis (23, 24). In SSc-affected skin and lungs, CD8+ T cells and NK cells did not exhibit signs of exhaustion. Instead, these cells were highly activated, with a notable disease-specific upregulation of CD7 co-stimulation. This upregulation appears to regulate the activation and effector phenotypes of both cytotoxic

T cells and NK cells. These findings differ from observations in other autoimmune diseases, potentially due to differences in autoantigen persistence and tissue regeneration. Unlike T1D, which targets non-regenerative pancreatic beta cells, SSc affects multiple organs, including regenerative tissues like the endothelium. This regenerative capacity may lead to recurrent antigen presentation, driving persistent or flaring immune responses, whereas the static nature of beta cells in T1D results in more stable autoantigen presentation (25-27).

The findings presented in this chapter highlight the therapeutic potential of targeting CD7 to mitigate immune cell-mediated skin and lung pathology in systemic sclerosis (SSc). The selective expression of CD7 on pathogenic cytotoxic T cells and NK cells, but not on tissue-resident T cells in healthy skin nor on other immune cells in SSc-affected/healthy skin, suggests that CD7 represents a promising therapeutic target. This specificity could enable the depletion of harmful cells while sparing other immune cells, potentially minimizing the side effects often associated with broader immunosuppressive therapies. Supporting this hypothesis, steroid-refractory acute graft-versus-host disease (GvHD) patients treated with anti-CD3/CD7 targeting immunotoxins did not exhibit signs of severe side effects such as cytokine release syndrome (28) that is often observed in patients treated with other depletive therapies such as CART cells (29).

Moreover, our study underscores the importance of understanding T cell activation in disease pathogenesis and designing novel therapies that target T cell costimulation via mechanisms distinct from those previously attempted, such as blocking the CTLA-4/CD28 co-stimulatory axis with abatacept. Abatacept, although explored as a therapeutic option, has shown limited efficacy in SSc (30). In our analysis on expression of activating and inhibitory receptors in SSc affected skin T cells, there were no significant differences in CTLA-4 gene expression between healthy individuals and patients with SSc, which may account for the lack of success with abatacept. In contrast, we found that CD7 co-stimulation exhibited the most significant up-regulation in SSc affected tissue T cells, suggesting that CD7 rather than CD28 co-stimulation might be more relevant in SSc tissue pathology.

Targeting the CD7/SECTM1 axis may offer an alternative and potentially more effective approach for addressing SSc-related fibrosis. A key advantage of this strategy is the specific upregulation of CD7 in proliferating and highly activated pathogenic T and NK cells, while naïve T and NK cells and other immune cells such as B cell and macrophages remain unaffected because they do not express CD7. This allows for precise targeting and a reduction in adverse effects, placing CD7targeting as an attractive therapeutic approach that is accompanied by reduced patient burden.

The **clinical implications of depleting CD7+ cells in SSc** are further supported by our case study, which demonstrated disease stabilization following the depletion of CD7+ cells using a combination of anti-CD3/CD7 immunotoxins. This case underscores the potential clinical benefits of this therapeutic approach. However, further clinical trials are essential to evaluate the efficacy, safety, and long-term outcomes of CD7-targeted therapies in a broader SSc patient population.

Future Perspectives

1. Development of CD7-Targeted Therapies

Advancing therapeutic strategies specifically targeting CD7 or its receptor SECTM1—such as immunotoxins, monoclonal antibodies, or cell-based approaches (e.g., anti-CD7 CAR T cells)—represents a promising avenue for treating early and diffuse cutaneous SSc. Elucidating the signalling pathways and interactions mediated by CD7 will enhance understanding of disease mechanisms and help identify additional therapeutic targets. Preclinical studies and clinical trials should aim to optimize the efficacy of these therapies in targeting tissue-resident pathogenic T and NK cells while minimizing potential adverse effects.

2. **Biomarker Potential of CD7**

The selective upregulation of CD7 on pathogenic T cells and NK cells highlights its potential as a biomarker for disease activity and progression in SSc. Specifically, CD7 expression could be utilized to identify SSc patients with early and severe disease manifestations, who are at risk of poor prognosis. Early identification and intervention are critical for improving outcomes in this subpopulation.

Notably, this thesis does not address whether CD7 activation in cytotoxic immune cells, observed during early disease stages, contributes to disease initiation or merely reflects generalized immune activation associated with early SSc. To clarify this, future research should include longitudinal studies of well-defined SSc patient cohorts, particularly those meeting the Very Early Diagnosis of Systemic Sclerosis criteria (VEDOSS) (31) that are presenting with puffy fingers for less than 3 years and specific-antibodies but without signs of SSc-associated progressive symptoms. Among this patient group often within a year, half of the patients exhibit progressive SSc disease complications.

Determining CD7 overexpression and the presence of activated cytotoxic immune cells in patients' affected tissues is expected to shed light on whether CD7 expression in cytotoxic immune cells may be associated with progression to SSc and thus being involved in SSc severe disease initiation.

Additionally, the development of diagnostic tools to detect and quantify CD7+ cells or CD7 gene expression could improve patient stratification and therapeutic monitoring. Such tools could also have applications beyond CD7-depletion therapies, such as evaluating the effectiveness of treatments like anti-CD19 CAR T cell therapy in mitigating cytotoxic immune-mediated pathology in SSc.

Exploration of CD7 in Other Autoimmune Diseases

Investigating the role of CD7 in other autoimmune conditions may uncover shared pathogenic mechanisms and expand the therapeutic potential of CD7targeted approaches beyond SSc. For example, in diseases like rheumatoid arthritis (RA) and Sjögren's syndrome (SjS), activated cytotoxic T cells play a significant role in driving tissue damage in the synovium and salivary glands, respectively (8, 13, 14, 32). Although in these studies CD7-costimulation was not studied, based on our results, it is plausible to speculate that activated T and NK cells in the RA synovium and SjS salivary glands also exhibit elevated CD7 expression, and their targeted depletion could prove beneficial in alleviating disease progression.

In conclusion, targeting CD7 presents a promising strategy for selectively depleting pathogenic cytotoxic T cells and NK cells in systemic sclerosis, potentially mitigating disease progression and improving patient outcomes. Further research is warranted to fully elucidate the therapeutic potential of CD7 inhibition in SSc and other autoimmune diseases.

Chapter 4: Developing a novel 3D hydrogel myofibroblast contraction model to unravel cytotoxic T cell-mediated skin pathology in SSc and other CTDs

Summary

In Chapter 3, we identified a previously underappreciated pathogenic role of cytotoxic CD8+ T cells, rather than CD4+ T cells, in promoting tissue pathology in SSc. Beyond their canonical functions, such as potentially targeting skin endothelial cells through the release of cytotoxic molecules, these cells also demonstrated noncanonical functions by contributing to tissue fibrosis. To gain deeper insights into the underlying mechanisms, Chapter 4 focuses on investigating the interactions between adaptive immune cells (particularly T cells) and myofibroblasts. This is achieved by developing 3D hydrogel models to elucidate how these interactions drive tissue contraction and stiffness—hallmarks of fibrotic diseases like SSc. Using allogeneic mismatching to model autoreactive immune responses, our findings reveal that CD8+ T cells are more effective than CD4+ T cells in inducing myofibroblast-mediated hydrogel contraction. Surprisingly, this effect is not attributable to cytotoxic mechanisms but instead depends on cytokine-driven pathways, particularly JAK/STAT3 and TGF β signalling. Targeting these pathways demonstrates an additive effect in mitigating myofibroblast contraction by inhibiting both immune cell and myofibroblast activation. These insights shed light on the role of non-canonical CD8+ T cells in driving fibrosis and highlight novel therapeutic strategies to halt cytotoxic T cell-induced pro-fibrotic manifestations in fibrotic diseases such as SSc.

Discussion Points

The findings of this chapter provide critical insights into the mechanisms by which non-canonical CD8+ T cells contribute to fibrosis, emphasizing their non-cytotoxic, cytokine-mediated activation of myofibroblasts. This challenges the conventional view of CD8+ T cells as primarily cytotoxic effectors in autoimmune and fibrotic contexts. Myofibroblast-mediated tissue contraction is a major pathological feature in (SSc) fibrosis, perpetuating a mechanical feedback loop that reinforces myofibroblast activation and tissue remodeling (33). Our experiments demonstrate that the co-culture of CD8+ T cells with myofibroblasts strongly induces hydrogel contraction. Remarkably, this contraction occurs independently of classical cytotoxic mechanisms such as apoptosis or necrosis, as evidenced by the absence of markers like caspase-3 activation and γH2AX. Instead, the effect appears to be mediated by soluble factors, as supernatant transfer from co-cultures replicated the contractile phenotype in unexposed mono-cultured myofibroblasts.

Recent studies (34) exploring the phenotype and functional role of tissue resident CD8+ cytotoxic T cell populations in CTDs have determined a clear distinction between CD8+GZMB+T cells and CD8+GZMK+T cells. Classic cytotoxic CD8+T cells express GZMB and perforin and kill target cells, while the novel population of CD8+T cells predominantly expressing GZMK were found to be the core CD8+T cell population in affected tissues of patients with RA (35) and other CTDs (no data on SSc) where their functional role was not classically cytotoxic but they contributed in the induction of inflammatory cytokine production by nearby cells. In chapter 3,

we demonstrated elevated presence of CD8+GZMB+ T cells and not CD8+GZMK+ T cells in SSc-affected skin, suggesting that SSc CD8+ T cell pathology may deviate from the other CTDs. We found that CD8+GZMB+ T cells in SSc were infiltrated in close proximity to blood vessels and did not only produce cytotoxic molecules but also pro-fibrotic cytokines. Functional experiments of this chapter validate these findings as 3D hydrogel co-culture of immune cells with myofibroblasts led to elevated expression of GZMB but not GZMK in CD8+ T cells. In contrast to our findings, cross-talk between myofibroblasts and CD8+GZMK+ T cells has been described in the context of CTD (36), cancer (37), allergy (38), and GvHD (39). This interaction is mediated in vivo by chemokines released by (myo)fibroblasts and chemokine receptors expressed on CD8+GZMK+ T cells. It is possible that the release and expression of such mediators are impaired in the current model due to in vitro culture conditions. Alternatively, GZMK upregulation may require a longer co-culture duration compared to GZMB, or the cytokines produced by the coculture may preferentially drive CD8+T cell differentiation toward the GZMB subset rather than the GZMK subset. Furthermore, CD8+GZMB+ T cells did not show evident signs of cytotoxicity towards myofibroblasts suggesting that the same CD8+GZMB+T cells may be involved in SSc vasculopathy by GZMB-mediated killing of endothelial cells (1) but also in SSc pro-fibrotic disease manifestations with the release of pro-fibrotic cytokines such as IL-6, TGFB and OSM.

In the developed co-culture model of this chapter, allogeneic mismatching was used to model T cell auto-reactivity due to the rarity of autoreactive T cells in SSc patients, such as less than 0.5% of CD4+ T cells responding to topoisomerase-1 in anti-topoisomerase-positive patients (40). This approach also reflects sclerodermatous skin manifestations seen in chronic GVHD, and conditions like morphea, lichen, or eosinophilic fasciitis (41) that involve both CD4+ and CD8+ T cells (42). Allogeneic activation of T cells typically depends on direct recognition of mismatched MHC molecules or peptides presented by them (43). Typically, T cells are activated in a polyclonal response, with CD4+ and CD8+ populations showing similar activation and contribution of naïve versus effector phenotype (44, 45). Here, we indeed observed comparable CD4+ T cell and CD8+ T cell activation levels at 24 hours, with activation increasing to 40-80% by 72 hours. This escalation may involve cytokine-driven bystander activation, as significant T cell proliferation was not detected within this timeframe (46). Although our model relies on MHCdriven T cell activation, we cannot rule out that the intensity of this activation may exceed that of autoimmune T cells. Thymic selection relies on the affinity of interactions between T cell receptor-peptide major histocompatibility complex glycoprotein (TCR-pMHC). Moderate-affinity TCR-pMHC interactions facilitate the development of functional T cells through positive selection and within this process a number of self-reactive T cells escape central tolerance. Conversely, high-affinity (strong binding) TCR-pMHC interactions typically induce apoptosis in self-reactive thymocytes through negative selection. In an alloreactive response, T cells recognize foreign MHC molecules (with or without peptide) and TCR affinity is higher because TCRs are not negatively selected against foreign MHC molecules. That may lead to stronger activation compared to autoreactive T cells (47). Given this critical role of TCR-MHC signalling strength in shaping T cell responses, our model might overestimate the activation strength of autoreactive T cells.

Despite similar levels of activation in CD4+ and CD8+ T cells, as indicated by the upregulation of markers like CD25 and CD69, **CD8+ T cells were more effective** in driving myofibroblast-mediated contraction. This effect correlates with their cytokine profile, particularly elevated IL-6 production, rather than cytotoxicity. While CD4+ T cells contributed to myofibroblast activation (48), their role was less pronounced, possibly reflecting differences in their signalling interactions or effector functions. Notably, these findings may be supported by the low presence of effector CD4+ T cells and the large infiltration of pro-fibrotic CD8+ T cells observed in SSc skin, particularly in early disease stages. These observations align with emerging evidence (35) that CD8+ T cells can adopt cytokine-producing roles in certain pathological contexts, similar to CD4+ T helper subsets. This cytokine-driven activation may be influenced by myofibroblast signalling or interactions with the extracellular matrix (ECM) (49), as seen in cancer-associated fibroblast models (50).

The 3D co-culture activated both immune cells and myofibroblasts, with myofibroblasts showing elevated HLA type 2 and IL-6 expression, indicating an immunomodulatory phenotype driven by STAT3 signalling, as tofacitinib (a JAK/STAT3 inhibitor) significantly reduced these genes. TGFβ signalling regulated fibroblast activation protein (FAP) and matrix molecules (COL1, COL3), while the activation marker PDPN responded to both tofacitinib and TGFβ inhibition. This 3D coculture model is particularly effective in studying the interplay between immune and myofibroblast pathology, offering a dynamic and physiologically relevant platform to investigate these processes. Unlike traditional 2D co-culture models, the 3D environment better replicates the structural and mechanical properties of native tissue, facilitating the study of cell-matrix interactions, spatial organization, and mechanical signalling. The ECM's molecular, physical, and mechanical properties regulate immune cell mobility, survival, and function. Conversely, the immune system maintains ECM health and repairs it after injury. Dysregulation in this partnership contributes to disease pathology (51). These

features make our 3D hydrogel model representative of in vivo conditions, enabling deeper insights into the cellular and molecular mechanisms driving fibrotic and autoimmune pathologies.

Our data highlights the **pivotal role of JAK/STAT3 and TGFß signalling** in driving tissue contraction. Both pathways are well-established (52, 53) contributors to fibrotic diseases, including SSc. CD8+ T cells in our model produced higher levels of IL-6, a known STAT3 activator, compared to CD4+ T cells. Inhibition of these pathways, using tofacitinib (JAK/STAT3 inhibitor) and SB-505124 (TGFB receptor inhibitor), reduced tissue contraction and myofibroblast activation, demonstrating an additive effect when combined. These findings underscore the complex signalling interplay between immune cells and myofibroblasts in SSc fibrosis and further exhibit the value of the developed in vitro model in unraveling immune cell-mediated myofibroblast activation pathways.

Finally, in Chapter 3, we have demonstrated that pathogenic CD7+ CD8+ T cells were particularly elevated in SSc patients with early and severe disease (diffuse cutaneous), indicating that CD8+ T cell-mediated inflammation is likely a hallmark of early SSc pathogenesis. The hydrogel model developed in this chapter effectively mimics SSc skin pathology and further underscores the central role of CD8+ T cells in early disease processes. Specifically, we found that early interactions (within 24 hours) between CD8+ T cells and myofibroblasts were critical in driving myofibroblast activation, and this activation was only reversible through immediate or early intervention (within 24 hours) using the targeted inhibitors described. After myofibroblast contraction was established, the used inhibitors could not reverse contraction. In this case myofibroblast contraction may be reversed by killing the highly activated and contractile myofibroblasts with other therapies such as FAPdirected photodynamic therapy (54). Collectively, these findings highlight the urgency of addressing autoimmune inflammation in the early stages of SSc to prevent irreversible fibrosis.

Future Perspectives

1. Combined Targeting of Cytokine Signalling Pathways

Applying therapeutic strategies to inhibit JAK/STAT3 and TGFB signalling in both T cells and myofibroblasts offers a promising avenue for treating immune-mediated fibrosis by dual targeting of immune and stromal cells. Combination therapies targeting these pathways could effectively mitigate tissue contraction and myofibroblast activation.

2. Investigating Soluble Mediators

Furthermore, identifying the specific soluble mediators responsible for myofibroblast activation in CD8+ T cell co-cultures, such as IL-6 and TGF β , will provide insights into their mechanistic roles and therapeutic potential. Here, we observed that production of these soluble mediators was dependent on cell-cell interactions, thus future therapies halting the physical interaction between cytotoxic T cells and myofibroblasts could also be another approach to halt tissue fibrosis.

3. Exploring T Cell-Myofibroblast Interactions in ECM Contexts

Investigating how ECM stiffness and composition and myofibroblast signalling modulate T cell functions could uncover novel mechanisms underlying immune cell-mediated fibrosis. Recently, reduced expression of inhibitory collagen receptors such as LAIR-1 in tissue immune cells have been linked to elevated skin fibrosis in mouse models of SSc (55). Increased presence of functional LAIR-1 could be a future approach to treat the dysregulated ECM in SSc and other fibrotic diseases.

4. Expanding the Immune Landscape

While our study focuses on T cells and myofibroblasts, other immune cells, such as macrophages, are known to orchestrate fibrosis. Future studies should include a broader immune landscape to capture the full spectrum of immune-fibroblast crosstalk. Apart from cytotoxic T cells and innate immune cells, it is of interest to explore the potential pro-fibrotic role of innate lymphoid cells and natural killer cells.

Conclusion

This chapter underscores the central role of CD8+ T cells in myofibroblast-mediated tissue contraction and fibrosis. Their cytokine-driven activation of myofibroblasts, mediated by JAK/STAT3 and TGF β signalling, presents novel therapeutic targets for fibrotic diseases like SSc. By advancing our understanding of immune-myofibroblast crosstalk, these findings pave the way for more effective and targeted treatments.

Chapter 5: Systemic Sclerosis-related Pulmonary Arterial Hypertension is characterized by distinct T helper response

Summary

In the previous chapters, we demonstrated that non-canonical CD8+ T cell-mediated autoimmune inflammation is evident in the early stages of SSc. Our

findings suggest that patients with early and severe disease may derive the greatest benefit from therapeutic interventions targeting these cells and the pathways they activate. However, SSc is a highly heterogeneous disease and is challenging to treat, with many patients developing severe organ and/or tissue involvement later in the disease course.

Chapter 5 of this thesis focuses on the potential involvement of the immune system in SSc-associated vascular abnormalities, which are frequently observed in later stages of the disease. In particular, this chapter explores the relationship between peripheral T cell subsets and severe vascular disease, with an emphasis on pulmonary arterial hypertension (PAH). PAH is a life-threatening vascular complication affecting approximately 12% of SSc patients, typically in advanced disease stages and accounts for 50% of SSc mortality rates (56). Using in-depth flow cytometric analysis, this study examines circulating T cells in a well-stratified cohort of SSc patients with more longstanding disease, with and without PAH, alongside age- and sex-matched healthy controls and patients with idiopathic nonautoimmune PAH (IPAH).

Our results reveal that SSc patients exhibited distinct T cell profiles, characterized by elevated frequencies of peripheral helper T (Tph) cells, CD4+GZMB+ T cells, and IL-4-expressing CD4+CD8+ T cells, alongside decreased levels of Th1 cells compared to healthy donors. Additionally, both CD4+CD28- and CD8+CD28- T cells were significantly enriched in SSc patients, displaying heightened cytokine and cytotoxic signatures. These findings underscore a dysregulated immune response in SSc. Importantly, the presence of PAH in SSc patients was associated with a unique T helper cell profile, marked by increased frequencies of Th17 and Tph cells. Together, these results suggest a potential link between specific T cell subsets and SSc-associated vascular complications, highlighting the role of autoimmune inflammation in the progression of severe vasculopathy. This chapter emphasizes the need for further investigation into these immune parameters to elucidate their contributions to disease pathology and to identify novel therapeutic targets for managing SSc-related vascular abnormalities.

Discussion Points

Consistent with prior studies (18, 57), in chapter 5 we confirmed an expansion of IL-4/IL-13 and granzyme B-expressing CD4+ and CD8+ T cells in SSc compared to healthy blood. This finding reinforces the role of pro-fibrotic type-2 T cells and cytotoxic T cells in the systemic manifestations of SSc.

In Chapter 3, we observed that in SSc-affected skin of patients with early and severe disease pathogenic T cells with both cytotoxic and pro-fibrotic effector functions were predominantly CD8+ rather than CD4+. However, in SSc peripheral blood (chapter 5) in a cohort of patients with more long-standing disease, both CD4+ and CD8+ T cells appear to exhibit these pathogenic characteristics. This discrepancy could potentially be explained by an initial response of CD8+ T cells, rather than CD4+ T cells, to nuclear antigens (e.g. DNA topoisomerase I, ScI70) present in SScaffected tissues. In a proportion of patients, the clinical manifestations remain unchanged after the initial phase. This benign disease course may hypothetically result from endogenous tolerogenic mechanisms, such as the shielding of autoantigens by tissue fibrosis. In contrast, patients with a disease course complicated by severe vasculopathy may continue to generate autoantigens. The abundance, type, or location of these autoantigens could trigger adaptive immune processes, including CD4+T cell activation and epitope spreading. This may, in turn, initiate a broader systemic response involving CD4+ T cells at later stages of the disease. Similar immune responses in the differential contribution of CD8+ versus CD4+ T cells are observed in the clearance of viral infections (58). Immune response to viral infections involves an initial activation of CD8+ T cells that eliminate infected cells. This is followed by a systemic CD4+ T cell response that supports and enhances the immune response, by promoting B cell activation.

In Chapter 3, we demonstrated that cytotoxic autoimmune inflammation is predominantly evident in patients with early (< 3 years from first non-Raynaud symptom) and diffuse cutaneous SSc. Only a small proportion of the SSc patient cohort in this study (7 out of 30 patients) were in the early stages of the disease. This is potentially a confounding factor since the low number of patients with early SSc in this cohort does not allow to confidently address T cell subtype differences between patients with early or late disease stages. In fact, exploratory analysis (*Figure 1*) exhibited an elevated presence of CD8+ T cells in blood of patients with early SSc, while CD4+ T cells were enriched in patients with late and more established disease (> 3 years from first non-Raynaud symptoms). These observations suggest that the relative contribution of effector T helper and cytotoxic T cells may change during a severe disease course; early disease processes in SSc (both locally and systemically) are driven by CD8+ T cells, while CD4+ T cells are likely more involved in severe and late onset disease manifestations such as PAH.

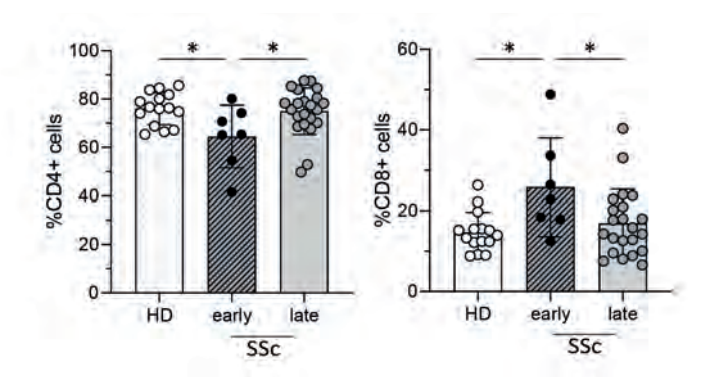


Figure 1. Percentage of circulating CD4+ T cells and CD8+ T cells in healthy donors (HD) and patients with early or late SSc.

Furthermore, in the blood circulation of SSc patients, we observed an expansion of both CD4+ and CD8+ exhausted-like T cell populations, characterized by the lack of expression of the co-stimulatory receptor CD28. These cells likely represent exhausted or hyporesponsive T cells resulting from chronic and recurrent activation triggered by persistent autoantigens (59). This finding has been previously reported in SSc (60) and other CTDs, such as RA (61-64) and SjS (65). What makes our findings particularly intriguing is that CD28-T cells in SSc blood exhibited elevated pro-fibrotic and cytotoxic functions compared to their CD28+ counterparts and that was particularly the case in SSc compared to healthy blood. This demonstrates that these T cells are not dysfunctional but remain functionally active. Similar observations have been made in SiS peripheral blood, where CD8+CD28- T cells displayed increased cytotoxicity and pro-inflammatory functions compared to their CD28+ counterparts (66). These results suggest that SSc blood circulation contains an increased proportion of CD28-'exhausted' T cells. However, rather than being anergic, these cells appear functionally adapted in a manner that may exacerbate tissue destruction. Since these cells lack CD28 co-stimulation, TCR;pMHC binding is unlikely to drive their expansion in SSc. Instead, it has been documented that CD8+CD28- T cells may expand in response to cytokines secreted by other innate and adaptive immune cells (67). Expansion of CD28 null T cells has been also linked to aging and viral infections e.g. with cytomegalovirus (CMV). In our cohort, patients and healthy controls were age matched making it unlikely that such differences are attributed to age. Unfortunately, were unable to retract information on CMV infection status of the included subjects, however, research from other autoimmune diseases such as SLE has shown that CMV can be not only a trigger but may also exacerbate an already aberrant expansion of these cells (68). This finding, together with analyses presented on chapter 3, may reinforce the limited effectiveness of targeting CD28 co-stimulation with abatacept in SSc (69), as CD28 co-stimulation does not appear to be necessary for T cells to exert their pathogenic effector functions. Of note, nearly all (in average 90.8%) of CD8+CD28-T cells in SSc blood express CD7 and can be effectively eliminated in vitro by anti-CD3/CD7-IT treatment (*Figure 2*), suggesting that this aberrant T cell population would be also targeted in vivo with CD7-directed therapies such as the one described in chapter 3.

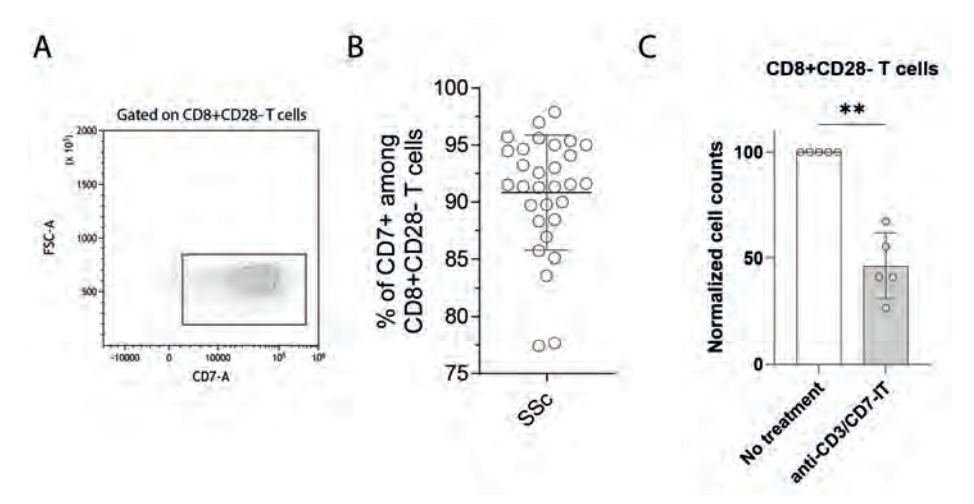


Figure 2. (A, B) Nearly all CD8+CD28-T cells express CD7. (C) CD8+CD28-T cells are eliminated in vitro by incubation of PHA-activated PBMCs with anti-CD3/CD7-IT treatment for 24 hrs.

By now, the implication of T cells in SSc-related inflammatory and pro-fibrotic manifestations is well established. However, the potential involvement of T cells in **SSc vascular complications**, such as PAH has not yet been explored. In Chapter 5 of this thesis, we present, for the first time, evidence that SSc patients with PAH exhibit a distinct T helper cell profile compared to those without PAH. Specifically, these patients show an elevated presence of T peripheral helper (Tph) and Th17 cells in their blood circulation. Of note, patients with idiopathic PAH (IPAH) did not differ significantly in percentage of Th17 and Tph cells compared to SSc patients, but they exhibited a unique Th2 enriched phenotype in their blood circulation. These findings suggest a potential involvement of distinct T helper-driven immune responses in the vascular complications of SSc. In SSc-PAH patients' serum elevated levels of the Th17 signature cytokine IL-17 have been observed (70, 71) reinforcing their involvement in disease although Th17 cells are not the only cells producing this cytokine. The increased presence of Th17 cells likely reflects the recruitment of inflammatory cells to the pulmonary arteries, contributing to their sustained vasoconstriction and vascular remodeling (72). This hypothesis is supported by studies showing that injection of Th17 but no other Thelper cells in immunodeficient mice was accompanied by microvascular PAH-like complications (73). Elevated Th17

polarization in PAH has been found to be mediated by disease modified monocyte derived dendritic cells (74). However, the potential mechanism of Th17-mediated vascular dysfunction in terms of the effect these cells have on primary endothelial cells in patients' affected tissues remains unclear. A definitive answer to this question is hampered by the inability of sampling and performing functional experiments with immune and stromal cells that reside in the pulmonary artery of SSc-PAH patients.

In addition to elevated Th17 cells, patients with SSc-PAH also exhibited increased percentages of Tph cells. This is a novel finding that has not been described before, and it suggests that humoral inflammation may be involved in SSc-PAH. This is because the main functional role of Tph cells is to help B cell maturation. class-switching and auto-antibody production. Furthermore, the presence of autoantibodies has been previously linked to development of SSc-related PAH compared to other forms of PAH (75, 76). Given that Tph cells play a central role in instructing B cells to produce antibodies, their enrichment in SSc-PAH may provide a mechanistic explanation for the elevated auto-antibody presence in SSc-PAH patients. However, it is still elusive whether these Tph cells are autoreactive or bystander. In these regards, examining the potential TCR specificity of these cells towards certain SSc autoantigens such as DNA topoisomerase I with tetramers or in vitro T cell activation assays may shed light to this question. This knowledge not only enhances our understanding of PAH pathogenesis in SSc but also identifies potentially novel therapeutic targets to halt or reverse the disease process.

Identifying T cell populations that correlate with PAH could lead to the development of novel biomarkers that assist in the early detection of this very severe and often fatal complication of SSc (77). Early diagnosis of PAH in SSc patients is critical for improving prognosis, as current diagnostic methods often detect PAH at more advanced stages (78). Early screening for PAH in patients with SSc identified a novel eight-protein biomarker panel that has the potential to assist in the detection of PAH (79). However, defining such biomarkers presents significant challenges often pertaining to large patient heterogeneity overlapping clinical features between SSc-PAH and other SSc-related disease complications. To address these challenges, we conducted analysis in a well-defined patient cohort with equal numbers of patients with or without PAH that did not exhibit other significantly different clinical parameters such as for example limited or cutaneous form of the disease or enriched presence for certain auto-antibody profiles. Detection of specific T cell subsets involved in SSc-PAH is expected to lead to the identification of more precise soluble biomarkers based on T cell profiles, improving early diagnosis of PAH in SSc patients. Unlike general inflammatory or autoantibody markers, which often reflect systemic immune activation or an indirect response, specific T cell subsets may perform better in early diagnosis of SSc-PAH and its severe complications. This direct involvement increases the likelihood that changes in these T cells will closely correlate with PAH development and progression, suggesting that T cell biomarkers may offer higher specificity and sensitivity for PAH. In the field of oncology, lymphocyte subsets and soluble T cell released biomarkers such as TRAIL and CD40L were proved more suitable in predicting disease progression compared to traditional systemic inflammatory biomarkers (80-82). Although these findings hold promise, validating T cell subsets as biomarkers will require robust, multicenter studies with diverse SSc cohorts. Addressing variability in disease presentation and comorbidities will be crucial to ensure the reproducibility and clinical applicability of our findings.

Finally, our findings indicate the potential for incorporating inflammation-targeted therapeutic approaches into the treatment strategy for PAH in SSc. PAH-specific medications currently in use such as prostacyclin, endothelin receptor antagonists and phosphodiesterase inhibitors are largely derived from studies on IPAH due to the smaller population of patients with SSc-PAH. Although SSc-PAH and idiopathic PAH share clinical and hemodynamic similarities, vasoactive therapy is known to be less effective in treating SSc-PAH (74, 83). This is likely due to the increased importance of autoimmune inflammation in causing or worsening PAH in SSc. However, the exact involvement of these T cell subsets in SSc-PAH pathology remains to be defined.

Future Perspectives

- 1. Validation of distinct T helper cell responses as Biomarkers: Future studies should aim to validate the identified T cell subsets as reliable biomarkers for PAH in larger, independent cohorts. This validation is crucial for assessing their clinical utility and their potential to enhance the early diagnosis of PAH in SSc patients. Additionally, investigating the infiltration of these T cell populations within the pulmonary vasculature of SSc-PAH patients, as well as exploring their potential correlation with circulating levels, is anticipated to strengthen their credibility as biomarkers. These efforts will contribute to a more robust understanding of their role in disease pathogenesis and their application in clinical practice.
- Functional Studies of expanded T Cell populations: Further research is
 essential to elucidate the functional roles of the expanded T cell populations
 in SSc-PAH. Understanding how these cells may contribute to vascular damage

will provide critical insights into their involvement in disease progression and may reveal novel therapeutic targets. Investigating this, in vitro coculture studies of sorted Th17 and Tph cells with human endothelial cells or vascular organoids are proposed as an initial step to assess their effects on endothelial cell function in comparison to other T cell subsets. Subsequently, animal models of PAH in SSc are expected to offer valuable opportunities to explore the mechanisms through which T cells contribute to microvascular dysfunction in greater detail. For instance, pharmacologic or genetic depletion of Th17 and Tph cells in the Fra-2 (Fos-related antigen-2) transgenic mouse model of systemic sclerosis is hypothesized to mitigate vascular remodeling in this model (84). These studies will provide a deeper understanding of the pathogenic role of T cells and inform the development of targeted therapies. Further research is needed to understand the functional roles of the expanded T cell populations in SSc with PAH. Investigating how these cells contribute to vascular damage will provide deeper insights into their involvement in disease progression and potentially uncover new therapeutic targets.

3. Therapeutic Targeting of pro-inflammatory T Cells: PAH-specific medications currently rely heavily on data extrapolated from IPAH studies, primarily due to the limited number of patients with SSc-PAH. If specific T cell subsets are confirmed to play a central role in PAH development, strategies aimed at modulating these immune cells could be explored as potential therapeutic approaches. Immune modulation, through targeted therapies or immune checkpoint inhibitors, could help reduce vascular inflammation and prevent further damage. Notably, a multicenter, doubleblind, randomized, placebo-controlled trial investigated the safety and efficacy of B cell depletion with rituximab for the treatment of SSc-PAH. The study found that low levels of soluble lymphocyte derived biomarkers were sensitive and specific predictors of a favorable response to rituximab (85). These findings suggest that assessing lymphocyte phenotypes and/or their soluble mediators could help identify patients who are more likely to benefit from certain immunotherapies. For example, in our patient cohort SSc-PAH patients with the highest levels of Tph cells, cells providing B cell help, are expected to benefit greatly from a B cell directed immunotherapy such as rituximab. Looking ahead, there is considerable potential for future drug trials specifically tailored to the SSc-PAH population, aiming to address the efficacy of targeting pro-inflammatory T cells to improve poor survival outcomes of SSc-PAH patients and their reduced responsiveness to current treatments.

In conclusion, this chapter demonstrates that T cell profiling in SSc patients with PAH offers valuable insights into the immunopathogenesis of vascular complications. The identification of T cell subsets associated with PAH severity has the potential to provide novel biomarkers for early diagnosis, improving patient outcomes. Further

research into the functional roles of these T cells and their potential as therapeutic targets could pave the way for more effective treatment strategies for patients with severe vasculopathy in SSc.

Chapter 6: A novel nuclear antigen-specific TRAIL+ CD4+ T cell subset with type 1 interferon stimulated gene signature regulates autoimmune responses in the active lymph nodes of patients with CTDs

In the previous chapters, we explored the pathogenic role of T cells in the blood and affected tissues of SSc patients, identifying specific cytotoxic and helper T cell subsets involved in the early and late stages of the disease. Similar patterns, implicating distinct CD4+ T cell and CD8+ T cell subsets in relation to different disease stages, pathological disease subsets and symptoms, have also been observed in other connective tissue diseases (CTDs) such as SjS (86). However, a critical question remains: are these pathogenic T cell subsets autoreactive—targeting specific autoantigens such as for example Scl70 in SSc or Ro60/La in SjS—and directly driving autoimmune processes, or do they constitute a pathogen reactive response, e.g. against virally infected cells, or arise as a byproduct of tissue inflammation mediated by innate immune mechanisms, e.g. elicited by DNA damage from environmental pollutants?

Antigen-specific T cell responses from affected tissues and locoregional active lymph nodes play a central role in regulating humoral immunity against pathogens, cancer, and autoantigens, promoting infection resolution and cancer targeting but also contributing to tissue destruction in autoimmunity (87). The effectiveness of autologous stem cell transplantation and anti-CD19 CAR T cell therapy highlights the importance of eliminating autoreactive immune responses in treating autoimmune CTDs (88, 89), however the mechanisms underlying CTD tissue antigen-specific T cell responses remain poorly understood.

To address this, Chapter 6 of this thesis shifts focus from the affected tissues to the lymph nodes (LNs) because the latter play a central role in propagating antigen-

specific T cell responses. By studying locoregional LNs, we aim to determine whether distinct T cell-mediated tissue pathologies seen across CTDs are orchestrated by autoreactive T cell responses withing active locoregional LNs. Importantly, these analyses were conducted not only in patients with SSc but also included SiS patients as a comparator group. SjS, another CTD characterized by reactivity to nuclear antigens, presents distinct pathological features of the affected exocrine glands, i.e. an extensive infiltrate of activated CD4+ T cells and B cells, and thereby provides a valuable contrast to SSc.

Summary

The characterization of autoreactive responses, particularly their phenotype and function within affected tissues and active lymph nodes, has been challenging due to technical difficulties in identifying and isolating these rare cell populations. To overcome this difficulty, in chapter 6, we developed a toolkit that combines 18-Fluorodeoxyglucose (FLT) positron emission tomography (PET) imaging, multiplex immunohistochemistry, single-cell RNA sequencing, and autoantigen T cell activation assays to detect, biopsy and analyze autoreactive T cell responses in patients' blood, LNs and affected tissues.

In the active lymph nodes of SiS patients, the autoreactive immune response to NAgs involved a strong interaction between APCs, B cells, and T cells, resulting in a broad CD4+ T cell and B cell-driven autoreactive response that explains the extensive APC/CD4+ T cell/B cell aggregates seen in inflamed SGs. In contrast, SSc displayed limited APC/T/B cell interactions in response to NAgs, largely due to the dominance of extrafollicular NAg-specific CD4+ TRAIL+ interferon-stimulated gene (ISG) signature T cells. These cells exhibited an immunoregulatory function by restricting plasma cell generation, reducing APC activation, and diminishing the effector CD4+ T cell-mediated B cell help response. Notably, these TRAIL+ CD4+ T cells were absent in non-reactive LNs and affected tissues of SSc patients, emphasizing their association with antigen-specific immune responses particularly withing inflamed LNs.

In SSc, the TRAIL+ CD4+ T cell subset was enriched, potentially contributing to the restricted APC-CD4+ T cell-B cell interactions and reduced antibody-mediated immune responses observed compared to the robust follicular and extrafollicular responses in SjS. Decreased soluble TRAIL levels in SSc cases with severe vascular complications underscored their potential role in moderating disease severity in SSc patients. These findings pave the way for designing novel (antigen-specific) immunotherapies that enhance TRAIL expression in autoreactive T cells to balance

Discussion points

The findings in this chapter highlight distinct immune mechanisms in regulating antinuclear antigen-specific responses in SjS and SSc LNs, underscoring the dual role of nuclear antigen-specific CD4+T cells in either enhancing or restricting systemic autoimmunity. Contrary to the longstanding belief that autoreactive CD4+ T cells primarily drive tissue damage and autoimmunity, our findings reveal a clear distinction between pathogenic and protective nuclear antigen-specific CD4+ T cell responses across different CTDs. In SiS, NAq-specific CD4+ T cells providing B cell help, enriched at follicular, extrafollicular, and affected tissue sites, exhibited significant TCR expansion and played a key role in germinal center-like structure formation, promoting high-affinity autoreactive antibody production and driving tissue inflammation, corresponding to the wide autoantibody repertoire typically observed in SiS (90). In contrast, these cells, as well as Th2 pro-fibrotic T cells that have been widely suggested to be involved in SSc fibrosis, were absent in SSc. Instead, we identified a novel TRAIL+ ISG CD4+ T cell subset in active LNs of SSc patients, which appears to suppress APC activation thereby reducing the expansion of autoreactive CD4+ effector T cells and limiting plasma cell differentiation in active LNs. These results suggest that CD4+TRAIL+ ISG T cells may prevent further autoimmune exacerbation by counteracting mechanisms like epitope spreading and affinity maturation, which could potentially explain the reduced antibody diversity and titers observed in SSc (91). The enriched presence of these cells in SSc active LNs and blood likely contributes to the milder antibody-mediated pathology in SSc compared to SiS (92-94).

TRAIL, a type II transmembrane protein of the TNF superfamily, closely resembles the Fas ligand and induces apoptosis by binding to death receptors (DR4/DR5), activating the caspase cascade. However, primary immune cells are generally resistant to TRAIL-induced apoptosis. Beyond its known role in cancer cell death, the broader function of TRAIL remains unclear. CD4+ TRAIL+ T cells have primarily been studied in peripheral blood and affected tissues in vasculopathy and atherosclerosis, where they contribute to disease activity by killing vascular smooth muscle cells, but no ISG gene signature has been reported in these cells. In contrast, we identified a novel subset of CD4+ TRAIL+ ISG T cells, predominantly found in the active lymph nodes of SSc and SjS patients, but rarely in blood or affected tissues. This subset uniquely co-expressed the death receptor TRAIL and a type I IFN gene signature, exhibiting a naïve-like phenotype with features of autoreactivity, relative

quiescence, and antigen specificity. Notably, antigen-specific CD4+ ISG T cells with TCR expansion were recently identified in systemic lupus erythematosus (95). The ISG response in these cells may have evolved as a regulatory mechanism to counteract proinflammatory autoreactive responses triggered by stromal tissue damage or viral infections that exploit APCs. As such, these cells may act as a protective brake on ANAg-specific humoral immune responses linked to tissue damage. The relative increase of these cells in SSc could result from a lowimmunogenic autoantigen response, potentially due to the absence of CD40L stimulation, or from a more antiviral-like immune response.

A protective role of TRAIL+CD4+ T cells towards robust adaptive immune response was further suggested by their spatial localization within active LNs. With the use of multiplex immunohistochemistry these cells were localized within lymph node T cell zones surrounding GC-like structures, potentially present to safe-guard an active humoral immune response. In SSc patients, where no GC-like structures were observed, these cells were dispersed throughout the tissue and in close proximity to DR4+APCs. Given that no effector NAg-specific CD4+ T cell were detected in SSc active LNs and affected skin, it is plausible to suggest that the differential regulation of NAq-specific TRAIL+CD4+ T cells in locoregional LNs of SiS compared to SSc contributes to the contrasting infiltration patterns of CD4+ T cells and B cells in SjS salivary glands versus SSc skin. In line with this hypothesis, recent single-cell RNA sequencing studies have showed a very limited infiltration of B cells in SSc skin (16). Also, in our study in Chapter 3, we found no increase in CD4+T cells in SSc skin compared to healthy skin.

In fact, in chapter 3 we showed that fibrosis in skin and lungs is driven by cytotoxic CD8+ T cells and NK cells producing pro-fibrotic cytokines, independent of plasma cell formation. Additionally, compared to SjS salivary glands, SSc-affected tissues and blood exhibited a dominant presence of antigen-reactive CD8+ T cells compared to CD4+ T cells, indicating that SSc skin vasculopathy and fibrosis is potentially driven by CD8+ autoreactive T cells. The significantly lower presence of autoreactive CD4+ compared to CD8+ effector T cells in SSc skin could be at least partially explained by our mechanistic in vitro data, exhibiting that blocking of the TRAIL-DR4 axis is involved in elevated generation of CD4 effector T cells. Still, in these experiments the effect of blocking this immunoregulatory axis towards generation of autoreactive effector CD8+ T cells was not examined. Nonetheless, like professional regulatory T cells (96, 97), this novel regulatory CD4+ TRAIL+ T cell subset may have a preferential effect towards restricting autoreactive effector CD4+ rather than CD8+ T cell responses. To our knowledge, the differential effect of TRAIL on CD4+ and CD8+ effector T cells has not been adequately examined, but it has been shown that TRAIL inhibits formation of effector Th17 cells (98). In line with this hypothesis, CD4+CD25+ Tregs can suppress the function of CD4 effector T cells by upregulating TRAIL in a TRAIL/DR5 but not FAS/FASL dependent manner (99).

Clinically, we found a negative correlation between systemic soluble TRAIL levels and SSc clinical parameters reflective of severe vascular complications such as N-terminal prohormone of brain natriuretic peptide and New York heart association functional class. The correlation between reduced TRAIL levels and disease severity in SSc patients, particularly in cases with pulmonary arterial hypertension (PAH), provides further evidence that supports a protective role of this novel T cell **subset** and highlights the potential of TRAIL+ T cells as biomarkers of disease activity and progression in SSc and other systemic CTDs. This hypothesis may be further supported by the elevated presence of T helper cells providing B cell help in SSc-PAH patients that we observed in the previous chapter. Likely low release of TRAIL reflects reduced presence of TRAIL+ CD4+ T cells in these patients, and this could be involved in the elevated B cell help CD4+ T cell profile in these patients' blood. Taken together, these findings suggest that in this subset of SSC patients, a severe disease course may result from the evasion of a CD4+ TRAIL+ ISG T cell regulatory response that leads to a stronger adaptive immune response and is possibly attributed to the prevalent tissue damage in these patients or to differential upregulation of surface receptors like CD40 in APCs. Likely, CD40 upregulation counteracts TRAIL expression leading to generation of effector CD4+CD40L+T cells, B cell activation and epitope spreading.

Nonetheless, such a protective role of TRAIL+ T cells still needs to be established in larger SSc patient cohorts. It is also to be examined whether TRAIL+CD4+ T cells exhibit similar regulatory functions in other CTDs such as RA and SLE. This is expected to potentially assist in the development of a therapeutic approach that can halt auto-antibody mediated pathology in more autoimmune diseases. Studies on animal models of RA (100, 101) and MS (98) have exhibited a protective role of TRAIL towards restricting disease symptoms, but whether the source of TRAIL was attributed to T cells or other immune cells remains elusive.

Future Perspectives

Validation of TRAIL+ CD4+ T Cell Function:

The unique ISG signature and antigen specificity of the TRAIL+CD4+ T cells offer potential biomarkers for disease stratification. To confirm this, large multicenter studies are required to validate the negative correlation between

serum levels of TRAIL and severe vascular disease complications. Furthermore, the role of TRAIL+ CD4+ T cells as regulatory mediators in systemic autoimmunity needs to be confirmed with mechanistic experiments in relevant animal models. For example, a specific knock down of TRAIL in CD4+ T cells in topoisomerase I-induced mouse model of SSc or the NOD mouse model is hypothesized to lead to increased fibrosis and elevated antibody production and salivary gland tissue damage respectively. Comparative studies of patients affected by other autoimmune and non-autoimmune conditions where TRAIL+ T cells have been implicated, such as myocardial infarction and vasculitis, could provide valuable insights into shared and disease-specific mechanisms of immune regulation.

Additionally, emergent single-cell technologies, such as high-resolution spatial transcriptomics, single-cell phosphoproteomics, and single-cell metabolomics, could provide deeper insights into the functional states and signalling dynamics of TRAIL+ CD4+ T cells in disease progression. Moreover, inducible CRISPR-Cas9-mediated knockdown of TRAIL in ex vivo assays using patient-derived lymph node biopsies, cultured PBMCs, or humanized SCID mouse models could further elucidate its immunoregulatory role and therapeutic potential in systemic autoimmunity.

Therapeutic Implications: 2.

Antigen-specific therapies offer the potential to target harmful autoreactive lymphocytes, such as autoreactive follicular T cells and plasma cells, while maintaining protective immune responses. Targeting the TRAIL-DR4 axis could provide novel strategies to modulate autoreactive immune responses in systemic autoimmunity. Our findings suggest that promoting TRAIL expression in autoreactive CD4+ T cells could form the basis for novel tolerogenic vaccine strategies. These vaccines could incorporate antigens relevant to SSc autoimmunity, such as topoisomerase-1, alongside adjuvants that selectively enhance TRAIL signalling. Alternatively, overexpressing immunodominant TCR sequences of CD4+TRAIL+ T cells could be another alternative to increase function of these cells. Such approaches may reduce systemic autoantibody production and associated pathology in CTDs. Additionally, novel immune checkpoint modulators targeting TRAIL pathways could promote TRAIL+ T cell differentiation to restore immune balance. While advancements have addressed challenges in similar approaches for cancer, key therapeutic hurdles remain, including minimizing off-target effects and identifying the optimal stage of disease for intervention.

Additionally, identification of the pathways mediating CD8+ T cell activation within active LNs and CTD affected tissues is vital in halting disease pathology in CTDs such as SSc, where tissue destruction seems to be primarily driven by cytotoxic immune cells. Incorporating adjuvants that inhibit dendritic cell-mediated CD8+ T cell activation may be necessary in tolerogenic vaccines. For instance, studies have demonstrated that vitamin D can modulate dendritic cell function, leading to reduced activation of CD8+ T cells (102).

Furthermore, analyses of this chapter did not only reveal TCR sequences with immunoregulatory role, but we also determined TCR sequences of pathogenic follicular and effector CD4+ T cells that were enriched in LN and salivary glands of patients with SiS. Building on the success of anti-CD19 CAR T cell therapy in systemic autoimmunity, designing CAR T cells to target pathogenic and immunodominant TCR sequences could offer a future therapeutic approach to selectively deplete pathogenic T cells while preserving B cells. Given the variability of such TCR sequences across different patients, however, developing a universal CAR T cell therapy targeting pathogenic TCRs presents significant challenges in terms of feasibility and cost. Instead, an alternative approach could involve engineering regulatory T cells (Tregs) with synthetic TCRs designed to modulate autoimmune responses in a more targeted manner. This strategy could provide a more tailored and regulatory mechanism to restore immune tolerance without the broad immunosuppressive effects associated with B cell depletion, thereby preserving immune function, reducing infection susceptibility, and improving vaccine responses in patients.

3. Broadening Applications to Other Autoimmune Diseases:

Investigating the role of TRAIL+ T cells in other autoimmune conditions such as systemic lupus erythematosus and rheumatoid arthritis could uncover shared regulatory pathways and extend therapeutic potential.

Conclusion

This chapter highlights the discovery of CD4+ TRAIL+ T cells as a regulatory subset uniquely associated with reactive LNs in SSc and SjS. These cells play a pivotal role in moderating antigen-specific immune responses, with a more pronounced regulatory function observed in SSc. The findings underscore the importance of TRAIL+ T cells in shaping disease outcomes and suggest their potential as therapeutic targets for mitigating autoimmune-mediated pathology. Further research is warranted to explore the mechanisms of driving TRAIL+ T cell

differentiation and to harness their regulatory capabilities for therapeutic benefit in systemic autoimmune diseases.

Overall conclusions and final considerations

The main objective of this thesis was to elucidate the role of autoreactive T cell responses in the pathology of SSc and other CTDs. Despite their potential involvement, the functional role of autoreactive T cells in active LNs and CTDaffected tissues remains poorly understood due to the challenges associated with detecting these rare cell populations. To address this gap, we developed an innovative toolkit that integrates advanced PET imaging of immunologically active tissues with single-cell multiomic technologies, multiplex immunohistochemistry, and functional in vitro assays to characterize autoreactive T cell responses in tissue.

The work presented in this thesis is the first to elucidate the distinct roles of nuclear antigen autoreactive T cells in immunologically divergent CTDs, such as SSc and SjS. These roles are linked to specific disease manifestations and significantly advance our understanding of the extent and level of involvement of different pathogenic T cell subsets in various CTDs, as well as in different disease stages in patients with SSc. In contrast to well-known B cell-driven CTDs like SjS, the disease pathology in SSc is primarily driven by autoreactive CD8+ T cells, rather than by effector CD4+ T cell-B cell interactions. This distinction is attributed to the differential orchestration of effector versus regulatory ANAq-specific responses originating from locoregional lymph nodes.

These findings prompt a relevant discussion on the long-standing debate regarding whether SSc is a CTD primarily driven by autoimmune responses. While the presence of disease-specific autoantibodies supports the involvement of humoral immune abnormalities, SSc also presents with significant vasculopathy and fibrosis, raising the question of whether autoimmunity is the primary driver or a secondary consequence of endothelial and fibroblast dysfunction. The findings of this thesis clarify this question and contribute to the ongoing debate, demonstrating that autoimmune inflammatory manifestations are prevalent in early disease stages of patients with severe disease. Furthermore, we exhibited distinct involvement of cytotoxic versus helper T cells in distinct disease stages and patient subtypes, which report on novel biomarkers of disease severity and progression. However, whether autoreactive responses play a role in disease initiation remains unexplored. To address this, we will utilize our developed toolkit in a unique patient cohort from our hospital, comprising individuals with very early vascular symptoms who may or may not progress to SSc (NCT03059979). Notably, half of these patients developed SSc with autoimmune and fibrotic features, providing an opportunity to investigate whether the autoreactive T cells and pathogenic processes identified in this thesis contribute to the transition from very early vascular dysfunction to fully progressed SSc.

Although this thesis highlights the role of the adaptive immune system in both early and late manifestations of SSc, it remains unclear whether targeting a single cell compartment, such as immune abnormalities driven by autoreactive T cells, is sufficient for effective treatment. Given the complex nature of SSc—characterized by immune activation, endothelial dysfunction, and fibrosis—this is unlikely. This notion is reinforced by the failure of current immune-modulating therapies, including the most effective strategies such as ASCT and anti-CD19 CAR T cells, to fully reverse fibrosis or restore vascular integrity. Our findings suggest that a combination of immune-targeting therapies and antifibrotic agents may yield better outcomes. However, the high toxicity profile of antifibrotic agents remains a significant challenge. Alternatively, specific elimination of the pathogenic autoreactive T cells in very early SSc disease stages, where fibrosis and vascular dysfunction is not yet established might be effective in preventing disease progression. According to this hypothesis and based on the promising results described in this thesis, we are currently running a proof-of-concept clinical trial of treating early SSc patients with anti-CD3/CD7 IT to assess whether depletion of the pathogenic cytotoxic immune cells in early disease stages can cause long-term disease remission.

References

- Maehara T, Kaneko N, Perugino CA, Mattoo H, Kers J, Allard-Chamard H, et al. Cytotoxic CD4+ T lymphocytes may induce endothelial cell apoptosis in systemic sclerosis. J Clin Invest. 2020:130(5):2451-64.
- Sun L, Su Y, Jiao A, Wang X, Zhang B. T cells in health and disease. Signal Transduction and Targeted Therapy. 2023;8(1):235.
- 3. El-Halwagi A, Agarwal SK. Insights into the genetic landscape of systemic sclerosis. Best Practice & Research Clinical Rheumatology. 2024;38(4):101981.
- Tsai S, Santamaria P. MHC Class II Polymorphisms, Autoreactive T, and Autoimmunity. Frontiers in Immunology, 2013:4.
- Acosta-Herrera M, Kerick M, Lopéz-Isac E, Assassi S, Beretta L, Simeón-Aznar CP, et al. Comprehensive analysis of the major histocompatibility complex in systemic sclerosis identifies differential HLA associations by clinical and serological subtypes. Annals of the Rheumatic Diseases. 2021;80(8):1040-7.
- Mayes Maureen D, Bossini-Castillo L, Gorlova O, Martin José E, Zhou X, Chen Wei V, et al. Immunochip Analysis Identifies Multiple Susceptibility Loci for Systemic Sclerosis. The American Journal of Human Genetics. 2014;94(1):47-61.
- Collier JL, Weiss SA, Pauken KE, Sen DR, Sharpe AH. Not-so-opposite ends of the spectrum: CD8(+) T cell dysfunction across chronic infection, cancer and autoimmunity. Nat Immunol. 2021;22(7):809-19.
- Moon J-S, Younis S, Ramadoss NS, Iyer R, Sheth K, Sharpe O, et al. Cytotoxic CD8+ T cells target citrullinated antigens in rheumatoid arthritis. Nature Communications. 2023;14(1):319.
- Wakasugi S, Akiyama M, Yoshimoto K, Inukai R, Matsuno Y, Ishigaki S, et al. OP0071 CX3CR1-POSITIVE CYTOTOXIC T CELLS SPECIFICALLY CONTRIBUTE TO THE PATHOGENESIS OF ELDERLY-ONSET AND DIFFICULT-TO-TREAT RHEUMATOID ARTHRITIS. Annals of the Rheumatic Diseases. 2024;83(Suppl 1):52-3.
- 10. Chang MH, Levescot A, Nelson-Maney N, Blaustein RB, Winden KD, Morris A, et al. Arthritis flares mediated by tissue-resident memory T cells in the joint. Cell Rep. 2021;37(4):109902.
- 11. Blanco P, Pitard V, Viallard J-F, Taupin J-L, Pellegrin J-L, Moreau J-F. Increase in activated CD8+ T lymphocytes expressing perforin and granzyme B correlates with disease activity in patients with systemic lupus erythematosus. Arthritis & Rheumatism. 2005;52(1):201-11.
- 12. Xiong H, Cui M, Kong N, Jing J, Xu Y, Liu X, et al. Cytotoxic CD161<sup>−</ sup>CD8⁺ T_{EMRA} cells contribute to the pathogenesis of systemic lupus erythematosus. eBioMedicine. 2023;90.
- 13. Kaneko N, Chen H, Perugino CA, Maehara T, Munemura R, Yokomizo S, et al. Cytotoxic CD8+T cells may be drivers of tissue destruction in Sjögren's syndrome. Scientific Reports. 2022;12(1):15427.
- 14. Tasaki S, Suzuki K, Nishikawa A, Kassai Y, Takiguchi M, Kurisu R, et al. Multiomic disease signatures converge to cytotoxic CD8 T cells in primary Sjögren's syndrome. Annals of the Rheumatic Diseases. 2017;76(8):1458-66.
- 15. Xu T, Zhu H-X, You X, Ma J-F, Li X, Luo P-Y, et al. Single-cell profiling reveals pathogenic role and differentiation trajectory of granzyme K+CD8+T cells in primary Sjögren's syndrome. JCI Insight. 2023;8(8).
- 16. Gur C, Wang SY, Sheban F, Zada M, Li B, Kharouf F, et al. LGR5 expressing skin fibroblasts define a major cellular hub perturbed in scleroderma. Cell. 2022;185(8):1373-88.e20.

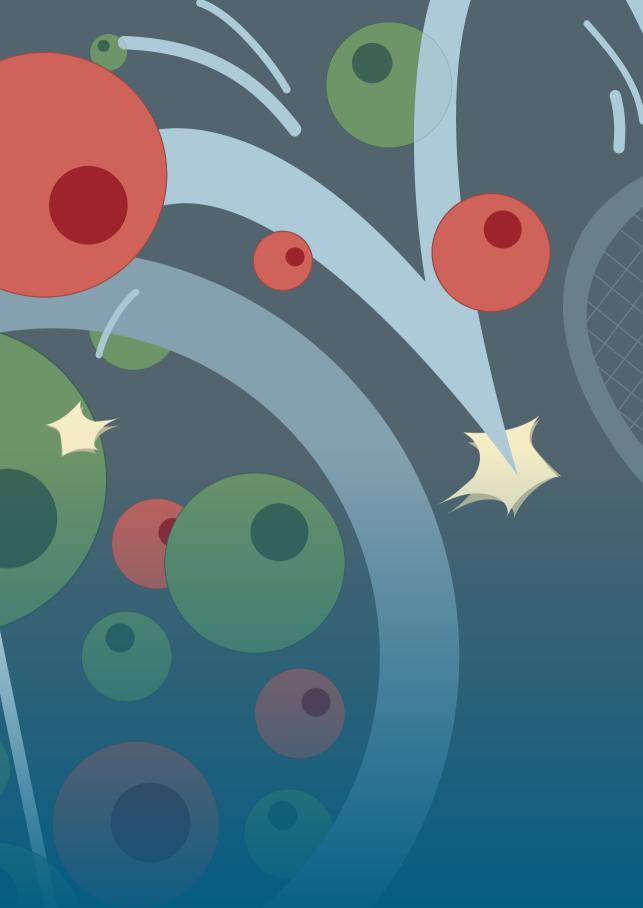
- 17. Padilla CM, Valenzi E, Tabib T, Nazari B, Sembrat J, Rojas M, et al. Increased CD8+ tissue resident memory T cells, regulatory T cells and activated natural killer cells in systemic sclerosis lungs. Rheumatology. 2023;63(3):837-45.
- 18. Fuschiotti P. Current perspectives on the role of CD8+T cells in systemic sclerosis. Immunol Lett. 2018;195:55-60.
- 19. Blank CU, Haining WN, Held W, Hogan PG, Kallies A, Lugli E, et al. Defining 'T cell exhaustion'. Nature Reviews Immunology. 2019;19(11):665-74.
- 20. Bender C, Rodriguez-Calvo T, Amirian N, Coppieters KT, von Herrath MG. The healthy exocrine pancreas contains preproinsulin-specific CD8 T cells that attack islets in type 1 diabetes. Sci Adv. 2020;6(42).
- 21. Cheuk S, Schlums H, Gallais Sérézal I, Martini E, Chiang SC, Marguardt N, et al. CD49a Expression Defines Tissue-Resident CD8(+) T Cells Poised for Cytotoxic Function in Human Skin. Immunity. 2017:46(2):287-300.
- 22. Wagner CA, Roqué PJ, Mileur TR, Liggitt D, Goverman JM. Myelin-specific CD8+T cells exacerbate brain inflammation in CNS autoimmunity. J Clin Invest. 2020;130(1):203-13.
- 23. McKinney EF, Lee JC, Jayne DR, Lyons PA, Smith KG. T cell exhaustion, co-stimulation and clinical outcome in autoimmunity and infection. Nature. 2015;523(7562):612-6.
- 24. Wiedeman AE, Muir VS, Rosasco MG, DeBerg HA, Presnell S, Haas B, et al. Autoreactive CD8+ T cell exhaustion distinguishes subjects with slow type 1 diabetes progression. J Clin Invest. 2020;130(1):480-90.
- 25. Singhaviranon S, Dempsey JP, Hagymasi AT, Mandoiu II, Srivastava PK. Low-avidity T cells drive endogenous tumor immunity in mice and humans. Nature Immunology. 2025;26(2):240-51.
- 26. Westcott PMK, Sacks NJ, Schenkel JM, Ely ZA, Smith O, Hauck H, et al. Low neoantigen expression and poor T cell priming underlie early immune escape in colorectal cancer. Nat Cancer. 2021:2(10):1071-85.
- 27. Zarour HM. Reversing T cell Dysfunction and Exhaustion in Cancer. Clin Cancer Res. 2016;22(8):1856-64.
- 28. Groth C, van Groningen LFJ, Matos TR, Bremmers ME, Preijers F, Dolstra H, et al. Phase I/II Trial of a Combination of Anti-CD3/CD7 Immunotoxins for Steroid-Refractory Acute Graft-versus-Host Disease. Biol Blood Marrow Transplant. 2019;25(4):712-9.
- 29. Frey N, Porter D. Cytokine Release Syndrome with Chimeric Antigen Receptor T Cell Therapy. Biol Blood Marrow Transplant. 2019;25(4):e123-e7.
- 30. Boleto G, Allanore Y, Avouac J. Targeting Costimulatory Pathways in Systemic Sclerosis. Front Immunol. 2018:9:2998.
- 31. Bellando-Randone S, Del Galdo F, Lepri G, Minier T, Huscher D, Furst DE, et al. Progression of patients with Raynaud's phenomenon to systemic sclerosis: a five-year analysis of the European Scleroderma Trial and Research group multicentre, longitudinal registry study for Very Early Diagnosis of Systemic Sclerosis (VEDOSS). Lancet Rheumatol. 2021;3(12):e834-e43.
- 32. Takemura S, Klimiuk PA, Braun A, Goronzy JrJ, Weyand CM. T Cell Activation in Rheumatoid Synovium Is B Cell Dependent 1. The Journal of Immunology. 2001;167(8):4710-8.
- 33. van Caam A, Vonk M, van den Hoogen F, van Lent P, van der Kraan P. Unraveling SSc Pathophysiology; The Myofibroblast. Front Immunol. 2018;9:2452.
- 34. Jonsson AH. Granzyme K(+) CD8 T cells in autoimmunity. Best Pract Res Clin Rheumatol. 2024;38(2):101930.
- 35. Jonsson AH, Zhang F, Dunlap G, Gomez-Rivas E, Watts GFM, Faust HJ, et al. Granzyme K(+) CD8 T cells form a core population in inflamed human tissue. Sci Transl Med. 2022;14(649):eabo0686.

- 36. Donado CA, Theisen E, Zhang F, Nathan A, Fairfield ML, Rupani KV, et al. Granzyme K activates the entire complement cascade. Nature. 2025.
- 37. Mao X, Xu J, Wang W, Liang C, Hua J, Liu J, et al. Crosstalk between cancer-associated fibroblasts and immune cells in the tumor microenvironment: new findings and future perspectives. Molecular Cancer. 2021;20(1):131.
- 38. Guo CL, Wang CS, Wang ZC, Liu FF, Liu L, Yang Y, et al. Granzyme K(+)CD8(+) T cells interact with fibroblasts to promote neutrophilic inflammation in nasal polyps. Nat Commun. 2024;15(1):10413.
- 39. Gao Y, Liu R, Shi J, Shan W, Zhou H, Chen Z, et al. Clonal GZMK⁺CD8⁺ T cells are identified as a hallmark of the pathogenesis of cGVHD-induced bronchiolitis obliterans syndrome after allogeneic hematopoietic stem cell transplantation. eBioMedicine. 2025;112.
- 40. Fava A, Cimbro R, Wigley FM, Liu QR, Rosen A, Boin F. Frequency of circulating topoisomerase-lspecific CD4 T cells predicts presence and progression of interstitial lung disease in scleroderma. Arthritis Res Ther. 2016;18(1):99.
- 41. Inamoto Y, Storer BE, Petersdorf EW, Nelson JL, Lee SJ, Carpenter PA, et al. Incidence, risk factors, and outcomes of sclerosis in patients with chronic graft-versus-host disease. Blood. 2013;121(25):5098-103.
- 42. Brüggen MC, Klein I, Greinix H, Bauer W, Kuzmina Z, Rabitsch W, et al. Diverse T cell responses characterize the different manifestations of cutaneous graft-versus-host disease. Blood. 2014;123(2):290-9.
- 43. Carnel N, Lancia HH, Guinier C, Benichou G. Pathways of Antigen Recognition by T Cells in Allograft Rejection. Transplantation. 2023;107(4):827-37.
- 44. DeWolf S, Grinshpun B, Savage T, Lau SP, Obradovic A, Shonts B, et al. Quantifying size and diversity of the human T cell alloresponse. JCI Insight. 2018;3(15).
- 45. Macedo C, Orkis EA, Popescu I, Elinoff BD, Zeevi A, Shapiro R, et al. Contribution of naïve and memory T cell populations to the human alloimmune response. Am J Transplant. 2009;9(9):2057-66.
- 46. Yosri M, Dokhan M, Aboagye E, Al Moussawy M, Abdelsamed HA. Mechanisms governing bystander activation of T cells. Front Immunol. 2024;15:1465889.
- 47. Kovalik J-P, Singh N, Mendiratta SK, Martin WD, Ignatowicz L, Van Kaer L. The Alloreactive and Self-Restricted CD4+ T Cell Response Directed Against a Single MHC Class II/Peptide Combination1. The Journal of Immunology. 2000;165(3):1285-93.
- 48. Koh CH, Lee S, Kwak M, Kim BS, Chung Y. CD8 T cell subsets: heterogeneity, functions, and therapeutic potential. Exp Mol Med. 2023;55(11):2287-99.
- 49. Chirivì M, Maiullari F, Milan M, Presutti D, Cordiglieri C, Crosti M, et al. Tumor Extracellular Matrix Stiffness Promptly Modulates the Phenotype and Gene Expression of Infiltrating T Lymphocytes. Int J Mol Sci. 2021;22(11).
- 50. Freeman P, Mielgo A. Cancer-Associated Fibroblast Mediated Inhibition of CD8+ Cytotoxic T Cell Accumulation in Tumours: Mechanisms and Therapeutic Opportunities. Cancers (Basel). 2020;12(9).
- 51. Sutherland TE, Dyer DP, Allen JE. The extracellular matrix and the immune system: A mutually dependent relationship. Science. 2023;379(6633):eabp8964.
- 52. Liu J, Wang F, Luo F. The Role of JAK/STAT Pathway in Fibrotic Diseases: Molecular and Cellular Mechanisms. Biomolecules. 2023;13(1).
- 53. Biernacka A, Dobaczewski M, Frangogiannis NG. TGF-β signalling in fibrosis. Growth Factors. 2011;29(5):196-202.

- Dorst DN, van Caam APM, Vitters EL, Walgreen B, Helsen MMA, Klein C, et al. Fibroblast Activation Protein Targeted Photodynamic Therapy Selectively Kills Activated Skin Fibroblasts from Systemic Sclerosis Patients and Prevents Tissue Contraction. International Journal of Molecular Sciences. 2021;22(23):12681.
- 55. Carvalheiro T, Marut W, Pascoal Ramos MI, García S, Fleury D, Affandi AJ, et al. Impaired LAIR-1-mediated immune control due to collagen degradation in fibrosis. J Autoimmun. 2024;146:103219.
- 56. Morrisroe K, Stevens W, Sahhar J, Rabusa C, Nikpour M, Proudman S, et al. Epidemiology and disease characteristics of systemic sclerosis-related pulmonary arterial hypertension: results from a real-life screening programme. Arthritis Research & Therapy. 2017;19(1):42.
- 57. Sakkas LI, Simopoulou T. Chapter 22 T cells in the pathogenesis of systemic sclerosis. In: Rezaei N, editor. Translational Autoimmunity: Academic Press; 2023. p. 447-74.
- 58. Rosendahl Huber S, van Beek J, de Jonge J, Luytjes W, van Baarle D. T cell responses to viral infections opportunities for Peptide vaccination. Front Immunol. 2014;5:171.
- 59. Paleja B, Low AHL, Kumar P, Saidin S, Lajam A, Nur Hazirah S, et al. Systemic Sclerosis Perturbs the Architecture of the Immunome. Front Immunol. 2020;11:1602.
- 60. Fox DA, Lundy SK, Whitfield ML, Berrocal V, Campbell P, Rasmussen S, et al. Lymphocyte subset abnormalities in early diffuse cutaneous systemic sclerosis. Arthritis Res Ther. 2021;23(1):10.
- 61. Pawlik A, Ostanek L, Brzosko I, Brzosko M, Masiuk M, Machalinski B, et al. The expansion of CD4+CD28-T cells in patients with rheumatoid arthritis. Arthritis Res Ther. 2003;5(4):R210.
- 62. Hooper M, Kallas E, Coffin D, Campbell D, Evans T, Looney R. Cytomegalovirus seropositivity is associated with the expansion of CD4+ CD28-and CD8+ CD28-T cells in rheumatoid arthritis. The Journal of rheumatology. 1999;26(7):1452-7.
- 63. Fasth AE, Snir O, Johansson AA, Nordmark B, Rahbar A, af Klint E, et al. Skewed distribution of proinflammatory CD4+ CD28 null T cells in rheumatoid arthritis. Arthritis research & therapy. 2007;9:1-11.
- 64. Gerli R, Schillaci G, Giordano A, Bocci EB, Bistoni O, Vaudo G, et al. CD4+ CD28– T lymphocytes contribute to early atherosclerotic damage in rheumatoid arthritis patients. Circulation. 2004;109(22):2744-8.
- 65. Smoleńska Ż, Pawłowska J, Zdrojewski Z, Daca A, Bryl E. Increased percentage of CD8+CD28— T cells correlates with clinical activity in primary Sjögren's syndrome. Cellular Immunology. 2012;278(1):143-51.
- Deng C, Wang A, Li W, Zhao L, Zhou J, Zhang W, et al. Involvement of expanded cytotoxic and proinflammatory CD28null T cells in primary Sjögren's syndrome. Clinical Immunology. 2024;261:109927.
- 67. Bullenkamp J, Mengoni V, Kaur S, Chhetri I, Dimou P, Astroulakis ZMJ, et al. Interleukin-7 and interleukin-15 drive CD4+CD28null T lymphocyte expansion and function in patients with acute coronary syndrome. Cardiovascular Research. 2020;117(8):1935-48.
- 68. Bano A, Pera A, Almoukayed A, Clarke THS, Kirmani S, Davies KA, et al. CD28 (null) CD4 T cell expansions in autoimmune disease suggest a link with cytomegalovirus infection. F1000Res. 2019;8.
- 69. Khanna D, Spino C, Johnson S, Chung L, Whitfield ML, Denton CP, et al. Abatacept in Early Diffuse Cutaneous Systemic Sclerosis: Results of a Phase II Investigator-Initiated, Multicenter, Double-Blind, Randomized, Placebo-Controlled Trial. Arthritis Rheumatol. 2020;72(1):125-36.

- 70. Seki N, Tsujimoto H, Tanemura S, Ishiqaki S, Takei H, Sugahara K, et al. Th17/IL-17A axis is critical for pulmonary arterial hypertension (PAH) in systemic sclerosis (SSc): SSc patients with high levels of serum IL-17A exhibit reduced lung functions and increased prevalence of PAH. Cytokine. 2024:176:156534.
- 71. Ono Y, Mogami A, Saito R, Seki N, Ishigaki S, Takei H, et al. Interleukin-17A is a potential therapeutic target predicted by proteomics for systemic sclerosis patients at high risk of pulmonary arterial hypertension. Scientific Reports. 2024;14(1):29484.
- 72. Zhong Y, Yu PB. Decoding the Link Between Inflammation and Pulmonary Arterial Hypertension. Circulation. 2022;146(13):1023-5.
- 73. Maston LD, Jones DT, Giermakowska W, Howard TA, Cannon JL, Wang W, et al. Central role of T helper 17 cells in chronic hypoxia-induced pulmonary hypertension. Am J Physiol Lung Cell Mol Physiol. 2017;312(5):L609-l24.
- 74. Hautefort A, Girerd B, Montani D, Cohen-Kaminsky S, Price L, Lambrecht BN, et al. T-helper 17 cell polarization in pulmonary arterial hypertension. Chest. 2015;147(6):1610-20.
- 75. Becker MO, Kill A, Kutsche M, Guenther J, Rose A, Tabeling C, et al. Vascular receptor autoantibodies in pulmonary arterial hypertension associated with systemic sclerosis. Am J Respir Crit Care Med. 2014;190(7):808-17.
- 76. Nunes JPL, Cunha AC, Meirinhos T, Nunes A, Araújo PM, Godinho AR, et al. Prevalence of autoantibodies associated to pulmonary arterial hypertension in scleroderma - A review. Autoimmun Rev. 2018;17(12):1186-201.
- 77. Almaaitah S, Highland KB, Tonelli AR. Management of Pulmonary Arterial Hypertension in Patients with Systemic Sclerosis. Integr Blood Press Control. 2020;13:15-29.
- 78. Vonk MC, Vandecasteele E, van Dijk AP. Pulmonary hypertension in connective tissue diseases, new evidence and challenges. European Journal of Clinical Investigation. 2021;51(4):e13453.
- 79. Bauer Y, de Bernard S, Hickey P, Ballard K, Cruz J, Cornelisse P, et al. Identifying early pulmonary arterial hypertension biomarkers in systemic sclerosis; machine learning on proteomics from the DETECT cohort. Eur Respir J. 2021;57(6).
- 80. Fang T, Yin X, Wang Y, Zhang L, Wang Y, Zhang X, et al. Lymphocyte subset is more suitable than systemic inflammatory response biomarker and immunoglobulin in constructing prognostic nomogram model for advanced gastric cancer. Heliyon. 2023;9(3):e14669.
- 81. Toiyama D, Takaha N, Shinnoh M, Ueda T, Kimura Y, Nakamura T, et al. Significance of serum tumor necrosis factor-related apoptosis-inducing ligand as a prognostic biomarker for renal cell carcinoma. Mol Clin Oncol. 2013;1(1):69-74.
- 82. Pazoki A, Dadfar S, Shadab A, Haghmorad D, Oksenych V. Soluble CD40 Ligand as a Promising Biomarker in Cancer Diagnosis. Cells. 2024;13(15):1267.
- 83. Montani D, Savale L, Natali D, Jaïs X, Herve P, Garcia G, et al. Long-term response to calcium-channel blockers in non-idiopathic pulmonary arterial hypertension. Eur Heart J. 2010;31(15):1898-907.
- 84. Maurer B, Distler JH, Distler O. The Fra-2 transgenic mouse model of systemic sclerosis. Vascul Pharmacol. 2013;58(3):194-201.
- 85. Zamanian RT, Badesch D, Chung L, Domsic RT, Medsger T, Pinckney A, et al. Safety and Efficacy of B cell Depletion with Rituximab for the Treatment of Systemic Sclerosis-associated Pulmonary Arterial Hypertension: A Multicenter, Double-Blind, Randomized, Placebo-controlled Trial. Am J Respir Crit Care Med. 2021;204(2):209-21.
- 86. Singh N, Cohen PL. The T cell in Sjogren's syndrome: force majeure, not spectateur. J Autoimmun. 2012:39(3):229-33.

- 87. Rojas M, Acosta-Ampudia Y, Heuer LS, Zang W, D MM, Ramírez-Santana C, et al. Antigen-specific T cells and autoimmunity. J Autoimmun. 2024;148:103303.
- 88. Henes J, Oliveira MC, Labopin M, Badoglio M, Scherer HU, Del Papa N, et al. Autologous stem cell transplantation for progressive systemic sclerosis: a prospective non-interventional study from the European Society for Blood and Marrow Transplantation Autoimmune Disease Working Party. Haematologica. 2021;106(2):375-83.
- 89. Müller F, Taubmann J, Bucci L, Wilhelm A, Bergmann C, Völkl S, et al. CD19 CAR T cell Therapy in Autoimmune Disease A Case Series with Follow-up. N Engl J Med. 2024;390(8):687-700.
- 90. Tong L, Koh V, Thong BY. Review of autoantigens in Sjögren's syndrome: an update. J Inflamm Res. 2017;10:97-105.
- 91. Alkema W, Koenen H, Kersten BE, Kaffa C, Dinnissen JWB, Damoiseaux J, et al. Autoantibody profiles in systemic sclerosis; a comparison of diagnostic tests. Autoimmunity. 2021;54(3):148-55.
- 92. Du AX, Gniadecki R, Osman M. Biomarkers of B cell activation in autoimmune connective tissue diseases: More than markers of disease activity. Clinical Biochemistry. 2022;100:1-12.
- 93. Marketos N, Koulouri V, Piperi EP, Georgaki ME, Nikitakis NG, Mavragani CP. Scleroderma-specific autoantibodies: Should they be included in the diagnostic work-up for Sjögren's syndrome? Seminars in Arthritis and Rheumatism. 2022;55:152026.
- 94. Andraos R, Ahmad A, Eriksson P, Dahlström Ö, Wirestam L, Dahle C, et al. Autoantibodies associated with systemic sclerosis in three autoimmune diseases imprinted by type I interferon gene dysregulation: a comparison across SLE, primary Sjögren's syndrome and systemic sclerosis. Lupus Sci Med. 2022;9(1).
- 95. Mori S, Kohyama M, Yasumizu Y, Tada A, Tanzawa K, Shishido T, et al. Neoself-antigens are the primary target for autoreactive T cells in human lupus. Cell. 2024;187(21):6071-87.e20.
- 96. Vignali DAA, Collison LW, Workman CJ. How regulatory T cells work. Nature Reviews Immunology. 2008:8(7):523-32.
- 97. Yang J, Brook MO, Carvalho-Gaspar M, Zhang J, Ramon HE, Sayegh MH, et al. Allograft rejection mediated by memory T cells is resistant to regulation. Proc Natl Acad Sci U S A. 2007;104(50):19954-9.
- 98. Chyuan IT, Tsai HF, Wu CS, Sung CC, Hsu PN. TRAIL-Mediated Suppression of T Cell Receptor Signalling Inhibits T Cell Activation and Inflammation in Experimental Autoimmune Encephalomyelitis. Front Immunol. 2018;9:15.
- 99. Ren X, Ye F, Jiang Z, Chu Y, Xiong S, Wang Y. Involvement of cellular death in TRAIL/DR5-dependent suppression induced by CD4+CD25+ regulatory T cells. Cell Death & Differentiation. 2007;14(12):2076-84.
- 100. Chyuan IT, Tsai HF, Liao HJ, Wu CS, Hsu PN. An apoptosis-independent role of TRAIL in suppressing joint inflammation and inhibiting T cell activation in inflammatory arthritis. Cell Mol Immunol. 2018;15(9):846-57.
- 101. Yao Q, Seol D-W, Mi Z, Robbins PD. Intra-articular injection of recombinant TRAIL induces synovial apoptosis and reduces inflammation in a rabbit knee model of arthritis. Arthritis Research & Therapy. 2005;8(1):R16.
- 102. Smolders J, Thewissen M, Damoiseaux J. Control of T cell activation by vitamin D. Nat Immunol. 2011;12(1):3; author reply -4.



Appendix

Samenvatting van de bevindingen van het proefschrift en klinische implicaties

Systemische sclerose (SSc) is een complexe reumatische bindweefselziekte die wordt gekenmerkt door vasculopathie, ontstekingen en fibrose van de huid en viscerale organen. Bij deze ziekte verliest het immuunsysteem van de patiënt tolerantie voor anti-nucleaire en andere auto-antigenen. Daarnaast vertoont SSc specifieke immunopathologische processen in aangetaste weefsels. Dit is in tegenstelling tot andere bindweefselziektes waarbij anti-nucleaire antigeenreactiviteit ook een rol speelt, zoals bij het syndroom van Sjogren (SjS). Zowel het ontstaan als de progressie van SSc worden sterk bepaald door (auto)immuunreacties. De heterogeniteit in (klinische) manifestaties, ontstaan en verloop van de ziekte vormt echter een uitdaging voor onderzoek en medische zorg. Ondanks grote inspanningen zijn er nog geen veilige en universeel toepasbare behandelingen ontwikkeld, met uitzondering van autologe stamceltransplantatie (ASCT) en mogelijk anti-CD19 CAR T-celtherapie. Tevens ontbreken er betrouwbare biomarkers voor het voorspellen en volgen van de ziekteprogressie. Dit is voornamelijk te wijten aan het onvolledige begrip van de onderliggende pathofysiologische mechanismen en initiërende factoren van de ziekte.

Dit proefschrift onderzoekt de rol van (autoreactieve) T-celresponsen bij pathologische processen als vasculopathie, fibrose en autoantilichaam-gemedieerde weefselafbraak in SSc en andere bindweefselziektes (SjS). Hieronder worden de belangrijkste bevindingen en hun implicaties samengevat. Daarna volgt er een diepgaande discussie over potentiële toekomstige therapeutische strategieën, die zich focust op de vertaling van laboratoriuminzichten naar klinische toepassingen.

Hoofdstuk 2 benadrukt de cruciale rol van het immuunsysteem bij SSc en het ontbreken van veilige, gerichte en curatieve behandelingen. T cellen sturen ontsteking, vasculopathie en fibrose en dragen bij aan zowel het verloop van vroege immuunreacties tot ziekteprogressie. Pro-fibrotische CD4+ en CD8+ T cellen die IL-4 en IL-13 produceren, dragen bij aan fibrose via myofibroblast-gemedieerde extracellulaire matrixafzetting. Andere T-cel-subtypes, waaronder Th17, Tph en Tregs, zijn ook betrokken bij ziekteprocessen, maar de bevindingen hierover zijn tegenstrijdig. Cytotoxische T cellen zijn in SSc-aangetaste huidweefsels aangetroffen en induceren vasculaire schade via apoptose van endotheelcellen. Hoewel onderzoek zich heeft gericht op de T-celsamenstelling in bloed en weefsels, ontbreekt er een uitgebreide analyse van de regulatie van (autoreactieve) T cellen

in bloed, lymfeklieren en aangetaste weefsels. Dit kennishiaat belemmert de ontwikkeling van gerichte therapieën. Huidige behandelingen, zoals ASCT, kunnen remissie bewerkstelligen maar kennen hoge mortaliteitsrisico's. Anti-CD19 CAR T-celtherapie toont veelbelovende resultaten, maar deze therapie slaagt er niet in om fibrose om te keren. Beide behandelingen onderstrepen de centrale rol van het immuunsysteem bij SSc, maar de hoge kosten, ernstige bijwerkingen en beperkte toepasbaarheid benadrukken de dringende behoefte aan gerichtere therapieën. Het verbeteren van methoden om pathogene T cellen te identificeren en doelgericht te behandelen, kan veiligere alternatieven bieden en de afhankelijkheid van intensieve behandelingen verminderen. Echter, cruciale vragen over T-celregulatie, autoreactiviteit en hun rol in de ziektepathologie vereisen verder onderzoek.

In hoofdstuk 3wordt verhoogde CD7-co-stimulatie als een marker van pathogene T- en NK-cellen in SSc-aangetaste huid en longen aangetoond, wat de rol van deze cellen in immuungemedieerde weefselpathologie benadrukt. Deze cellen vertonen een cytotoxisch, pro-inflammatoir en pro-fibrotisch genexpressieprofiel, met name in vroege en ernstige stadia van SSc. CD7-co-stimulatie is betrokken bij hun effectorfuncties en gerichte depletie van CD7+ cellen verminderde fibroblastcontractie en stabiliseerde zelfs de ziekte bij een patiënt met ernstige diffuse cutane SSc. Deze bevindingen suggereren dat CD7-gerichte therapieën een nieuwe aanpak zouden kunnen zijn om immuun gemedieerde weefselschade bij SSc te verminderen, met mogelijke voordelen voor patiënten met vroege en ernstige ziekte.

In hoofdstuk 4 is het onderzoek naar cytotoxische T cellen vervolgt en dit onderzoek toont aan dat niet-canonieke CD8+ T cellen, in tegenstelling tot CD4+ T cellen, de primaire drijvers van fibrose in SSc zijn. Deze cellen activeren myofibroblasten en induceren contractie via cytokine-gemedieerde mechanismen, met name via JAK/ STAT3- en TGFβ-signaleringspaden, en niet door directe cytotoxiciteit. Gerichte remming van deze signaleringspaden had een additief effect in het verminderen van fibrose door zowel immuuncel- als myofibroblastactivatie te onderdrukken. Deze bevindingen benadrukken de potentie van therapeutische interventies die gericht zijn op het blokkeren van cytokine-gemedieerde CD8+ T-celactivatie als een strategie om fibrose in SSc te remmen en ziekteprogressie tegen te gaan.

Hoofdstuk 5 beschrijft de immuundisregulatie geassocieerd met SScgerelateerde pulmonale arteriële hypertensie (PAH), een ernstige vasculaire complicatie. Patiënten met SSc-PAH vertonen specifieke T-celprofielen, waaronder verhoogde Tph- en Th17-cellen. Dit immuunprofiel onderstreept de rol van autoimmuunontsteking bij de ontwikkeling van PAH en suggereert een mogelijke link tussen specifieke T-cel-subsets en vasculaire complicaties. Klinisch gezien benadrukken deze bevindingen de noodzaak van immuungerichte benaderingen om PAH bij SSc-patiënten effectiever te diagnosticeren en te behandelen.

Hoofdstuk 6 richt zich op antigeen specifieke T-celresponsen in de actieve lymfeklieren van patiënten met SSc en SjS. Dit hoofdstuk onthult dat SjS wordt gekenmerkt door sterke interacties tussen APC-CD4+ T cellen en B cellen die auto-immuniteit aansturen, terwijl SSc wordt gekenmerkt door een unieke TRAIL+ CD4+ T-cel-subset met een interferon-gestimuleerd genexpressieprofiel. Deze subset reguleert immuunresponsen door overmatige plasmacelvorming en autoantilichaam productie te beperken. Opmerkelijk is dat gereduceerde TRAIL-waarden correleren met ernstige vasculaire complicaties, wat de beschermende rol van TRAIL benadrukt. Deze bevindingen suggereren dat het versterken van TRAIL-expressie in autoreactieve T cellen kan dienen als een nieuwe immuuntherapeutische strategie om de balans tussen immuun activatie en -onderdrukking te herstellen en autoantilichaam-gemedieerde schade te verminderen.

Algemene conclusies en slotbeschouwingen

Het hoofddoel van dit proefschrift was om de rol van autoreactieve T-celresponsen bij de pathologie van systemische sclerose (SSc) en andere bindweefselziekten te ontrafelen. Ondanks hun veronderstelde betrokkenheid blijft de functionele rol van autoreactieve T cellen in actieve lymfeklieren en aangetaste weefsels slecht begrepen. Dit komt voornamelijk vanwege de uitdagingen bij het detecteren van deze zeldzame celpopulaties. Om dit gebrek aan wetenschappelijke kennis te verhelpen, hebben we een innovatieve toolkit ontwikkeld die geavanceerde PET-imaging van immunologisch actieve weefsels integreert met single-cell multiomics technologieën, multiplex immunhistochemie en functionele in-vitro-assays om autoreactieve T-celresponsen in weefsels te karakteriseren.

Het onderzoek in dit proefschrift is het eerste dat de verschillende rollen van nucleaire antigeen (NAg) autoreactieve T cellen in immunologisch uiteenlopende bindweefselziektes zoals SSc en SjS in kaart brengt. Deze rollen zijn gekoppeld aan specifieke ziekteverschijnselen en kennis hiervan draagt bij aan ons begrip van de mate en de betrokkenheid van verschillende pathogene T-celsubsets in diverse bindweefselziektes en in verschillende ziektefasen bij patiënten met SSc. In tegenstelling tot B-celgemedieerde bindweefselziektes zoals SjS, wordt de ziektepathologie in SSc voornamelijk aangedreven door autoreactieve CD8+T cellen, in plaats van door effector-CD4+T-cel-B-cel interacties. Dit verschil wordt

toegeschreven aan de verschillende wijze van organisatie en regulatie van effectorversus regulatoire NAg-specifieke responsen in locoregionale lymfeklieren.

Bovenstaande bevindingen stimuleren het langlopende debat of SSc primair wordt aangedreven door auto-immuunresponsen. Hoewel de aanwezigheid van ziektespecifieke autoantilichamen de betrokkenheid van humorale immuunafwijkingen ondersteunt, presenteert SSc zich ook met significante vasculopathie en fibrose. Dit roept de vraag op of auto-immuniteit de primaire drijvende kracht is, of slechts een secundair gevolg van endotheel- en fibroblastdysfunctie. De bevindingen uit dit proefschrift dragen bij aan het voortdurende debat door aan te tonen dat auto-immuunontstekingsverschijnselen optreden in de vroege ziektefasen van patiënten. Daarnaast hebben we een duidelijke betrokkenheid van cytotoxische versus helper-T cellen aangetoond in verschillende ziektefasen en patiëntensubtypen, wat bijdraagt aan de identificatie van nieuwe biomarkers voor ziekte-ernst en progressie. Echter, de vraag of autoreactieve responsen een rol spelen in de initiatie van de ziekte blijft onbeantwoord. Om dit te onderzoeken, zullen we onze ontwikkelde toolkit toepassen op een unieke patiëntencohort uit het Radboudumc, bestaande uit individuen met zeer vroege vasculaire symptomen die mogelijk wel of niet later progressie naar SSc vertonen (NCT03059979). Opmerkelijk is dat de helft van deze patiënten uiteindelijk SSc met auto-immuun en fibrotische kenmerken ontwikkelde, wat ons de kans biedt om te onderzoeken of de in dit proefschrift geïdentificeerde autoreactieve T cellen en pathogene processen bijdragen aan de transitie van zeer vroege vasculaire dysfunctie naar volledig ontwikkelde SSc.

Hoewel de bevindingen in dit proefschrift de rol van het adaptieve immuunsysteem impliceert in zowel vroege als late manifestaties van SSc, blijft het onduidelijk of het gericht aanpakken van een enkele celcompartiment, zoals de door autoreactieve T cellen gedreven immuunafwijkingen, voldoende is voor een effectieve behandeling. Gezien de complexe aard van SSc—gekenmerkt door immuunactivatie, endotheliale disfunctie en fibrose—lijkt dit onwaarschijnlijk. Deze gedachtegang wordt ondersteund door het falen van huidige immuunmodulerende therapieën, inclusief de meest effectieve strategieën zoals ASCT en anti-CD19 CAR-T cellen, om fibrose volledig om te keren of vasculaire integriteit te herstellen. Onze bevindingen suggereren dat een combinatie van immuungerichte therapieën en antifibrotische middelen betere resultaten kan opleveren. Echter, het hoge toxiciteitsprofiel van antifibrotische middelen blijft een grote uitdaging. Als alternatief kan de specifieke eliminatie van pathogene autoreactieve T cellen in zeer vroege stadia van SSc, waarin fibrose en vasculaire disfunctie nog niet zijn

vastgesteld, effectief zijn in het voorkomen van ziekteprogressie. Op basis van deze hypothese en de veelbelovende resultaten beschreven in dit proefschrift, voeren we momenteel een "proof-of-concept" klinische studie uit waarbij vroege SSc-patiënten worden behandeld met anti-CD3/CD7 immunotoxines (IT) om te beoordelen of depletie van pathogene cytotoxische immuuncellen in vroege ziektefasen kan leiden tot langdurige ziekte-remissie.

Research Data Management Plan

Ethics and privacy

This thesis is based on research involving human participants (on both newly obtained data and analysis of previously published data), conducted in compliance with applicable national and international laws, regulations, guidelines, ethical codes, and Radboudumc policy. A designated Medical Ethics Review Committee has granted approval to perform these studies, and each specific file number is mentioned in the methods section of each chapter. As instructed by the Dutch law, data collection from electronic patient files was carried out by personnel with a treatment relationship with the patient (clinicians) with the participant's consent. All participants provided informed consent for the collection and processing of their data for this research project.

Data collection and storage

In vitro culture data for chapters 3-6 were obtained from laboratory experiments that involved anonymous human materials from either healthy individuals or patients. For chapters 3, 5 and 6, clinical data were extracted from patient files included in electronic health records through EPIC application. Raw data from laboratory systems and measurements along with processed data and documentation are archived in our department's server and are only accessible by project members working at Radboudumc.

Data sharing according to the FAIR principles

All studies included in this thesis are published open access. The single-cell RNA sequencing data that were generated in chapter 6 are publicly available for reuse through the data repository of the NCBI Gene Expression Omnibus (GEO). Data was made reproducible by including elaborate documentation of the research protocols, methods and scripts that were used.

List of publications

Papadimitriou TI, Singh P, van Caam A, Vonk M, van der Horst-Bruinsma I, van der kraan P, Aarntzen E, Huijnen M, Koenen H, Thurlings R. Single-cell Multi-omics Analysis of Reactive Lymph Nodes, Affected Tissues, and Blood Reveals a Naive-like CD4+TRAIL+ T Cell Population That Differentially Directs Effector Anti-nuclear Antigen Reactive Responses in Patients with Sjogren's Syndrome and Systemic Sclerosis [abstract]. Arthritis Rheumatol. 2024; 76 (suppl 9)

Papadimitriou TI, Singh P, van Caam A, et al. CD7 activation regulates cytotoxicity-driven pathology in systemic sclerosis, yielding a target for selective cell depletion. Ann Rheum Dis. 2024;83(4):488-498. Published 2024 Mar 12. doi:10.1136/ard-2023-224827

Papadimitriou TI, van Caam A, van der Kraan PM, Thurlings RM. Therapeutic Options for Systemic Sclerosis: Current and Future Perspectives in Tackling Immune-Mediated Fibrosis. Biomedicines. 2022;10(2):316. Published 2022 Jan 29. doi:10.3390/biomedicines10020316

Papadimitriou TI, Lemmers JMJ, van Caam APM, et al. Systemic sclerosis-associated pulmonary arterial hypertension is characterized by a distinct peripheral T helper cell profile. Rheumatology (Oxford). Published online March 29, 2024. doi:10.1093/rheumatology/keae190

Papadimitriou TI, van Essen A, Willemse M, et al. CD8+ T cells drive myofibroblast activation and contraction via JAK/STAT3 and TGF β signalling. bioRxiv 2025.03.05.641635; doi: https://doi.org/10.1101/2025.03.05.641635

Venrooij K, Papadimitriou TI, Dorst D, Bonger K. Depleting autoreactive B cells using targeted photodynamic therapy . ACS Pharmacology & Translational Science. DOI: 10.1021/acsptsci.5c00332

X. Chen, TI Papadimitriou, A. H. G. van Essen, et al., "Mitochondrial Activity Regulates Human T Helper 17 Differentiation and Function," Immunology (2025): 1–14, https://doi.org/10.1111/imm.70037

Acknowledgements

Σα βγεις στον πηγαιμό για την Ιθάκη, να εύχεσαι νάναι μακρύς ο δρόμος, γεμάτος περιπέτειες, γεμάτος γνώσεις. Τους Λαιστρυγόνας και τους Κύκλωπας, τον θυμωμένο Ποσειδώνα μη φοβάσαι, τέτοια στον δρόμο σου ποτέ σου δεν θα βρεις, αν μέν' η σκέψις σου υψηλή, αν εκλεκτή συγκίνησις το πνεύμα και το σώμα σου αγγίζει. Κ. Π. Καβάφης – "Ιθάκη"

As you set out for Ithaka
hope the voyage is a long one,
full of adventure, full of discovery.
Laistrygonians and Cyclops,
angry Poseidon—don't be afraid of them:
you'll never find things like that on your way
as long as you keep your thoughts raised high,
as long as a rare excitement
stirs your spirit and your body.
C.P. Cavafy – "Ithaka"

These past four years as a PhD student have been an incredible journey, made possible by the amazing people around me who made this journey smooth and enjoyable. I am truly grateful to all who offered their support, encouragement, and belief in me along the way.

First of all, I am incredibly grateful to my PhD supervisors—**Dr. Rogier Thurlings**, **Dr. Hans Koenen**, **Dr. Arjan van Caam**, and **Prof. Dr. Peter van der Kraan**—whose support and unwavering mentorship have been invaluable from the very beginning.

Rogier, thank you for your exceptional guidance and support throughout my entire PhD journey. From the very start, you placed your trust in me and my abilities, allowing me to take the lead on our projects with confidence. It's been truly rewarding to see how this project evolved—from establishing and optimizing techniques during the challenging times of the pandemic to applying them to unravel complex mechanistic questions in autoreactive T cell biology in systemic connective tissue disease. Your boundless enthusiasm, motivation, and open-door policy were instrumental in keeping the project moving forward and ensuring its timely completion. I especially appreciated our in-depth scientific discussions—whether in focused meetings, over WhatsApp messages in the evenings, or even with a drink in hand during conferences. These moments not only enriched my thinking but also made the process genuinely enjoyable. Thank you for consistently encouraging me to attend conferences and present our work; your support greatly boosted my confidence and opened doors for future collaborations. I will carry your quidance with me throughout my career.

Hans, thank you for always being so kind and supportive. Your pragmatic and down-to-earth approach played a key role in making this thesis feasible. I learned a great deal from you, particularly in mastering flow cytometry and understanding how to approach complex T cell biology. You were always present at our progress meetings, ensuring I stayed on track, and I am truly grateful for the opportunity to have worked under your supervision.

Peter, I would like to express my sincere gratitude for your support and guidance as my promoter. While you were not involved in the day-to-day aspects of the project, your presence and encouragement were always reassuring. I deeply appreciated your kindness, thoughtful feedback during key moments, and your help with all the formal and administrative aspects of the PhD process. Your trust in me and steady support played an important role in bringing this thesis to completion.

Last but certainly not least, a very special thank you to you, **Arjan**. From the early days of 2018, when I did my first master's internship with you, I was immediately inspired by your research approach and your ability to explain complex biological concepts in a clear and accessible way. You were the one who inspired me to pursue a PhD in the rheumatology department, and I'm very grateful for your trust in me and for introducing me to Rogier as the right candidate for this project. As my daily supervisor, you were outstanding—always available to advise and support me, both practically and conceptually, at every step of the way. Most importantly, I want to thank you for being there during the difficult moments, offering mental support, and helping me find solutions that kept me going. Sharing my concerns with you made a real difference. Our scientific discussions were among the most enjoyable parts of my daily routine, and I will always look back on them with appreciation.

I would also like to extend my heartfelt thanks to **Dr. Ypke van Oosterhout**, with whom I had the privilege of working closely throughout my PhD. Our collaboration on exploring the effectiveness of selective T and NK cell depletion in systemic sclerosis—using the drug developed by his company—has been one of the most exciting and rewarding parts of this journey. Together, we navigated the entire process from preclinical studies to a proof-of-concept clinical trial, which was both a scientific and personal milestone. Ypke, I am deeply grateful for your mentorship, trust in me, and the collaborative spirit with which you approached our work. Leading the experimental part of the trial with your support has been a valuable learning experience that I will always carry with me. Thank you, Ypke, for your confidence, openness, and for being such a valuable and committed partner in this endeavor.

I would like to extend my sincere appreciation to the assessment committee—**Prof. Dr. Annemiek van Spriel**, **Prof. Dr. Esther de Jong**, and **Prof. Dr. Aline Bozec**—for their time, effort, and critical evaluation of my work.

My dear paranymphs, **Massis** and **Nienke**—firstly, thank you for accepting this role and for all the effort you've put into making this day so special.

Nienke, you have been there from the very beginning of this journey. We've shared not only the ups and downs of the PhD process, but also countless moments outside the lab—hobbies, travels, and after-work fun activities—that brought balance and joy to these intense years. Your kindness, eagerness to help, and thoughtful presence have meant a great deal to me. You were always there with a listening ear, a warm smile, and a willingness to support me in any way you could. I couldn't have asked for a better companion throughout this journey. I wish you all the best for your future plans.

Massis, your support has been equally invaluable. You were always ready to help with practical matters, but what I appreciated most was your impact on my wellbeing. You taught me how to approach challenges with calm and perspective, and I learned from you how to cope with every situation—both in and outside the lab. Your steady presence and thoughtful advice helped me stay grounded, and I'm truly grateful for your friendship and support.

No PhD journey is complete without the incredible support of the dedicated lab technicians of the Reuma Lab. **Elly** and **Birgitte**, you have been there for me since day one, and you hold a special place in my heart. Always helpful, knowledgeable, and ready to lend a hand whenever needed, your patience and meticulous approach were invaluable—especially during high-pressure moments—and played a crucial role in ensuring the quality and timely publication of our work. I am particularly grateful for the way you prioritized my experiments during critical times, such as rebuttal deadlines. Even more than your technical support, I deeply appreciate the personal and unconditional care you offer. You were there not only with your hands, but with your hearts as well. Talking to you was always a relief, and I have always felt you were more than colleagues—more like my lab mums. I truly feel fortunate to have had you by my side throughout this journey. **Monique**, thank you for your valuable help with our Luminex measurements and your critical contribution to collecting patient samples. **Annet** and **Onno**, thank you for your essential assistance and for always being available whenever needed.

I would also like to extend my sincere thanks to **Dr. Prashant Singh** and **Prof. Martijn Huijnen**, whose expertise and contributions on the bioinformatic analyses were vital to the success of my project and its resulting publications. **Prashant**, it was a pleasure working closely with you. Your deep knowledge and analytical skills made a significant impact on the quality of our data analysis. I truly appreciated the clarity you brought to our complex datasets. **Martijn**, thank you for your valuable supervision and for providing the guidance and structure that supported our bioinformatics work. Your input was essential in shaping the analytical framework of the project. I am grateful to both of you for your support and collaboration throughout my PhD.

I would also like to thank **Dr. Erik Aarntzen** and **Dr. Ruben Smeets**, who, although not official supervisors, played a supervisory role throughout my PhD. **Erik**, your involvement in the imaging aspects of my thesis was incredibly valuable, and I truly appreciated your guidance and support in navigating this complex part of the project. **Ruben**, your input on the in vitro assays was equally essential. Your feedback was always sharp, creative, and out-of-the-box, and your enthusiasm and encouragement made a real difference. I'm grateful for the time and energy you both invested in my work, and I feel fortunate to have had you as part of my PhD journey.

I would also like to thank **Dr. Marije Koenders**, a core member of our Adaptive Immunity group, for her valuable feedback and continuous support throughout my PhD. Your thoughtful insights during discussions helped sharpen my thinking and improve the quality of my work. Beyond your scientific input, I truly appreciated your kindness, positivity, and caring nature. You always brought a warm and encouraging atmosphere to the lab, and it was a pleasure to work alongside you.

I would also like to thank all my amazing colleagues at the Reuma Lab for creating the most enjoyable and supportive working environment I could have hoped for. Thank you for the many fruitful and challenging discussions, as well as the fun and cheerful moments we shared. It was a true joy working with Martijn, Djulio, Daphne, Esmeralda, Wessel, Arjen, Henk, Fons, Peng, Thea, Emma, and more recently with Anne, Angela, Pedro, Sharona, Donna, Linda. Your presence in the lab, during meetings, and on our lab day outings made each day more pleasant and motivating. A special mention goes to you, Xinlai. From day one, we were in this together as part of the T cell group, sharing countless moments—the highs, the lows, and everything in between. I sincerely enjoyed working alongside you in the lab, and I am deeply grateful for your friendship, your support, and your

unwavering presence throughout this journey. Thank you for always being there for me. I wish you all the very best in everything that lies ahead.

I would also like to express my heartfelt thanks to the clinicians of our Department of Rheumatology—the rheumatologists and nurses—whose support was essential for the clinical aspects of my research. Your help with patient inclusion and your valuable feedback from a clinical perspective greatly enriched the translational relevance of my work. In particular, I would like to thank **Jackie**, **Madelon**, and **Sander** for the close and inspiring collaboration we shared, especially through our common interest in systemic sclerosis and our joint publications. Your clinical insights, enthusiasm for research, and willingness to engage in scientific discussions were incredibly motivating and helped bridge the gap between bench and bedside.

I would also like to extend my sincere gratitude to **Prof. Irene van der Horst-Bruinsma**, head of our department. Although we got to know each other more closely in the later stages of my PhD, I am truly thankful for your support and genuine interest in me and my work. Your presence at every one of my conference presentations—always sitting next to me, offering encouragement—meant a great deal and gave me the confidence to present with pride. Your support has been both empowering and deeply appreciated.

I would also like to thank **Laura Wingens** from the Molecular Biology Department for her invaluable support and dedication. Working closely together to optimize the single-cell RNA sequencing platform was one of the most rewarding aspects of my PhD. As pioneers of this technique at Radboud, we faced many challenges, but your commitment, precision, and collaborative spirit were key in establishing robust and reliable protocols. I truly appreciated your perseverance and teamwork, which laid the foundation for high-quality sequencing data and meaningful results. It was a pleasure to share this journey with you.

I am also very grateful for the inspiring collaboration with the Tumor Immunology Department. **Prof. Jolanda de Vries**, thank you for your sharp and insightful feedback on my project. Your ability to quickly identify key points and provide clear, constructive suggestions truly elevated the quality of my work.

I would also like to thank my colleagues from the Laboratory of Medical Immunology (LMI), with whom I had the pleasure of working during my PhD. This shared PhD experience provided me with valuable insights and opportunities for learning. **Bram**, I am especially grateful for your guidance in mastering flow cytometry.

Your expertise and willingness to teach were instrumental in building a strong foundation for my experimental work. **Xuehui**, thank you for your involvement in our progress meetings and for the collaborative work we did together on company-related projects—your contributions were always thoughtful and appreciated. **Dimitri**, thank you for your sharp feedback and the amazing ideas you shared with me that significantly elevated my project. I truly enjoyed the discussions during our Friday morning single-cell RNAseq meetings. To the fellow PhD students and technicians I interacted with—**Manon**, **Annemijn**, **Laurien**, **Ezgi**, **Aysel**, **Vera**, **Judith**, **Guilherme**—thank you for the friendly atmosphere, helpful exchanges, and occasional scientific discussions. Although our interactions were mostly during the early phases of my PhD, they were meaningful and contributed to a positive and collaborative environment.

I would also like to express my appreciation to the brilliant Bachelor's and Master's students I had the pleasure of supervising during my PhD—Marieke, Noor, Michelle, Lizan, Anne, Merel, Malou, Sidney, Tijmen and Jilke. Thank you for your valuable help in the lab; I learned a great deal from each of you, and I hope I was able to support and guide you well during your internships. I wish you all the very best in your future endeavors, both professionally and personally.

To all my friends in the Netherlands and across Europe—Marciano, Ruby, Payam, Michael, Luka, Peter and all the members of Hoogeveldt's Gang 39—thank you for being a source of laughter, comfort, and perspective throughout this journey. Whether it was a spontaneous weekend getaway with the 5 Muskulöse Männer, a late-night talk about life in Payam's place, or sharing good food, wines and beers at Ruby's and Marciano's place, a long bike ride to drinks beers at Beers Michael, your presence helped keep me grounded and reminded me of the world beyond pipettes and protocols. I deeply cherish the memories we've made and the unwavering support you've shown me over the years. You've made this chapter not only bearable but beautiful—and for that, I am truly grateful. I look forward to all the new adventures we'll take on next, near or far.

Now, it's time to go back to my roots in Greece—where my journey truly began. I am deeply grateful to my family, whose love and support have been the foundation of everything I've achieved. To my mother, **Sevi**, and my father, **Giorgos**—thank you for your unwavering belief in me, for the sacrifices you made, and for showing me the value of perseverance. To my brother, **Marios**—thank you for your steady encouragement and for always cheering me on, no matter the distance. And to my

beloved grandmother, **Arhondia**—your wisdom and gentle strength have guided me more than you know.

A special acknowledgment to my godmother **Julieta**, godfather **Nikos** and their daughters **Dimitra-Maria** and **Dione-Alcestis**. Nona mou, your love and support from the very beginning of my studies shaped the path I walked with confidence and courage and filled me with countless of love and care that supported every difficulty. Without your guidance and generosity, I would not be standing where I am today. None mou, your presence, advice, unwavering support and care have been a quiet but powerful force—thank you both from the bottom of my heart.

To **Stelios**—my best friend, brother, and most trusted confidant—thank you for always being there and for being someone I can rely on without hesitation. Our friendship, which began during our bachelor studies, has grown into one of the most meaningful relationships in my life. You've always shown genuine interest in my research, asking about every detail, and for me, those conversations were not only comforting but almost meditative. Talking to you helped me process challenges and find clarity. I deeply appreciate the way you've stood by me through every phase of this journey. I want to take this moment to tell you how much I believe in you. I know you will achieve great things in life, and I'll always be cheering you on. Thank you for being the incredible person you are.

To my companion, life partner, and soulmate—Paola Konstantina Strepi: I consider myself incredibly lucky to have found you. Since 2019, when you first stole my heart, you have been my unwavering source of strength and belief. Thank you for your incredible support during the most challenging moments of my PhD journey. You always remained positive about my project and believed in me, even during the darkest times, when I struggled to believe in myself. Your thoughtful surprises, the uplifting trips you organized, and the joy you brought into my life helped me recharge and navigate the challenges with more ease. I'm also deeply grateful for your honest advice and for setting an example of how to be direct and stand up for myself—something I truly learned from you and will carry forward. Looking back at everything we've shared, it feels surreal that we've come this far together. I can't wait to experience all the moments our future holds. Thank you for always being by my side. I am endlessly grateful for you, Paola. I would also like to thank your big wonderful family—Eleni and Leonidas and the loved ones from Volos; Vangelis, **Tzouli**, **Vefa**, **Stefania**—for their warmth, kindness, and support throughout these years. **Efi**, I truly enjoyed our scientific discussions and all the cooking sessions we shared, which brought both inspiration and joy. Nikola, thank you for your thoughtful advice and for always offering a grounded and insightful perspective. I feel very fortunate to have become part of such a caring and supportive family.

Department: Rheumatology/Medical Immunology

PhD period: **08/10/2020 – 31/12/2024** PhD Supervisor(s): **Prof. P.M van der Kraan**

PhD Co-supervisor(s): Dr R.M Thurlings, H.J.P.M Koenen, A. van Caam

Training activities	Hours
Courses	
Introduction course to R (2020)	12.00
DGS - GS Introduction Day (2020)	7.00
GSL - Introduction Day (2020)	8.00
RIMLS - Introduction course "In the lead of my PhD" (2021)	15.00
RTC Microscopy Course I mage Analysis with FIJI (2021)	16.00
RU - Effective Writing Strategies (2021)	84.00
Radboudumc - Scientific integrity (2022)	20.00
Getting ready for your first grant application (2024)	24.00
Radboudumc - eBROK course (2024)	42.00
Seminars	
Research integrity round: Recognition and Rewards for Radboudumc Academics (2020)	2.00
Research Integrity Round: The dark side of science (2021)	2.00
Research Integrity Round: The challenges of collaboration	2.00
with profit and non-profit organisations (2021)	
Research Integrity Round (2021)	2.00
"Weten en Eten" training seminar (2022)- Oral Presentation	8.00
NVLE Najaarsdag 2023 (2023)- Oral Presentation	10.00
Detective project patient day (2024)- Oral Presentation	8.00
Conferences	
PhD Retreat (2021)- Poster Presentation	8.00
New Frontiers Symposium Translational Glycoscience (2021)	16.00
European workshop for Rheumatology 2022 (2022)- Poster Presentation	16.00
NVVI Winterschool 2022 (2022)- Oral Presentation	16.00
RIMLs PhD Retreat 2022 (2022)- Poster Presentation	16.00
NVVR Najaarsdagen (2022) - Oral Presentation	8.00
European workshop for Rheumatology research (2023)- Oral Presentation	28.00
NVVI Lunteren 2023 (2023)	20.00
EULAR Congress 2023 (2023)- Oral Presentation	40.00
8th Systemic sclerosis World Congress (2024)- Poster Presentation	28.00
European workshop for Rheumatology research 2024 (2024)- Poster Presentation	28.00
FASEB Immunoreceptors and Immunotherapy (2024)- Oral Presentation	28.00
ACR Convergence 2024 (2024)- Oral Presentation	28.00
NVVI Annual Meeting 2024 (2024)- Oral Presentation	16.00
<u> </u>	10.00
Teaching activities	
Lecturing Most the DhD workshop (2021)	16.00
Meet the PhD workshop (2021)	16.00
Workshop in single-cell RNA sequencing and flow cytometry in the	16.00
Honours program for bachelor Biomedical students (2021)	1600
Teaching assistance in master courses "Inflammatory disease"	16.00
(BMS74) and "Advanced Immunology"(BMS88) (2021)	4.00
Workshop (2022)	4.00
Teaching assistance in master course "Inflammatory diseases" BMS 74 (2023)	8.00

Supervision of internships / other	
Supervision Bachelor student internship (2021)	24.00
Supervising master students internship (2022)	56.00
Supervising master student internship (2022)	56.00
Master student internship supervision (2023)	56.00
Master Student Internship Supervision (2023)	56.00
Master student supervision (2023)	56.00
Master student internship supervision (2024)	56.00
Total	978.00

Awards/Distinctions

- Co-applicant in 450€K Health Holland grant to develop novel human in vitro models to study SSc pathogenesis
- Best abstract award in EULAR Congress 2023 held in Milan, Italy
- Awarded by the patient organization NVLE as the best scientist performing basic research for systemic sclerosis in the Netherlands for the year of 2023
- Travel bursary award to attend EWRR Conference 2023
- Travel bursary award to attend EULAR Congress 2023
- Best poster award in EWRR Conference 2024 held in Genoa, Italy
- Travel bursary award to attend EWRR Conference 2024
- Travel bursary award to attend ACR Convergence 2024
- Travel bursary award to attend EULAR Congress 2024
- Travel bursary award to attend FASEB Immunoreceptors and Immunotherapy Conference 2024
- Kao Family Foundation SCTC Young Investigator Travel Award
- Co-applicant in grants (total 1M) from Radboudumc Holding and a Dutch investment syndicate to conduct a proof-of concept clinical trial of using anti-CD3/CD7-IT to deplete autoreactive T cells and halt disease progression in patients with early diffuse cutaneous systemic sclerosis

Abbreviations

Abbreviation	Full term
2D	Two-dimensional
3D	Three-dimensional
6MWD	6 min walk distance
7-AAD	7-aminoactinomycin D
ACA	Anticentromere antibodies

ACR American college of rheumatology

ACTA2 Actin alpha 2

AIM Activation-induced marker assay
ALK4/5/7 Activin receptor-like kinase 4/5/7

ANA Antinuclear antibodies
ANAg Antinuclear antigen

ANCA Antineutrophil cytoplasmic antibodies

ANOVA Analysis of variance

ANP32B Acidic nuclear phosphoprotein 32 family member B

ant-Scl70 Anti-scleroderma-70

ANXA1 Annexin A1

APC Antigen presenting cell

APRIL A proliferation-inducing ligand

ARA Anti-reticulin antibodies

ASCT Autologous stem cell transplantation

AT1R Angiotensin II type 1 receptor

ATA Anti-topoisomerase antibodies

ATCC American type culture collection

ATP Adenosine triphosphate
BAFF B cell activating factor

BANK1 B cell scaffold protein with ankyrin repeats 1

BCL6 B cell lymphoma 6
BCR B cell receptor
Beffs B effector cells
BFA Brefeldin A

BLK B lymphoid tyrosine kinase

Bregs B regulatory cells

CAR Chimeric antigen receptor
Cas9 CRISPR-associated protein 9

Chemokine (C-C motif) ligand 3
Carbontetrachloride
C-C motif chemokine ligand 4
Chemokine (C-C motif) ligand 4
Chemokine (C-C motif) ligand 5
C-C chemokine receptor type 4
C-C chemokine receptor type 6
C-C chemokine receptor type 7
Cluster of differentiation 11c
Cluster of differentiation 137
Cluster of differentiation 14
Cluster of differentiation 154
Cluster of differentiation 163
Cluster of differentiation 19
Cluster of differentiation 1c
Cluster of differentiation 2
Cluster of differentiation 20
Cluster of differentiation 20
Cluster of differentiation 204
Cluster of differentiation 21
Cluster of differentiation 22
Cluster of differentiation 25
Cluster of differentiation 25
Tumor necrosis factor receptor superfamily member 10B
Cluster of differentiation 27
Cluster of differentiation 28
Cluster of differentiation 3
Cluster of differentiation 30
Cluster of differentiation 34
Cluster of differentiation 38
Cluster of differentiation 4
Cluster of differentiation 40
CD40 ligand
Cluster of differentiation 45
Cluster of differentiation 45RA
Cluster of differentiation 56
Cluster of differentiation 69
Cluster of differentiation 69

CD7 Cluster of differentiation 7
CD79A Cluster of differentiation 79A
CD8 Cluster of differentiation 8
CD86 Cluster of differentiation 86
CD90 Cluster of differentiation 90
CD95 Cluster of differentiation 95

cDNA Complementary DNA

CDR3 Complementarity-determining region 3

CENP-A Centromere protein A
CENP-B Centromere protein B
cGAS Cyclic GMP-AMP synthase

CITE-seq Cellular indexing of transcriptomes and epitopes by sequencing

CLIP Class II-associated invariant chain peptide

CLR Centered log ratio
CMV Cytomegalovirus

COL1A1 Collagen type I alpha 1 chain
COL3A1 Collagen type III alpha 1 chain

CRISPR Clustered regularly interspaced short palindromic repeats

CRP C-reactive protein
CS Corticosteroids

CT Computed tomography
CTDs Connective tissue diseases

CTGF Connective tissue growth factor

CTLA-4 Cytotoxic T lymphocyte-associated protein 4

CTLs Cytotoxic T cells

CXCL11 Chemokine (C-C motif) ligand 9
CXCL13 Chemokine (C-C motif) ligand 13
CXCL4 Chemokine (C-C motif) ligand 4
CXCL8 Chemokine (C-C motif) ligand 8
CXCR3 C-X-C motif chemokine receptor 3
CXCR4 C-X-C motif chemokine receptor 4
CXCR5 C-X-C motif chemokine receptor 5

CYC Cyclophosphamide

DAMPs Damage-associated molecular patterns

DcR1 Decoy receptor 1
DcR2 Decoy receptor 2

dcSSc Diffuse cutaneous systemic sclerosis

DDX58 DEAD box polypeptide 58

DEGs Differentially expressed genes
DEPs Differentially expressed proteins

DHX58 DExH-box helicase 58

DLCO Diffusing capacity for carbon monoxide

DMARDs Disease-modifying antirheumatic drugs

DMEM Dulbecco's modified eagle medium

DMSO Dimethyl sulfoxide
DNA Deoxyribonucleic acid

DR4

DR5 Death receptor 5

dsRNA Double-stranded RNA

DUSP1 Dual specificity phosphatase 1
DYG Differential dynamic genes

EAE Experimental autoimmune encephalomyelitis
EANM European association of nuclear medicine

ECM Extracellular matrix

EMT Epithelial/endothelial-mesenchymal transition

ENA Extractable nuclear antigen

ESC/ERS European society of cardiology/European respiratory society

ETAR Endothelin-1 type A receptor

EULAR European League against Rheumatism
EUSTAR European scleroderma trials and research

FACS Fluorescence-activated cell sorting

FAS Fibroblast activation protein
FAS First apoptosis signal

FASL Fas ligand

FASTQ Text-based format for storing nucleotide sequences

FCGR3A Fc fragment of IgG receptor Illa

FCS Fetal calf serum

FDA Food and Drug Administration

FDC Follicular dendritic cell

FFPE Formalin-fixed paraffin-embedded

FGFBP2 Fibroblast growth factor binding protein 2

FGFR Fibroblast growth factor receptor

FLT 18F-fluorothymidine

FN1 Fibronectin 1

FOXP3 Forkhead box P3

Fra-2 Fos-related antigen 2

FSC Forward scatter

FVC Forced vital capacity

FVD Fixable viability dye

GAPDH Glyceraldehyde-3-phosphate dehydrogenase

GATA-3 GATA binding protein 3

GC Germinal center

GEO Gene expression omnibus
GFR Glomerular filtration rate

GNLY Granulysin

GvHD Graft-versus-host disease

GWAS Genome-wide association study

GZMA Granzyme A
GZMB Granzyme B
GZMB Granzyme B
GZMH Granzyme H
GZMK Granzyme K
GZMK Granzyme K
GZMZ Granzyme Z

H₂O₂ Hydrogen Peroxide

HAVCR2 Hepatitis A virus cellular receptor 2

HC Healthy control
HD Healthy donor

HDF Human dermal fibroblasts
HE Hematoxylin and eosin
HLA Human leykocyte antigen

HLA-ABC Human leukocyte antigen A, B, C

HLA-DPB1 Human leykocyte antigen-DP beta chain 1
HLA-DQB1 Human leykocyte antigen-DQ beta chain 1
HLA-DR Human leukocyte antigen-DR isotype
HLA-DRB1 Human leykocyte antigen-DR beta chain 1

HPS Human pooled serum

HRCT High-resolution computed tomography

ICAM-1 Adhesion molecule 1

ICOS Inducible T cell co-stimulator

IFIH1 Interferon induced with helicase C domain 1

IFITs Interferon-induced proteins with tetratricopeptide repeats

IFNAR1/2 Interferon alpha/beta receptor 1 and 2

IFNGR Interferon gamma receptor

IFN-α Interferon-alpha
IFN-γ Interferon-gamma
IgG Immunoglobulin G
IHC Immunohistochemistry

IL-1 Interleukin 1 Interleukin 10 IL-10 IL-12 Interleukin 12 IL-13 Interleukin 5 IL-15 Interleukin 15 Interleukin 17 IL-17 Interleukin 1 beta IL-1β IL-2 Interleukin 2 IL-21 Interleukin 21 IL-22 Interleukin 22 IL-25 Interleukin 25

IL2RA Interleukin 2 receptor alpha chain

IL-33 Interleukin 33
IL-4 Interleukin 4
IL-6 Interleukin 6
IL-6 Interleukin 13

IL7R Interleukin 7 receptor

IL-9 Interleukin 9

ILCs innate lymphoid cells
ILD Interstitial lung disease
INKT Invariant natural killer T cells

IPAH Idiopathic pulmonary arterial hypertension

IPF Idiopathic pulmonary fibrosis
IRF5 Interferon regulatory factor 5
IRF7 Interferon regulatory factor 7
IRF8 Interferon regulatory factor 8
ISG Interferon-stimulated gene
ISG15 Interferon-stimulated gene 15

IT Immunotoxin JAK Janus kinases

KLRD1 Killer cell lectin like receptor D1
LAG3 Lymphocyte activation gene 3

LAIR-1 Leukocyte-associated immunoglobulin-like receptor 1

LASP1 LIM and SH3 protein 1

lcSSc Limited cutaneous systemic sclerosis

LDH Lactate dehydrogenase

LN Lymph node

LR test Likelihood ratio test

IY6F Lymphocyte antigen 6 family member E

MACS Magnetic-activated cell sorting MAIT Mucosal-associated invariant T cells

MDA-5 Melanoma differentiation-associated protein 5

MDRD Modification of Diet in Renal Disease

MeSH **Medical Subject Headings**

MHC Major histocompatibility complex

MKI67 Marker of proliferation Ki-67 MLR Mixed lymphocyte reaction MMF Mycophenolate mofetil MMP9 Matrix metallopeptidase 9 MMPs Matrix metalloproteinases

moAb Monoclonal antibody mRNA messenger RNA

mRSS Modified Rodman skin thickness score

MS Multiple sclerosis MTX Methotrexate

MX1 MX dynamin like GTPase 1

Nuclear Antigen NAg

NCAM1 Neural cell adhesion molecule 1 NES Normalized enrichment score National institutes of health NIH

NK Natural killer

NKG7 Natural killer cell granule protein 7 NMF Non-negative matrix factorization

NMMII Non muscle myosin type 2 NOD Non-obese diabetic mice NOS Nitric oxide synthase

NP H1N1 Nucleoprotein of influenza A virus H1N1 subtype NR4A1 Nuclear receptor subfamily 4 group A member 1 NR4A2 Nuclear receptor subfamily 4 group A member 2 NR4A3 Nuclear receptor subfamily 4 group A member 3

Nt-proBNP N-terminal pro b-type natriuretic peptide

NYHA New york heart association OASL 2'-5'-oligoadenylate synthetase like

OSEM Ordered subset expectation maximization

OSM Oncostatin M

OX40 Cluster of differentiation 134
PAH Pulmonary arterial hypertension
PAM Prediction analysis for microarrays
PBMCs Peripheral blood mononuclear cells

PBS Phosphate-buffered saline PCA Principal component analysis

PD-1 Programmed death-1

PDCD1 Programmed cell death protein 1
pDCs Plasmacytoid dendritic cells
PDGF Platelet derived growth factor

PDPN Podoplanin

PET Positron emission tomography
PFTs Pulmonary function tests
PHA Phytohemagglutinin

PLOD2 Procollagen-lysine,2-oxoglutarate 5-dioxygenase 2

PMA Phorbol 12-myristate 13-acetate poly IC Polyinosinic-polycytidylic acid

Poly-HRP Polymer-conjugated horseradish peroxidase

PRDM1 PR domain zinc finger protein 1

PRF1 Perforin 1

pSTAT3 phosphorylated STAT3
PTGDS Prostaglandin D2 synthase

QILD Quantitative interstitial lung disease qPCR Quantitative polymerase chain reaction

RA Rheumatoid arthritis
RCT Randomized control trials
RIG-1 Retinoic acid-inducible gene I

RNA Ribonucleic acid

RORC RAR-related orphan receptor C
ROS Reactive oxygen species
RP Raynaud's phenomenon

RPMI Roswell park memorial institute medium

RPS27A Ribosomal protein S27a RT Room temperature

RTX Rituximab

SCID Severe combined immunodeficiency

SCOT Cyclophosphamide or transplantation trial

SD Standard deviation

SEB Staphylococcal enterotoxin B SECTM1 Secreted and transmembrane 1

SELL Selectin L

SG Salivary gland

SIE Serum-induced expression

SjS Sjogren's syndrome SLC Scleroderma lung study

SLE Systemic lupus erythematosus

SMAD2 SMAD family member 2

SPV-T3a Sample processing variable T3a

SSc Systemic sclerosis SSC Side scatter

ssGSEA Single-sample gene set enrichment analysis

STAP Key to active participation

STAT1 Signal transducer and activator of transcription 1 STAT3 Signal transducer and activator of transcription 3

STING Stimulator of interferon genes SUV Standardized uptake value

T1D Type 1 diabetes

TBET T-box transcription factor TBX21 TBP TATA-box binding protein

TBX21 T-box transcription factor 21

TCF7 Transcription factor 7

TCR T cell receptor TCZ Tocilizumab

Extrafollicular T cells Tef Texh Exhausted T cells Tfh T follicular helper

TGFB1 Transforming growth factor beta 1 TGF-β Transforming growth factor-beta

Th/To Thymus/thymocyte Th1 Thelper type 1 Th17 Thelper type 17 Th2 Thelper type 2 Th9 Thelper type 9

Thprm Hypofunctional tissue resident T cells

TIGIT T cell immunoreceptor with Ig and ITIM domains

TIM-3 T cell immunoglobulin and mucin-domain containing-3

TKs Tyrosine kinases
TLR Toll-like receptor
TMPO Thymopoietin

Tncm Naïve/central memory T cells

TNFRSF9 Tumor necrosis factor receptor superfamily member 9
TNFSF10 Tumor necrosis factor ligand superfamily member 10

TNF-α Tumor necrosis factor alpha

Tph T peripheral helper
Tprolif Proliferating T cells

Tqcm Quiescent tissue-resident T cells

TRAIL Tumor necrosis factor-related apoptosis-inducing ligand

Tregs T regulatory cells

TRGC2 T cell receptor gamma constant 2

Trm Tissue-resident memory T cells

TSLP Thymic stromal lymphopoietin

t-SNE T-distributed stochastic neighbor embedding

TSS Total skin score

UMAP Uniform manifold approximation and projection

US United states

USA United States of America

VC Vital capacity

VCAM-1 Vascular cell adhesion molecule 1

VDJ Variable, diversity, and joining gene segments

VEDOSS Very early diagnosis of systemic sclerosis

VEGFR Vascular endothelial growth factor receptor

viSNE Visualization of t-SNE

WHO World health organization

WT1 Wilms tumor 1

XCL1 Chemokine (C motif) ligand 1
ZFP36L2 Zinc finger protein 36 like 2
α-SMA Smooth muscle actin-alpha

γH2AX Phosphorylated H2A histone family member X

Curriculum vitae

Education and Professional Experience

After earning my PharmD from Aristotle University of Thessaloniki in 2016, I moved to the Netherlands in 2017. There, I received scholarship and completed a MSc in Biomedical Sciences at Radboud University Medical Center with "Excellent" distinction in 2019, focusing on the role of TGF-β in regulatory T cell autoimmunity. I then served as a voluntary research assistant in Experimental Rheumatology at Radboudume, investigating myeloid cells' role in autoimmune T cell suppression. In October 2020 I was offered a PhD position in the interface between Rheumatology and Medical Immunology at Radboudumc, where I have to date supervised six MSc theses and mentored four PhD students.

Research Focus

During my PhD, I developed an innovative pipeline that combines PET-CT imaging, ultrasound-guided biopsies, in vitro co-culture models, and single-cell analyses to detect and target autoimmune reactive B- and T cells in systemic autoimmunity. I actively shared this expertise with lab members and colleagues, significantly improving research design and execution within our department. The recognition of the developed toolkit's utility led to invitation to teach these techniques at labs outside the Netherlands, further expanding its impact and fostering new international collaborations.

In a recent study published in the top rheumatology journal Annals of the Rheumatic diseases (IF 27), I identified the CD7 receptor as a specific marker for pathogenic immune cells in systemic sclerosis tissues (chapter 3). It was demonstrated that CD7-targeted therapeutic depletion with a novel drug could halt disease progression. This research, which involved collaboration with Prof. Ido Amit's group at the Weizmann Institute, earned me the Best Basic Science Award at the 2023 EULAR meeting and was orally presented at six conferences. Based on these promising results, we received a patent and we have since launched a spinoff company to perform a proof-of-concept clinical trial, funded by Radboudumc Holding and a Dutch investment syndicate, to assess the therapeutic potential of the CD7-targeting compound in systemic sclerosis.

Collaborations and Recognitions

Recently, I collaborated with Prof. Georg Schett's team at Friedrich Alexander University of Erlangen, Germany, which pioneered anti-CD19 CAR T therapy for lupus erythematosus. We are currently investigating the molecular mechanisms

of this treatment using the toolkit I developed during my PhD. My PhD research, titled "Towards Curative Treatment for Rheumatic Systemic Autoimmune Diseases: Detection and Elimination of Pathogenic Immune Cells," earned the 2023 NVLE (Dutch Patient Organization for rheumatology research) Award for the most promising young investigator in systemic sclerosis research in the Netherlands. My work has garnered significant attention from academic and social media platforms, enabling me to advocate for systemic autoimmunity patients and receive valuable feedback from those who see hope in my research.

Outlook

The development of a novel co-culture 3D model (chapter 4) to study adaptive immune–stromal cell interactions led to a Reuma Nederland grant (Human Measurement Model) in collaboration with Professor Linde Meyaard, Utrecht University. Within this research line, we aim to further improve the current model to reflect all three disease hallmarks of systemic sclerosis; also vascular dysfunction on top of the autoimmunity and fibrosis that are already modeled. Final goal is to standardize the model to be used for high throughput drug screening.

I am planning to write a Rubicon grant to visit Professor Cornelia Weyand's lab at Stanford University and the Mayo Clinic to gain expertise on CD4+TRAIL+ T cells. This collaboration will build on my findings from Chapter 6 and further explore the metabolic role of these cells in regulating systemic rheumatic disease, with the goal of bringing this knowledge and the novel techniques back to the Netherlands.



